Synthetic, Biomimetic and Chemoenzymatic Studies of Meroterpenoid Natural Products

Thesis submitted for the degree of Doctor of Philosophy

Lauren Ashleigh Marie Murray

B. Sc. (Hons.) Chemistry

Department of Chemistry

The University of Adelaide

Nov, 2020

Table of Contents

Acknowledgements

Firstly, I would like to thank my supervisor, Assoc. Prof. Jonathan George for his guidance throughout my PhD. I am extremely grateful to have been given such interesting projects throughout my candidature, and for the opportunities and collaborations these projects have led to. Jonathan's passion for synthetic chemistry alongside his skills and experience in biomimetic synthesis have inspired me throughout my PhD and influenced my future studies. I am very thankful to Jonathan for sending me to conferences within Australia and the USA, as well as encouraging me to study abroad.

Next, I would like to thank our collaborators at Scripps Institution of Oceanography in San Diego, California, the Moore Lab. I am extremely thankful to Prof. Bradley Moore for welcoming me into his lab, twice, and truly making Scripps my home away from home. His knowledge and guidance towards this project was inimitable. I would equally like to thank my mentor, Asst. Prof. Shaun McKinnie for his constant guidance and direction during my time at Scripps. I am so grateful for his thoughts, extensive knowledge and friendship throughout my studies abroad and beyond. I would also like to thank the entire Moore lab for inviting me into their labs and lives, my time at Scripps truly allowed me to advance as a multidisciplinary scientist.

I would like to acknowledge and thank all the members of the George Group, past and present, for your support throughout my PhD. To Henry, thank you for your help with my biomimetic total synthesis. To Aaron, thank you for being my sounding board over the years, your depth of knowledge and willingness to give guidance and assistance is something I will always be grateful for. To Stefania, thank you for being my lab bestie since the day you arrived. Your support, company and kindness throughout this journey has been unwavering, and our friendship is something I will cherish forever.

To my undergraduate friends who have joined me on this PhD rollercoaster, Kathryn, Begbie and Alex, it has been a pleasure and an honour to study with you. I wish you all the best in your future endeavours, and I know you will all go on to do great things. To everyone else who has become a part of our Friday beer family, thank you for keeping me sane.

I would also like to thank my family and friends for all of their support over the years, I could not have done it without you. To my Mum and Dad, your constant support throughout my studies and over my entire life has been unwavering. Your ability to ensure that I was always able to do anything I put my mind to has been incredible, and something I am eternally grateful for. To my brothers, thank you for teaching me how to stand up for myself. Your competitive spirits and constant belief in my abilities has always kept me striving to reach my full potential. To my friends, thank you for standing by me in all of my endeavours, academic and otherwise.

Finally, to my partner Nick, your patience, love and support over the past 3 years has been incredible. You are the light of my life, and I cannot wait to see where the future takes us.

Abstract

Meroterpenoid natural products are interesting bioactive molecules produced by both terrestrial and marine organisms in nature. In *Streptomyces* bacteria, these natural products are derived from the polyketide 1,3,6,8-tetrahydroxynaphthalene (THN), giving a structurally complex group of antibiotic molecules. The biological activity and interesting scaffolds of these natural products has inspired many attempts at their chemical synthesis. This thesis will highlight how biosynthetic studies of these compounds has inspired their biomimetic and chemoenzymatic syntheses, gaining insight into their biosynthesis.

The naphterpins and marinones are two families of naphthoquinone-based meroterpenoids, isolated form *Streptomyces* bacteria. Biosynthetic speculation inspired the first total syntheses of two members from the naphterpin and marinone families, 7-demethylnaphterpin and debromomarinone, mimicking the entire proposed biosynthetic pathway. In validation of this biogenetic hypothesis, proposed biosynthetic intermediates from these biomimetic total syntheses were used in chemoenzymatic studies. These studies stimulated the discovery of multiple enzymes responsible for interconverting several of the proposed biosynthetic intermediates within these natural product biosyntheses, therefore confirming the biosynthetic proposal.

Following these biomimetic total syntheses, a concise and divergent strategy for the synthesis of more members from the naphterpin and marinone families was developed. This approach utilised a plethora of pericyclic reactions, enabling the efficient synthesis of six meroterpenoid natural products, in the absence of protecting group strategies. This synthetic approach facilitated the first total synthesis of naphterpin in five steps from 2,5-dimethoxyphenol, alongside similar syntheses of 7-demethylnaphterpin and debromomarinone. Late-stage

oxidation and bromination reactions were also investigated, resulting in the first total syntheses of naphterpins B and C, and isomarinone.

Declaration

I certify that this work contains no material which has been accepted for the award of any other degree or diploma in my name, in any university or other tertiary institution and, to the best of my knowledge and belief, contains no material previously published or written by another person, except where due reference has been made in the text. In addition, I certify that no part of this work will, in the future, be used in a submission in my name, for any other degree or diploma in any university or other tertiary institution without the prior approval of the University of Adelaide and where applicable, any partner institution responsible for the joint-award of this degree.

I give permission for the digital version of my thesis to be made available on the web, via the University's digital research repository, the Library Search and also through web search engines, unless permission has been granted by the University to restrict access for a period of time.

I acknowledge the support I have received for my research through the provision of an Australian Government Research Training Program Scholarship.

25/11/2020

Lauren Ashleigh Marie Murray Date

List of Abbreviations

AIBN	Azobisisobutyronitrile
antiSMASH	Antibiotics & Secondary Metabolite Analysis Shell
ATP	Adenosine Triphosphate
BGC	Biosynthetic Gene Cluster
BLAST	Basic Local Alignment Search Tool
CAN	Ceric Ammonium Nitrate
CoA	Coenzyme A
COSY	Correlated Spectroscopy
cm^{-1}	Wavenumber(s)
d	Doublet
DBU	1,8-Diazabicyclo[5.4.0]undec-7-ene
DDQ	2,3-Dichloro-5,6-Dicyano-1,4-Benzoquinone
DMAPP	Dimethylallyl Pyrophosphate
DMSO	Dimethyl Sulfoxide
DMF	*N,N*-Dimethylformamide
DPMVA	Diphosphomevalonate
EDDA	Ethylenediaminediacetate
EDTA	Ethylenediaminetetraacetic Acid
EIC	Extracted Ion Chromatogram
ESI	Electrospray Ionization
EtOAc	Ethyl Acetate
FPP	Farnesyl Pyrophosphate
FT	Fourier Transform
GPP	Geranyl Pyrophosphate
h	Hour(s)
HEPES	(4-(2-Hydroxyethyl)-1-Piperazineethanesulfonic Acid)
HMBC	Heteronuclear Multiple Bond Connectivity
HMG	3-Hydroxy-3-Methyl-Glutaryl
HPLC	High Performance Liquid Chromatography
IBX	2-Iodoxybenzoic Acid

IC_{50}	Half Maximal Inhibitory Concentration
IPP	Δ^3-Isopentenyl Pyrophosphate
IR	Infrared Spectrum
J	Coupling Constant
KHMDS	Potassium Hexamethyldisilazide
LDA	Lithium Diisopropylamide
m	Multiplet
m/z	Mass Units
MCD	Monochlorodimedone
MEP	Methylerythritol Phosphate
MES	2-(N-Methylmorpholino)-Ethanesulfonic Acid
MHz	Megahertz
MIC	Minimum Inhibitory Concentration
MOM	Methoxymethyl
mp	Melting Point
MRSA	Methicillin Resistant Staphylococcus Aureus
MS	Mass Spectrum
MVA	Mevalonate
NBS	*N*-Bromosuccinimide
NCS	*N*-Chlorosuccinimide
NaHMDS	Sodium Hexamethyldisilazide
NMR	Nuclear Magnetic Resonance
NOESY	Nuclear Overhauser Effect Spectroscopy
Phyre	Protein Homology/Analogy Recognition Engine
PMVA	Phosphomevalonate
PP	Pyrophosphate
ppm	Parts Per Million
PPTS	Pyridinium *para*-Toluenesulfonate
p-TsOH	*para*-Toluenesulfonic Acid
q	Quartet
R_f	Retention Factor
ROESY	Rotating Frame Nuclear Overhauser Effect Spectroscopy

RP	Reverse Phase
rt	Room Temperature
s	Singlet
SAM	*S*-Adenosyl Methionine
SAR	Structure Activity Relationship
t	Triplet
TEMPO	(2,2,6,6-Tetramethylpiperidin-1-yl)oxyl
THC	Tetrahydrocannabinol
THCA	Tetrahydrocannabinolic Acid
THF	Tetrahydrofuran
THN	1,3,6,8-Tetrahydroxynaphthalene
THNS	1,3,6,8-Tetrahydroxynaphthalene Synthase
TLC	Thin Layer Chromatography
TMS	Tetramethylsilane
TOF	Time of Flight
UV	Ultraviolet Light
VCPO	Vanadium-Dependent Chloroperoxidase
VHPO	Vanadium-Dependent Haloperoxidase

CHAPTER 1

Thesis Introduction

1.1 Meroterpenoid Natural Products

The organic compounds produced in nature can be separated into two distinct classes, known as primary and secondary metabolites.[1] Primary metabolites are molecules present in the pathways essential for life, including nucleic acids, proteins, lipids and polysaccharides. They also play a crucial role in pathways for the generation and storage of energy, such as the citrate cycle, glycolysis and amino acid metabolism.[1] Many of these primary metabolites are shared across multiple organisms, however secondary metabolites are often specific to certain genera or species. Secondary metabolites are molecules that are not essential for the life of the producing organism, however they commonly give an environmental or evolutionary advantage. These secondary metabolites are produced by bacteria, fungi and plants, and are more commonly referred to as natural products.

Many of the fundamental building blocks in primary metabolism are also crucial in secondary pathways that lead to the synthesis of natural products.[2] These natural product frameworks include polyketides, terpenes, alkaloids and peptides.[1] Alkaloid natural products contain one or more basic nitrogen atoms, embedded within a heterocyclic ring. These nitrogen atoms originate from essential amino acids, similar to peptide natural products, which are typically constructed though the cyclisation of linear peptide chains. The thioester acetyl coenzyme A (acetyl-CoA) (**1.01**) plays a crucial role in both primary and secondary metabolism. In secondary metabolism, acetyl-CoA (**1.01**) is converted through the fatty acid or polyketide synthesis pathways to malonyl-CoA (**1.02**), or alternatively through the mevalonate pathway to mevalonic acid (mevalonate, **1.03**).[3] Malonyl-CoA (**1.02**) is then used in the biosynthesis of fatty acids and polyketides, while mevalonate (**1.03**) is used in the biosynthesis of steroids and terpenes (Scheme 1.01).

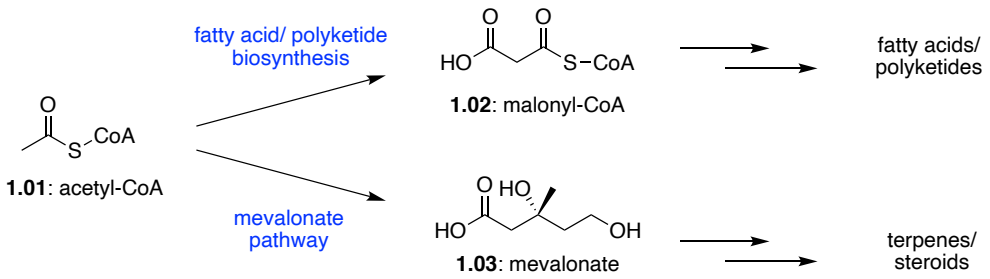

Scheme 1.01: Biosynthesis of different natural product classes from acetyl-CoA (**1.01**).

Malonyl-CoA (**1.02**) is synthesised through the ATP-dependent carboxylation of acetyl-CoA (**1.01**) with the biotin-dependent enzyme, acetyl-CoA carboxylase (Scheme 1.02).[4]

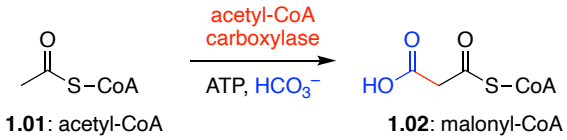

Scheme 1.02: Formation of malonyl-CoA (**1.02**) through carboxylation of acetyl-CoA (**1.01**) with biotin-dependent acetyl-CoA carboxylase enzyme.[4]

In both fatty acid and polyketide biosynthesis, the malonyl-CoA subunit is transferred to the thiol of an acyl carrier protein,[5,6] where the polyketide chain is elongated (Scheme 1.03).[3] This elongation process begins with an enzyme-catalysed decarboxylation of the malonyl thioester **1.04** to form the acetyl-CoA carbanion **1.05**, accompanied by the irreversible loss of CO_2. Carbanion **1.05** can then undergo a Claisen condensation with **1.06** to form diketide **1.07**. This decarboxylative Claisen condensation is then repeated to extend the β-keto thioester chain to afford a polyketide (**1.08**) of desired length. Alternatively, in fatty acid biosynthesis, diketide **1.07** will undergo a series of reduction and dehydration reactions in addition to elongation to give a fatty acid (**1.09**).

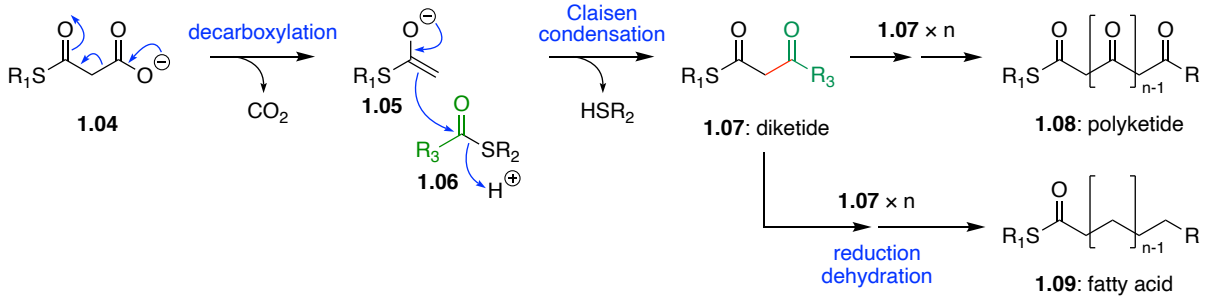

Scheme 1.03: Chain elongation in fatty acid and polyketide biosynthesis.[3]

These linear polyketonic chains are susceptible to condensation, dehydration and aromatization reactions to form diverse polyketide natural product scaffolds (Scheme 1.01). Many of the unique scaffolds found in polyketide natural products are known to have potent therapeutic properties. For example, aromatic tetracycle doxycycline (**1.10**)[7] and macrolactone erythromycin (**1.11**)[3] are both potent antibiotics, while lovastatin (**1.12**) is a decalin-containing drug used clinically to lower cholesterol.[8] The insecticide xanthone (**1.13**) is part of a much larger xanthone natural product family, known for their diverse pharmacological properties.[9] Lasalocid (**1.14**) is a coccidiostat and an antibacterial agent.[10]

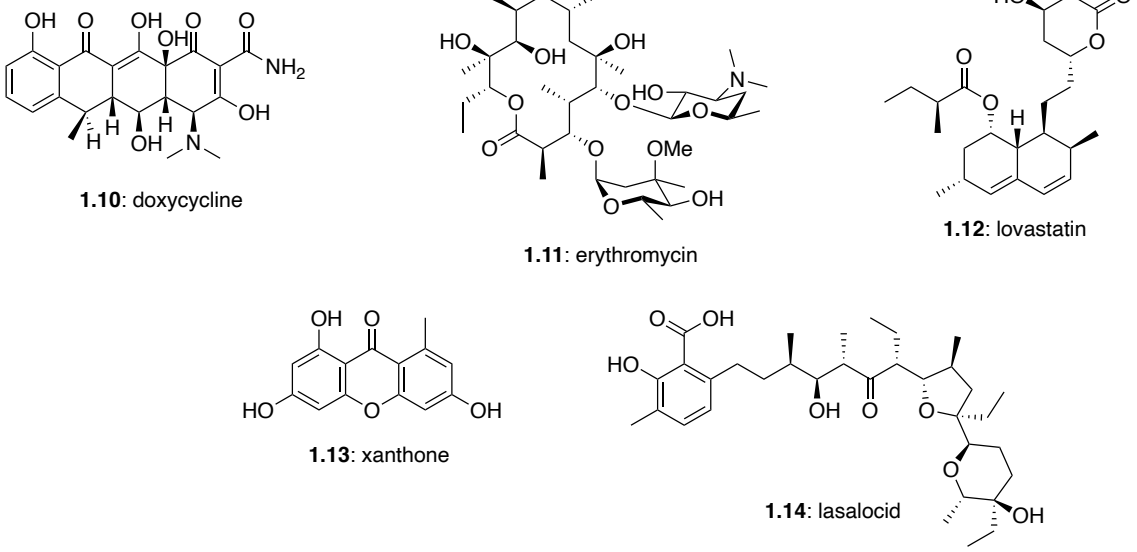

Figure 1.01: Examples of diverse polyketide natural product scaffolds.[3,7–10]

Terpene and terpenoids are the most abundant class of natural products, and are frequently isolated from plants, fungi and green algae. These natural products are derived from five-carbon isoprene units and are biosynthesised from Δ^3-isopentenyl pyrophosphate (IPP) and dimethylallyl pyrophosphate (DMAPP). In eukaryotes, archaea and most bacteria, these two building blocks are biosynthesised from the classical pathway, also known as the mevalonate pathway (Scheme 1.04).[1] The mevalonate pathway begins with the enzyme-catalysed condensation of two acetyl-CoA (**1.01**) subunits to form malonyl-CoA (**1.02**). A third condensation reaction is then catalysed by HMG-CoA synthase with **1.01** to give the intermediate HMG-CoA (**1.15**). Subsequent four electron reduction of **1.15** with HMG-CoA reductase affords mevalonate (**1.03**). Two successive phosphorylations at C1 with MVA and PMVA kinases generates mevalonate pyrophosphate (**1.16**). A third phosphorylation at the C3 alcohol gives **1.17**, followed by decarboxylation and loss of P_i to yield IPP (**1.18**). Formation of DMAPP (**1.19**) is achieved through enzyme-catalysed isomerisation, giving an equilibrium between the two regioisomers **1.18** and **1.19**.

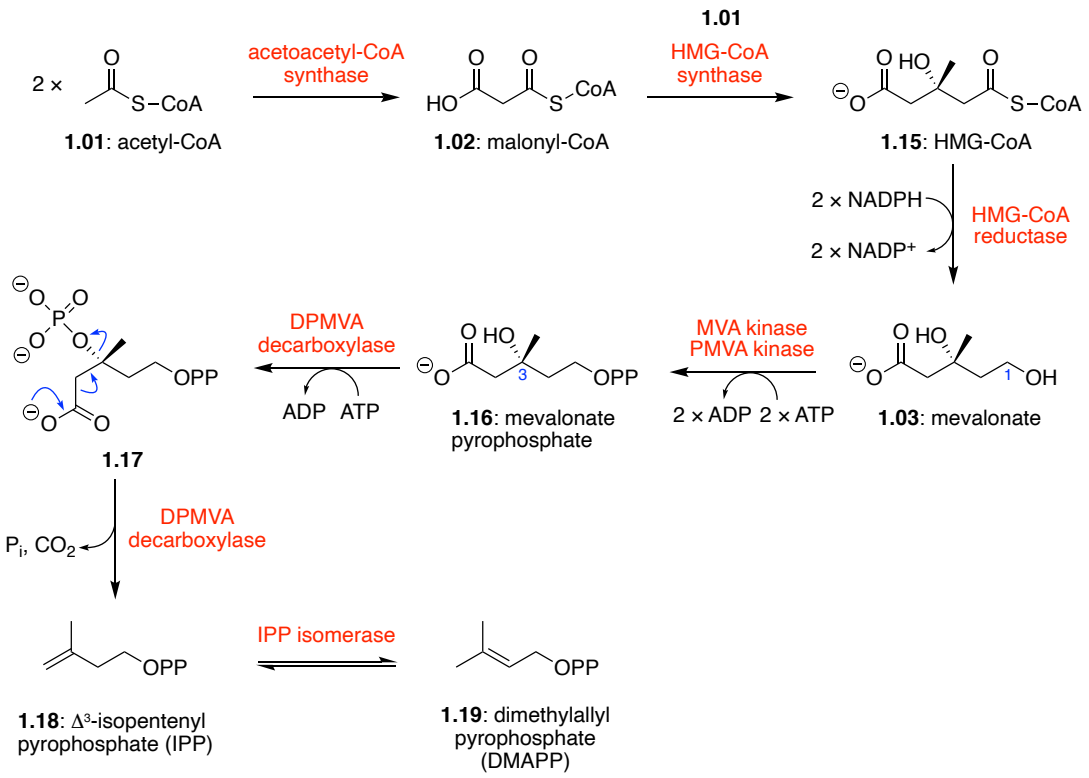

Scheme 1.04: Mevalonate pathway leading to the synthesis of IPP (**1.18**) and DMAPP (**1.19**) in equilibrium.[1]

A second biosynthetic pathway leading to the formation of IPP (**1.18**) also exists, known as the non-classical pathway or the methylerythritol phosphate (MEP) pathway.[11] This pathway relies on the condensation of primary metabolites pyruvate and glyceraldehyde-3-phosphate for the formation of MEP. Subsequent tailoring steps result in the formation of **1.18** and **1.19**. The MEP pathway is found in plants, fungi, and archaea.[12]

The elongation of these five carbon prenyl groups can occur through head-to-tail addition of IPP (**1.18**) to DMAPP (**1.19**) (Scheme 1.05).[1] This elongation begins with the formation of the cationic species **1.20** and **1.21**, through dissociation of the C1-OPP group from DMAPP (**1.19**). Nucleophilic attack from the regioisomer IPP (**1.18**) then results in the formation of the C-10 monoterpene geranyl pyrophosphate (GPP) (**1.22**). Subsequent alkylation results in the C-15

sesquiterpene farnesyl pyrophosphate (**1.23**), followed by C-20 diterpene geranylgeranyl pyrophosphate (**1.24**) and so on.

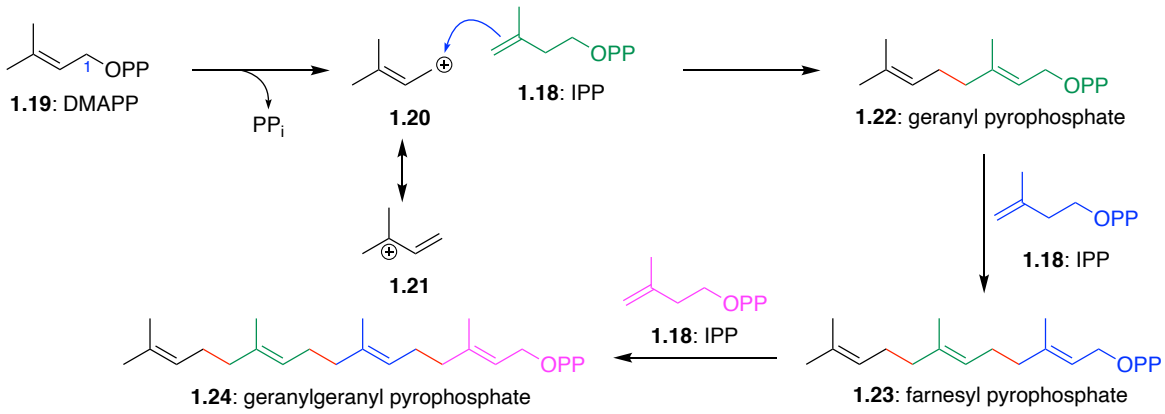

Scheme 1.05: Chain elongation of DMAPP (**1.19**) through head-to-tail addition of IPP (**1.18**).

Electrophilic cyclisation of these linear terpenes can produce a wide variety of cyclic natural products (Scheme 1.02).[1] Terpene natural products consist of a hydrocarbon framework (**1.25-1.28**), while their oxygen containing counterparts are referred to as terpenoids (**1.29-1.33**). Historically, the most abundant source of terpene and terpenoid natural products has been from plants, where they are responsible for many well-known flavours and fragrances. Limonene (**1.25**) and citral (**1.31**) are the two major components found in citrus fruit peels, while lavandulol (**1.33**) is found in a variety of essential oils including lavender oil.[13,14]

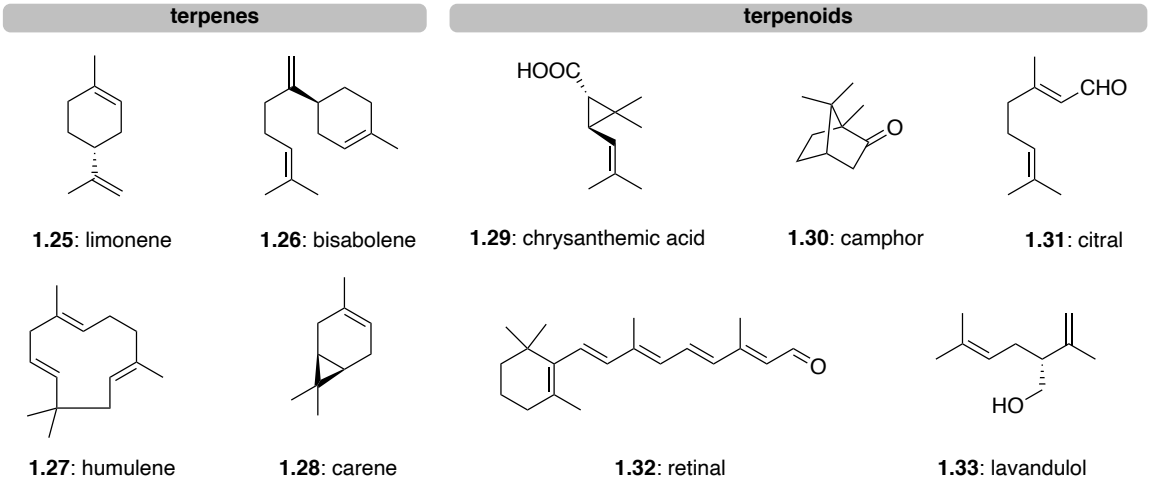

Figure 1.02: Examples of terpene and terpenoid natural products.[1]

Meroterpenoids are natural products of mixed biosynthetic origin, derived partially from a terpenoid co-substrate.[15,16] These hybrid molecules are broadly produced in nature by bacteria, fungi, plants, algae and animals, and combine terpenoid building blocks with polyketides, phenols, alkaloids, and amino acids to achieve exceptional chemical diversity.[17–20] Some notable examples include antidepressant hyperforin (**1.34**),[21,22] psychoactive drug tetrahydrocannabinol (**1.35**)[20,23] and immunosuppressant mycophenolic acid (**1.36**)[24] (Scheme 1.03).

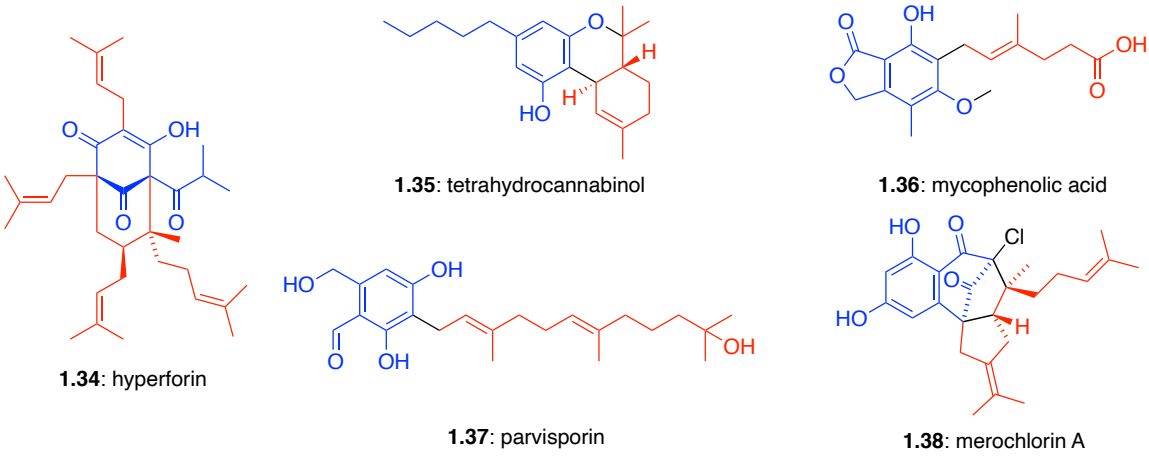

Figure 1.03: Meroterpenoid natural products. Terpene derived fragment highlighted in red, and polyketide derived fragment highlighted in blue.[21–26]

Mycophenolic acid (**1.36**) is a meroterpenoid natural product with broad biological activity, most commonly known for its immunosuppressive properties.[27] Mycophenolic acid (**1.36**) is biosynthetically derived from both the polyketide and terpene biosynthetic pathways, and involves methylation reactions from *S*-adenosyl methionine (SAM) (Scheme 1.06).[24] Biosynthetically, 5-methylorsellinic acid (**1.39**) is synthesised from one molecule of acetyl-CoA (**1.01**), three molecules of malonyl-CoA (**1.02**) and one molecule of SAM, under the control of a polyketide synthase MpaC. Next, chimeric P450 monooxygenase and hydrolase enzyme, MpaDE, converts **1.39** to phthalide **1.40** through hydroxylation of the C-6 methyl group, followed by lactonization. Farnesylation of **1.40** is catalysed by prenyltransferase enzyme MpaA with **1.23** to give **1.41**, which is then proposed to undergo oxidative cleavage with MpaH to give demethylmycophenolic acid (**1.42**).[24] Subsequent methylation with MpaG in the presence of SAM affords the natural product mycophenolic acid (**1.36**). The biosynthesis of **1.36** demonstrates how meroterpenoid natural products can be formed from the union of two distinct biosynthetic pathways.

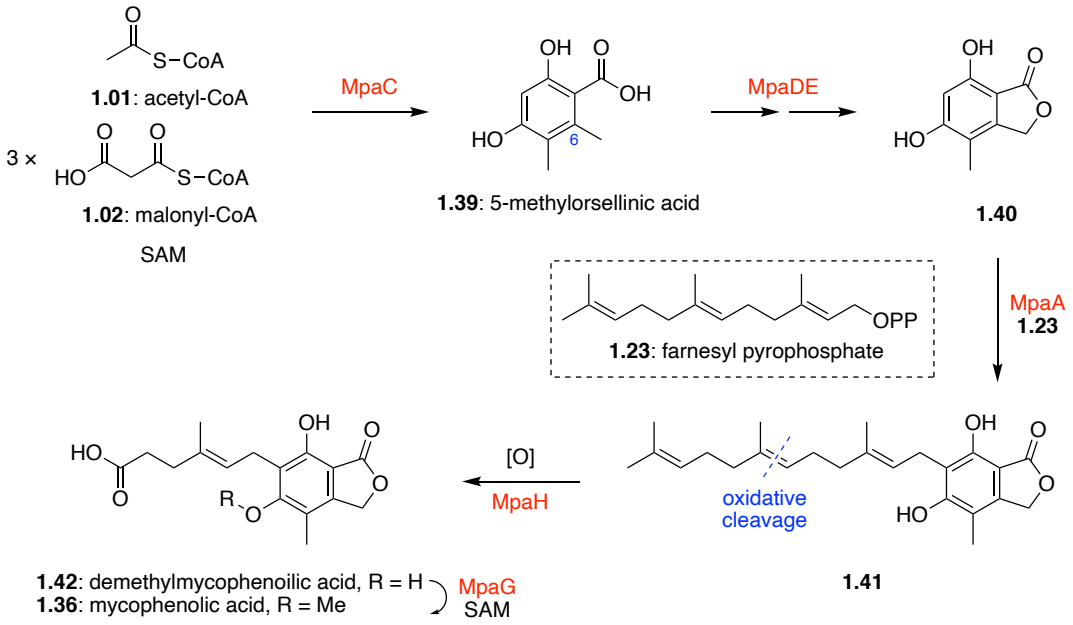

Scheme 1.06: Biosynthesis of mycophenolic acid (**1.36**).[24]

1.2 Biomimetic Synthesis of Natural Products

The isolation of natural products has contributed to the discovery of new therapeutic agents for decades.[28,29] The novel scaffolds of these molecules often result in interesting biological activities with the potential to act as effective agents in the treatment of human disease. Studies have shown that in the last four decades, ~40% of new approved drugs were natural products or natural product derivatives.[28] This data emphasises the importance of natural product discovery and derivatisation. Natural products themselves are often isolated in sub-milligram to milligram quantities from their natural source. Consequently, accessing these biologically active molecules through chemical synthesis in a laboratory is necessary to produce the quantities required for clinical trials and commercial availability.

One such approach to accessing these natural products is to mimic key steps from the proposed or known biosynthetic pathway. This approach is known as biomimetic synthesis. Although the term biomimetic synthesis was coined by Breslow in 1972,[30] the first example of such as synthesis was the biomimetic total synthesis of tropinone (**1.43**) completed by Robinson in 1917 (Scheme 1.07).[31] This synthesis mimicked the biosynthesis of tropinone (**1.43**) employing sequential Mannich reactions. Starting from three simple starting materials, succinaldehyde (**1.44**), methylamine (**1.45**) and 3-oxopentanedioic acid (**1.46**), this approach was able to rapidly build the molecular complexity of this bicyclic structure.

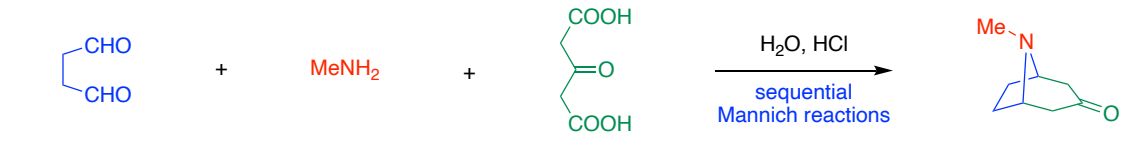

1.44: succinaldehyde **1.45**: methylamine **1.46**: 3-oxopentanedioic acid **1.43**: tropinone

Scheme 1.07: Robinson's 1917 biomimetic synthesis of tropinone (**1.43**).[31]

This biomimetic approach has since been expanded to the synthesis of many natural product scaffolds, including the synthesis of steroid and terpenoid natural products.[32] These biomimetic syntheses commonly utilise polyene cyclisation cascade reactions to mimic the polyene cyclase reactions found in nature.[33] This strategy was employed by van Tamelen[34] in the biomimetic synthesis of allopregnanolone (**1.47**) (Scheme 1.08). Treatment of epoxide **1.48** with $BF_3 \cdot OEt_2$ and ethylene carbonate (**1.49**) catalysed a cascade cyclisation, generating four new rings and seven new stereocentres, to give **1.47** in one pot.

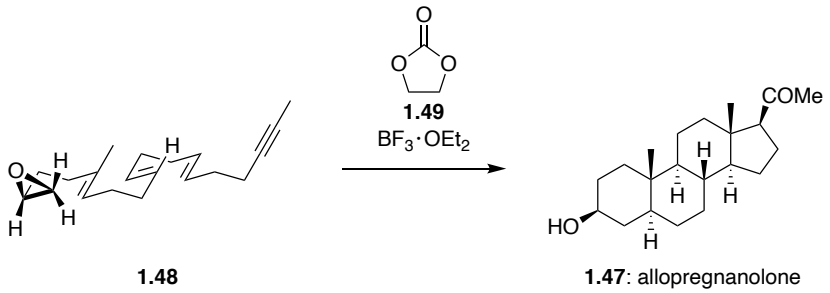

Scheme 1.08: Key polyene cyclisation in van Tamelen's biomimetic synthesis of allopregnanolone (**1.47**).[34]

Considering the biosynthetic origin of these complex natural products throughout a chemical synthesis continues to inspire and improve synthetic strategies, with the potential to rapidly build molecular complexity. Our ability to mirror the innate reactivity of these molecules using synthetic chemistry is crucial in accessing these important bioactive natural products.

1.3 Previous Studies on Marine Meroterpenoid Natural Products

Over the past four decades, marine and soil-derived streptomycete bacteria have been discovered from several families of naphthoquinone-based meroterpenoids.[35] These natural products have been linked through biosynthetic speculation and ^{13}C-labelling studies to the key aromatic polyketide building block 1,3,6,8-tetrahydroxynaphthalene (THN, **1.50**). In bacteria, THN (**1.50**) is biosynthesised by the condensation and aromatisation of five malonyl-CoA (**1.02**) subunits under the control of a THN synthase (THNS) enzyme (Scheme 1.09).[36] This is achieved by bacterial THN synthases using a simple type III polyketide synthase homodimeric structure.[37]

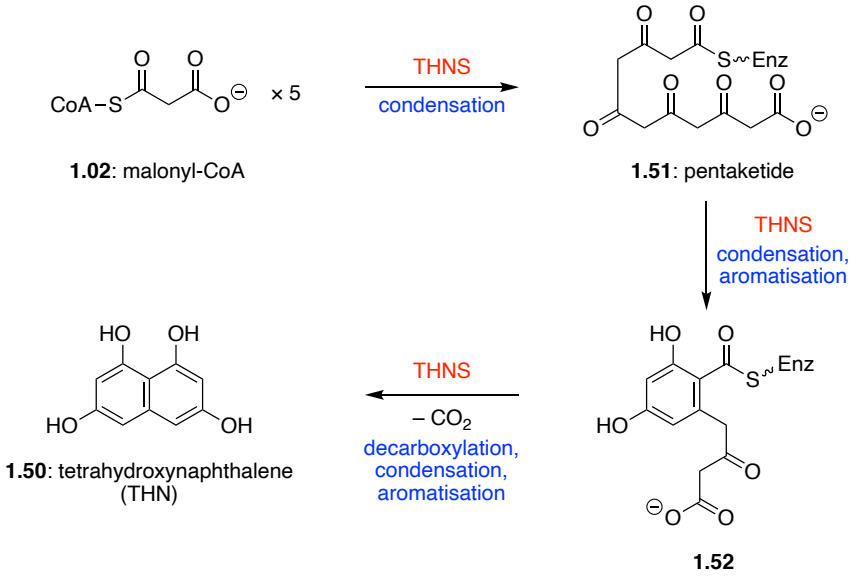

Scheme 1.09: Biosynthesis of 1,3,6,8-tetrahydroxynaphthalene (THN, **1.50**).[36]

Several THN synthases have previously been involved in the biosynthesis of bacterial meroterpenoids, including Mcl17 (merochlorins)[26] and NapB1 (napyradiomycins)[38]. The previous work on these marine meroterpenoids has shown that the merochlorins[26] and napyradiomycins[39] are derived directly from THN, with oxidation, halogenation and cyclisation steps occurring after the initial prenylation of the THN core (Figure 1.04). Aromatic prenyltransferase enzymes are responsible for catalysing electrophilic aromatic substitution

reactions between prenyl donors, including prenyl, geranyl and farnesyl pyrophosphate, with the nucleophilic C-2 and C-4 positions of THN (**1.50**).[40] Subsequently, vanadium-dependent haloperoxidase (VHPO) enzymes are responsible for catalysing a variety of reactions, including direct halogenation, oxidative dearomatisation, halocyclization and α-hydroxyketone rearrangements, to give complex meroterpenoid molecular architectures such as **1.38**, **1.53**, **1.54**, **1.55**, **1.56** and **1.57**.[41] The work presented in this thesis will focus on the synthesis and biosynthesis of the marinone and naphterpin families of natural products.

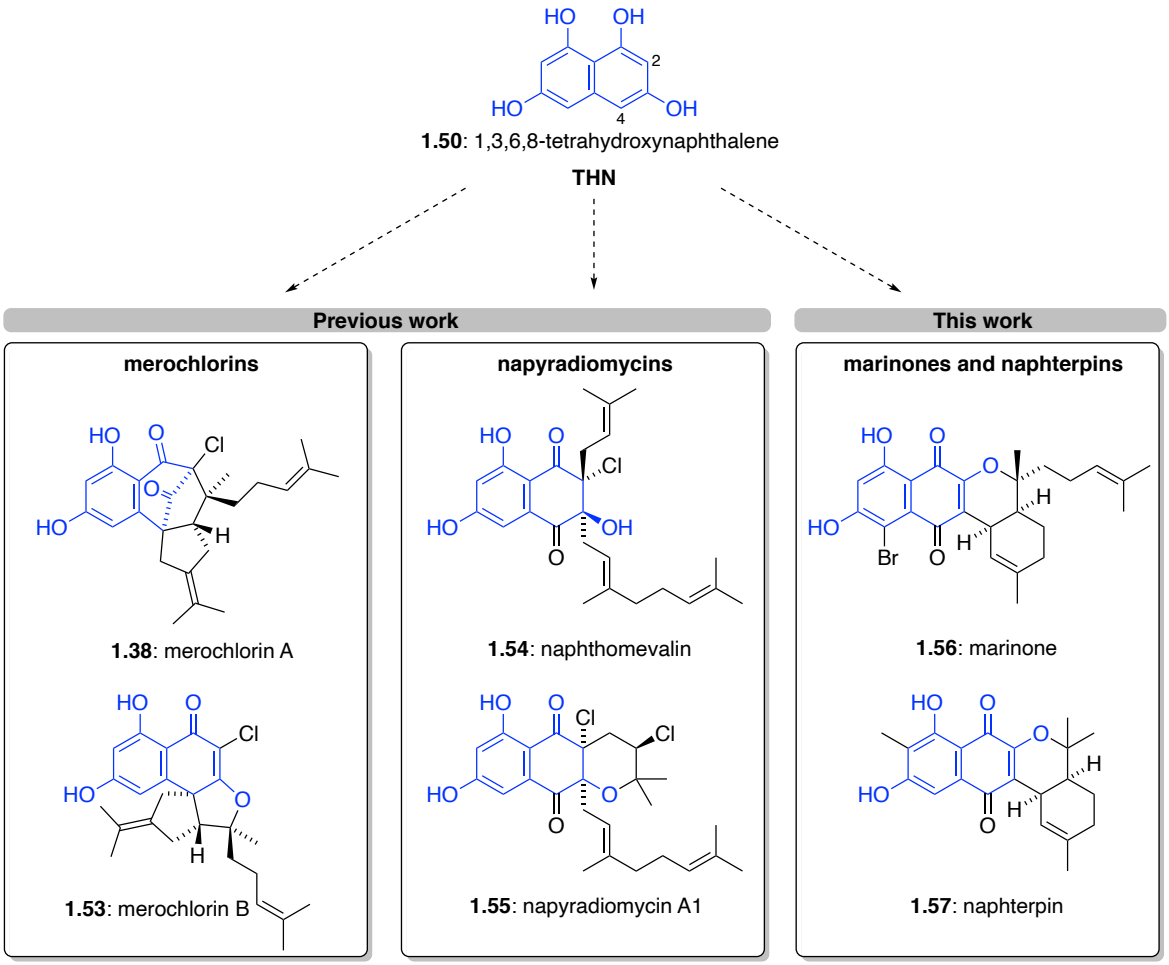

Figure 1.04: Families of meroterpenoid natural products biosynthesised from THN (**1.50**).

1.4 References

(1) Walsh, C. T.; Tang, Y. *Natural Product Biosynthesis: Chemical Logic and Enzymatic Machinery*; Royal Society of Chemistry, 2017.
(2) Mouncey, N. J.; Otani, H.; Udwary, D.; Yoshikuni, Y. *J. Ind. Microbiol. Biotechnol.* **2019**, *46*, 273.
(3) Staunton, J.; Weissman, K. J. *Nat. Prod. Rep.* **2001**, *18*, 380.
(4) Broussard, T. C.; Price, A. E.; Laborde, S. M.; Waldrop, G. L. *Biochemistry* **2013**, *52*, 3346.
(5) Majerus, P. W.; Alberts, A. W.; Vagelos, P. R. *J. Biol. Chem.* **1965**, *240*, 618.
(6) Majerus, P. W.; Alberts, A. W.; Vagelos, P. R. *Proc. Natl. Acad. Sci. U.S.A.* **1965**, *53*, 410.
(7) Aronson, J. K.; Meyler, L. In *Meyler's Side Effects of Drugs: The International Encyclopedia of Adverse Drug Reactions and Interactions*; Elsevier Science: Amsterdam, 2016; pp 1086–1090.
(8) Maron, D. J.; Fazio, S.; Linton, M. F. *Circulation* **2000**, *101*, 207.
(9) Mazimba, O.; Nana, F.; Kuete, V.; Singh, G. S. *Xanthones and Anthranoids from the Medicinal Plants of Africa*; Elsevier Inc., 2013.
(10) Minami, A.; Oguri, H.; Watanabe, K.; Oikawa, H. *Curr. Opin. Chem. Biol.* **2013**, *17*, 555.
(11) Rohmer, M. *Nat. Prod. Rep.* **1999**, *16*, 565.
(12) Lichtenthaler, H. K. *Annu. Rev. Plant Biol.* **1999**, *50*, 47.
(13) Demissie, Z. A.; Erland, L. A. E.; Rheault, M. R.; Mahmoud, S. S. *J. Biol. Chem.* **2013**, *288*, 6333.
(14) Sharmeen, J. B.; Mahomoodally, F. M.; Zengin, G.; Maggi, F. *Molecules* **2021**, *26*, 666.
(15) Cornforth, J. W. *Chem. Br.* **1968**, *4*, 102.
(16) Geris, R.; Simpson, T. J. *Nat. Prod. Rep.* **2009**, *26*, 1063.
(17) Matsuda, Y.; Abe, I. *Nat. Prod. Rep.* **2016**, *33*, 26.
(18) Li, S.-M. *Nat. Prod. Rep.* **2010**, *27*, 57.
(19) Gallagher, K. A.; Fenical, W.; Jensen, P. R. *Curr. Opin. Biotechnol.* **2010**, *21*, 794.
(20) Appendino, G.; Chianese, G.; Taglialatela-Scafati, O. *Curr. Med. Chem.* **2011**, *18*, 1085.
(21) Gurevich, A. I.; Dobrynin, V. N.; Kolosov, M. N.; Popravko, S. A.; Ryabova, I. D.; Chernov, B. K.; Derbentseva, N. A.; Aizenman, B. E.; Garagulya, A. D. *Antibiot. Khimioterapi* **1971**, *16*, 510.
(22) Bystrov N. S., Chernov, B. K., Dobrynin V. N., Kolosov, M. N. *Tetrahedron Lett.* **1975**, *16*, 2791.
(23) Gaoni, Y.; Mechoulam, R. *J. Am. Chem. Soc.* **1964**, *86*, 1646.
(24) Halle, M. B.; Lee, W.; Yudhistira, T.; Kim, M.; Churchill, D. G. *European J. Org. Chem.* **2019**, *2019*, 2315.
(25) Nozawa, Y.; Sugawara, K.; Stachybotrin, C. *J. Antibiot.* **1997**, *50*, 641.
(26) Kaysser, L.; Bernhardt, P.; Nam, S. J.; Loesgen, S.; Ruby, J. G.; Skewes-Cox, P.; Jensen, P. R.; Fenical, W.; Moore, B. S. *J. Am. Chem. Soc.* **2012**, *134*, 11988.
(27) Bennett, W. M. *J. Am. Soc. Nephrol.* **2003**, *14*, 2414.
(28) Newman, D. J.; Cragg, G. M. *J. Nat. Prod.* **2020**, *83*, 770.
(29) Atanasov, A. G.; Zotchev, S. B.; Dirsch, V. M.; Supuran, C. T. *Nat. Rev. Drug Discov.* **2021**, *20*, 200.
(30) Breslow, R. *Chem. Soc. Rev.* **1972**, *1*, 553.
(31) Robinson, R. J. *J. Chem. Soc., Trans.* **1917**, *111*, 762.
(32) Yoder, R. A.; Johnston, J. N. *Chem. Rev.* **2005**, *105*, 4730.

(33) Brunoldi, E.; Luparia, M.; Porta, A.; Zanoni, G.; Vidari, G. *Curr. Org. Chem.* **2006**, *10*, 2259.
(34) van Tamelen, E. E.; Leiden, T. M. *J. Am. Chem. Soc.* **1982**, *104*, 2061.
(35) Moore, B. S. *Synlett* **2018**, *29*, 401.
(36) Funa, N.; Ohnishi, Y.; Fujli, I.; Shibuya, M.; Ebizuka, Y.; Horinouchi, S. *Nature* **1999**, *400*, 897.
(37) Austin, M. B.; Izumikawa, M.; Bowman, M. E.; Udwary, D. W.; Ferrer, J. L.; Moore, B. S.; Noel, J. P. *J. Biol. Chem.* **2004**, *279*, 45162.
(38) Winter, J. M.; Moffitt, M. C.; Zazopoulos, E.; McAlpine, J. B.; Dorrestein, P. C.; Moore, B. S. *J. Biol. Chem.* **2007**, *282*, 16362.
(39) Miles, Z. D.; Diethelm, S.; Pepper, H. P.; Huang, D. M.; George, J. H.; Moore, B. S. *Nat. Chem.* **2017**, *9*, 1235.
(40) Tello, M.; Kuzuyama, T.; Heide, L.; Noel, J. P.; Richard, S. B. *Cell. Mol. Life Sci.* **2008**, *65*, 1459.
(41) Winter, J. M.; Moore, B. S. *J. Biol. Chem.* **2009**, *284*, 18577.

CHAPTER 2

Biomimetic Total Synthesis of Naphterpin and Marinone Natural Products

Carbon atoms of 7-demethylnaphterpin, debromomarinone and related synthetic intermediates are numbered throughout this chapter as follows:

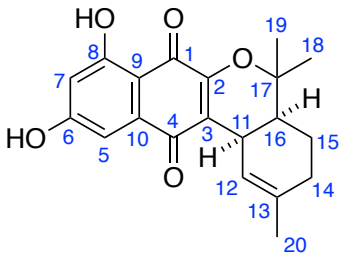

7-demethylnaphterpin

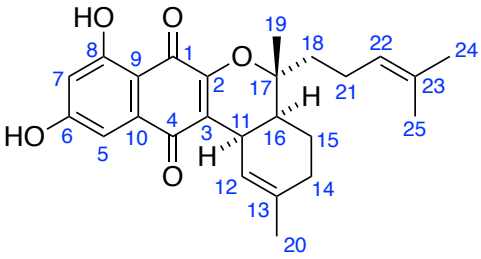

debromomarinone

Parts of this chapter have been published as follows:

Murray, L. A. M.; McKinnie, S. M. K.; Pepper, H. P.; Erni, R.; Miles, Z. D.; Cruickshank, M. C.; López-Pérez, B.; Moore, B. S.; George, J. H. *Angew. Chem. Int. Ed.* **2018**, *57*, 11009.

Parts of this chapter were adapted from the following review:

Murray, L. A. M.; McKinnie, S. M. K.; Moore, B. S.; George, J. H. *Nat. Prod. Rep.* **2020**, *37*, 1334.

2.1 Introduction

2.1.1 Halogenated Natural Products

Halogenation of natural products is a recurrent modification found in nature, often linked to the bioactivity of these secondary metabolites.[1] These halogenated compounds exhibit a diverse range of biological activities, including both anticancer and antibiotic properties.[2] To date, there are over 5000 halogenated natural products, with chlorination being the most prevalent modification.[2] The structural diversity of these halogenated natural products in nature is widespread, ranging from simple halogenated aromatic phenols to more complex terpenoids, polyketides, oligopeptides, and alkaloids.[3] While the majority of these organohalogen natural products are of marine origin, their isolation spans both marine and terrestrial organisms including plants, algae, sponges, corals, bacteria, cyanobacteria and fungi.[4]

Many examples of these organohalogen natural products possess remarkable biological activities with a wide range of applications (Figure 2.01). The dichloride chloramphenicol (**2.01**) is a clinically relevant broad-spectrum antibiotic,[5,6] while β-lactone salinosporamide A (**2.02**) is an extremely potent anticancer agent.[7,8] The chlorine substituents of the glycopeptide antibiotic vancomycin (**2.03**) are responsible for the molecule's clinically active conformation, used to treat many life threatening infections such as multiple-drug resistant *S. aureus* infections.[9,10] In a physiological context, the thyroid prohormone thyroxine (**2.04**) is activated and deactivated through modifications to the number of iodine atoms attached to the bicyclic core.[11] Finally, sesterterpenes neomangicol A (**2.05**) and B (**2.06**) are two halogenated natural products, differing only by the halogen on their terminal olefin, and both found to have cytotoxic activity against a variety of cancer cell lines.[12] The incredible variety of fascinating chemical structures and potent biological activity of these organohalogen natural products continues to inspire the chemical synthesis of these valuable molecules.

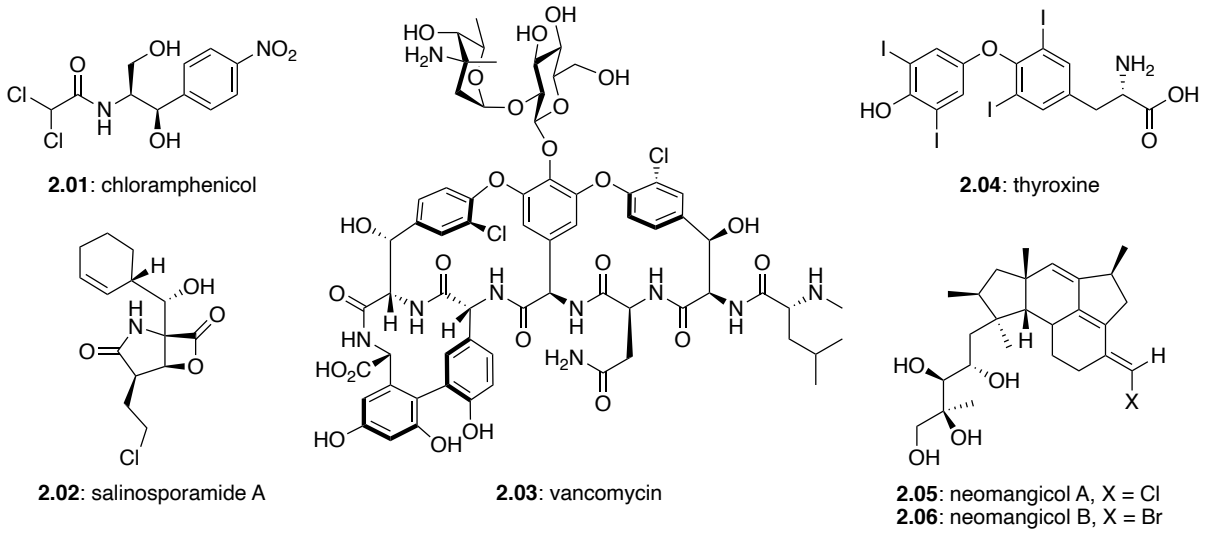

Figure 2.01: Examples of halogenated organic natural products.[5–11]

2.1.2 Vanadium-Dependent Haloperoxidases

With an abundance of halogenated natural products being continuously isolated from a wide variety of organisms, the enzymes responsible for their halogenation have become of increasing interest. After the first halogenating enzyme, haem chloroperoxidase (CPO),[13] was discovered in the 1960s, many other halogenating enzymes including haem haloperoxidases, non-haem iron halogenases, and non-metallo haloperoxidases have been discovered from a variety of different organisms.[14] Most of these enzymes are oxidative, and require the use of a substrate such as molecular oxygen or hydrogen peroxide to generate the reactive halogen species for catalysis.[15]

Investigation into the halogenation of marine natural products has identified one such class of halogenating enzymes, vanadium-dependent haloperoxidases (VHPOs). VHPOs employ a vanadate prosthetic group, capable of utilising hydrogen peroxide to oxidise a halide ion into a reactive electrophilic intermediate. As vanadium is the second most abundant transition metal in the ocean, VHPOs are prevalent among marine organisms and have been identified in species of marine bacteria, fungi and algae.[15] These VHPO enzymes are thought to be responsible for almost all halogenation events in marine natural products.[1]

The VHPO catalytic cycle (Scheme 2.01) begins with coordination of H_2O_2 to the vanadium centre through Lewis acid/base interactions, forming the intermediate peroxide. Next the peroxide, which is activated through charge separation, undergoes nucleophilic attack from a halide ion, breaking the newly formed peroxide bond. Subsequent protonation of the resultant hypohalite species by an incoming water molecule generates the reactive hypohalous acid (HOX). Hypohalous acids are the chemical equivalent of an electrophilic halogen (X^+) and will readily react with nucleophilic substrates such as aromatic rings and alkenes, leading to a variety of halogenated natural products. In the absence of a nucleophilic substrate, the hypohalous acid will react with another H_2O_2 molecule, generating singlet O_2.[16] As a result, the substrate must bind to the active site for halogenation to occur, arising in high substrate specificity and stereoselectivity.

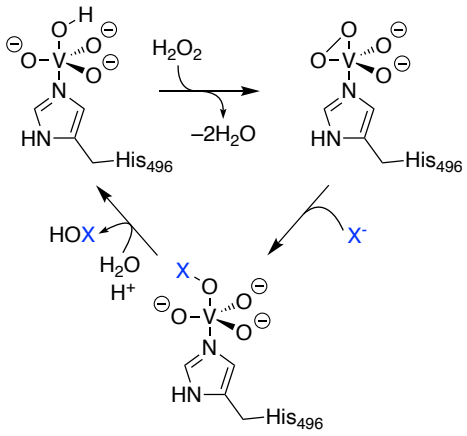

Scheme 2.01: VHPO catalytic cycle.[15]

The classification of a VHPO is dependent on the most electronegative halogen oxidised, therefore vanadium-dependent chloroperoxidases (VCPOs) can oxidise chloride, bromide and iodide, while vanadium-dependent bromoperoxidases (VBPOs) can only oxidise bromide and iodide.[16] During the catalytic cycle, these enzymes undergo no change in oxidation state at the vanadium centre and consequently do not suffer from oxidative inactivation during turnover. As a result, VHPOs present as attractive biocatalysts in synthetic applications.[15]

One such example is the VBPO-catalysed conversion of the sesquiterpene (*E*)-(+)-nerolidol (**2.07**) to α- (**2.10**), β- (**2.11**) and γ-snyderol (**2.12**) (Scheme 2.02).[17] The marine VBPO, isolated from red algae, was found to catalyse the asymmetric, regioselective and diastereoselective bromination of the C10-C11 olefinic bond in **2.08**. The resultant bromonium ion **2.08** undergoes nucleophilic attack from the internal alkene to form carbocation **2.09**, followed by one of three alternative elimination reactions to give α- (**2.10**), β- (**2.11**) and γ-snyderol (**2.12**). As the bromination takes place in the active site of the enzyme, all three natural products are formed as single enantiomers.

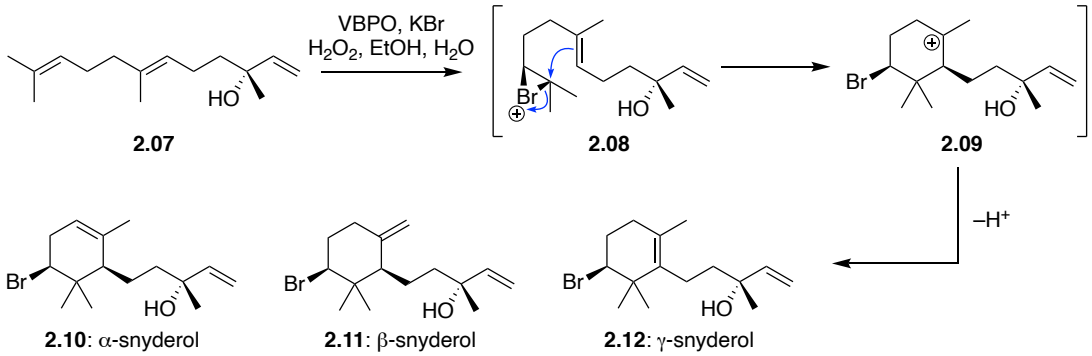

Scheme 2.02: VBPO-catalysed biosynthesis of marine natural products α- (**2.10**), β- (**2.11**) and γ-snyderol (**2.12**).[17]

2.1.3 The α-Hydroxyketone Rearrangement

The 1,2-rearrangement or 1,2-shift reaction is a class of organic reactions involving the migration of H or alkyl groups from one atom to an adjacent atom, within the same molecule. This reaction is observed in the biosynthesis of many natural products and has proven to be an important tool for synthetic chemists in for the total synthesis of complex molecules.

A common example of this 1,2-shift is the Wagner-Meerwein rearrangement, in which a hydrogen, alkyl or aryl group migrates from one carbon atom to the adjacent carbon atom *via* a carbocationic intermediate.[18] This migration occurs to favour the formation of the more stable carbocation, particularly in the case where alternatives such as S_N1 or E1 reactions are not possible. The Wagner-

Meerwein rearrangement is a key reaction in the biosynthesis of terpene natural products, as can be observed in the biosynthesis of camphene (**2.13**) (Scheme 2.03).[19] Reduction of camphor (**2.14**) gives secondary alcohol isoborneol (**2.15**). Acid-catalysed dehydration of **2.15** occurs through protonation to give **2.16**, followed by dehydration to form carbocation **2.17**. The key Wagner-Meerwein rearrangement then takes place to give **2.18**, followed by proton loss to form camphene (**2.13**).

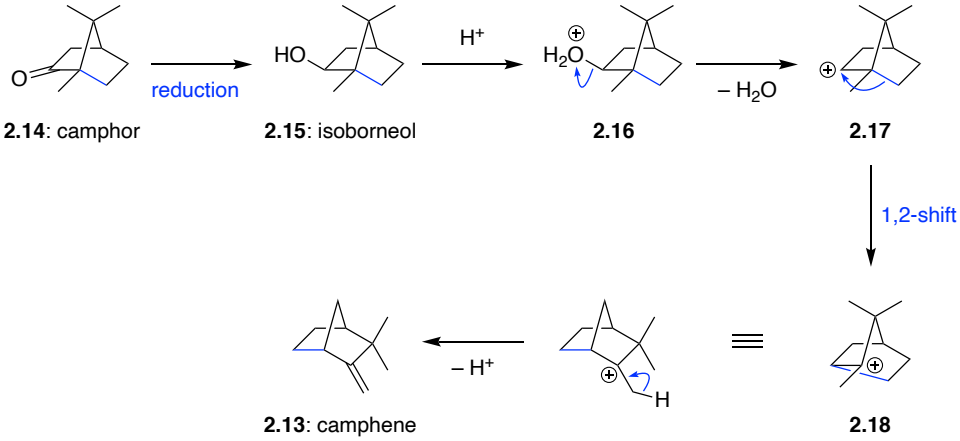

Scheme 2.03: Wagner-Meerwein rearrangement in the formation of camphene (**2.18**).

This reaction is also employed in the biosynthesis of more complex natural products such as the conversion of terpenoid natural product betulin (**2.19**) to form allobetulin (**2.20**) (Scheme 2.04).[20] Protonation of the terminal alkene of **2.19** gives the intermediate carbocation **2.21**, which can then undergo a ring expansion through a 1,2-shift. The resulting carbocation **2.22** is then trapped by the primary alcohol to afford the natural product allobetulin **2.20**.

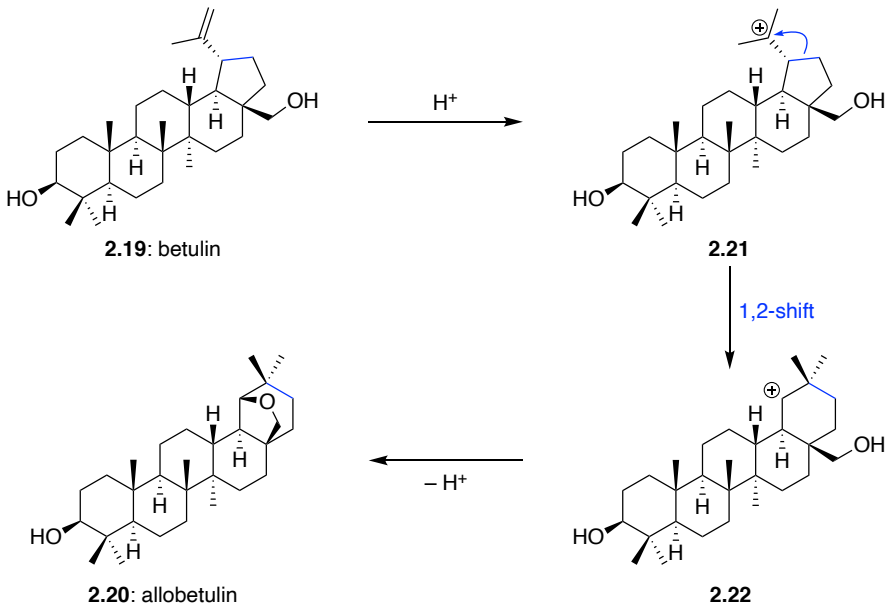

Scheme 2.04: Wagner-Meerwein rearrangement in the formation of allobetulin (**2.20**).[20]

The α-hydroxyketone rearrangement (or α-ketol rearrangement) is a 1,2-rearrangement of an α-hydroxy carbonyl compound to form an isomeric product. This rearrangement is commonly induced synthetically by treatment of a suitable α-hydroxy aldehyde or ketone with a Lewis or Brønsted acid, base or through heat.[21] This reaction varies mechanistically dependent on the reaction conditions (Scheme 2.05), however the alkyl shift and ketone formation are simultaneous in all cases. Under acidic conditions (Scheme 2.05, **A**), coordination of the carbonyl oxygen occurs, initiating bond migration. Under basic conditions (Scheme 2.05, **B**), deprotonation of the hydroxy group occurs prior to the rearrangement. Under thermal conditions (Scheme 2.05, **C**), the reaction proceeds *via* intramolecular proton transfer.

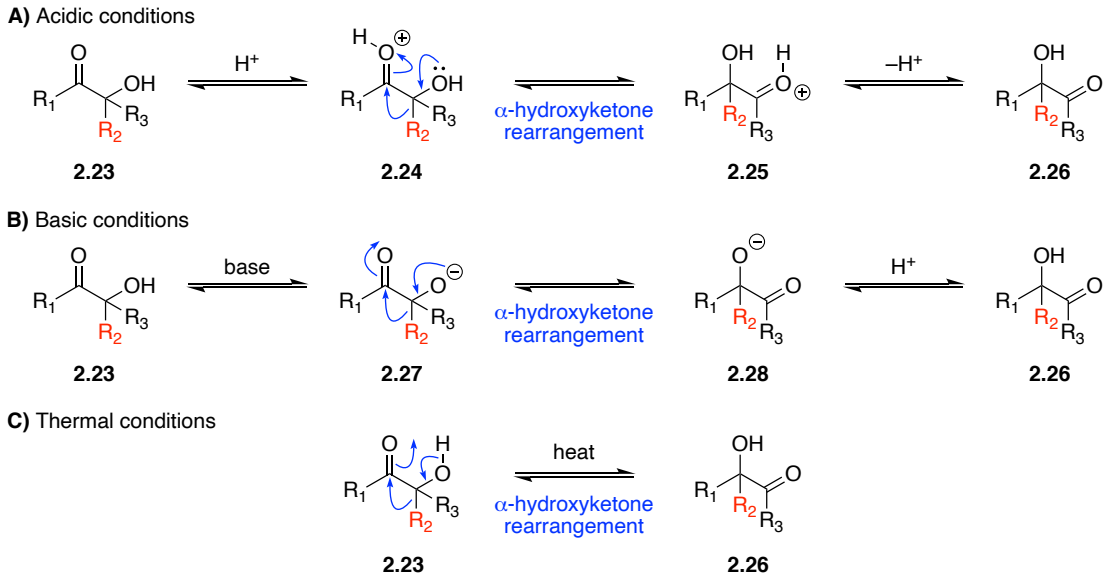

Scheme 2.05: Mechanism of the α-hydroxyketone rearrangement under **A)** acidic, **B)** basic and **C)** thermal conditons.[21]

Due to the inherent reversibility of the α-hydroxyketone rearrangement, the products of these reactions are favoured when they are more thermodynamically stable than their precursors. This is commonly achieved through the release of ring strain,[21] however this concept must be carefully considered when designing a synthesis involving this rearrangement.

In 2017, Gademann and co-workers implemented an α-hydroxyketone rearrangement in the first enantioselective total synthesis of the sesquiterpenoid natural product, periconianone A (**2.29**) (Scheme 2.06).[22] This synthesis followed a biogenetic proposal to furnish the complex cage-like framework of **2.29**. Treatment of α-ketocarbinol **2.30** with $Ca(OMe)_2$ catalysed the desired α-hydroxyketone rearrangement to afford the α-allylated hydroxyenone **2.31** in 70% yield. This rearrangement enabled the stereoselective installation of the C-7 carbinol. From key intermediate **2.31**, the total synthesis of complex tricarbocycle periconianone A (**2.29**) was completed.

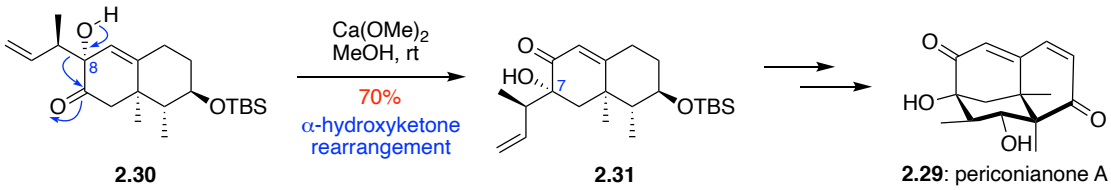

2.30 **2.31** **2.29**: periconianone A

Scheme 2.06: Key α-hydroxyketone rearrangement in Gademann's total synthesis of periconianone A (**2.29**).[22]

2.1.4 Naphterpin and Marinone Families of Natural products

The naphterpins and marinones are meroterpenoid families of natural products, isolated from actinobacteria. They are characterised by a common naphthoquinone ring system and cyclised C-3 geranyl or farnesyl side chains (Figure 2.02). Both families also contain terpene derived *cis*-fused 6-6 ring systems and are structurally related to the napyradiomycin[23,24] and merochlorin[25] families.

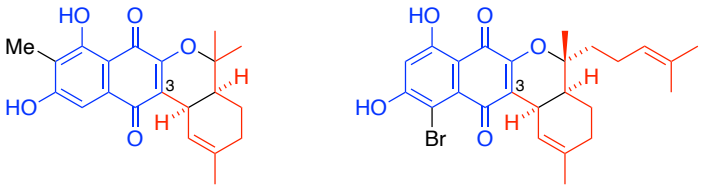

2.32: naphterpin **2.33**: marinone

Figure 2.02: Naphterpin (**2.32**) and marinone (**2.33**) meroterpenoid natural products containing common naphthoquinone ring system (blue) and cyclised C-3 prenyl side chains (red).

Naphterpin (**2.32**) was the first member of this family to be discovered, isolated from *Streptomyces* sp. CL190 in 1990.[26] The producing organism was found in a soil sample collected from Ishigaki Island, Japan. Naphterpin was found to suppress lipid peroxidation in rat homogenate system with an IC_{50} value of 5.3 μg/mL, however showed no antibacterial or antifungal properties on the cell lines tested. Oxidised derivatives naphterpin B (**2.34**) and C (**2.35**) were later isolated from the same producing organism (Figure 2.03).[27] Naphterpins B (**2.34**) and C (**2.35**) were also found to suppress lipid peroxidation in rat homogenate system with IC_{50} values of 6.5 μg/mL and 6.0 μg/mL,

respectively. In 2018, radical scavengers naphterpin D (**2.36**) and E (**2.37**) were isolated from *Streptomyces* sp. CNQ-509, found in a sediment sample collected near La Jolla, California.[28]

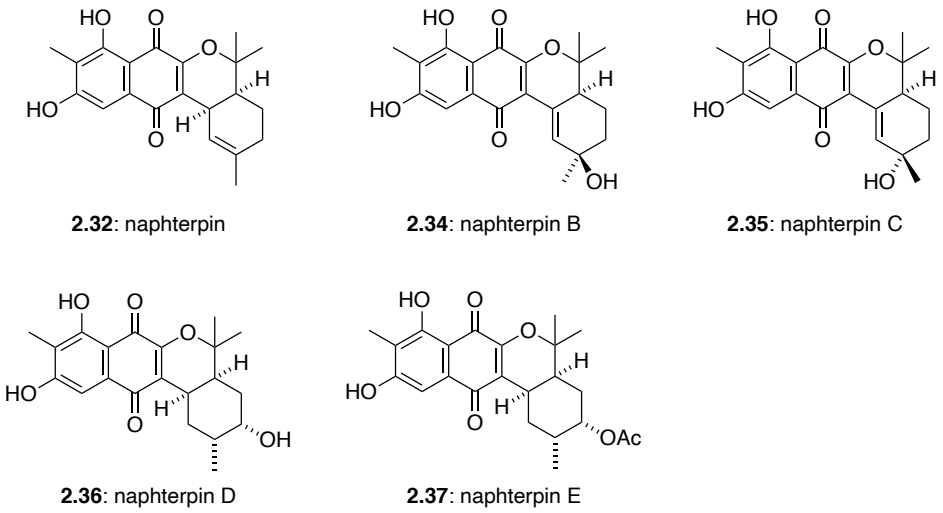

2.32: naphterpin **2.34**: naphterpin B **2.35**: naphterpin C

2.36: naphterpin D **2.37**: naphterpin E

Figure 2.03: The naphterpin family of meroterpenoid natural products.

In 1992, naphterpin analogue 7-demethylnaphterpin (**2.38**) was isolated from *Streptomyces prunicolor*.[29] Despite the absence of the C-7 methyl group, 7-demethylnaphterpin possessed similar antioxidative properties to naphterpin, and was found to inhibit the lipid peroxidase in rat liver microsomes with IC_{50} = 9 μg/mL. 7-Demethylnaphterpin (**2.38**) had been previously isolated in 1991 as part of the naphthgeranine family of natural products, therefore it is also referred to as naphthgeranine A (Figure 2.04).[30]

Several other oxidised members of the naphthgeranine family have been isolated from Streptomycete bacteria. These members contain highly oxidised terpene-derived ring systems, presumably the result of cytochrome P450 mediated C-H oxidations. Naphthgeranines A-E (**2.38**-**2.42**) were isolated from *Streptomyces violaceus* Tü 3556, a bacterial strain found in a soil sample collected in Nepal.[30] The less oxidised members, naphthgeranines A (**2.38**) and B (**2.39**), showed only weak antibacterial and antifungal activities, with the more polar **2.39** being less active. Naphthgeranines A-C (**2.38**-**2.40**) were found to have moderate cytocidal activity against various tumour cell lines *in vitro*.

Naphthgeranine F (**2.43**), the only naphthgeranine oxidised on the C-18 methyl was later isolated from the same bacteria, *Streptomyces violaceus* Tü 3556.[31] This compound was found to have weak antibacterial activity against Gram-positive bacteria (*Bacillus subtilis* ATCC6051, *Bacillus brevis* ATCC9999, *Streptomyces viridochromogenes* Tü 57), with similar MIC values to that of naphthgeranine C (**2.40**). In 2016 two naphthgeranine analogues, 12-hydroxy-naphthgeranine A (**2.44**) and isonaphthgeranine C (**2.45**) were isolated from *Streptomyces* sp. XZYN-4.[32] Additionally, 12-hydroxy-naphthgeranine A (**2.44**) was found to have moderate activity against *Aspergillus niger*.

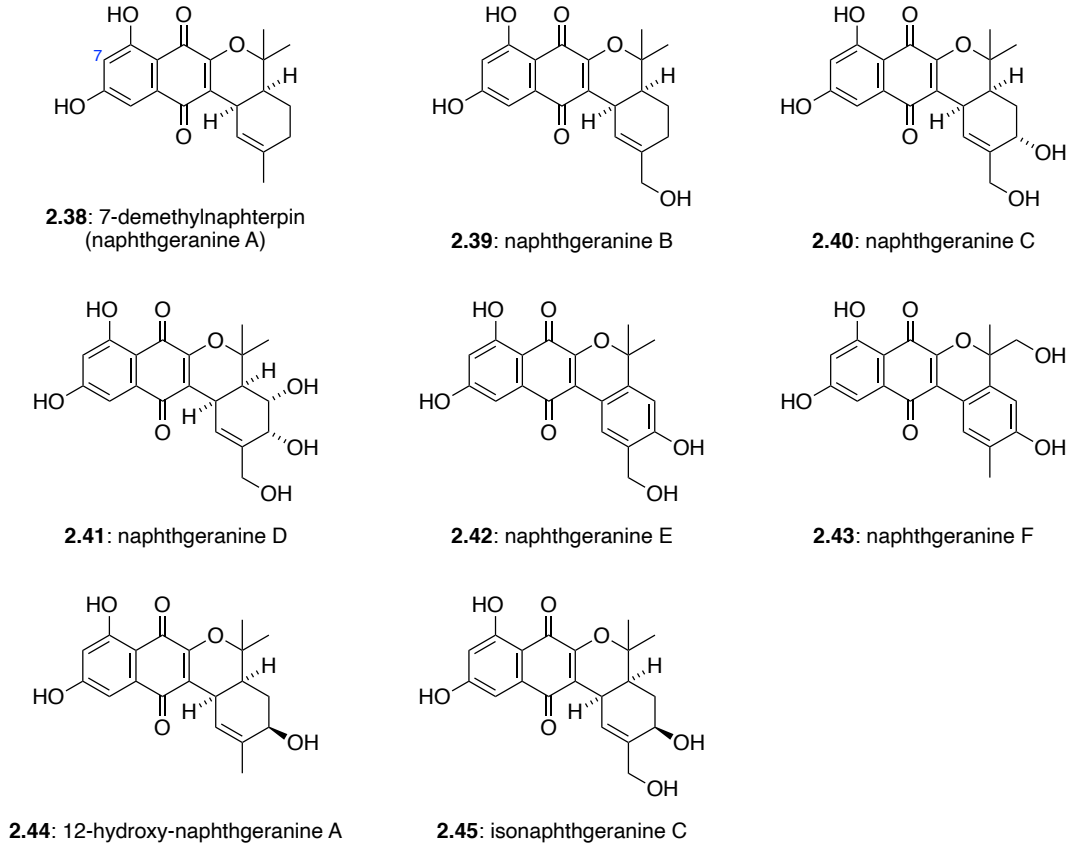

Figure 2.04: The naphthgeranine family of meroterpenoid natural products.

In 1992, two farnesyl-derived naphthoquinone natural products debromomarinone (**2.46**) and marinone (**2.33**) were first isolated from the culture broth of an unidentified marine actinomycete *Streptomyces* sp. CNB-632 (Figure 2.05).[33] These two metabolites showed significant structural similarities to that of the naphterpin and naphthgeranine families, and were shown to possess

considerable *in vitro* antibacterial activity against Gram-positive bacteria. Marinone (**2.33**) possesses activity against *Bacillus subrifis* (MIC 1 μg/mL) and debromomarinone (**2.46**) is active against *Staphylococcus aureus*, *S. epidermis*, *S. pneumoniae* and *S. pyogenes* with MIC values ranging from 1-2 μg/mL. In 2000, three related natural products isomarinone (**2.47**), hydroxydebromomarinone (**2.48**) and methoxydebromomarinone (**2.49**) were isolated from a taxonomically-novel marine actinomycete strain CNH-099.[34] These marinone analogues were found in a sediment sample at Batiquitos Lagoon, California, and were shown to have moderate *in vitro* cytotoxicity against the HCT-116 colon carcinoma cell line with IC_{50} values of approximately 8 μM.

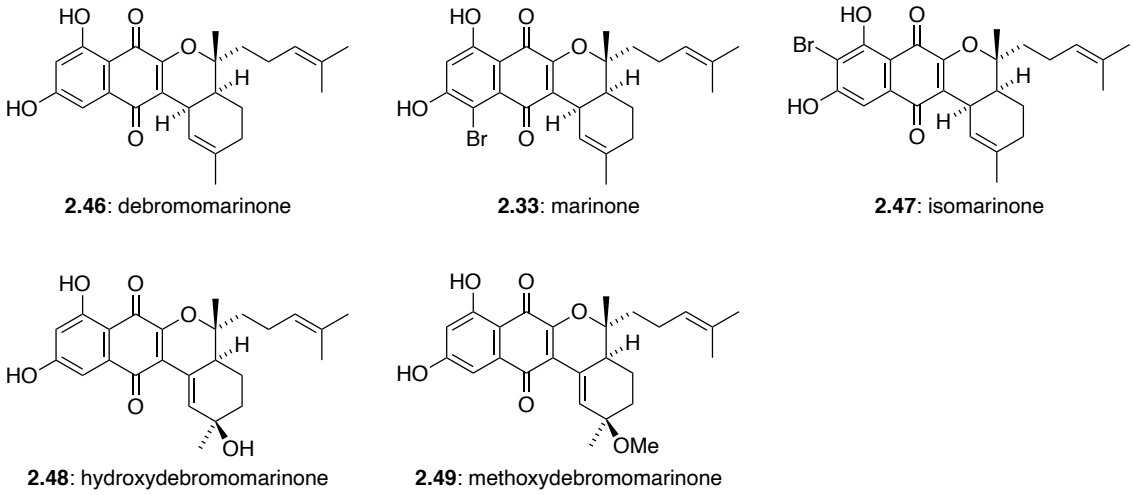

Figure 2.05: The marinone family of meroterpenoids.

A structurally unique compound, neomarinone (**2.50**), was co-isolated with these marinone metabolites from the marine actinomycete strain CNH-099 (Figure 2.06).[34] The originally proposed structure of neomarinone was revised to be **2.50** on the basis of ^{13}C labelling studies, combined with 2D NMR spectroscopy.[35] Neomarinone showed moderate *in vitro* cytotoxicity against HCT-116 colon carcinoma cells with an IC_{50} value of 10 μM.

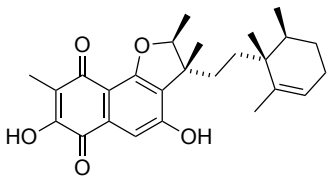

2.50: neomarinone

Figure 2.06: Structure of neomarinone (**2.50**).

2.1.5 Early Biosynthetic Studies of the Naphterpin and Marinone Families

To establish the early biosynthetic origins of naphthoquinone-based streptomycete meroterpenoids, early biosynthetic studies focused on stable isotope labelling with ^{13}C-labelled acetate. In 1990, Seto and colleagues reported isotope incorporation results showing that naphterpin is likely to originate from the coupling of THN and GPP precursors (Scheme 2.07).[36] The isotope labelling patterns established that the isoprene units originate from the mevalonate pathway.

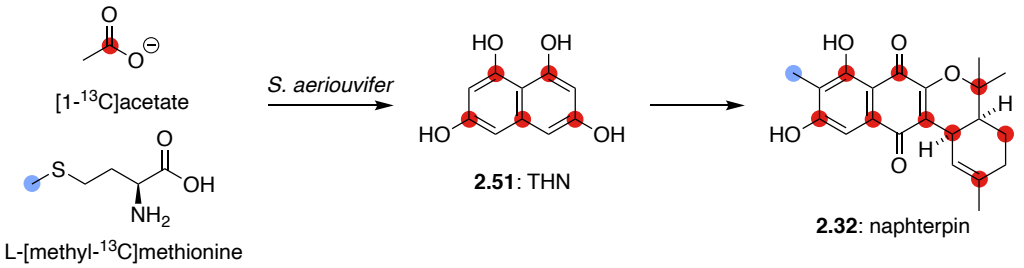

Scheme 2.07: Labelling pattern of naphterpin from [1-^{13}C]acetate and L-[methyl-^{13}C]methionine.[36]

Despite structural similarities of naphterpin (**2.32**) and debromomarinone (**2.46**), Moore and co-workers discovered that the isoprenoid units in both **2.46** and neomarinone (**2.50**) differed in origin.[35] Results of ^{13}C-acetate studies revealed a symmetrically labelled naphthoquinone core, indicating a common THN building block, however no enrichment was observed in the sesquiterpene-derived carbons of **2.46** and **2.50** (Figure 2.07). Alternatively, feeding experiments using ^{13}C-labelled glucose were shown to enrich the terpenoid fragments of these molecules. These results suggest the origin of the farnesyl pyrophosphate (FPP) precursor is consistent with a non-mevalonate or methyl D-

erythritol-4-phosphate (MEP) pathway. These findings also lead to the structural revision of neomarinone, revealing that the original structure proposed on isolation by Fenical[34] was incorrect, with the correct structure shown in Figure 2.07.

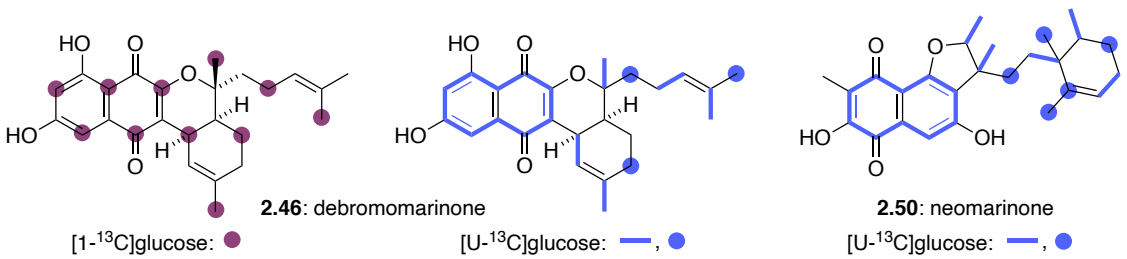

Figure 2.07: Incorporation of ^{13}C-labelled precursors in debromomarinone and neomarione.[35]

In 2006, the groups of Dairi[37] and Heide[38] reported the first connections between clustered biosynthetic genes and the chemistry they exhibit for the structurally similar naphthoquinone-based meroterpenoids, furaquinocin D (**2.52**) and furanonaphthoquinone I (**2.53**), isolated from *Streptomyces* bacterium (Figure 2.08).

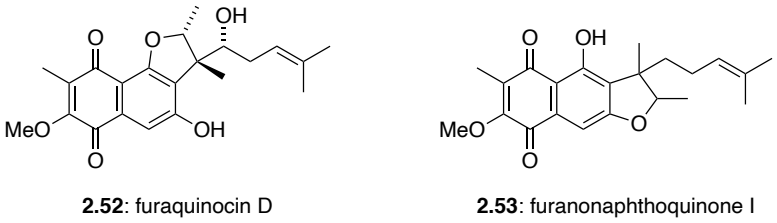

Figure 2.08: Meroterpenoids furaquinocin D (**2.52**) and furanonaphthoquinone I (**2.53**).

Shortly after, the napyradiomycin biosynthetic gene cluster was discovered and validated by the Moore group, utilising heterologous expression studies.[39] These early meroterpenoid gene cluster studies confirmed that the shared THN fragment originates from a type III polyketide synthase, initially discovered by Horinouchi and colleagues.[40] In *Streptomyces* bacteria this homodimeric enzyme is responsible for pigmented melanin production, in addition to its significance in meroterpenoid biosynthesis.[41] These gene clusters were also found to contain a complete set of

isoprenoid biosynthesis encoding genes *via* the mevalonate pathway as well as an ABBA prenyltransferase, first established for naphterpin biosynthesis by Kuzuyama.[42]

2.1.6 Biosynthetic Studies and Biomimetic Total Synthesis of the Merochlorins

The first THN-based meroterpenoids to have their complete biosynthesis determined were merochlorins A (**2.54**) and B (**2.55**). The insight gained from this biosynthetic logic would eventually lead to multiple biomimetic syntheses and assist in the discovery of multiple biosynthetic pathways of related meroterpenoid natural products.

In 2012, Fenical and Moore reported the isolation and biosynthetic gene cluster (BGC) of the merochlorin family of natural products.[25] The *mcl* BGC was identified through mutagenesis and heterologous expression, confirming that merochlorins A-D (**2.54**-**2.57**) shared the same biogenesis, despite their differing carbon skeletons (Scheme 2.08). The merochlorins can be divided into two structurally different groups, dependent on whether the C_{15} isoprene sidechain is attached at the C-4 (**2.54** and **2.55**) or C-3 (**2.56** and **2.57**) position of the THN biosynthetic precursor.

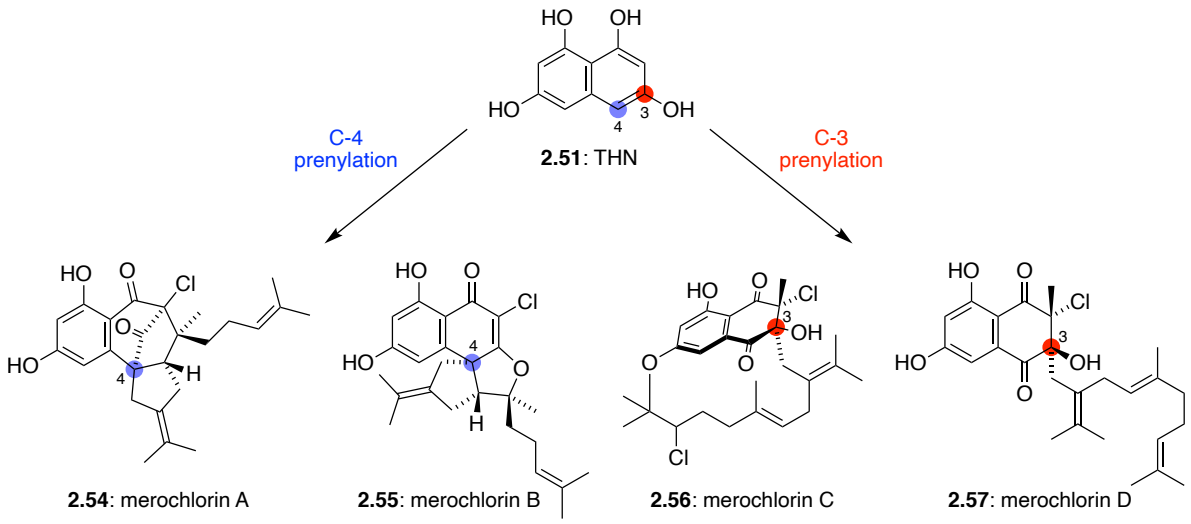

Scheme 2.08: Structures of merochlorins A-D.[25]

Between the heterologous expression in *Streptomyces coelicolor* and knockout experiments in the native *Streptomyces* CNH-189 strain, the genes responsible for merochlorin biosynthesis were identified (Scheme 2.09).[43] Firstly, THN synthase Mcl17 is responsible for converting five molecules of malonyl coenzyme A (**2.58**) into THN (**2.51**). Prenyltransferase Mcl22 was then found to assemble the branched isoprene unit from an unusual head-to-torso condensation of **2.59** and **2.60** to give the isoprene building block isosesquilavandulyl pyrophosphate (**2.61**). Subsequent C-4 alkylation of **2.51** with sesquiterpene **2.61** was catalysed by prenyltransferase Mcl23 to give pre-merochlorin (**2.62**). Finally, VHPO Mcl24 was found to independently convert **2.62** to merochlorin A (**2.54**) and B (**2.55**). This cascade began with chlorination at C-2, followed by oxidative dearomatisation to form carbocation **2.63**. After subsequent cyclisation, intermediate **2.64** could then undergo a stepwise [5+2] or [3+2] cycloaddition to give merochlorin A (**2.54**) or B (**2.55**), respectively.

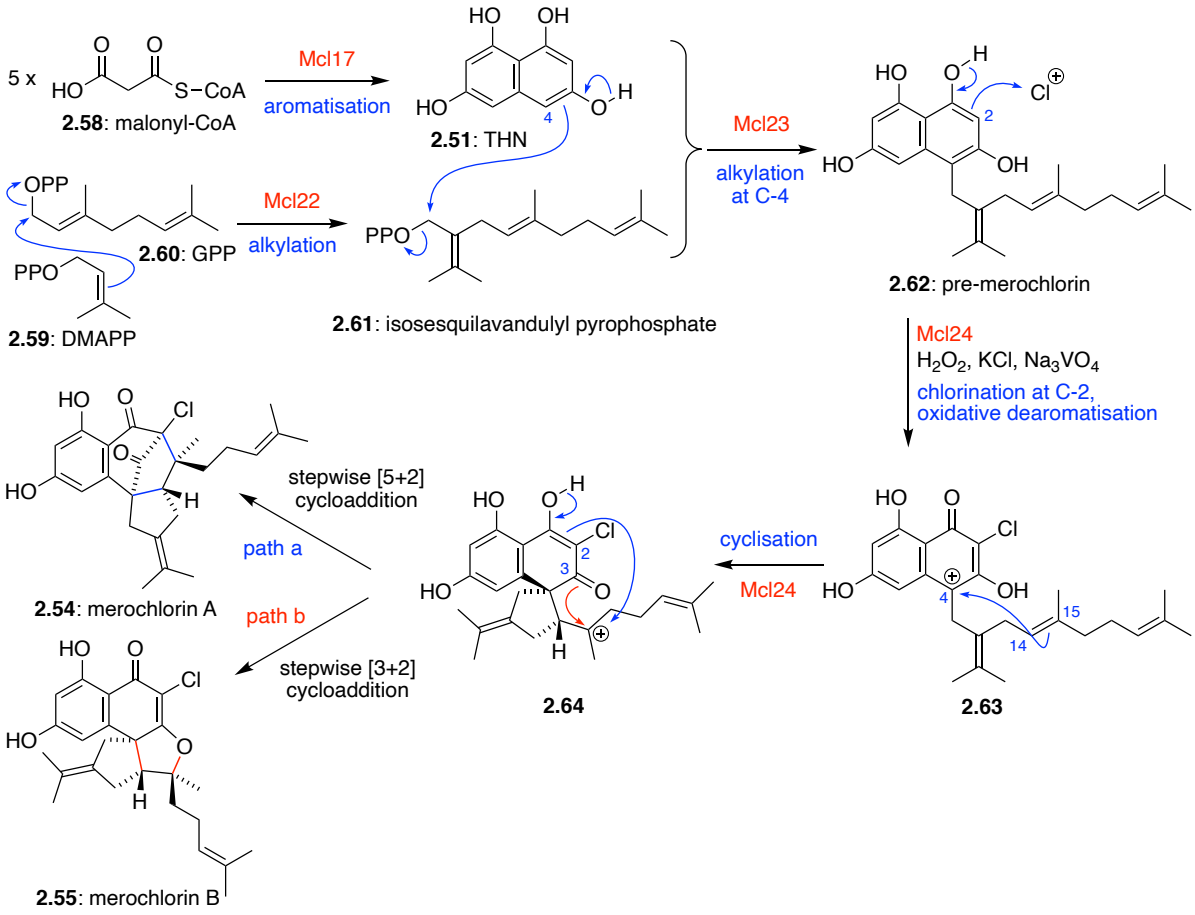

Scheme 2.09: Biosynthesis of merochlorins A (**2.54**) and B (**2.55**).

Interestingly, further investigation into these reactions discovered the potential for Mcl24 to initiate further structural diversity in the merochlorin pathway, dependent on the pH of the reaction.[44,45] While Mcl24 consistently catalysed the chlorination and oxidative dearomatisation of pre-merochlorin (**2.62**), under mildly basic conditions (pH 8.0), the dearomatised intermediate (**2.63**) was preferentially hydrated at C-4 to give tertiary alcohol **2.66** in favour of cyclisation to intermediate **2.64** (Scheme 2.10). The source of this C-4 hydroxyl group was confirmed to be from water, not the co-substrate hydrogen peroxide or atmospheric oxygen through studies using $H_2{}^{18}O$. Mcl24 then facilitated a second chlorination at C-2 to give dichloride **2.67**, followed by an enzyme-catalysed α-hydroxyketone rearrangement, shifting the branched isoprene moiety from the C-4 to the C-3 position, giving **2.68**. Both experimental and computational analysis has proven this 1,2-suprafacial shift to be thermodynamically favourable, only following di-substitution of the C-2 position in the THN ring.[45] Although unanticipated, the discovery of this pH-dependent 1,2-shift rationalised the biosynthesis of the abundant C-3 prenylated meroterpenoid natural products.

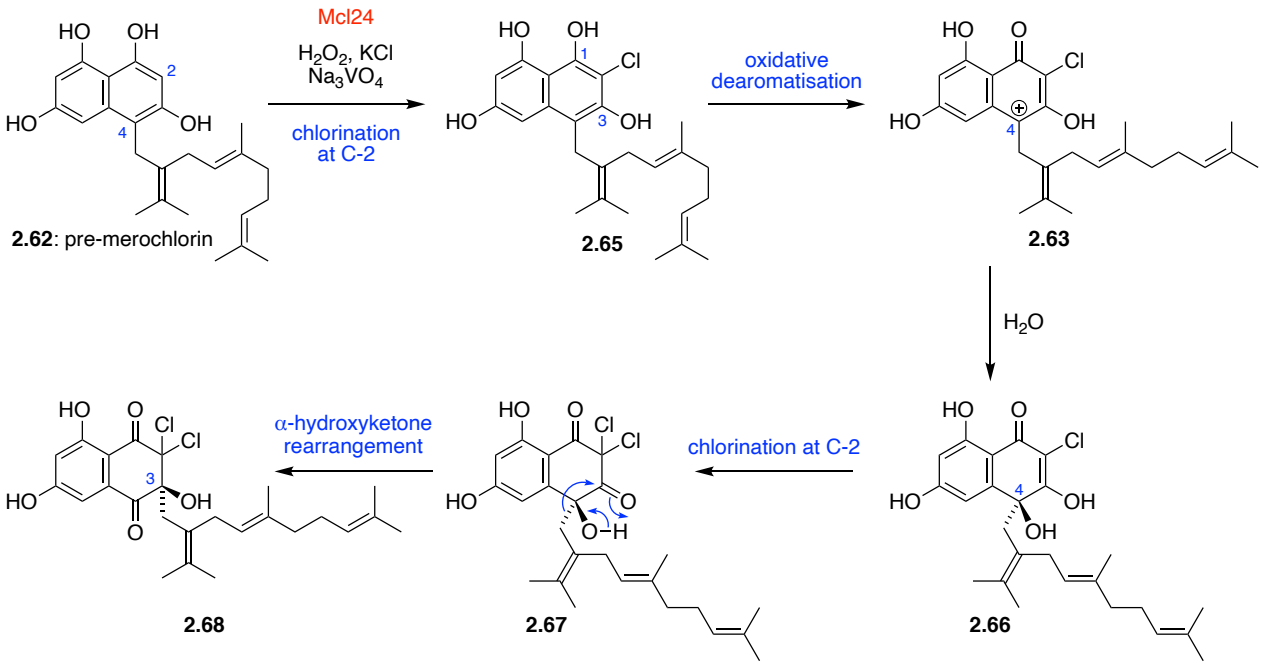

Scheme 2.10: VHPO-catalysed α-hydroxyketone rearrangement under basic pH conditions.

The chemical logic of this pH dependence extends to the biosynthesis of merochlorin C (**2.56**) and D (**2.57**). In this case, Mcl24-catalysed di-chlorination at the C-2 position would be replaced with a stereoselective methylation by a SAM-dependent methyltransferase giving **2.69** (Scheme 2.11). With di-substitution and the C-2 position, an analogous Mcl24-catalysed α-hydroxyketone rearrangement would generate merochlorin D (**2.57**). Subsequent VHPO-catalysed chlorination and cyclisation would give macrocycle merochlorin C (**2.56**). Genetic evidence suggested a second merochlorin VHPO gene, *mcl40*, may be responsible for the entropically-challenging cyclisation of the 15-membered macrocyclic chloro-ether ring in merochlorin C, however this is yet to be confirmed though *in vitro* recombinant enzymology due to protein expression and insolubility issues.[43]

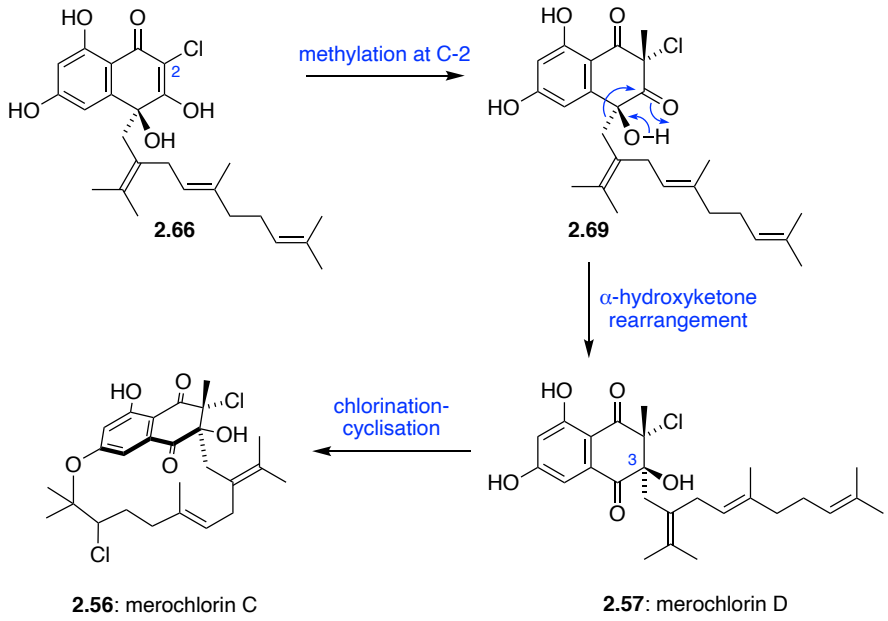

Scheme 2.11: Proposed biosynthetic pathway to merochlorin C (**2.56**) and D (**2.57**).

In 2013, George and co-workers established the first biomimetic total synthesis of merochlorin A (**2.54**), closely anticipating its biosynthetic pathway (Scheme 2.12).[46] The synthetic route began with a Friedel-Crafts acylation of methyl 3,5-dimethoxyphenylacetate (**2.70**) with chloroacetyl chloride to afford chloroketone **2.71**. Base-induced aromatisation of **2.71** was achieved with NaOMe *via* a Dieckmann cyclisation, giving phenolate anion **2.72**. Subsequent C-4 alkylation with

"isosesquilavandulyl bromide" **2.73** (accessed in three steps from geranyl bromide) gave **2.74**. Unexpectedly, the basic conditions of the alkylation reaction resulted in partial *E*/*Z* isomerisation at the C14-C15 alkene. Treatment of **2.74** with $Pb(OAc)_4$ in $CHCl_3$ induced a cascade of oxidative dearomatisation and cyclisation to give **2.75**, the dimethyl ether of merochlorin A. Under these reaction conditions, no formation of the merochlorin B scaffold was observed. Subsequent deprotection of **2.75** was achieved under two consecutive Krapcho demethylations to give racemic merochlorin A (**2.54**).

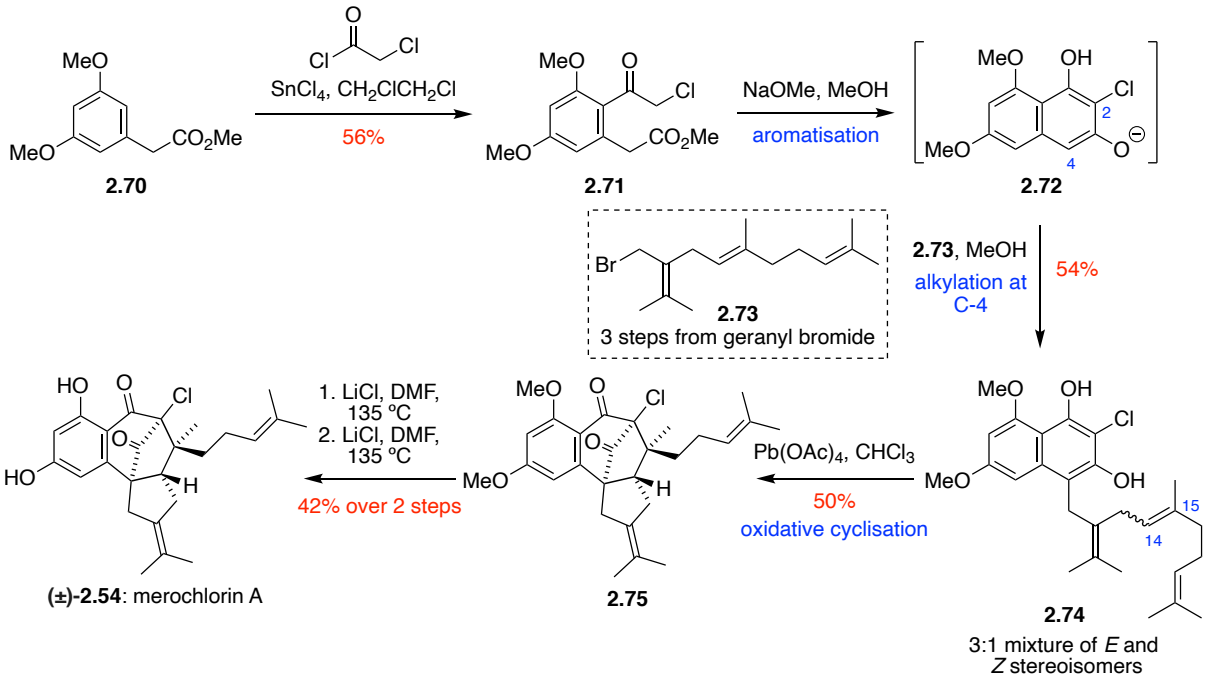

Scheme 2.12: George's biomimetic total synthesis of (±)-merochlorin A (**2.54**).[46]

Following George's biomimetic synthesis of merochlorin A, Trauner,[47] Moore,[43] Zhang and Tang[48] and Carreira[49] were able to successfully synthesise merochlorins A (**2.54**) and B (**2.55**), however no published syntheses of merochlorins C (**2.56**) or D (**2.57**) exist to date.[50]

2.1.7 Biosynthetic Studies and Biomimetic Total Synthesis of the Napyradiomycins

During studies into the merochlorin biosynthetic pathway, it was discovered that VHPO Mcl24, catalysed an unprecedented pH-dependent α-hydroxyketone rearrangement under basic conditions, shifting the prenyl sidechain from the C-4 o the C-3 position of THN (Scheme 2.10 above). It was predicted that this alkyl shift would allow access to the many meroterpenoid natural products with a C-3 attachment of the isoprene sidechain, including the napyradiomycins,[23,24] marinone,[33,34] and naphterpin.[26]

Following this chemical logic, the biosynthetic pathway to the napyradiomycin natural products was proposed (Scheme 2.13). Geranylation of the THN ring (**2.51**) at the C-4 position with GPP (**2.60**) would give **2.76**, which could then undergo VCPO-catalysed C-2 chlorination to give **2.77** followed by dearomatisation and hydration to afford intermediate **2.78**. Subsequent prenylation at C-2 with DMAPP (**2.59**) would then allow the necessary di-substitution to facilitate the α-hydroxyketone rearrangement of **2.79** to naphthomevalin (**2.80**), the structurally simplest member of the napyradiomycin family of natural products. Successive chloronium-mediated cyclisations with a hydroxyl or alkenyl nucleophile would produce napyradiomycins A1 (**2.81**) and B1 (**2.82**) respectively. It was predicted that these challenging synthetic reactions would occur under the stereocontrol of putative VHPO enzymes.

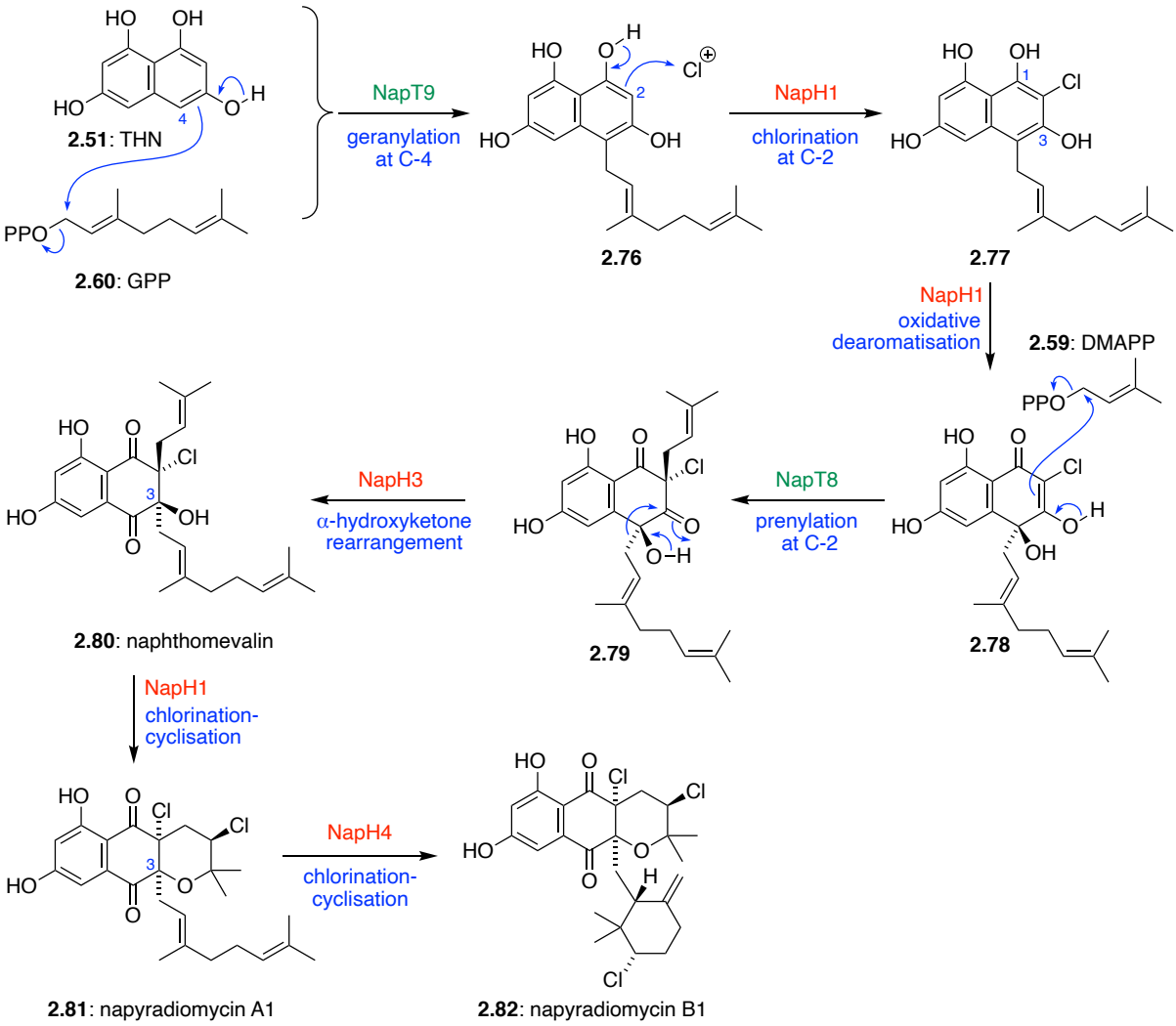

Scheme 2.13: Proposed biosynthesis of the napyradiomycins.

Inspired by the proposed biosynthesis of the napyradiomycins (Scheme 2.13), George and Moore went on to achieve the biomimetic total synthesis of naphthomevalin (**2.80**) (Scheme 2.14).[45] The synthesis began by converting methyl 3,5-dimethoxyphenylacetate (**2.70**) into protected THN derivative (**2.83**) over four steps. Selective Pd-catalysed C-4 geranylation with carbonate **2.84** gave **2.85**. Subsequent oxidative dearomatisation with $Pb(OAc)_4$ and dichlorination with NCS gave an intermediate geminal dichloride, which then underwent selective mono-dechlorination with LDA and acetate hydrolysis to give **2.86**. Diastereoselective prenylation at C-2, followed by acid-catalysed MOM deprotection gave intermediate **2.79**. Heating **2.79** in toluene induced the desired thermal α-hydroxyketone rearrangement to afford racemic naphthomevalin (**2.80**). All of the synthetic intermediates in this synthesis were prime for facile MOM deprotection, therefore giving access to

enzyme substrates and synthetic standards for investigation into the biosynthetic pathway through chemoenzymatic studies.

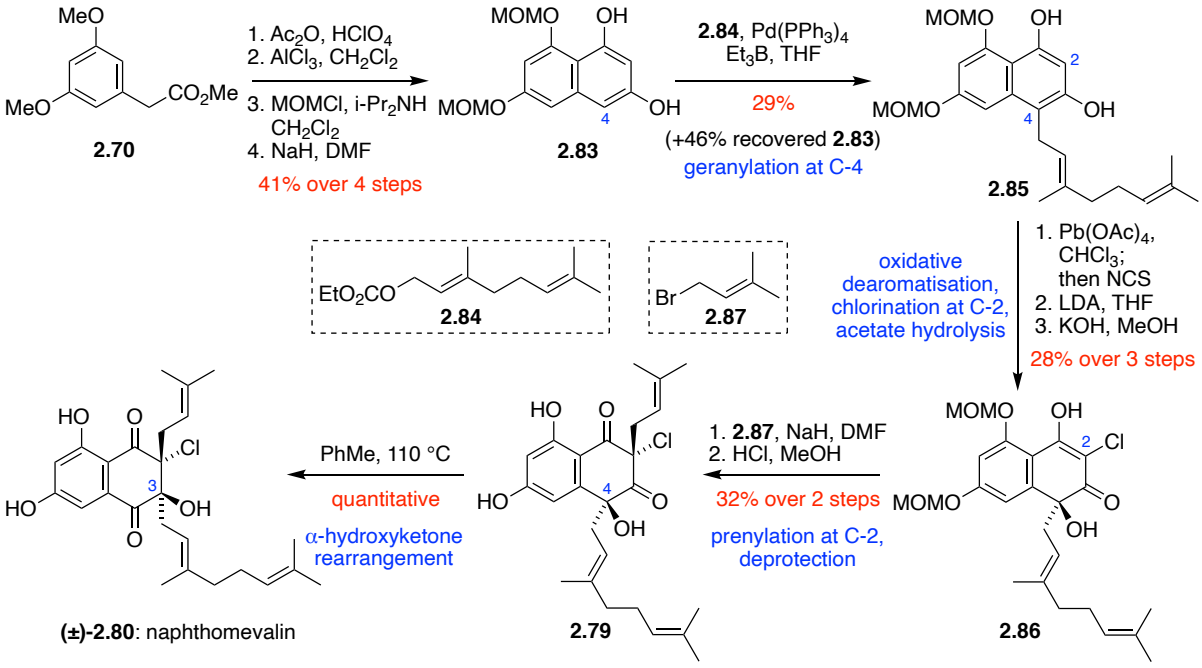

Scheme 2.14: George's biomimetic total synthesis of (±)-naphthomevalin (**2.80**).[45]

After confirming the chemical viability of the proposed biosynthetic pathway, the chemically synthesised putative biosynthetic intermediates were used as substrates and synthetic standards for newly discovered enzymes. Analogous to the putative biosynthesis of merochlorin C (**2.56**) and D (**2.57**), NapT8 was discovered to catalyse a diastereoselective aromatic prenylation at the C-2 position of the THN ring in **2.78** with prenyl donor DMAPP (**2.59**) to give **2.79** (Scheme 2.15). Substitution at the C-2 position enabled the thermodynamically favourable α-hydroxyketone rearrangement, shifting the geranyl substituent of **2.79** from C-4 to C-3, establishing the naphthoquinone core of **2.80**. Although this reaction could occur spontaneously *in vitro*, the addition of VHPO homologue NapH3 was found to significantly accelerate the reaction. Access to these synthetic substrates ultimately led to elucidation of the entire biosynthetic pathway of naphthomevalin (**2.80**), napyradiomycin A1 (**2.81**) and napyradiomycin B1 (**2.82**).[51]

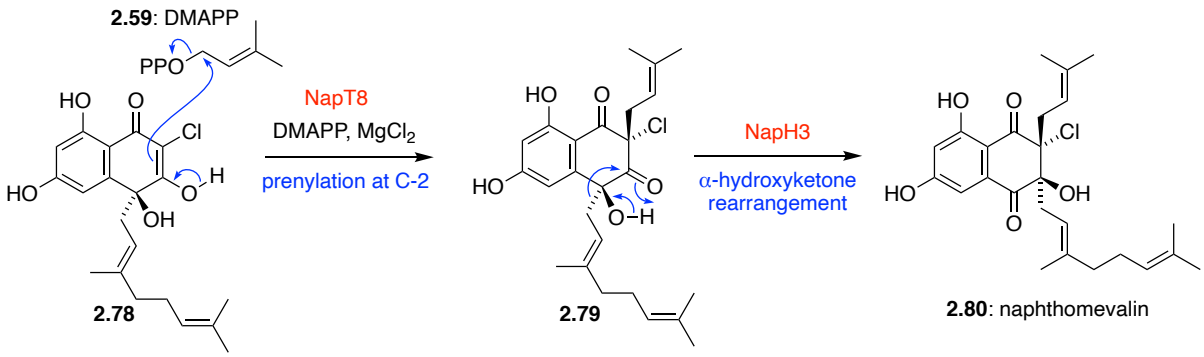

Scheme 2.15: Nap-T8 catalysed prenylation at C-2 followed by NapH3 catalysed α-hydroxyketone rearrangement.[45]

2.1.8 Proposed Biosynthesis of Naphterpin and Marinone Natural Products

Early isotope labelling studies revealed that both the naphterpin and marinone families of natural products are derived from THN (**2.51**), despite their conflicting oxidation patterns. In addition, the terpene substituents of the naphterpins and marinones reside at the C-3 position, despite the C-2 and C-4 positions of **2.51** being nucleophilic. These observations implied a potential α-hydroxyketone rearrangement to shift the terpene sidechain,[52] and form the correct substitution pattern of these molecules, similar to that demonstrated in the merochlorin and napyradiomycin biosyntheses.[45] The key difference between the naphterpin and marinone biosynthetic pathways is the length of the terpene sidechain, with the naphterpins incorporating a geranyl subunit while the marinones incorporate a farnesyl group. Our proposed biosynthesis of the naphterpin and marinone families of natural products is outlined below.

Firstly, THN (**2.51**) is biosynthesised by the condensation of 5 malonyl-coenzyme A units followed by aromatisation with a type III polyketide synthase, namely THN synthase.[40,41] Next, THN (**2.51**) is subjected to C-4 alkylation with either geranyl pyrophosphate (GPP) (**2.60**) or farnesyl pyrophosphate (FPP) (**2.88**) to give intermediate **2.76** or **2.89** (Scheme 2.16). In 2005, Kuzuyama and co-workers discovered three genes from the naphterpin BGC, including a THN synthase and an aromatic prenyltransferase.[42] This aromatic prenyltranferase Orf2 (renamed NphB[53]) was found to have

relaxed substrate specificity toward various hydroxyl-containing aromatic acceptors; however, THN was never evaluated as a substrate. This prenyltransferase was confirmed to be crucial in naphterpin biosynthesis, as a mutant *Streptomyces* sp. CL190 strain containing a disruption in the Orf2 gene abolished naphterpin production. More recently in 2015, Kaysser and co-workers sequenced the genome of a debromomarinone (**2.46**) producing organism, *Streptomyces* sp. CNQ-509.[54] Analysis of this genome discovered a putative gene cluster for the biosynthesis of a hybrid polyketide-terpenoid containing a putative THN synthase, two putative prenyltransferase enzymes (CnqP3 and CnqP4), and two putative vanadium-dependent chloroperoxidase genes. This gene cluster closely mimics that of complex meroterpenoid antibiotics such as the merochlorins.[25,43] *In vitro* prenyltransferase activity studies of Cnq3 and Cnq4 found that both putative prenyltransferases were active, with CnqP3 showing significant promiscuity towards aromatic substrates and isoprenoid donor molecules, however THN (**2.51**) or FPP (**2.88**) were never tested as substrates. From these studies we propose that C-4 alkylation of THN is putatively catalysed by aromatic prenyltranferase NphB in naphterpin biosynthesis and CnqP3 or CnqP4 in marinone biosynthesis.

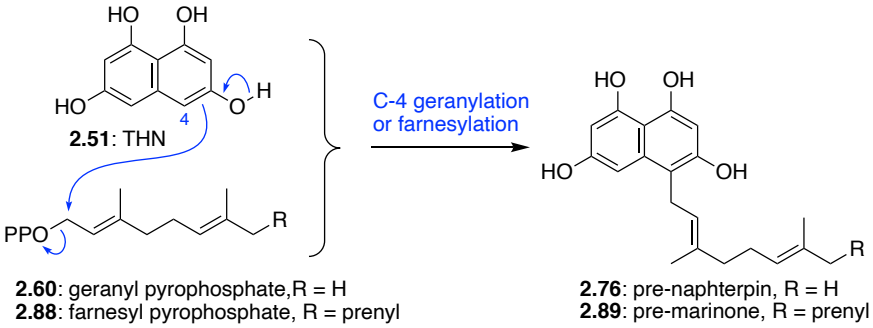

Scheme 2.16: C-4 alkylation of THN (**2.51**) with either geranyl pyrophosphate (**2.60**) or farnesyl pyrophosphate (**2.88**).

We then propose that **2.76**/**2.89** would undergo VCPO-catalysed oxidative dearomatisation to give **2.90**/**2.91** followed by two successive chlorination steps at C-2 to give monochlorides **2.78**/**2.92** and dichlorides **2.93**/**2.94** (Scheme 2.17). Next, **2.93**/**2.94** would be subjected to a VCPO-catalysed

α-hydroxyketone rearrangement to shift the terpene substituent from C-4 to C-3, giving **2.95**/**2.96**. Computational studies have shown this reaction to be thermodynamically favourable.[45] An analogous sequence of chlorination, dearomatisation and 1,2-shift is catalysed by the VCPO Mcl24 in merochlorin biosynthesis (Scheme 2.10/2.11).[45]

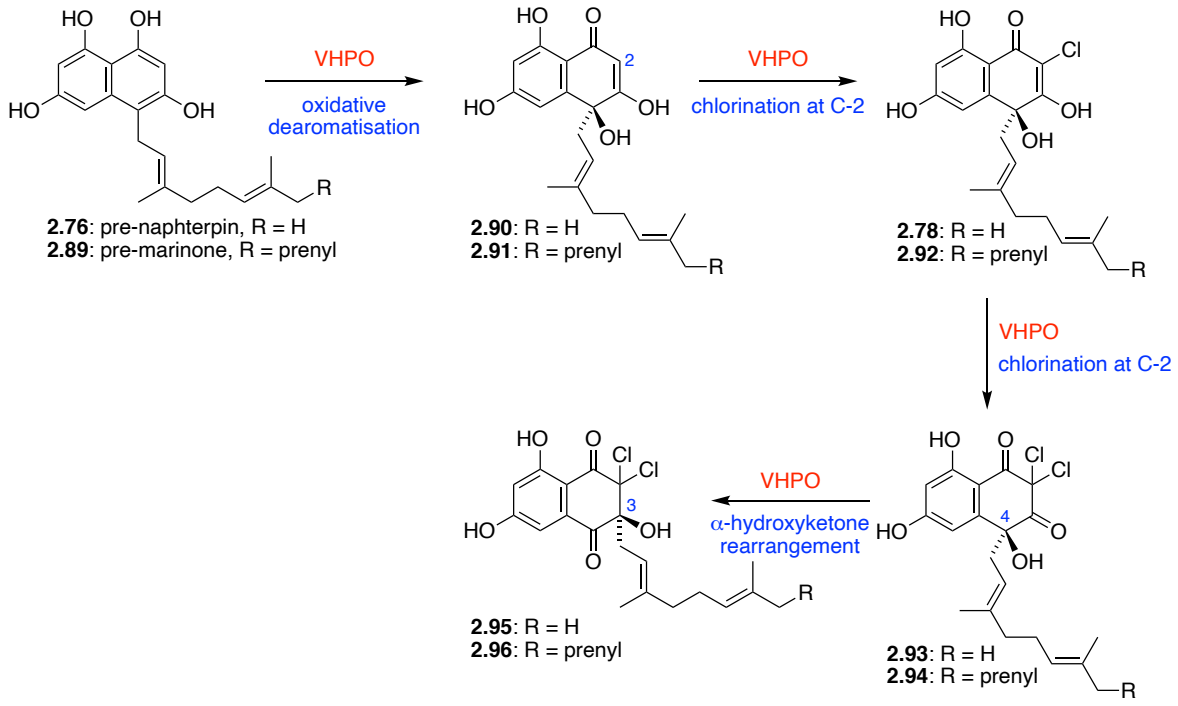

Scheme 2.17: Proposed VHPO-catalysed oxidative dearomatisation, chlorination and α-hydroxyketone rearrangement.

At this stage, treatment of **2.95**/**2.96** with mildly basic conditions should induce cyclisation to form α-chloroepoxides **2.97**/**2.98** (Scheme 2.18). A similar epoxidation has been proposed in the biosynthesis of A80915G from naphthomevalin.[55,56] Additionally, a small number of marine α-chloroepoxide natural products have previously been reported,[57,58] however they are yet to be proposed as intermediates in any biosynthetic pathways. Next, we propose that the α-chloroepoxides **2.97**/**2.98** could be converted to hydroxynaphthoquinones **2.99**/**2.100** *via* reductive dehalogenation. Encouragingly, the C-7 methylated analogue of **2.99**, which we propose as a direct biosynthetic precursor to naphterpin (**2.32**), has been previously isolated as a *Streptomyces* metabolite.[59]

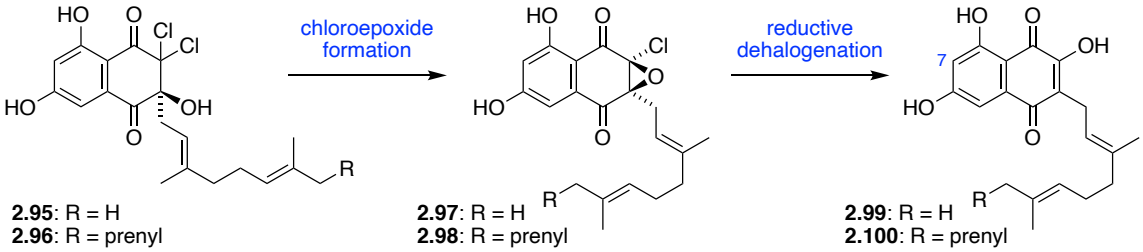

Scheme 2.18: Chloroepoxide formation and reductive dehalogenation.

Associated reductions of naphthoquinone epoxides to give naphthoquinones have been proposed as biosynthetic reactions, and used in the biomimetic synthesis of zeylanone (**2.102**)[60] (Scheme 2.19) and juglocombins.[61]

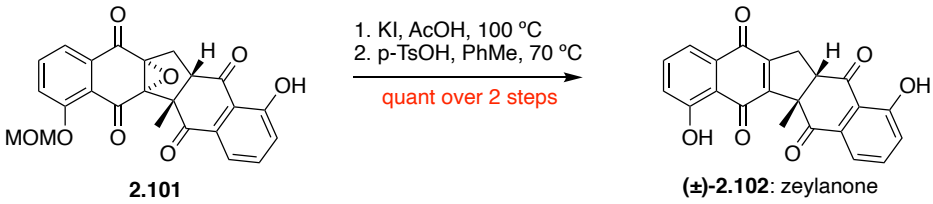

Scheme 2.19: Final step in Kuramochi's biomimetic total synthesis of zeylanone.[60]

Oxidation and facile *E*-to-*Z* alkene isomerization of **2.99**/**2.100** would give reactive enones **2.103**/**2.104**, which could then undergo the final intramolecular Diels-Alder reaction to give 7-demethylnaphterpin (**2.38**) and debromomarinone (**2.46**) (Scheme 2.20).

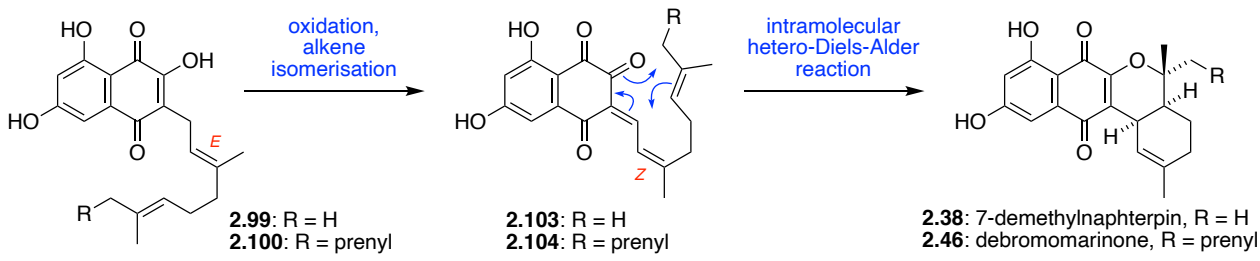

Scheme 2.20: Oxidation, *E*-to-*Z* alkene isomerisation and intramolecular Diels-Alder reaction.

The naphterpins and marinones were isolated as enantiopure compounds, therefore we speculate that the late stage oxidative cyclisation of achiral **2.99**/**2.100** must be under enzymatic stereocontrol.[62] A similar oxidative cyclisation is observed in the biosynthesis of Δ^1-tetrahydrocannabinolic acid (**2.106**) from cannabigerolic acid (**2.105**) catalysed by THCA synthase (Scheme 2.21).[63,64] Oxidation of hydroxyquinones **2.99**/**2.100** also has literature precedent in the biosynthesis of marine *Streptomyces* metabolite chlorizidine A.[65]

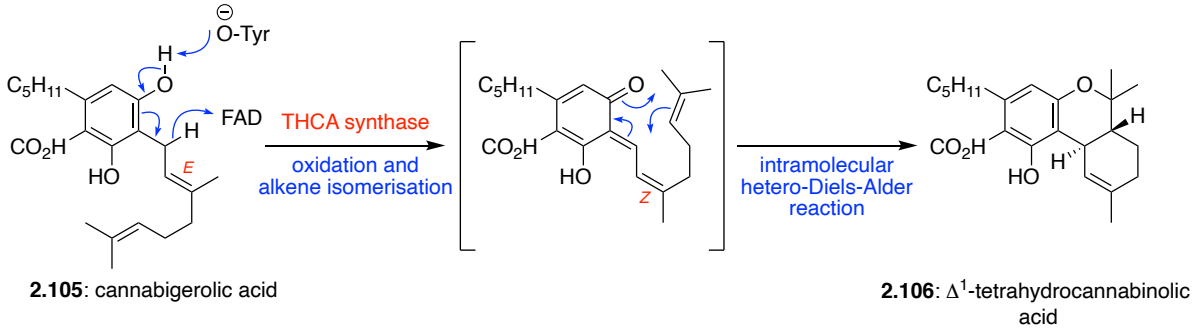

2.105: cannabigerolic acid

2.106: Δ^1-tetrahydrocannabinolic acid

Scheme 2.21: Proposed mechanism of tetrahydrocannabinol biosynthesis.[63,64]

Finally, a late stage bromination at C-5 or C-7 of **2.46** would give marinone (**2.33**) or isomarinone (**2.47**), respectively (Scheme 2.22).

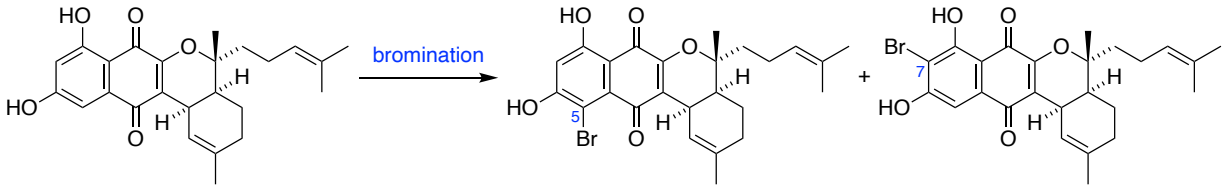

2.46: debromomarinone

2.33: marinone

2.47: isomarinone

Scheme 2.22: Bromination of debromomarinone (**2.46**).

Despite an absence of chlorine in these natural products, we envisaged that the THN ring could be selectively oxidised through a cryptic chlorination, promoting the predicted α-hydroxyketone rearrangement. This hypothesis was supported by the clustering of VCPO and aromatic

prenyltransferase homologues with a THN synthase in the preliminary genomic analysis of the putative marinone genome from *Streptomyces* sp. CNQ-509.[54]

2.1.9 Project Aims

The primary objective of this research was to investigate our biosynthetic proposal for both the naphterpin and marinone families of natural products by completing their biomimetic total syntheses.

Mimicking the entire biosynthetic pathway of these natural products would allow us access to each proposed biosynthetic intermediate for chemoenzymatic studies, giving the potential for elucidation of their biosynthetic pathways. The initial synthetic targets of this research would be the two simplest members of the naphterpin and marinone families, 7-demethylnaphterpin (**2.38**) and debromomarinone (**2.46**) shown in Figure 2.09.

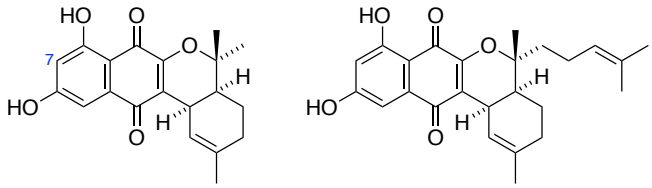

2.38: 7-demethylnaphterpin **(±)-2.46**: debromomarinone

Figure 2.09: Primary natural product targets.

Moore and George have previously reported two VCPO enzymes, Mcl24 and NapH3,[45] responsible for catalysing α-hydroxyketone rearrangements to shift terpene sidechains from C-4 to C-3 in merochlorin and napyradiomycin biosynthesis, respectively (Scheme 2.23). Given the similarities in biosynthetic proposal, we believed this biosynthetic logic would extend to the naphterpins and marinones for this key step.

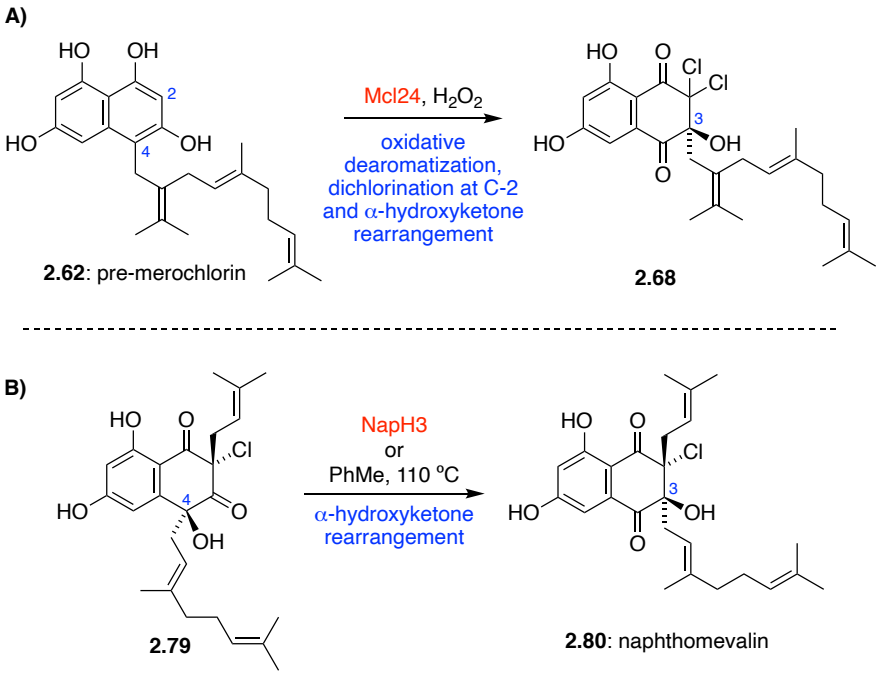

Scheme 2.23: VCPO enzymes currently known to catalyse α-hydroxyketone rearrangements A) Mcl24 in merochlorin biosynthesis B) NapH3 in napyradiomycin biosynthesis.

In order to investigate this biosynthetic proposal, an alkylated, dearomatized and dichlorinated THN-derivative such as (**2.93**/**2.94**) would be prepared, using chemistry analogous to that in the total synthesis of naphthomevalin (**2.80**) (Scheme 2.24). If successful, we would then investigate the analogous α-hydroxyketone rearrangement, followed by formation of α-chloroepoxides **2.97**/**2.98**. Subsequent reductive dehalogenation would give hydroxyquinones **2.99**/**2.100** followed by oxidation and alkene isomerisation to form reactive enones **2.103**/**2.104**. These enone intermediates **2.103**/**2.104** are then prime to undergo the final intramolecular hetero-Diels-Alder reaction to generate the tetracyclic core of the 7-demethylnaphterpin (**2.38**) or debromomarinone (**2.46**), depending on the length of the sidechain. With **2.46** in hand, we could then explore its conversion into marinone (**2.33**) or isomarinone (**2.47**) through bromination at C-5 or C-7, respectively. This approach would lead to the first biomimetic total synthesis of these meroterpenoid natural products, and their only total synthesis at this time.

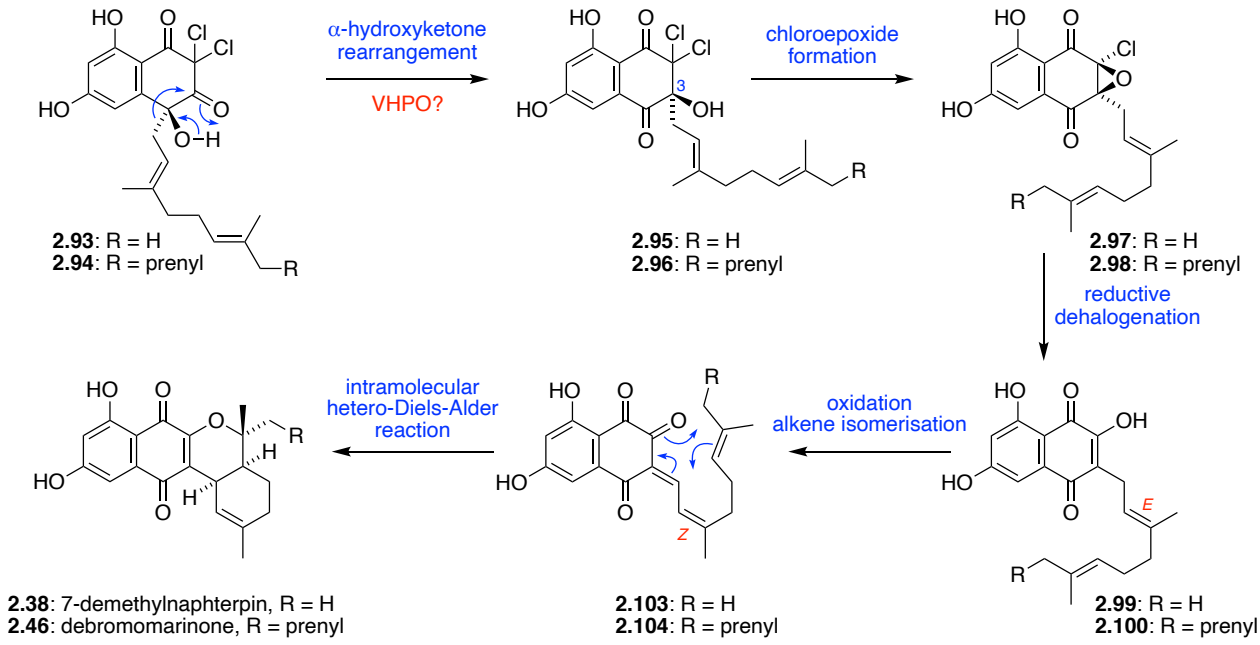

Scheme 2.24: Proposed synthetic and biosynthetic studies on the marinones.

The success of this α-hydroxyketone rearrangement would strongly suggest that these molecules are synthesised through a sequence of VCPO-catalysed reactions, similar to that of the merochlorins and the napyradiomycins, therefore confirming our hypothesis of cryptic chlorination events. The completion of these biomimetic total syntheses has the potential to generate several biosynthetic intermediates. These intermediates will be used in chemoenzymatic assays to ascertain the reactivity and function of putative VHPO enzymes from the putative marinone BGC, thus elucidating key steps within the biosynthetic pathway.

2.2 Results and Discussion

2.2.1 Retrosynthetic Analysis of 7-Demethylnaphterpin and Debromomarinone

Previous syntheses of both the merochlorin and napyradiomycin natural products gave us great precedent for the synthesis of THN intermediates towards the naphterpin and marinone families. We predicted that the cis-fused cyclohexane and pyran rings of 7-demethylnaphterpin (**2.38**) and debromomarinone (**2.46**) could be formed through an intramolecular hetero-Diels-Alder reaction of reactive enones **2.103**/**2.104**, which would be unveiled through oxidation and alkene isomerisation of hydroxyquinones **2.99**/**2.100** (Scheme 2.25). The synthesis of hydroxyquinones **2.99**/**2.100** would be achieved through reductive dehalogenation of α-chloroepoxides **2.97**/**2.98**.

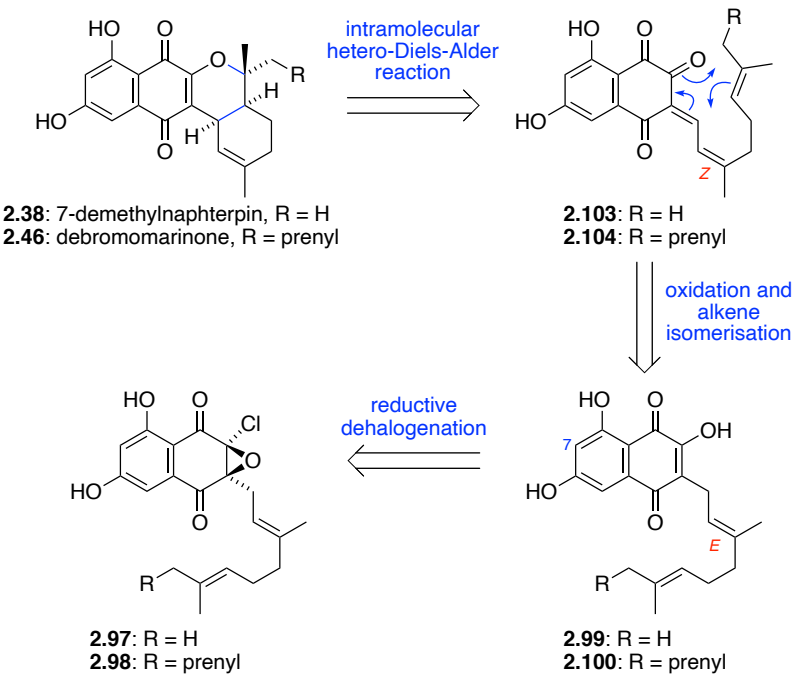

Scheme 2.25: Retrosynthetic analysis of 7-demethylnaphterpin (**2.38**) and debromomarinone (**2.46**).

We envisaged that α-chloroepoxides **2.107**/**2.108** could be formed through cyclisation of dichlorinated intermediates **2.109**/**2.110** under mildly basic conditions (Scheme 2.26). The predicted α-hydroxyketone rearrangement of **2.111**/**2.112** would then shift the geranyl or farnesyl sidechain from the C-4 to the C-3 position to afford intermediates **2.109**/**2.110**. Dichlorides **2.111**/**2.112** would

be formed through dichlorination at the C-2 position of dearomatised intermediates **2.113**/**2.114**. Wessely[66,67] oxidation of the alkylated THN intermediate **2.85**/**2.115** would give access to a dearomatised ring system, containing all of the required oxygen atoms in the final natural products. Considering our previous synthesis of naphthomevalin, we decided that the di-MOM protected pre-naphterpin/marinone structure (**2.85**/**2.115**) could be accessed by the same Pd(0) catalysed alkylation between di-MOM protected THN (**2.83**) and geranyl/farnesyl carbonate (**2.84**/**2.116**).[45,68] The di-MOM protected THN would be synthesised using our previously published synthesis.[45]

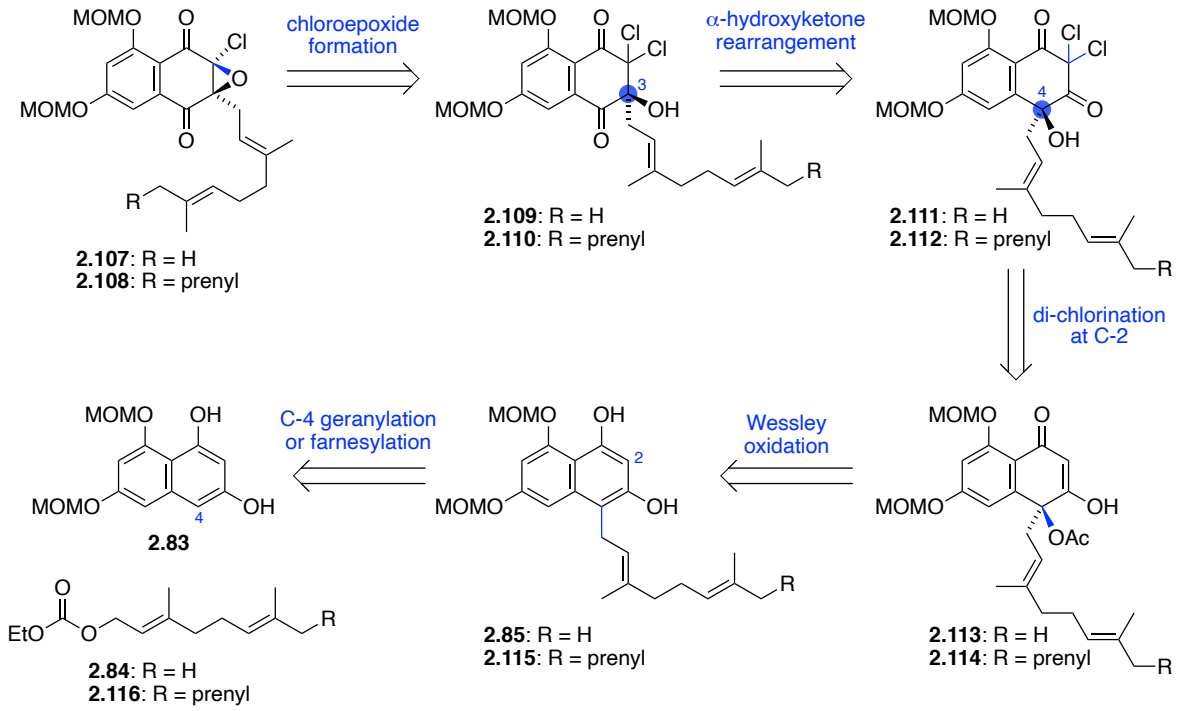

Scheme 2.26: Retrosynthetic analysis of key intermediates **2.107**/**2.108**, R = H or prenyl.

2.2.2 Biomimetic Total Synthesis of 7-Demethylnaphterpin

The first step of this synthesis involved the gram scale preparation of a di-protected THN intermediate for alkylation. In the presence of air, THN (**2.51**) is known to readily oxidise to flaviolin, therefore we proposed the use of a partially protected intermediate to simplify the synthesis. Previous literature reports show that THN can be synthesised from the commercially available chromotropic acid disodium salt (**2.117**) through a technically challenging alkali fusion reaction, utilising molten NaOH

(Scheme 2.27).[69–72] This reaction was not practical for our laboratory as the equipment needed to perform this reaction, both reliably and safely, was not available.

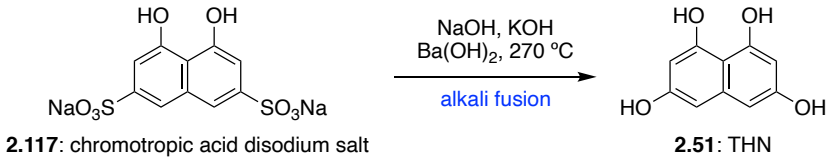

2.117: chromotropic acid disodium salt

2.51: THN

Scheme 2.27: Previous literature synthesis of THN (**2.51**) from chromotropic acid disodium salt.

The second literature approach for the synthesis of THN compounds was first employed by Bycroft and Roberts in 1963.[73] More recently it has been adapted by Barrow[74,75] in 2005 (Scheme 2.28), and Akai[76] in 2007. This two-step approach involved a Friedel-Crafts acylation of commercially available methyl 3,5-dimethoxyphenolacetate (**2.70**) to give **2.117**, followed by formation of the second aromatic ring **2.118** through a Dieckmann-type condensation between an aryl ketone and an ester.

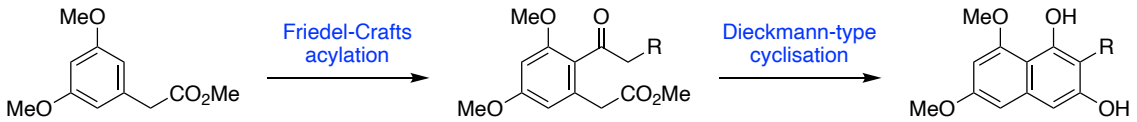

2.70 **2.117** **2.118**

Scheme 2.28: Previous literature approach to synthesise substituted 1,3-dihydroxy-6,8-dimethoxynaphthalene **2.118**.[75]

A similar synthetic approach was taken by George and Pepper in their previous biomimetic syntheses of merochlorin A.[77] This reaction was found to be very reliable and scalable, confirming that this aromatization approach was a more suitable approach to access THN type intermediates. Methyl ether protecting groups were found successful for the synthesis of merochlorin A due to their robust nature, however removal in the final deprotection step required the harsh conditions of LiCl in DMF at 135 °C. As the focus of our new synthesis towards naphterpin and debromomarinone was to access, and therefore deprotect, each proposed biosynthetic intermediate, we anticipated the need for a more

labile protecting group that could still survive the reaction conditions throughout the synthetic sequence.

Two previous syntheses of napyradiomycin A1,[78,79] alongside a previous synthesis of naphtomevalin[45] involved the protection of phenols with MOM ether protecting groups. In each of these cases the MOM ether was successfully cleaved as the final synthetic step. MOM ethers are known to be stable to most reaction conditions, with the exception of acid hydrolysis, therefore we were confident that they would be compatible with our synthesis.

As the MOM protected methyl 3,5-dihydroxyphenylacetate was not commercially available, this synthesis began with the commercially available methyl 3,5-dimethoxyphenylacetate (**2.70**) (Scheme 2.29).[45] Friedel-Crafts acylation of **2.70** with Ac_2O gave the intermediate methyl ketone, followed by demethylation using $AlCl_3$ to afford **2.119**. Bis-MOM protection followed by base-induced aromatisation with NaH *via* a Dieckmann-type cyclization gave the protected THN derivative **2.83**.

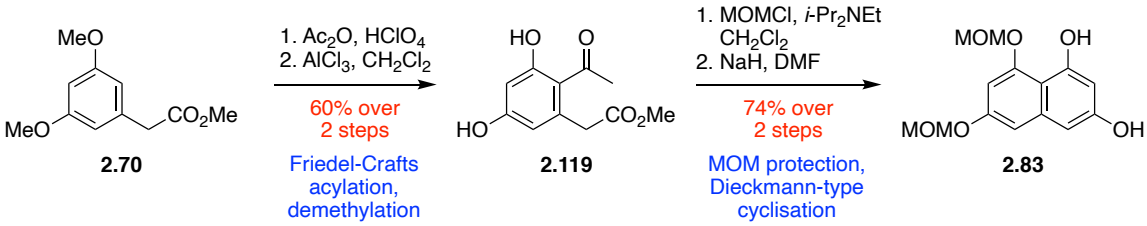

Scheme 2.29: Synthesis of di-MOM protected THN **2.83**.

With the protected THN intermediate **2.83** in hand, we could now attempt the desired Pd-catalysed Tsuji-Trost alkylation with geranyl carbonate (**2.84**) (Scheme 2.30).[45,68] This strategy had also been employed previously by Moore *et. al.* in their synthesis towards the merochlorins,[43] and later in George's synthesis of the napyradiomycins.[45] Ethyl geranyl carbonate (**2.84**) was synthesised in one step from geraniol and ethyl chloroformate.[80] Much like what was observed in the napyradiomycin synthesis, this reaction was slow and was never driven to completion, resulting in recovery of a

significant proportion of starting material. Despite attempts to change variables such as temperature, time, scale, ratios of reagents and catalytic loading, the outcome of the reaction was unchanged. Unable to improve the yield of this reaction, it was routinely performed on 10 g scale, heating at 50 °C for 2 h. On purification by column chromatography, unreacted starting material **2.83** was isolated and recycled. Next, Wessely oxidation of **2.85** with $Pb(OAc)_4$ gave oxidatively dearomatised intermediate **2.113** *in situ*, followed by dichlorination with NCS at C-2 to give **2.120** in a one-pot process. A two-step process was originally attempted, however we faced difficulties with yield reproducibility in the Wessely oxidation step. Coupling these two reactions solved this problem as the chlorinated product **2.120** was found to be more stable.

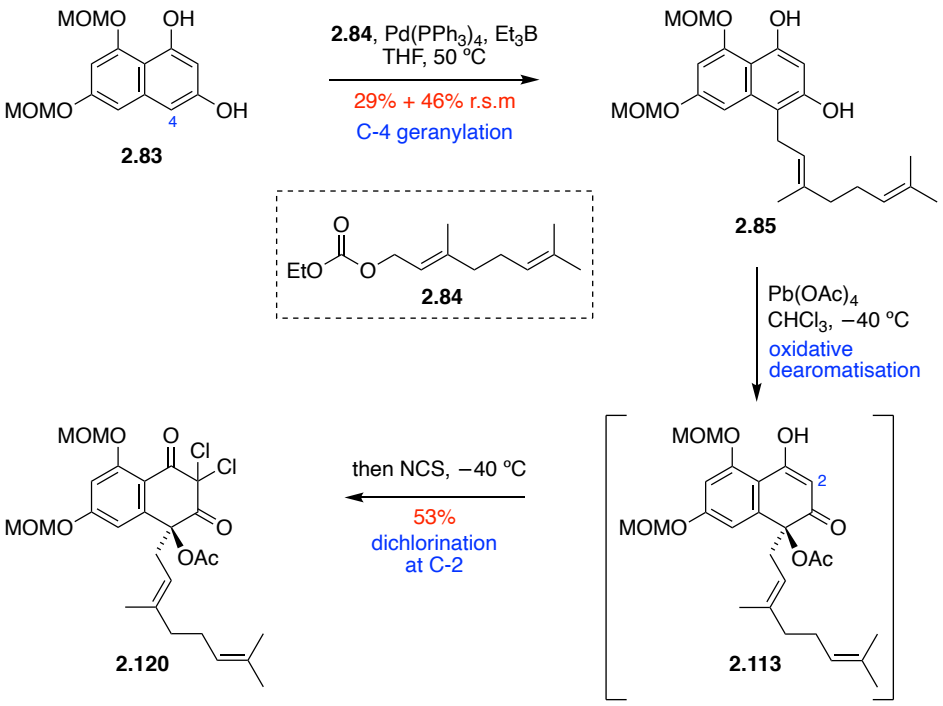

Scheme 2.30: Total synthesis of dichlorinated intermediate **2.120**.

Next we attempted acetate hydrolysis of dichlorinated intermediate **2.120** (Scheme 2.31). Under standard conditions of KOH in MeOH at rt, TLC analysis showed a mixture of products, however none of the isolated products matched the desired alcohol **2.111**. NMR analysis of the major product determined it to be compound **2.121**. This compound is presumably formed by a competing haloform

reaction, resulting in fragmentation as a result of nucleophilic attack of methoxide onto the C-3 carbonyl group, cleaving the C2-C3 bond. Substituting KOH for K_2CO_3 gave analogous results.

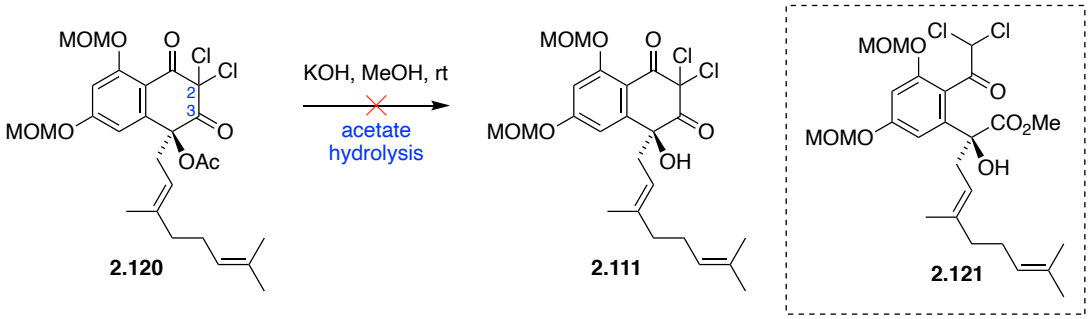

Scheme 2.31: Unsuccessful conditions for acetate hydrolysis of **2.120**.

Thankfully, this undesired haloform reaction could be circumvented by LDA-mediated dechlorination prior to acetate hydrolysis (Scheme 2.32). Treatment of dichloride **2.120** with LDA at –78 °C resulted in the formation of two polar products by TLC analysis. ^{1}H NMR analysis of the isolated compounds confirmed their structures to be **2.122** and **2.86**. These results showed that the desired dichlorination event was occurring, with some acetate cleavage under the reaction conditions, however this could not be pushed to completion. Although these two compounds could be separated and isolated by column chromatography, it was made difficult due to their high polarity and similarity in R_f. Consequently, this mixture of compounds were routinely subjected to the next reaction as a mixture.

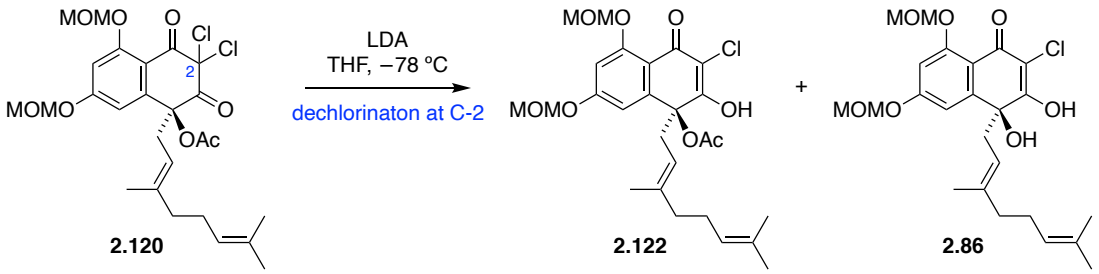

Scheme 2.32: Dechlorination of **2.120**.

The hydrolysis on the monochlorinated system avoided the previously observed haloform reaction, however two new products were observed by TLC. ^{1}H NMR analysis showed a mixture of compounds **2.86** and **2.123** (Scheme 2.33). Consequently, MOM-deprotection of the C-8 hydroxyl had occurred to some extent under the reaction conditions. Regardless of extreme caution taken in acidification upon workup, mono-deprotection was always observed to some extent.

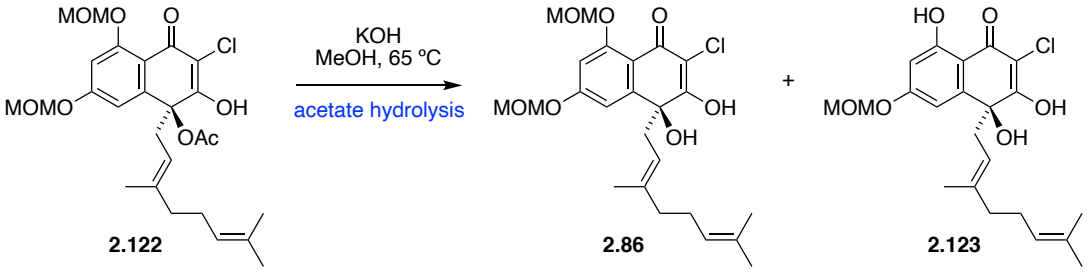

2.122 **2.86** **2.123**

Scheme 2.33: Acetate hydrolysis of **2.122**.

Due to the high polarity of these molecules, the crude mixture of products was taken through to the next chlorination step. Chlorination of the mixture of mono-chlorinated intermediates proceeded smoothly at -78 ºC, producing separable intermediates **2.111** and **2.124** in 32% and 21% yield, respectively (Scheme 2.34). At this stage it was impossible to know if di-MOM protection was crucial to the success of this synthesis. If not, we envisaged pushing the mono-deprotection to completion in the hydrolysis step, increasing the yield of the dichlorinated intermediate **2.124** to predictably over 50%.

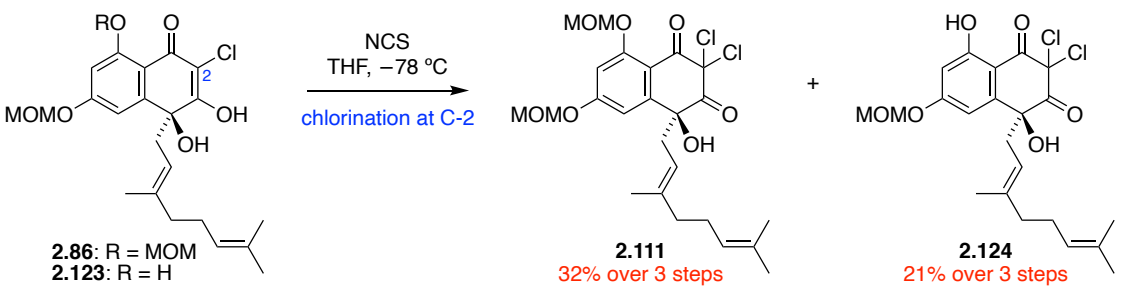

2.86: R = MOM
2.123: R = H

2.111
32% over 3 steps

2.124
21% over 3 steps

Scheme 2.34: NCS chlorination at C-2.

With the desired 1,3-diketone structure locked due to full substitution at the C-2 position, we could now replicate the α-hydroxyketone rearrangement previously employed in the synthesis of naphthomevalin, shifting the geranyl substrate from the C-4 to the C-3 position.[45] At this stage, it made sense to attempt this key rearrangement with both **2.111** and **2.124**. The 1,2-shift of a prenyl moiety in these α-hydroxyketone rearrangements is often catalysed by base, Brønsted or Lewis acid or heat.[21] In the case of naphthomevalin, basic conditions catalysed a fragmentation reaction similar to Scheme 2.31, while Lewis and Brønsted acids failed to promote any reaction at all. Therefore, thermal conditions were explored, discovering that reflux in toluene gave complete conversion. With this knowledge, we too attempted a thermal rearrangement (Scheme 2.35). Satisfyingly, refluxing 1,3-diketone **2.124** in toluene resulted in the formation of a product with an almost identical R_f to the starting material by TLC analysis. ^{1}H, ^{13}C and 2D NMR analysis confirmed the product to be the desired 1,2-shift product **2.125**.

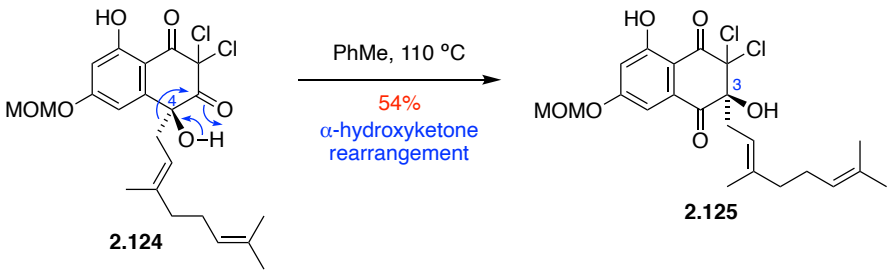

Scheme 2.35: α-Hydroxyketone rearrangement.

The yields of this reaction did not rival that of its naphthomevalin counterpart, which was found to be consistently quantitative. Instead, yields of this reaction were unreliable and often fluctuated between 20-70%. Changes in reaction variables including temperature, time and dilution were found to show little improvement to the reaction outcome. This reaction was also found to have scalability issues and was therefore routinely performed on ~100 mg scale, heated at reflux for 20 h in toluene before cooling to room temperature. Shortened reaction times showed remaining starting material. This posed bigger issues as clean separation of the starting material from the product was impossible

by column chromatography. Multiple attempts to set up identical side by side reactions would regularly result in different product ratios, due to the formation of an undesired side product. Although we had initially isolated this side product, identification proved difficult by NMR analysis as any structure we proposed seemed to defy synthetic logic. Following successful crystallisation of this product, single-crystal X-ray crystallography led to the crystal structure and identification of the side product **2.126** (Scheme 2.36).

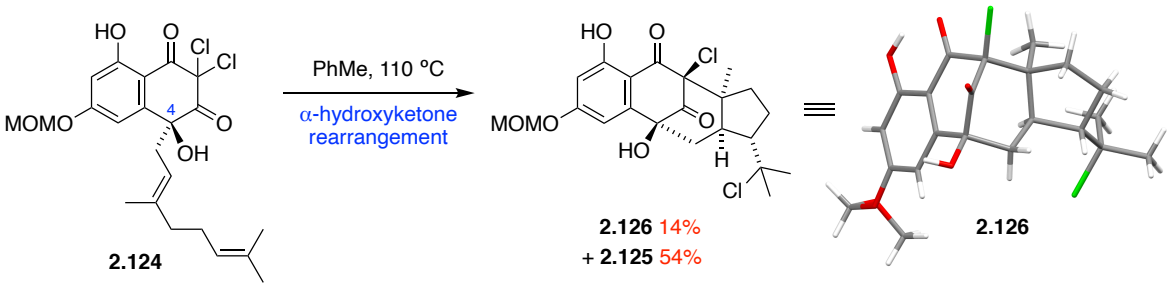

Scheme 2.36: Synthesis of side product **2.126** and crystal structure.

Intriguingly, it appeared that the formation of **2.126** was the product of an atom transfer radical cyclisation (ATRC) mechanism. This reaction is commonly employed in the preparation of functionalised 4-10 membered ring systems, utilising a transition metal catalyst such as copper or ruthenium.[81–83] In 2006 Yang and co-workers reported a series of copper(I) chloride-catalysed chlorine atom transfer radical cyclisations on α-dichlorinated β-keto ester substrates, with striking similarity to that observed in our thermal reaction (Scheme 2.37).[84] In this example, CuCl abstracts a chlorine atom from the substrate **2.127** to generate the tertiary radical **2.128** and $CuCl_2$. Subsequently, a sequence of 6-*endo* and 5-*exo* cyclisations to give **2.129**, followed by abstraction of a chlorine atom from $CuCl_2$, affords the 6,5-*cis* tandem cyclisation product **2.130** as a mixture of epimers.

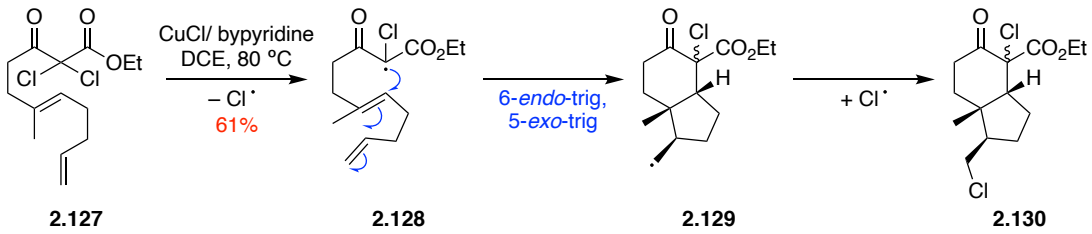

Scheme 2.37: Literature example of a copper(I)-catalysed chlorine transfer radical cyclisation.[84]

Dismissing the unlikely situation in which trace metal contamination (e.g. from a stirrer bar) had occurred, our reaction contained no metal catalyst, however, the sequence of cyclisations did mimic that observed by Yang. This suggested an analogous mechanism to give side product **2.126** (Scheme 2.38). We propose that homolysis of one carbon-chlorine bond in **2.124** would give corresponding tertiary radical **2.131**. This intermediate could then undergo a 6-*endo*-trig, 5-*exo*-trig cyclisation cascade to give secondary radical **2.132**. Subsequent chlorine atom abstraction would give the isolated side product **2.126**.

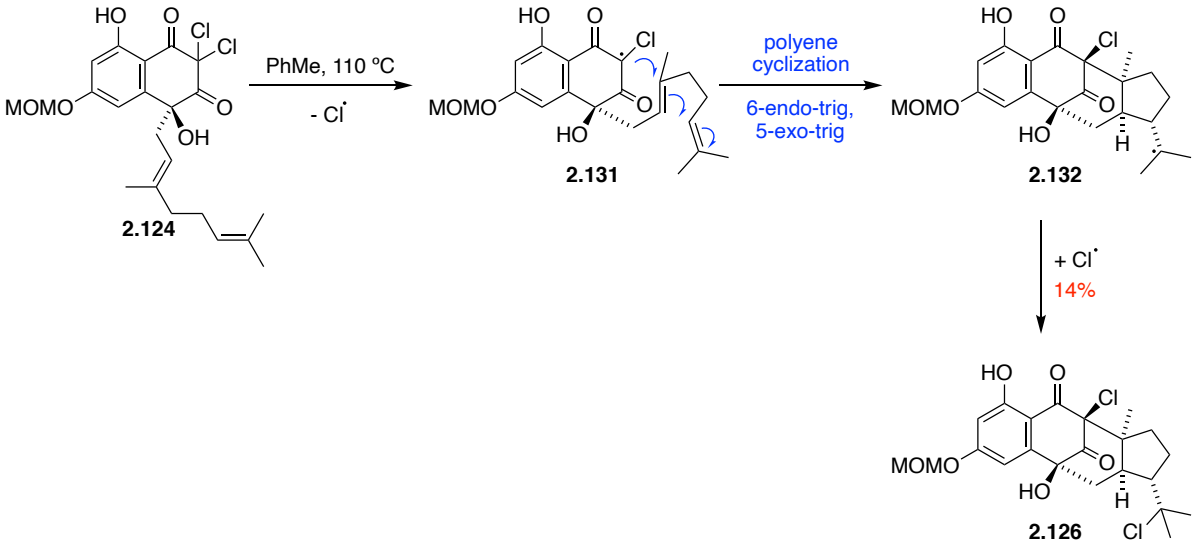

Scheme 2.38: Proposed chlorine transfer radical cyclisation mechanism to form **2.126**.

With this proposal in mind, we speculated that the addition of a radical trap to the reaction conditions could increase the production of the desired α-ketol rearrangement product, and therefore give a more reliable yield. Addition of the radical inhibitor 2,6-di-tert-butyl-4-methylphenol (BHT)[85] to the

reaction showed no improvement. Interestingly, the addition of radical initiator azobisisobutyronitrile (AIBN) with $SnBu_3H$ did not increase the amount of **2.126** produced. At this stage, we were unsure if this reaction really was driven *via* a radical mechanism. Attempting the reaction using Yang's CuCl-catalysed conditions (Scheme 2.39), the expected 6-*endo* and 5-*exo* cyclisation sequence occurred, forming **2.126** in 25% yield.

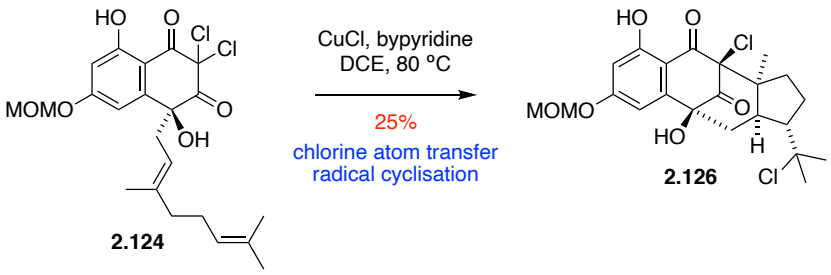

Scheme 2.39: Copper(I)-catalysed chlorine transfer radical cyclisation to give **2.126**.

Although this result gave us promising insight into the mechanism of this side reaction, optimisation of the desired α-ketol reaction conditions using radical traps proved unsuccessful and did not improve the product yield.

In addition to testing the mono-protected intermediate **2.124,** we decided to investigate if the yield would be improved by attempting the α-hydroxyketone rearrangement on the di-MOM protected intermediate **2.111** (Scheme 2.40). This reaction progressed in the same manner as the mono-protected intermediate **2.124**, giving the desired product **2.109** in 46% yield. Although this was not a poor yield for this reaction, it was not higher than that previously achieved on **2.124**.

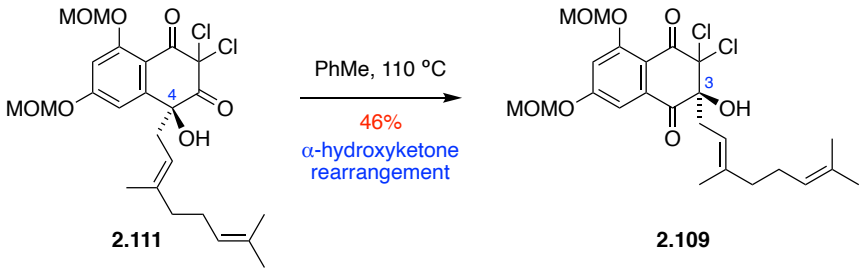

Scheme 2.40: α-Hydroxyketone rearrangement on di-MOM protected intermediate **2.111**.

With this in mind, we conceded that avoiding partial MOM deprotection during acetate hydrolysis (Scheme 2.33) seemed impossible. As a result, it was decided to further acidify the reaction during workup to push the mono-deprotection to completion. Simplifying this reaction to form one product increased the overall yield of this hydrolysis sequence to 65% over three steps (Scheme 2.41).

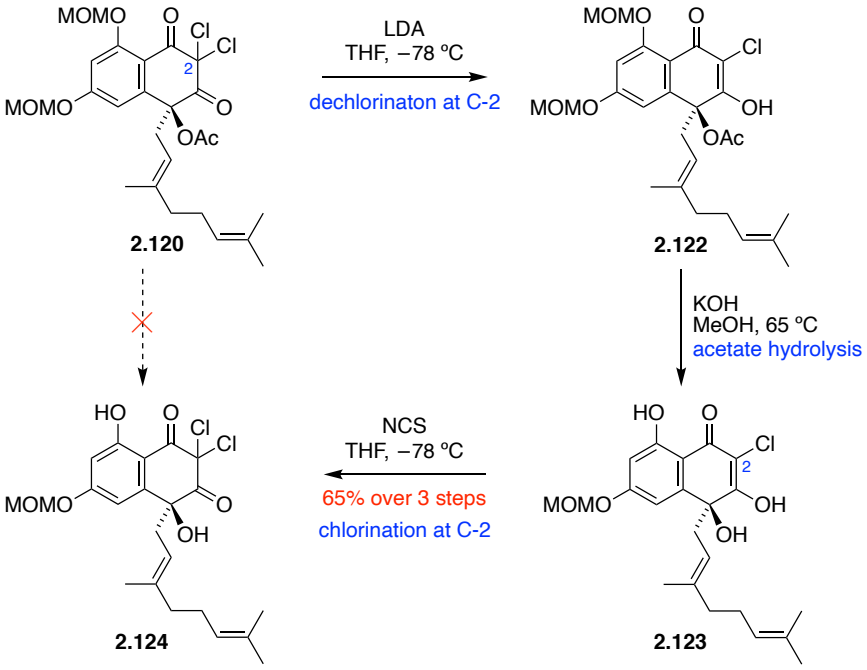

Scheme 2.41: Revised acetate hydrolysis sequence to give **2.124**.

With our reaction conditions established for the α-hydroxyketone rearrangement, we were set to proceed with the desired α-chloroepoxide formation. Several bases were screened in order to catalyse the desired epoxidation, resulting in no product formation or degradation. Treatment of dichloride

2.125 with Cs_2CO_3 in THF at 0 ºC gave the desired α-chloroepoxide **2.133** (Scheme 2.42). Although initially in quite poor yields, increasing the reaction time spent at 0 ºC and care taken monitoring the reaction by TLC led to a fair yield of 57%.

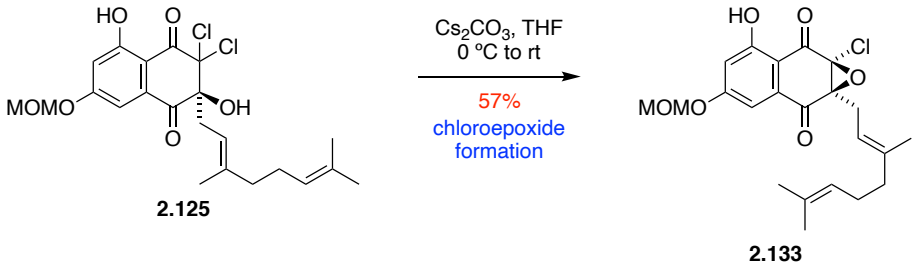

Scheme 2.42: α-Chloroepoxide formation.

The next step in this synthetic sequence was to perform a reductive dehalogenation. Similar reductive dehalogenations had been performed in literature, catalysed by Zn, a Zn-Cu couple or thermolysis.[86,87] In 2011, Kotoku and co-workers showed that they were able to perform a similar reductive ring opening of their iodo-epoxide utilising Zn powder in MeOH with quantitative yield during, their synthesis of cortistatin A.[87] Subjection of **2.133** to Kotoku conditions of Zn powder in MeOH at reflux showed rapid formation of a new product by TLC analysis (Scheme 2.43). This new product was found to have a similar but lower R_f than the starting material, and after isolation, NMR analysis confirmed the reductive dehalogenation was successful, giving hydroxyquinone **2.134** in 92% yield. Leaving this reaction for longer reactions times at reflux significantly decreased the yield.

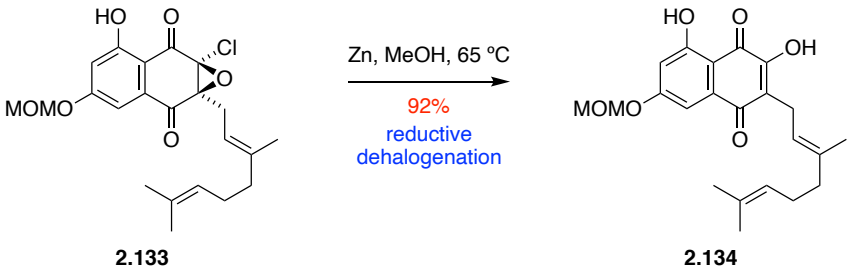

Scheme 2.43: Reductive dehalogenation of **2.133**.

With **2.134** in hand, we were now in a position to test our proposed oxidative cyclisation to give the natural product 7-demethylnaphterpin (**2.38**). In this case, we hoped that subjecting geranylated hydroxyquinone **2.134** to oxidative conditions would induce allylic oxidation on the geranyl sidechain to yield intermediate **2.135**. Subsequent elimination of water and facile double-bond isomerisation would yield *ortho*-quinone methide **2.103**, which could then undergo the desired intramolecular hetero Diels-Alder reaction to afford 7-demethylnaphterpin (**2.38**) (Scheme 2.44).

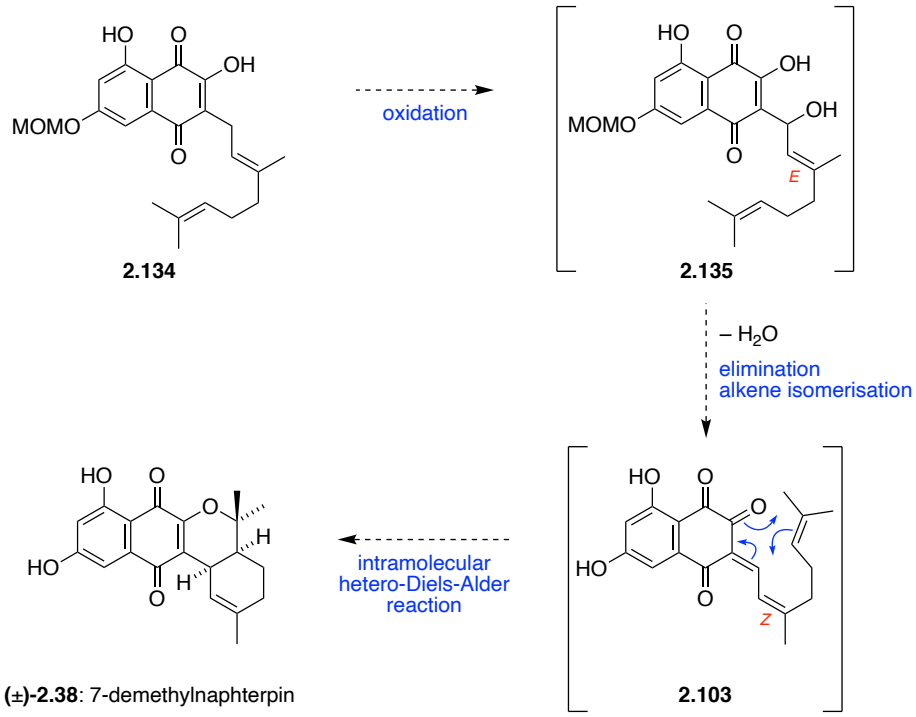

Scheme 2.44: Proposed oxidative cyclisation of **2.134** to give 7-demethylnaphterpin.

A similar biosynthetic proposal was described by Trauner and co-workers in their studies towards the synthesis of antimalarial naphthoquinones pyranokunthone A (**2.139**) and B (**2.141**) (Scheme 2.45).[88] This proposal suggested that after oxidation of **2.136**, intermediate **2.137** could then undergo elimination of water and facile *E* to *Z* alkene isomerisation to form **2.138** which would then undergo the desired hetero Diels-Alder reaction to give the natural product pyranokunthone A (**2.139**). In the alternative pathway, **2.137** would undergo dehydration to give intermediate **2.140**, which would then undergo an oxa-6π-electrocyclisation to form pyranokunthone B (**2.141**). Intriguingly, it was found

experimentally that the oxa-6π-electrocyclization was kinetically favoured over the intramolecular hetero Diels-Alder reaction in these systems.

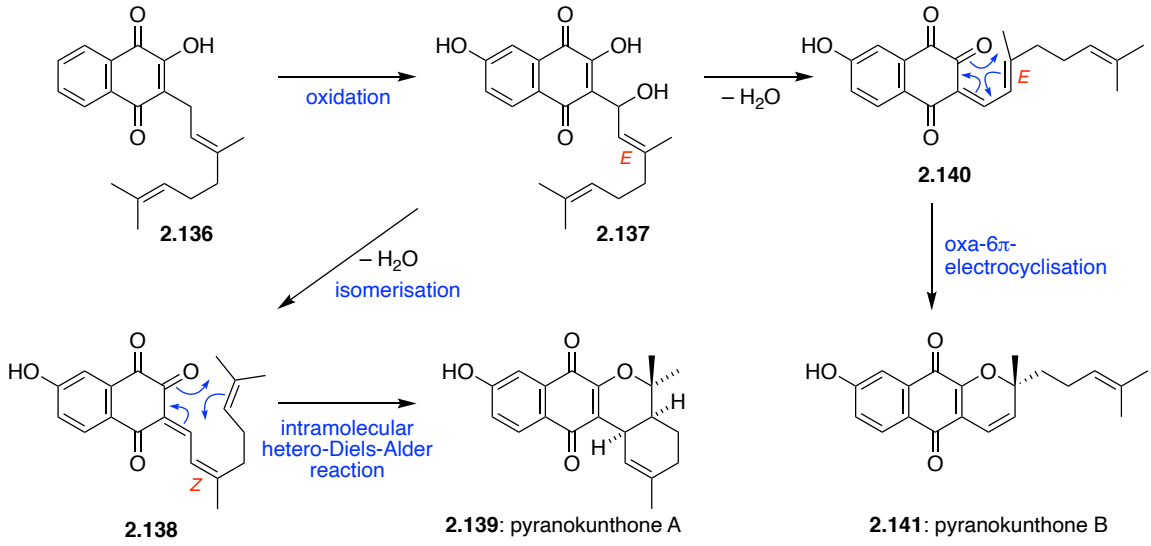

Scheme 2.45: Biosynthetic proposal for pyranokunthone A (**2.139**) and B (**2.141**).

Literature examples show that such *o*-quinone methide intermediates have previously been generated by oxidation with Ag_2O.[89] A similar approach was taken in the oxidative formation of α,β-unsaturated ketones as part of the biomimetic total syntheses of the hyperjapones and hyperjaponols.[90,91] In the example of hyperjapone A (**2.145**) (Scheme 2.46), the known natural product norflavesone (**2.142**) was oxidised using TEMPO and Ag_2O in tandem to form the α,β-unsaturated ketone (**2.144**) *in situ*. This intermediate then underwent an intermolecular Diels-Alder reaction with humulene (**2.143**), forming the natural product hyperjapone A (**2.145**).

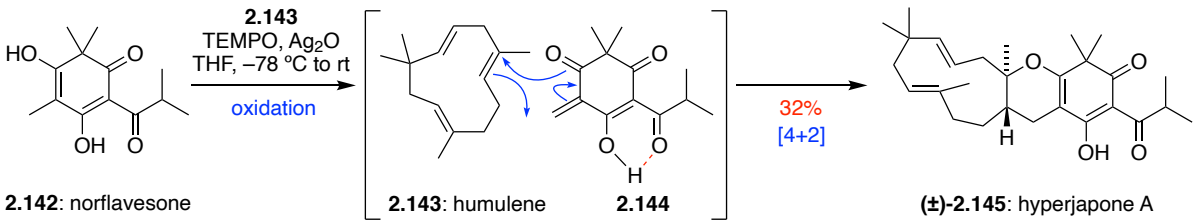

Scheme 2.46: George's biomimetic synthesis of hyperjapone A (**2.145**).[90]

We proposed that we could extend this logic for our intramolecular Diels-Alder reaction. Unfortunately, exposure of **2.134** to TEMPO and Ag_2O showed only degradation in our system. Screening alternative oxidants such as CAN, DDQ and IBX were also unsuccessful, leading to either no reaction or decomposition of the starting material. With this in mind, we decided to try hypervalent iodine oxidant $PhI(OAc)_2$ with TEMPO. This combination had shown previous success in the biomimetic total synthesis of hyperguinone B (**2.148**) (Scheme 2.47).[92] It was proposed that this reaction proceeds *via* a selective hydride abstraction by the *in situ* generated TEMPO cation to generate the *o*-quinone methide intermediate **2.147**, which undergoes a 6π-electrocyclization to give natural product hyperguinone B (**2.148**).

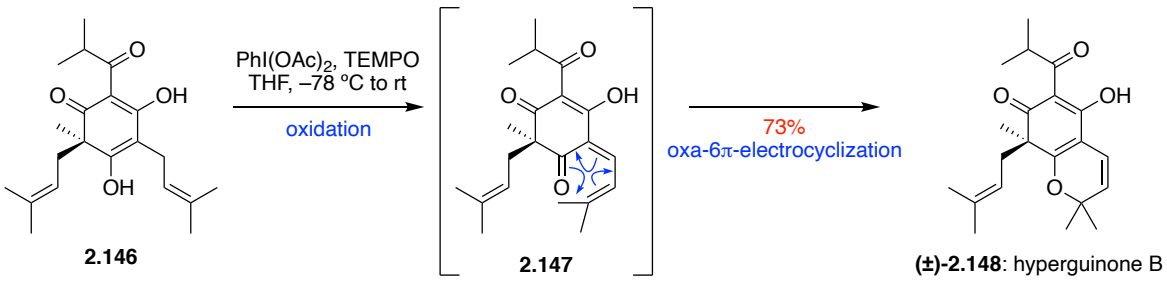

Scheme 2.47: George's biomimetic total synthesis of hyperguinone B (**2.148**).[92]

Treatment of hydroxynaphthoquinone **2.134** with $PhI(OAc)_2$ in the presence of TEMPO (Scheme 2.48) resulted in the formation of a new product by TLC. Isolation and NMR analysis confirmed the major product to be paraquinone **2.149** in 78% yield. As discussed previously, 6π-electrocyclisation is usually kinetically favoured over the intramolecular hetero Diels-Alder reaction is such systems.[88]

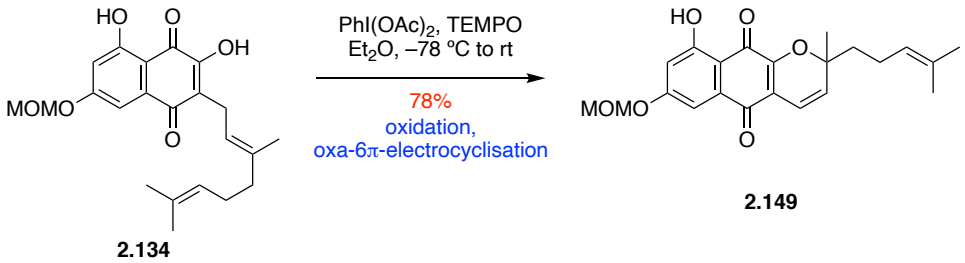

Scheme 2.48: Oxa-6π-electrocyclisation of **2.134**.

At this stage it was clear that oxidation and alkene isomerisation to achieve the desired intramolecular hetero Diels-Alder reaction of intermediate **2.134** would prove difficult. With oxa-6π-electrocyclisation product **2.149** in hand, we decided to take advantage of the reversibility of this reaction. Trauner and co-workers had shown some success in this area through Lewis-acid-promoted electrocyclic ring opening.[88] Different conditions were screened, including Lewis acids, Brønsted acids and even some bases, as well as different solvents. To our excitement, we discovered that heating **2.149** in EtOH with $SnCl_4$ formed a major product as a single spot by TLC analysis. NMR analysis showed that this spot was indeed **2.38**, which had undergone the desired cascade of retro-oxa-6π-electrocyclisation, alkene isomerisation, and a final intra-molecular hetero-Diels–Alder reaction to afford (±)-7-demethylnaphterpin (**2.38**) (Scheme 2.49). Additionally, C-6 MOM deprotection was also achieved under these reaction conditions. However, the ^{1}H NMR spectrum also showed the presence of a minor impurity, thought to be the trans-fused ring system as a result of the final Diels-Alder reaction. Thankfully, recrystallisation of the orange solid with EtOAc gave pure (±)-7-demethylnaphterpin (**2.38**) in 39% yield. This was the first ever synthesis of this natural product, and the first member of the naphterpin family to be synthesised in literature.

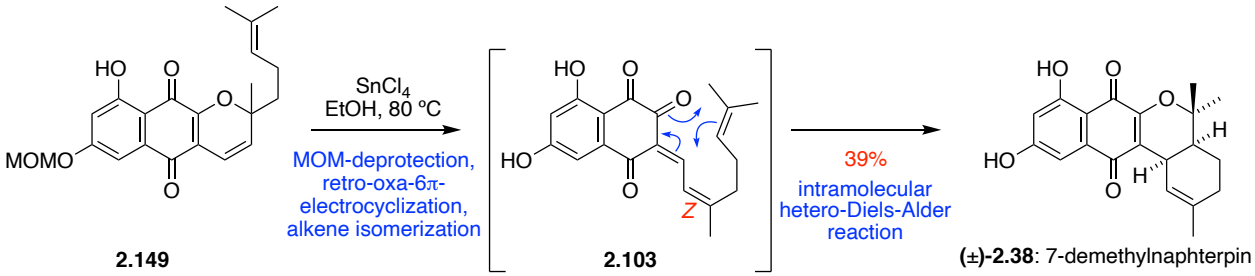

Scheme 2.49: Cascade of retro-oxa-6π-electrocyclisation, alkene isomerisation, and a final intra-molecular hetero-Diels–Alder reaction to afford (±)-7-demethylnaphterpin (**2.38**).

The ^{1}H and ^{13}C data of our synthetic 7-demethylnaphterpin (**2.38**) matched with the literature data for the natural product as shown in Table 2.01.

Table 2.01: ^{1}H and ^{13}C NMR data of natural[29] and synthetic 7-demethylnaphterpin (**2.38**) in $CDCl_3$.

Position	Natural **2.38**, ^{1}H NMR	Synthetic **2.38**, ^{1}H NMR, 500 MHz	Natural **2.38**, ^{13}C NMR	Synthetic **2.38**, ^{13}C NMR, 125 MHz
1			183.1	183.0
2			153.0	153.2
3			123.8	123.7
4			183.6	184.0
5	7.09	7.19 (d, *J* = 2.1 Hz, 1H)	108.3	108.6
6			162.9	163.4
7	6.53	6.56 (d, *J* = 2.1 Hz, 1H)	107.2	107.3
8			164.3	164.4
9			108.9	108.7
10			135.0	134.8
11	3.48	3.49 (m, 1H)	31.1	31.1
12	6.04	6.03 (d, *J* = 4.0 Hz, 1H)	120.0	119.9
13			136.1	136.2
14	1.95	1.95 (m, 2H)	29.7	29.7
15	1.95, 1.28	1.95 (m, 1H) 1.28 (m, 1H)	20.4	20.4
16	1.76	1.77 (ddd, *J* = 12.1, 6.1, 2.8 Hz, 1H),	39.7	39.7
17			80.6	80.8
18	1.55	1.55 (s, 3H),	25.7	25.6
19	1.33	1.34 (s, 3H),	25.0	25.0
20	1.66	1.67 (s, 3H)	23.5	23.6
OH-6	6.37	6.89 (s, 1H)		
OH-8	11.92	11.91 (s, 1H)		

2.2.3 Biomimetic Total Synthesis of Debromomarinone

Now that we had established the entire biomimetic synthesis of 7-demethylnaphterpin (**2.38**) with good reproducibility and in acceptable yields, we moved our focus to accessing the simplest member of the marinone family, debromomarinone (**2.46**). The key difference between these two natural products is the length of their terpene sidechain, with the naphterpins incorporating a geranyl subunit while the marinones integrate a farnesyl group. With this in mind, we proposed a synthesis analogous to 7-demethylnaphterpin, alkylating THN using farnesyl carbonate instead of geranyl carbonate.

The synthesis began utilising the same di-MOM-protected THN **2.83**. Applying our Pd-mediated C-4 alkylation with farnesyl carbonate **2.116** as the electrophile gave intermediate **2.115** in almost identical yields to that observed in the analogous geranylation reaction (Scheme 2.50). Wessely oxidation of **2.115** using $Pb(OAc)_4$ followed by dichlorination with NCS proceeded smoothly, giving dichlorinated intermediate **2.150** in slightly higher yields than that of the naphterpin system.

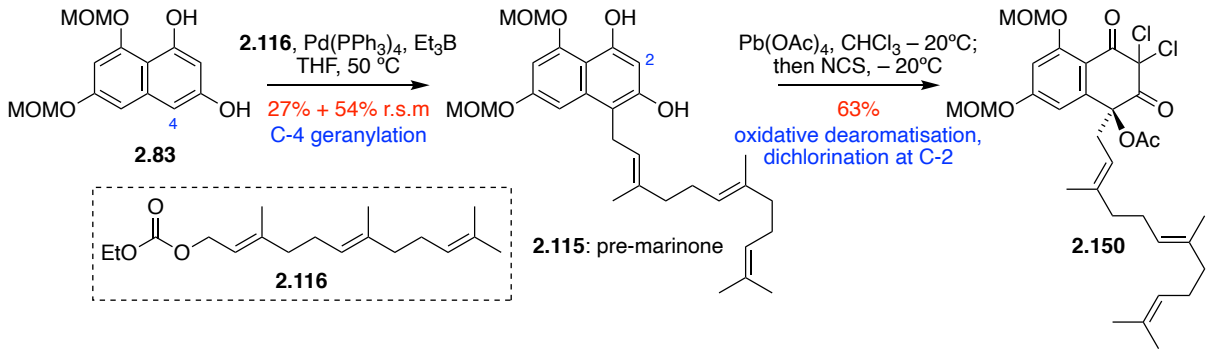

Scheme 2.50: Alkylation, oxidative dearomatisation and dichlorination.

Again, our 3-step procedure of LDA-mediated dechlorination, acetate hydrolysis and re-chlorination of geminal dichloride **2.150** gave tertiary alcohol **2.151** in good yields over 3 steps (Scheme 2.51). Applying our established α-hydroxyketone rearrangement conditions, heating **2.151** in toluene at reflux shifted the farnesyl side chain from the C-4 to the C-3 position to give **2.152** in 54% yield. To the best of our knowledge, this is the first report of a α-hydroxyketone rearrangement inducing the 1,2-shift of a farnesyl substituent, and the longest carbon chain to undergo this rearrangement to date.[21]

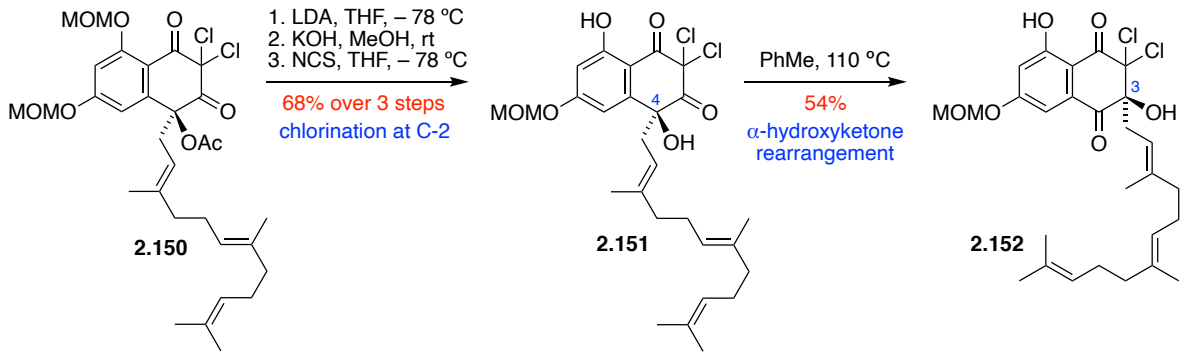

Scheme 2.51: Acetate hydrolysis and α-hydroxyketone rearrangement.

Treatment of **2.152** with Cs_2CO_3 formed the α-chloroepoxide **2.153**, which then underwent the desired reductive dehalogenation with Zn in MeOH to give **2.154** (Scheme 2.52).

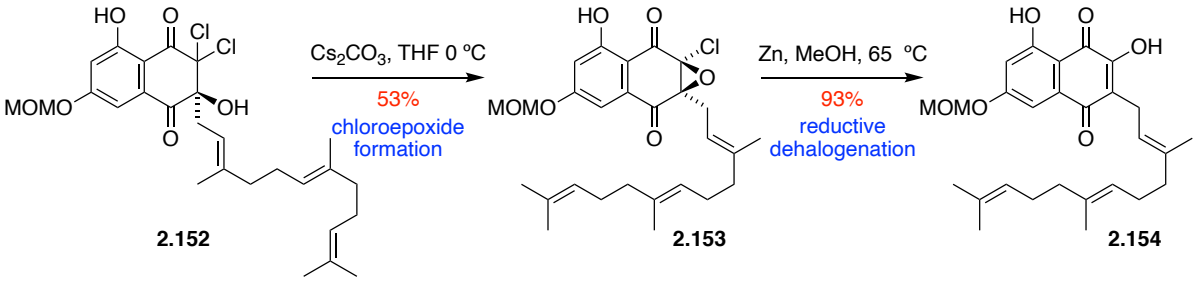

Scheme 2.52: α-Chloroepoxide formation and reductive dehalogenation.

Exposure of hydroxynaphthoquinone **2.154** to optimised oxidation conditions of TEMPO/$PhI(OAc)_2$ gave tricycle **2.155** through an oxa-6π-electrocyclisation (Scheme 2.53). Heating **2.155** in EtOH with $SnCl_4$ resulted in the same cascade of retro-oxa-6π-electrocyclisation, alkene isomerisation, and a final intramolecular hetero-Diels-Alder reaction to afford (±)-debromomarinone (**2.46**) in 16% yield. This final step was in lower yield than that observed in the naphterpin system, seemingly due to the instability of the exposed prenyl group of **2.155** in the presence of $SnCl_4$.

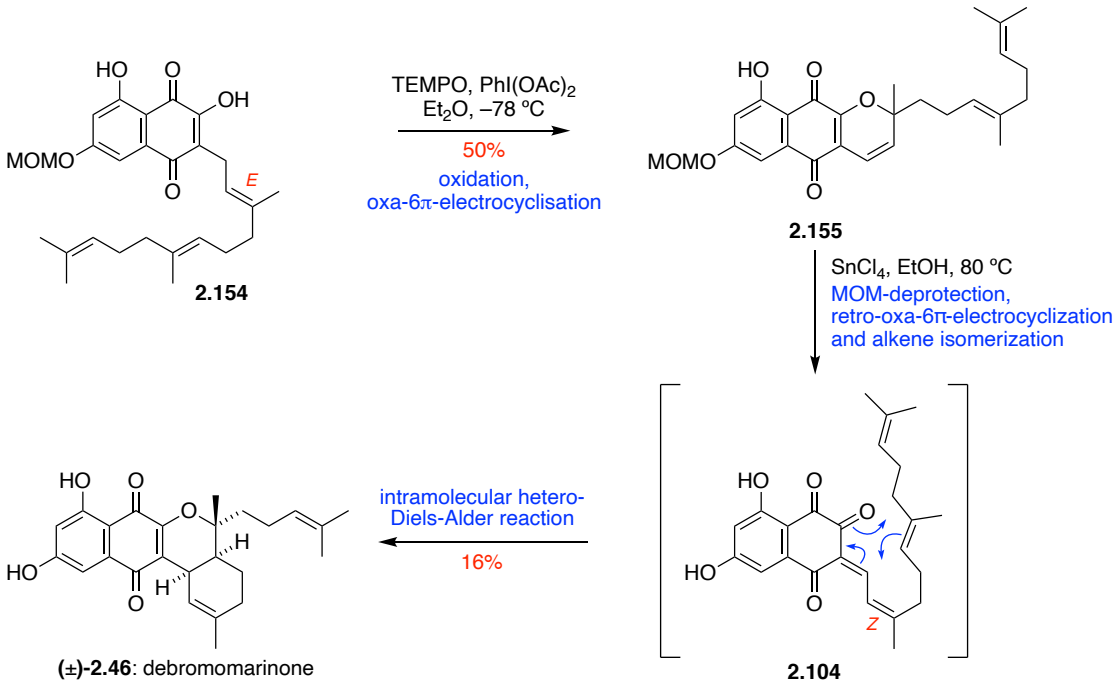

Scheme 2.53: Synthesis of (±)-debromomarinone (**2.46**).

Pleasingly, comparisons between ^{1}H and ^{13}C NMR for the synthetic and natural debromomarinone were found to be a match (Table 2.02). This was the first total synthesis of debromomarinone, and the first synthesis of a member from the marinone family.

Table 2.02: ^{1}H NMR and ^{13}C NMR data of natural[33,35] and synthetic debromomarinone (**2.46**) in CD_3OD.

Position	Natural **2.46**, ^{1}H NMR	Synthetic **2.46**, ^{1}H NMR, 500 MHz	Natural **2.46**, ^{13}C NMR	Synthetic **2.46**, ^{13}C NMR, 125 MHz
1			182.5	182.8
2			153.0	153.3
3			123.8	123.9
4			184.0	184.1
5	6.83 (d, *J* = 2.5 Hz)	6.96 (d, *J* = 2.4 Hz)	107.8	108.5
6			164.4	163.7
7	6.10 (d, *J* = 2.5 Hz)	6.42 (d, *J* = 2.4 Hz,)	106.9	107.3
8			165.1	164.5
9			109.0	108.9
10			134.5	134.7
11	3.39 (t, *J* = 5.0 Hz)	3.42 (t, *J* = 6.0 Hz)	30.7	30.9
12	6.03 (d, *J* = 5.0 Hz)	6.01 (d, *J* = 5.0 Hz)	119.9	119.9
13			135.9	136.2
14	2.00 m	2.00 m	29.6	29.7
15	1.31 (dt, *J* = 6.0, 12.0 Hz), 2.00 m	1.29 m 2.00 m	20.0	20.2
16	1.88 (ddd, *J* = 3.0, 6.0, 12.0 Hz)	1.90 (ddd, *J* = 3.0, 6.0, 12.0 Hz)	37.2	37.4
17			82.9	83.1
18	1.63 m	1.64 m	36.5	36.7
19	1.49 s	1.49 s	22.4	22.6
20	1.66 s	1.66 s	23.3	23.5
21	2.00 m	2.00 m	22.0	22.2
22	5.08 (t, *J* = 7.0)	5.07 (t, *J* = 7.2 Hz)	123.0	123.1
23			132.3	132.5
24	1.60 s	1.59 s	25.4	25.6
25	1.55 s	1.54 s	17.4	17.6

2.3 Conclusions

The first total syntheses of the naphterpin natural product 7-demethylnaphterpin (**2.38**) was achieved in 10 steps from our previously reported di-MOM protected THN compound (**2.83**) in 0.9% overall yield (Scheme 2.54). An analogous synthesis was used to complete the first total synthesis of the marinone natural product debromomarinone (**2.46**) in 0.2% overall yield.

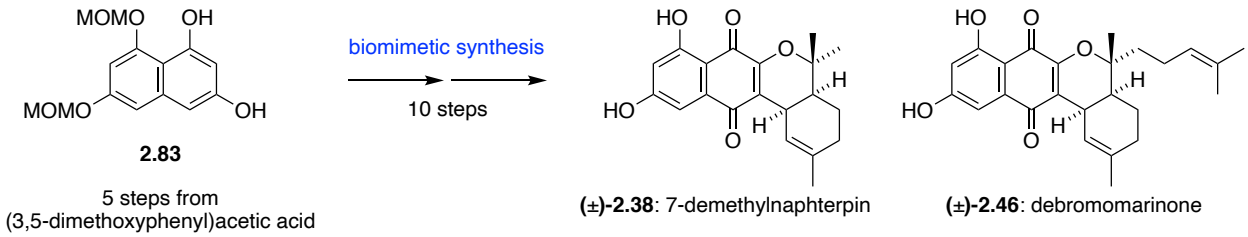

Scheme 2.54: Summary of the biomimetic total synthesis of 7-demethylnaphterpin (**2.38**) and debromomarinone (**2.46**).

Inspired by our biosynthetic proposals towards these two natural products, we were able to achieve an α-ketol rearrangement, involving the 1,2-shift of both a geranyl and farnesyl substituent. Thermal conditions of refluxing **2.124/2.151** in toluene were found to give the most consistent results, to give **2.125/2.152** (Scheme 2.55). The success of this key biomimetic synthetic step furnished a naphthoquinone skeleton containing the crucial substitution pattern that would ultimately lead to the synthesis of these natural products.

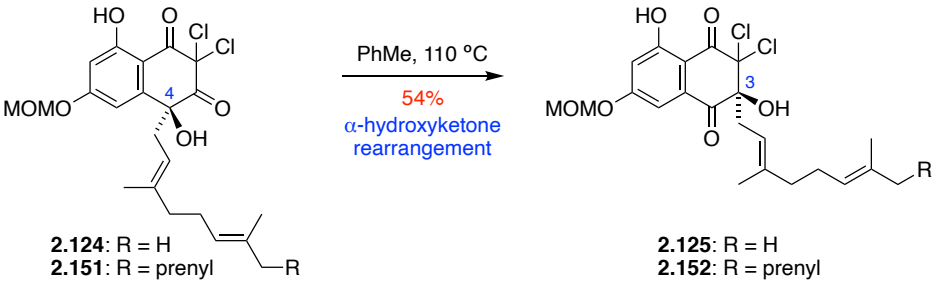

Scheme 2.55: Thermal α-ketol rearrangement of **2.124/2.151**.

Some difficulties were experienced in the oxidation and alkene isomerisation of our proposed hydroxynaphthoquinone intermediates **2.134**/**2.154**, as biosynthetically we propose this to be our penultimate intermediate. Despite extensive screening, oxidative conditions of $PhI(OAc)_2$ with TEMPO were found to promote the kinetically favoured oxa-6π-electrocyclisation to give the tricyclic intermediates **2.149**/**2.155** (Scheme 2.56). Although we were unable to directly overcome this issue, heating **2.149**/**2.155** with $SnCl_4$ in EtOH was able to promote the cascade of retro-oxa-6π-electrocyclisation, alkene isomerisation, and a final intramolecular hetero-Diels-Alder reaction to afford the natural products (±)-7-demethylnaphterpin (**2.38**) and (±)-debromomarinone (**2.46**).

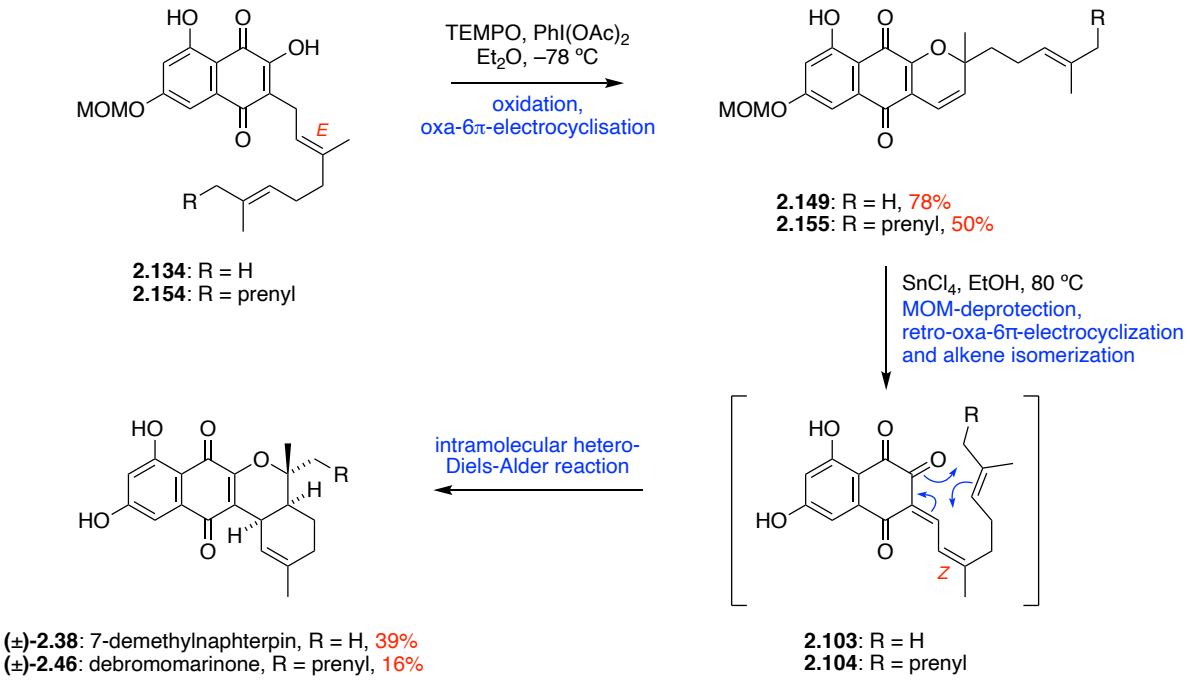

Scheme 2.56: Final synthetic steps in the formation of (±)-7-demethylnaphterpin (**2.38**) and (±)-debromomarinone (**2.46**).

More efficient strategies could be imagined for constructing these natural products. For example, a previous non-biomimetic synthesis of a protected form of **2.38** was achieved.[93] However, the value of this synthesis was not focussed towards the final destination, but in the journey, as each step of this synthesis represents a potential biosynthetic intermediate (after facile MOM deprotection). Having access to each of these potential biosynthetic intermediates opened up the possibility to

discover and characterise enzymes responsible for the biosynthesis of naphterpin and marinone natural products. This work will be discussed in detail in Chapter 3. Although we hope to explore the synthesis of more members from the naphterpin and marinone families of natural products, this biomimetic synthesis did not produce sufficient quantities of these natural products to screen further reaction conditions. As such, a more efficient synthesis to access these natural products would be required.

2.4 Supporting Information

2.4.1 General Methods

All chemicals used were purchased from commercial suppliers and used as received. All reactions were performed under an inert atmosphere of N_2. All organic extracts were dried over anhydrous magnesium sulfate. Thin layer chromatography was performed using aluminium sheets coated with silica gel F_{254}. Visualization was aided by viewing under a UV lamp and staining with ceric ammonium molybdate or $KMnO_4$ stain followed by heating. All R_f values were measured to the nearest 0.05. Flash column chromatography was performed using 40-63 micron grade silica gel. Melting points were recorded on a Reichart Thermovar Kofler microscope apparatus and are uncorrected. Infrared spectra were recorded using an FT-IR spectrometer as the neat compounds. High field NMR spectra were recorded using a 500 MHz spectrometer (^{1}H at 500 MHz, ^{13}C at 125 MHz) or a 600 MHz spectrometer (^{1}H at 600 MHz, ^{13}C at 150 MHz) as stated. Solvent used for spectra were $CDCl_3$ unless otherwise specified. ^{1}H chemical shifts are reported in ppm on the δ-scale relative to TMS (δ 0.0) and ^{13}C NMR are reported in ppm relative to $CDCl_3$ (δ 77.00). Multiplicities are reported as (br) broad, (s) singlet, (d) doublet, (t) triplet, (q) quartet, (quin) quintet, (sext) sextet, (hept) heptet and (m) multiplet. All *J*-values were rounded to the nearest 0.1 Hz. ESI high-resolution mass spectra were recorded on an ESI-TOF mass spectrometer.

2.4.2 Experimental Procedures

Synthesis of 7-demethylnaphterpin

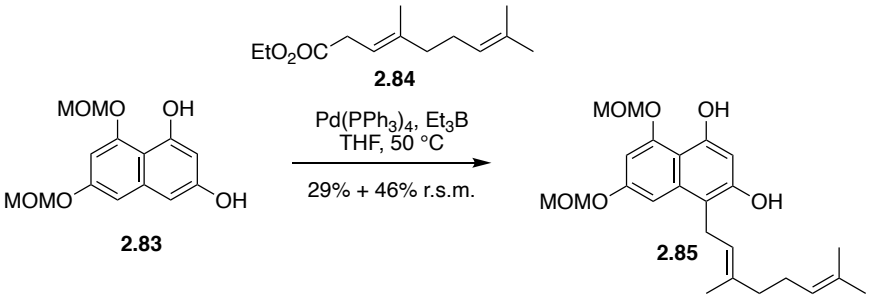

A solution of **2.83**[45] (7.50 g, 26.7 mmol), ethyl geranyl carbonate (**2.84**) (9.06 g, 40.0 mmol) and $Pd(PPh_3)_4$ (1.56 g, 1.35 mmol) in THF (100 mL) was degassed. Et_3B (1.0 M in THF, 40.0 mL, 40.0 mmol) was then added and the resultant mixture was stirred at 50 °C for 2 h. The mixture was cooled, quenched with *sat*. NH_4Cl solution (100 mL) and extracted with Et_2O (2 x 100 mL). The combined organic layers were washed with brine (100 mL) dried over anhydrous $MgSO_4$, filtered and concentrated *in vacuo*. The residue was purified by flash chromatography (petrol/EtOAc 5:1 → 3:1) to yield **2.85** (3.28 g, 29%) as a brown gum along with recovered starting material (3.46 g, 46%).

Data for 2.85:

R_f = 0.20 (3:1, petrol/EtOAc)

IR (neat): 3378, 2915, 1622, 1602, 1378, 1287, 1138, 1019, 990, 909, 816 cm^{-1}

^{1}H-NMR (500 MHz, $CDCl_3$): δ 9.24 (s, 1H), 7.08 (d, *J* = 2.1 Hz, 1H), 6.71 (d, *J* = 2.1 Hz, 1H), 6.40 (s, 1H), 5.41 (s, 2H), 5.25 (s, 2H), 5.21 (t, *J* = 6.7 Hz, 1H), 5.06 (t, *J* = 6.8 Hz, 1H), 3.59 (d, J = 6.6 Hz, 1H), 3.58 (s, 3H), 3.52 (s, 3H), 2.13 – 1.99 (m, 4H), 1.88 (s, 3H), 1.66 (s, 3H), 1.58 (s, 3H).

^{13}C-NMR (125 MHz, $CDCl_3$): δ 155.6, 155.3, 154.0, 153.3, 137.1, 136.7, 131.7, 124.0, 122.6, 109.7, 107.4, 101.1, 100.5, 98.8, 95.8, 94.6, 56.9, 56.1, 39.7, 26.6, 25.6, 24.5, 17.7, 16.3.

HRMS (ESI): calculated for $C_{24}H_{33}O_6$ 417.2277 $[M+H]^+$, found 417.2268.

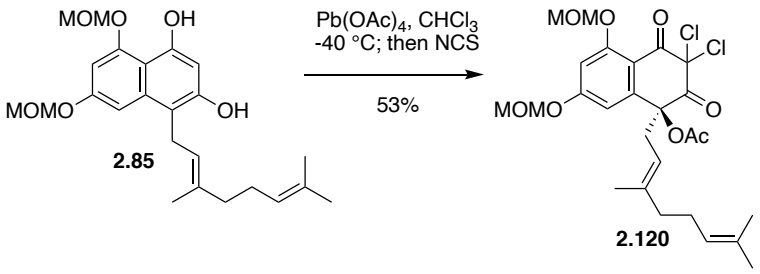

To a solution of **2.85** (234 mg, 0.576 mmol) in $CHCl_3$ (8 mL) at −40 °C was added $Pb(OAc)_4$ (268 mg, 0.604 mmol) in small portions. The mixture was stirred at −40 °C for 5 min before NCS (147 mg, 1.04 mmol) was added portion wise. The mixture was stirred at −40 °C for a further 20 min before $Na_2S_2O_3$ (20 mg) was added. The mixture was warmed to rt, filtered through a short pad of SiO_2 and concentrated *in vacuo*. The residue was purified by flash chromatography (petrol/EtOAc 5:1) to yield **2.120** (166 mg, 53%) as a yellow oil.

Data for 2.120:

R_f = 0.20 (3:1, petrol/EtOAc)

IR (neat): 2917, 1753, 1719, 1599, 1324, 1225, 1147, 1019, 972, 924 cm^{-1}

^{1}H-NMR (500 MHz, $CDCl_3$): δ 6.90 (d, *J* = 2.2 Hz, 1H), 6.72 (d, *J* = 2.2 Hz, 1H), 5.30 (d, *J* = 6.8 Hz, 1H), 5.28 (d, *J* = 6.8 Hz, 1H), 5.23 (d, *J* = 7.0 Hz, 1H), 5.20 (d, *J* = 7.0 Hz, 1H), 5.02 (t, *J* = 6.8 Hz, 1H), 4.92 (t, *J* = 7.3 Hz, 1H), 3.53 (s, 3H), 3.48 (s, 3H), 2.96 (dd, *J* = 14.2, 8.0 Hz, 1H), 2.73 (dd, *J* = 14.3, 7.4 Hz, 1H), 2.14 (s, 3H), 2.04 – 1.90 (m, 4H), 1.66 (s, 3H), 1.58 (s, 3H), 1.41 (s, 3H).

^{13}C-NMR (125 MHz, $CDCl_3$): δ 190.7, 178.5, 169.2, 162.8, 159.8, 143.4, 141.9, 131.7, 123.8, 113.7, 113.6, 105.4, 104.0, 94.9, 94.4, 82.1, 81.4, 56.7, 56.6, 40.4, 39.8, 26.0, 25.7, 20.4, 17.6, 16.3.

HRMS (ESI): calculated for $C_{26}H_{33}Cl_2O_8$ 543.1552 $[M+H]^+$, found 543.1554

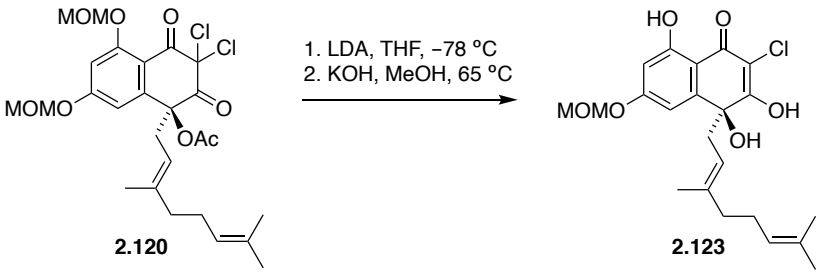

2.120 **2.123**

To a solution of **2.120** (2.35 g, 4.32 mmol) in THF (70 mL), was added LDA (2.0 M in THF, 6.49 mL, 13.0 mmol) at −78 ºC. The mixture was stirred at −78 ºC for 30 min. The mixture was quenched with 0.5 M HCl (80 mL) and extracted with EtOAc (3 × 50 mL). The combined organic extracts were washed with brine (100 mL), dried over $MgSO_4$, filtered and concentrated *in vacuo*. The resultant yellow oil was dissolved in MeOH (60 mL), and KOH (970 mg, 17.3 mmol) was added at rt. The mixture was heated at reflux for 2 h before cooling to rt. 1 M HCl (80 mL) was added and the mixture was stirred at rt for 10 min before extracting with EtOAc (3 × 60 mL). The combined organic extracts were washed with brine (150 mL), dried over $MgSO_4$, filtered and concentrated *in vacuo* to give **2.123** as a brown oil which was used in the next step without further purification.

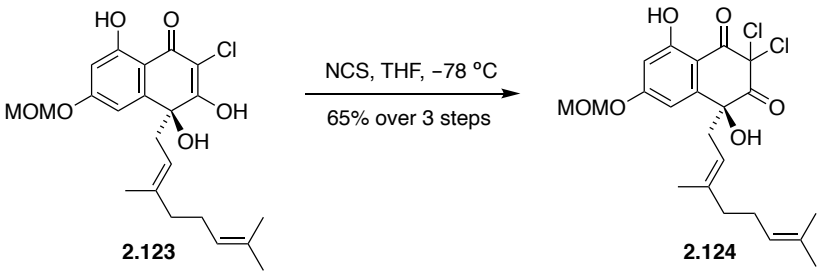

To a solution of **2.123** (crude from previous step, <4.32 mmol) in THF (50 mL) was added NCS (519 mg, 3.89 mmol) at −78 ºC. The reaction mixture was stirred at −78 ºC for 25 min. The mixture was warmed to rt, quenched with $Na_2S_2O_3$ (50 mg), filtered through celite and concentrated *in vacuo*. The residue was purified by flash chromatography on SiO_2 (7:1, petrol/EtOAc) to give **2.124** (1.29 g, 65% over 3 steps) as an orange oil.

Data for 2.124:

R_f = 0.35 (4:1, petrol/EtOAc)

IR (neat): 3478, 2969, 2916, 1747, 1619, 1571, 1444, 1375, 1289, 1253, 1148 cm^{-1}.

^{1}H NMR (500 MHz, $CDCl_3$): δ 11.61 (s, 1H), 6.94 (d, *J* = 2.4 Hz, 1H), 6.65 (d, *J* = 2.4 Hz, 1H), 5.27 (d, *J* = 6.8 Hz, 1H), 5.24 (d, *J* = 6.8 Hz, 1H), 5.05 (t, *J* = 6.6 Hz, 1H), 4.99 (t, *J* = 7.1 Hz, 1H), 3.84 (s, 1H), 3.48 (s, 3H), 2.71 (dd, *J* = 14.6, 8.8 Hz, 1H), 2.62 (dd, *J* = 14.6, 6.2 Hz, 1H), 2.10 – 1.99 (m, 4H), 1.70 (s, 3H), 1.59 (s, 3H), 1.50 (s, 3H).

^{13}C NMR (125 MHz, $CDCl_3$): δ 193.9, 186.3, 166.3, 166.1, 145.0, 143.3, 131.9, 123.7, 115.0, 107.3, 105.8, 103.1, 94.1, 79.5, 77.8, 56.6, 45.4, 39.7, 26.1, 25.6, 17.6, 16.4.

HRMS (ESI): calculated for $C_{22}H_{27}Cl_2O_6$ 457.1185 $[M+H]^+$, found 457.1170.

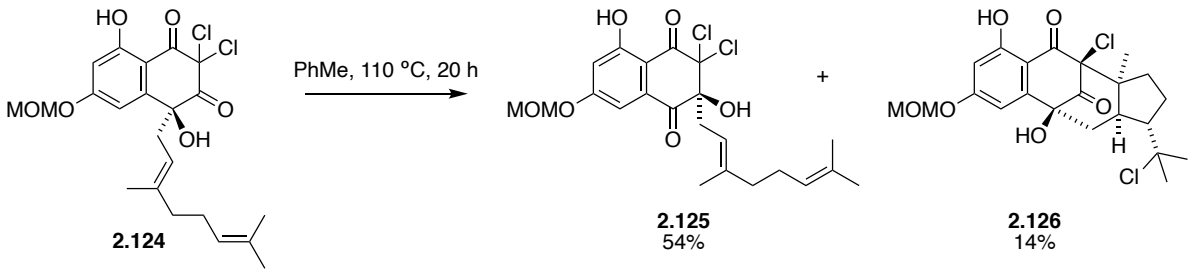

A solution of **2.124** (1.50 g, 3.28 mmol) in PhMe (150 mL) was stirred at 110 ºC for 20 h. The mixture was cooled to rt and concentrated *in vacuo*. The residue was purified by flash chromatography on SiO_2 (4:1, petrol/EtOAc) to give **2.125** (802 mg, 54%) as a yellow oil.

Data for 2.125:

R_f = 0.55 (3:2, petrol/EtOAc)

IR (neat): 3478, 2969, 2916, 1748, 1619, 1571, 1487, 1375, 1289, 1253, 1148 cm^{-1}.

^{1}H NMR (500 MHz, $CDCl_3$): δ 11.43 (s, 1H), 7.17 (d, *J* = 2.4 Hz, 1H), 6.94 (d, *J* = 2.4 Hz, 1H), 5.29 (d, *J* = 7.0 Hz, 1H), 5.26 (d, *J* = 7.0 Hz, 1H), 5.00 (t, *J* = 6.7 Hz, 1H), 4.88 (t, *J* = 7.9 Hz, 1H), 4.43 (s, 1H), 3.49 (s, 3H), 2.80 (dd, *J* = 14.6, 6.5 Hz, 1H), 2.35 (dd, *J* = 14.2, 9.1 Hz, 1H), 2.00 – 1.85 (m, 4H), 1.70 (s, 3H), 1.58 (s, 3H), 1.21 (s, 3H).

^{13}C NMR (125 MHz, $CDCl_3$): δ 193.7, 187.1, 165.5, 164.6, 141.4, 133.3, 131.8, 123.6, 115.0, 109.6, 109.1, 108.0, 94.3, 90.4, 85.7, 56.7, 39.7, 36.3, 26.2, 25.6, 17.7, 16.0.

HRMS (ESI): calculated for $C_{22}H_{27}Cl_2O_6$ 457.1185 $[M+H]^+$, found 457.1176.

Further elution gave **2.126** (210 mg, 14%) as a white solid.

Data for 2.126:

R_f = 0.15 (3:2, petrol/EtOAc)

Mp = 159 – 160 °C

IR (neat): 3477, 2968, 1746, 1616, 1573, 1385, 1280, 1218, 1146, 1069, 1004 cm^{-1}

^{1}H NMR (500 MHz, $CDCl_3$): δ 11.96 (s, 1H), 6.92 (d, *J* = 2.3 Hz, 1H), 6.67 (d, *J* = 2.3 Hz, 1H), 5.28 (d, *J* = 6.8 Hz, 1H), 5.26 (t, *J* = 6.8 Hz, 1H), 3.95 (s, 1H), 3.50 (s, 3H), 2.62 (dd, *J* = 13.8, 6.8 Hz, 1H), 2.13 (td, *J* = 9.6, 3.2 Hz, 1H), 2.04 (dd, *J* = 13.8, 12.3 Hz, 1H), 1.96 – 1.82 (m, 2H), 1.82 – 1.68 (m, 2H), 1.68 – 1.60 (m, 1H), 1.46 (s, 3H), 1.44 (s, 3H), 1.18 (s, 3H).

^{13}C NMR (125 MHz, $CDCl_3$): δ 200.2, 191.6, 165.4, 164.5, 146.0, 109.3, 105.5, 103.5, 94.2, 89.2, 77.6, 71.8, 61.7, 58.8, 56.7, 52.6, 43.4, 35.2, 32.3, 30.1, 25.9, 23.6.

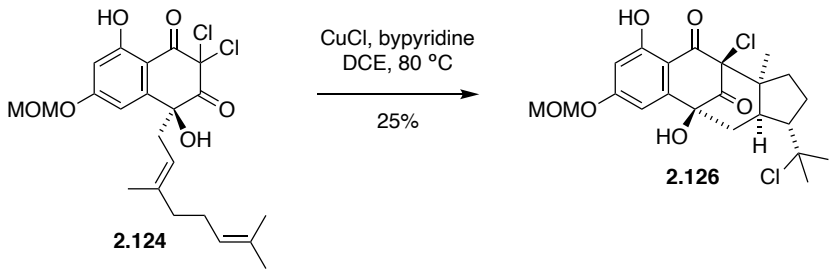

To a solution of **2.124** (92 mg, 0.20 mmol) in DCE (5 mL) was added CuCl (6 mg, 0.06 mmol) and bipyridine (9 mg, 0.06 mmol) at rt. The reaction was stirred at 80 ºC for 17 h. The mixture was cooled to rt, diluted with H_2O (20 mL) and extracted with EtOAc (3 × 15 mL). The combined organic extracts were washed with brine (20 mL), dried over $MgSO_4$, filtered and concentrated *in vacuo*. The residue was purified by flash chromatography on SiO_2 (4:1, petrol/EtOAc) to give **2.126** (23 mg, 25%) as a white solid.

Data for 2.126 matches that reported above.

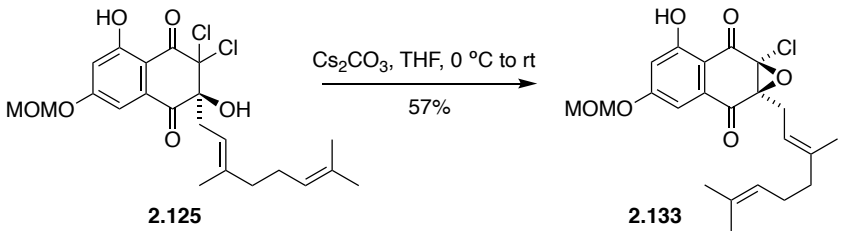

2.125 **2.133**

To a solution of **2.125** (532 mg, 1.16 mmol) in THF (40 mL) was added Cs_2CO_3 (1.14 g, 3.49 mmol) at 0 ºC. The reaction was stirred at 0 ºC for 1 h. The mixture was then warmed to rt and stirred for a further 1.5 h. The mixture was quenched with saturated NH_4Cl solution (50 mL) and extracted with EtOAc (2 × 30 mL). The combined organic extracts were dried over $MgSO_4$, filtered and concentrated *in vacuo*. The residue was purified by flash chromatography on SiO_2 (4:1, petrol/EtOAc) to give **2.133** (277 mg, 57%) as a yellow oil.

Data for 2.133:

R_f = 0.50 (3:2, petrol/EtOAc)

IR (neat): 3108, 2967, 2923, 1699, 1664, 1609, 1488, 1380, 1280, 1146 cm^{-1}

^{1}H NMR (500 MHz, $CDCl_3$): δ 11.47 (s, 1H), 7.25 (d, *J* = 2.5 Hz, 1H), 6.88 (d, *J* = 2.5 Hz, 1H), 5.26 (d, *J* = 6.9 Hz, 1H), 5.24 (d, *J* = 6.9 Hz, 1H), 5.19 (t, *J* = 6.7 Hz, 1H), 5.03 (t, *J* = 6.9 Hz, 1H), 3.47 (s, 3H), 3.36 (dd, *J* = 14.6, 7.7 Hz, 1H), 2.67 (dd, *J* = 14.6, 6.8 Hz, 1H), 2.10 – 1.99 (m, 4H), 1.78 (s, 3H), 1.62 (s, 3H), 1.57 (s, 3H).

^{13}C NMR (125 MHz, $CDCl_3$): δ 187.33, 187.32, 164.9, 164.9, 164.4, 140.5, 133.5, 131.5, 123.9, 115.1, 109.9, 109.3, 107.9, 94.2, 80.9, 67.8, 56.6, 39.8, 26.4, 26.0, 25.6, 17.6, 16.6.

HRMS (ESI): calculated for $C_{22}H_{24}ClO_6$ 419.1261 $[M-H]^-$, found 419.1273.

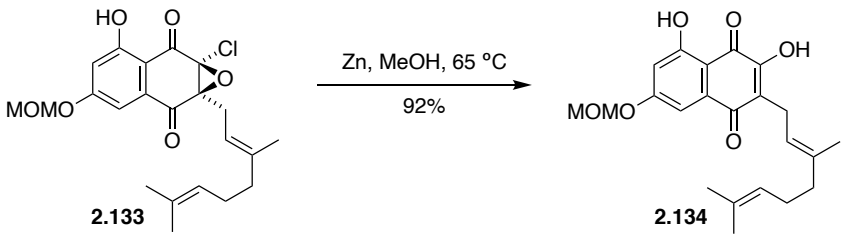

To a solution of **2.133** (560 mg, 1.33 mmol) in MeOH (50 mL) was added Zn powder (174 mg, 2.66 mmol) at rt. The reaction was stirred at 65 ºC for 15 min. The mixture was cooled to rt, quenched with saturated NH_4Cl solution (40 mL) and stirred for a further 10 min before extraction with EtOAc (3 × 30 mL). The combined organic extracts were washed sequentially with saturated NH_4Cl solution (50 mL) and brine (50 mL), dried over $MgSO_4$, filtered and concentrated *in vacuo*. The residue was purified by flash chromatography on SiO_2 (4:1 → 1:1, petrol/EtOAc gradient elution) to give **2.134** (474 mg, 92%) as an orange solid.

Data for 2.134:

R_f = 0.75 (2:1, petrol/EtOAc)

Mp = 114 - 116 °C

IR (neat): 3364, 2923, 1645, 1621, 1605, 1487, 1313, 1237, 1146 cm^{-1}

^{1}H NMR (500 MHz, $CDCl_3$): δ 11.21 (s, 1H), 7.30 (d, *J* = 2.4 Hz, 1H), 6.75 (d, *J* = 2.3 Hz, 1H), 5.26 (s, 2H), 5.17 (t, *J* = 7.0 Hz, 1H), 5.05 (t, *J* = 6.8 Hz, 1H), 3.48 (s, 3H), 3.27 (d, *J* = 7.3 Hz, 2H), 2.09 – 1.93 (m, 4H), 1.77 (s, 3H), 1.63 (s, 3H), 1.57 (s, 3H).

^{13}C NMR (125 MHz, $CDCl_3$): δ 183.3, 182.9, 164.7, 163.7, 152.7, 137.3, 134.5, 131.4, 124.2, 123.8, 119.3, 110.0, 108.0, 107.1, 94.1, 56.6, 39.7, 26.6, 25.6, 22.5, 17.6, 16.2.

HRMS (ESI): calculated for $C_{22}H_{27}O_6$ 387.1808 $[M+H]^+$, found 387.1795.

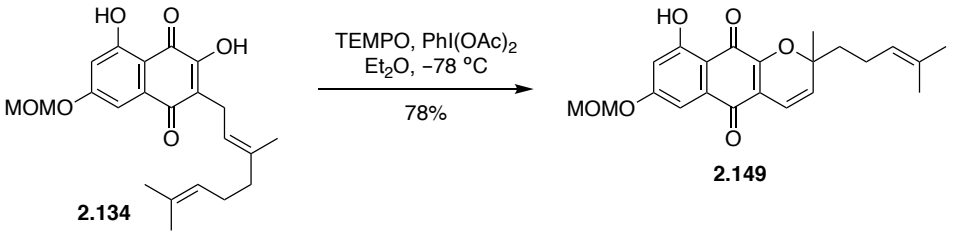

To a solution of **2.134** (452 mg, 1.17 mmol) in Et_2O (40 mL) was added $PhI(OAc)_2$ (416 mg, 1.29 mmol) and TEMPO (219 mg, 1.40 mmol) at −78 ºC. The reaction was stirred at −78 ºC for 1 h. The mixture was then warmed to rt and stirred overnight. The mixture was filtered through SiO_2, washing with Et_2O and concentrated *in vacuo*. The residue was purified by flash chromatography on SiO_2 (9:1, petrol/EtOAc) to give **2.149** (353 mg, 78%) as a red oil.

Data for 2.149:

R_f = 0.50 (4:1, petrol/EtOAc)

IR (neat): 3363, 2970, 2925, 1646, 1621, 1573, 1487, 1387, 1378, 1315, 1237, 1147 cm^{-1}

^{1}H NMR (500 MHz, $CDCl_3$): δ 12.06 (s, 1H), 7.26 (d, *J* = 2.5 Hz, 1H), 6.76 (d, *J* = 2.4 Hz, 1H), 6.65 (d, *J* = 10.1 Hz, 1H), 5.64 (d, *J* = 10.1 Hz, 1H), 5.26 (s, 2H), 5.09 (t, *J* = 7.1 Hz, 1H), 3.49 (s, 3H), 2.19 – 2.05 (m, 2H), 1.95 (ddd, *J* = 14.3, 10.0, 6.5 Hz, 1H), 1.69 (ddd, *J* = 14.2, 10.3, 5.7 Hz, 1H), 1.63 (s, 3H), 1.56 (s, 3H), 1.52 (s, 3H).

^{13}C NMR (125 MHz, $CDCl_3$): δ 182.8, 180.6, 164.1, 163.8, 153.0, 133.3, 132.3, 129.4, 123.3, 117.6, 115.9, 109.7, 109.1, 107.8, 94.1, 83.4, 56.5, 41.6, 27.5, 25.6, 22.6, 17.7.

HRMS (ESI): calculated for $C_{22}H_{25}O_6$ 385.1651 $[M+H]^+$, found 385.1643.

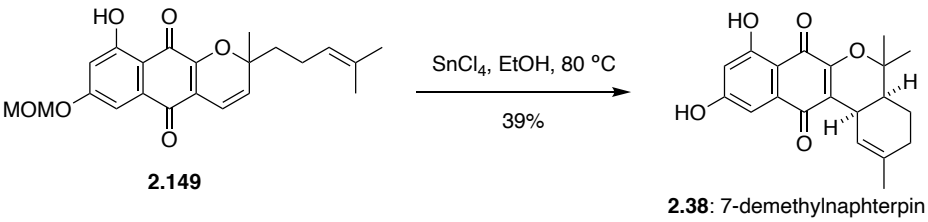

To a solution of **2.149** (20 mg, 0.059 mmol) in EtOH was added $SnCl_4$ (3 drops) at rt. The reaction was stirred at 80 ºC for 1.5 h. The mixture was cooled to rt, quenched with 1 M HCl solution (5 mL) and extracted with CH_2Cl_2 (2 × 10 mL). The combined organic extracts were dried over $MgSO_4$, filtered and concentrated *in vacuo*. The residue was purified by flash chromatography on SiO_2 (4:1, petrol/EtOAc) to give a 4:1 mixture of 7-demethylnaphterpin **2.38** to an unknown impurity (16 mg, 77%). Recrystallisation from EtOAc gave 7-demethylnaphterpin **2.38** (8 mg, 39% overall yield) as an orange solid.

Data for 2.38:

R_f = 0.60 (1:1, petrol/EtOAc)

Mp = 255 - 257 ºC

IR (neat): 3344, 2921, 1625, 1600, 1572, 1458, 1335, 1285, 1220, 1159, 1126 cm^{-1}

^{1}H NMR (500 MHz, $CDCl_3$): δ 11.91 (s, 1H), 7.19 (d, *J* = 2.1 Hz, 1H), 6.89 (s, 1H), 6.56 (d, *J* = 2.1 Hz, 1H), 6.03 (d, *J* = 4.0 Hz, 1H), 3.49 (s, 1H), 2.02 – 1.95 (m, 2H), 1.93 (m, 1H), 1.77 (ddd, *J* = 12.1, 6.1, 2.8 Hz, 1H), 1.67 (s, 3H), 1.55 (s, 3H), 1.34 (s, 3H), 1.33 – 1.28 (m, 1H).

^{13}C NMR (125 MHz, $CDCl_3$): δ 184.0, 183.0, 164.4, 163.4, 153.2, 136.2, 134.8, 123.7, 119.9, 108.7, 108.6, 107.3, 80.8, 39.7, 31.1, 29.7, 25.6, 25.0, 23.6, 20.4.

HRMS (ESI): calculated for $C_{20}H_{19}O_5$ 339.1232 $[M-H]^-$, found 339.1238.

Synthesis of debromomarinone

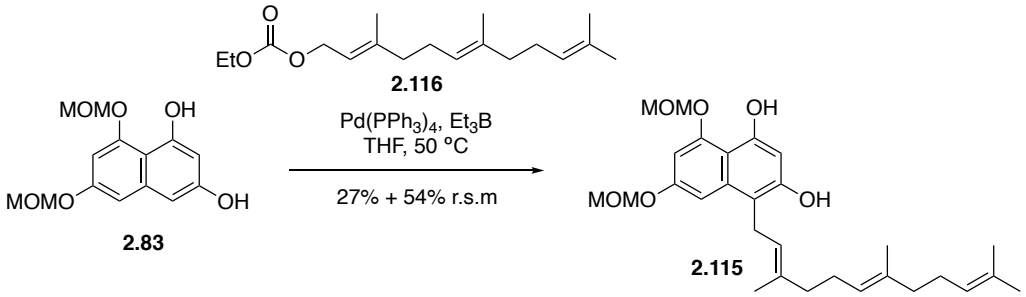

A solution of **2.83** (12.0 g, 42.8 mmol), ethyl farnesyl carbonate **2.116** (12.7 g, 42.8 mmol) and $Pd(PPh_3)_4$ (2.48 g, 2.15 mmol) in THF (125 mL) was degassed. Et_3B (1.0 M in THF, 65.0 mL, 65.0 mmol) was then added at the resultant mixture was stirred at 50 ºC for 2 h. The mixture was cooled, quenched with *sat.* NH_4Cl solution (150 mL) and extracted with Et_2O (2 x 100). The combined organics were washed with brine (200 mL) dried over anhydrous $MgSO_4$, filtered and concentrated *in vacuo*. The residue was purified by flash chromatography on SiO_2 (petrol/EtOAc, 5:1 $\rightarrow$ 3:1 gradient elution) to give **2.115** (5.64 g, 27%) as brown oil along with recovered starting material **2.83** (6.49 g, 54%).

Data for 2.115:

R_f = 0.25 (3:1, petrol/EtOAc)

IR (neat): 3373, 2913, 1623, 1378, 1287, 1138, 1022, 910, 832 cm^{-1}.

^{1}H NMR (500 MHz, $CDCl_3$): δ 9.30 (s, 1H), 7.09 (d, *J* = 2.1 Hz, 1H), 6.71 (d, *J* = 2.1 Hz, 1H), 6.45 (s, 1H), 6.08 (s, 1H), 5.40 (s, 2H), 5.27 (s, 2H), 5.23 (t, *J* = 6.1 Hz, 1H), 5.11 (t, *J* = 6.6 Hz, 1H), 5.09 (t, *J* = 7.0 Hz, 1H), 3.61 (d, *J* = 6.8 Hz, 2H), 3.57 (s, 3H), 3.54 (s, 3H), 2.14 – 1.94 (m, 8H), 1.90 (s, 3H), 1.69 (s, 3H), 1.61 (s, 3H), 1.59 (s, 3H).

^{13}C NMR (125 MHz, $CDCl_3$): δ 155.5, 155.2, 153.7, 153.1, 136.8, 136.0, 135.0, 131.1, 124.4, 124.1, 123.1, 110.4, 107.2, 101.2, 100.5, 98.7, 95.7, 94.5, 56.8, 56.1, 39.7, 39.7, 26.7, 26.6, 25.7, 24.3, 17.6, 16.3, 16.0.

HRMS (ESI): calculated for $C_{29}H_{40}O_6Na$ 507.2717 $[M+Na]^+$, found 507.2721.

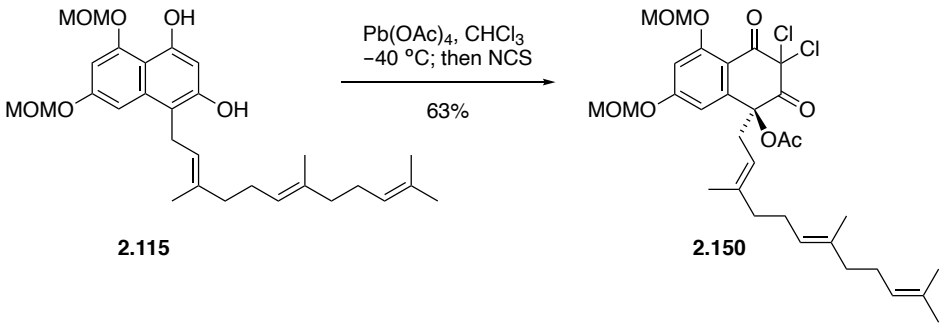

2.115 **2.150**

To a solution of **2.115** (11.0 g, 22.7 mmol) in $CHCl_3$ (150 mL) was addded $Pb(OAc)_4$ (10.6 g, 23.8 mmol) portion wise at – 20 ºC. The mixture was stirred at – 20 ºC for 5 min before NCS (5.76 g, 43.4 mmol) was added portion wise at – 20 ºC. The mixture was stirred at – 20 ºC for a further 20 min before $Na_2S_2O_3$ (100 mg) was added. The mixture was warmed to rt, filtered through a short pad of SiO2 and concentrated *in \vacuo*. The residue was purified by flash chromatography on SiO_2 (4:1, petrol/EtOAc) to give **2.150** as a yellow oil (8.70 g, 63%).

Data for 2.150:

R_f = 0.20 (3:1, petrol/EtOAc)

IR (neat): 2915, 1753, 1719, 1600, 1324, 1225, 1147, 1019, 973 cm^{-1}.

^{1}H NMR (500 MHz, $CDCl_3$): δ 6.90 (d, *J* = 2.4 Hz, 1H), 6.72 (d, *J* = 2.4 Hz, 1H), 5.30 (d, *J* = 6.8 Hz, 1H), 5.28 (d, *J* = 6.9 Hz, 1H), 5.23 (d, *J* = 7.0 Hz, 1H), 5.20 (d, *J* = 7.0 Hz, 1H), 5.07 (t, *J* = 6.1 Hz, 1H), 5.05 (t, *J* = 6.9 Hz, 1H), 4.92 (t, *J* = 7.8 Hz, 1H), 3.53 (s, 3H), 3.48 (s, 3H), 2.96 (dd, *J* = 14.2, 8.1 Hz, 1H), 2.72 (dd, *J* = 14.3, 7.4 Hz, 1H), 2.14 (s, 3H), 2.08 – 1.89 (m, 8H), 1.67 (s, 3H), 1.59 (s, 3H), 1.57 (s, 3H), 1.41 (s, 3H).

^{13}C NMR (125 MHz, $CDCl_3$): δ 190.9, 178.6, 169.3, 162.9, 159.9, 143.6, 142.1, 135.5, 131.5, 124.5, 123.9, 113.8, 113.8, 105.5, 104.2, 95.1, 94.5, 82.3, 81.6, 56.8, 56.7, 40.5, 40.0, 39.8, 26.9, 26.2, 25.8, 20.6, 17.8, 16.5, 16.1.

HRMS (ESI): calculated for $C_{31}H_{40}Cl_2O_8Na$ 633.1992 $[M+Na]^+$, found 633.1987.

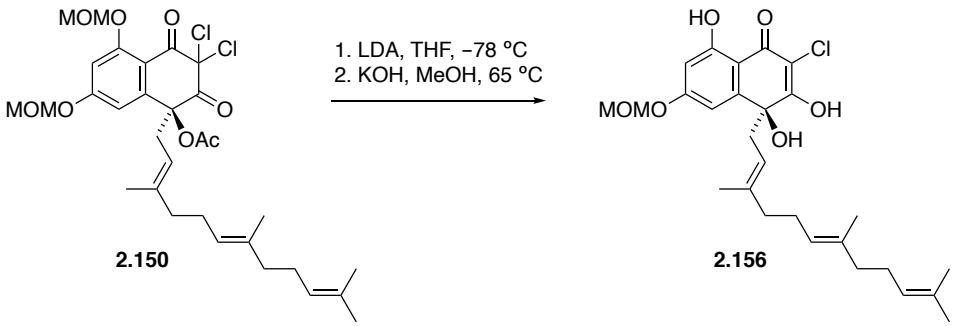

To a solution of **2.150** (11.2 g, 18.3 mmol) in THF (150 mL), was added LDA (2.0 M in THF, 27.5 mL, 54.9 mmol) at −78 ºC. The mixture was stirred at −78 ºC for 30 min. The mixture was quenched with 1 M HCl (150 mL) and extracted with EtOAc (3 × 100 mL). The combined organic extracts were washed with brine (300 mL), dried over $MgSO_4$, filtered and concentrated *in vacuo*. The resultant yellow oil was dissolved in MeOH (150 mL), and KOH (4.11 g, 73.2 mmol) was added at rt. The mixture was heated at reflux for 2 h before cooling to rt. 1 M HCl (150 mL) was added and the mixture was stirred at rt for 10 min before extracting with EtOAc (3 × 100 mL). The combined organic extracts were washed with brine (300 mL), dried over $MgSO_4$, filtered and concentrated *in vacuo* to give **2.156** as a brown oil which was used in the next step without further purification.

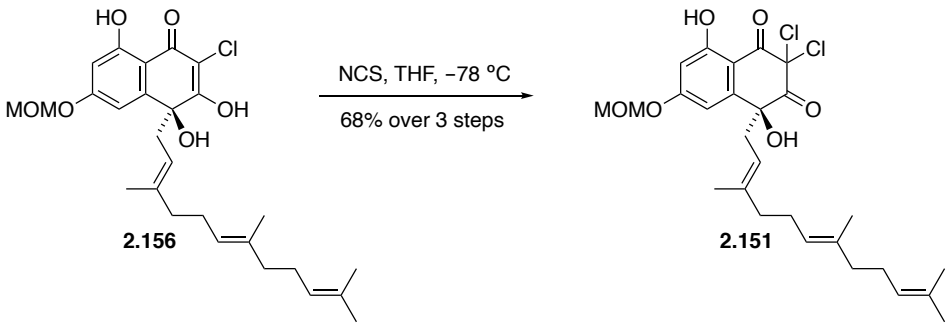

To a solution of **2.156** (crude from previous step, <18.3 mmol) in THF (100 mL) at −78 ºC was added NCS (2.44 mg, 18.3 mmol). The reaction mixture was stirred at −78 ºC for 25 min. The mixture was warmed to rt, quenched with $Na_2S_2O_3$ (100 mg), filtered through celite and concentrated *in vacuo*. The residue was purified by flash chromatography on SiO_2 (8:1, petrol/EtOAc) to give **2.151** as an orange oil (6.50 g, 68% over 3 steps).

Data for 2.151:

R_f = 0.40 (3:1, petrol/EtOAc)

IR (neat): 3388, 2923, 1748, 1622, 1452, 1105, 1163, 857, 732 cm^{-1}.

^{1}H NMR (500 MHz, $CDCl_3$): δ 11.62 (s, 1H), 6.95 (d, *J* = 2.4 Hz, 1H), 6.67 (d, *J* = 2.4 Hz, 1H), 5.28 (d, *J* = 6.8 Hz, 1H), 5.25 (d, *J* = 6.8 Hz, 1H), 5.09 (t, *J* = 6.6 Hz, 1H), 5.08 (t, *J* = 6.8 Hz, 2H), 5.01 (t, *J* = 7.5 Hz, 2H), 3.77 (s, 1H), 3.49 (s, 3H), 2.73 (dd, *J* = 14.7, 8.8 Hz, 1H), 2.63 (dd, *J* = 14.6, 6.2 Hz, 1H), 2.11 – 1.98 (m, 8H), 1.68 (s, 3H), 1.61 (s, 6H), 1.52 (s, 3H).

^{13}C NMR (125 MHz, $CDCl_3$): δ 194.2, 186.6, 166.5, 166.4, 145.2, 143.7, 135.9, 131.5, 124.5, 123.7, 115.1, 107.6, 106.1, 103.4, 94.4, 79.7, 78.0, 56.9, 45.7, 40.0, 39.8, 26.9, 26.4, 25.9, 17.8, 16.8, 16.2.

HRMS (ESI): calculated for $C_{27}H_{33}Cl_2O_6$ 523.1660 $[M-H]^-$, found 523.1658.

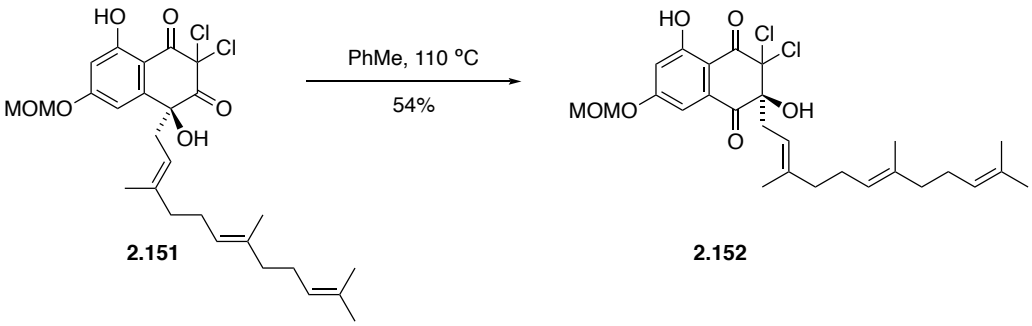

2.151 **2.152**

A solution of **2.151**(1.07 g, 2.04 mmol) in PhMe (120 mL) was stirred at 110 ºC for 16 h. The mixture was cooled to rt and concentrated *in vacuo*. The residue was purified by flash chromatography on SiO_2 (4:1, petrol/EtOAc) to give **2.152** as a yellow oil (574 mg, 54%).

Data for 2.152:

R_f = 0.45 (3:1, petrol/EtOAc)

IR (neat): 3380, 2917, 1712, 1656, 1614, 1580, 1349, 1248, 1096, 810 cm^{-1}.

^{1}H NMR (500 MHz, $CDCl_3$): δ 11.44 (s, 1H), 7.18 (d, *J* = 2.4 Hz, 1H), 6.95 (d, *J* = 2.4 Hz, 1H), 5.30 (d, *J* = 6.9 Hz, 1H), 5.26 (d, *J* = 7.0 Hz, 1H), 5.09 (t, *J* = 7.1 Hz, 1H), 5.03 (t, *J* = 6.8 Hz, 1H), 4.89 (t, *J* = 7.8 Hz, 1H), 4.44 (s, 1H), 3.49 (s, 3H), 2.80 (dd, *J* = 14.5, 6.4 Hz, 1H), 2.36 (dd, *J* = 14.5, 8.8 Hz, 1H), 2.10 – 1.86 (m, 8H), 1.68 (s, 3H), 1.60 (s, 3H), 1.58 (s, 3H), 1.22 (s, 3H).

^{13}C NMR (125 MHz, $CDCl_3$): δ 193.8, 187.2, 165.6, 164.7, 141.6, 135.6, 133.5, 131.4, 124.4, 123.7, 115.1, 109.8, 109.3, 109.2, 108.2, 94.5, 90.6, 85.8, 56.8, 39.8, 39.8, 26.9, 26.4, 25.8, 17.8, 16.2, 16.1.

HRMS (ESI): calculated for $C_{27}H_{34}Cl_2O_6Na$ 547.1625 $[M+Na]^+$, found 547.1607.

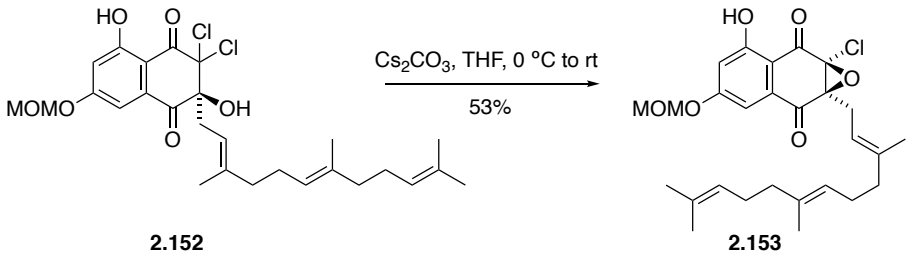

2.152 **2.153**

To a solution of **2.152** (576 mg, 1.10 mmol) in THF (30 mL) was added Cs_2CO_3 (1.07 g, 3.29 mmol) at 0 ºC. The reaction was stirred at 0 ºC for 1.5 h. The mixture was then warmed to rt and stirred for a further 1.5 h. The mixture was quenched with saturated NH_4Cl solution (50 mL) and extracted with EtOAc (2 × 30 mL). The combined organic extracts were dried over $MgSO_4$, filtered and concentrated *in vacuo*. The residue was purified by flash chromatography on SiO_2 (9:1, petrol/EtOAc) to give **2.153** (286 mg, 53%) as a yellow oil.

Data for 2.153:

R_f = 0.50 (3:1, petrol/EtOAc)

IR (neat): 2915, 1703, 1662, 1612, 1375, 1148, 1076, 1019, 950, 826 cm^{-1}.

^{1}H NMR (500 MHz, $CDCl_3$): δ 11.46 (s, 1H), 7.25 (d, *J* = 2.5 Hz, 1H), 6.87 (d, *J* = 2.5 Hz, 1H), 5.26 (d, *J* = 6.9 Hz, 1H), 5.24 (d, *J* = 6.9 Hz, 1H), 5.19 (t, *J* = 6.9 Hz, 1H), 5.04 (t, *J* = 6.8 Hz, 1H), 5.03 (t, *J* = 7.0 Hz, 1H), 3.47 (s, 3H), 3.35 (dd, *J* = 14.6, 7.7 Hz, 1H), 2.67 (dd, *J* = 14.7, 6.8 Hz, 1H), 2.13 – 1.86 (m, 8H), 1.78 (s, 3H), 1.66 (s, 3H), 1.57 (s, 3H), 1.26 (s, 3H).

^{13}C NMR (125 MHz, $CDCl_3$): δ 187.50, 187.47, 165.1, 164.6, 140.7, 135.3, 133.6, 131.4, 124.4, 123.9, 115.3, 110.1, 109.5, 108.1, 94.4, 81.1, 68.0, 56.8, 39.9, 39.8, 26.9, 26.4, 26.2, 25.8, 17.8, 16.8, 16.2.

HRMS (ESI): calculated for $C_{27}H_{33}Cl_2O_6$ 523.1660 $[M+Cl]^+$, found 523.1666

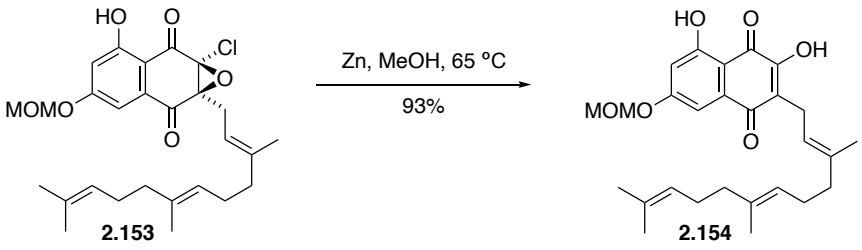

To a solution of **2.153** (190 mg, 0.389 mmol) in MeOH (8 mL) was added Zn powder (50 mg, 0.76 mmol) at rt. The reaction was stirred at 65 ºC for 15 min. The mixture was cooled to rt, quenched with 1 M HCl solution (20 mL) and stirred for a further 10 min before extraction with EtOAc (3 × 10 mL). The combined organic extracts were washed sequentially with 1 M HCl (20 mL) and brine (20 mL), dried over $MgSO_4$, filtered and concentrated *in vacuo*. The residue was purified by flash chromatography on SiO_2 (6:1 petrol/EtOAc) to give **2.154** (163 mg, 93%) as a yellow solid.

Data for 2.154:

R_f = 0.35 (3:1, petrol/EtOAc)

Mp: 96 - 101 °C

IR (neat): 3368, 3123, 2918, 1646, 1620, 1606, 1571, 1486, 1314, 1238, 1146, 1081 cm^{-1}.

^{1}H NMR (500 MHz, $CDCl_3$): δ 11.21 (s, 1H), 7.35 (s, 1H), 7.29 (d, *J* = 2.3 Hz, 1H), 6.74 (d, *J* = 2.3 Hz, 1H), 5.26 (s, 2H), 5.18 (t, *J* = 6.8 Hz, 1H), 5.06 (t, *J* = 7.0 Hz, 1H), 5.04 (t, *J* = 8.5 Hz, 1H), 3.48 (s, 3H), 3.27 (d, *J* = 7.4 Hz, 2H), 2.10 – 1.88 (m, 8H), 1.78 (s, 3H), 1.66 (s, 3H), 1.56 (s, 6H).

^{13}C NMR (125 MHz, $CDCl_3$): δ 183.5, 183.0, 164.8, 163.9, 152.9, 137.5, 135.1, 134.7, 131.3, 124.5, 124.1, 124.0, 119.5, 110.1, 108.2, 107.3, 94.3, 56.7, 39.8, 39.8, 26.9, 26.6, 25.8, 22.7, 17.8, 16.4, 16.1.

HRMS (ESI): calculated for $C_{27}H_{35}O_6$ 455.2428 $[M+H]^+$, found 455.2429.

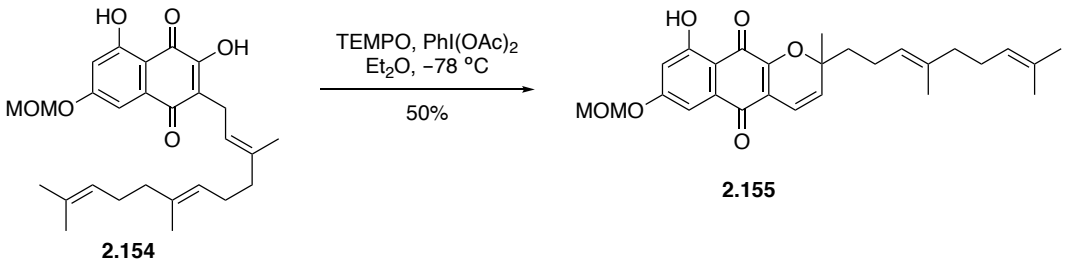

To a solution of **2.154** (163 mg, 0.359 mmol) in Et_2O (10 mL) was added $PhI(OAc)_2$ (126 mg, 0.394 mmol) and TEMPO (67 mg, 0.43 mmol) at −78 ºC. The reaction was stirred at −78 ºC for 1 h. The mixture was then warmed to rt and stirred for a further 16 h. The mixture was filtered through SiO_2, washing with Et_2O and concentrated *in vacuo*. The residue was purified by flash chromatography on SiO_2 (10:1, petrol/EtOAc) to give **2.155** (81 mg, 50%) as a red oil.

Data for 2.155:

R_f = 0.45 (3:1, petrol/EtOAc)

IR (neat): 2916, 1646, 1620, 1573, 1377, 1316, 1224, 1146, 940, 736 cm^{-1}.

^{1}H NMR (500 MHz, $CDCl_3$): δ 12.05 (s, 1H), 7.27 (d, *J* = 2.4 Hz, 1H), 6.77 (d, *J* = 2.4 Hz, 1H), 6.65 (d, *J* = 10.1 Hz, 1H), 5.65 (d, *J* = 10.1 Hz, 1H), 5.25 (s, 2H), 5.10 (t, *J* = 6.8 Hz, 1H), 5.06 (t, *J* = 6.9 Hz, 1H), 3.48 (s, 3H), 2.17 – 2.11 (m, 2H), 2.07 – 1.90 (m, 5H), 1.74 – 1.68 (m, 1H), 1.67 (s, 3H), 1.58 (s, 3H), 1.56 (s, 3H), 1.52 (s, 3H).

^{13}C NMR (125 MHz, $CDCl_3$): δ 182.8, 180.6, 164.1, 163.8, 153.0, 136.0, 133.3, 131.4, 129.5, 124.2, 123.1, 117.7, 115.9, 109.7, 109.2, 107.9, 94.1, 83.4, 56.5, 41.6, 39.6, 27.5, 26.6, 25.7, 22.5, 17.6, 16.0.

HRMS (ESI): calculated for $C_{27}H_{33}O_6$ 453.2272 $[M+H]^+$, found 453.2277.

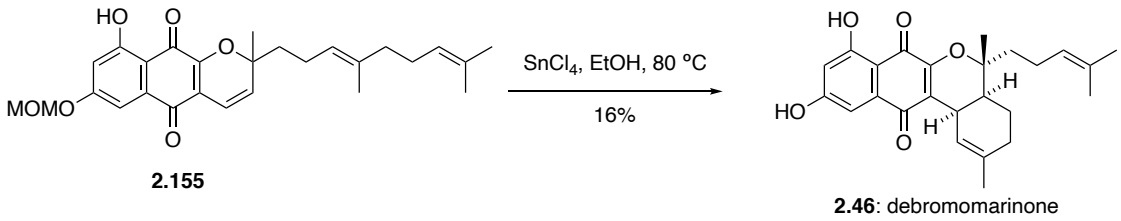

To a solution of **2.155** (81 mg, 0.18 mmol) in EtOH (8 mL) was added $SnCl_4$ (3 drops) at rt. The reaction was stirred at 80 ºC for 3 h. The mixture was cooled to rt, quenched with 1 M HCl solution (10 mL) and extracted with EtOAc (3 × 5 mL). The combined organic extracts were washed with brine (10 mL) dried over $MgSO_4$, filtered and concentrated *in vacuo*. The residue was purified by flash chromatography on SiO_2 (4:1, petrol/EtOAc) to give debromomarinone **2.46** (12 mg, 16%) as an orange solid.

Data for 2.46:

R_f = 0.30 (3:1, petrol/EtOAc)

Mp: 83 – 88 °C

IR (neat): 3296, 2923, 1630, 1586, 1324, 1221, 1160, 1007, 768 cm^{-1}.

^{1}H NMR (500 MHz, $CDCl_3$): δ 11.90 (s, 1H), 7.22 (d, *J* = 2.4 Hz, 1H), 6.57 (d, *J* = 2.3 Hz, 1H), 6.03 (d, *J* = 4.3 Hz, 1H), 5.02 (t, *J* = 7.0 Hz, 1H), 3.46 (t, *J* = 5.9 Hz, 1H), 2.10 – 1.89 (m, 5H), 1.89 (dddd, *J* = 12.0, 5.8, 3.0 Hz, 1H), 1.72 – 1.60 (m, 2H), 1.67 (s, 3H), 1.62 (s, 3H), 1.56 (s, 3H), 1.52 (s, 3H), 1.38 – 1.30 (m, 1H).

^{13}C NMR (125 MHz, $CDCl_3$): δ 184.3, 183.0, 164.6, 163.9, 153.4, 136.4, 134.9, 132.6, 124.1, 123.3, 120.1, 109.0, 108.7, 107.5, 83.3, 37.5, 36.9, 31.0, 29.9, 25.7, 23.7, 22.8, 22.4, 20.4, 17.8.

^{1}H NMR (500 MHz, CD_3OD): δ 6.96 (d, *J* = 2.4 Hz, 1H), 6.42 (d, *J* = 2.3 Hz, 1H), 6.01 (d, *J* = 5.0 Hz, 1H), 5.07 (t, *J* = 7.2 Hz, 1H), 3.41 (t, *J* = 5.9 Hz, 2H), 2.14 – 1.92 (m, 5H), 1.90 (ddd, *J* = 11.7, 6.1, 2.8 Hz, 1H), 1.70 – 1.60 (m, 2H), 1.66 (s, 3H), 1.59 (s, 3H), 1.54 (s, 3H), 1.49 (s, 3H), 1.33 – 1.25 (m, 2H).

^{13}C NMR (125 MHz, CD_3OD): δ 184.8, 183.9, 167.0, 165.6, 154.2, 136.9, 136.1, 132.9, 124.9, 124.8, 121.4, 109.6, 108.8, 107.3, 83.9, 39.0, 37.6, 32.2, 30.6, 25.8, 23.7, 23.2, 22.6, 21.4, 17.6.

HRMS (ESI): calculated for $C_{25}H_{29}O_5$ 409.2010 $[M+H]^+$, found 409.2017

2.4.3 Single Crystal X-ray Data

A single crystal was mounted in Paratone-N oil on a MiTeGen micromount. X-ray diffraction data were collected at 150(2) K on an Oxford X-calibur single crystal diffractometer using Mo Kα radiation.[94] The data set was corrected for absorption using a multi-scan method, and the structure solved by direct methods (SHELXS)[95,96] and refined by full-matrix least squares on F2 by SHELXL,[97] interfaced through the programs X-Seed (version 4)[98]and Olex2.[99]All non-hydrogen atoms were refined anisotropically and hydrogen atoms were included as invariants at geometrically estimated positions, unless specified otherwise. A series of EADP, ISOR and DFIX restraints was used to allow refinement of the disordered $C(CH_3)_2Cl$ substituent. Table S1 lists the X-ray experimental data and refinement parameters for the crystal structures. Perspective views of the structure of **2.126** is shown in Figure SI-2.1.

Full details of the structure determinations have been deposited with the Cambridge Crystallographic Data Centre as CCDC 1863976. Copies of this information may be obtained free of charge from The Director, CCDC, 12 Union Street, Cambridge CB2 1EZ, U.K. (fax, +44-1223-336-033; e-mail, deposit@ccdc.cam.ac.uk).

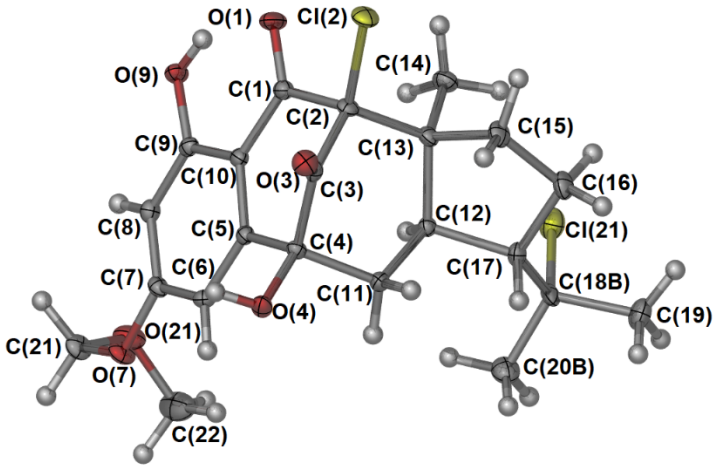

(a)

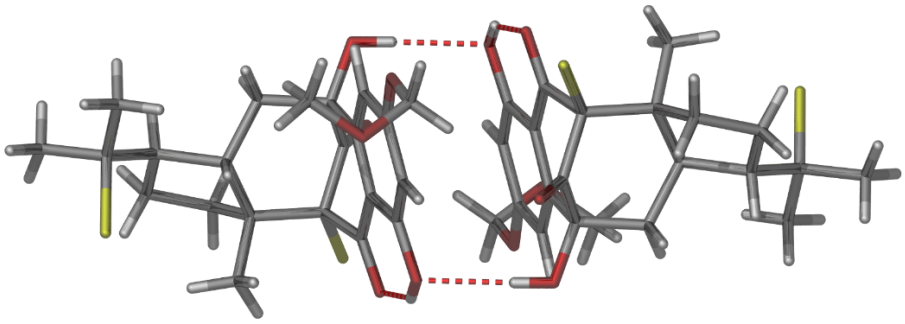

(b)

Figure SI-2.1: Perspective views of (a) the labelled asymmetric unit (only the minor component of the disorder 0.35 occupancy is shown) and (b) the hydrogen bonded dimer in the structure of **2.126**). Carbon – grey, hydrogen – white, oxygen – red, chlorine – yellow. The intramolecular and intermolecular hydrogen bonding parameters are: $D_{O9\text{-}H\cdots O1}$ = 2.55 Å, $angle_{O9\text{-}H\cdots O1}$ = 146.2° and $D_{O4\text{-}H\cdots O9}$ = 2.94 Å, $angle_{O4\text{-}H\cdots O9}$ = 175.2°, respectively.

Table SI-2.1. X-ray experimental data for **2.126**.

Compound	**2.126**
CCDC number	1841960
cif	16-HP-61
Empirical formula	$C_{22}H_{26}Cl_2O_6$
Formula weight	457.33
Crystal system	triclinic
Space group	P-1
a (Å)	7.9638(3)
b (Å)	11.5702(4)
c (Å)	12.7239(4)
α (°)	63.836(3)
β (°)	84.162(3)
γ (°)	82.250(3)
Volume ($Å^3$)	1041.50(7)
Z	2
Density (calc.) (Mg/m^3)	1.458
Absorption coefficient (mm^{-1})	0.350
F(000)	480.0
Crystal size (mm^3)	0.58 × 0.21 × 0.11
2θ range for data collection (º)	6.81 to 58.732
Reflections collected	36801
Observed reflections [*R*(*int*)]	5285 [R_{int} = 0.0466]
Data/restraints/parameters	5285/21/288
Goodness-of-fit on F2	1.027
R_1 [$I>2\sigma(I)$]	0.0363
wR_2 (all data)	0.0877
Largest diff. peak and hole ($e.Å^{-3}$)	0.39/-0.33

2.5 References

(1) Neumann, C. S.; Fujimori, D. G.; Walsh, C. T. *Chem. Biol.* **2008**, *15*, 99.
(2) Gribble, G. W. *Mar. Drugs* **2015**, *13*, 4044.
(3) Agarwal, V.; Miles, Z. D.; Winter, J. M.; Eustáquio, A. S.; El Gamal, A. A.; Moore, B. S. *Chem. Rev.* **2017**, *117*, 5619.
(4) Gribble, G. W. *Environ. Chem.* **2015**, *12*, 396.
(5) Dinos, G. P.; Athanassopoulos, C. M.; Missiri, D. A.; Giannopoulou, P. C.; Vlachogiannis, I. A.; Papadopoulos, G. E.; Papaioannou, D.; Kalpaxis, D. L. *Antibiotics* **2016**, *5*.
(6) Barclay, C.; Anderson, R. J.; Groundwater, P. W.; Todd, A.; Worsley, A. J. In *Antibacterial agents*; John Wiley & Sons, Inc., 2012; pp 231–242.
(7) Groll, M.; Huber, R.; Potts, B. C. M. *J. Am. Chem. Soc.* **2006**, *128*, 5136.
(8) Kale, A. J.; McGlinchey, R. P.; Lechner, A.; Moore, B. S. *ACS Chem. Biol.* **2011**, *6*, 1257.
(9) McCormick, M. H.; McGuire, J. M.; Pittenger, G. E.; Pittenger, R. C.; Stark, W. M. *Antibiot Annu* **1955**, *3*, 606.
(10) Harris, C. M.; Kannan, R.; Kopecka, H.; Harris, T. M. *J. Am. Chem. Soc.* **1985**, *107*, 6652.
(11) Bianco, A. C.; Salvatore, D.; Gereben, B.; Berry, M. J.; Larsen, P. R. *Endocr. Rev.* **2002**, *23*, 38.
(12) Renner, M. K.; Jensen, P. R.; Fenical, W. *J. Org. Chem.* **1998**, *63*, 8346.
(13) Hager, L. P.; Morris, D. R.; Brown, F. S.; Eberwein, H. *J. Biol. Chem.* **1966**, *241*, 1769.
(14) Butler, A.; Sandy, M. *Nature* **2009**, *460*, 848.
(15) Winter, J. M.; Moore, B. S. *J. Biol. Chem.* **2009**, *284*, 18577.
(16) Butler, A.; Carter-Franklin, J. N. *Nat. Prod. Rep.* **2004**, *21*, 180.
(17) Carter-Franklin, J. N.; Butler, A. *J. Am. Chem. Soc.* **2004**, *126*, 15060.
(18) Hanson, J. R. *Compr. Org. Synth.* **1991**, *3*, 705.
(19) Croteau, R.; Satterwhite, D. M. *J. Biol. Chem.* **1989**, *264*, 15309.
(20) Dehaen, W.; Mashentseva, A. A.; Seitembetov, T. S. *Molecules* **2011**, *16*, 2443.
(21) Paquette, L. A.; Hofferberth, J. E. *Org. React.* **2003**, *62*, 477.
(22) Liffert, R.; Linden, A.; Gademann, K. *J. Am. Chem. Soc.* **2017**, *139*, 16096.
(23) Shiomi, K.; Iinuma, H.; Hamada, M.; Naganawa, H. *J. Antibiot.* **1986**, *39*, 487.
(24) Shiomi, K.; Nakamura, H.; Naganawa, H.; Isshiki, K.; Takeuchi, T.; Umezawa, H.; Iitaka, Y. *J. Antibiot.* **1986**, *39*, 494.
(25) Kaysser, L.; Bernhardt, P.; Nam, S. J.; Loesgen, S.; Ruby, J. G.; Skewes-Cox, P.; Jensen, P. R.; Fenical, W.; Moore, B. S. *J. Am. Chem. Soc.* **2012**, *134*, 11988.
(26) Shin-ya, K.; Imai, S.; Furihata, K.; Hayakawa, Y.; Kato, Y.; Vanduyne, G. D.; Clardy, J.; Seto, H. *J. Antibiot.* **1990**, *43*, 444.
(27) Takagi, H.; Motohashi, K.; Miyamoto, T.; Shin-ya, K.; Furihata, K.; Seto, H. *J. Antibiot.* **2005**, *58*, 275.
(28) Park, J.-S.; Kwon, H. C. *Mar. Drugs* **2018**, *16*, 90.
(29) Shin-ya, K.; Shimazu, A.; Hayakawa, Y.; Seto, H. *J. Antibiot.* **1992**, *45*, 124.
(30) Wessels, P.; Göhrt, A.; Zeeck, A.; Gohrt, A.; Zeeck, A. *J. Antibiot.* **1991**, *44*, 1013.
(31) Volkmann, C.; Hartjen, U.; Zeeck, A.; Fiedler, H.-P. *J. Antibiot.* **1995**, *48*, 522.
(32) Lu, C.; Yang, C.; Xu, Z. *Rec. Nat. Prod.* **2016**, *10*, 430.
(33) Pathirana, C.; Jensen, P. R.; Fenical, W. *Tetrahedron Lett.* **1992**, *33*, 7663.
(34) Hardt, I. H.; Jensen, P. R.; Fenical, W. *Tetrahedron Lett.* **2000**, *41*, 2073.
(35) Kalaitzis, J. A.; Hamano, Y.; Nilsen, G.; Moore, B. S. *Org. Lett.* **2003**, *5*, 4449.

(36) Shin-ya, K.; Furihata, K.; Hayakawa, Y.; Seto, H. *Tetrahedron Lett.* **1990**, *31*, 6025.
(37) Kawasaki, T.; Hayashi, Y.; Kuzuyama, T.; Furihata, K.; Itoh, N.; Seto, H.; Dairi, T. *J. Bacteriol.* **2006**, *188*, 1236.
(38) Haaqen, Y.; Glück, K.; Fay, K.; Kammerer, B.; Gust, B.; Heide, L. *ChemBioChem* **2006**, *7*, 2016.
(39) Winter, J. M.; Moffitt, M. C.; Zazopoulos, E.; McAlpine, J. B.; Dorrestein, P. C.; Moore, B. S. *J. Biol. Chem.* **2007**, *282*, 16362.
(40) Funa, N.; Ohnishi, Y.; Fujli, I.; Shibuya, M.; Ebizuka, Y.; Horinouchi, S. *Nature* **1999**, *400*, 897.
(41) Austin, M. B.; Izumikawa, M.; Bowman, M. E.; Udwary, D. W.; Ferrer, J. L.; Moore, B. S.; Noel, J. P. *J. Biol. Chem.* **2004**, *279*, 45162.
(42) Kuzuyama, T.; Noel, J. P.; Richard, S. B. *Nature* **2005**, *435*, 983.
(43) Teufel, R.; Kaysser, L.; Villaume, M. T.; Diethelm, S.; Carbullido, M. K.; Baran, P. S.; Moore, B. S. *Angew. Chem. Int. Ed.* **2014**, *53*, 11019.
(44) McKinnie, S. M. K.; Miles, Z. D.; Moore, B. S. *Methods Enzymol.* **2018**, *604*, 405.
(45) Miles, Z. D.; Diethelm, S.; Pepper, H. P.; Huang, D. M.; George, J. H.; Moore, B. S. *Nat. Chem.* **2017**, *9*, 1235.
(46) Pepper, H. P.; George, J. H. *Angew. Chem. Int. Ed.* **2013**, *52*, 12170.
(47) Meier, R.; Strych, S.; Trauner, D. *Org. Lett.* **2014**, *16*, 2634.
(48) Yang, H.; Liu, X.; Li, Q.; Li, L.; Zhang, J. R.; Tang, Y. *Org. Biomol. Chem.* **2015**, *14*, 198.
(49) Brandstätter, M.; Freis, M.; Huwyler, N.; Carreira, E. M. *Angew. Chem. Int. Ed.* **2019**, *58*, 2490.
(50) Murray, L. A. M.; McKinnie, S. M. K.; Moore, B. S.; George, J. H. *Nat. Prod. Rep.* **2020**, *37*, 1334.
(51) McKinnie, S. M. K.; Miles, Z. D.; Jordan, P. A.; Awakawa, T.; Pepper, H. P.; Murray, L. A. M.; George, J. H.; Moore, B. S. *J. Am. Chem. Soc.* **2018**, *140*, 17840.
(52) Katsuyama, Y.; Li, X. W.; Müller, R.; Nay, B. *ChemBioChem* **2014**, *15*, 2349.
(53) Kuzuyama, T. *J. Antibiot.* **2017**, *70*, 811.
(54) Leipoldt, F.; Zeyhle, P.; Kulik, A.; Kalinowski, J.; Heide, L.; Kaysser, L. *PLoS One* **2015**, *10*, 1.
(55) Fukuda, D. S.; Mynderse, J. S.; Baker, P. J.; Berry, D. M.; Boeck, L. D.; Yao, R. C.; Mertz, F. P.; Nakatsukasa, W. M.; Mabe, J.; Ott, J.; Counter, F. T.; Ensminger, P. W.; Allen, N. E.; Alborn, W. E.; Hobbs, J. N. *J. Antibiot.* **1990**, *43*, 623.
(56) Henkel, T.; Zeeck, A. *J. Antibiot.* **1991**, *44*, 665.
(57) Stadler, M.; Anke, H. *J. Antibiot.* **1993**, *46*, 968.
(58) Watanabe, K.; Sekine, M.; Iguchi, K. *J. Nat. Prod.* **2003**, *66*, 1434.
(59) Shitakawa, H.; Nakajima, S.; Hirayama, M.; Kondo, H.; Ojiri, K.; Suda, H. JP11349522, 1999.
(60) Maruo, S.; Nishio, K.; Sasamori, T.; Tokitoh, N.; Kuramochi, K.; Tsubaki, K. *Org. Lett.* **2013**, *15*, 1556.
(61) Kamo, S.; Yoshioka, K.; Kuramochi, K.; Tsubaki, K. *Angew. Chem. Int. Ed.* **2016**, *55*, 10317.
(62) Tang, M. C.; Zou, Y.; Watanabe, K.; Walsh, C. T.; Tang, Y. *Chem. Rev.* **2017**, *117*, 5226.
(63) Taura, F.; Morimoto, S.; Shoyama, Y. *J. Am. Chem. Soc.* **1995**, *117*, 9766.
(64) Shoyama, Y. Y.; Tamada, T.; Kurihara, K.; Takeuchi, A.; Taura, F.; Arai, S.; Blaber, M.; Shoyama, Y. Y.; Morimoto, S.; Kuroki, R. *J. Mol. Biol.* **2012**, *423*, 96.
(65) Mantovani, S. M.; Moore, B. S. *J. Am. Chem. Soc.* **2013**, *135*, 18032.
(66) Wessely, F.; Lauterbach-Keil, G.; Sinwel, F. *Monatsh. Chem.* **1950**, *81*, 811.

(67) Wessely, F.; Sinwel, F. *Monatsh. Chem.* **1950**, *811*, 1055.
(68) Kimura, M.; Fukasaka, M.; Tamaru, Y. *Synthesis (Stuttg).* **2006**, No. 21, 3611.
(69) Pittelkow, M.; Boas, U.; Christensen, J. B. *Org. Lett.* **2006**, *8*, 5817.
(70) Snyder, S. A.; Tang, Z. Y.; Gupta, R. *J. Am. Chem. Soc.* **2009**, *131*, 5744.
(71) Schätzle, M. A.; Flemming, S.; Husain, S. M.; Richter, M.; Günther, S.; Müller, M. *Angew. Chem. Int. Ed.* **2012**, *51*, 2643.
(72) Ichinose, K.; Ebizuka, Y.; Sankawa, U. *Chem. Pharm. Bull.* **2001**, *49*, 192.
(73) Bycroft, B. W.; Roberts, J. C. *J. Chem. Soc.* **1963**, 4868.
(74) McCulloch, M. W. B.; Barrow, R. A. *Tetrahedron Lett.* **2005**, *46*, 7619.
(75) McCulloch, M. W. B.; Barrow, R. A. *Molecules* **2005**, *10*, 1272.
(76) Akai, S.; Kakiguchi, K.; Nakamura, Y.; Kuriwaki, I.; Dohi, T.; Harada, S.; Kubo, O.; Morita, N.; Kita, Y. *Angew. Chem. Int. Ed.* **2007**, *46*, 7458.
(77) Pepper, H. P.; George, J. H. *Angew. Chem. Int. Ed.* **2013**, *52*, 12170.
(78) Tatsuta, K.; Yoshimoto, T.; Gunji, H.; Okado, Y.; Takahashi, M. *Chem. Lett.* **2002**, *31*, 14.
(79) Snyder, S. A.; Tang, Z. Y.; Gupta, R. *J. Am. Chem. Soc.* **2009**, *131*, 5744.
(80) Houssame, S.; Anane, H.; Firdoussi, L.; Karim, A. *Cent. Eur. J. Chem.* **2008**, *6*, 470.
(81) Clark, A. J. *European J. Org. Chem.* **2016**, 2231.
(82) Nagashima, H.; Seki, K.; Nobuyasu, O.; Wakamatsu, H.; Itoh, K.; Tomo, Y.; Tsuji, J. *J. Org. Chem.* **1990**, *55*, 985.
(83) Naota, T.; Takaya, H.; Murahashi, S. I. *Chem. Rev.* **1998**, *98*, 2599.
(84) Yang, D.; Yan, Y.-L. L.; Zheng, B.-F. F.; Gao, Q.; Zhu, N.-Y. Y. *Org. Lett.* **2006**, *8*, 5757.
(85) Yehye, W. A.; Rahman, N. A.; Ariffin, A.; Abd Hamid, S. B.; Alhadi, A. A.; Kadir, F. A.; Yaeghoobi, M. *Eur. J. Med. Chem.* **2015**, *101*, 295.
(86) Templeton, J. F.; Kumar, V. P. S.; El-Sheikh, A. A. M.; Zeglam, T. H.; Marat, K. *J. Chem. Soc. Perkin Trans. 1* **1988**, 1961.
(87) Kotoku, N.; Sumii, Y.; Kobayashi, M. *Org. Lett.* **2011**, *13*, 3514.
(88) Malerich, J. P.; Maimone, T. J.; Elliott, G. I.; Trauner, D. *J. Am. Chem. Soc.* **2005**, *127*, 6276.
(89) Liao, D.; Li, H.; Lei, X. *Org. Lett.* **2012**, *14*, 18.
(90) Lam, H. C.; Spence, J. T. J.; George, J. H. *Angew. Chem. Int. Ed.* **2016**, *55*, 10368.
(91) Lam, H. C.; Phan, Q. D.; Sumby, C. J.; George, J. H. *Aust. J. Chem.* **2018**, *71*, 649.
(92) George, J. H.; Hesse, M. D.; Baldwin, J. E.; Adlington, R. M. *Org. Lett.* **2010**, *12*, 3532.
(93) Tapia, R. A.; Alegría, L.; Valderrama, J. A.; Cortés, M.; Pautet, F.; Fillion, H. *Tetrahedron Lett.* **2001**, *42*, 887.
(94) CrysAlisPro 1.171.38.43d: Rigaku Oxford Diffraction 2015.
(95) Sheldrick, G. M. *Acta Crystallogr. Sect. A Found. Crystallogr.* **2008**, *64*, 112.
(96) Sheldrick, G. M. *Acta Crystallogr. Sect. A Found. Crystallogr.* **2015**, *71*, 3.
(97) Sheldrick, G. M. *Acta Crystallogr. Sect. C Struct. Chem.* **2015**, *71*, 3.
(98) Barbour, L. J. *J. Supramol. Chem.* **2001**, *1*, 189.
(99) Dolomanov, O. V.; Bourhis, L. J.; Gildea, R. J.; Howard, J. A. K.; Puschmann, H. *J. Appl. Crystallogr.* **2009**, *42*, 339.

2.6 Appendix

2.6.1 NMR Spectra

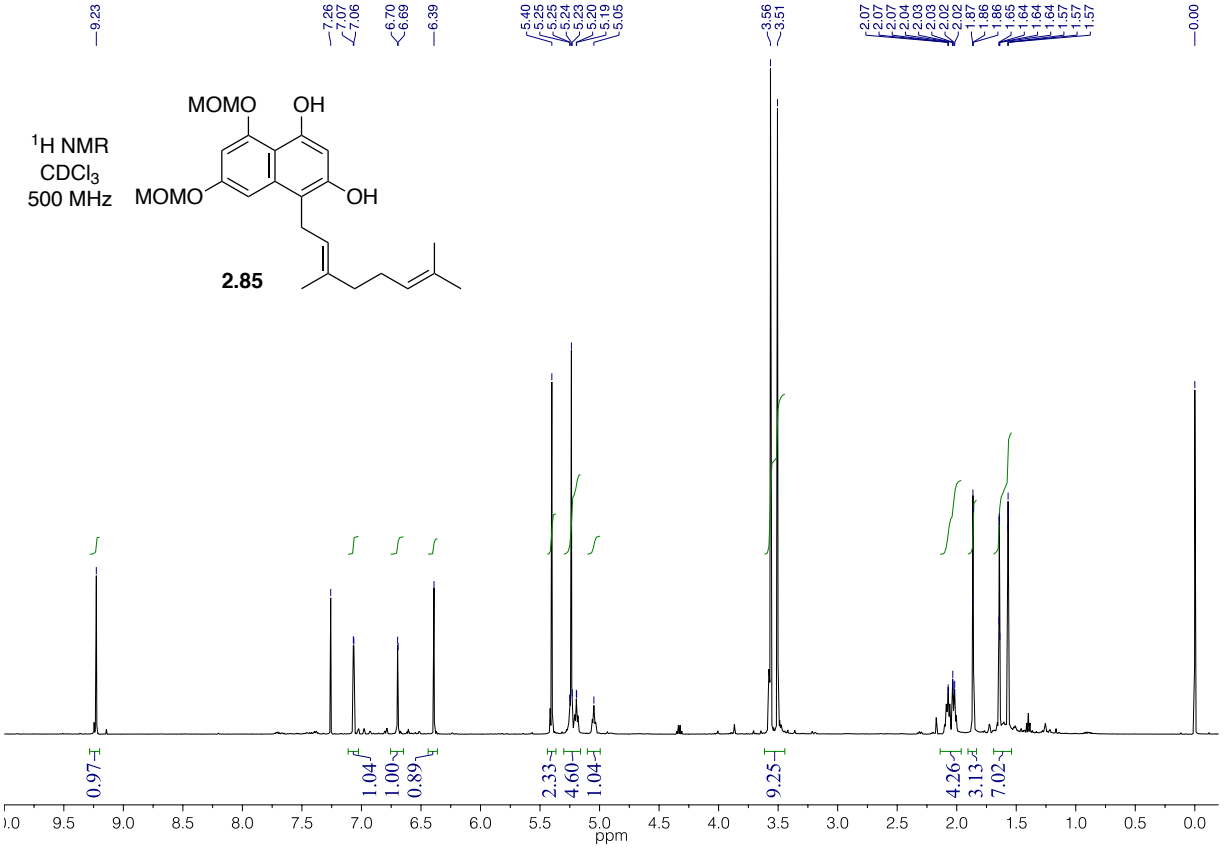

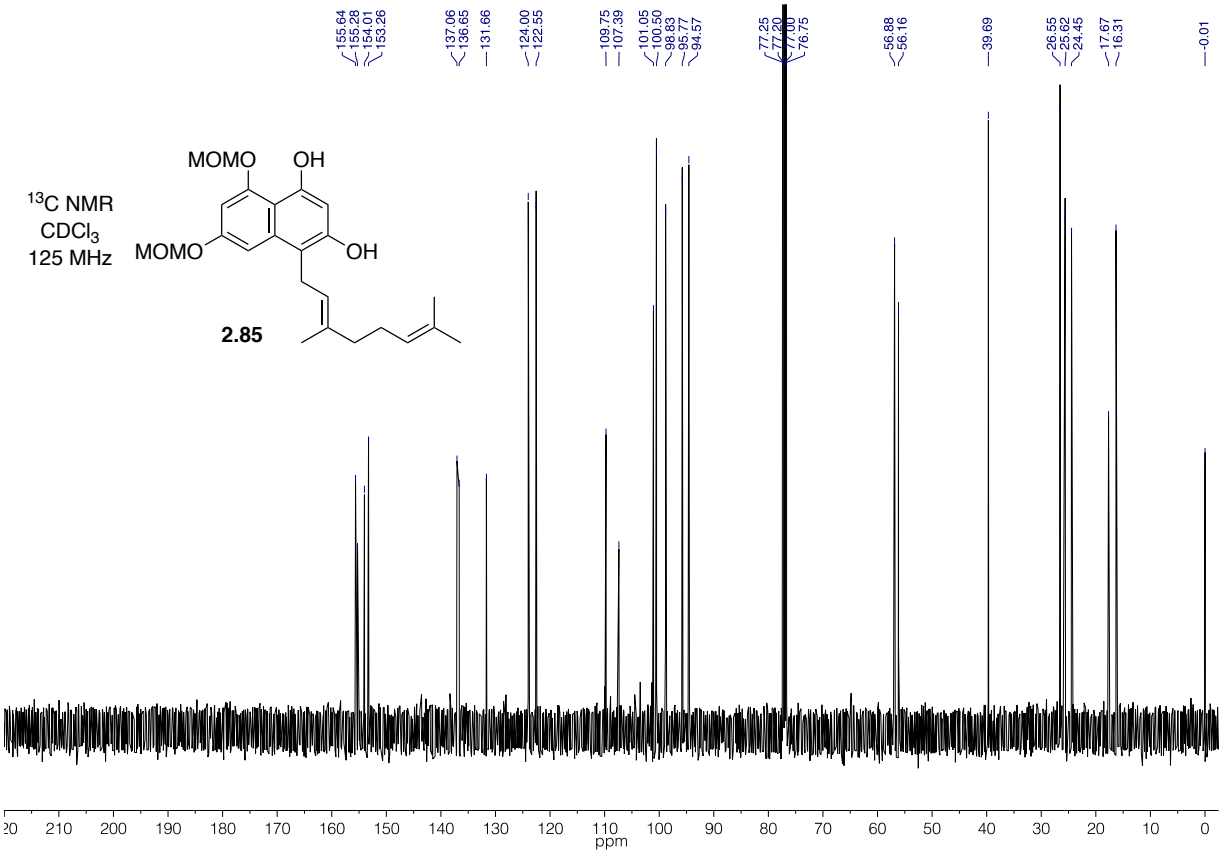

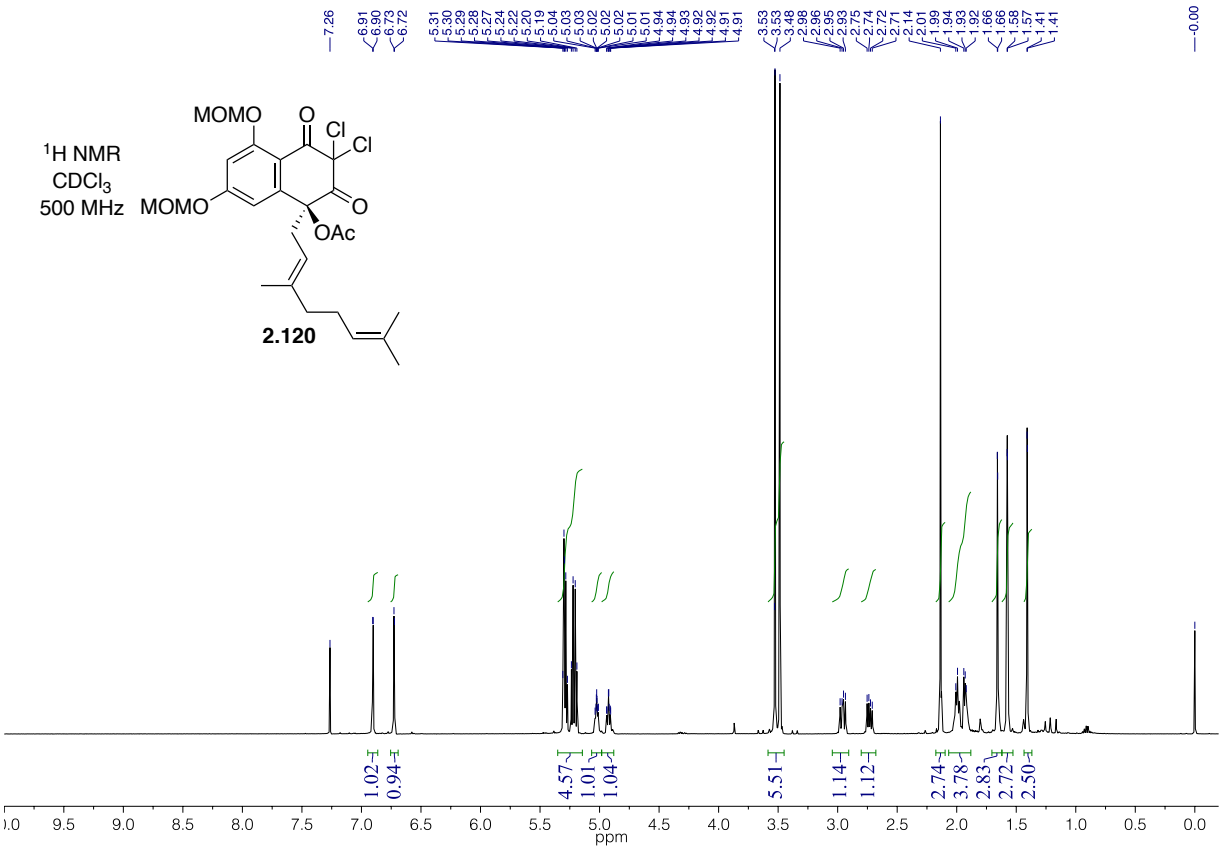
^{1}H NMR
$CDCl_3$
500 MHz
MOMO
O
Cl
Cl
MOMO
O
OAc
2.120
7.26
6.91
6.90
6.73
6.72
5.31
5.30
5.29
5.28
5.27
5.24
5.22
5.20
5.19
5.04
5.03
5.02
5.02
5.02
5.01
5.01
4.94
4.94
4.93
4.92
4.92
4.91
4.91
3.53
3.53
3.48
3.48
2.96
2.95
2.93
2.75
2.74
2.72
2.71
2.14
2.01
1.99
1.94
1.93
1.92
1.66
1.66
1.58
1.57
1.41
1.41
0.00
1.02
0.94
4.57
1.01
1.04
5.51
1.14
1.12
2.74
3.78
2.83
2.72
2.50
ppm

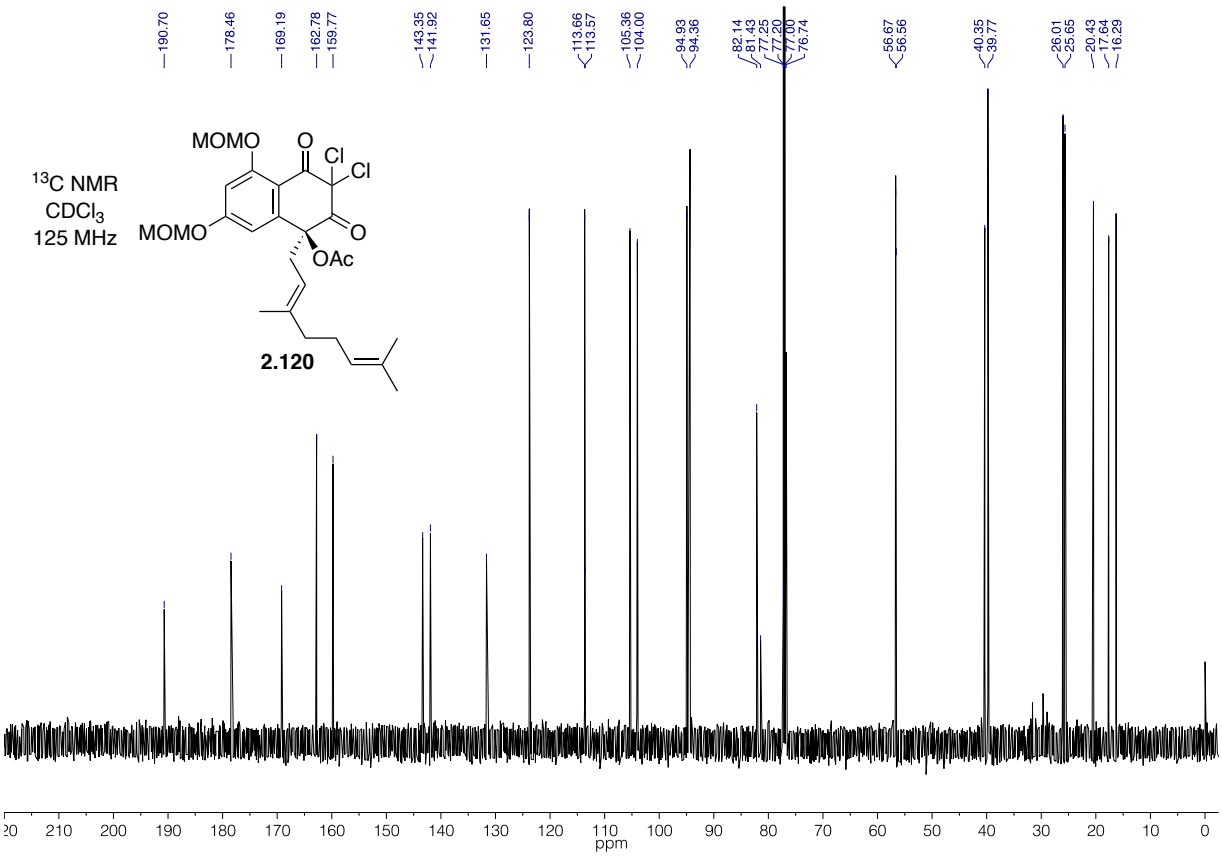
^{13}C NMR
$CDCl_3$
125 MHz
MOMO
O
Cl
Cl
MOMO
O
OAc
2.120
190.70
178.46
169.19
162.78
159.77
143.35
141.92
131.65
123.80
113.66
113.57
105.36
104.00
94.93
94.36
82.14
81.43
77.25
77.20
76.74
56.67
56.56
40.35
39.77
26.01
25.65
20.43
17.64
16.29
ppm

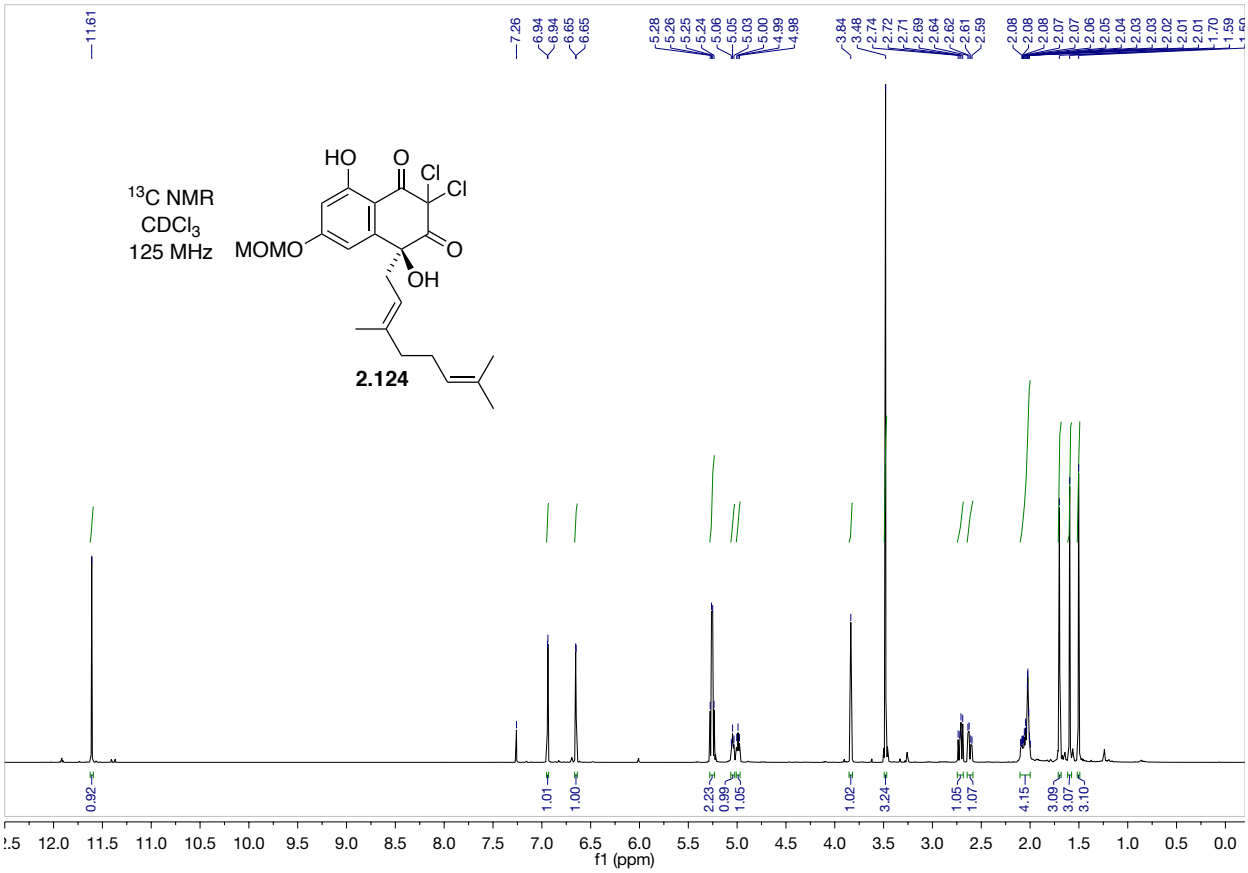
^{13}C NMR
$CDCl_3$
125 MHz
HO
O
Cl
Cl
MOMO
O
OH
2.124
f1 (ppm)

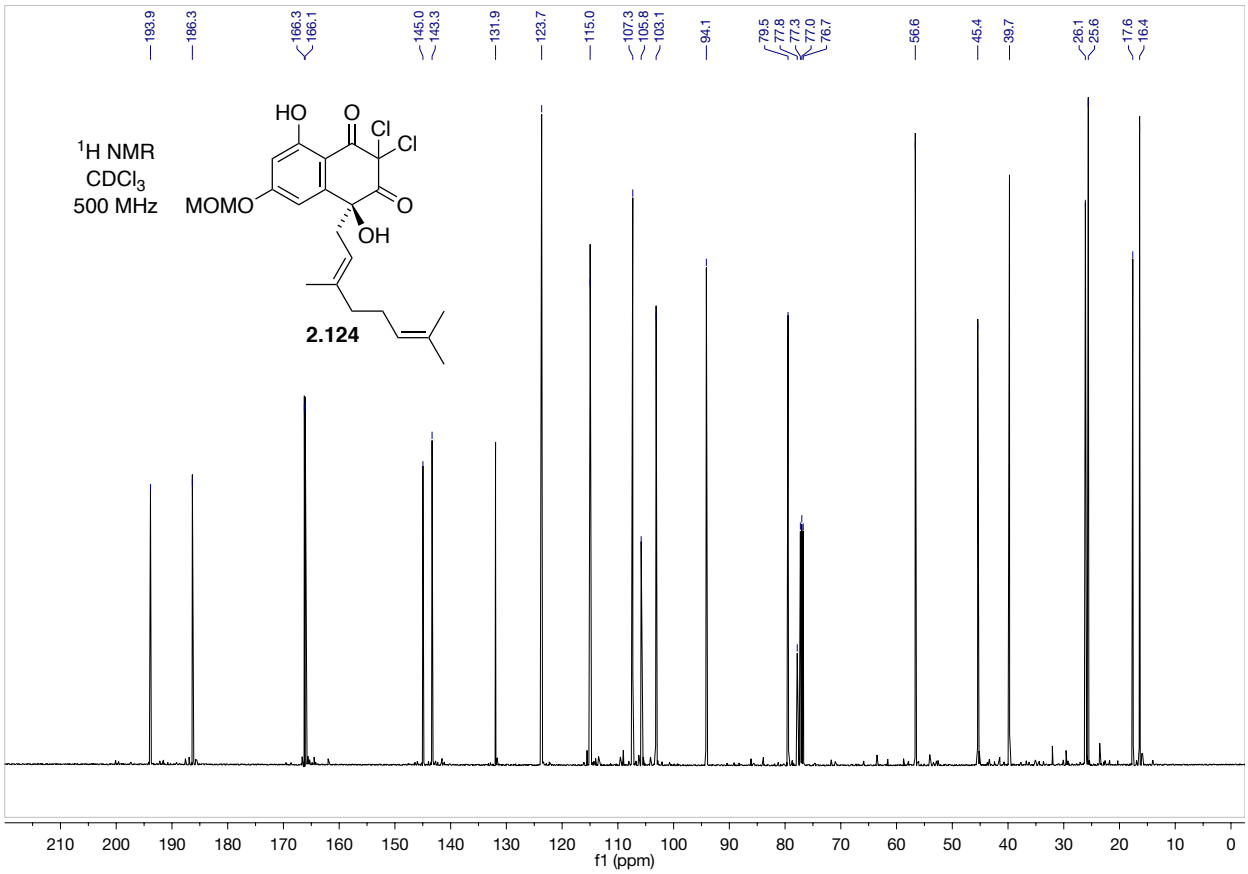
^{1}H NMR
$CDCl_3$
500 MHz
HO
O
Cl
Cl
MOMO
O
OH
2.124
f1 (ppm)

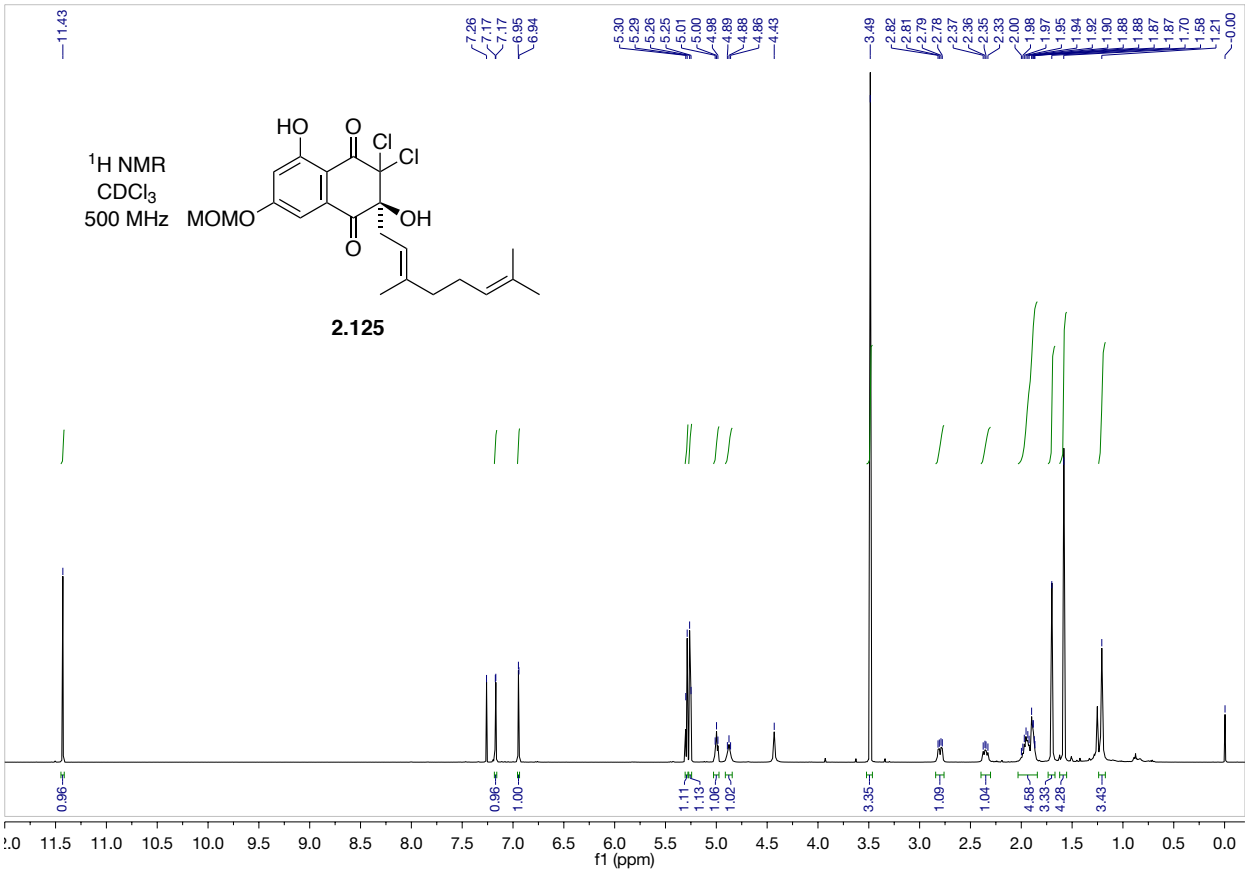
^{1}H NMR
$CDCl_3$
500 MHz
HO
O
Cl
Cl
MOMO
OH
O
2.125
f1 (ppm)

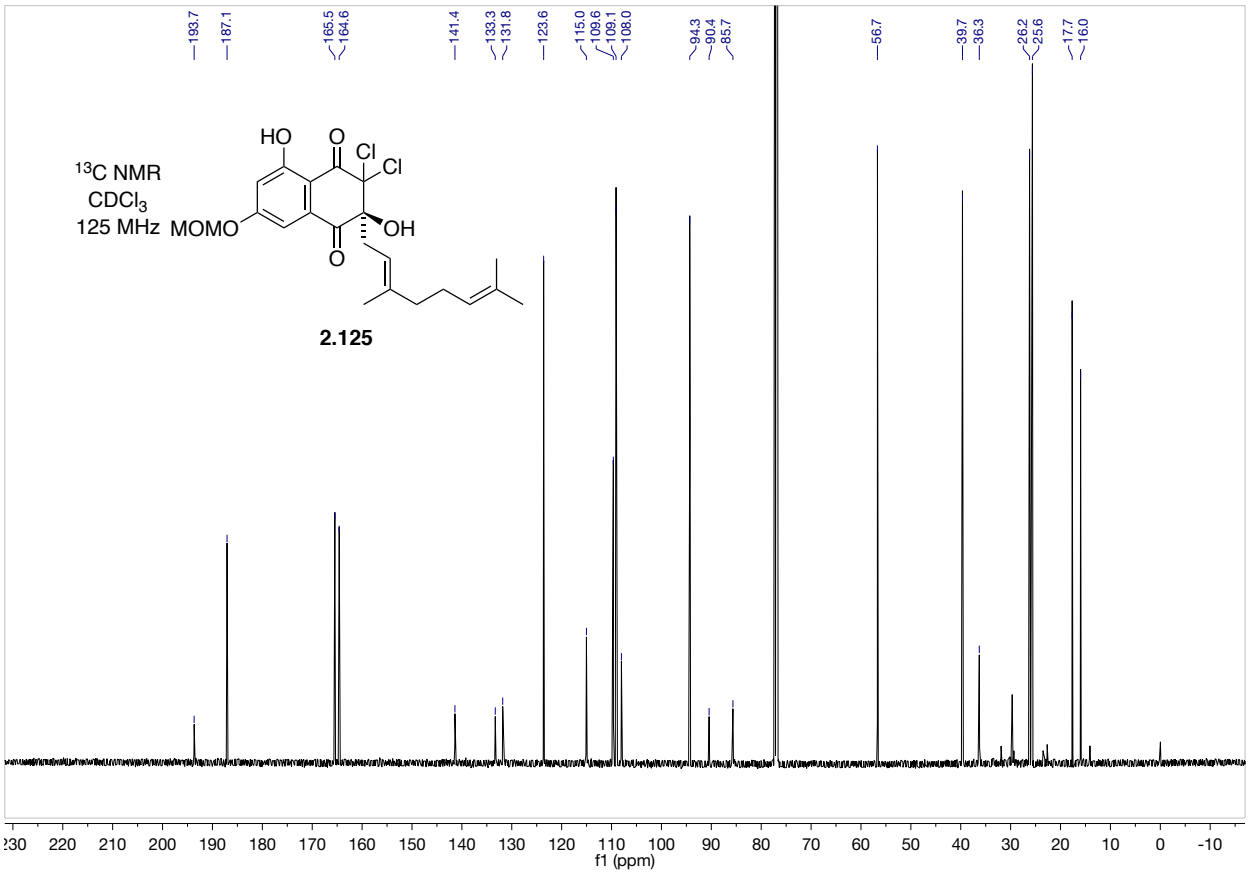
^{13}C NMR
$CDCl_3$
125 MHz
HO
O
Cl
Cl
MOMO
OH
O
2.125
f1 (ppm)

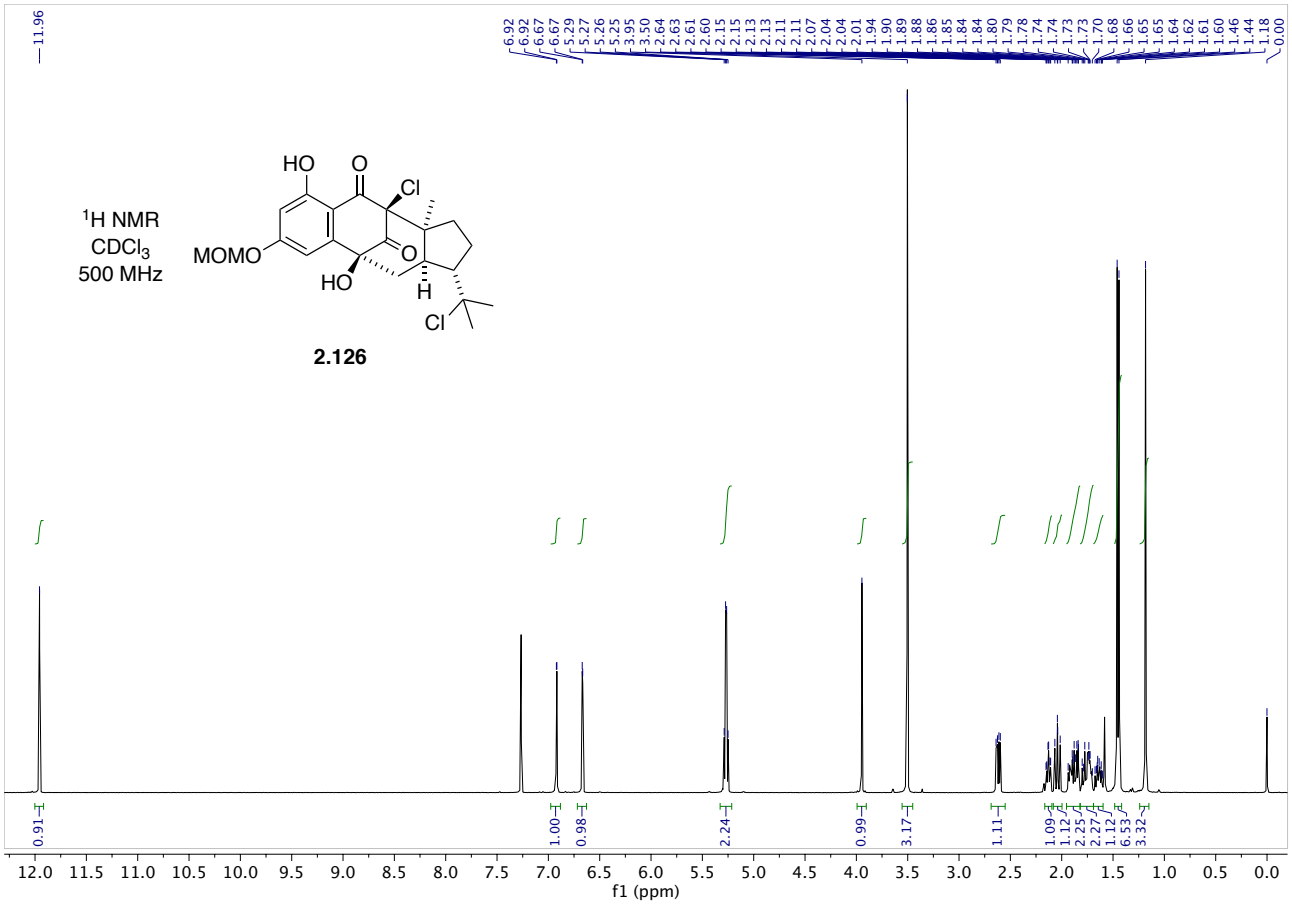
^{1}H NMR
$CDCl_3$
500 MHz
HO
O
Cl
MOMO
O
HO
H
Cl
f1 (ppm)

2.126

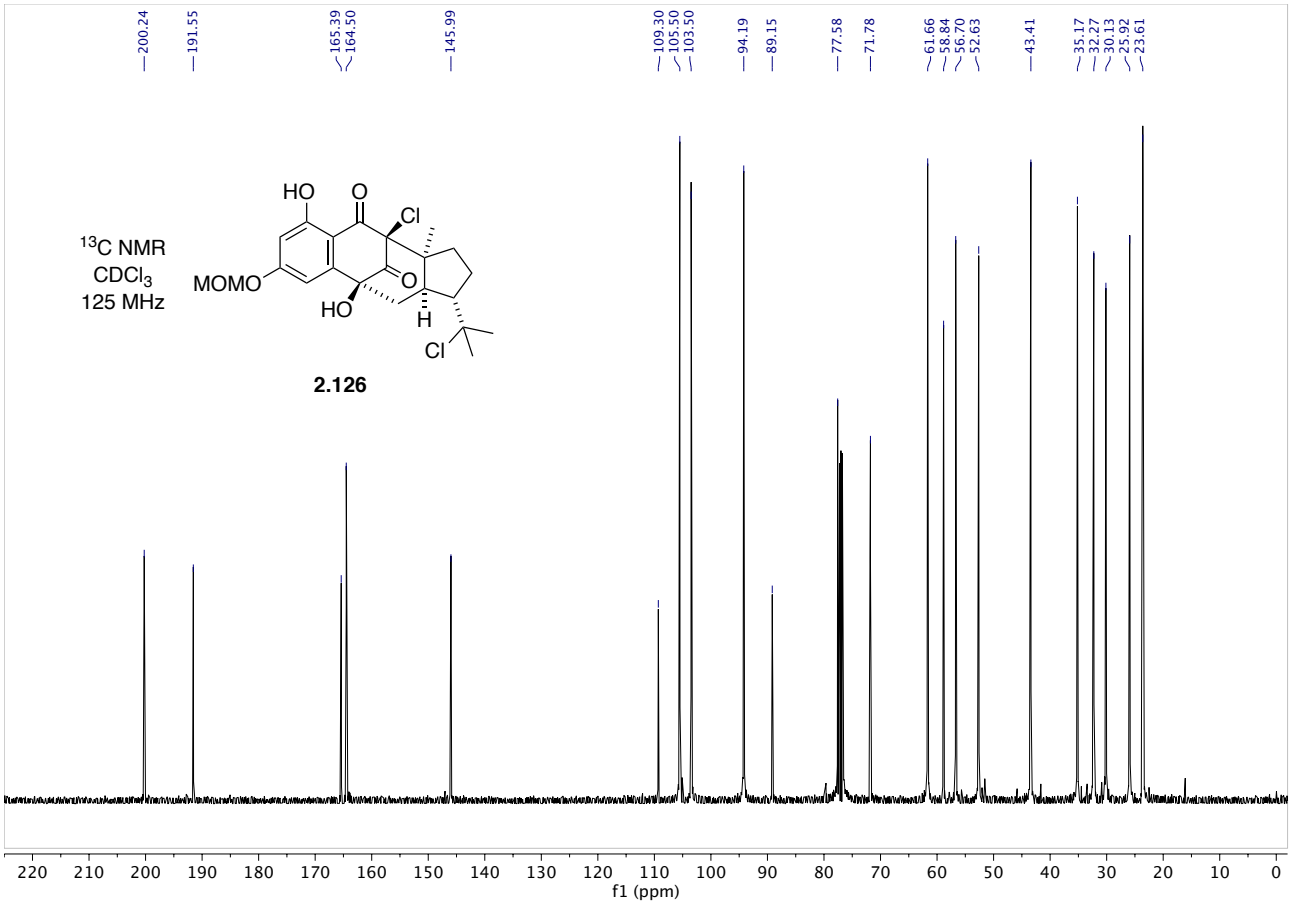
^{13}C NMR
$CDCl_3$
125 MHz
HO
O
Cl
MOMO
O
HO
H
Cl
f1 (ppm)

2.126

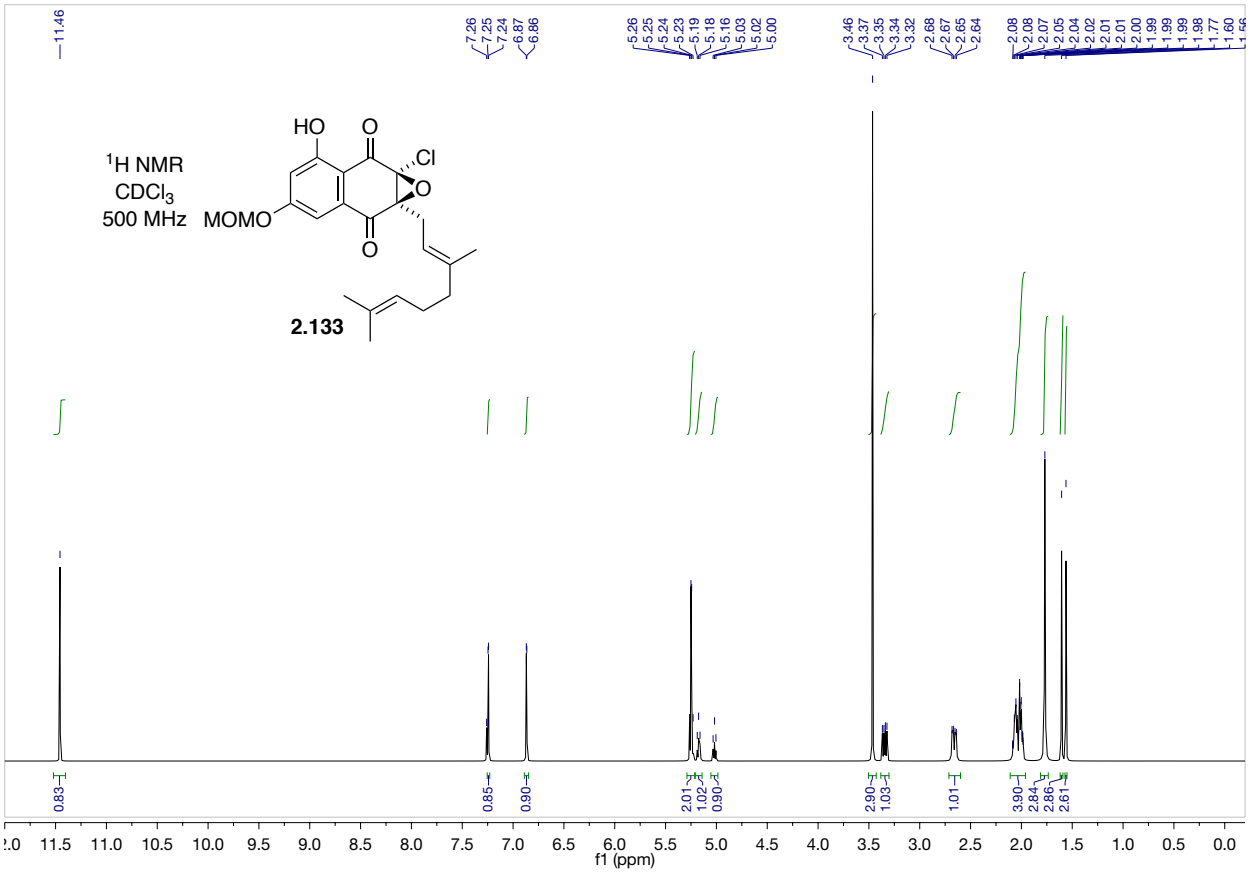
^{1}H NMR
$CDCl_3$
500 MHz
HO
O
Cl
O
MOMO
O
2.133
f1 (ppm)

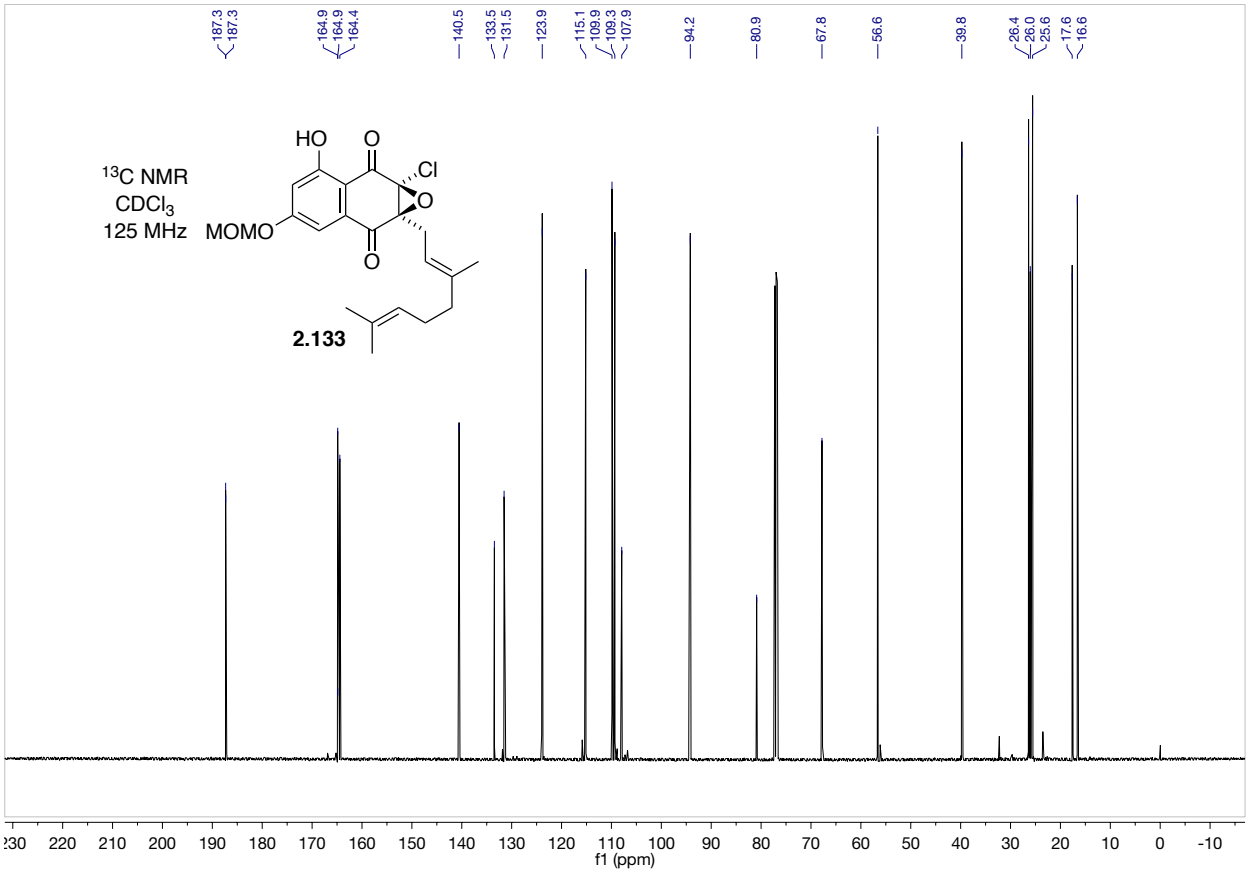
^{13}C NMR
$CDCl_3$
125 MHz
HO
O
Cl
O
MOMO
O
2.133
f1 (ppm)

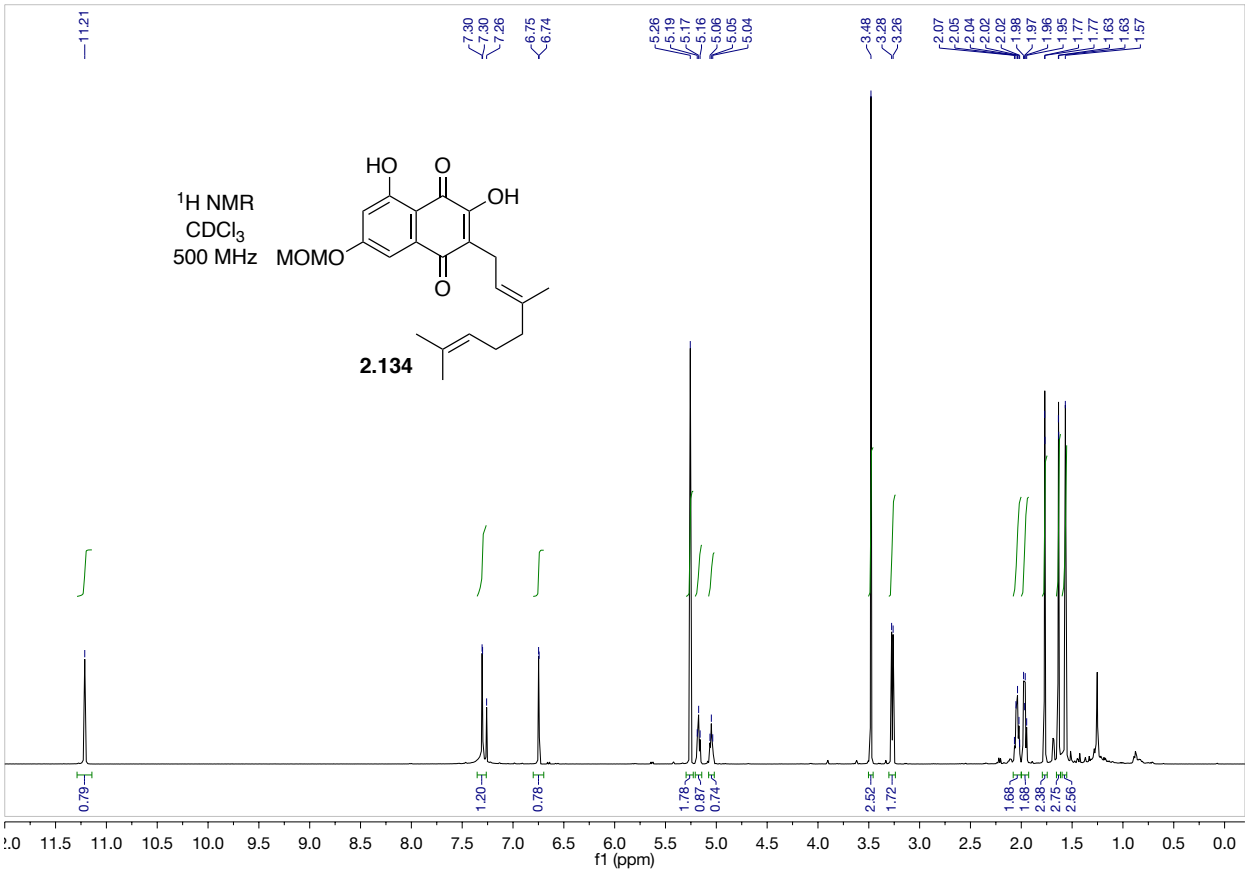
^{1}H NMR
$CDCl_3$
500 MHz
HO
O
OH
MOMO
O
2.134
f1 (ppm)

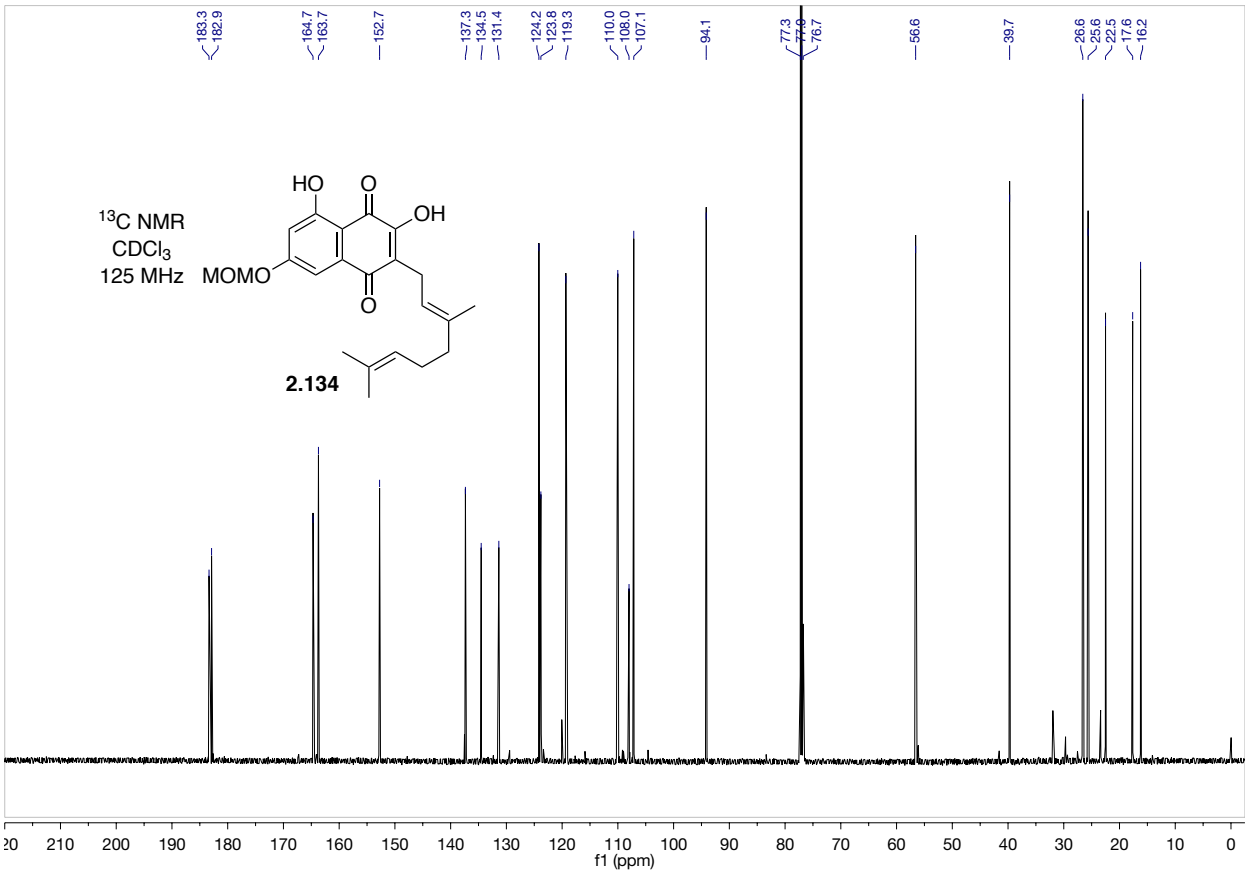
^{13}C NMR
$CDCl_3$
125 MHz
HO
O
OH
MOMO
O
2.134
f1 (ppm)

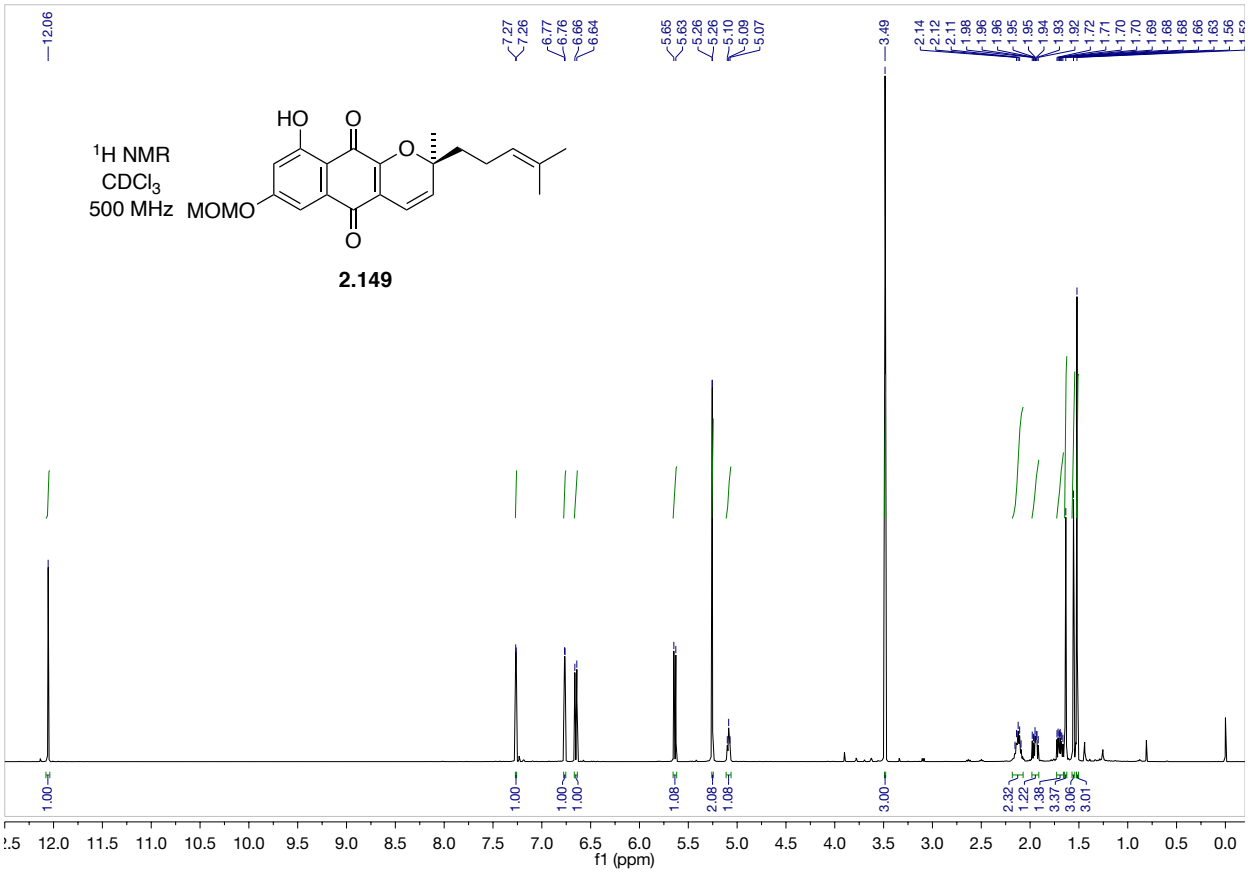
^{1}H NMR
$CDCl_3$
500 MHz
HO
O
O
MOMO
O
2.149
f1 (ppm)

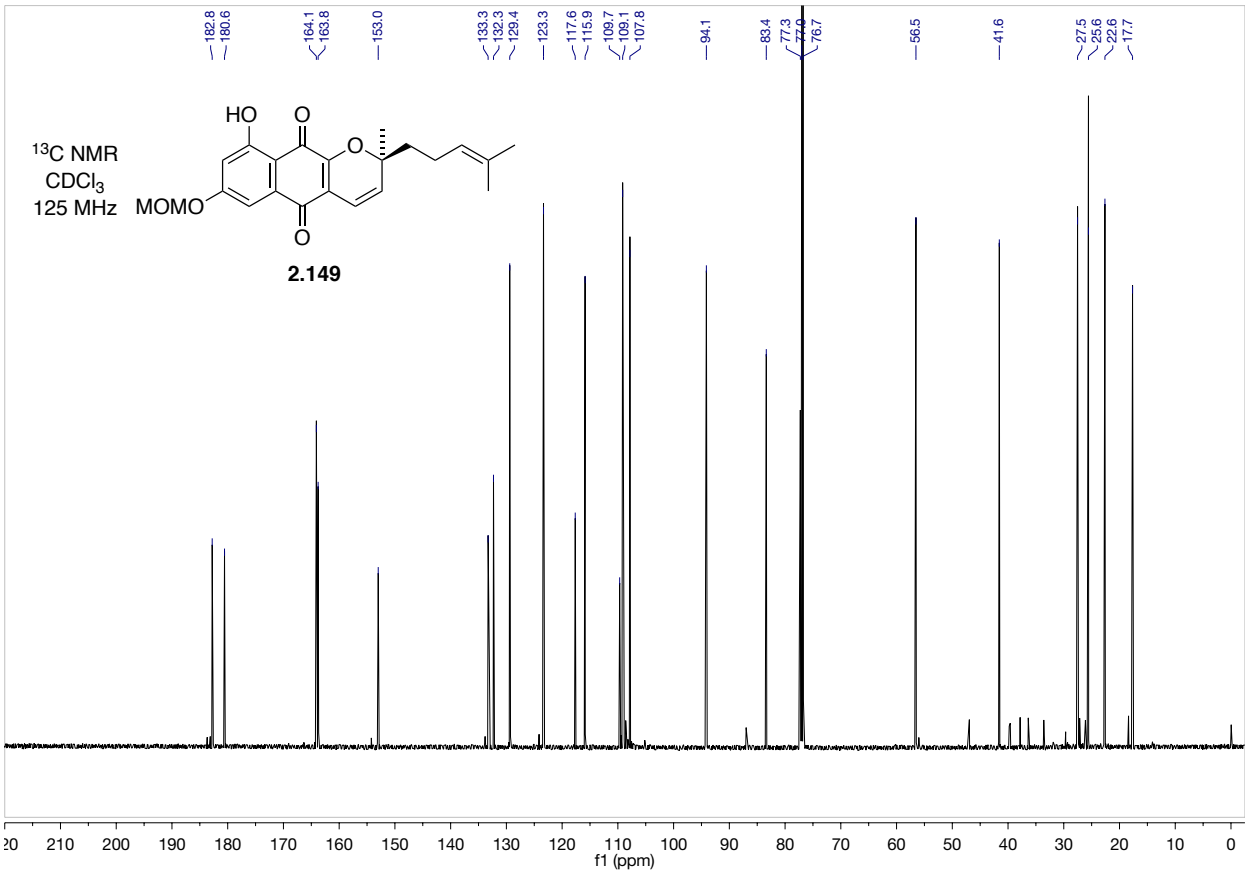
^{13}C NMR
$CDCl_3$
125 MHz
HO
O
O
MOMO
O
2.149
f1 (ppm)

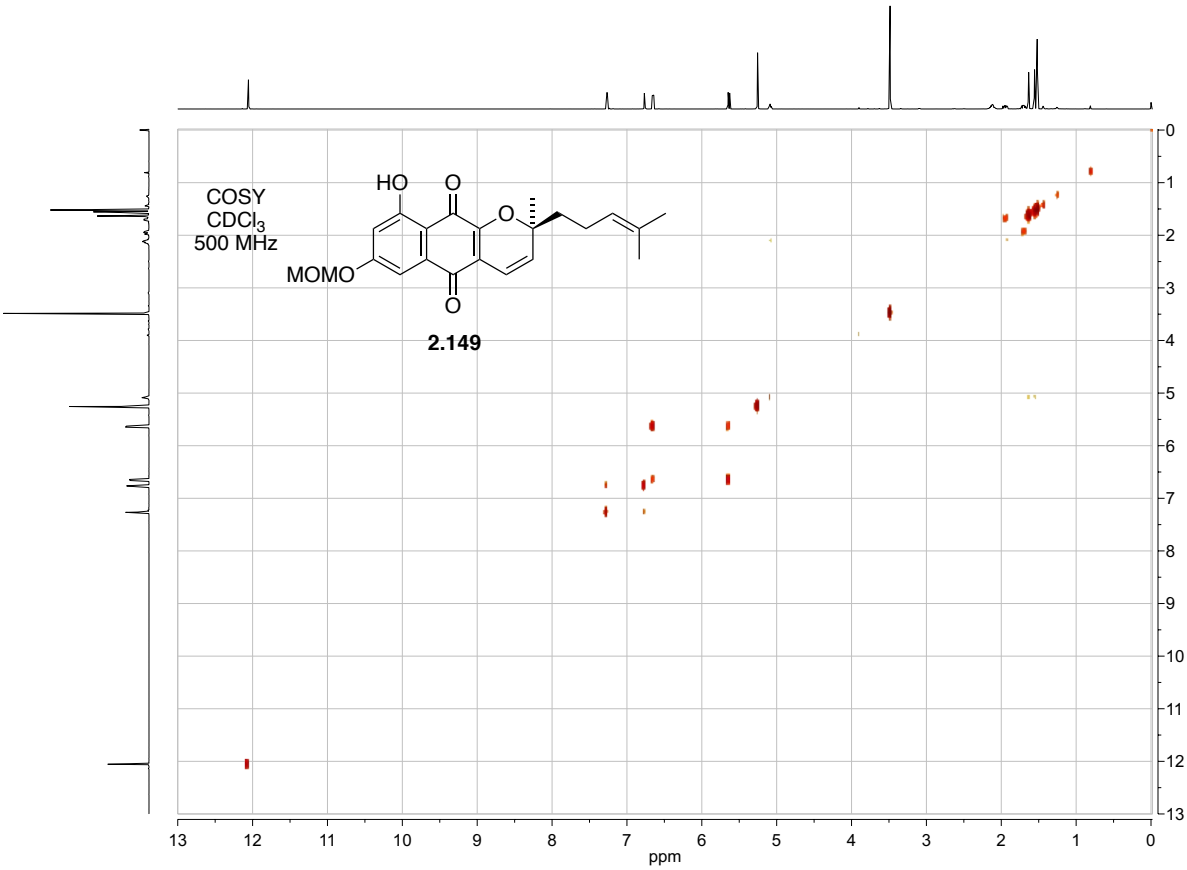
COSY
CDCl3
500 MHz
HO
O
O
MOMO
O
2.149
ppm

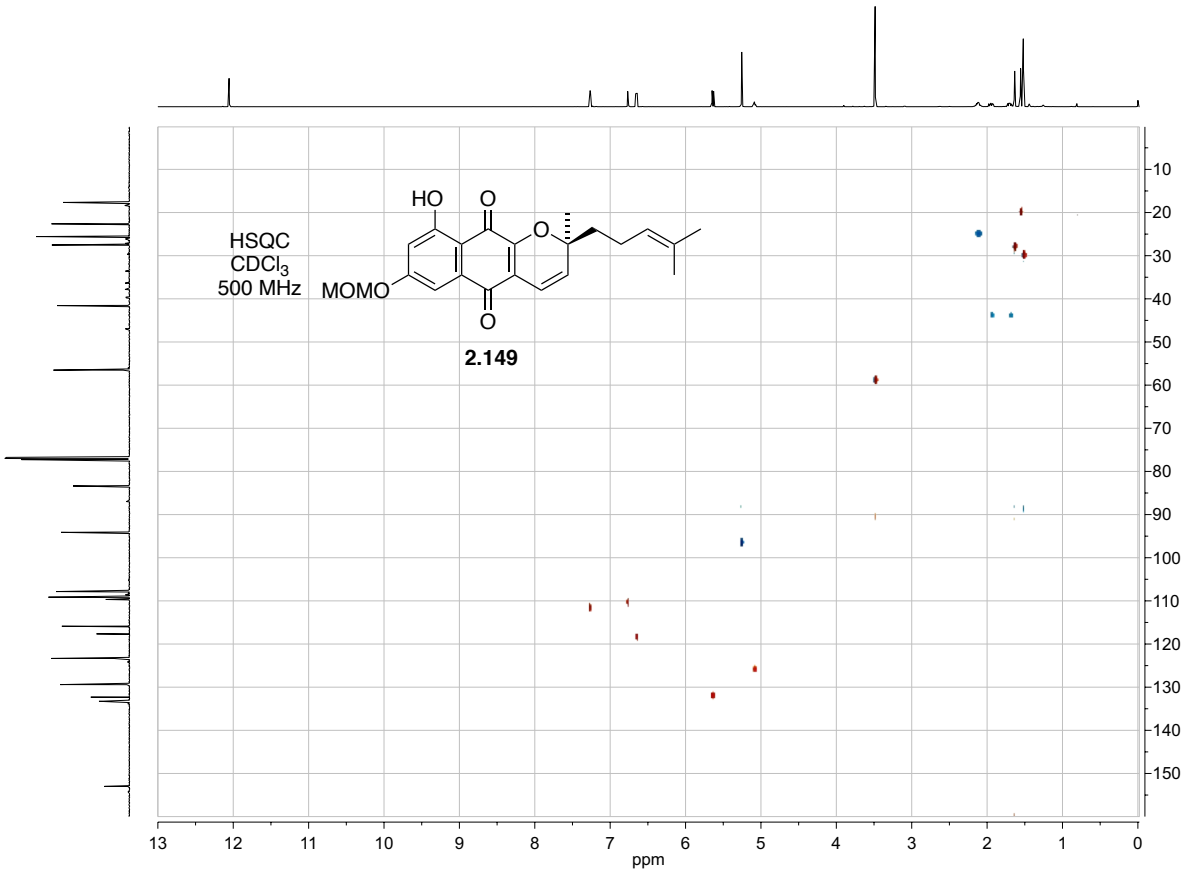
HSQC
CDCl3
500 MHz
HO
O
O
MOMO
O
2.149
ppm

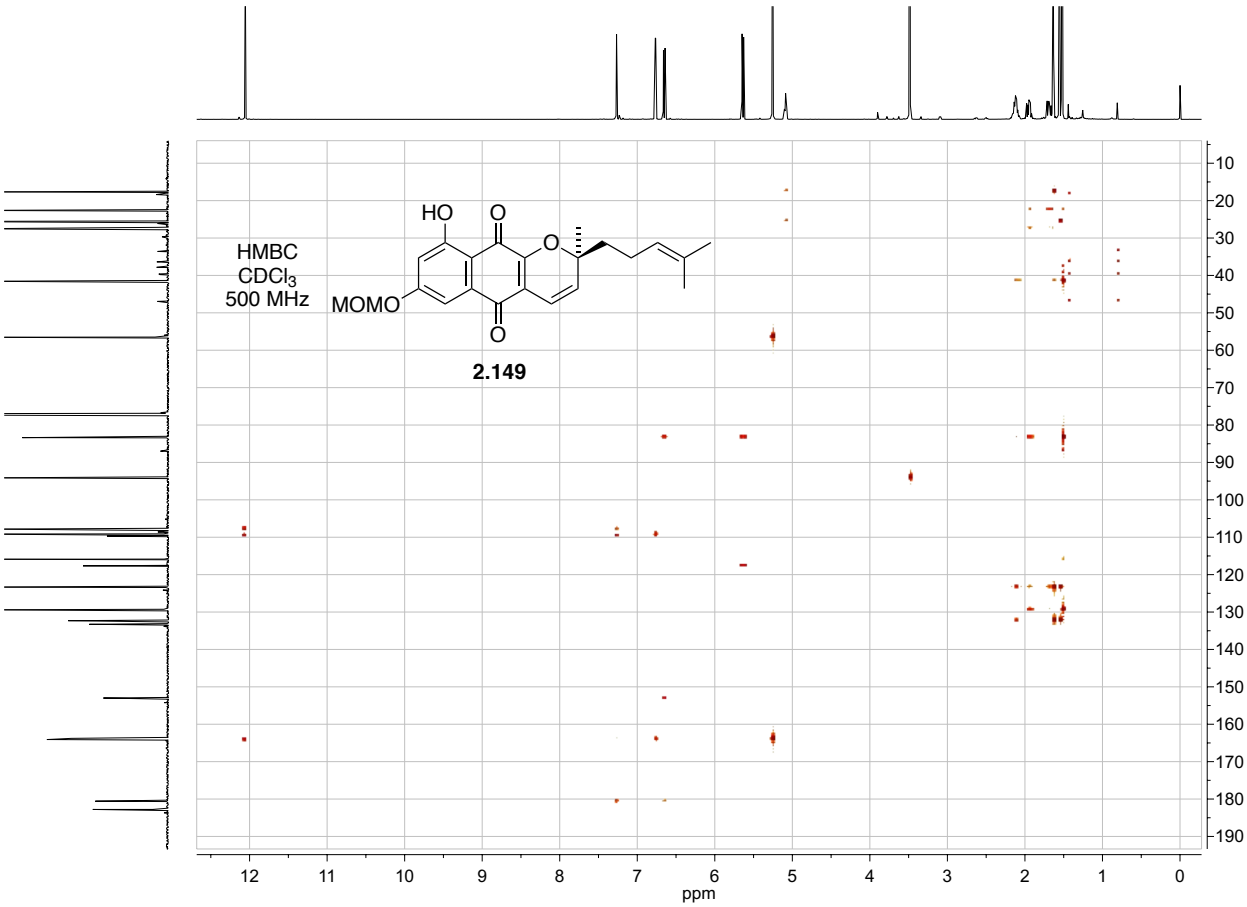
HMBC
CDCl3
500 MHz
HO
O
O
MOMO
O
2.149
ppm

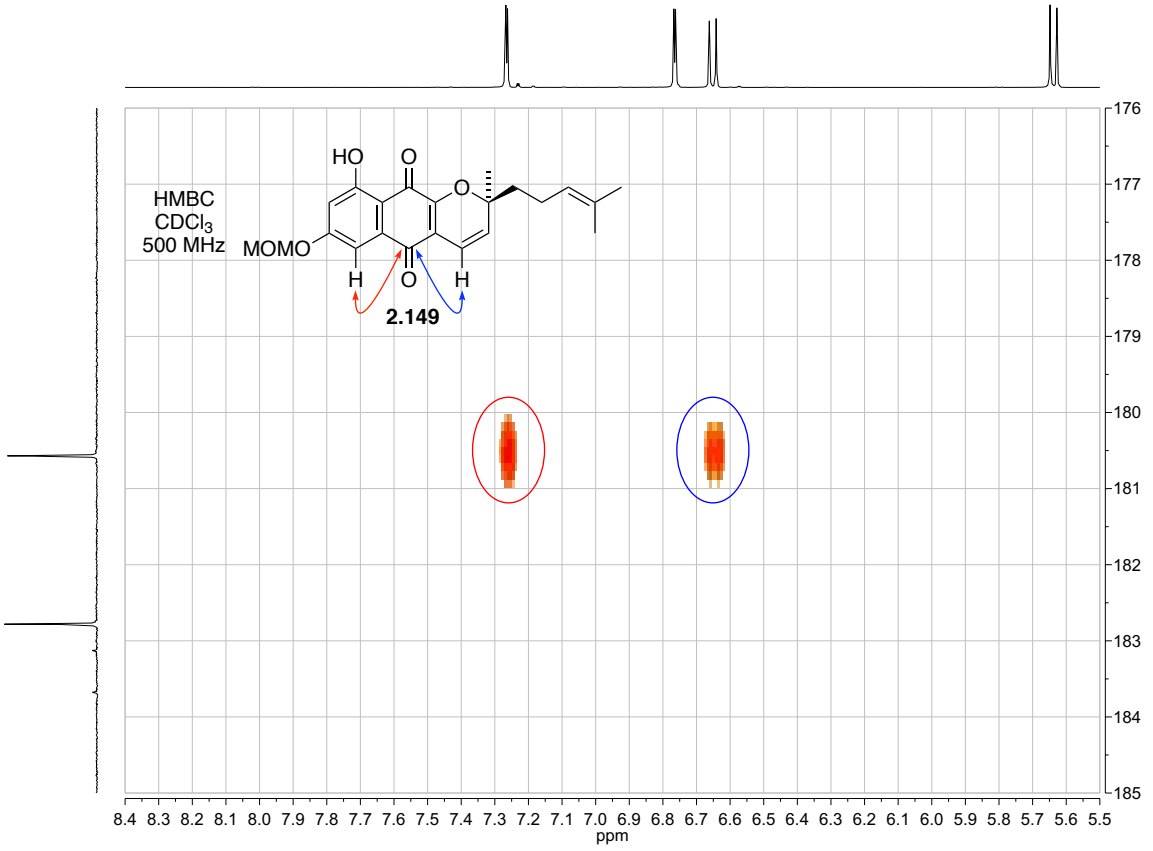
HMBC
CDCl3
500 MHz
HO
O
O
MOMO
H
O
H
2.149
ppm

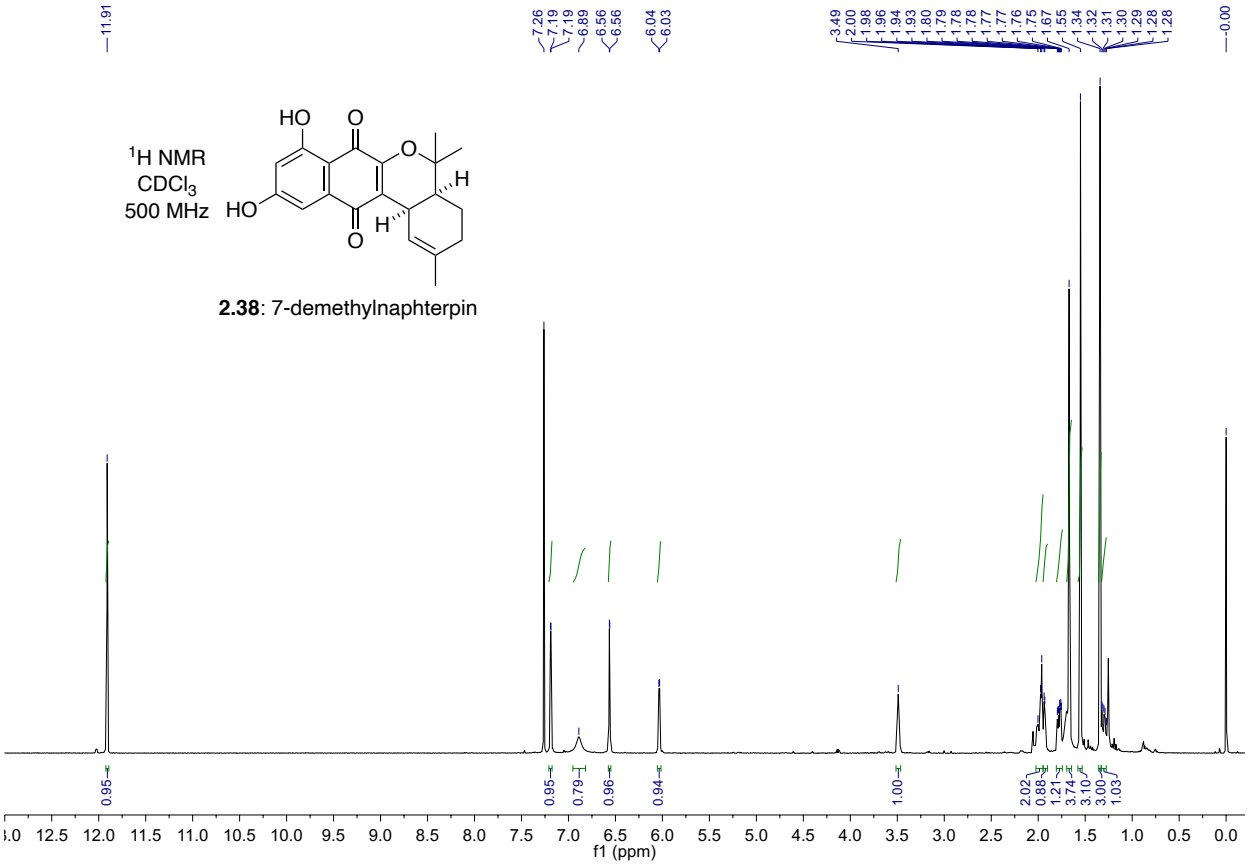
^{1}H NMR
$CDCl_3$
500 MHz
HO
O
O
O
H
HO
H
2.38: 7-demethylnaphterpin
f1 (ppm)

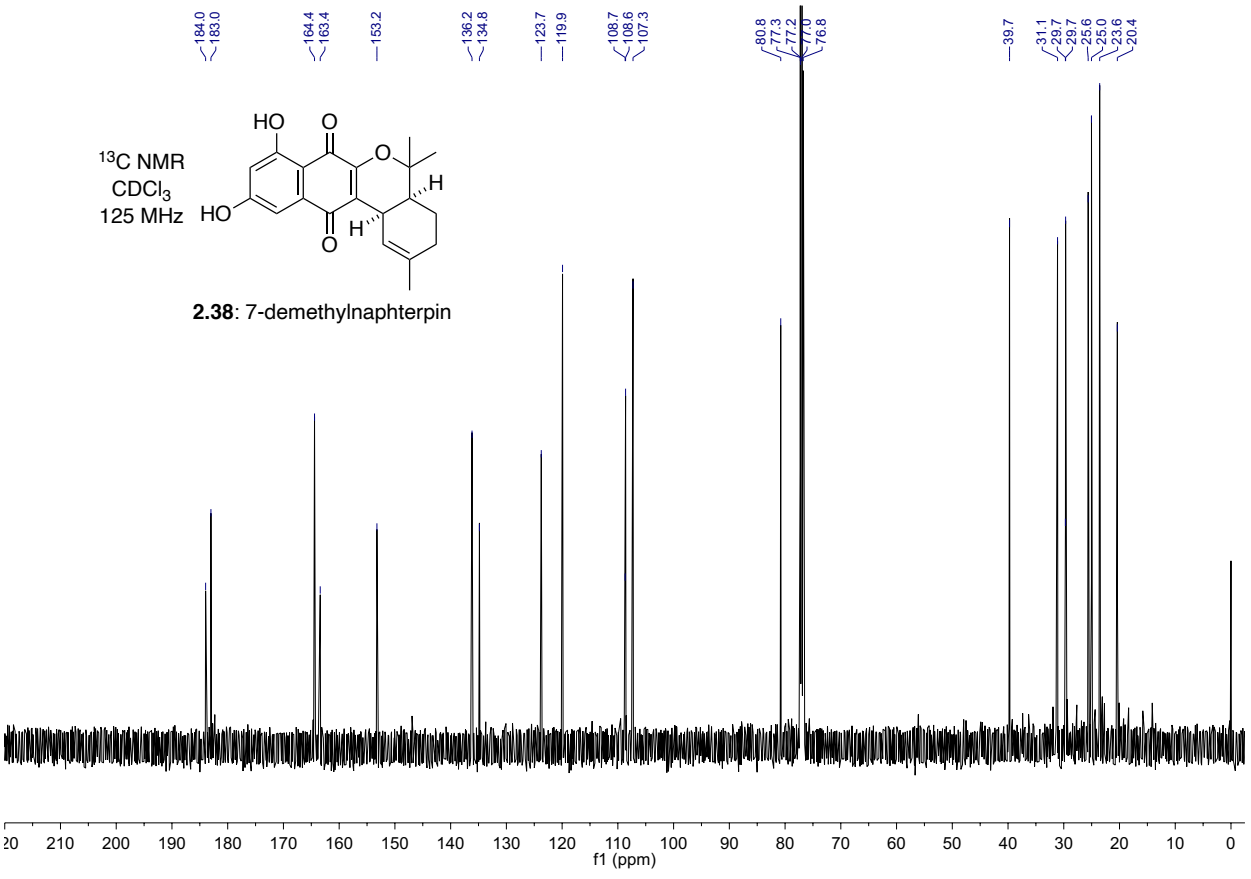
^{13}C NMR
$CDCl_3$
125 MHz
HO
O
O
O
H
HO
H
2.38: 7-demethylnaphterpin
f1 (ppm)

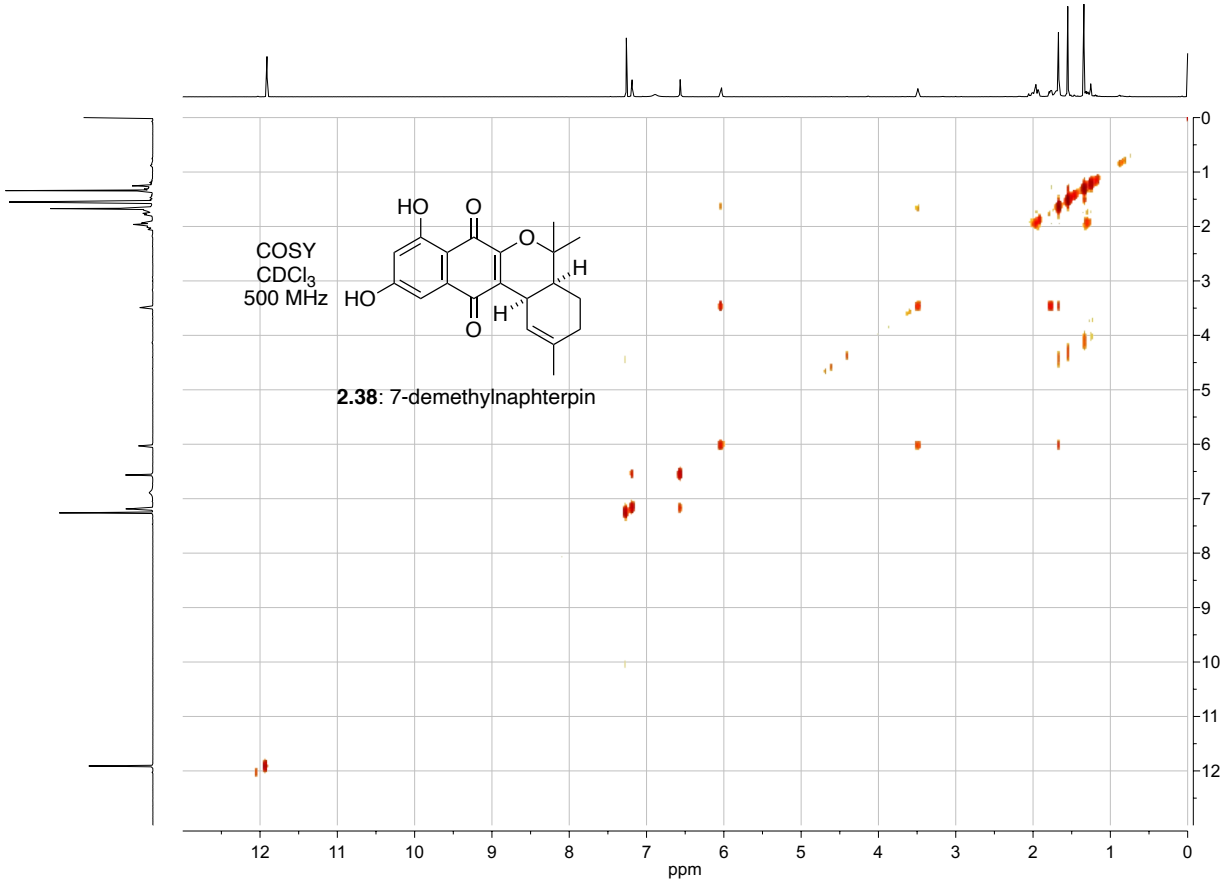
COSY
CDCl3
500 MHz
HO
O
O
H
HO
H
O
2.38: 7-demethylnaphterpin
ppm

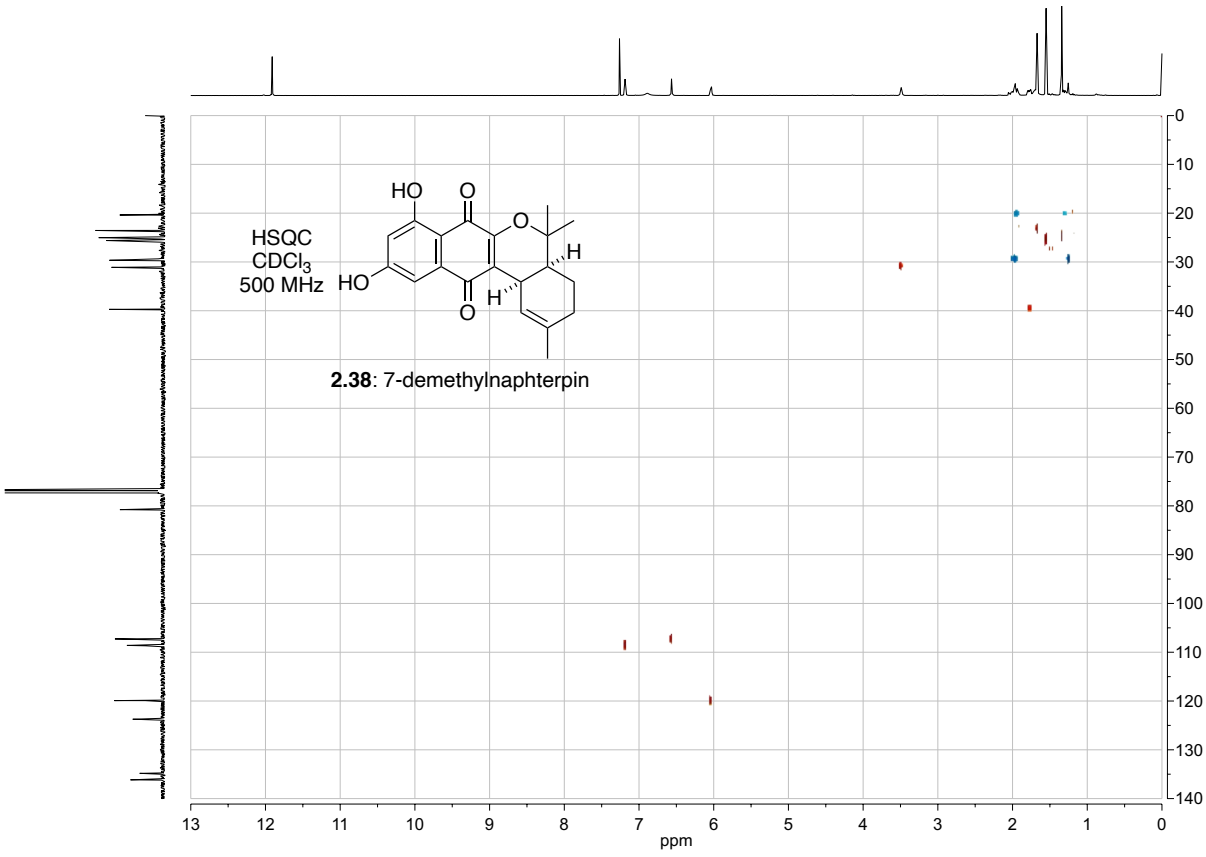
HSQC
CDCl3
500 MHz
HO
O
O
H
HO
H
O
2.38: 7-demethylnaphterpin
ppm

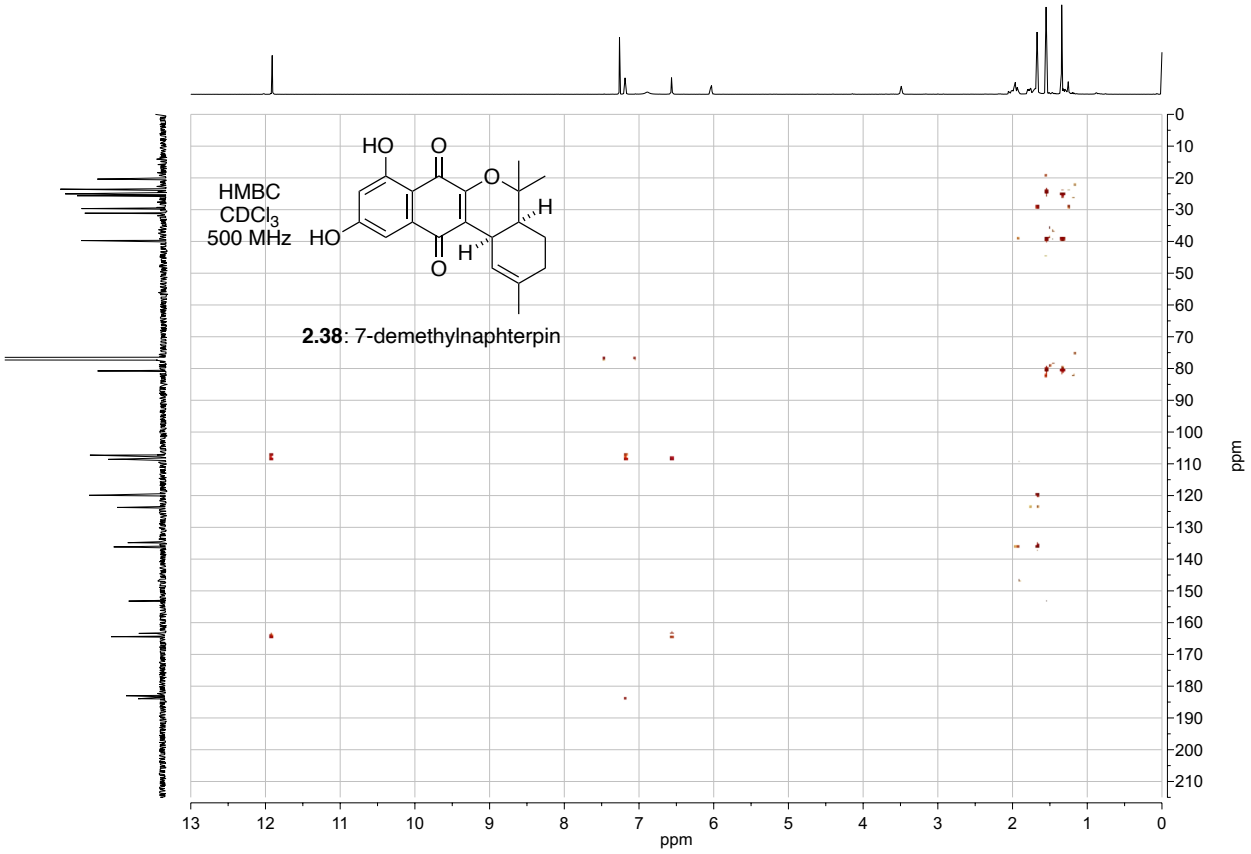
HMBC
CDCl3
500 MHz
HO
O
O
H
HO
H
O
2.38: 7-demethylnaphterpin
ppm
ppm

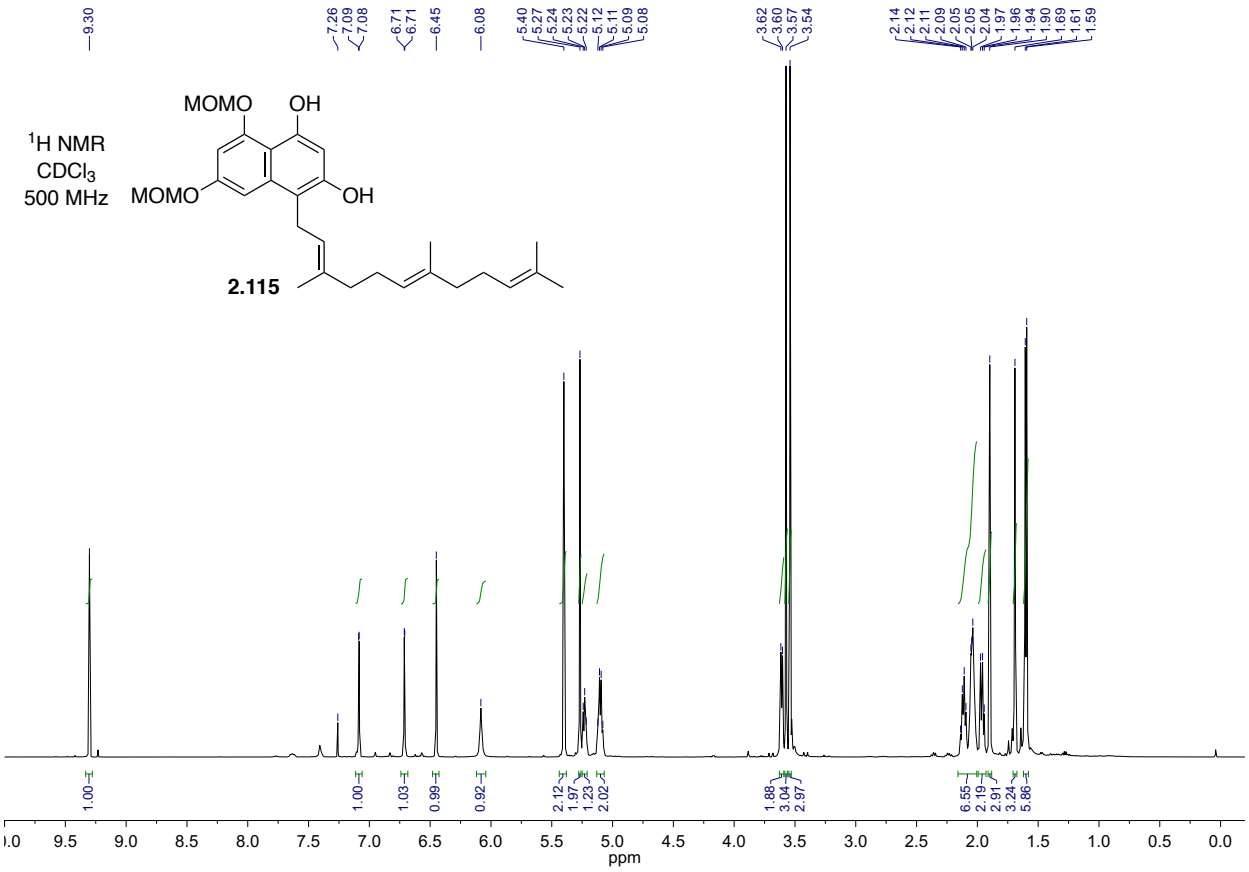
9.30
7.26
7.09
7.08
6.71
6.71
6.45
6.08
5.40
5.27
5.24
5.23
5.22
5.12
5.11
5.09
5.08
3.62
3.60
3.57
3.54
2.14
2.12
2.11
2.09
2.05
2.05
2.04
1.97
1.96
1.94
1.90
1.69
1.61
1.59
1H NMR
CDCl3
500 MHz
MOMO
OH
MOMO
OH
2.115
1.00
1.00
1.03
0.99
0.92
2.12
1.97
1.23
2.02
1.88
3.04
2.97
6.55
2.19
2.91
3.24
5.86
ppm

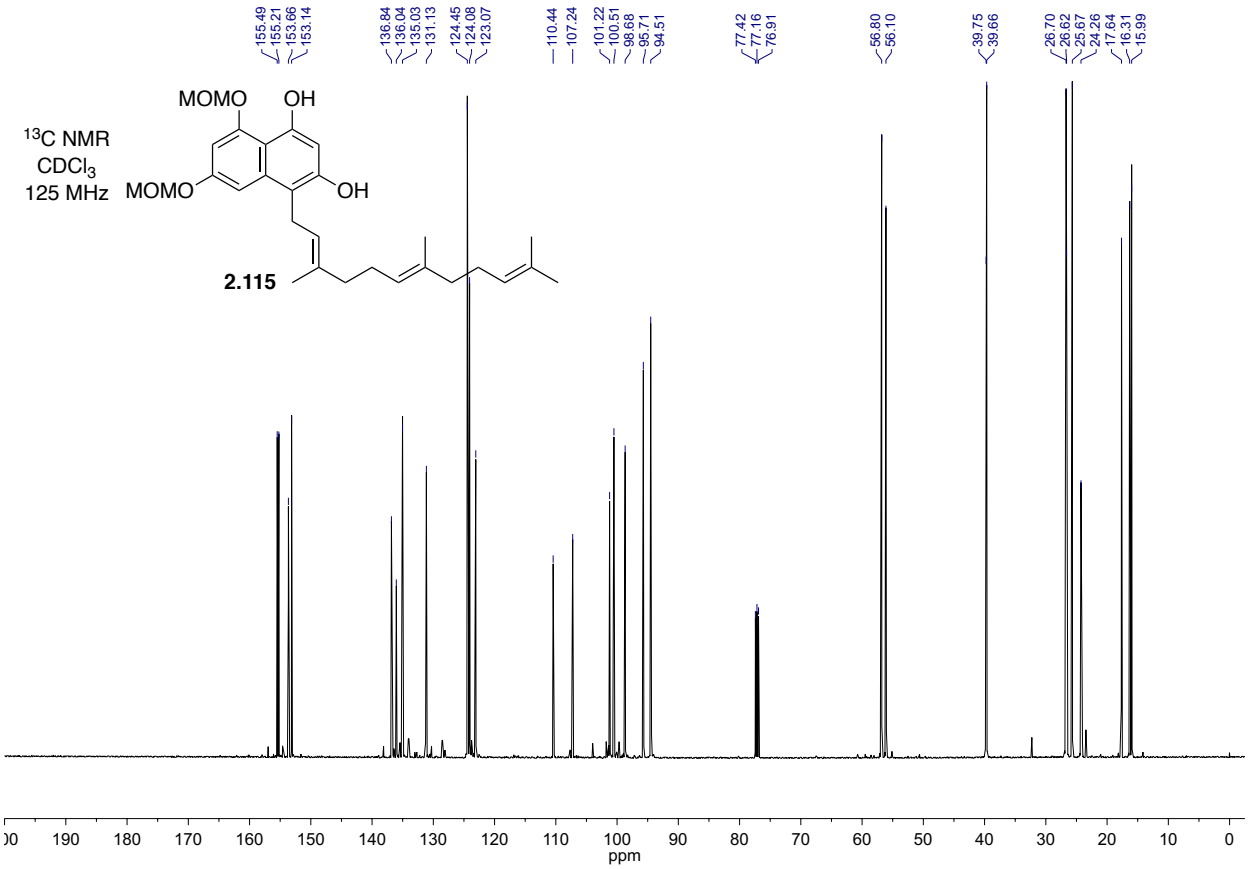
155.49
155.21
153.66
153.14
136.84
136.04
135.03
131.13
124.45
124.08
123.07
110.44
107.24
101.22
100.51
98.68
95.71
94.51
77.42
77.16
76.91
56.80
56.10
39.75
39.66
26.70
26.62
25.67
24.26
17.64
16.31
15.99
13C NMR
CDCl3
125 MHz
MOMO
OH
MOMO
OH
2.115
ppm

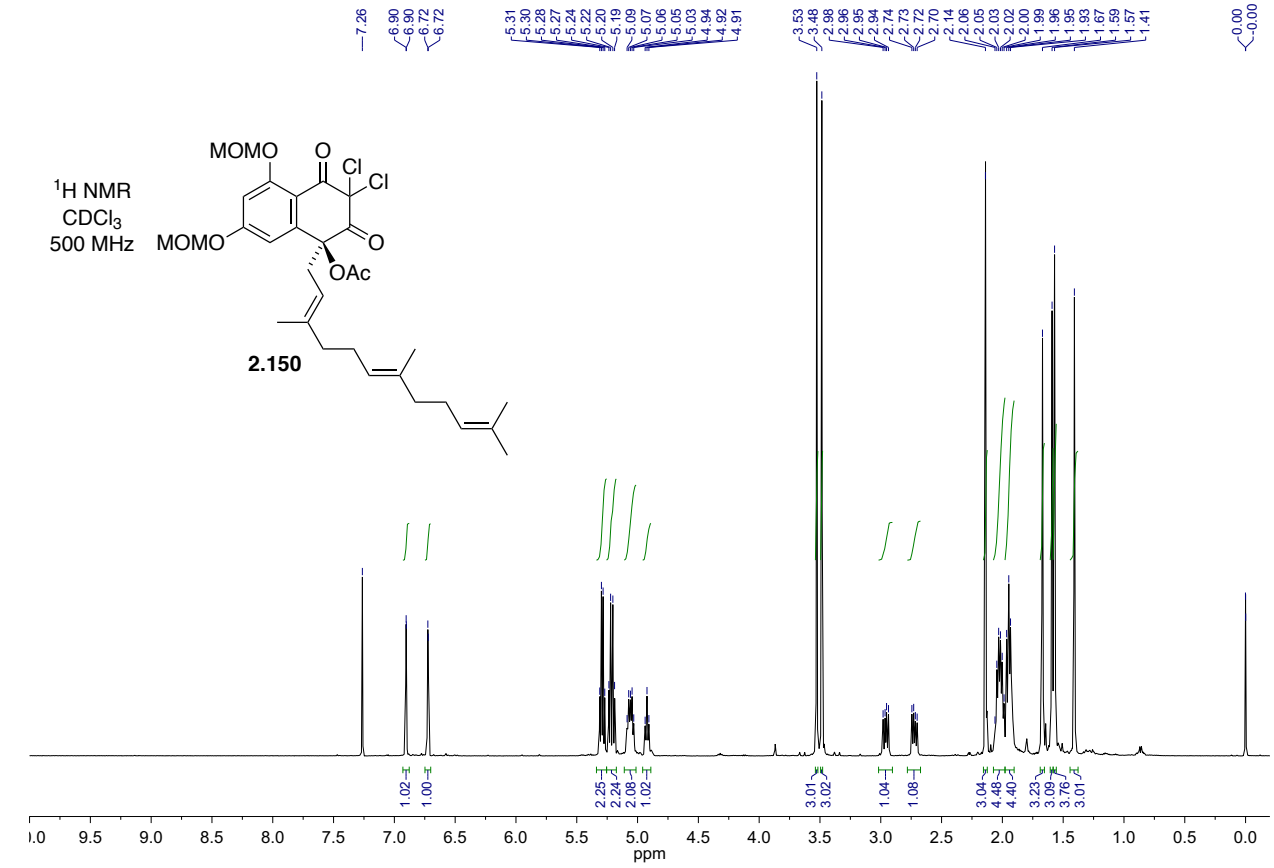
^{1}H NMR
$CDCl_3$
500 MHz
MOMO
MOMO
Cl
Cl
O
O
OAc
2.150
ppm

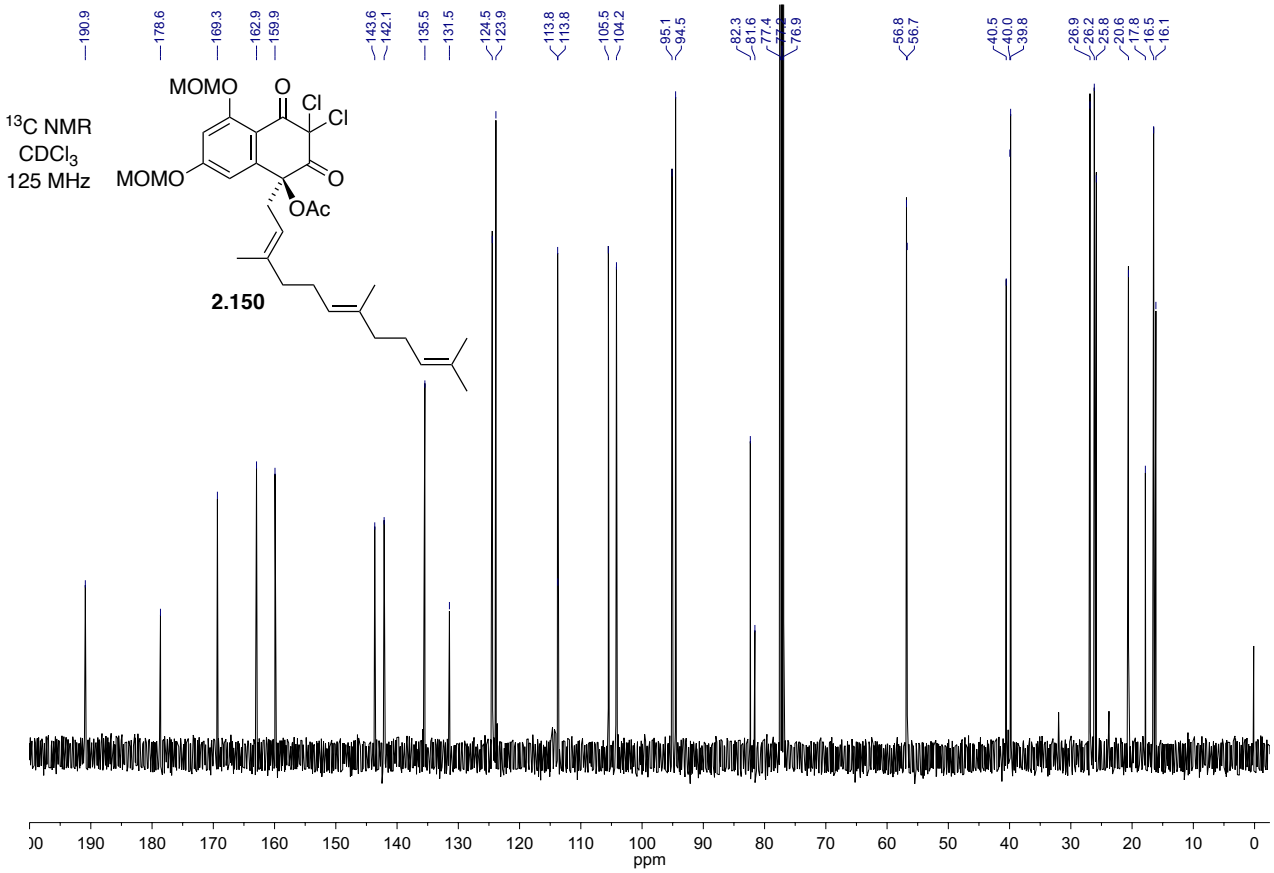
^{13}C NMR
$CDCl_3$
125 MHz
MOMO
MOMO
Cl
Cl
O
O
OAc
2.150
ppm

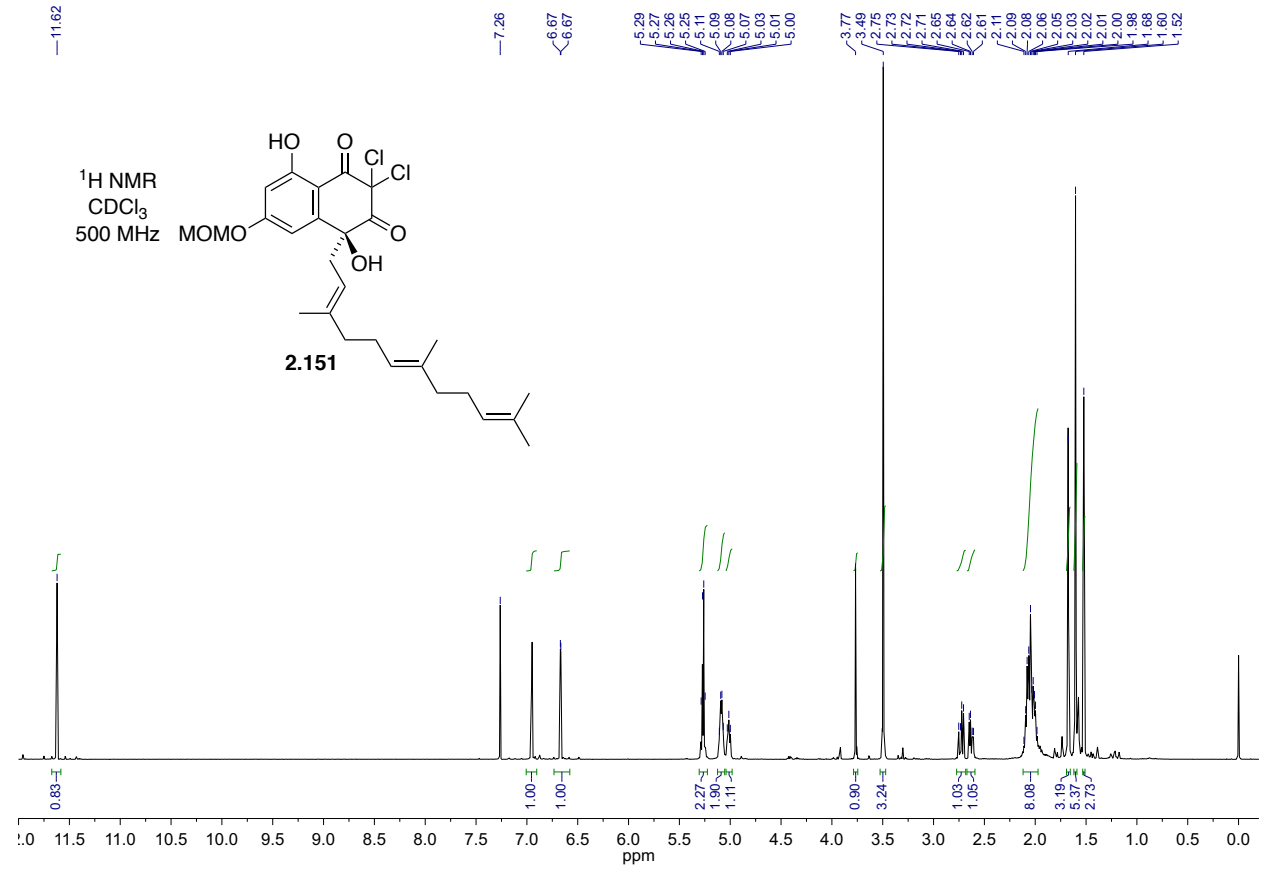
^{1}H NMR
$CDCl_3$
500 MHz
HO
O
Cl
Cl
MOMO
O
OH
2.151
ppm

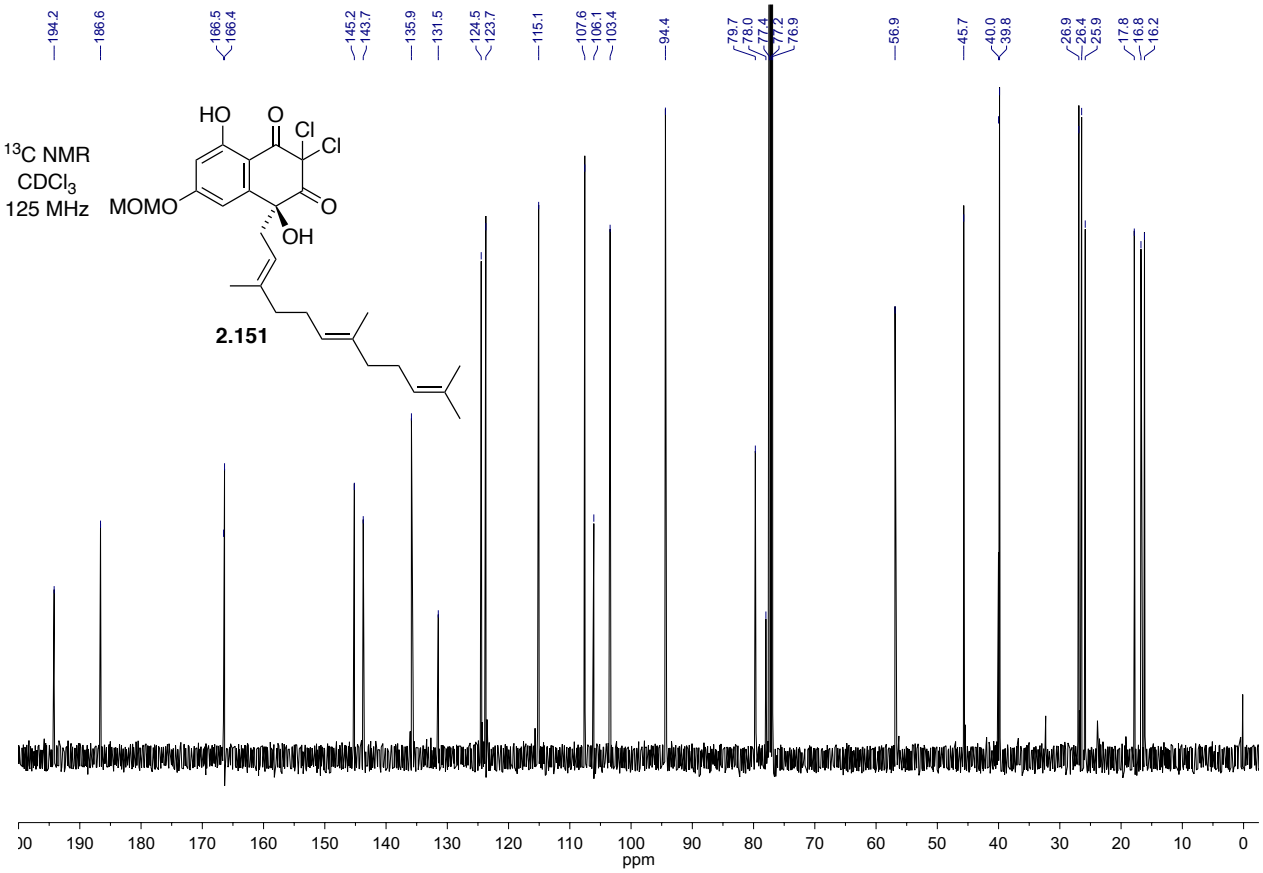
^{13}C NMR
$CDCl_3$
125 MHz
HO
O
Cl
Cl
MOMO
O
OH
2.151
ppm

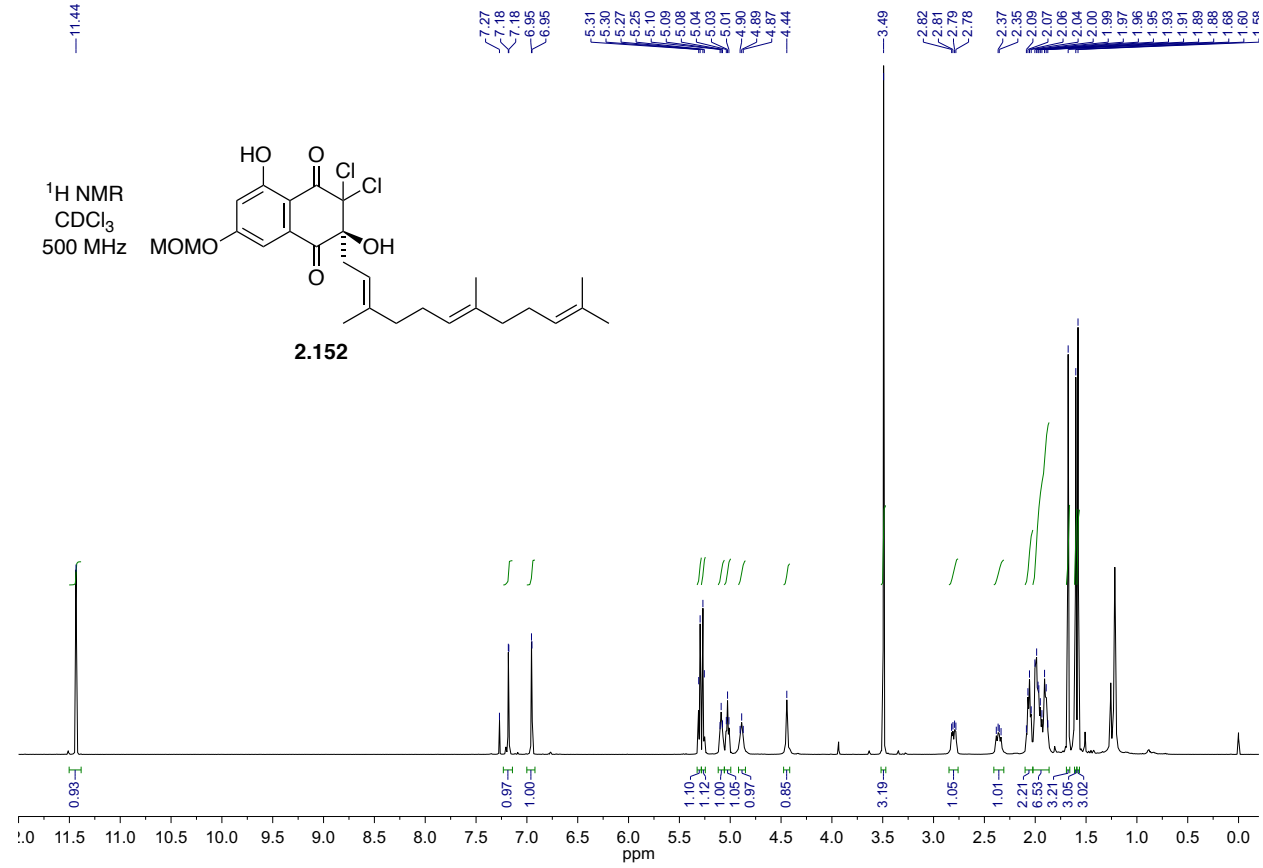
^{1}H NMR
$CDCl_3$
500 MHz
HO
O
Cl
Cl
MOMO
OH
O
2.152
ppm

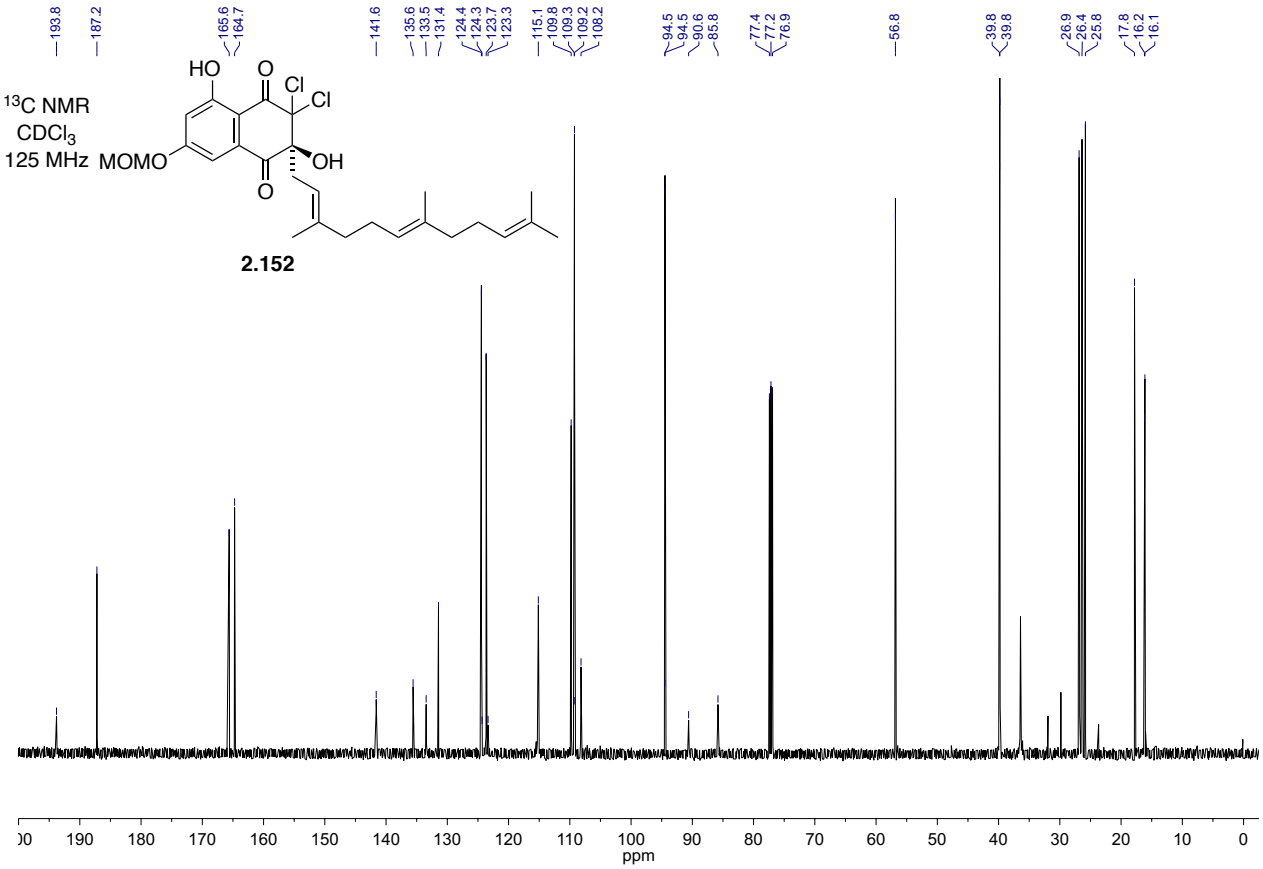
^{13}C NMR
$CDCl_3$
125 MHz
HO
O
Cl
Cl
MOMO
OH
O
2.152
ppm

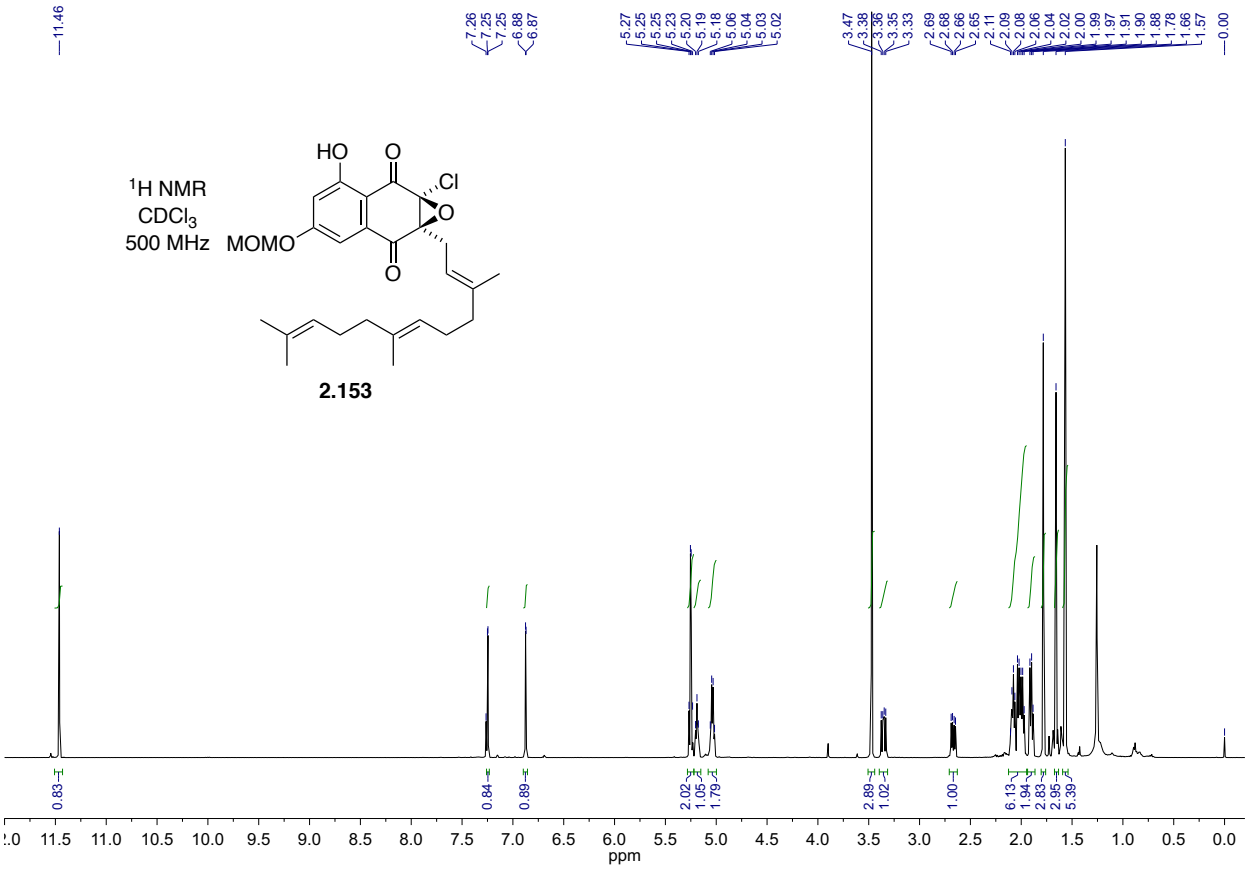
^{1}H NMR
$CDCl_3$
500 MHz
HO
O
Cl
O
MOMO
O
2.153
ppm

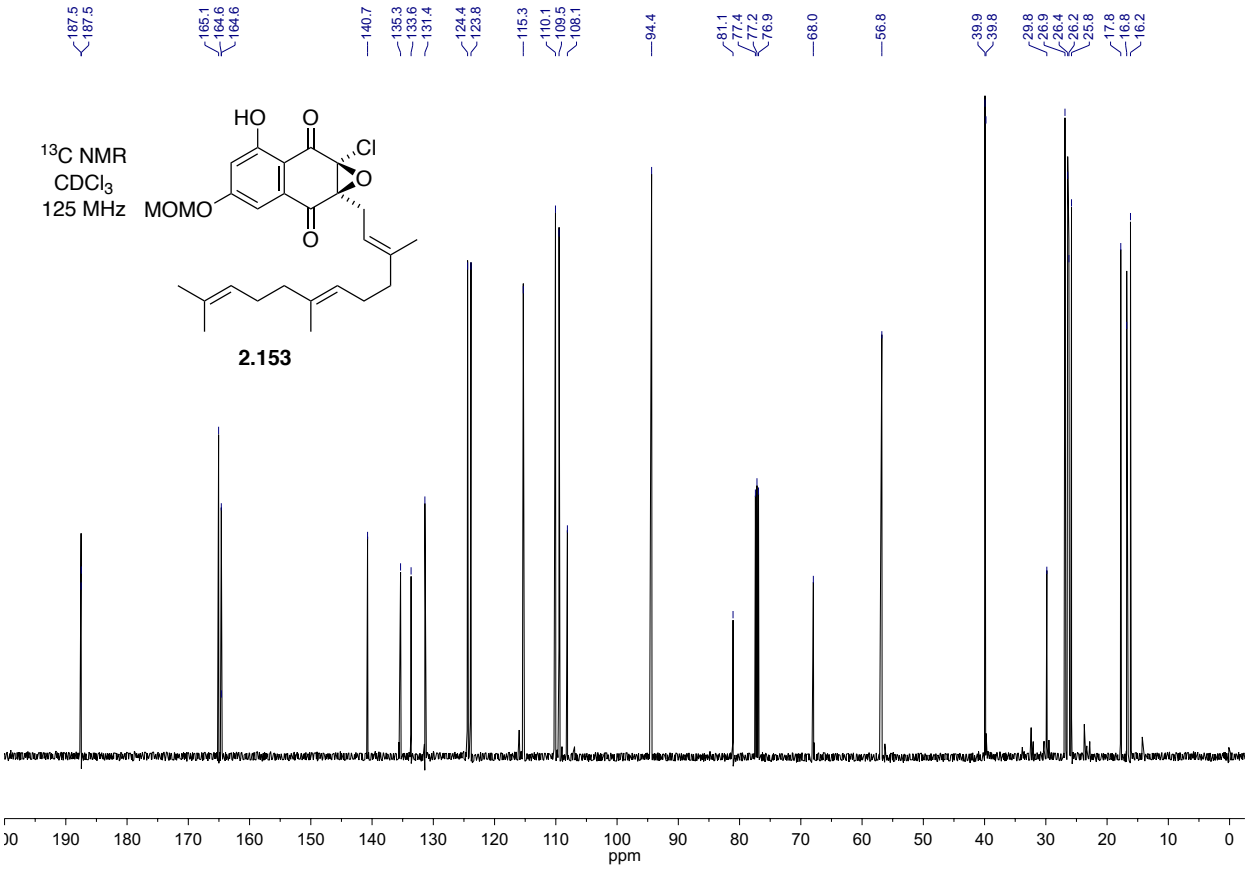
^{13}C NMR
$CDCl_3$
125 MHz
HO
O
Cl
O
MOMO
O
2.153
ppm

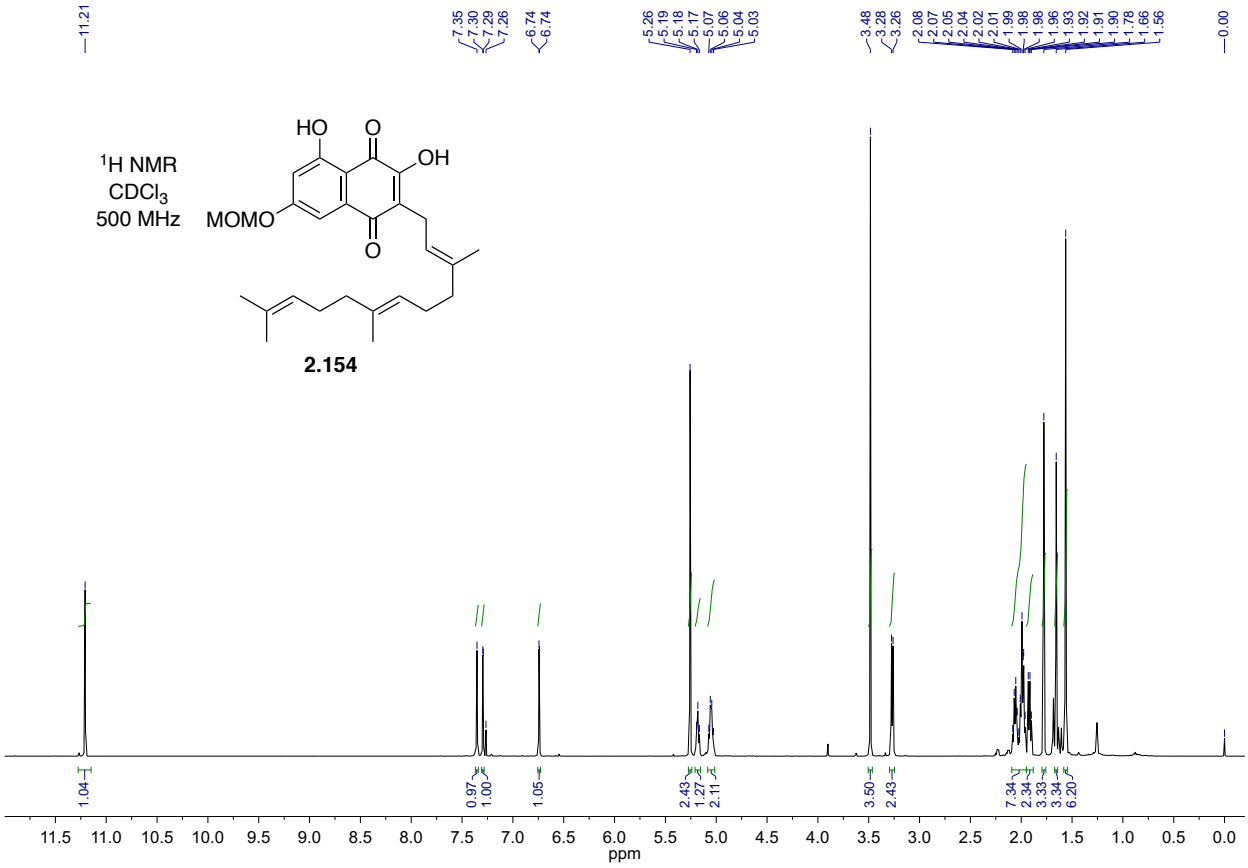
11.21
7.35
7.30
7.29
7.26
6.74
6.74
5.26
5.19
5.18
5.17
5.07
5.06
5.04
5.03
3.48
3.28
3.26
2.08
2.07
2.05
2.04
2.02
2.01
1.99
1.98
1.98
1.96
1.93
1.92
1.91
1.90
1.78
1.66
1.56
0.00
1H NMR
CDCl3
500 MHz
HO
O
OH
MOMO
O
2.154
1.04
0.97
1.00
1.05
2.43
1.27
2.11
3.50
2.43
7.34
2.34
3.33
3.34
6.20
11.5 11.0 10.5 10.0 9.5 9.0 8.5 8.0 7.5 7.0 6.5 6.0 5.5 5.0 4.5 4.0 3.5 3.0 2.5 2.0 1.5 1.0 0.5 0.0
ppm

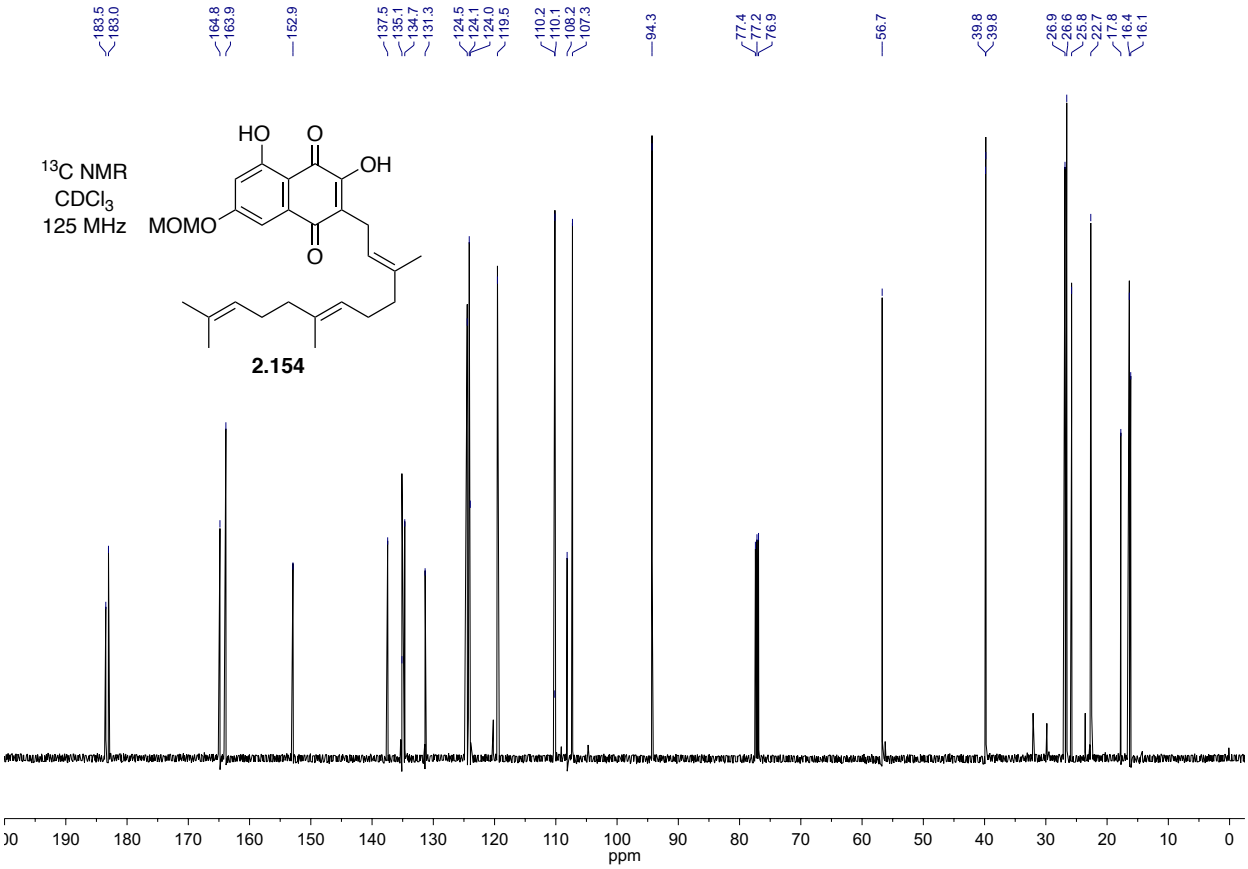
183.5
183.0
164.8
163.9
152.9
137.5
135.1
134.7
131.3
124.5
124.1
124.0
119.5
110.2
110.1
108.2
107.3
94.3
77.4
77.2
76.9
56.7
39.8
39.8
26.9
26.6
25.8
22.7
17.8
16.4
16.1
13C NMR
CDCl3
125 MHz
HO
O
OH
MOMO
O
2.154
190 180 170 160 150 140 130 120 110 100 90 80 70 60 50 40 30 20 10 0
ppm

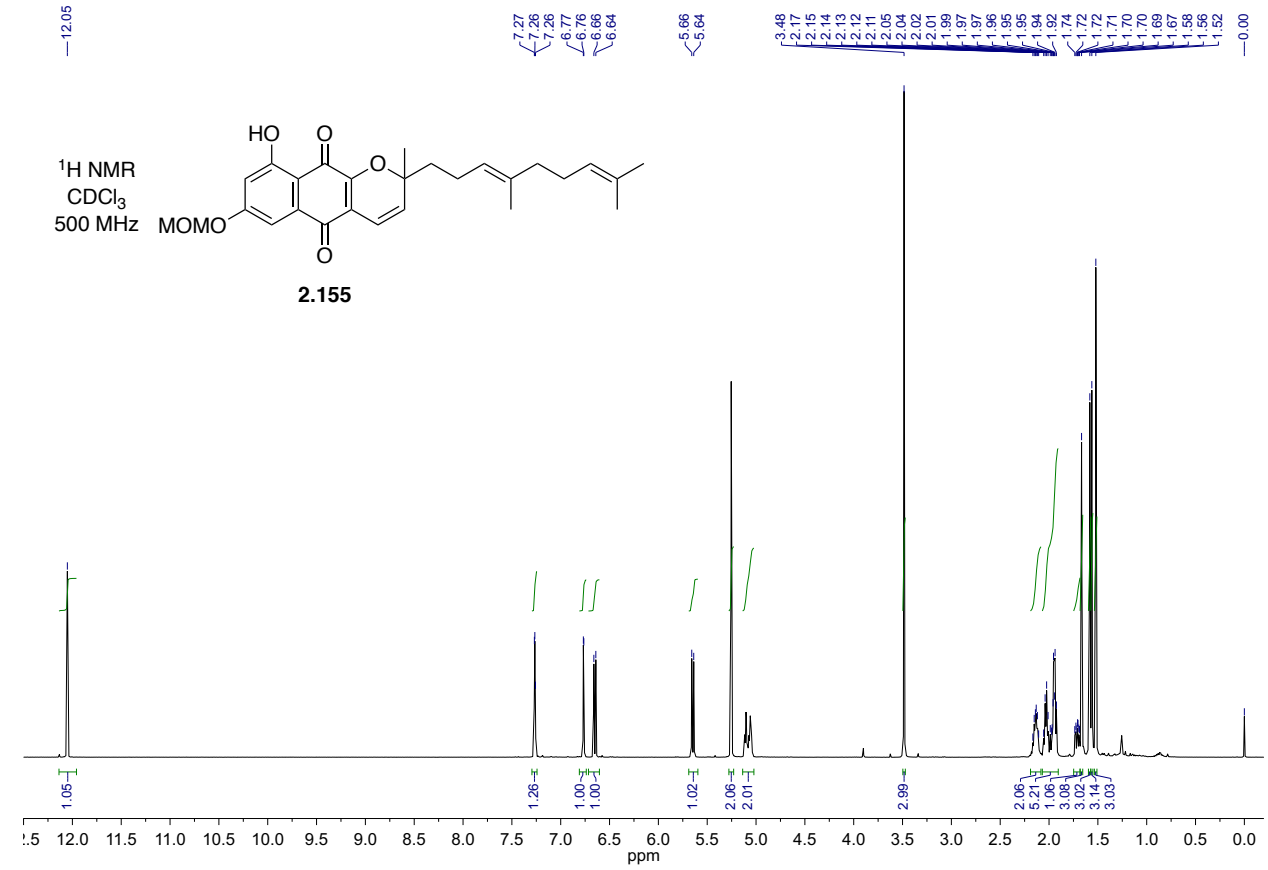
^{1}H NMR
$CDCl_3$
500 MHz
HO
O
O
MOMO
O
2.155
ppm

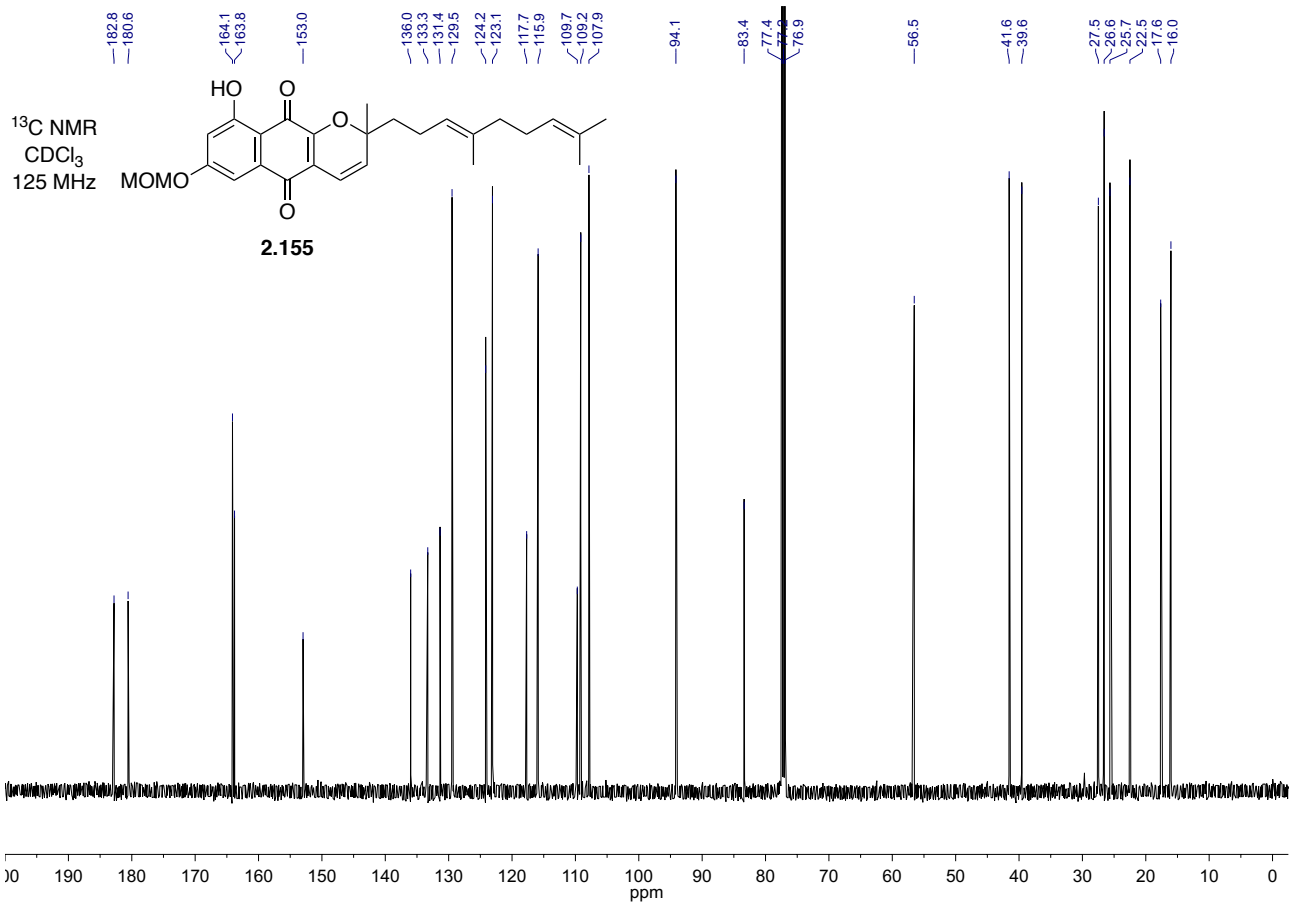
^{13}C NMR
$CDCl_3$
125 MHz
HO
O
O
MOMO
O
2.155
ppm

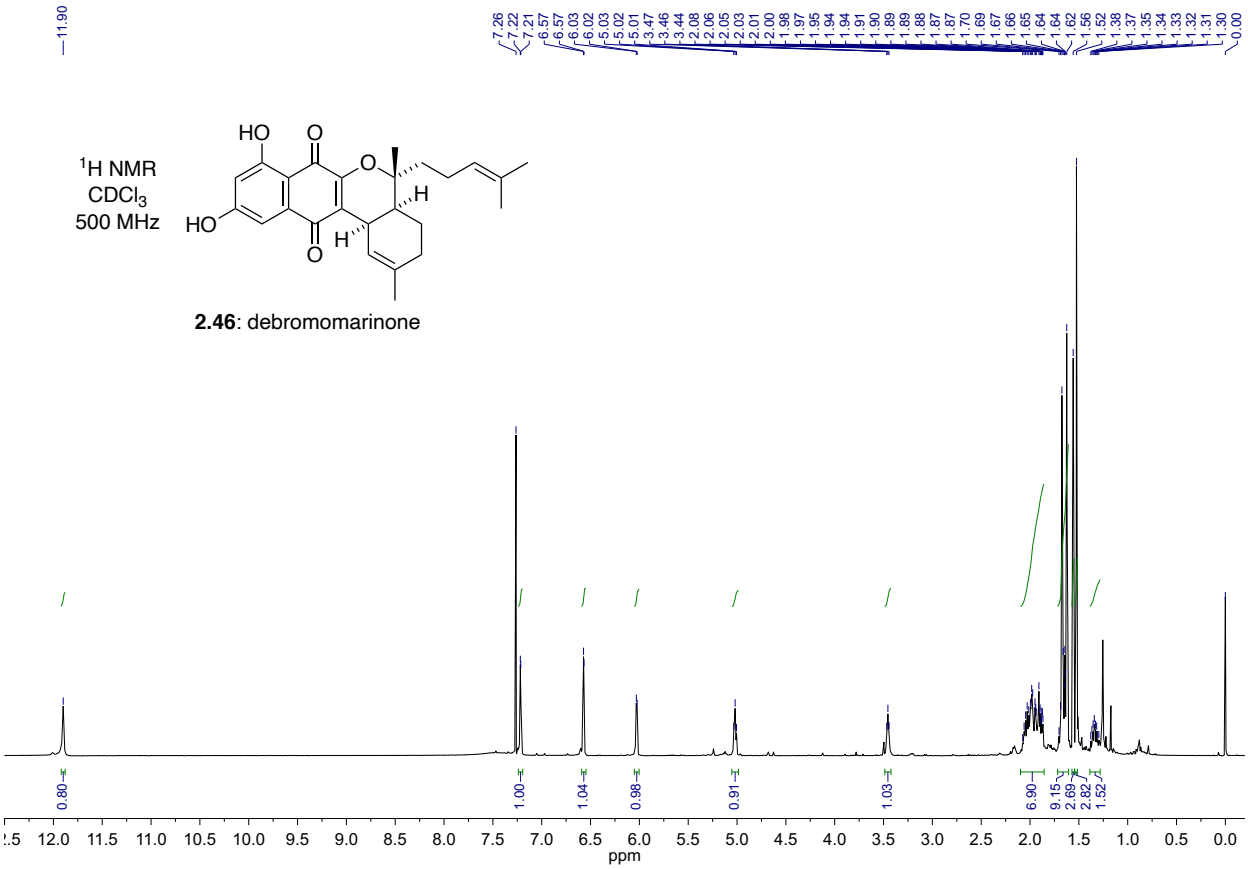

2.46: debromomarinone

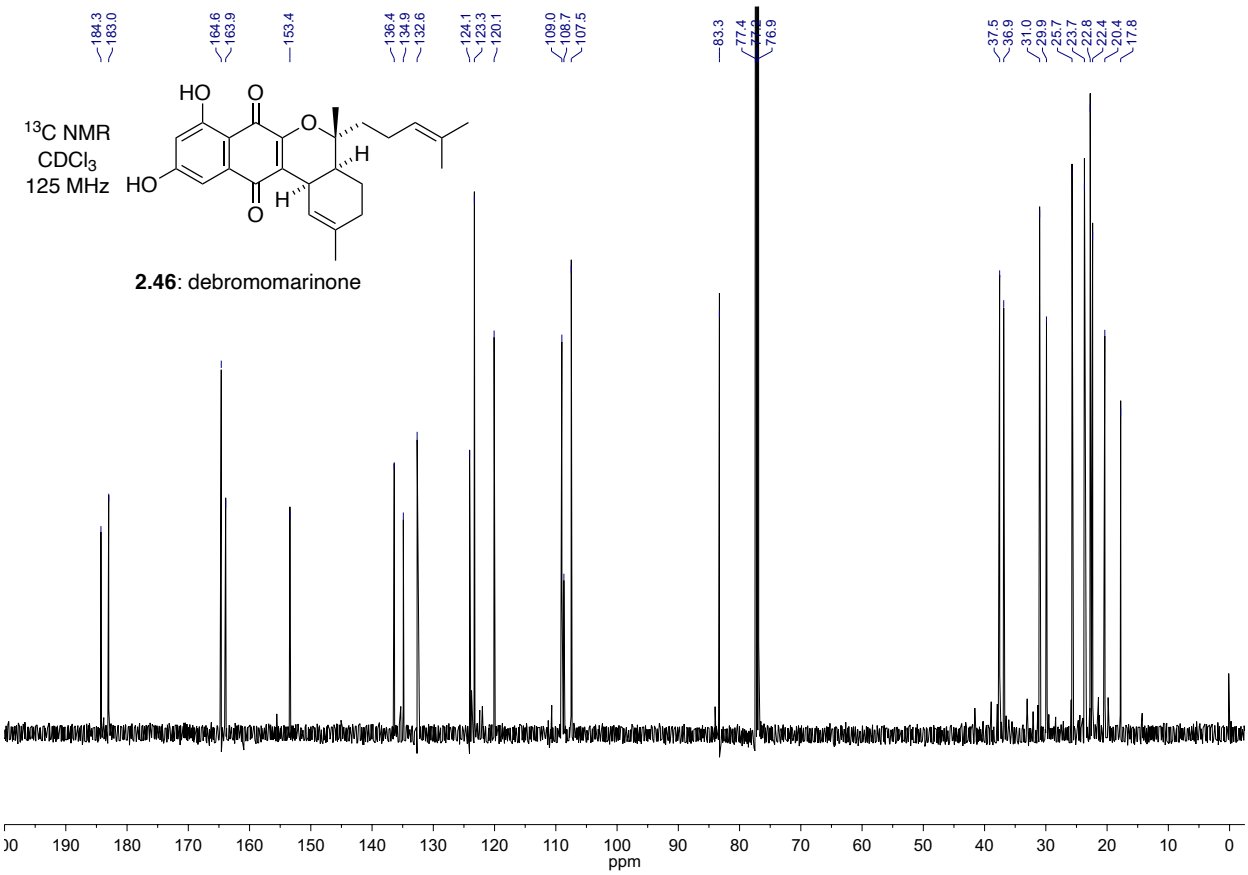

2.46: debromomarinone

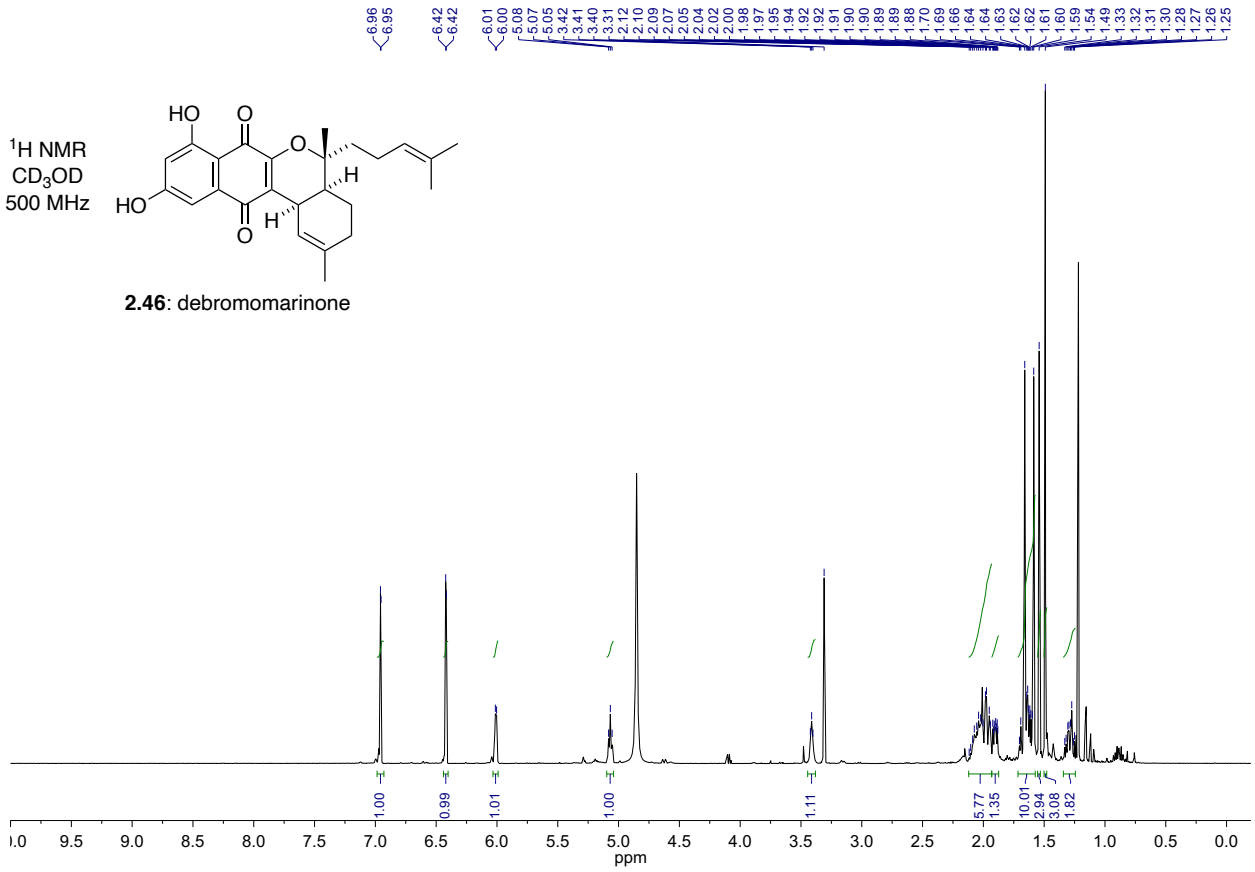

2.46: debromomarinone

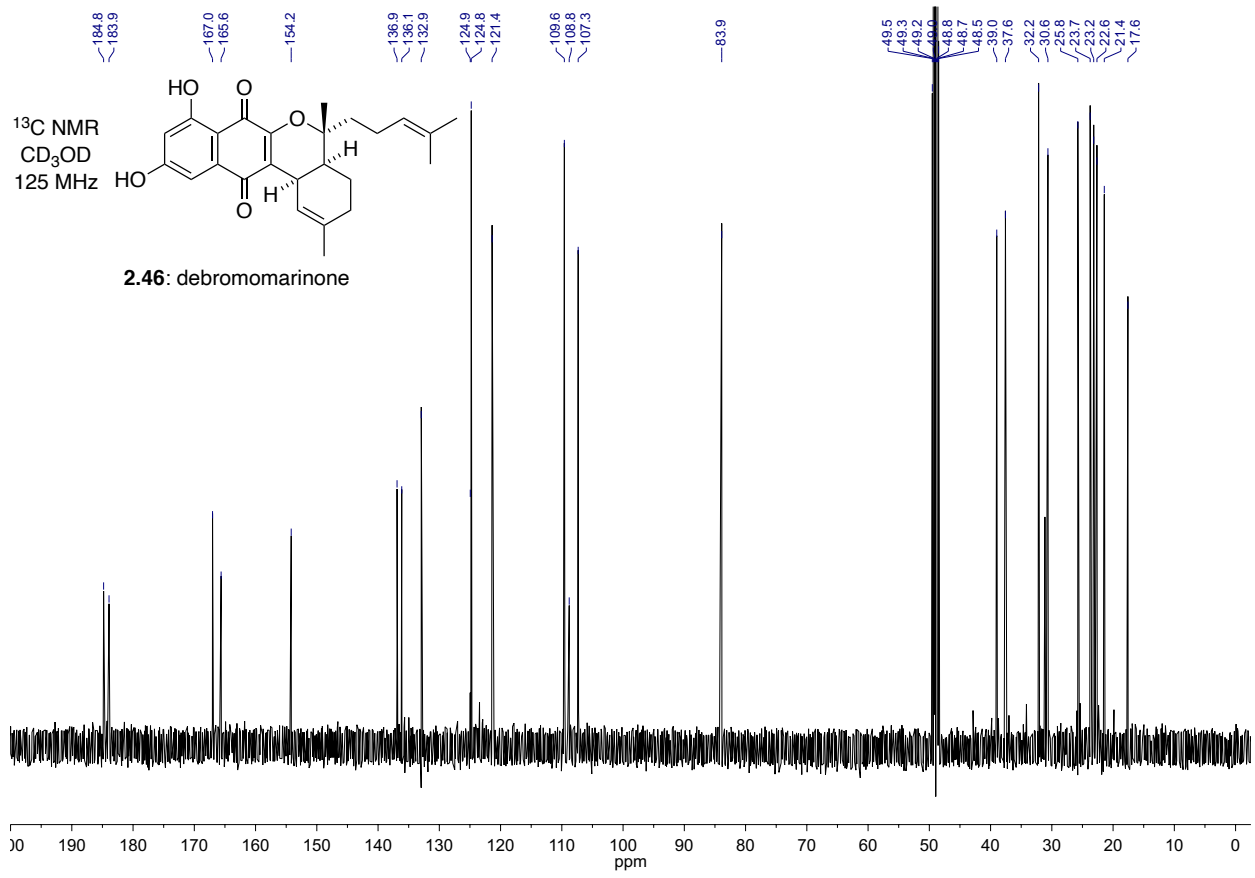

2.46: debromomarinone

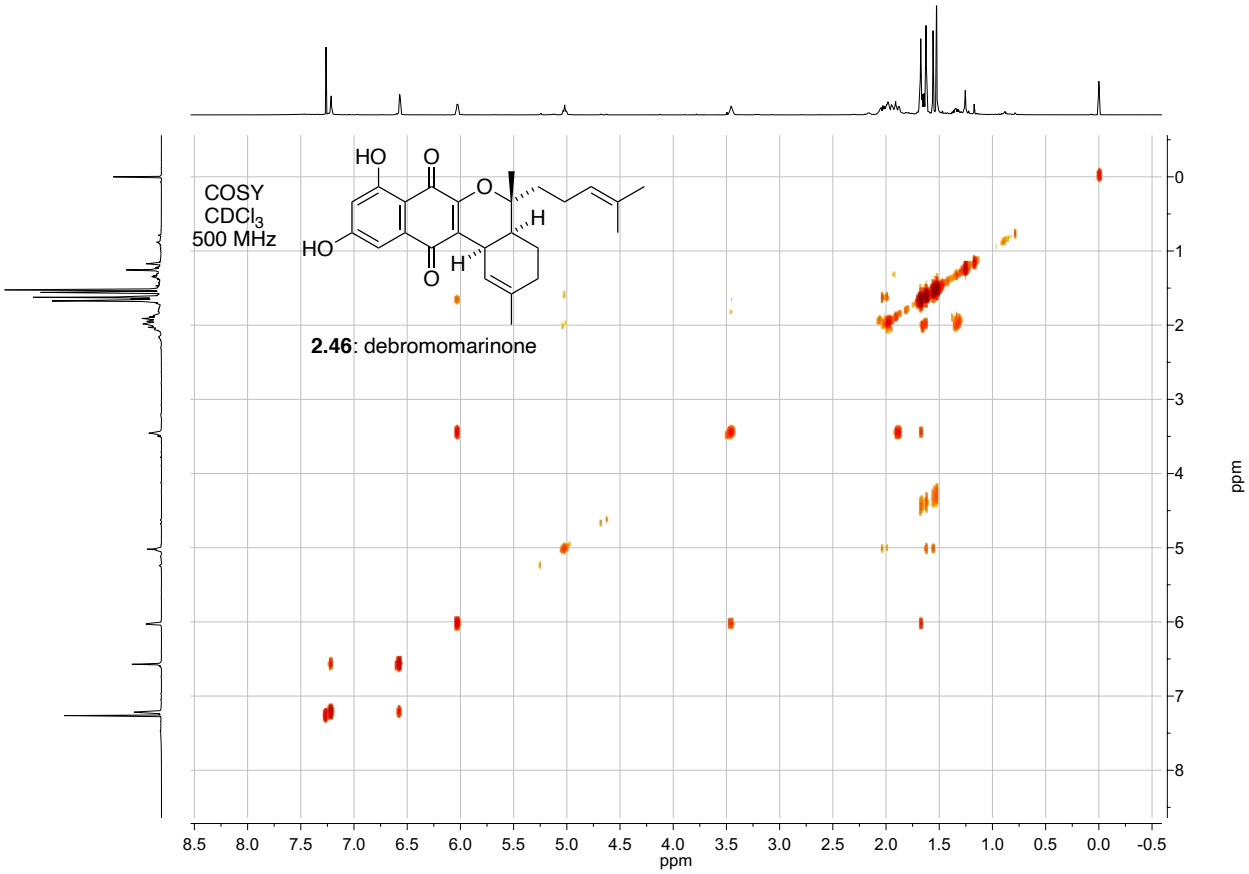
COSY
CDCl3
500 MHz
HO
O
O
H
HO
H
O
2.46: debromomarinone
ppm
ppm

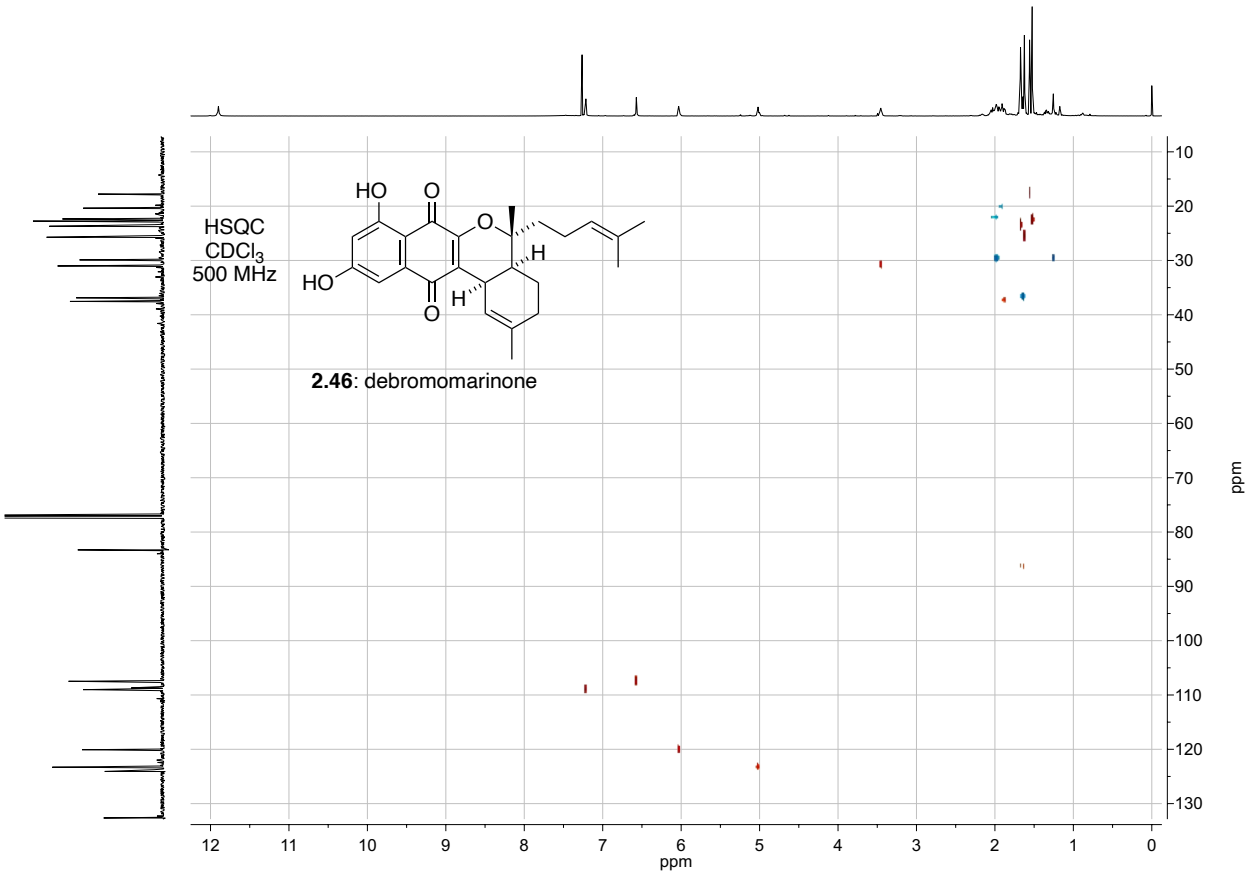
HSQC
CDCl3
500 MHz
HO
O
O
H
HO
H
O
2.46: debromomarinone
ppm
ppm

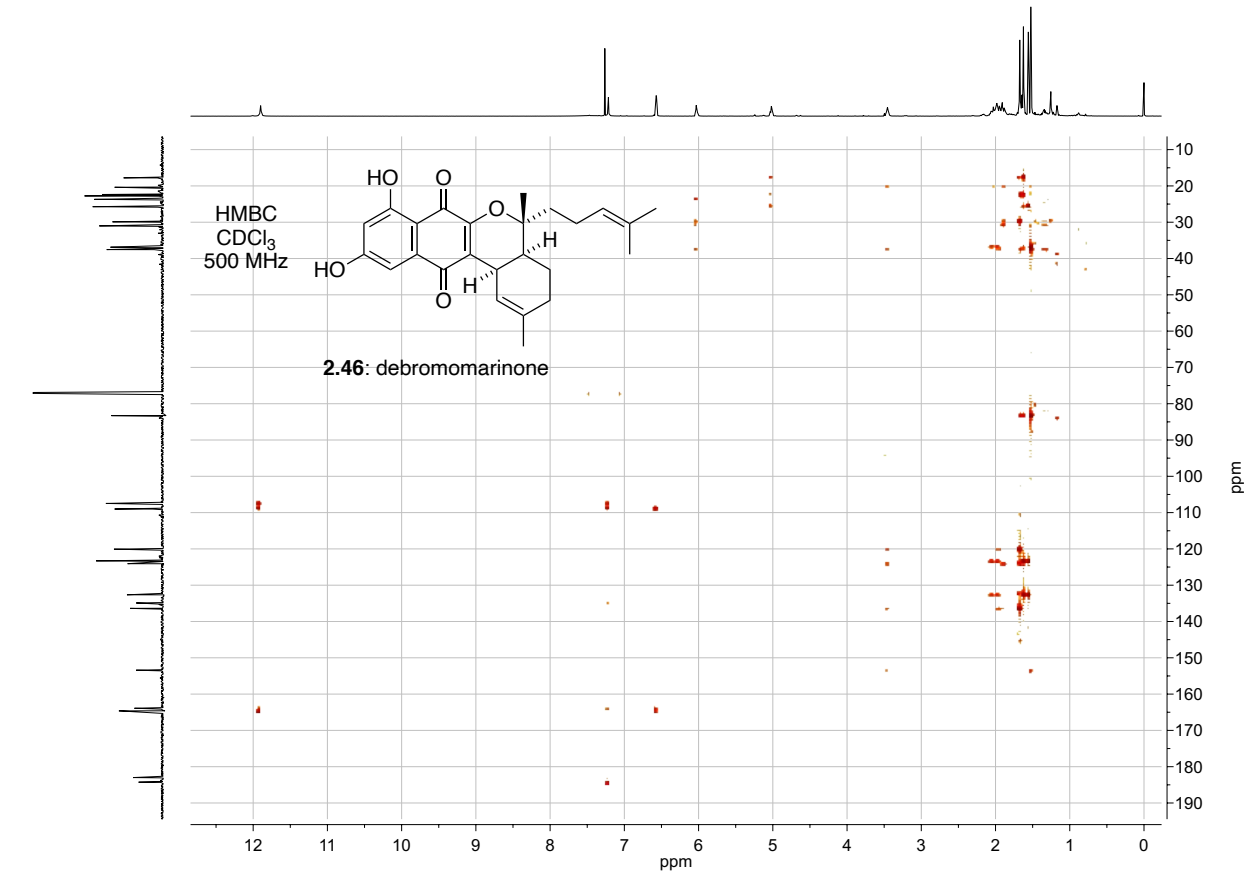
HMBC
CDCl3
500 MHz
HO
O
O
H
HO
H
O
2.46: debromomarinone
ppm
ppm

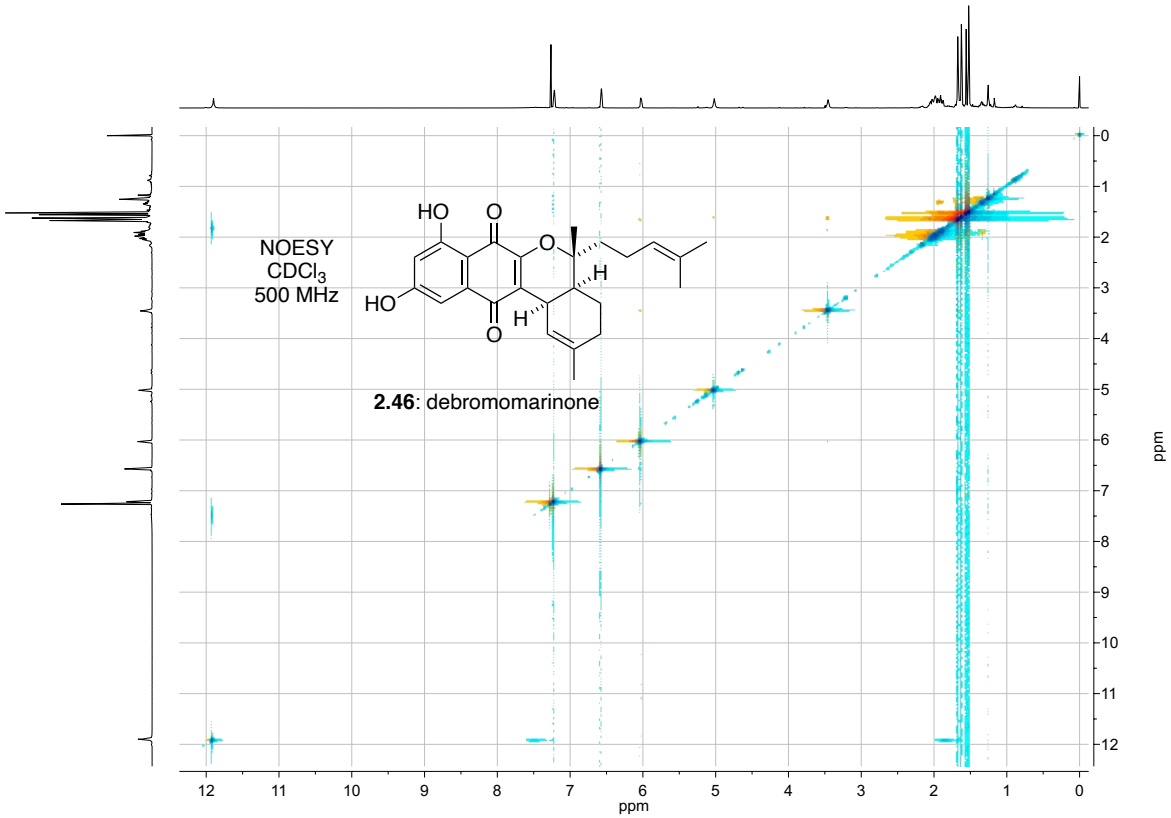
NOESY
CDCl3
500 MHz
HO
O
O
H
HO
H
O
2.46: debromomarinone
ppm
ppm

CHAPTER 3

Chemoenzymatic Studies of Naphterpin and Marinone Natural Products

Carbon atoms of 7-demethylnaphterpin, debromomarinone and related synthetic intermediates are numbered throughout this chapter as follows:

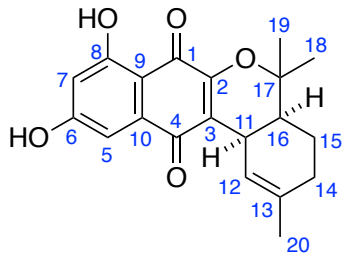

7-demethylnaphterpin

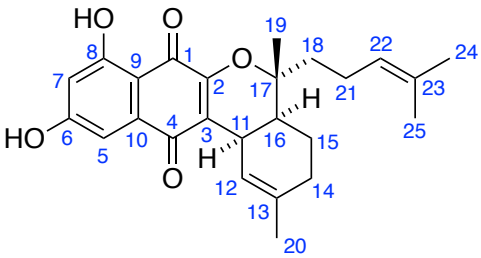

debromomarinone

Parts of this chapter have been published as follows:

Murray, L. A. M.; McKinnie, S. M. K.; Pepper, H. P.; Erni, R.; Miles, Z. D.; Cruickshank, M. C.; López-Pérez, B.; Moore, B. S.; George, J. H. *Angew. Chem. Int. Ed.* **2018**, *57*, 11009.

3.1 Introduction

3.1.1 Biosynthetic Gene Clusters

Natural products, also known as secondary metabolites, are assembled in nature *via* a complex ensemble of biosynthetic machinery within the cell. In the case of bacteria as well as some fungi and plants, the genes which encode the production of secondary metabolites often cluster together within their genomes, known as biosynthetic gene clusters (BGCs).[1] The extent of this clustering varies significantly, both within and between organisms. BGCs often contain all of the genes required for the biosynthesis of each natural product precursor, as well as assembly and tailoring of the scaffold, resistance, exportation and regulation.[2] The expression of these BGCs is highly controlled within the cell, dependent on gene regulation, protein folding, and a series of post-translational modifications.[2] These cellular processes also rely on the availability of substrates and co-factors, required for each step in the biosynthetic pathway. Advances in sequencing technologies have identified thousands of BGCs, however with so many limiting factors, it is predicted that only 10-20% of BGCs can be functionally expressed in the laboratory using current technologies.[2]

3.1.2 Genome Mining

In the past, classical natural product discovery methods were centred around microbial fermentation, and screening culture extracts for biological activity.[2] This method proved valuable for identifying early antibiotics, however more recently has resulted in the re-isolation of many known compounds. Additionally, these techniques are extremely laborious, highlighting the need for a more targeted approach. The introduction of next-generation sequencing, and bioinformatic tools have significantly increased the rate of novel secondary metabolite discovery through an approach known as “genome mining”. Genome mining utilises bioinformatic tools, alongside the genomes of sequenced organisms to identify

previously uncharacterized natural product BGCs. As a result, insight can be gained into the class of compounds these natural product BGCs encode, and in some cases, even predict the structures themselves.[3] Computational softwares such as antiSMASH[4,5] and BLAST[6] allow the natural product potential of a DNA sequence to be predicted, somewhat instantaneously. While genome mining continues to considerably increase opportunities for natural product discovery,[7] there remains a disparity between the number of BGCs we are able to identify, which far exceed our ability to detect the natural products they encode. Additionally, we cannot overlook the continual discovery of novel BGCs and novel enzymes, which cannot be predicted using bioinformatic tools. As such, it is important that we continue to use a combination of genome mining and studies based on functional characterisation in order to elucidate biosynthetic pathways and continue to discover novel and diverse enzyme catalysts.

3.1.3 Chemoenzymatic Investigations into Biosynthetic Pathways

Nature has long developed elegant strategies for the synthesis of complex natural products, employing sophisticated enzyme catalysts. In recent years, the use of biocatalytic transformations in chemical synthesis have become an important tool, due to an enzyme's unparalleled ability to catalyse regioselective and stereoselective reactions under mild reaction conditions.[8] This synergistic approach can also be applied to the elucidation of biosynthetic pathways, utilising a combination of chemical synthesis and genome mining.

This chemoenzymatic approach has previously unveiled the biosynthesis of two naphthoquinone-derived meroterpenoid natural product families, the merochlorins and the napyradiomycins.[9] In both cases, the completion of a biomimetic total synthesis allowed access to each of the proposed biosynthetic intermediates within the biosynthetic pathway. A

combination of these intermediates and recombinant proteins was then used to interrogate the biosynthesis of these natural products through *in vitro* chemoenzymatic assays.

The success of these chemoenzymatic studies later resulted in the complete elucidation of the napyradiomycin biosynthetic pathway form THN (**3.01**) and organic pyrophosphate precursors (Scheme 3.01).[10] Construction of key intermediate **3.02** was achieved through alkylation with Mg^{2+}-dependent aromatic ABBA prenyltransferases (NapT8, NapT9), alongside oxidative dearomatisation and chlorination facilitated by a VHPO (NapH1). VHPO NapH3 was found to catalyse the key α-hydroxyketone rearrangement of **3.02**, shifting the geranyl substituent from the C-4 to the C-3 position, forming the simplest member of the napyradiomycin family, naphthomevalin (**3.03**). Subsequent chlorination with NapH1 promoted cyclisation to form napyradiomycin A1 (**3.04**), which could then undergo NapH4-catalysed chlorination and cyclisation to form napyradiomycin B1 (**3.05**). The elucidation of this biosynthetic pathway also resulted in the one-pot total *in vitro* enzyme syntheses of napyradiomycin A1 (**3.04**) and napyradiomycin B1 (**3.05**). The chemoenzymatic application of these recombinant napyradiomycin enzymes completed the enantioselective synthesis of **3.04** and **3.05** in a protecting group-free manner. To date, these molecules are yet to be chemically synthesised, highlighting the utility of biocatalysis in complex natural product synthesis.

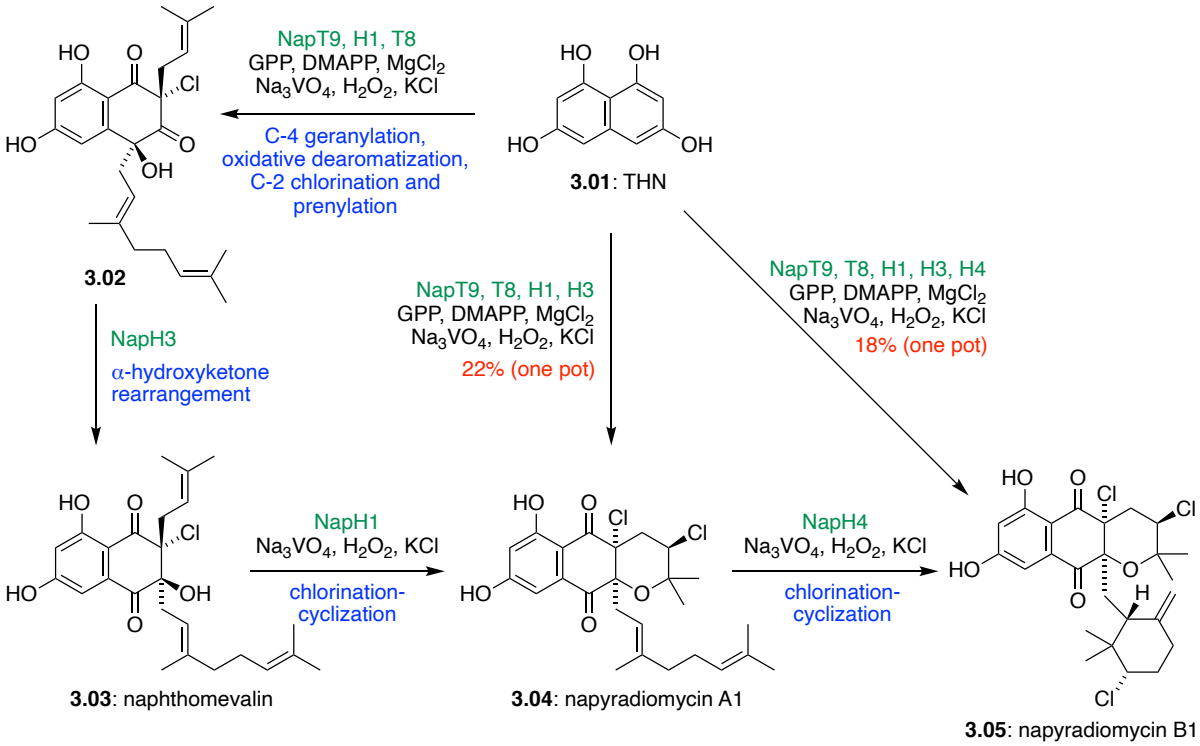

Scheme 3.01: Fully elucidated biosynthetic pathway from THN to napyradiomycin B1 (**3.05**) and chemoenzymatic, one-pot total syntheses of napyradiomycins A1 (**3.04**) and B1 (**3.05**).[10]

3.1.4 Project Aims

With an established biomimetic total synthesis of 7-demethylnaphterpin (**3.06**) and debromomarinone (**3.07**) (Chapter 2), our next objective was to elucidate the entire biosynthetic pathway towards these two natural products (Scheme 3.02).

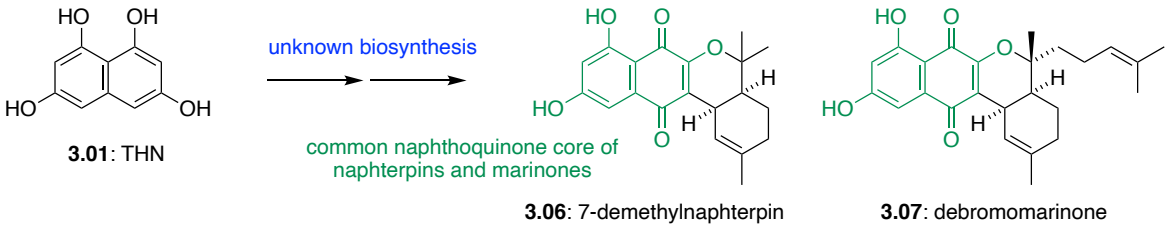

Scheme 3.02: Previously unknown biosynthesis of the desired naphthoquinone substitution in naphterpin and marinone natural products form the biosynthetic precursor, THN (**3.01**).

The aim of this project was to characterise the key transformations in the naphterpin and marinone biosynthetic pathways utilising the chemical synthesis of our proposed biomimetic intermediates and a chemoenzymatic approach. As part of our biochemical approach, we would heterologously express and purify target enzymes present in the putative marinone biosynthetic gene cluster. The function of these enzymes could then be investigated through *in vitro* enzyme assays with our chemically synthesised biosynthetic intermediates.

In 2015, the draft genome of the marinone-producing bacterium *Streptomyces* sp. CNQ-509 was sequenced and reported.[11] This genome was found to contain a BGC, including a THN synthase, prenyltransferase and, most significant to us, three genes putatively encoding VHPO enzymes. Additionally, these genes were found to have homology to Mcl24 and NapH3, the enzymes which catalyse an α-hydroxyketone rearrangement in the merochlorin and napyradiomycin biosyntheses, respectively.[9] Based on our established biochemistry of the merochlorin and napyradiomycin VCPO enzymes, we proposed a similar sequence of reactions could be catalysed by these putative VCPO enzymes in the naphterpin and marinone biosynthetic pathways. Elucidation of key steps in this biosynthetic pathway would allow us to better understand the role of bacterial VHPOs in natural product biosynthesis. Additionally, evidence of these VHPOs converting our key biosynthetic intermediates in this biosynthesis would support our biosynthetic proposal of cryptic halogenation events in these non-halogenated natural products.

3.2 Results and Discussion

3.2.1 Synthesis of Biosynthetic Intermediates

With our completed biomimetic synthetic route to 7-demethylnaphterpin (**3.06**) and debromomarinone (**3.07**) in place, we set out to synthesise all of our deprotected intermediates for use in our chemoenzymatic assays. As all of our synthetic intermediates featured MOM protecting groups, we envisaged facile deprotection employing acidic conditions to form our biosynthetic intermediates.

Firstly, dimethoxy protected THN (**3.10**) was prepared according to previous literature conditions (Scheme 3.03).[12] This synthesis avoided the requirement for demethylation followed by MOM protection, as we envisaged demethylation would be achievable on this simple scaffold to afford THN (**3.01**).

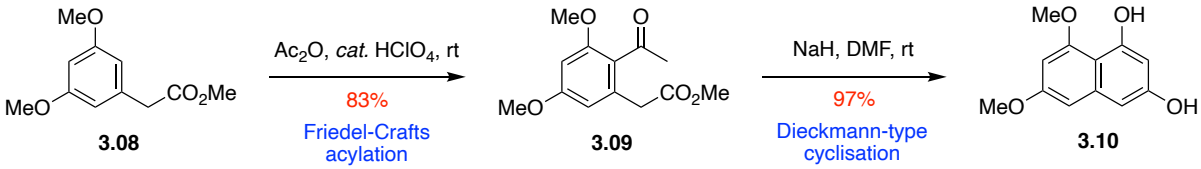

Scheme 3.03: Synthesis of di-methoxy protected THN (**3.10**).[13]

Demethylation had previously been achieved on **3.10** employing Lewis acid BBr_3.[14] Treatment of **3.10** with BBr_3 was also successful in our hands, giving deprotected THN (**3.01**) in moderate yield (Scheme 3.04), with data matching the literature procedure. THN is highly sensitive to oxidation and was therefore handled with great care and stored under inert gas. Given the instability of this compound, it was used immediately in the next step.

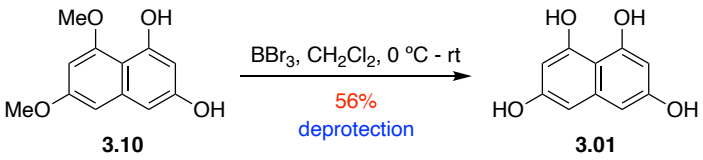

Scheme 3.04: Deprotection of **3.10** to give THN **3.01.**

Alkylation of THN was performed under our previous Pd-catalysed Tsuji-Trost conditions with both geranyl (**3.11a**) and farnesyl (**3.11b**) carbonate to form pre-naphterpin (**3.12a**) and pre-marinone (**3.12b**), respectively. The equivalents of each carbonate were decreased in these cases to avoid multiple alkylation events. This reaction was slow and was therefore left for extended reaction times in an attempt to increase yield. Due to the instability of the deprotected THN intermediates (**3.12a**/**3.12b**), column chromatography was achieved under an argon atmosphere, placing all fractions in sealed vials under argon in an attempt to minimise degradation prior to concentration. The product was then stored under argon at –20 ºC for a minimum amount of time before use.

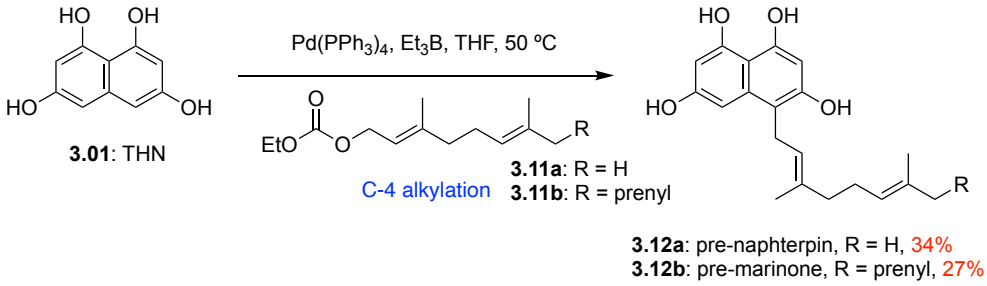

Scheme 3.05: Alkylation of THN (**3.01**) with geranyl (**3.12a**) or farnesyl (**3.12b**) ethyl carbonate.

In an attempt to avoid continuing the synthesis with the unstable and deprotected intermediates (**3.12a**/**3.12b**), we decided to synthesise the oxidative dearomatisation products through the MOM protected intermediates (**3.13a**/**3.13b**). Oxidative dearomatisation was achieved under

our standard Wessely oxidation conditions, followed by acetate hydrolysis using KOH. Facile MOM deprotection with HCl in MeOH was employed, giving the desired dearomatised intermediates **3.14a**/**3.14b** (Scheme 3.06). The yield over three steps was found to be much lower for the marinone derivative (**3.14b**) as a consequence of low yields for the acetate hydrolysis and deprotection steps.

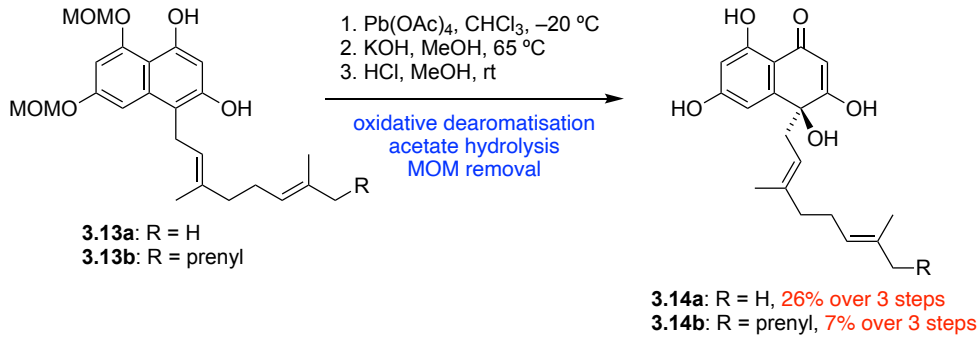

Scheme 3.06: Oxidative dearomatisation, acetate hydrolysis and MOM deprotection of **3.13a**/**3.13b**.

Mono deprotection of **3.15a**/**3.15b** was also achieved using HCl in MeOH to give deprotected monochlorides **3.16a**/**3.16b** (Scheme 3.07).

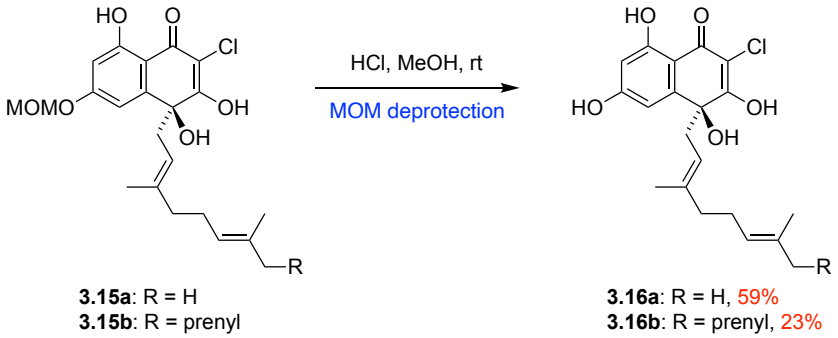

Scheme 3.07: MOM deprotection of α-chloroenols **3.15a**/**3.15b**.

Diketones **3.17a**/**3.17b** were mono deprotected using HCl in MeOH, giving both the geranyl and farnesyl dichloride compounds **3.18a**/**3.18b** in moderate yields.

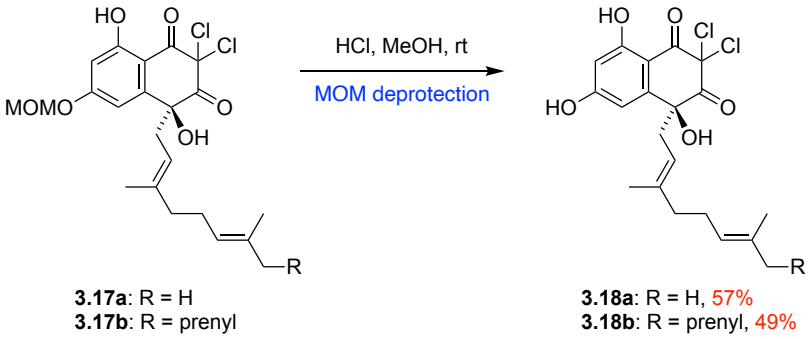

Scheme 3.08: MOM deprotection of dichlorides **3.17a**/**3.17b**.

The α-hydroxyketone rearrangement intermediates **3.19a**/**3.19b** were deprotected using HCl in MeOH, giving both rearranged products **3.20a**/**3.20b** (Scheme 3.09). Due to the inherently reactive nature of epoxides, we knew that deprotection of the protected α-chloroepoxide under acidic conditions would most likely result in hydrolysis. Therefore, we envisaged that the best route would be to cyclise the already deprotected geminal dichlorides **3.20a**/**3.20b**. This reaction proceeded as previously observed on the protected analogue to form **3.21a**/**3.21b**, however the yield of the farnesyl system was shown to significantly decrease. This decrease in yield was believed to be the result of degradation during the reaction process, observed when monitoring the reaction by TLC.

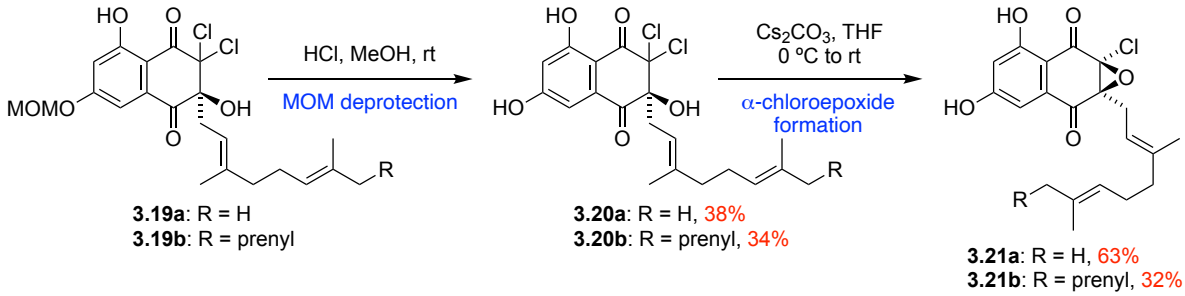

Scheme 3.09: Synthesis of deprotected dichlorides **3.20a**/**3.20b** and α-chloroepoxides **3.21a**/**3.21b**.

Synthesis of the deprotected hydroxyquinones from **3.22a**/**3.22b** was found to be slightly more challenging, as MOM deprotection with HCl in MeOH proved messy and low yielding. Literature precedent suggested that the weak acid, pyridinium *p*-toluenesulfonate (PPTS), could act as a milder alternative for MOM deprotection.[15,16] To our delight, treatment of **3.22a**/**3.22b** with PPTS in *t*-BuOH at reflux achieved the desired intermediates **3.23a**/**3.23b** in good yields (Scheme 3.10).

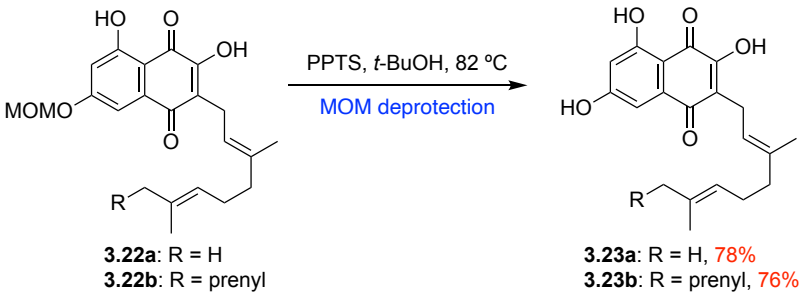

Scheme 3.10: MOM deprotection of hydroxynaphthoquinones **3.22a**/**3.22b**.

The success of these deprotections was extremely encouraging, as we now had access to each proposed biosynthetic intermediate in milligram quantities, for use as starting materials and synthetic standards in chemoenzymatic assays.

3.2.2 Chemoenzymatic Assays

Following the synthesis of all the deprotected synthetic intermediates on pathway to both 7-demethylnaphterpin (**3.06**) and debromomarinone (**3.07**), we were interested in the chemoenzymatic transformation of these intermediates, in validation of our proposed biosynthetic pathway. We anticipated that our alkylated THN intermediates, pre-naphterpin (**3.12a**) and pre-marinone (**3.12b**), could undergo a series of VHPO-catalysed reactions, in a similar sequence to that of naphthomevalin.[9] This theory was supported by the recent publication of a marinone-producing *Streptomyces* sp. CNQ-509 draft genome, containing VHPO homologues.[11,17] If this sequence of VCPO-catalysed reactions was successful, we would then continue to explore the biosynthetic gene cluster of these natural products, and investigate enzymes responsible for interconverting our proposed late stage biosynthetic intermediates into the natural products themselves.

Moore and co-workers had previously published a significant contribution to the literature in VHPO enzymes, including their work in napyradiomycin and merochlorin biosynthesis.[18–21] These overlapping research interests led to collaboration between the Moore and George research groups, resulting in a joint synthetic and biosynthetic effort to interrogate the biosynthesis of the merochlorin and napyradiomycin families of natural products.[9] Amongst other successes, this research led to the discovery of a VCPO, NapH3, responsible for the key α-hydroxyketone rearrangement forming the natural product, naphthomevalin (**3.03**) (Scheme 3.11). This discovery was made by exploring the reactivity of our synthesised biosynthetic intermediate **3.02** with the NapH3 enzyme, isolated from *Streptomyces* sp. CNQ- 525. This reaction is analogous to one of the biosynthetic steps in our proposed pathway to the naphterpin and marinone families of natural products.

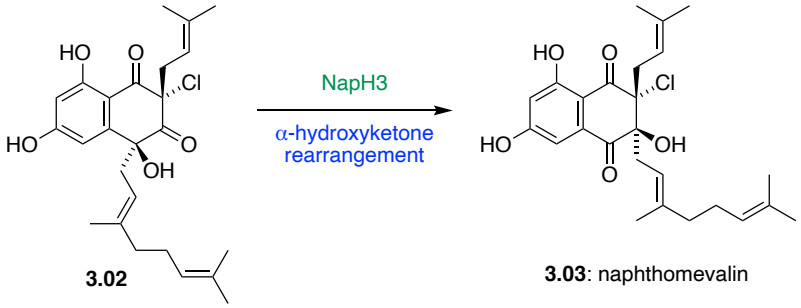

Scheme 3.11: α-Hydroxyketone rearrangement of **3.02** to form naphthomevalin (**3.03**).

With the success of our previous collaborations with the Moore research group, we extended an invitation to once again join forces in an attempt to use both synthetic chemistry and biochemistry to prove our biosynthetic proposal for the naphterpin and marinone families of natural products. I was fortunate enough to undertake this work personally at Scripps Institution of Oceanography, University of California, San Diego, under the supervision of Prof. Bradley Moore and Assistant Prof. Shaun McKinnie.

3.2.2 Heterologous Expression and Purification of VHPOs

Due to our previous success and familiarity with VHPOs in our chemoenzymatic assays, the heterologous expression and purification of these enzymes became our first target. The function of the genes within the putative marinone BGC were initially predicted using the basic local alignment search tool (BLAST) and are outlined in Figure 3.01.[6]

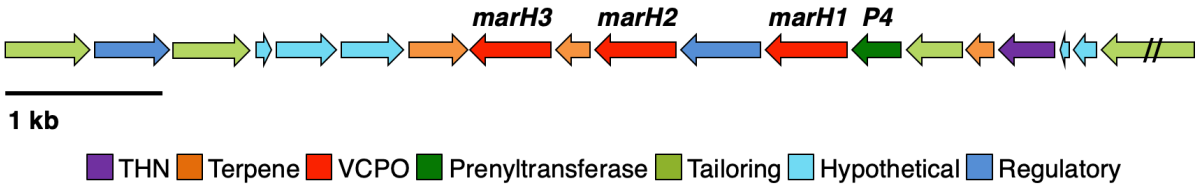

Figure 3.01: Graphical representation of the putative marinone biosynthetic gene cluster from *Streptomyces* sp. CNQ-509. Genes have been annotated with their proposed function. Putative VCPO genes *marH1*, *marH2*, and *marH3* are highlighted in red.

In order to commence *in vitro* chemoenzymatic assays with these VHPO enzymes, the three VCPO homologues *marH1*, *marH2*, and *marH3* were cloned from the *Streptomyces* sp. CNQ-509 putative marinone biosynthetic gene cluster and heterologously expressed in *Escherichia coli*. The recombinant proteins containing a *N*-terminal His_6-tag were then purified using Ni^{2+} affinity chromatography (see 3.4.2 Biochemical Methods).

3.2.3 Preliminary Activity Studies of VHPO Enzymes

The halogenating activity of these three VHPO enzymes was investigated employing a monochlorodimedone (MCD) (**3.24**) assay. This assay is commonly used as an analytical method for the identification of VHPOs.[22–24] MCD (**3.24**) is a monohalogenated 1,3-diketone that is brominated or chlorinated through diffusible hypohalous acids produced in the presence of an active VHPO enzyme, to form the dihalogenated species **3.25** (Scheme 3.12).

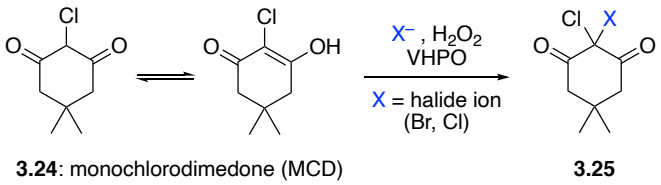

Scheme 3.12: Conversion of monochlorodimedone (**3.24**) to **3.25**.

This reaction is easily monitored spectrophotometrically as MCD absorbs UV light at 290 nm. Monitoring the loss of absorbance at 290 nm is proportional to the brominating or chlorinating activity of the halogenating enzyme.

Our intention was to use this assay to determine the activity of the putative marinone VCPOs, MarH1, MarH2, and MarH3. Methods are outlined in biochemical methods section 3.4.2, alongside more detailed descriptions by Wever *et al.*[23] and McKinnie *et al.*[24] Our initial experiments tested the activity of the three VHPOs under slightly acidic (pH 6.0) and slightly basic (pH 8.0) conditions. After a two-minute equilibration time, H_2O_2 was added to the reaction and monitored for an additional 5 minutes. If no decrease in absorbance was observed after this time, KBr was added to the reaction, and monitored for an additional 8 minutes. The result of these experiments are outlined at pH 6.0 and pH 8.0 in Figure 3.02 and Figure 3.03 below.

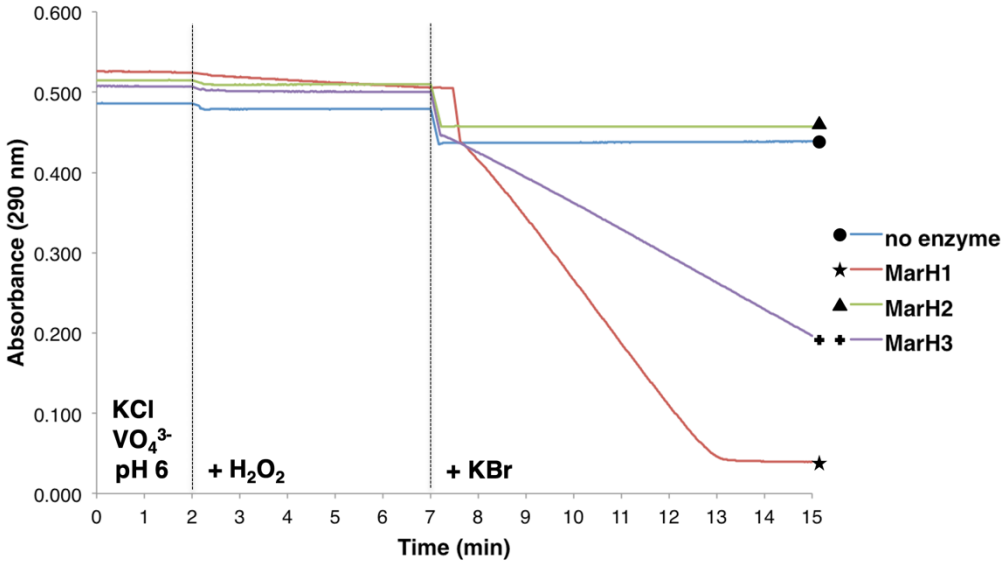

Figure 3.02: Monochlorodimedone (MCD) assay of MarH VCPO homologues at pH 6.0.

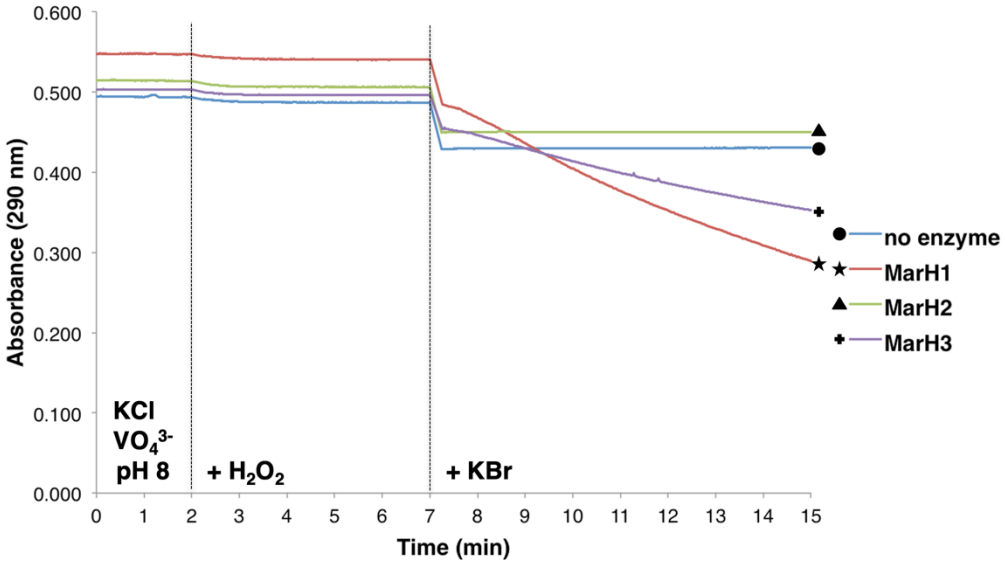

Figure 3.03: Monochlorodimedone (MCD) assay of MarH VCPO homologues at pH 8.0.

As shown above, only MarH1 and MarH3 exhibited halogenation activity in the presence of bromide anions, consistent with other *Streptomyces* spp. VCPO enzymes.[24]

To investigate these VHPO enzymes further, we needed to clarify if they were purified with vanadium bound in their active site. This would be particularly important for the generation of assay conditions. In a similar manner, an MCD assay was performed with the two active MarH enzymes, MarH1 and MarH3. Initially, reaction components were allowed to equilibrate for 2 minutes in the absence of sodium vanadate. After no reaction was observed, sodium vanadate was added to the reaction mixture and the reaction was monitored for an additional 13 minutes (Figure 3.04).

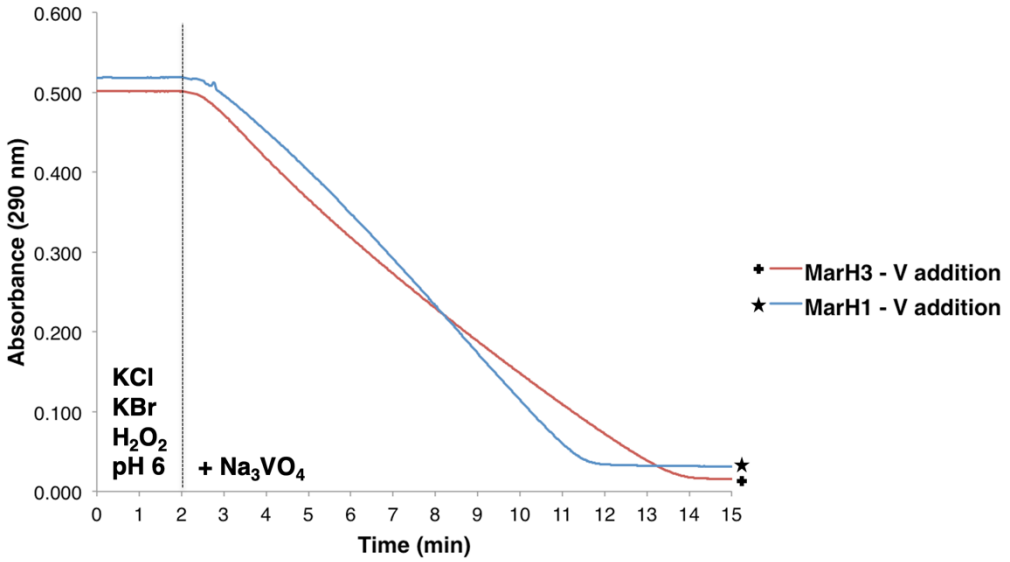

Figure 3.04: Monochlorodimedone (MCD) assay of MarH1 and MarH3 VCPO homologues at pH 6.0 adding sodium vanadate at 2 minutes.

A decrease in absorbance at 290 nm was only observed following the addition of exogenous sodium vanadate. This result indicated that recombinant MarH1 and MarH3 enzymes did not have vanadium bound in their active sites, and that negligible time was required to incorporate vanadate in order to restore catalysis. This information further confirmed the VHPO activity of both MarH1 and MarH3.

3.2.4 Enzyme Assays with MarH1, MarH2 and MarH3

With the synthetic intermediates and recombinant MarH enzymes in hand, we could then explore if these enzymes were capable of converting our proposed biosynthetic intermediates from both the naphterpin and marinone families of natural products. Despite not having access to the equivalent recombinant enzymes from the putative naphterpin BGC, we were hopeful that the active site of the MarH enzymes would still catalyse these transformations with the shorter side chain of naphterpin.

Considering similarities to the napyradiomycin biosynthetic pathway, we predicted that one or a combination of the MarH enzymes would catalyse the oxidative dearomatisation, C-2 dichlorination and α-hydroxyketone rearrangement on both the pre-naphterpin (**3.12a**) and pre-marinone substrates (**3.12b**) (Scheme 3.13).

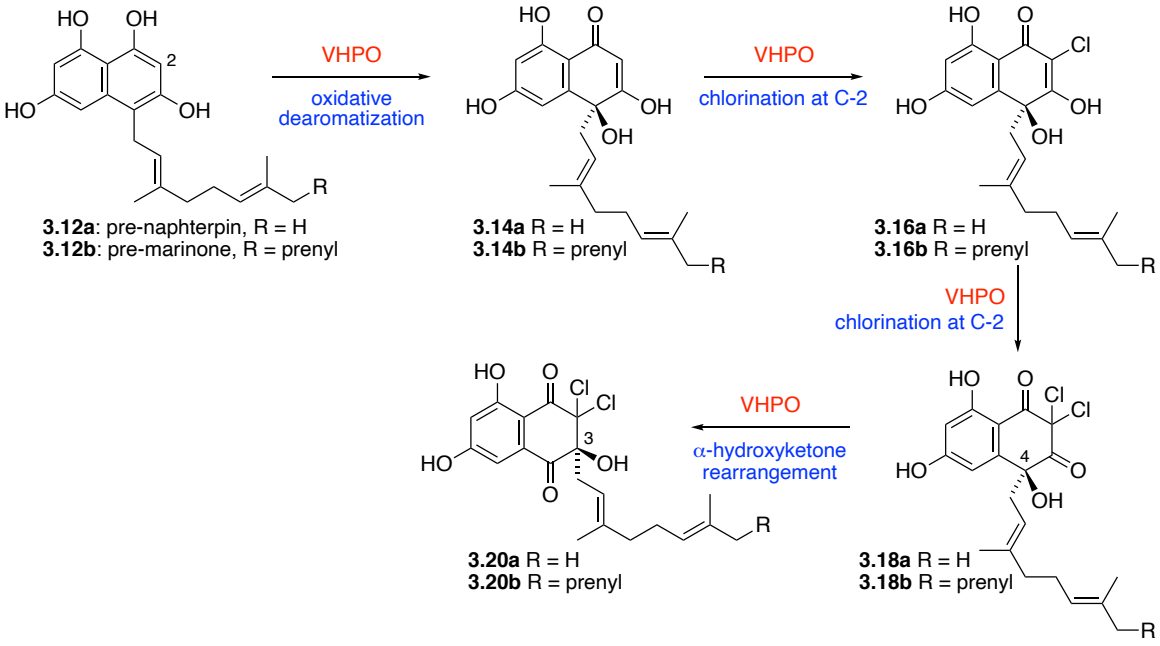

Scheme 3.13: Proposed VHPO-catalysed reactions in the naphterpin and marinone biosynthetic pathway.

Two of the VHPO homologues, MarH1 and MarH3, exhibited good potential given their halogenation activity on our initial MCD assays. Although MarH2 was not found to have activity based on our initial MCD assay, there was still the possibility it could play an important role in the biosynthesis. This could be analogous to the VCPO enzyme NapH3, which was found to have no bromination or chlorination activity in MCD assays. Later it was established that NapH3 catalysed the key α-hydroxyketone rearrangement in the napyradiomycin biosynthetic pathway (Scheme 3.11).[9,10]

3.2.5 Activity of MarH1 on Pre-marinone

I*n vitro* experiments began thorough characterisation of reactions between pre-marinone (**3.12b**) and the recombinant MarH enzymes. The formation of biosynthetic intermediates was then monitored with reverse-phase HPLC (Figures 3.05-3.11). The established reaction conditions included MarH enzyme, KCl, sodium orthovanadate and hydrogen peroxide (see 3.4.2 Biochemical Methods). Unsure of the optimal reaction conditions, all assays were initially run in duplicate, both at pH 6.0 and pH 8.0.

Incubation of MarH1 with **3.12b** at pH 8.0 in the presence of varying equivalents of H_2O_2 resulted in formation of the C-2 monochlorinated intermediate **3.16b** through the oxidatively dearomatised intermediate **3.14b** after 18 h (Figure 3.05). The interconversion of **3.12b** to our proposed biosynthetic intermediates was the first step towards confirmation of our proposed biosynthetic pathway. This reaction was found to proceed with one equivalent of H_2O_2, however the reaction could not be pushed further with excess H_2O_2.

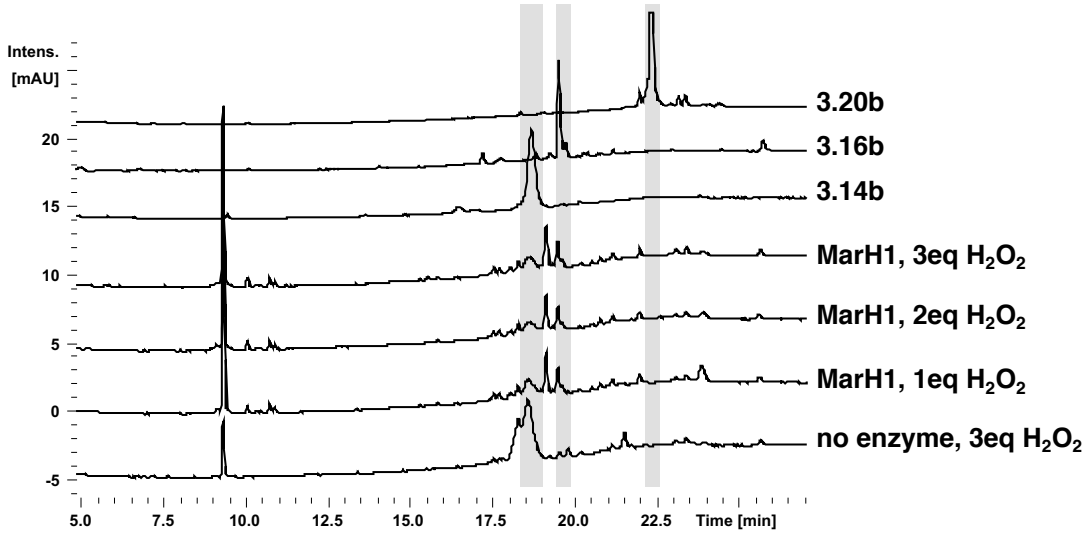

Figure 3.05: RP-HPLC-MS analysis (λ = 300 nm) of *in vitro* MarH1 incubation with **3.12b** in the presence of variable equivalents of hydrogen peroxide (pH 8.0, 18 h), and comparison to synthetic standards **3.14b**, **3.16b**, and **3.20b**.

To investigate this reaction further, this experiment was repeated with one equivalent of H_2O_2, measuring the conversion at shorter time points. Here we could observe the conversion of pre-marinone **3.12b** to the oxidatively dearomatised product **3.14b** after 1 h, followed by slower conversion to monochlorinated intermediate **3.16b** at 3 h, and finally almost complete conversion at 18 h. Although some of the oxidatively dearomatised product **3.14b** was observed in the no enzyme control, overall this conversion was shown to be much faster and cleaner in the presence of MarH1. These experiments were also repeated at pH 6.0, however pH 8.0 was found to give a much cleaner conversion (see 3.4.2 Biochemical Methods, Figures SI-3.11 – SI-3.12 for pH 6.0 experiments).

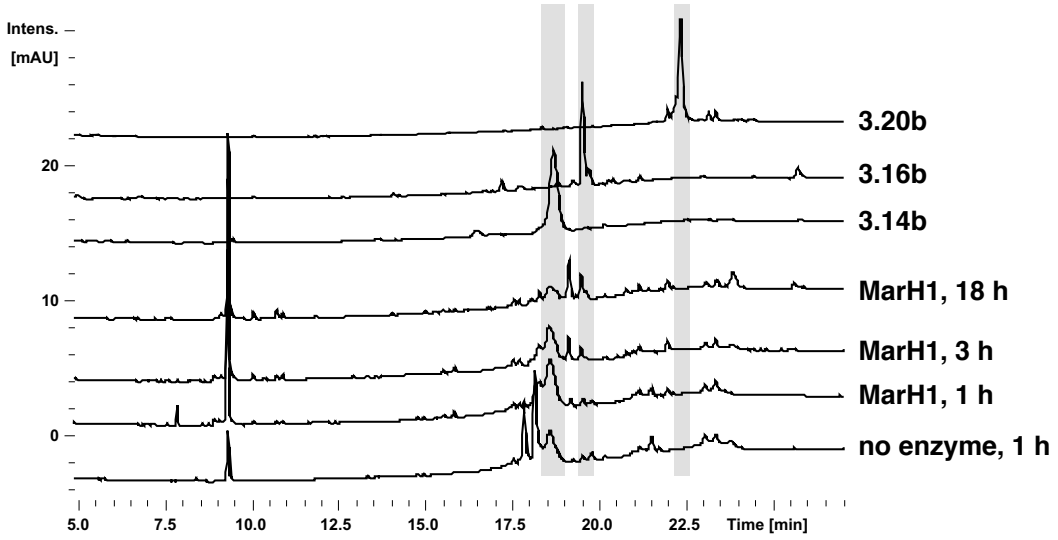

Figure 3.06: RP-HPLC-MS analysis (λ = 300 nm) of *in vitro* MarH1 incubation with **3.12b** over time (pH 8.0, 1 equiv. hydrogen peroxide), and comparison to synthetic standards **3.14b**, **3.16b**, and **3.20b**.

3.2.6 Activity of MarH3 on Pre-marinone

With the preliminary role of MarH1 established, we turned our attention to the role of MarH3. Again, unsure of its function, we subjected pre-marinone (**3.12b**) to the same reaction conditions (KCl, Na_3VO_4, pH 8.0) in the presence of MarH3 using varied equivalents of H_2O_2 (Figure 3.07). At higher equivalents of H_2O_2, the formation of a peak corresponding to the α-hydroxyketone rearrangement product **3.20b** was observed.

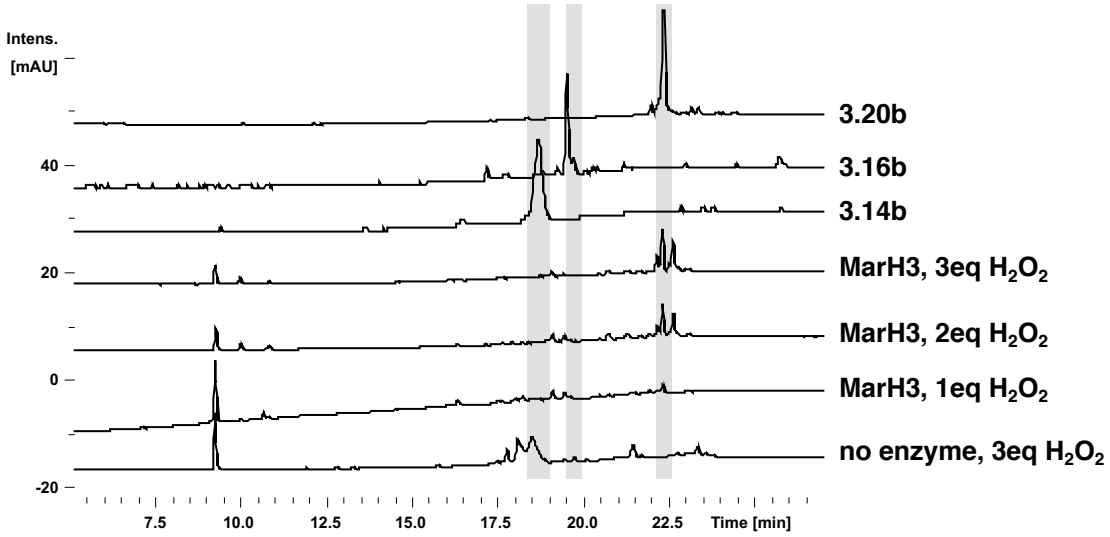

Figure 3.07: RP-HPLC-MS analysis (λ = 300 nm) of *in vitro* MarH3 incubation with **3.12b** in the presence of variable equivalents of hydrogen peroxide (pH 8.0, 18 h), and comparison to synthetic standards **3.14b**, **3.16b**, and **3.20b**.

Next, the conversion of pre-marinone **3.12b** to **3.20b** was monitored at shorter time intervals, with three equivalents of H_2O_2 (Figure 3.08). After 1 h, small quantities of both the oxidatively dearomatised product **3.14b** and the monochlorinated species **3.16b** could be observed. At 3 h, the monochlorinated species **3.16b** was still present, however formation of the α-hydroxyketone rearrangement product **3.20b** could be detected. After 18 h, all of the monochlorinated species **3.16b** appeared to be converted to **3.20b**. Again, these experiments were repeated at pH 6.0, however pH 8.0 was found to be the more suitable pH (see 3.4.2 Biochemical Methods, Figures SI-3.13 – SI-3.14 for pH 6.0 experiments).

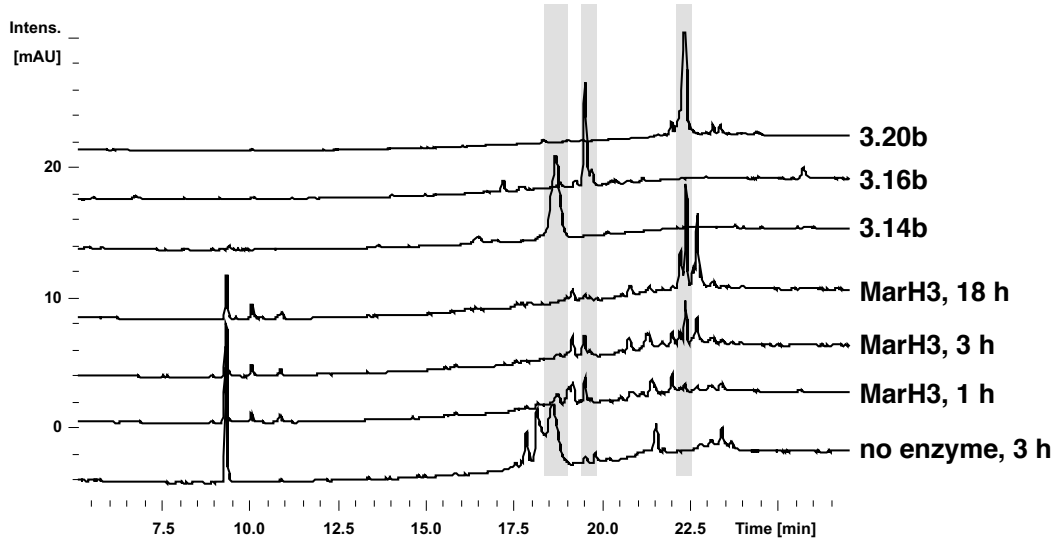

Figure 3.08: RP-HPLC-MS analysis (λ = 300 nm) of *in vitro* MarH3 incubation with **3.12b** over time (pH 8.0, 3 equiv. hydrogen peroxide), and comparison to synthetic standards **3.14b**, **3.16b**, and **3.20b**.

3.2.7 Sequential activities of MarH1, then MarH3 on Pre-marinone

With the results from these initial studies, MarH1 was observed to convert pre-marinone **3.12b** to the monochloride intermediate **3.16b**. Despite incubation with excess H_2O_2, MarH1 was not found to further catalyse chlorination and rearrangement of **3.16b** to **3.20b**. Incubation of **3.12b** with MarH3 was found to catalyse the additional chlorination at C-2 and the desired α-hydroxyketone rearrangement to form **3.20b**.

With this knowledge in hand, we predicted that a combination of the two enzymes would result in clean conversion of pre-marinone **3.12b** to the α-hydroxyketone rearrangement product **3.20b**. In the presence of Na_3VO_4 and two equivalents of H_2O_2, MarH1 was found to catalyse the oxidative dearomatisation and C-2 monochlorination of pre-marinone (**3.12b**) to give **3.16b** (Figure 3.09). After 18 h, MarH3 was added to the reaction, with an additional equivalent of H_2O_2. The reaction was then monitored at 1, 3 and 24 hours, showing the conversion of

monochloride intermediate **3.16b** to the dichlorinated rearranged product **3.20b**. Again pH 8.0 was found to be the optimal pH for this reaction (see 3.4.2 Biochemical Methods, Figure SI-3.15 for pH 6.0 experiment).

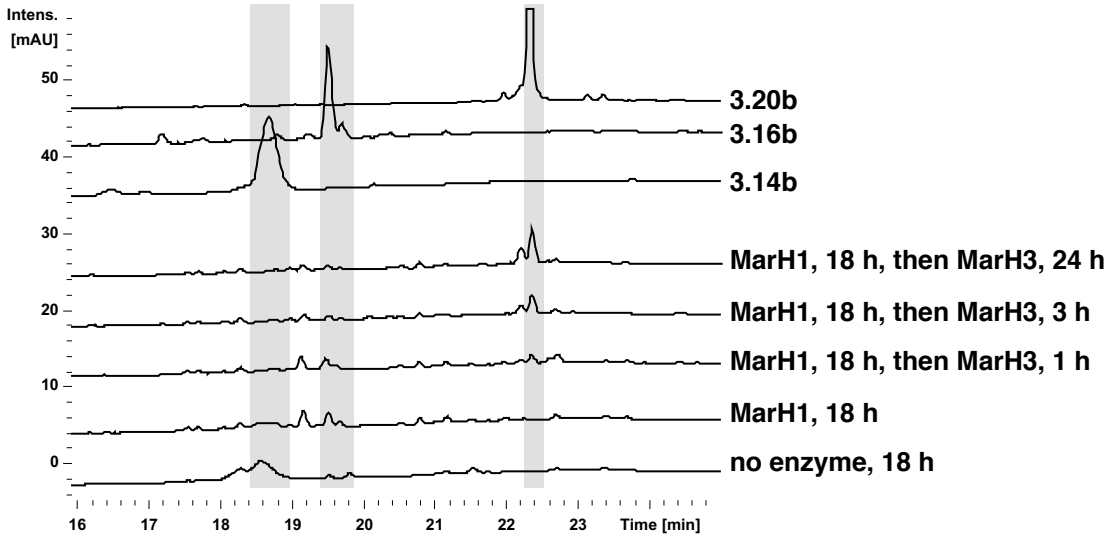

Figure 3.09: RP-HPLC-MS analysis (λ = 300 nm) of *in vitro* incubation of **3.12b** with MarH1 (pH 8.0, 2 equiv. hydrogen peroxide, 18 h) followed by MarH3 (1 additional equiv. hydrogen peroxide, variable time), and comparison to synthetic standards **3.14b**, **3.16b**, and **3.20b**.

3.2.8 Activity of MarH2 on Pre-marinone

Despite the lack of activity shown by recombinant MarH2 in the MCD assays, we were curious as to its role within the putative marinone BGC. We envisaged MarH2 as a putative partner protein to another MarH enzyme, helping to catalyse one of the desired reactions in the marinone biosynthetic pathway.

To test this hypothesis, we subjected our pre-marinone substrate (**3.12b**) to the standard *in vitro* reaction conditions of MarH1 in the presence of Na_3VO_4, two equivalents of H_2O_2 at pH 8.0 (Figure 3.10). After 18 h, we confirmed the formation of monochloride **3.16b** prior to the

addition of either recombinant MarH3 or co-incubation of recombinant MarH2 and MarH3, alongside an additional equivalent of H_2O_2. Unfortunately, the combination of MarH2/H3 was found to have no significant effect on the reaction when compared to the reaction with MarH3 alone, still forming the α-ketol product **3.20b**. The same was true for a duplicate experiment run at pH 6.0 (see 3.4.2 Biochemical Methods, Figure SI-3.16 for pH 6.0 experiment).

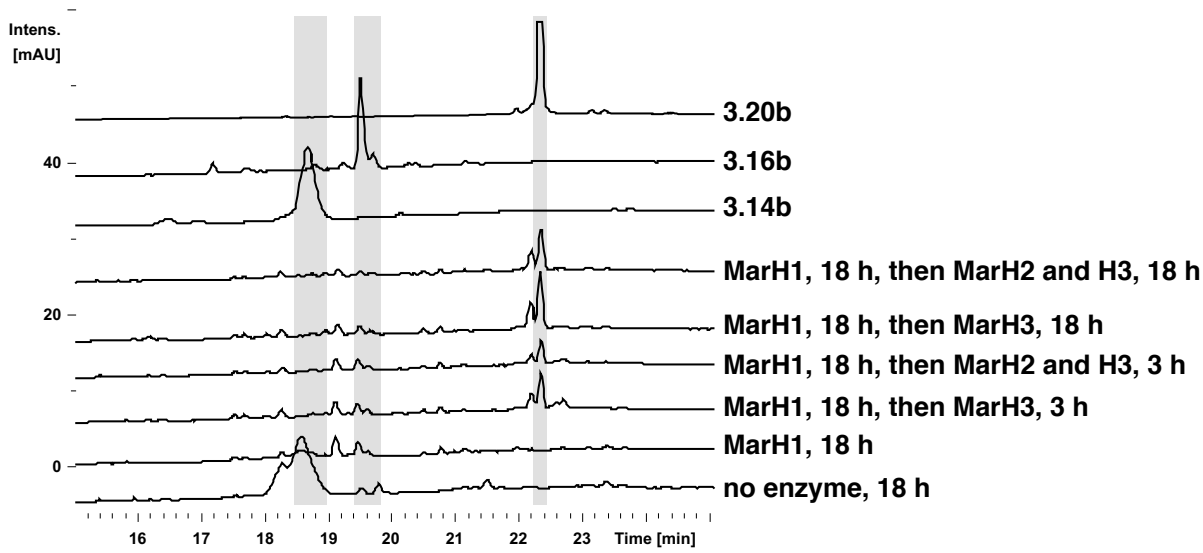

Figure 3.10: RP-HPLC-MS analysis (λ = 300 nm) of *in vitro* incubation of **3.12b** with MarH1 (pH 8.0, 2 equiv. hydrogen peroxide, 18 h) followed by MarH3 with or without MarH2 (1 additional equiv. hydrogen peroxide, variable time), and comparison to synthetic standards **3.14b**, **3.16b**, and **3.20b**.

With no apparent influence on the conversion of monochloride **3.16b** to **3.20b**, we decided to investigate whether MarH2 would influence the activity of MarH3 in conversion of pre-marinone to **3.12b** in an analogous way to MarH1. A direct comparison of *in vitro* activity of MarH3 was undertaken on pre-marinone, with and without co-incubation of MarH2 (Figure 3.11). Timepoints were taken at 1, 3 and 18 hours, comparing the products of both reactions. MarH2 seemed to have little influence on MarH3, and at longer time points showed decreased

conversion of monochloride **3.16b** to the rearranged dichloride **3.20b**. A duplicate experiment was also run at pH 6.0 with mimicked results (see 3.4.2 Biochemical Methods, Figure SI-3.17 for pH 6.0 experiment).

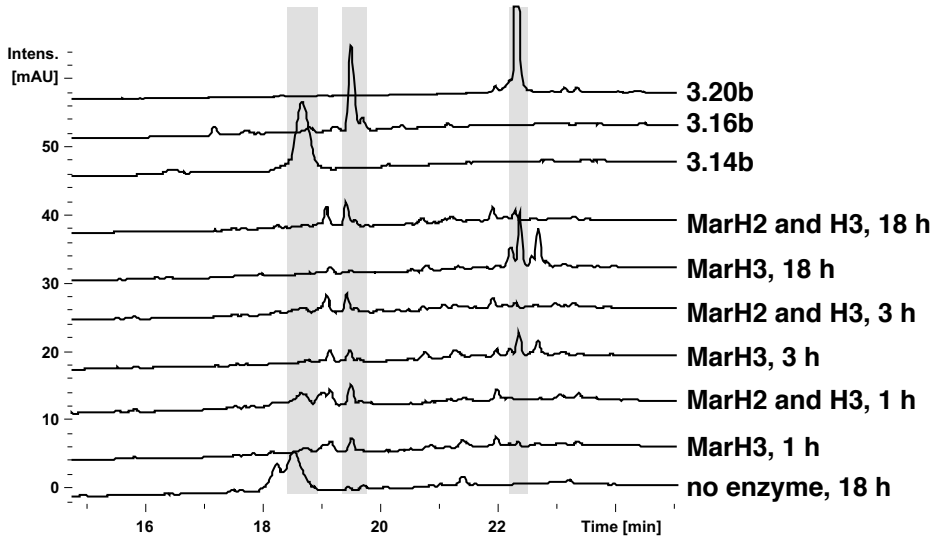

Figure 3.11: RP-HPLC-MS analysis (λ = 300 nm) of *in vitro* incubation of **3.12b** with MarH3 over time (pH 8.0, 3 equiv. hydrogen peroxide) with or without MarH2, and comparison to synthetic standards **3.14b**, **3.16b**, and **3.20b**.

MarH2 failed to show any catalytic halogenating or α-hydroxyketone rearrangement activities on the tested meroterpenoid substrates, despite testing both individually and co-incubated with other MarH enzymes. This outcome supports the result of the previous MCD assay, in which MarH2 was the only putative VCPO of the three MarH enzymes to show no halogenating ability. With this in mind we decided to further investigate the genetic sequence of MarH2. Despite the high sequence similarity of MarH2 with other VCPO enzymes, closer investigation showed a substitution of the key vanadate coordinating histidine residue[18] with an asparagine (Figure 3.12). This substitution would explain the absence of halogenating activity in this

enzyme, however further investigation is needed to determine if this enzyme plays an unprecedented role in marinone biosynthesis.

```
MarH1      HFPTWTDFTQKCGASRVWGGVHFRKTVETSIAFGEQFGDMAHEFVQKHIKGEVED----      523
Mcl40      HFHTWAEFNKACAESRVWGGVHFRKTVQQSLIYGEQFGDLAHEFVNRHVKGNIKTDTRN      531
NapH1      HIPTWTDFTRTCATSRVWGGVHFQTTVDRTIDFGEQFGDLAHEFVQRHVKGDVKD----      527
NapH4      SFPTWTDFNKRCAYSRLDGGVHFKKTVERSMAFGEQFGDLAHDFIQRHVKGEGDG----      396
NapH3      TWATWTDFENDCATSRVWAGAHFTKTAETSLAFGTQFGDLAHTFVQRHINGDVKD----      478
MarH2      NYGTWTTFVRDAALSRVWAGVNFTKTAERSVEFGKQFGDLAHEFVQRHVSGEAED----      516
MarH3      HYGTWTEFVKDCGYSRLWAGVHFTTTVERSMEFGTQFGDLAYEFAQKYIKGDVED----      518
Mcl24      HWDTWTRFTRDCADSRVWGGVHFQTTVDRSIEWGAQFGDRAHQFLQRHIKGEVS-----      517
```

Figure 3.12: Multiple sequence alignment of VHPO homologues (C-terminal truncated region) from *Streptomyces* sp. meroterpenoid gene clusters. Sequence alignment was performed using Clustal Omega.[25] The key vanadate-coordinating histidine residue, highlighted in red, is mutated to an asparagine residue, highlighted in blue, in MarH2 (full Figure SI-3.6).

3.2.9 Activity of MarH1 and MarH3 on Pre-naphterpin

With the activity of MarH1 and MarH3 established in the marinone biosynthesis, our next focus was to determine if this biosynthetic logic could be extended to the naphterpin family of natural products, differing only by the length of the prenyl sidechain.

With the recombinant MarH enzymes in hand, we first investigated if MarH1 could convert pre-naphterpin **3.12a** to monochloride **3.16a**. Under analogous *in vitro* assay conditions to that of the marinone system, MarH1 was observed to convert pre-naphterpin to oxidatively dearomatised product **3.14a**, followed by monochlorination at C-2 to form **3.16a** (Figure 3.13).

Again, increased equivalents of H_2O_2 was not found to promote further chlorination of the substrate. This promising result mimicked that of the marinone system as we had hoped.

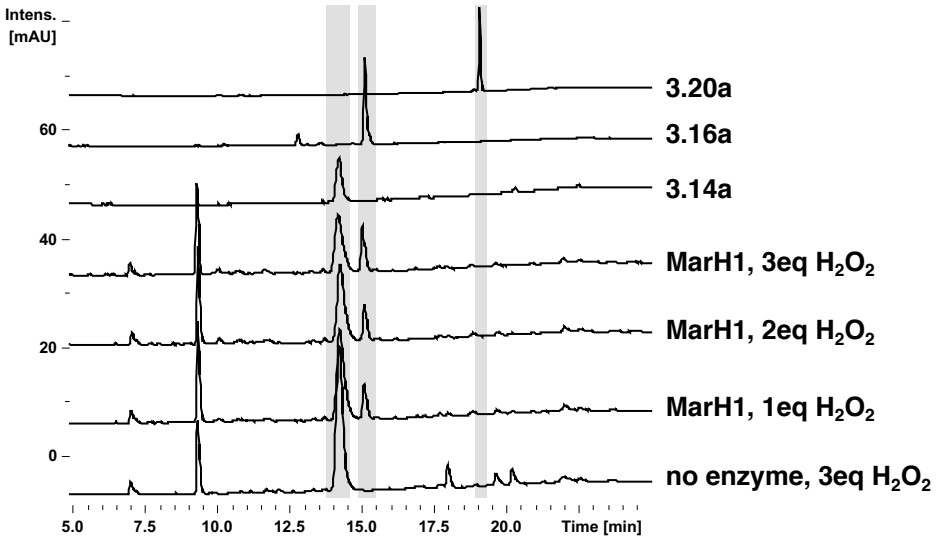

Figure 3.13: RP-HPLC-MS analysis (λ = 300 nm) of *in vitro* MarH1 incubation with **3.12a** in the presence of variable equivalents of hydrogen peroxide (pH 8.0, 18 h), and comparison to synthetic standards **3.14a**, **3.16a**, and **3.20a**.

After investigating this reaction at decreased time points (Figure 3.14), we observed almost exclusive production of the oxidatively dearomatised product **3.14a** after 1 h. The oxidatively dearomatised product **3.14a** was then slowly converted to the monochlorinated species **3.16a** between 3 – 18 h.

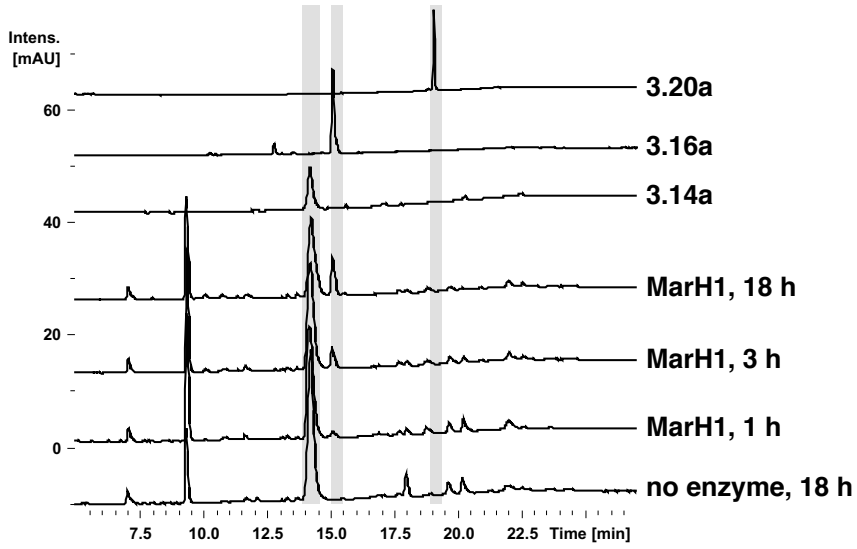

Figure 3.14: RP-HPLC-MS analysis (λ = 300 nm) of *in vitro* MarH1 incubation with **3.12a** over time (pH 8.0, 3 equiv. hydrogen peroxide), and comparison to synthetic standards **3.14a**, **3.16a**, and **3.20a**.

With MarH1 showing analogous catalysis in both the naphterpin and marinone systems, we moved our attention to MarH3. Incubation of pre-naphterpin (**3.12a**) with MarH3 was investigated. As predicted from the marinone system, MarH3 was capable of catalysing oxidative dearomatisation of pre-naphterpin to form **3.14a**, followed by monochlorination at the C-2 position to give **3.16a** as shown by MarH1. After 3 hours, MarH3 then began to catalyse a second chlorination event, followed by an α-hydroxyketone rearrangement to give **3.20a**.

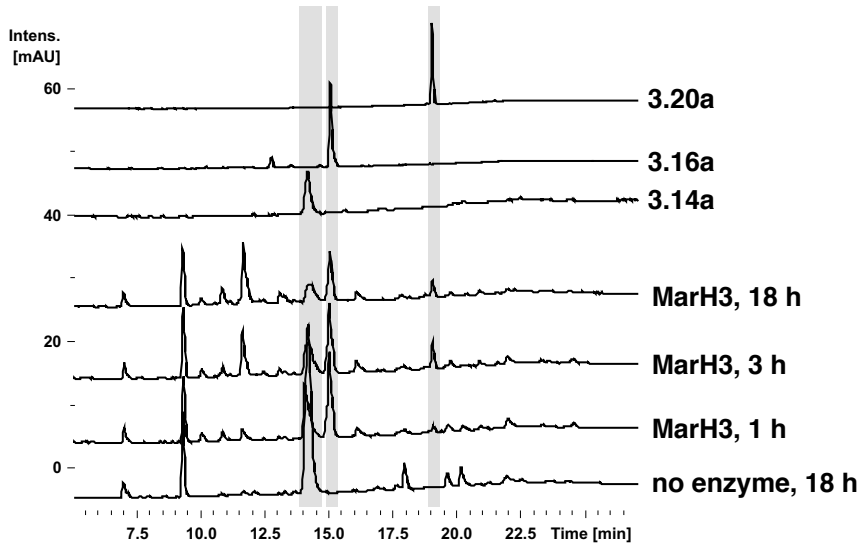

Figure 3.15: RP-HPLC-MS analysis (λ = 300 nm) of *in vitro* MarH3 incubation with **3.12a** over time (pH 8.0, 3 equiv. hydrogen peroxide), and comparison to synthetic standards **3.14a**, **3.16a**, and **3.20a**.

These results suggested the same sequence of reactions as observed for the marinone system. With this in mind, *in vitro* experiments were run with sequential addition of these enzymes (Figure 3.16). As expected, MarH1 converted pre-naphterpin (**3.12a**) to the oxidatively dearomatised product **3.14a**, followed by C-2 monochlorination to **3.16a**. MarH3 was then responsible for the second chlorination event, which promoted the α-hydroxyketone rearrangement to give **3.20a**.

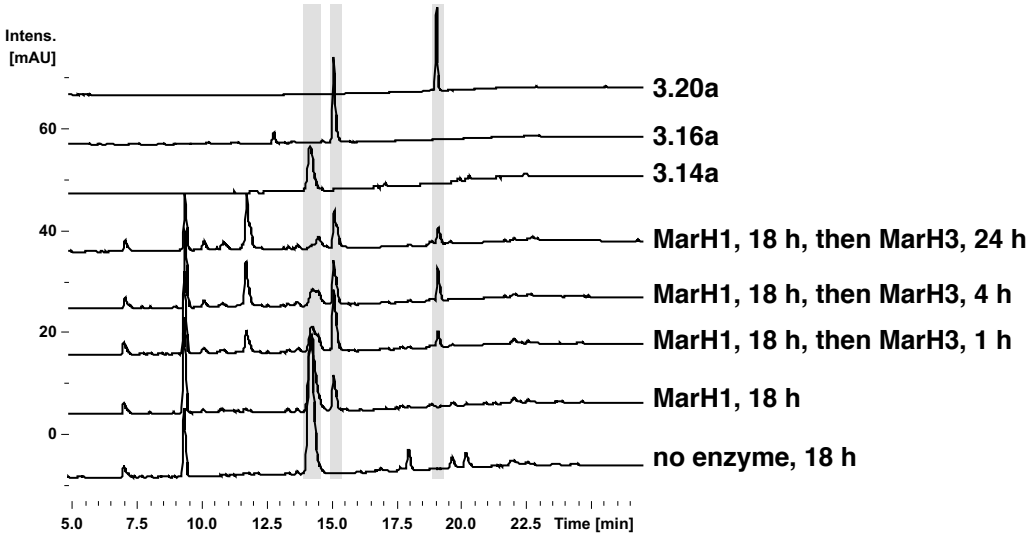

Figure 3.16: RP-HPLC-MS analysis (λ = 300 nm) of *in vitro* incubation of **3.12a** with MarH1 (pH 8.0, 3 equiv. hydrogen peroxide, 18 h) followed by MarH3 (1 additional equiv. hydrogen peroxide, variable time), and comparison to synthetic standards **3.14a**, **3.16a**, and **3.20a**.

This result had successfully confirmed our hypothesis that *Streptomyces* bacteria utilise VCPO enzymes to oxidise THN derivatives *via* cryptic chlorination in the biosynthesis of the naphterpin and marinone family of meroterpenoid natural products.

3.2.10 Activity of MarH3 on Racemic Dearomatized Substrates

At this stage, we were confident that we had elucidated two VCPO enzymes, responsible for catalysing oxidative dearomatisation and dichlorination and an α-hydroxyketone rearrangement, converting pre-marinone (**3.12b**) and pre-naphterpin (**3.12a**) to **3.20b** and **3.20a**, respectively. In order to confirm the success of each individual conversion, we investigated the activity of MarH3 on the chemically synthesised substrates.

In vitro incubation of oxidatively dearomatised synthetic substrate **3.14b** with MarH3 (pH 8.0, two equivalents H_2O_2, 18 h) resulted in conversion to the C-2 monochlorinated intermediated

3.16b. Next, *in vitro* incubation of monochlorinated synthetic substrate **3.16b** with MarH3 (pH 8.0, one equivalent H_2O_2, 18 h) resulted in a second C-2 chlorination event, followed by an α-hydroxyketone rearrangement to afford **3.20b**. As these synthetic substrates were racemic, an expected conversion of approximately 50% was observed, suggesting that these enzymes are specific for one enantiomer.

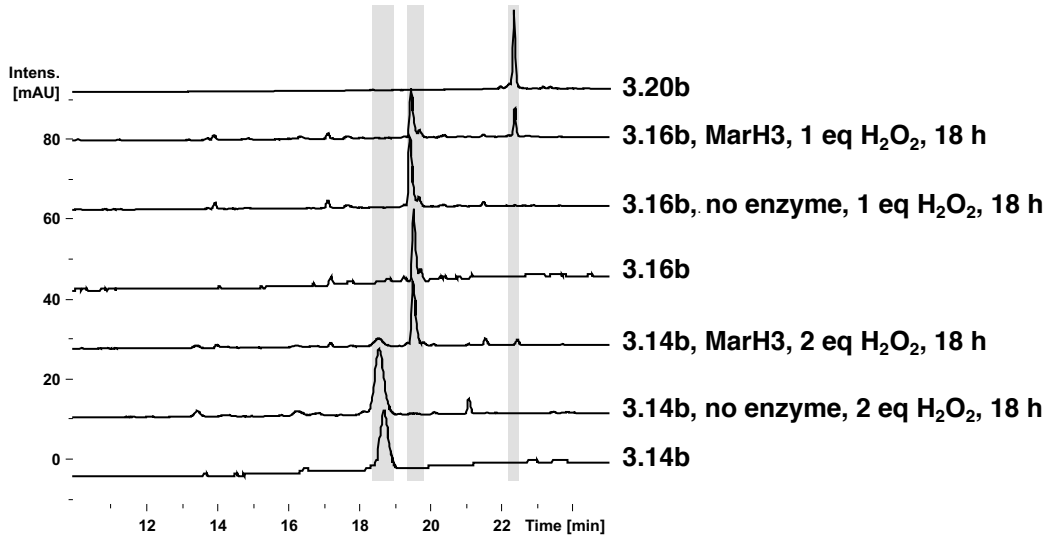

Figure 3.17: RP-HPLC-MS analysis (λ = 300 nm) of *in vitro* incubation of racemic synthetic substrates (**3.14b**/**3.16b**) with MarH3 (pH 8.0, variable quantities of hydrogen peroxide, 18 h), and comparison to synthetic standards **3.14b**, **3.16b**, and **3.20b**.

The same results were observed for the naphterpin synthetic intermediates. Again, *in vitro* incubation of MarH3 with oxidatively dearomatised synthetic substrate **3.14a** (pH 8.0, two equivalents H_2O_2, 18 h) resulted in conversion to the monochlorinated intermediated **3.16a**. Synthetic monochlorinated intermediate **3.16a** was then converted to **3.20a** through incubation with MarH3 (pH 8.0, one equivalent H_2O_2, 18 h). As expected, no more than approximately 50% of the racemic synthetic substrates were converted.

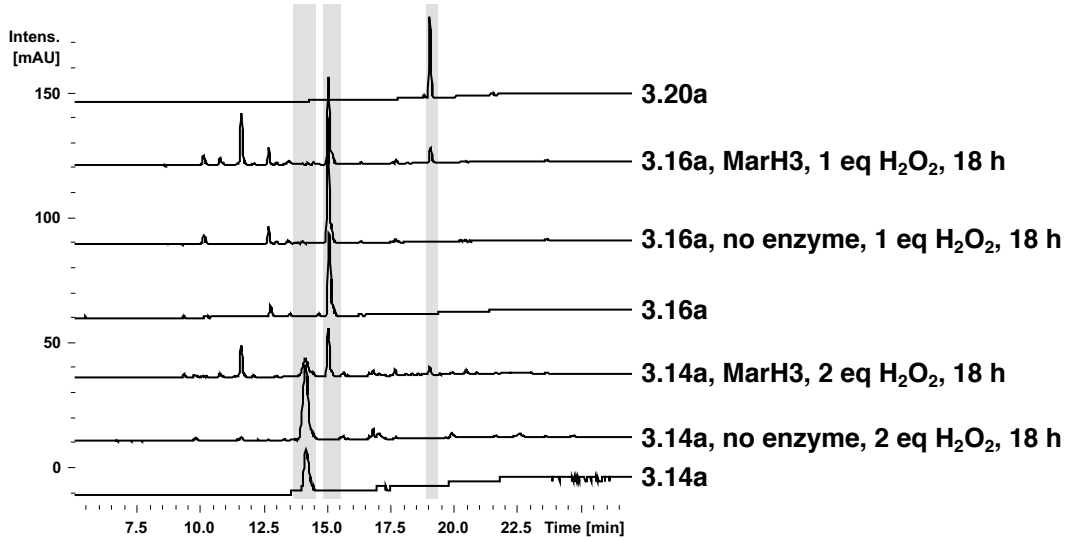

Figure 3.18: RP-HPLC-MS analysis (λ = 300 nm) of *in vitro* incubation of racemic synthetic substrates (**3.14a**/**3.16a**) with MarH3 (pH 8.0, variable quantities of hydrogen peroxide, 18 h), and comparison to synthetic standards **3.14a**, **3.16a**, and **3.20a**.

These results confirmed that cryptic halogenation plays a key role in both the naphterpin and marinone biosynthetic pathways. Here we confirmed that VCPO enzymes MarH1 and MarH3 were able to selectively oxidise and chlorinate the THN ring. Additionally, MarH3 was found to catalyse a second chlorination event, promoting the key α-hydroxyketone rearrangement required to give these natural product scaffolds (Scheme 3.14). While some redundancy was observed between these two enzymes, the combination of these enzymes was found to significantly improve the conversion of these reactions as well as decrease observed by-products. Biologically, we propose that these genes are regulated differently to help efficiently construct these molecules with minimal by-products. There is also the possibility of inherent redundancy of these genes, due to their evolution within the BGC.

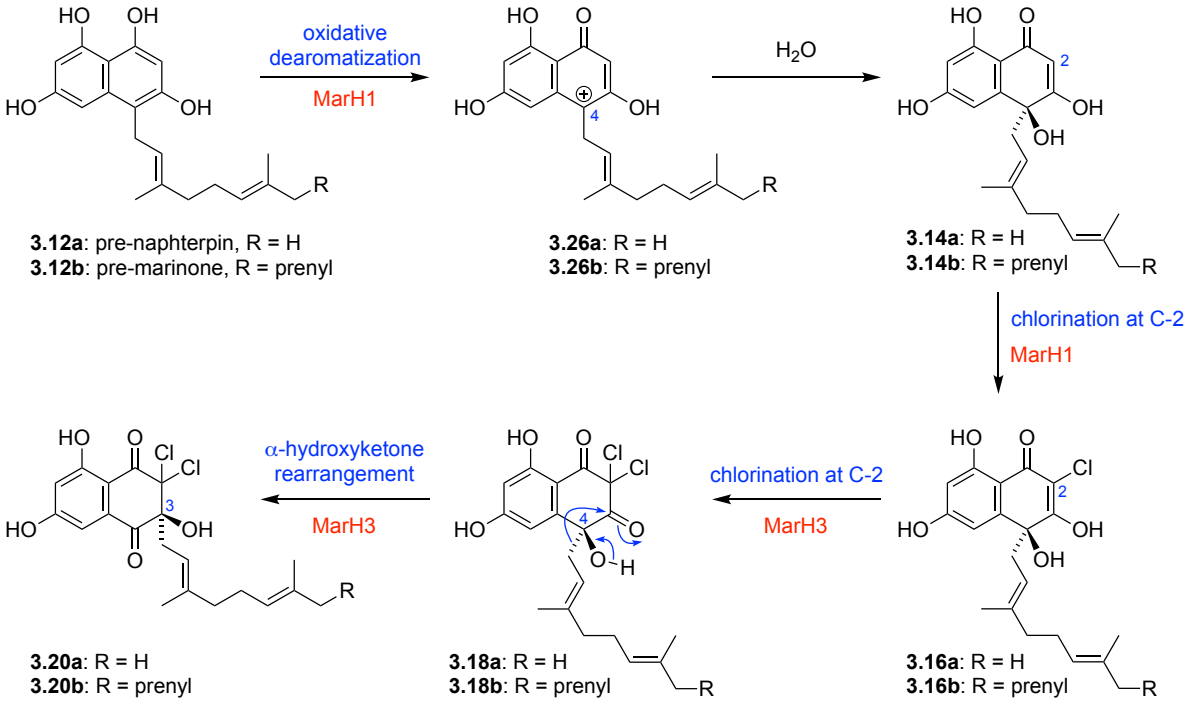

Scheme 3.14: Summary of the activity of MarH enzymes.

3.2.11 Investigation into Putative *O*-Methyltransferase Enzyme MarO

After successfully confirming the cryptic chlorination of THN intermediates in the naphterpin and marinone biosynthesis, we were enthusiastic to elucidate the enzymes responsible for catalysing the final steps in these biosynthetic pathways.

Returning our focus to the putative marinone genome from *Streptomyces* sp. CNQ-509,[11] we were interested in investigating genes which may be responsible for late stage interconversion of our proposed biosynthetic intermediates. The previously annotated genome predicted a putative S-adenosyl-methionine (SAM)-dependent *O*-methyltransferase enzyme *marO* (Figure 3.19).

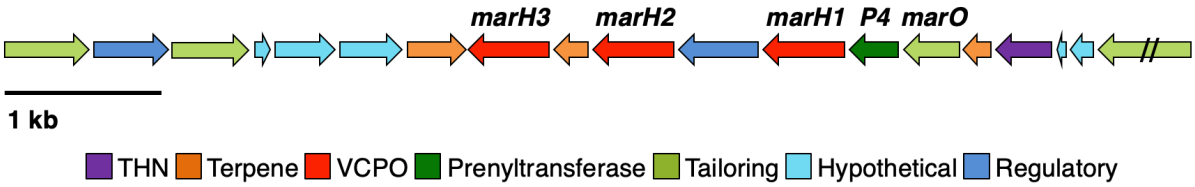

Figure 3.19: Graphical representation of the putative marinone biosynthetic gene cluster from *Streptomyces* sp. CNQ-509. Genes have been annotated with their proposed function. Putative SAM-dependent *O*-methyltransferase gene is annotated as *marO*.

In classical examples, SAM-dependant *O*-methyltransferase enzymes catalyse the transfer of the SAM (**3.27**) methyl group to the free hydroxyl group of an acceptor molecule, such as proteins and secondary metabolites through an S_N2 mechanism (Scheme 3.15).[26]

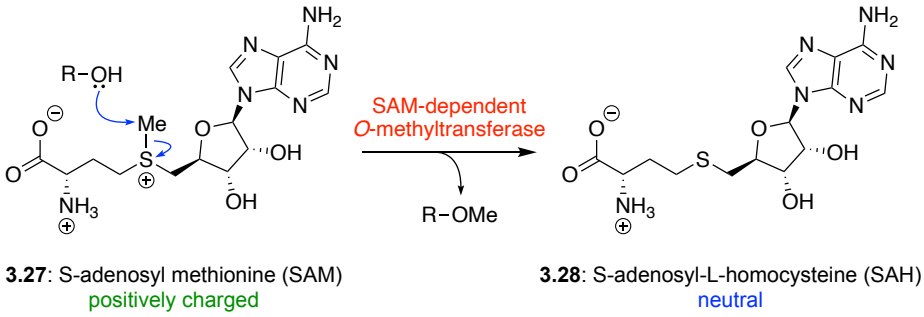

3.27: S-adenosyl methionine (SAM)
positively charged

3.28: S-adenosyl-L-homocysteine (SAH)
neutral

Scheme 3.15: Common S_N2 mechanism of methylation *via* SAM-dependent *O*-methyltransferase enzymes.[26]

In addition to their canonical methyltransferase activity, SAM-dependent enzymes have been shown to catalyse a variety of different reactions from typical alkylation reactions to hetero-Diels-Alder, Alder-ene and cyclopropanation reactions in natural product biosynthesis.[26–29]

In 2017, Tang and co-workers reported an inverse electron demand hetero-Diels–Alder reaction catalysed by a SAM-dependent *O*-methyltransferase enzyme, LepI (Scheme 3.16).[27]

In this example, LepI was able to catalyse the dehydration of **3.29** to afford the intermediate *o*-quinone methide **3.30**. In the presence of LepI, **3.30** underwent a hetero-Diels-Alder reaction to give leporin C (**3.31**). In the absence of LepI, a spontaneous intramolecular Diels-Alder reaction occurred to give cyclohexene **3.32**.

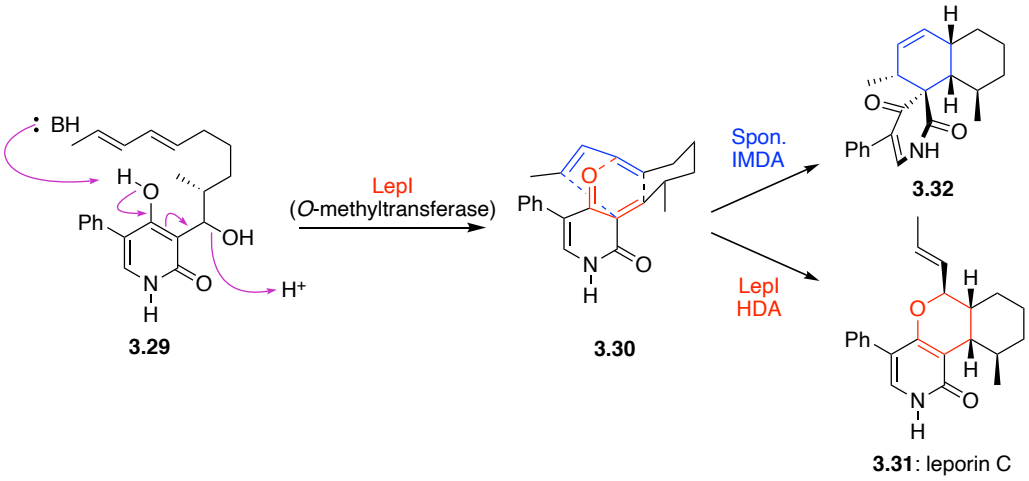

Scheme 3.16: LepI catalysed inverse electron demand hetero-Diels-Alder (HDA) in the biosynthesis of leporin C.[27]

As the marinone biosynthesis did not involve a distinct *O*-methylation step, we postulated that MarO could be responsible for catalysing late stage reactions in the marinone biosynthesis, similar to that observed by Tang and co-workers above.

3.2.12 Heterologous Expression and Purification of MarO

To obtain the desired enzyme, the *O*-methyltransferase homologue *marO* was cloned from the *Streptomyces* sp. CNQ-509 putative marinone biosynthetic gene cluster and heterologously expressed in *Escherichia coli*. The recombinant protein containing a *N*-terminal His_6-tag was purified using Ni^{2+} affinity chromatography (see 3.4.2 Biochemical Methods).

3.2.13 Activity of MarO

With the purified recombinant *O*-methyltransferase enzyme MarO in hand, the function of this enzyme within the putative marinone genome could now be investigated. Having previously synthesised all of our proposed biosynthetic intermediates, these could be utilised for chemoenzymatic assays.

Utilising the previously isolated VHPO enzymes, MarH1 and Mar H3, the initial steps in the marinone and naphterpin biosynthetic pathways had been elucidated, giving the dichlorinated intermediates **3.20a**/**3.20b**. With the unknown activity of MarO, the next linear step in the proposed marinone and naphterpin biosyntheses was the conversion of **3.20a**/**3.20b** to the α-chloroepoxides **3.21a**/**3.21b** (Scheme 3.17).

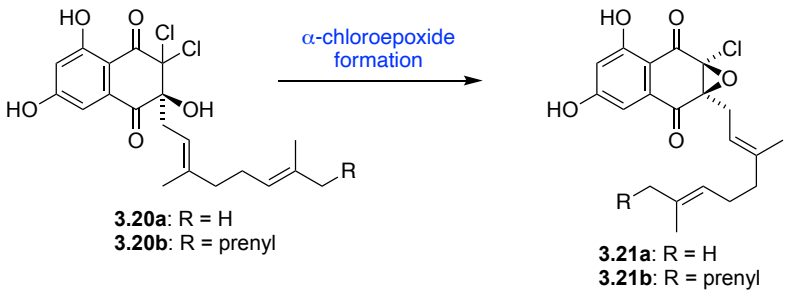

Scheme 3.17: Proposed α-chloroepoxide formation in marinone and naphterpin biosynthesis. R = prenyl in marinone system, R=H in naphterpin system.

Uncertain whether SAM had been co-isolated within the MarO active site, initial chemoenzymatic assays were run in both the presence and absence of exogenous SAM. *In vitro* incubation of the dichlorinated synthetic substrate **3.20b** with recombinant MarO (pH 8.0, 3 h) in both the presence and absence of SAM resulted in conversion to the α-chloroepoxide **3.21b** (Scheme 3.20). Additionally, conversion to **3.21b** was observed in the no enzyme control. This

result suggested that the formation of **3.21b** may be occurring spontaneously within the cell and is not enzyme catalysed.

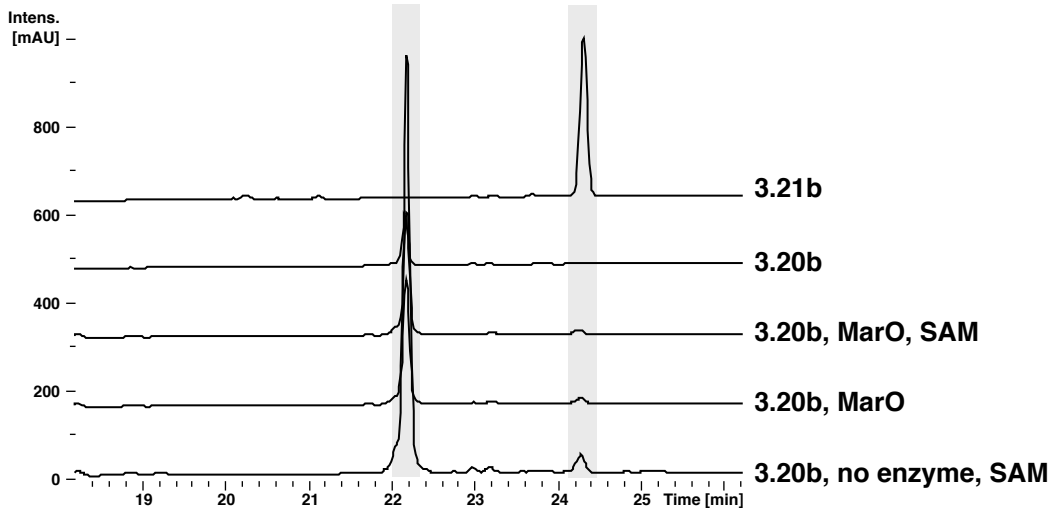

Figure 3.20: RP-HPLC-MS analysis (λ = 254 nm) of *in vitro* incubation of **3.20b** with MarO over time (pH 8.0) with or without SAM, and comparison to synthetic standards **3.20b**, and **3.21b**.

Following the formation of chloroepoxides **3.21a**/**3.21b**, the next biosynthetic step would involve reductive dehalogenation to give hydroxyquinones **3.23a**/**3.23b** (Scheme 3.18).

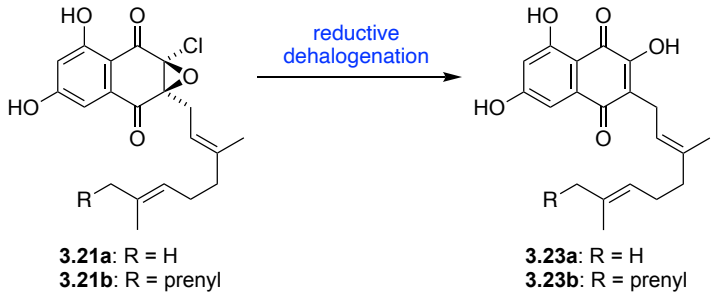

Scheme 3.18: Proposed reductive dehalogenation in marinone and naphterpin biosynthesis. R = prenyl in marinone system, R=H in naphterpin system.

I*n vitro* experiments began with incubation of α-chloroepoxide **3.21b** with MarO at pH 8.0 in both the presence and absence of SAM. After 30 min, conversion of **3.21b** to hydroxyquinone **3.23b** was observed (Figure 3.21). Irrespective of the presence of MarO, it was observed that the remaining starting material **3.21b** was converted to a new peak observed in Figure 3.21 at 18.9 min. Attempts to minimise formation of this side product were unsuccessful, leading us to believe its formation was the result of epoxide hydrolysis under the reaction conditions.

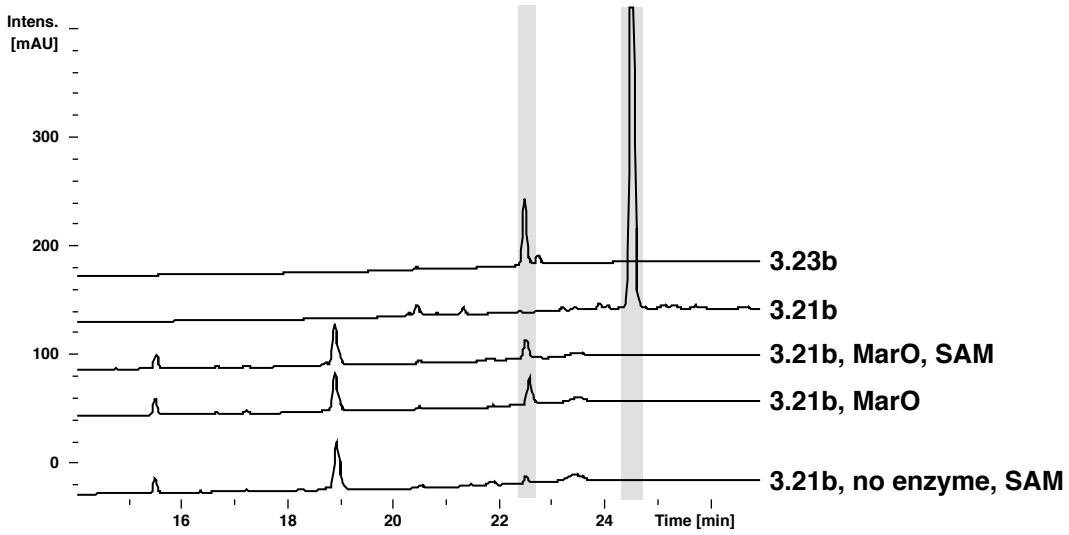

Figure 3.21: RP-HPLC-MS analysis (λ = 254 nm) of *in vitro* incubation of **3.21b** with MarO (pH 8.0, 3 h) in the presence and absence of SAM, and comparison to synthetic standards **3.21b** and **3.23b**.

The same result was observed on the naphterpin system, as chloroepoxide **3.21a** was converted to hydroxyquinone **3.23a** when treated with MarO in both the presence and absence of SAM (Figure 3.22). Again, the unavoidable hydrolysis product was observed at 14.6 min.

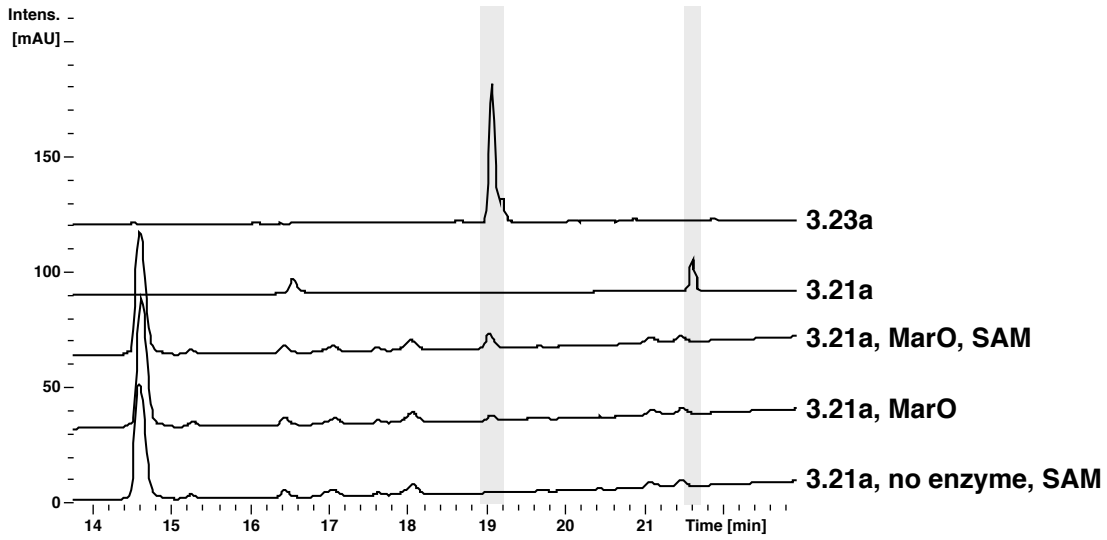

Figure 3.22: RP-HPLC-MS analysis (λ = 254 nm) of *in vitro* incubation of **3.21a** with MarO (pH 8.0, 3 h) in the presence and absence of SAM, and comparison to synthetic standards **3.21a** and **3.23a**.

This conversion was somewhat unexpected as we had previously envisaged that this *O*-methyltransferase, MarO, may be responsible for the catalysing the final oxidation step in the marinone biosynthesis, followed by alkene isomerisation and an intramolecular hetero Diels-Alder reaction. By comparison with synthetic standards and mass, it appeared that MarO catalysed only the initial reductive dehalogenation reaction, and not the subsequent oxidation and cyclisation steps.

Although examples of enzyme catalysed reductive dehalogenations are present in literature,[30] to the best of our knowledge, this is the first example of such a reaction being catalysed by an *O*-methyltransferase homologue.

As the assay proceeded in both the presence and absence of exogenous SAM, we predicted that SAM was copurified with MarO and remained bound in the active site. Following a procedure published by Tang and co-workers,[27] the presence of SAM in the active site was investigated through LC-MS detection of SAM degradation products, L-homoserine lactone and methylthioadenine (MTA), in the supernatant of heat denatured MarO (Scheme 3.19).

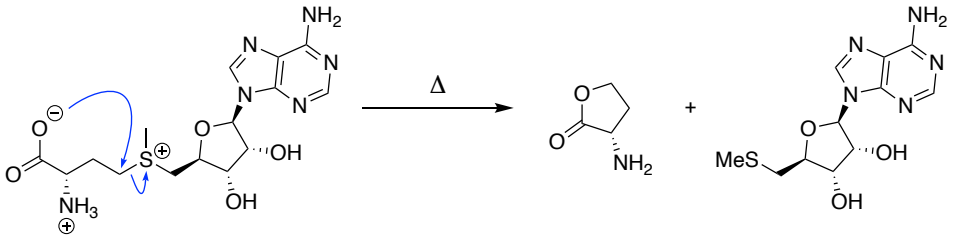

3.27: S-adenosyl methionine (SAM)

3.33: L-homoserine lactone

3.34: methylthioadenine (MTA)

Scheme 3.19: Thermal cleavage of SAM to give L-homoserine lactone and MTA.[27]

Denaturation of MarO with both MeCN and heat (100 ºC) followed by LC-MS analysis confirmed that SAM was copurified with MarO, due to the presence of both SAM (**3.27**) and degradation product MTA (**3.34**) in the supernatant (Figure 3.23).

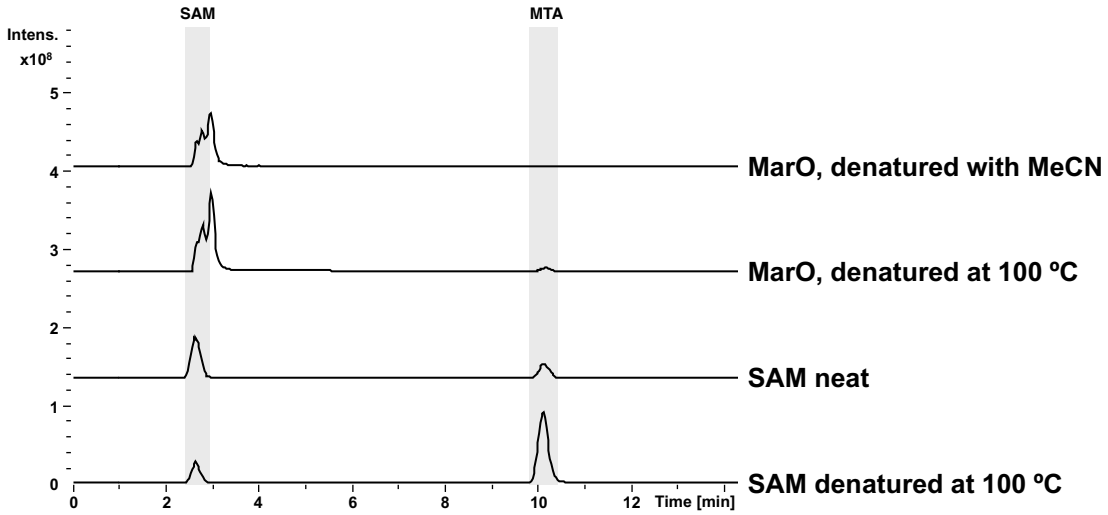

Figure 3.23: RP-HPLC-MS analysis confirming that purified MarO retains SAM. Extracted ion chromatograms (EICs) are shown using positive ionisation. Assay analytes extracted for MTA [M+H] = 298.1, and SAM [M+H] = 399.1, *m/z* values ± 0.2 Da. MarO was denatured at 100 ºC for 10 min, showing a single peak corresponding to MTA, matching commercial SAM denatured under the same conditions. MarO denatured with acetonitrile was found to also contain SAM in the supernatant, matching the commercial sample.

3.2.14 Early Mechanistic Studies of MarO

In our previous biomimetic synthesis, the reductive dehalogenation of chloroepoxides **3.21a**/**3.21b** was achieved using Zn powder. With this in mind, we were determined to confirm that this reaction was taking place within the enzyme active site, and not as a consequence of any co-purified metals. To confirm this, another enzyme assay was completed introducing **3.21a** to the assay conditions in which MarO had been pre-incubated in the presence of metal chelator ethylenediaminetetraacetic acid (EDTA) (Figure 3.24). As observed from Figure 3.24, the desired reductive dehalogenation reaction occurred in all experiments containing MarO. This was the case irrespective of the presence of EDTA, and therefore presumably, no trace metals were responsible for catalysing this reaction.

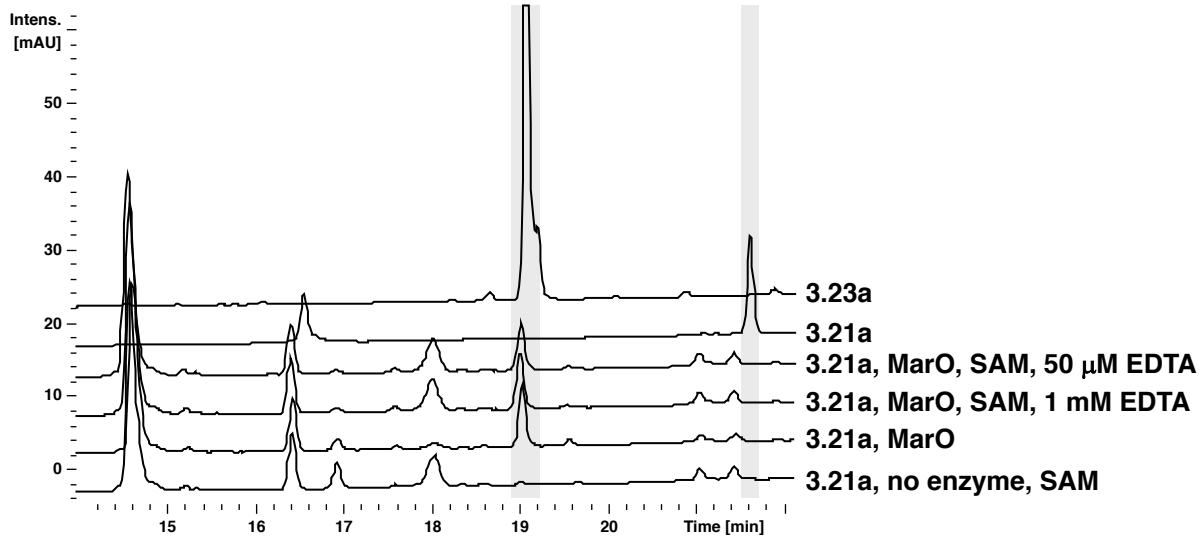

Figure 3.24: RP-HPLC-MS analysis (λ = 300 nm) of *in vitro* incubation of **3.21a** with MarO (pH 8.0, 3 h) in the presence of SAM and 50 μM to 1 mM EDTA. Comparison to standard incubation of **3.21a** with MarO and no enzyme assay, alongside synthetic standards **3.21a** and **3.23a**.

An additional assay was also run to confirm that nothing within the assay buffer was responsible for catalysing this reaction. To achieve this, the enzyme in buffer solution was centrifuged through an Amicon (10000 MWCO) concentration filter, removing any enzyme from the solution. Chloroepoxide **3.21a** was then treated under the assay conditions in the presence of the buffer solution and SAM, and in the absence of MarO. As observed in Figure 3.25, the reductive dehalogenation reaction did not occur in the presence of the enzyme buffer solution, only in the presence of the enzyme MarO. This result further established that MarO was responsible for catalysing this transformation.

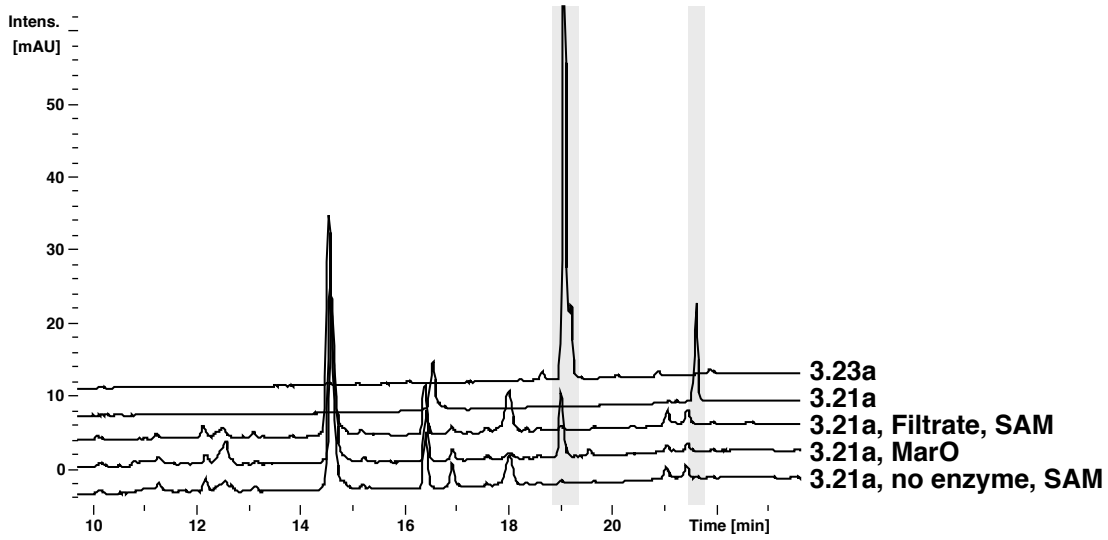

Figure 3.25: RP-HPLC-MS analysis (λ = 300 nm) of *in vitro* incubation of **3.21a** with filtered enzyme buffer (pH 8.0, 3 h) in the presence of SAM. Comparison to standard incubation of **3.21a** with MarO and no enzyme assay, alongside synthetic standards **3.21a** and **3.23a**.

At this stage we were confident that the enzyme MarO was playing a crucial role in the catalysis of this reaction, however we were yet to confirm if this reaction was occurring within the active site. Consequently, we decided to investigate whether this reductive dehalogenation could still be catalysed in the presence of the denatured enzyme. MarO was denatured by treatment with 0.1% formic acid in MeCN. The following assay was run in the presence of the denatured enzyme and SAM (Figure 3.26), however again showed that only the non-denatured MarO enzyme could catalyse this reaction.

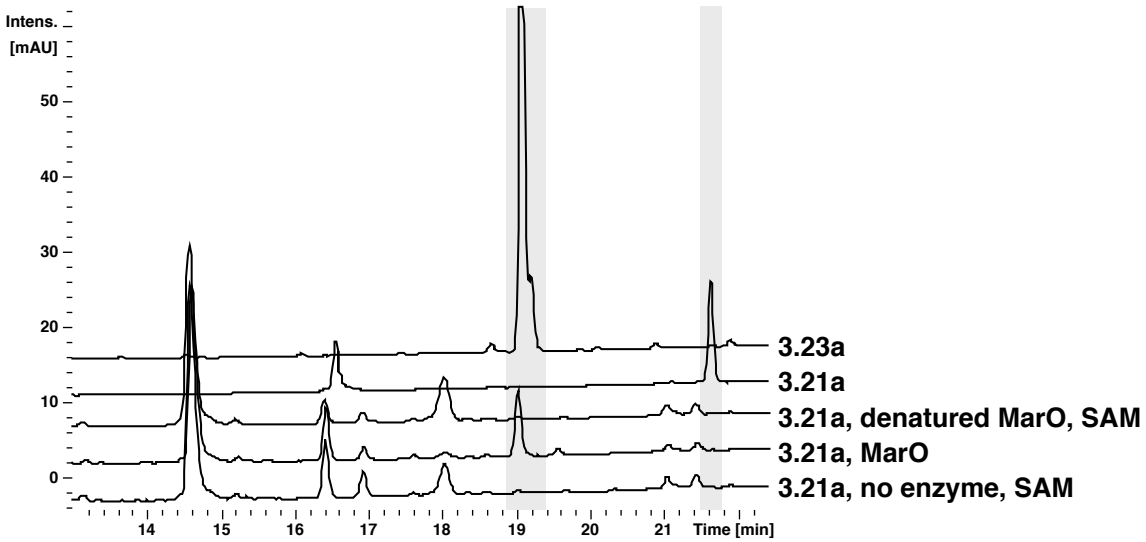

Figure 3.26: RP-HPLC-MS analysis (λ = 300 nm) of *in vitro* incubation of **3.21a** with denatured (MeCN, 0.1% formic acid) enzyme (pH 8.0, 3 h) in the presence of SAM. Comparison to standard incubation of **3.21a** with MarO and no enzyme assay, alongside synthetic standards **3.21a** and **3.23a**.

While catalytically active, the mechanism by which MarO achieved the reductive dehalogenation of **3.21a** was unknown. With the presence of SAM in the active site confirmed, we were curious to investigate its role within this reaction. Although the mechanism of most SAM-catalysed reactions are not extensively characterised, they are most commonly driven by the electrophilic character of the carbon centres adjacent to the positively charged sulfur atom of SAM.[31]

In order to determine the role of SAM in this reaction, the first step was to remove the co-purified SAM from the enzyme's active site. This was achieved through denaturation of the SAM-bound holoenzyme MarO with urea, followed by dialysis and re-folding to give the apoenzyme (see 3.4.2 Biochemical Methods). The refolded protein was then purified by size exclusion chromatography to remove any protein aggregates. The apoenzyme was denatured,

and the lysate analysed by LC-MS to confirm the absence of SAM using the same protocol as above (Figure 3.27). MarO holoenzyme denatured with heat and denatured with 0.1% formic acid in acetonitrile were shown to contain SAM through the presence of SAM degradation product MTA, matching commercial SAM denatured by heat. No presence of SAM was observed in apoenzyme denatured under the same conditions, confirming that SAM had been successfully removed from the MarO active site.

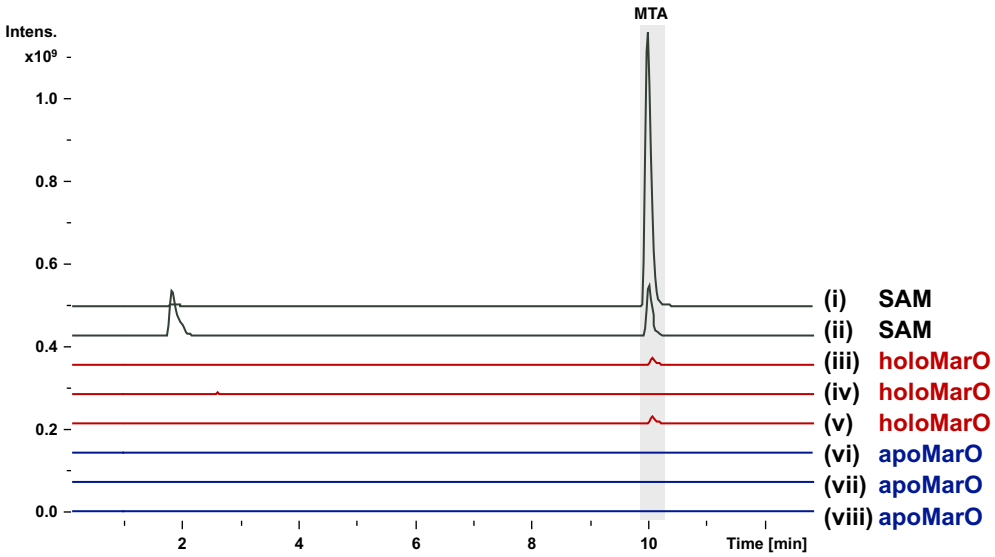

Figure 3.27: RP-HPLC-MS analysis confirming that SAM was successfully removed from MarO active site. Extracted ion chromatograms (EICs) are shown using positive ionisation. Assay analytes extracted for MTA [M+H] = 298.1, *m/z* values ± 0.2 Da. MarO holoenzyme and MarO apoenzyme denoted as holoMarO and apoMarO, respectively. LC−MS profiles of (i) SAM denatured at 100 ºC for 10 min, (ii) an authentic reference of SAM, (iii) holoMarO denatured with 0.1% formic acid in MeCN, (iv) holoMarO denatured MeCN, (v) holoMarO denatured at 100 ºC for 10 min, (vi) apoMarO denatured with 0.1% formic acid in MeCN, (vii) apoMarO denatured MeCN, (viii) apoMarO denatured at 100 ºC for 10 min. Experimental details are described in 3.4.2 Biochemical Methods)

After successfully removing SAM from the active site, we could now investigate its role in the catalysis of the reductive dehalogenation reaction. MarO enzymatic assays were performed in the absence of SAM (**3.27**), alongside the presence of SAM competitive inhibitor S-adenosyl-L-homocysteine[32] (SAH) (**3.28**) and the positively-charged SAM mimic, sinefungin[33] (**3.35**) (Figure 3.28) following literature procedure (Figure 3.29).[27]

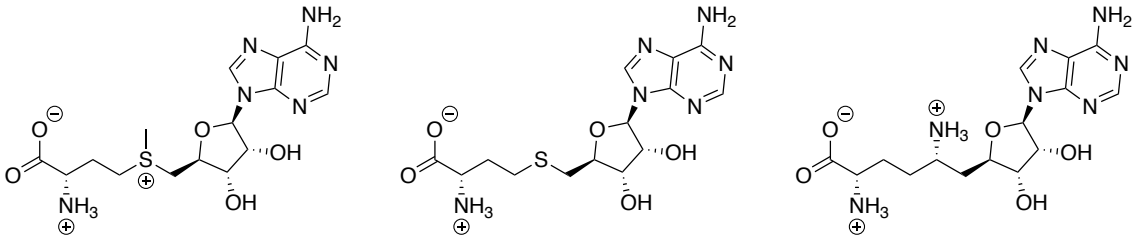

Figure 3.28: SAM (**3.27**) analogues SAH (**3.28**) and sinefungin (**3.35**) used in MarO assay.

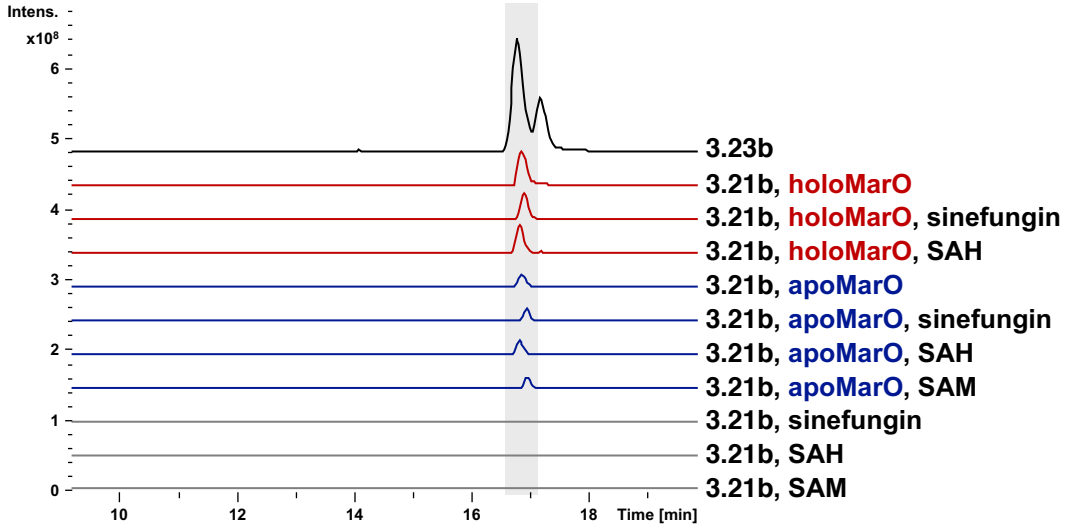

Figure 3.29: RP-HPLC-MS extracted ion chromatogram (EIC) analysis investigating the role of SAM in the MarO active site. Extracted ion chromatograms (EICs) are shown using negative ionisation. Assay analytes extracted for **3.23b** [M-H] = 409.2, *m/z* values ± 0.2 Da. *In vitro* incubation of **3.21b** with MarO holoenzyme (holoMarO) or apoenzyme (apoMarO) (pH 8.0, 1 h) in the presence and absence of exogenous SAM, SAH and sinefungin, and comparison to synthetic standard **3.23b**.

The results of these assays showed that MarO was active, irrespective of the presence or absence of a co-substrate. Despite our previous hypothesis of a SAM-dependent reaction, SAM was not required within the active site for the reaction to take place. The presence of the positively charged SAM molecule or its positively charged analogue, sinefungin, was found to have no substantial impact on the assay outcome. Neutrally charged co-substrate SAH, the demethylated analogue of SAM, has previously been identified as a competitive inhibitor of methyltransferase enzymes.[34] Introduction of SAH (**3.28**) to these *in vitro* assays exhibited no inhibition of this reaction. These results established that SAM is not an essential component of the catalysis demonstrated by MarO, and therefore this positive charge does not play a key role in these reactions as we had previously predicted.

At this stage, we anticipated that protein residues within the active site of MarO must be responsible for catalysing this reductive dehalogenation. Therefore, the most tangible experiment to confirm the formation of the product **3.23b** was decided to be 1D and 2D NMR analysis. In order to complete a milligram scale *in vitro* synthesis of **3.23b**, a total of 20 x 1 mL assays were run concurrently, following the procedure outlined in 3.4.2 Biochemical Methods. Following work-up and purification, ^{1}H NMR analysis of the enzymatic product and the previously prepared synthetic standard were found align almost perfectly, despite minor impurities present in the enzymatic spectrum (Figure 3.30). Further comparison of 2D NMR data, alongside our previous retention time and MS data confirmed the formation of hydroxyquinone **3.23b** as the product of this enzyme catalysed reductive dehalogenation.

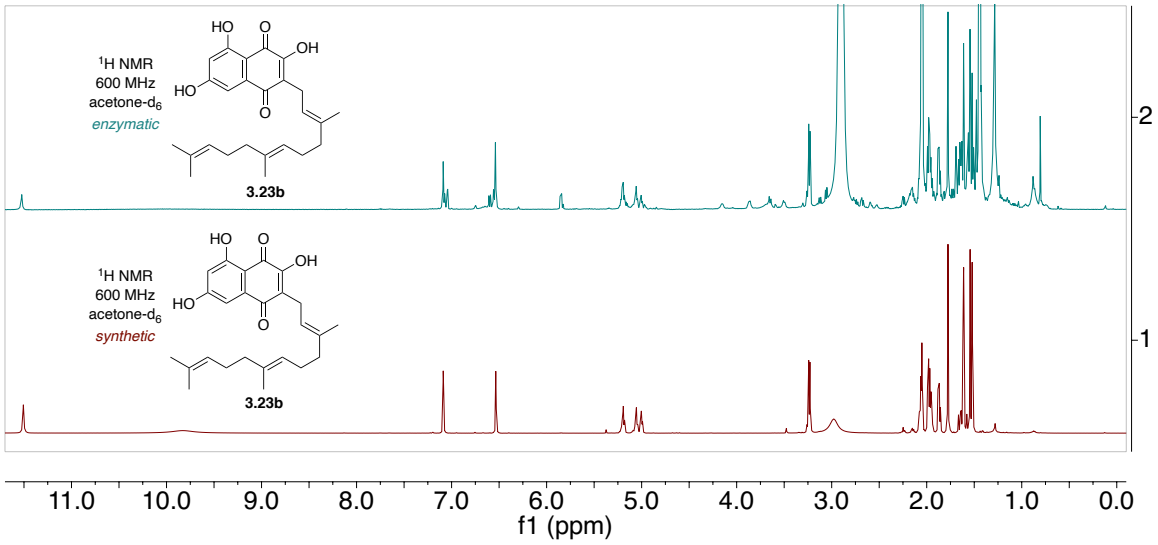

Figure 3.30: Comparison of ^{1}H NMR spectra of enzymatic (top) and synthetic (bottom) **3.23b**.

With these results, we remain confident that the putative *O*-methylransferase enzyme MarO is responsible for the reductive dehalogenation of chloroepoxides **3.21a**/**3.21b** to form hydroxyquinones **3.23a**/**3.23b**. Further work to characterize the MarO enzyme is currently

underway through crystallisation studies. Insight into the structure of this enzyme could identify the mechanism behind this unprecedented reductive dehalogenation reaction.

3.2.15 Investigation into MarX1, MarX2, MarX3, Mar4

Following our tentative assignment of MarO as a reductive dehalogenase, we turned our focus to the enzymes responsible for catalysing the final steps in the marinone biosynthesis. We predicted that from hydroxyquinone intermediate **3.23b**, the final steps in the biosynthesis would proceed through a cascade of oxidation, alkene isomerisation and an intramolecular hetero Diels-Alder reaction to give debromomarinone (**3.07**) (Scheme 3.20).

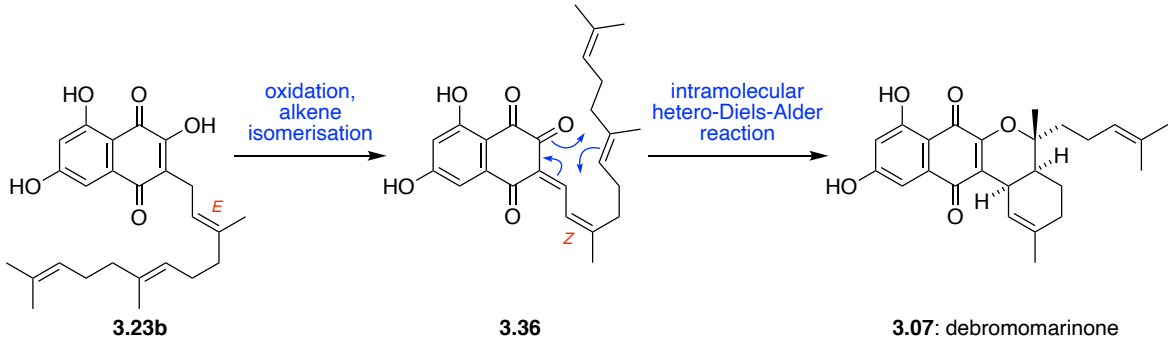

3.23b **3.36** **3.07**: debromomarinone

Scheme 3.20: Proposed final reaction cascade in debromomarinone (**3.07**) biosynthesis.

Utilising the genome annotation tool, BLAST,[6] four genes of interest were identified within the putative marinone gene cluster. These four genes were tentatively labelled *marX1*, *marX2*, *marX3* and *marX4* (Figure 3.31). Genes *marX1*, *marX2* and *marX3* were all predicted as "hypothetical proteins", denoting a large open reading frame without a previously characterised homologue in the protein database. Both *marX2* and *marX3* were also identified as containing PEP-cterm domains, often associated with an *N*-terminal signal peptide. The fourth gene, *marX4*, was identified as an aromatic ring hydroxylase, possibly FAD-binding.

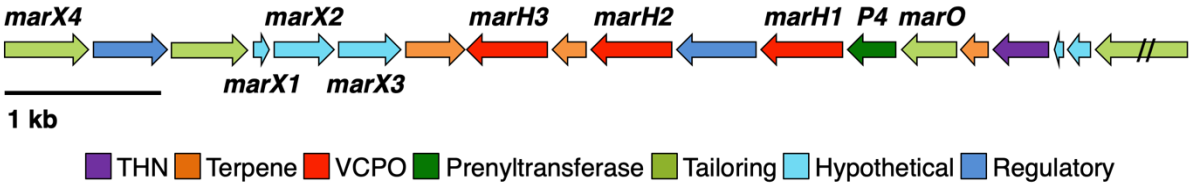

Figure 3.31: Graphical representation of the putative marinone biosynthetic gene cluster from *Streptomyces* sp. CNQ-509. Tentatively labelled genes *marX1*, *marX2*, *marX3* and *marX4* are denoted above.

Examining the literature, we had previously noted a similar oxidative cyclisation as that predicted for the marinone biosynthetic pathway in the biosynthesis of Δ^1-tetrahydrocannabinolic acid (THCA, **3.37**) (Scheme 3.21). In this case, an FAD dependent oxidoreductase enzyme, THCA synthase, is responsible for the oxidative cyclisation of cannabigerolic acid (**3.38**) to give **3.37** through the same cascade of oxidation, alkene isomerisation and intramolecular hetero-Diels-Alder reactions that we propose in the marinone biosynthesis.[35,36]

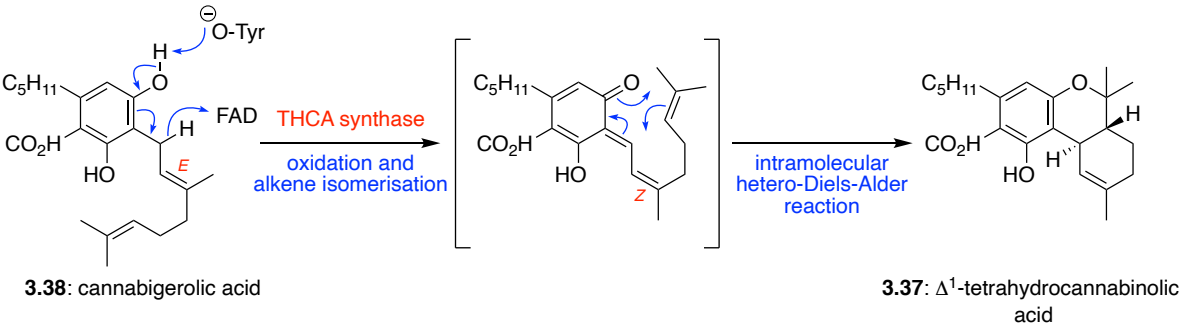

Scheme 3.21: Proposed mechanism of tetrahydrocannabinol biosynthesis.

With this in mind, the structural homology of the putative aromatic ring hydroxylase MarX4 was also investigated using the Protein Homology/Analogy Recognition Engine, Phyre2.[37] MarX4 was shown to have 25% similarity with a FAD-dependent [4+2] cyclase, PyrE3 from

the pyrroindomycins biosynthetic pathway.[38] These results suggested that the putative aromatic ring hydroxylase enzyme, MarX4, with the potential for FAD binding could be responsible for catalysing the final oxidative cyclisation in the marinone biosynthesis.

Alternatively, we were unsure of the function of the hypothetical proteins MarX1, MarX2 and MarX3. In this case Phyre2 and BLAST were also used to predict the function on these enzymes. Hypothetical protein MarX1 was found to have structural homology to a monooxygenase enzyme, ActVA-Orf6, from *Streptomyces coelicolor*.[39] This enzyme is known to catalyse the oxidation of an aromatic substrate, in the absence of any cofactors, metal ions or prosthetic groups, usually associated with the activation of molecular oxygen. Both *marX2* and *marX3* were found to have sequence homology to two genes ScyE and ScyD, predicted to be involved in the biosynthesis of the natural sunscreen scytonemin from *Nostoc punctiforme* ATCC 29133.[40–42] Interestingly, *scyD* appeared to be a duplication of the *scyE* gene, suggesting a highly conserved pseudogene within the gene cluster.

3.2.16 Heterologous Expression and Purification of MarX1, MarX2, MarX3 and MarX4.

To obtain the putative aromatic ring hydroxylase *marX4*, the gene was cloned from the *Streptomyces* sp. CNQ-509 putative marinone biosynthetic gene cluster and heterologously expressed in *Escherichia coli*. The recombinant protein containing a *N*-terminal His_6-tag was then purified using Ni^{2+} affinity chromatography (see 3.4.2 Biochemical Methods).

Hypothetical genes *marX1*, *marX2* and *marX3* were cloned from the *Streptomyces* sp. CNQ-509 putative marinone biosynthetic gene cluster. Both *marX2* and *marX3* were predicted to contain *N*-terminal signal peptides, commonly leading to the secretion of these proteins from

the cell. In order to avoid this issue, the protein sequence of the signal peptide in both MarX2 and MarX3 was identified using the bioinformatics prediction server SignalP-5.0.[43] From this information, primers were created to clone only the desired DNA sequence, without the signal peptide. Following PCR, all genes were individually cloned with a *N*-terminal His_6-tag and heterologously expressed in *Escherichia coli*. Recombinant protein MarX1 was then purified using Ni^{2+} affinity chromatography (see 3.4.2 Biochemical Methods). Recombinant proteins MarX2 and MarX3 were found to have poor expression and the crude lysate was used in preliminary assays.

3.2.17 Preliminary studies of MarX4

Investigations into the final oxidative cyclisation cascade began with the putative aromatic ring hydroxylase enzyme, MarX4. Within the numerous literature examples of enzyme mediated Diels-Alder reactions in natural product biosynthesis,[44–48] there are several examples in which FAD-dependent enzymes are responsible for catalysing this [4+2] cycloaddion.[36,38,49] After purification of MarX4 through Ni^{2+} affinity chromatography, we observed a strong yellow colour indicating that FAD was co-purified with the enzyme. In order to accurately investigate the presence of FAD, MarX4 was denatured under three different conditions; MeOH, 0.1% formic acid in MeCN and heat (95 ºC for 10 min). LC-MS analysis of the supernatant was then compared to a commercial sample of FAD, confirming the presence of FAD within the active site of MarX4.

The *in vitro* activity of MarX4 was investigated through assays with hydroxyquinone **3.23b**, in the hope it would be converted to the natural product, debromomarinone **3.07** (Scheme 3.22). Unsure of any exogenous cofactors required by MarX4, assays were run in the presence of flavin and nicotinamide cofactors (FAD and $NADP^+$), and cofactor regeneration enzymes SsuE

and phosphite dehydrogenase enzyme (PtdH). $FADH_2$ would be regenerated *in situ* by *E. coli* flavin reductase SsuE,[50] which in turn oxidizes NADPH to $NADP^+$. $NADP^+$ would then be recycled to NADPH *in situ* using $NADP^+$ reductase/phosphite dehydrogenase PtdH and sodium phosphite.[51,52] Assay conditions, alongside both SsuE and PtdH enzymes were obtained from Dr. Hanna Luhavaya.[52] Unfortunately, *in vitro* incubation of **3.23b** under these assay conditions was not found to result in any reaction, with only the starting material observed (see 3.4.2 Biochemical Methods). Additional assays were also attempted in the absence of PtdH and the presence of NADPH, however these were also unsuccessful.

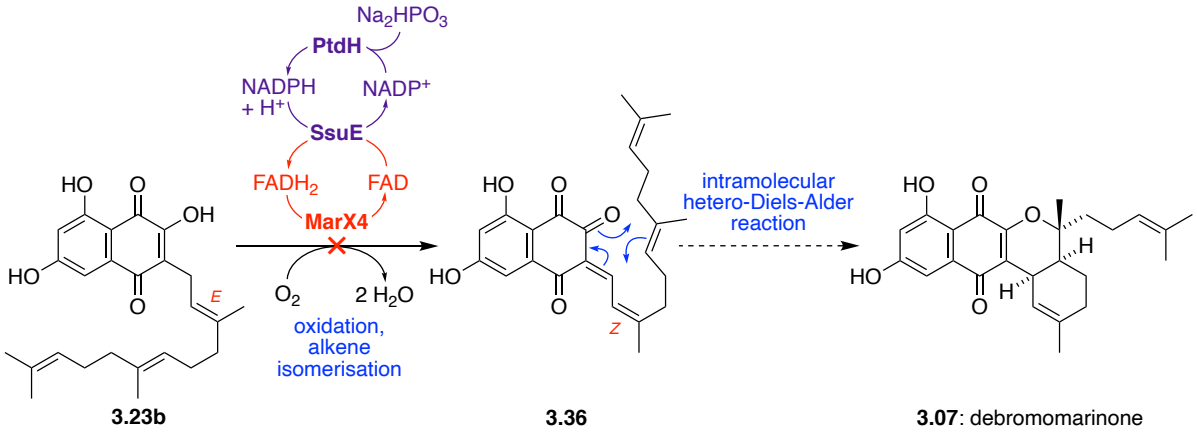

Scheme 3.22: Assay conditions for attempted oxidation of **3.23b**.

A similar set of assay conditions was also implemented to investigate if MarX4 was capable of catalysing the final bromination of debromomarinone (**3.07**) to give the natural products marinone (**3.39**) or isomarinone (**3.40**) (Scheme 3.23). An analogous assay was used to discover the halogenating activity of flavin-dependent halogenase, Bmp2, in the biosynthesis of tetrabromopyrrole.[51] In this system, the halide (Br^-) would be oxidised in the presence of O_2 and FAD to generate an electrophilic halogen, which could then react with nucleophilic substrate **3.07** within the active site. Despite multiple attempts, treatment of **3.07** under these

reaction conditions yielded no reaction, with only starting material observed. Additional assays were attempted in the absence of PtdH and the presence of NADPH. These conditions are analogous to that of Bmp5, a flavin-dependent phenol brominase enzyme, which does not require flavin reductase to regenerate $FADH_2$ *in situ*,[53] however these conditions were also unsuccessful on our substrate.

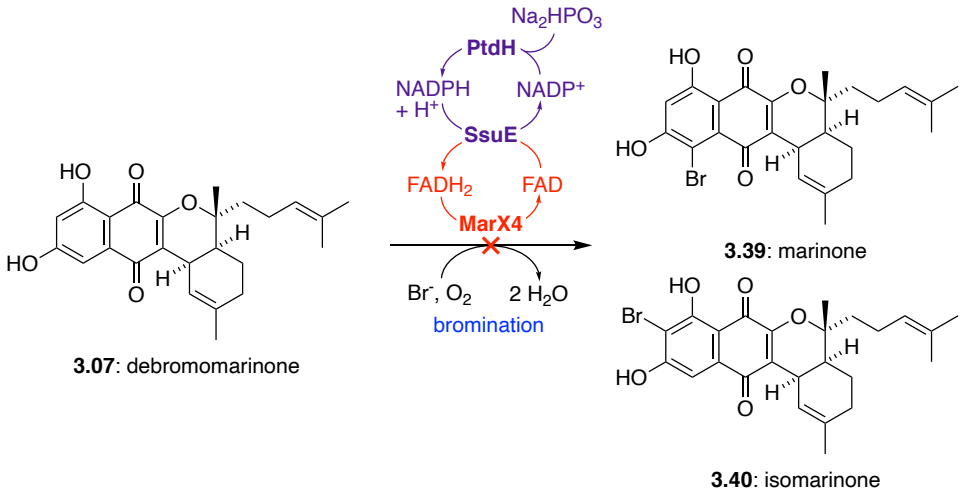

Scheme 3.23: Proposed enzymatic bromination of debromomarinone (**3.07**) to afford marinone (**3.39**) and/or isomarinone (**3.40**).

At this stage, the role of MarX4 within the putative marinone BGC remains unknown. As the *marX4* gene appears to flank the putative BGC, there is a possibility that this gene resides outside of the gene cluster itself. It is also possible that the necessary exogenous co-factors were not provided within our preliminary *in vitro* assays, and therefore further studies towards the activity of this enzyme are being investigated.

3.2.18 Preliminary studies of MarX1, MarX2, MarX3

As our isolated MarX4 enzyme was not found to catalyse the final oxidative cyclisation cascade under our assay conditions, we moved our focus to investigate the activity of the three hypothetical proteins MarX1, MarX2 and MarX3 on hydroxyquinone **3.23b**.

Preliminary assays were run using the cell lysate of *E. coli* heterologously expressing MarX1, MarX2 and MarX3, individually. The *in vitro* activity of these enzymes was investigated using lysates containing individual enzymes, as well as a combination of all three enzyme lysates, however analysis by LC-MS showed only starting material for all assays investigated.

As MarX1 was shown to have the highest expression from protein gel electrophoresis, this protein was further purified by Ni^{2+} affinity chromatography. *In vitro* incubation of **3.23b** with purified MarX1 was investigated, however only starting material was observed.

As MarX1, MarX2 and MarX3 were annotated to be hypothetical proteins, there is little known about their function, or which cofactors they may require to be active. Further investigation into these three hypothetical enzymes is required to determine their role within the marinone BGC. Investigations into the enzymes responsible for catalysing the final steps in the marinone and naphterpin biosynthetic pathways are still ongoing. The success of these studies has the potential to lead to a complete *in vitro* enzymatic synthesis of these complex natural product scaffolds.

3.3 Conclusions

The completed biomimetic total synthesis of 7-demethylnaphterpin (**3.06**) and debromomarinone (**3.07**) gave access to each proposed biosynthetic intermediate for use in chemoenzymatic assays, after facile MOM deprotection. This allowed for investigation into the complete biosynthesis of these meroterpenoid natural products.

In these studies, it was discovered that *Streptomyces* bacteria are capable of using VCPO enzymes to selectively oxidise THN derivatives through cryptic chlorination events in the biosynthesis of the naphterpin and marinone families of natural products. This biosynthetic sequence began with a VCPO-mediated chlorination and oxidative dearomatisation of **3.12a**/**3.12b** through **3.41a**/**3.41b** to give intermediate carbocations **3.26a**/**3.26b** (Scheme 3.24). Nucleophilic attack from water gave intermediate enols **3.14a**/**3.14b**, followed by C-2 monochlorination to afford **3.16a**/**3.16b.** All reactions in this sequence were catalysed by VCPO enzyme MarH1, in the presence of H_2O_2, KCl and Na_3VO_4.

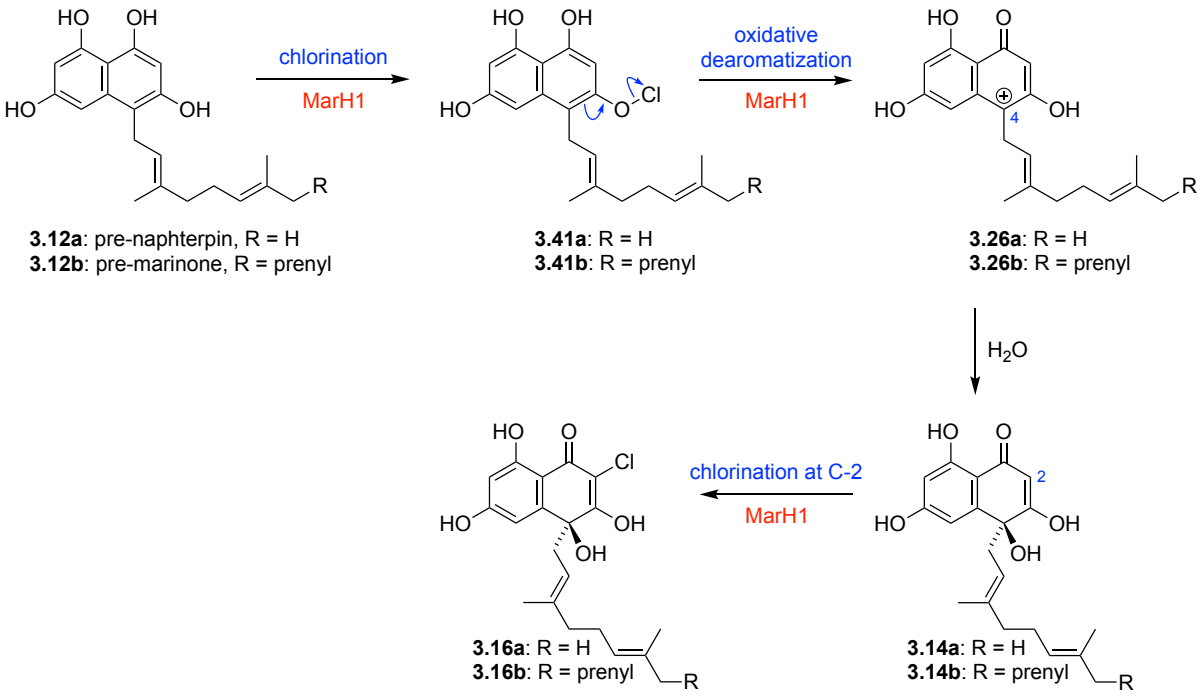

Scheme 3.24: Oxidative dearomatisation and monochlorination catalysed by VCPO MarH1.

VCPO enzyme MarH3 in the presence of H_2O_2, KCl and Na_3VO_4 was found to catalyse the second C-2 chlorination event of chloroenols **3.16a**/**3.16b** to give geminal dichlorides **3.18a**/**3.18b** (Scheme 3.25). Formation of these dichlorinated substrates **3.18a**/**3.18b** promoted an α-hydroxyketone rearrangement, shifting the alkyl sidechain from the C-4 to the C-3 position of the THN ring to give **3.20a**/**3.20b**.

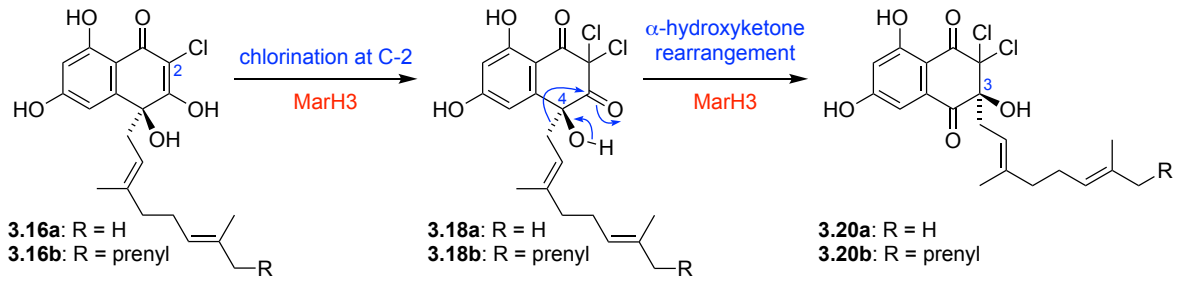

Scheme 3.25: Chlorination and α-hydroxyketone rearrangement catalysed by VCPO MarH3.

Chloroepoxide formation from **3.20a**/**3.20b** was found to occur spontaneously *in vitro*, requiring no recombinant enzymes (Scheme 3.26). Preliminary *in vitro* assays with α-chloroepoxides **3.21a**/**3.21b** found that the predicted SAM-dependent *O*-methyltransferase enzyme MarO was capable of catalysing the anticipated reductive dehalogenation to form achiral hydroxyquinone intermediates **3.23a**/**3.23b**. Despite being co-isolated with SAM, this enzyme was not found to be SAM-dependent, and therefore the mechanism of this reaction requires further studies.

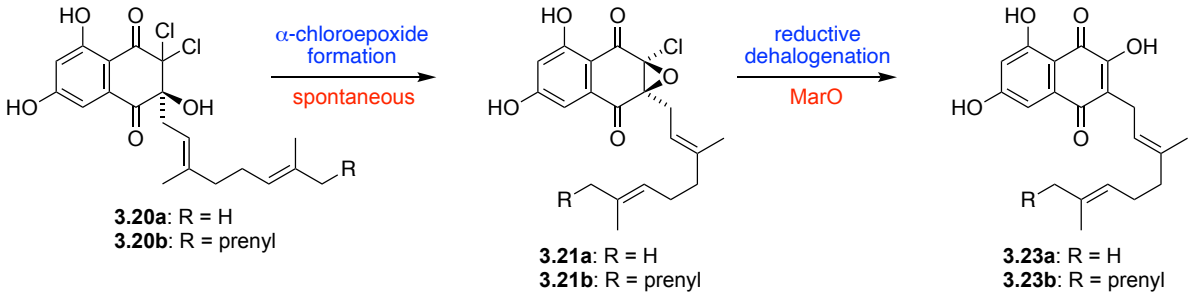

Scheme 3.26: Spontaneous α-chloroepoxide formation followed by MarO catalysed reductive dehalogenation.

The final oxidative cyclisation cascade (Scheme 3.27) to transform **3.23a**/**3.23b** into the natural products 7-demethylnaphterpin (**3.06**) and debromomarinone (**3.07**) was investigated with four individual enzymes, tentatively named MarX1, MarX2, MarX3 and MarX4. As both 7-demethylnaphterpin (**3.06**) and debromomarinone (**3.07**) were isolated as enantiopure compounds, we propose that the oxidation and cyclisation of achiral intermediates **3.23a**/**3.23b** must occur under enzymatic control.

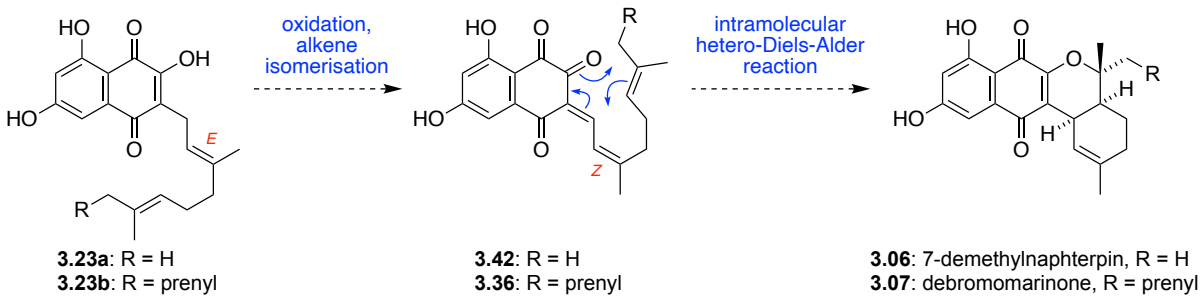

3.23a: R = H
3.23b: R = prenyl

3.42: R = H
3.36: R = prenyl

3.06: 7-demethylnaphterpin, R = H
3.07: debromomarinone, R = prenyl

Scheme 3.27: Proposed oxidative cyclisation cascade to form naphterpin and marinone natural products.

Preliminary *in vitro* assays with MarX enzymes found no activity on hydroxyquinone substrate **3.23b**. As little is known about the structure and function of these enzymes, it is possible that further cofactors may be required for their activity. Despite the inactivity of these MarX enzymes, we are confident that an enzyme or enzymes within the marinone BGC are capable of catalysing these reactions. Further work to discover and characterize the enzymes that control the final steps in the naphterpin and marinone biosynthetic pathways are underway.

3.4 Supporting Information

3.4.1 Chemical Methods

General Methods

All chemicals used were purchased from commercial suppliers and used as received. All reactions were performed under an inert atmosphere of N_2. All organic extracts were dried over anhydrous magnesium sulfate. Thin layer chromatography was performed using aluminium sheets coated with silica gel F_{254}. Visualization was aided by viewing under a UV lamp and staining with ceric ammonium molybdate or $KMnO_4$ stain followed by heating. All R_f values were measured to the nearest 0.05. Flash column chromatography was performed using 40-63 micron grade silica gel. Melting points were recorded on a Reichart Thermovar Kofler microscope apparatus and are uncorrected. Infrared spectra were recorded using an FT-IR spectrometer as the neat compounds. High field NMR spectra were recorded using a 500 MHz spectrometer (^{1}H at 500 MHz, ^{13}C at 125 MHz) or a 600 MHz spectrometer (^{1}H at 600 MHz, ^{13}C at 150 MHz) as stated. Solvent used for spectra were $CDCl_3$ unless otherwise specified. ^{1}H chemical shifts are reported in ppm on the δ-scale relative to TMS (δ 0.0) and ^{13}C NMR are reported in ppm relative to $CDCl_3$ (δ 77.16). Multiplicities are reported as (br) broad, (s) singlet, (d) doublet, (t) triplet, (q) quartet, (quin) quintet, (sext) sextet, (hept) heptet and (m) multiplet. All *J*-values were rounded to the nearest 0.1 Hz. ESI high-resolution mass spectra were recorded on an ESI-TOF mass spectrometer.

Experimental Procedures

Synthesis of Naphterpin Biosynthetic Intermediates

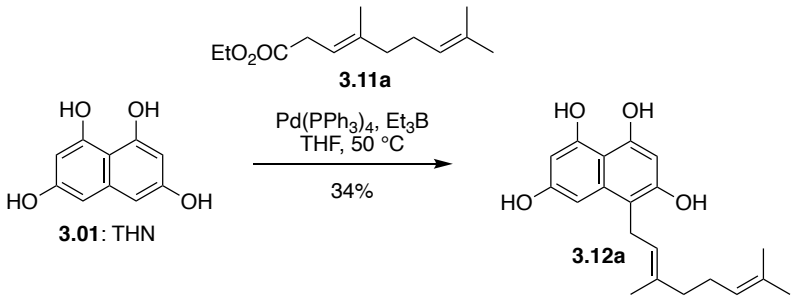

A solution of THN (**3.01**) (318 mg, 1.66 mmol), ethyl geranyl carbonate (**3.11a**) (250 mg, 1.10 mmol) and $Pd(PPh_3)_4$ (64 mg, 0.055 mmol) in THF (4 mL) was degassed. Et_3B (1.0 M in THF, 1.66 mL, 1.66 mmol) was then added and the resultant mixture was stirred at 50 °C for 2 days under an Ar atmosphere. The mixture was cooled, quenched with saturated NH_4Cl solution (30 mL) and extracted with EtOAc (3 × 30 mL). The combined organic layers were washed with brine (30 mL), dried over $MgSO_4$, filtered and concentrated *in vacuo*. The residue was triturated using cold hexanes, and further purified *via* silica flash chromatography under an Ar atmosphere (4:1 petrol/EtOAc, 1.25% AcOH), to yield **3.12a** (124 mg, 34%) as a light brown powder.

Data for 3.11a:

R_f = 0.45 (1:1 petrol/EtOAc, 1.25% AcOH)

IR (EtOAc cast): 3391 (br), 2974, 2922, 1623, 1528, 1480, 1377, 1295, 1213, 1158 cm^{-1}

^{1}H NMR (600 MHz, d_6-DMSO): δ 10.64 (s 1H), 9.11 (s, 1H), 8.96 (s, 1H), 8.32 (s, 1H), 6.28 (d, *J* = 2.0 Hz, 1H), 6.00 (s, 1H), 5.90 (d, *J* = 1.9 Hz, 1H), 5.08-5.01 (m, 2H), 3.31 (d, *J* = 6.5 Hz, 2H), 2.02-1.96 (m, 2H), 1.92-1.88 (m, 2H), 1.77 (s, 3H), 1.58 (s, 3H), 1.52 (s, 3H).

^{13}C NMR (150 MHz, d_6-DMSO): δ 157.4, 154.1, 153.8, 151.5, 135.9, 133.0, 130.7, 129.2, 124.4, 124.2, 110.0, 107.0, 106.7, 96.6, 40.1, 26.3, 25.5, 23.4, 17.6, 16.2.

HRMS (ESI): calculated for $C_{20}H_{23}O_4$ 327.1602 $[M-H]^-$, found 327.1603.

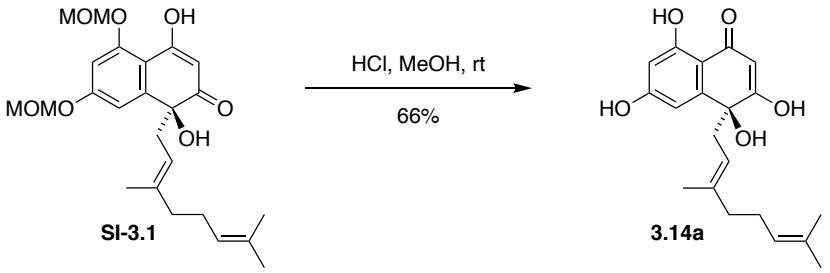

To a solution of **SI-3.1** (98 mg, 0.23 mmol) in MeOH (4 mL) was added 32% HCl (0.4 mL). The mixture was stirred at rt for 16 h. The mixture was diluted with H_2O (15 mL) and extracted with EtOAc (3 x 10 mL). The combined organic layers were washed with brine (20 mL) dried over $MgSO_4$, filtered and concentrated *in vacuo*. The residue was purified by flash chromatography (petrol /EtOAc, 2:1) to yield pure **3.14a (**52 mg, 66%) as a brown solid.

Data for 3.14a:

R_f = 0.05 (1:1 petrol/EtOAc)

Mp: 100 – 104 °C

IR (neat): 3254, 2915, 1590, 1231, 1157, 1007 cm^{-1}

major tautomer

^{1}H-NMR (500 MHz, acetone-*d_6*): δ 13.24 (s, 1H), 12.53 (s, 1H), 6.76 (d, *J* = 2.2 Hz, 1H), 6.23 (d, *J* = 2.2 Hz, 1H), 5.55 (s, 1H), 4.98 (t, *J* = 6.7 Hz, 1H), 4.69 (t, *J* = 7.4 Hz, 1H), 2.91 (dd, *J* = 13.1, 8.2 Hz, 1H), 2.55 (dd, *J* = 13.1, 7.4 Hz, 1H), 1.91 – 1.78 (m, 4H), 1.62 (s, 3H), 1.53 (s, 3H), 1.40 (s, 3H).

all peaks

^{13}C-NMR (125 MHz, acetone-*d_6*): δ 192.7, 178.4, 166.1, 165.4, 151.2, 142.3, 133.6, 126.7, 120.0, 119.8, 119.5, 111.0, 108.7, 107.7, 107.4, 105.3, 104.7, 104.4, 104.1, 76.1, 52.6, 46.2, 45.4, 45.2, 42.4, 29.2, 29.0, 27.5, 19.5, 18.2, 17.9.

HRMS (ESI): calculated for $C_{20}H_{23}O_5$ 343.1551 $[M-H]^-$, found 343.1161.

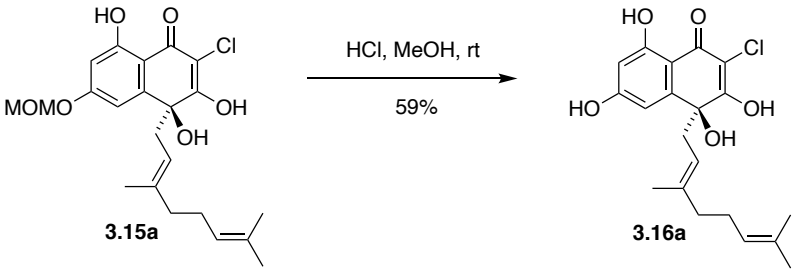

To a solution of **3.15a** (326 mg, 0.698 mmol) in MeOH (8 mL), was added 32% HCl (0.8 mL). The mixture was stirred at rt for 16 h. The mixture was diluted with H_2O (20 mL) and extracted with EtOAc (3 x 15 mL). The combined organic layers were washed with brine (30 mL), dried over $MgSO_4$, filtered and concentrated *in vacuo*. The residue was triturated with cold CH_2Cl_2 to yield **3.16a** (163 mg, 59%) as an off white solid.

Data for 3.16a:

R_f = 0.05 (6:1 CH_2Cl_2/MeOH)

Mp: 172 − 175 °C

IR (neat): 3340, 3159, 2925, 1645, 1604, 1587, 1455, 1323, 1206, 1147, 1009, 829 cm^{-1}.

^{1}H-NMR (500 MHz, acetone-*d*$_6$): δ 13.02 (s, 1H), 6.78 (d, *J* = 2.3 Hz, 1H), 6.28 (d, *J* = 2.3 Hz, 1H), 4.99 (t, *J* = 6.9 Hz, 1H), 4.63 (t, *J* = 7.5 Hz, 1H), 2.94 (dd, *J* = 13.1, 8.6 Hz, 1H), 2.52 (dd, *J* = 13.1, 7.4 Hz, 1H), 1.93 – 1.75 (m, 4H), 1.62 (s, 3H), 1.54 (s, 3H), 1.39 (s, 3H).

^{13}C-NMR (125 MHz, acetone-*d*$_6$): δ 183.8, 164.1, 163.8, 148.2, 141.5, 131.9, 125.1, 125.0, 118.1, 117.3, 108.7, 106.0, 102.8, 102.7, 44.5, 40.7, 27.6, 25.8, 17.8, 16.2.

HRMS (ESI): calculated for $C_{20}H_{22}ClO_5$ 377.1161 $[M-H]^-$, found 377.1170.

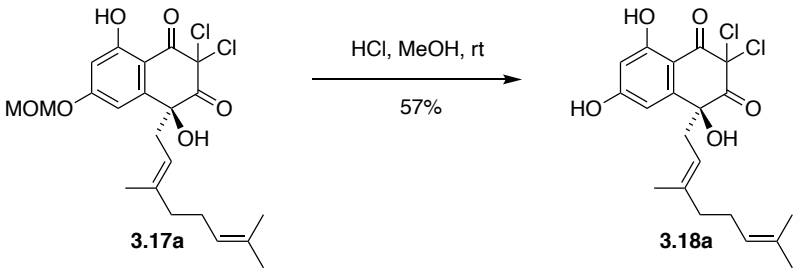

To a solution of **3.17a** (110 mg, 0.24 mmol) in MeOH (4 mL), was added 32% HCl (0.4 mL) at rt. The mixture was stirred at rt for 24 h. The mixture was diluted with brine (20 mL) and extracted with EtOAc (3 x 10 mL). The combined organic layers were dried over $MgSO_4$, filtered and concentrated *in vacuo*. The residue was purified by flash chromatography (9:1 → 4:1, petrol/EtOAc gradient elution) to yield **3.18a** (57 mg, 57%) as a pale yellow oil.

Data for 3.18a:

R_f = 0.20 (petrol/EtOAc, 3:1)

IR (neat): 3376, 2918, 1748, 1621, 1585, 1453, 1309, 1258, 1164, 856 cm^{-1}

^{1}H-NMR (500 MHz, $CDCl_3$): δ 11.70 (s, 1H), 6.95 (s, 1H), 6.82 (d, *J* = 2.4 Hz, 1H), 6.46 (d, *J* = 2.4 Hz, 1H), 5.07 (t, *J* = 6.5 Hz, 1H), 5.00 (t, J = 7.0 Hz, 1H), 3.86 (s, 1H), 2.73 (dd, *J* = 14.6, 7.0 Hz, 1H), 2.65 (dd, *J* = 14.6, 6.1 Hz, 1H), 2.15 – 2.01 (m, 4H), 1.72 (s, 3H), 1.62 (s, 3H), 1.53 (s, 3H)

^{13}C-NMR (125 MHz, $CDCl_3$): δ 193.9, 186.2, 166.6, 166.0, 145.7, 143.7, 132.2, 123.7, 115.0, 106.9, 105.4, 103.4, 79.5, 77.9, 45.5, 39.8, 26.2, 25.7, 17.7, 16.5

HRMS (ESI): calculated for $C_{20}H_{23}Cl_2O_5$ 413.0923 $[M+H]^+$, found 413.0898.

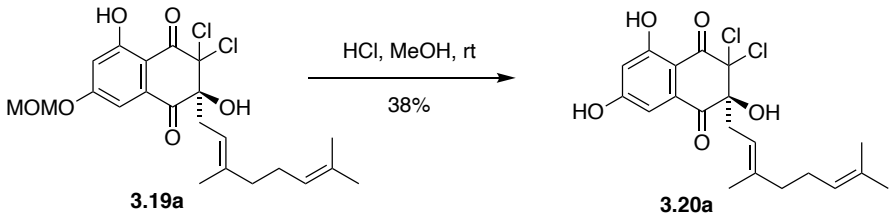

3.19a **3.20a**

To a solution of **3.19a** (230 mg, 0.503 mmol) in MeOH (10 mL), was added 32% HCl (1.0 mL) at rt. The mixture was stirred at rt for 40 h. The mixture was diluted with brine (20 mL) and extracted with EtOAc (3 x 15 mL). The combined organic layers were dried over $MgSO_4$, filtered and concentrated *in vacuo*. The residue was purified by flash chromatography (9:1, petrol/EtOAc) to yield **3.20a** (79 mg, 38%) as an orange oil.

Data for 3.20a:

R_f = 0.30 (petrol/EtOAc, 3:1)

IR (neat): 3377, 2919, 1712, 1656, 1613, 1580, 1350, 1248, 1172, 1095, 810 cm^{-1}

^{1}H-NMR (500 MHz, $CDCl_3$): δ 11.46 (s, 1H), 7.03 (d, *J* = 2.0 Hz, 1H), 6.75 (d, *J* = 1.9 Hz, 1H), 6.64 (s, 1H), 6.56 (s, 1H), 5.00 (t, *J* = 6.7 Hz, 1H), 4.87 (t, *J* = 6.8 Hz, 1H), 4.44 (s, 1H), 2.81 (dd, *J* = 14.5, 6.2 Hz, 1H), 2.37 (dd, *J* = 14.2, 8.5 Hz, 1H), 2.03 – 1.83 (m, 4H), 1.70 (s, 3H), 1.59 (s, 3H), 1.24 (s, 3H).

^{13}C-NMR (125 MHz, $CDCl_3$): δ 193.7, 186.9, 165.7, 163.9, 141.6, 133.7, 131.9, 123.6, 114.9, 109.4, 108.5, 107.7, 90.4, 85.7, 39.7, 36.3, 26.2, 25.7, 17.7, 16.1.

HRMS (ESI): calculated for $C_{20}H_{23}Cl_2O_5$ 413.0923 $[M+H]^+$, found 413.0914.

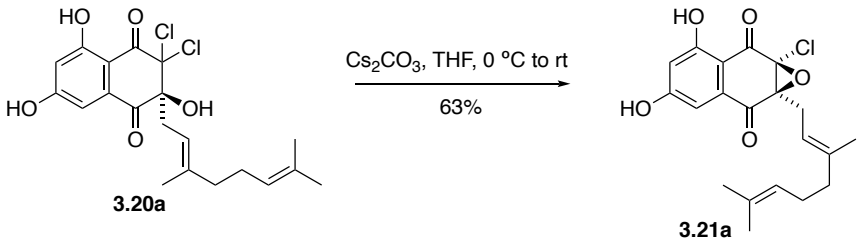

To a solution of **3.20a** (59 mg, 0.13 mmol) in THF (7 mL) was added Cs_2CO_3 (126 mg, 0.39 mmol) at -78 °C. The reaction was stirred at -78 °C for 20 mins prior to being warmed to 0 °C and stirred for a further 2 h. The mixture was then warmed to rt and stirred for a further 1 h. The mixture was quenched with saturated NH_4Cl solution (10 mL) and extracted with EtOAc (3 × 15 mL). The combined organic extracts were dried over $MgSO_4$, filtered and concentrated *in vacuo*. The residue was purified by flash chromatography on SiO_2 (9:1, petrol/EtOAc) to give **3.21a** (31 mg, 63%) as a yellow oil.

Data for 3.21a:

R_f = 0.55 (3:2, petrol/EtOAc)

IR (neat): 3439, 2968, 2923, 1699, 1665, 1614, 1453, 1407, 1348, 1159, 1097, 1043 cm^{-1}

^{1}H NMR (500 MHz, $CDCl_3$): δ 11.51 (s, 1H), 7.11 (d, *J* = 2.4 Hz, 1H), 6.69 (d, *J* = 2.4 Hz, 1H), 6.45 (s, 1H), 5.17 (t, *J* = 6.9 Hz, 1H), 5.03 (t, *J* = 6.6 Hz, 1H), 3.35 (dd, *J* = 14.7, 7.6 Hz, 1H), 2.67 (dd, *J* = 14.7, 6.8 Hz, 1H), 2.11 – 2.04 (m, 2H), 2.04 – 1.99 (m, 2H), 1.77 (s, 3H), 1.61 (s, 3H), 1.57 (s, 3H).

^{13}C NMR (125 MHz, $CDCl_3$): δ 187.9, 187.4, 165.4, 163.9, 140.9, 134.1, 131.8, 124.0, 115.2, 109.6, 109.3, 107.8, 81.0, 68.0, 39.9, 26.6, 26.2, 25.8, 17.8, 16.8.

HRMS (ESI): calculated for $C_{20}H_{20}ClO_5$ 375.1005 $[M–H]^–$, found 375.1010.

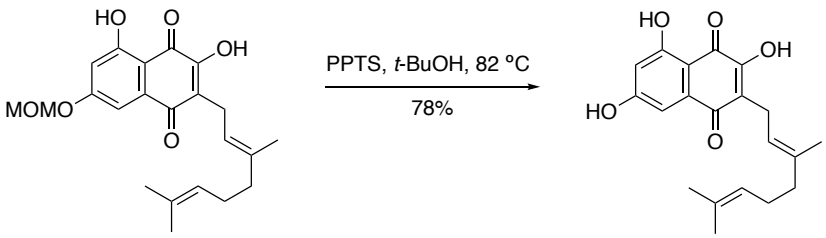

3.22a **3.23a**

To a solution of **3.22a** (37 mg, 0.08 mmol) in *t*-BuOH (5 mL), was added PPTS (123 mg, 0.49 mmol). The mixture was stirred at 82 °C for 6 h. The mixture was cooled, quenched with saturated H_2O (10 mL) and extracted with EtOAc (3 x 10 mL). The combined organic layers were washed with brine (20 mL), dried over $MgSO_4$, filtered and concentrated *in vacuo*. The residue was purified by flash chromatography on SiO_2 (9:1 → 6:1, petrol/EtOAc gradient elution) to yield **3.23a** (25 mg, 78 %) as an orange solid.

Data for 3.23a:

R_f = (3:1, petrol/EtOAc)

IR (neat): 3336, 2971, 2921, 1642, 1592, 1579, 1487, 1455, 1341, 1295, 1244, 1159 cm^{-1}

^{1}H NMR (500 MHz, acetone-d_6): δ 11.48 (s, 1H), 9.73 (s, 1H), 7.08 (d, *J* = 2.3 Hz, 1H), 6.52 (d, *J* = 2.3 Hz, 1H), 5.20 (td, *J* = 7.3, 1.4 Hz, 1H), 5.04 (tt, *J* = 7.1, 1.5 Hz, 1H), 3.23 (d, *J* = 7.2 Hz, 2H), 2.05 – 2.01 (m, 2H), 1.98 – 1.93 (m, 2H), 1.77 (s, 3H), 1.58 (s, 3H), 1.54 (s, 3H).

^{13}C NMR (125 MHz, acetone-d_6): δ 184.1, 184.0, 166.5, 165.0, 155.1, 136.9, 135.9, 131.7, 125.0, 124.1, 121.3, 109.5, 108.1, 107.0, 40.4, 27.3, 25.8, 23.0, 17.7, 16.4.

HRMS (ESI): calculated for $C_{20}H_{23}O_5$ 343.1545 $[M+H]^+$, found 343.1547.

Synthesis of Marinone Biosynthetic Intermediates

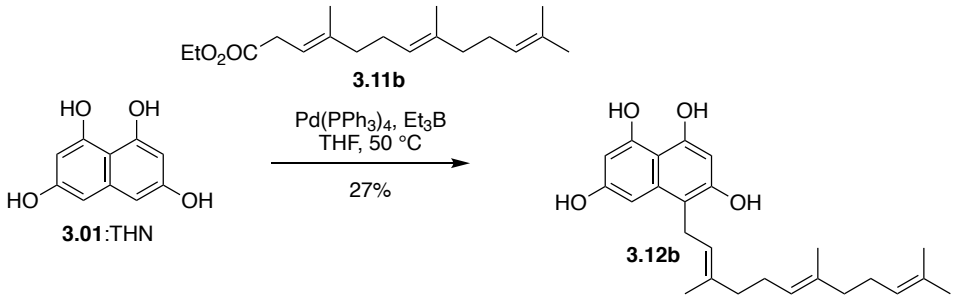

A solution of THN (**3.01**) (220 mg, 1.14 mmol), ethyl farnesyl carbonate (**3.11b**) (336 mg, 1.14 mmol) and $Pd(PPh_3)_4$ (69 mg, 0.057 mmol) in THF (10 mL) was degassed. Et_3B (1.0 M in THF, 1.71 mL, 1.71 mmol) was then added and the resultant mixture was stirred at 50 °C for 18 h under an Ar atmosphere. The mixture was cooled, quenched with saturated NH_4Cl solution (20 mL) and extracted with EtOAc (3 x 20 mL). The combined organic layers were washed with brine (50 mL), dried over $MgSO_4$, filtered and concentrated *in vacuo*. The residue was purified *via* silica flash chromatography under an Ar atmosphere (5:1 → 2:1 petrol/EtOAc, 1.25% AcOH), to yield **3.12b** (122 mg, 27%) as a brown oil.

Data for 3.12b:

R_f = 0.45 (1:1, petrol/EtOAc, 1.25% AcOH)

IR (neat): 3337 (br), 2973, 1607, 1377, 1273, 1088, 1046, 879 cm^{-1}.

^{1}H NMR (600 MHz, d_6-DMSO): δ 9.09 (s, 1H), 8.95 (s, 1H), 6.30 (d, *J* = 2.1 Hz, 1H), 6.01 (s, 1H), 5.91 (d, *J* = 2.1 Hz, 1H), 5.10 – 5.02 (m, 3H), 3.33 (d, *J* = 6.7 Hz, 2H), 2.04 – 1.93 (m, 4H), 1.93 – 1.86 (m, 4H), 1.78 (s, 3H), 1.61 (s, 3H), 1.53 (s, 3H), 1.53 (s, 3H).

^{13}C NMR (150 MHz, d_6-DMSO): δ 157.4, 154.1, 153.8, 151.5, 135.9, 134.3, 133.0, 130.6, 124.4, 124.2, 124.0, 107.1, 106.9, 96.7, 96.6, 95.8, 26.4, 26.2, 25.6, 17.6, 16.2, 15.8.

HRMS (ESI): calculated for $C_{25}H_{32}O_4H$ 379.2379 $[M+H]^+$, found 379.2371.

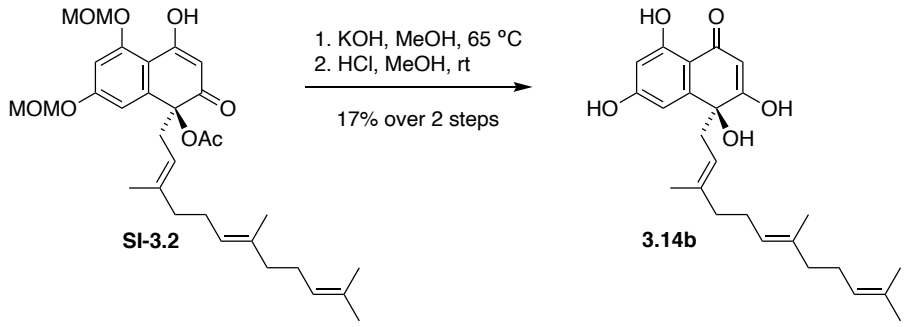

To a solution of **SI-3.2** (263 mg, 0.485 mmol) in MeOH (10 mL) was added KOH (109 mg, 1.94 mg) at rt. The mixture was heated at 65 °C for 4 h. The mixture was cooled, quenched with 1 M HCl (20 mL) and extracted with EtOAc (3 x10 mL). The combined organic extracts were washed with brine (20 mL), dried over $MgSO_4$, filtered and concentrated *in vacuo*. The residue was dissolved in MeOH (8 mL), 32% HCl (0.8 mL) was added and the mixture was stirred at rt for 16 h. The mixture was diluted with 1 M HCl (15 mL) and extracted with EtOAc (3 x 10 mL). The combined organics were washed with brine, dried over $MgSO_4$, filtered and concentrated *in vacuo*. The residue was triturated with cold CH_2Cl_2 to yield **3.14b** (33 mg, 17%) as a pale brown solid.

Data for 3.14b:

R_f = 0.15 (CH_2Cl_2/MeOH, 20:1)

Mp = 122 -126 °C

IR (neat): 3176, 2916, 1589, 1452, 1376, 1160, 1115, 1007, 851 cm^{-1}

major tautomer

^{1}H-NMR (500 MHz, $CDCl_3$): δ 13.23 (s, 1H), 9.86 (s, 2H), 9.12 (s, 1H), 6.77 (d, *J* = 2.3 Hz, 1H), 6.24 (d, *J* = 2.2 Hz, 1H), 5.55 (s, 1H), 5.07 (t, *J* = 6.8 Hz, 1H), 5.02 (t, *J* = 6.6 Hz, 1H), 4.70 (t, *J* = 7.6 Hz, 1H), 2.91 (dd, *J* = 13.2, 8.3 Hz, 1H), 2.55 (dd, *J* = 13.2, 7.4 Hz, 1H), 2.11 – 1.78 (m, 8H), 1.64 (s, 3H), 1.58 (s, 3H), 1.55 (s, 3H), 1.40 (s, 3H).

minor tautomer

^{1}H-NMR (500 MHz, $CDCl_3$): δ 12.53 (s, 1H), 9.86 (s, 1H), 6.82 (d, *J* = 2.3 Hz, 1H), 6.32 (d, *J* = 2.4 Hz, 1H), 5.17 (t, *J* = 7.6 Hz, 1H), 5.10 (t, *J* = 6.8 Hz, 1H), 5.08 (t, *J* = 6.6 Hz, 1H), 4.08 (d, *J* = 19.4 Hz, 1H), 3.48 (d, *J* = 19.3 Hz, 1H), 2.72 (dd, *J* = 14.8, 7.6 Hz, 1H), 2.64 (dd, *J* = 14.8, 7.2 Hz, 1H), 2.11 – 1.78 (m, 8H), 1.65 (s, 3H), 1.60 (s, 3H), 1.59 (s, 3H), 1.54 (s, 3H).

all peaks

^{13}C-NMR (125 MHz, $CDCl_3$): δ 204.0, 197.0, 190.9, 176.6, 166.4, 166.0, 164.3, 163.6, 150.6, 149.4, 140.8, 140.7, 135.8, 135.6, 131.6, 131.5, 125.2, 125.2, 124.9, 124.8, 124.8, 118.0, 117.7, 109.2, 106.9, 105.9, 103.5, 102.6, 102.3, 81.0, 74.4, 50.8, 43.6, 43.4, 40.6, 40.6, 40.4, 40.4, 32.7, 27.5, 27.4, 27.2, 25.8, 25.3, 17.8, 17.7, 16.4, 16.2, 16.1, 16.0.

HRMS (ESI): calculated for $C_{25}H_{33}O_5$ 413.2328 $[M+H]^+$, found 413.2323.

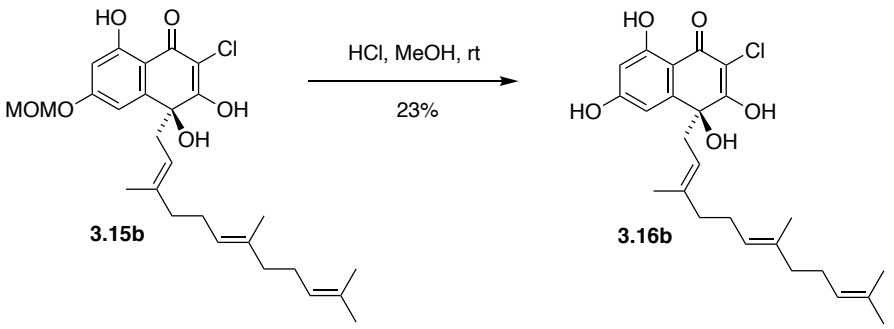

To a solution of **3.15b** (333 mg, 0.745 mmol) in MeOH (12 mL), was added 32% HCl (1.2 mL) at rt. The mixture was stirred at rt for 16 h. The mixture was diluted with 1 M HCl (20 mL) and extracted with EtOAc (3 x 15 mL). The combined organic layers were washed with brine (30 mL), dried over $MgSO_4$, filtered and concentrated *in vacuo*. The residue was triturated with cold CH_2Cl_2 to yield **3.16b** (76 mg, 23%) as a pale brown solid.

Data for 3.16b:

R_f = 0.05 (CH_2Cl_2/MeOH, 10:1)

Mp = 162 – 164 °C

IR (neat): 3347, 3159, 2922, 1638, 1587, 1456, 1148, 1008, 830 cm^{-1}

^{1}H-NMR (500 MHz, $CDCl_3$): δ 12.78 (s, 1H), 9.46 (s, 1H), 6.80 (d, *J* = 2.3 Hz, 1H), 6.30 (d, *J* = 2.3 Hz, 1H), 5.48 (s, 1H), 5.08 (t, *J* = 7.0 Hz, 1H), 5.02 (t, *J* = 6.9 Hz, 1H), 4.60 (t, *J* = 7.7 Hz, 1H), 2.97 (dd, *J* = 13.0, 8.6 Hz, 1H), 2.55 (dd, *J* = 13.0, 8.6 Hz, 1H), 2.06 – 1.79 (m, 8H), 1.64 (s, 3H), 1.58 (s, 3H), 1.56 (s, 3H), 1.40 (s, 3H).

^{13}C-NMR (125 MHz, $CDCl_3$): δ 184.0, 170.5, 164.2, 164.1, 148.2, 141.9, 135.7, 131.5, 125.2, 124.8, 124.8, 116.9, 108.5, 106.0, 102.8, 76.1, 44.1, 40.6, 40.4, 27.5, 27.4, 25.8, 17.7, 16.2, 16.0.

HRMS (ESI): calculated for $C_{25}H_{32}ClO_5$ 447.1933 $[M+H]^+$, found 447.1930.

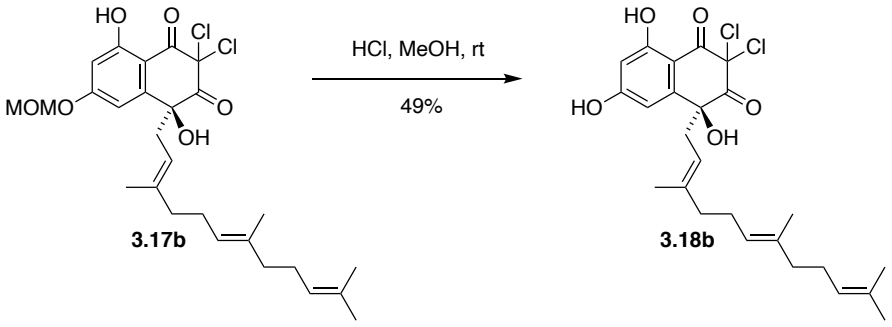

To a solution of **3.17b** (196 mg, 0.373 mmol) in MeOH (6 mL), was added 32% HCl (0.6 mL) at rt. The mixture was stirred at rt for 24 h. The mixture was diluted with 1 M HCl (20 mL) and extracted with EtOAc (3 x 10 mL). The combined organic layers were washed with brine (20 mL), dried over $MgSO_4$, filtered and concentrated *in vacuo*. The residue was purified by flash chromatography on SiO_2 (4:1, petrol/EtOAc) to yield **3.18b** (88 mg, 49%) as a yellow oil.

Data for 3.18b:

R_f = 0.15 (petrol/EtOAc, 3:1)

IR (neat): 3388, 2923, 2854, 1748, 1622, 1452, 1163, 857, 732 cm^{-1}

^{1}H-NMR (500 MHz, $CDCl_3$): δ 11.69 (s, 1H), 7.26 (s, 1H), 6.83 (d, *J* = 2.3 Hz, 1H), 6.45 (d, *J* = 2.3 Hz, 1H), 5.09 (t, *J* = 6.8 Hz, 1H), 5.08 (t, *J* = 6.8 Hz, 1H), 5.01 (t, *J* = 7.7 Hz, 1H), 3.90 (s, 1H), 2.74 (dd, *J* = 14.7, 8.8 Hz, 1H), 2.65 (dd, *J* = 14.7, 6.1 Hz, 1H), 2.14 – 1.96 (m, 8H), 1.67 (s, 3H), 1.60 (s, 3H), 1.53 (s, 3H), 1.26 (s, 3H).

^{13}C-NMR (125 MHz, $CDCl_3$): δ 194.1, 186.3, 166.7, 166.1, 145.8, 144.0, 135.9, 131.6, 124.4, 123.7, 114.9, 107.1, 105.6, 103.6, 79.8, 78.0, 45.6, 40.0, 39.8, 26.9, 26.4, 25.8, 17.8, 16.7, 16.2.

HRMS (ESI): calculated for $C_{25}H_{29}Cl_2O_5$ 479.1398 $[M-H]^-$, found 479.1394.

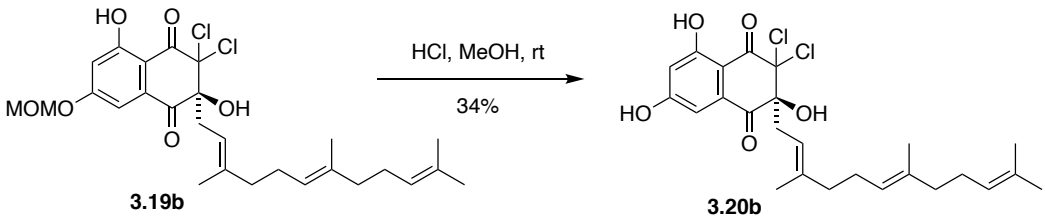

To a solution of **3.19b** (295 mg, 0.561 mmol) in MeOH (10 mL), was added 32% HCl (1.0 mL) at rt. The mixture was stirred at rt for 24 h. The mixture was diluted with 1 M HCl (20 mL) and extracted with EtOAc (3 x 15 mL). The combined organic layers were washed with brine (30 mL), dried over $MgSO_4$, filtered and concentrated *in vacuo*. The residue was purified by flash chromatography on SiO_2 (4:1, petrol/EtOAc) to yield **3.20b** (83 mg, 31%) as an orange oil along with recovered starting material (101 mg, 34%).

Data for 3.20b:

R_f = 0.20 (petrol/EtOAc, 3:1)

IR (neat): 3380, 2917, 1712, 1656, 1614, 1580, 1349, 1248, 1168, 1095, 810 cm^{-1}

^{1}H-NMR (500 MHz, $CDCl_3$): δ 11.45 (s, 1H), 7.09 (s, 1H), 7.03 (d, *J* = 2.4 Hz, 1H), 6.76 (d, *J* = 2.4 Hz, 1H), 5.10 (t, *J* = 7.0 Hz, 1H), 5.02 (t, *J* = 6.4 Hz, 1H), 4.88 (t, *J* = 7.4 Hz, 1H), 4.47 (s, 1H), 2.81 (dd, *J* = 14.6, 6.5 Hz, 1H), 2.37 (dd, *J* = 14.4, 8.6 Hz, 1H), 2.16 (s, 1H), 2.09 – 1.88 (m, 8H), 1.68 (s, 3H), 1.60 (s, 3H), 1.58 (s, 3H), 1.25 (s, 3H).

^{13}C-NMR (125 MHz, $CDCl_3$): δ 193.9, 187.0, 165.9, 164.3, 141.8, 135.7, 133.8, 131.7, 124.5, 123.6, 115.0, 109.6, 108.7, 107.7, 90.6, 85.9, 39.8, 36.5, 26.9, 26.4, 25.8, 17.8, 16.3, 16.1.

HRMS (ESI): calculated for $C_{25}H_{31}Cl_2O_5$ 481.1543 $[M+H]^+$, found 481.1538.

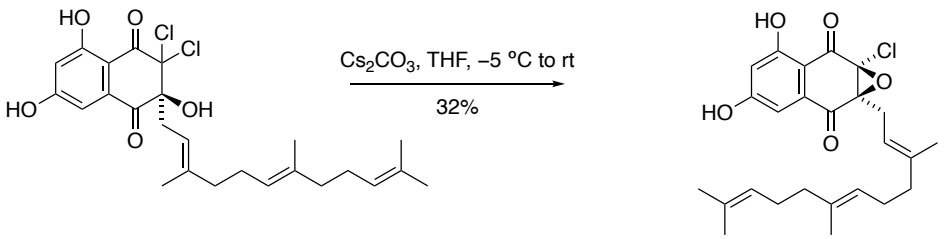

3.20b **3.21b**

To a solution of **3.20b** (131 mg, 0.27 mmol) in THF (7 mL) was added Cs_2CO_3 (266 mg, 0.82 mmol) at –5 °C. The reaction was stirred at –5 °C for 1 h. The mixture was then warmed to rt and stirred for a further 2 h. The mixture was quenched with 1 M HCl solution (10 mL) and extracted with EtOAc (3 × 10 mL). The combined organic extracts were dried over $MgSO_4$, filtered and concentrated *in vacuo*. The residue was purified by flash chromatography on SiO_2 (9:1, petrol/EtOAc) to give **3.21b** (39 mg, 32%) as a yellow residue.

Data for 3.21b:

R_f = 0.25 (3:1, petrol/EtOAc)

IR (neat): 3441, 2963, 2922, 2854, 1696, 1639, 1614, 1451, 1402, 1351, 1318, 1161 cm^{-1}

^{1}H NMR (500 MHz, $CDCl_3$): δ 11.50 (s, 1H), 7.09 (d, *J* = 2.5 Hz, 1H), 6.83 (s, 1H), 6.68 (d, *J* = 2.5 Hz, 1H), 5.18 (t, *J* = 7.2 Hz, 1H), 5.04 (t, *J* = 6.5 Hz, 2H), 3.35 (dd, *J* = 14.7, 7.7 Hz, 1H), 2.67 (dd, *J* = 14.7, 6.8 Hz, 1H), 2.11 – 2.05 (m, 2H), 2.05 – 1.97 (m, 4H), 1.92 – 1.88 (m, 2H), 1.77 (s, 3H), 1.66 (s, 3H), 1.57 (s, 3H).

^{13}C NMR (125 MHz, $CDCl_3$): δ 188.0, 187.3, 165.4, 164.0, 140.9, 135.4, 134.0, 131.5, 124.5, 123.8, 115.3, 109.6, 109.3, 107.7, 81.1, 67.9, 39.9, 39.8, 29.8, 26.9, 26.4, 26.2, 25.8, 17.8, 16.8, 16.2.

HRMS (ESI): calculated for $C_{25}H_{30}ClO_5$ 445.1782 $[M+H]^+$, found 445.1773.

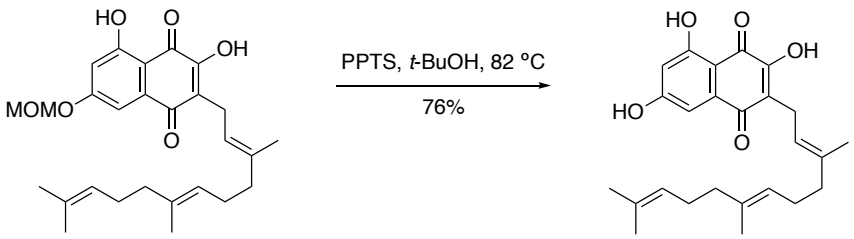

3.22b **3.23b**

To a solution of **3.22b** (37 mg, 0.08 mmol) in *t*-BuOH (5 mL), was added PPTS (123 mg, 0.49 mmol). The mixture was stirred at 82 °C for 6 h. The mixture was cooled, quenched with H_2O (10 mL) and extracted with EtOAc (3 x 10 mL). The combined organic layers were washed with brine (20 mL), dried over $MgSO_4$, filtered and concentrated *in vacuo*. The residue was purified by flash chromatography on SiO_2 (9:1 → 6:1, petrol/EtOAc gradient elution) to yield **3.23b** (25 mg, 76%) as an orange solid.

Data for 3.23b:

R_f = 0.30 (3:1, hexane/EtOAc)

IR (neat): 3340, 2964, 2918, 1591, 1484, 1343, 1247, 1158 cm^{-1}

^{1}H NMR (500 MHz, acetone-d_6): δ 11.50 (s, 1H), 9.78 (s, 1H), 7.09 (d, *J* = 2.3 Hz, 1H), 6.54 (d, *J* = 2.4 Hz, 1H), 5.19 (t, *J* = 7.3 Hz, 1H), 5.06 (t, *J* = 7.0 Hz, 1H), 5.01 (t, *J* = 7.0 Hz, 1H), 3.24 (d, *J* = 7.4 Hz, 2H), 2.92 (s, 1H), 2.10 – 2.04 (m, 2H), 2.03 – 1.91 (m, 4H), 1.92 – 1.83 (m, 2H), 1.78 (s, 3H), 1.61 (s, 3H), 1.55 (s, 3H), 1.52 (s, 3H).

^{13}C NMR (125 MHz, acetone-d_6): δ 184.1, 184.0, 166.5, 165.0, 155.2, 136.8, 135.9, 135.5, 131.6, 125.1, 124.8, 124.1, 121.4, 109.5, 108.1, 106.9, 40.4, 40.4, 27.4, 26.9, 25.8, 23.0, 17.6, 16.3, 16.1.

HRMS (ESI): calculated for $C_{25}H_{29}O_5$ 409.2019 $[M–H]^–$, found 409.2020.

3.4.2 Biochemical Methods

Cloning of *Streptomyces* sp. CNQ-509 *marH1*, *marH2*, and *marH3*:

Putative *mar* VCPO genes from *Streptomyces* sp. CNQ-509 (GenBank accession number CP011492)[11] were amplified from genomic DNA using standard PCR conditions using the following primers at the indicated annealing temperatures:

MarH1: Fwd - 5′– AAACATATGACGACCGGACACTCTCC–3′

MarH1: Rev - 5′– ATAAAGCTTTCAGTCCTCGACCTCACCCTTG–3′ (annealing temp. 59 °C)

MarH2: Fwd - 5′– ATACATATGATGACGACGTCCGGAAGCTCCTCC–3′

MarH2: Rev - 5′– ATTAAGCTTTCAGTCCTCGGCCTCGCCCGAG–3′ (annealing temp. 71 °C)

MarH3: Fwd - 5′– ATACATATGACGTCCGGAAACTCCTCCTCCGC–3′

MarH3: Rev - 5′– ATTAAGCTTTCAGTCCTCCACGTCGCCCTTGATG–3′ (annealing temp. 66 °C)

The resulting PCR products were digested with restriction enzymes NdeI and HindIII, and subsequently ligated into a similarly digested pET28a vector (Novagen) for expression of *N*-terminally His_6-tagged MarH1, MarH2, and MarH3.

Cloning of *Streptomyces* sp. CNQ-509 *marO*:

MarO: Fwd - 5′– ATACATATGACACAAGGAGCCACACTCG –3′

MarO: Rev - 5′– ATAAAGCTTTCACCGGACCTTCGTGGCGGAG –3′

The resulting PCR products were digested with restriction enzymes NdeI and HindIII, and subsequently ligated into a similarly digested pET28a vector (Novagen) for expression of *N*-terminally His_6-tagged MarO.

Cloning of *Streptomyces* sp. CNQ-509 *marX4*:

MarX4: Fwd - 5′– AAACATATGGAAGCCATCGAAGTTCCGGTTCTGATCGTG –3′

MarX4: Rev - 5′– AAAAAGCTTCTAGCCGTGCCGGGTGCCGC –3′ (annealing temp. 55 °C)

Gibson Overhangs:

For NdeI p28: Fwd - 5′– GGTGCCGCGCGGCAGCCAT –3′

Rev XhoI p28: Fwd - 5′– GGTGGTGGTGGTGCTCGAG –3′

The resulting PCR products were digested with restriction enzymes NdeI and Xhol, and subsequently ligated into a similarly digested pET28a vector (Novagen) *via* Gibson Assembly.[54,55] Gibson assembly was achieved using NEBuilder® HiFi DNA Assembly Master Mix, following the provided protocols to give *N*-terminally His_6-tagged MarX4.

Cloning of *Streptomyces* sp. CNQ-509 *marX1*, *marX2*, and *marX3*:

MarX1: Fwd - 5′– GGTGCCGCGCGGCAGCCATATGAGCGTCCGCATGTTCCGTGCCAAGATC –3′

MarX1: Rev - 5′– GGTGGTGGTGGTGCTCGAGTCAGTAGAAGAGGCGGTACGAGCCGAGTGACG –3′

(annealing temp. 70 °C)

MarX2: Fwd - 5′– GGTGCCGCGCGGCAGCCATGAGAAGGGTTCGGGCACGCTGTCCGG –3′

MarX2: Rev -5′– GGTGGTGGTGGTGCTCGAGTCAGCCGATCTTGACGACCTCGCCCTGGTC –3′

(annealing temp. 70 °C)

MarX3: Fwd - 5′– GGTGCCGCGCGGCAGCCATGACCACGGCCGGGGCTCGGGCACG –3′

MarX2: Rev -5′– GGTGGTGGTGGTGCTCGAGTCAGCCGATCTTGATGACCTCTCCCTTGTCCCAGTCGCC –3′ (annealing temp. 70 °C)

Gibson Overhangs:

For NdeI p28: Fwd - 5′– GGTGCCGCGCGGCAGCCAT –3′

Rev XhoI p28: Fwd - 5′– GGTGGTGGTGGTGCTCGAG –3′

The resulting PCR products were digested with restriction enzymes NdeI and Xhol, and subsequently ligated into a similarly digested pET28a vector (Novagen) *via* Gibson Assembly.[54,55] Gibson assembly was achieved using NEBuilder® HiFi DNA Assembly Master Mix, following the provided protocols to give *N*-terminally His_6-tagged MarX1, MarX2 and MarX3.

Expression of *Streptomyces* sp. CNQ-509 enzymes

Mar enzymes were expressed, purified, and assayed following a general literature procedure.[24] *E. coli* BL21-Gold(DE3) cells (Agilent Technologies) containing the pET28a:*mar* genes were individually grown in 1L of TB broth containing 50 μg/mL kanamycin with shaking (200 rpm) at 37 °C until an OD_{600} of approximately 0.6. The temperature was decreased to 18 °C and cells were grown for an additional 1 h. Protein expression was induced by the addition of 0.1 mM IPTG (final concentration) and allowed to grow overnight at 18 °C. The next day, cells were harvested by centrifugation (7000 x *g*), resuspended in buffer A (50 mM Tris-HCl (pH 8.0), 0.5 M NaCl, and 25 mM imidazole) and stored at -80 °C.

General purification of *Streptomyces* sp. CNQ-509 enzymes

Cell pellets were thawed and sonified on ice with stirring using a Branson digital sonifier (40% amplitude) and a 15 s on/45 s off cycle over 40 minutes. The lysate was centrifuged for 40 minutes at 17000 x *g* at 4 °C to pellet insoluble material. Clarified lysate was loaded onto a 5 mL HisTrap FF column (GE Healthcare) previously equilibrated with buffer A. The column was washed with 25 mL of buffer A, and then washed with a gradient of 0-10% buffer B (50 mM Tris-HCl (pH 8.0), 0.5 M NaCl, and 500 mM imidazole) over 10 mL. The column was washed with 50 mL of 10% buffer B to elute weakly bound proteins, then *mar* enzymes were eluted in a gradient of 10-100% buffer B over 60 mL. Fractions containing Mar enzymes were identified by SDS-PAGE (12%), pooled, and concentrated to under 2.5 mL using an Amicon Ultra-15 30 kDa cutoff concentrator (EMD Millipore) by centrifugation at 3500 x *g*, 4 °C. Concentrated protein was loaded onto a PD-10 desalting column (GE Healthcare) pre-equilibrated with >5 column volumes of cold storage buffer (25 mM HEPES-NaOH (pH 8.0), 200 mM NaCl, 5% glycerol), and eluted in 3.5 mL of the same buffer. Proteins were concentrated as described above and their concentration determined using the Bradford method and bovine serum albumin as a standard. Mar enzyme aliquots were frozen on dry ice and stored at -80 °C until needed. Typical production yields: MarH1 10 - 20 mg/L; MarH2 30 - 40 mg/L; MarH3 20 - 45 mg/L; MarO 100 - 160 mg/L; MarX4 113 mg/L; MarX1 11 mg/L.

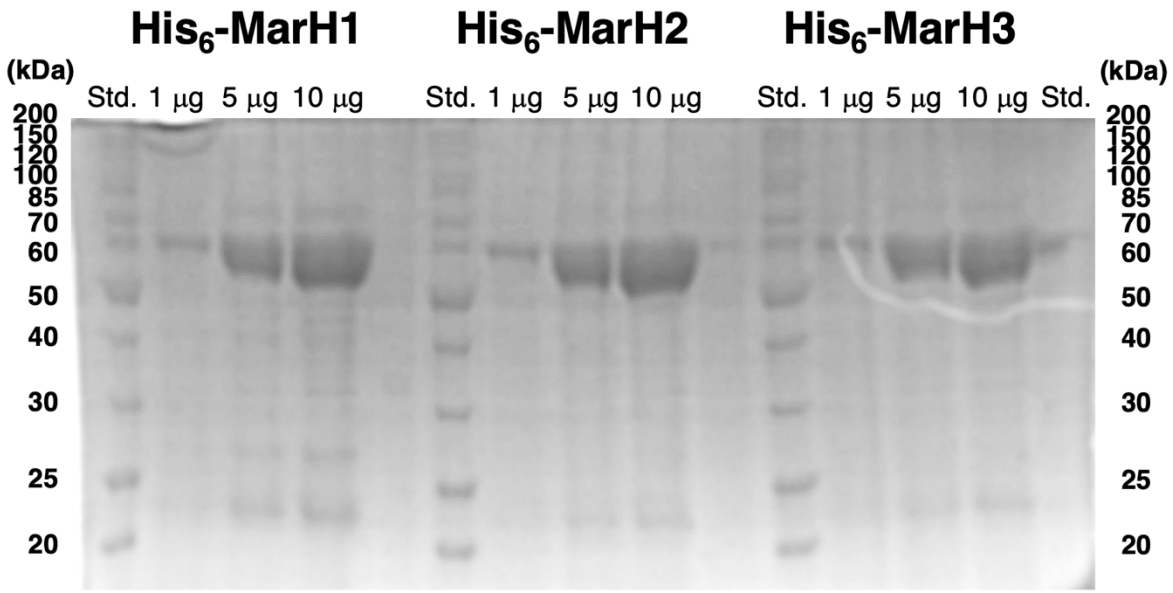

Figure SI-3.1: SDS-PAGE gel (12%) of purified MarH1, MarH2, and MarH3. The bands are consistent with the predicted molecular weights of His_6-MarH1 (59.6 kDa), His_6-MarH2 (58.3 kDa), and His_6-MarH3 (58.8 kDa). All proteins were judged to be ~90% pure based on band intensities.

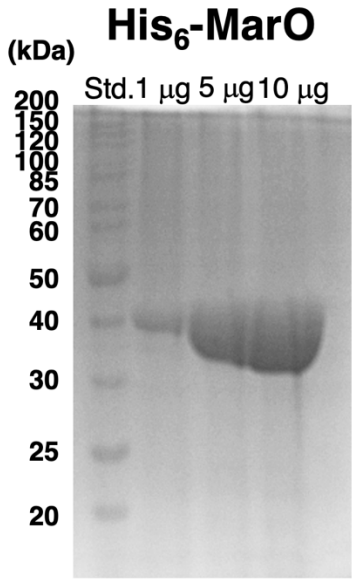

Figure SI-3.2: SDS-PAGE gel (12%) of purified MarO. The bands are consistent with the predicted molecular weight of His_6-MarO (41.3 kDa). Protein was judged to be ~90% pure based on band intensities.

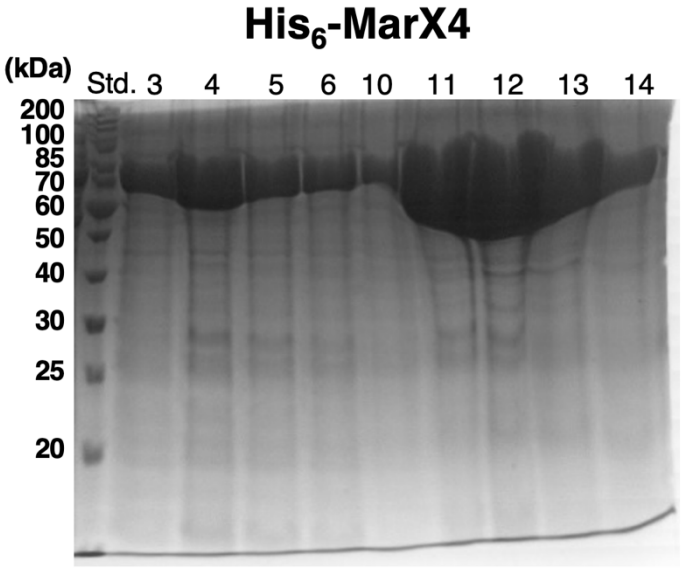

Figure SI-3.3: SDS-PAGE gel (12%) of MarX4 during FPLC purification. The bands are consistent with the predicted molecular weight of His_6-MarX4 (66.2 kDa).

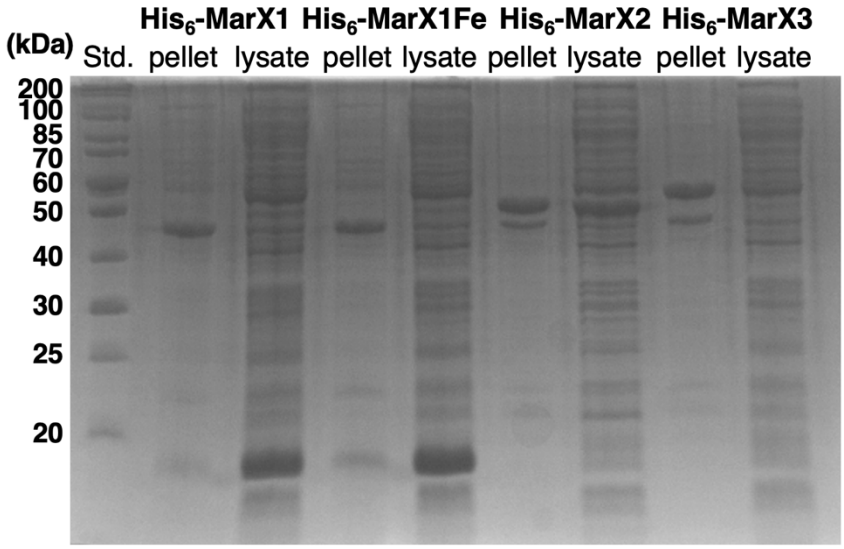

Figure SI-3.4: SDS-PAGE gel (12%) of MarX1, MarX2, and MarX3 pellet and crude lysate. Bands present in the crude lysate are consistent with the predicted molecular weights of His_6-MarX1 (13.7 kDa), His_6-MarX2 (39.2 kDa), and His_6-MarX3 (41.2 kDa). His_6-MarX1Fe was MarX1 protein expressed in the presence of $FeSO_4$.

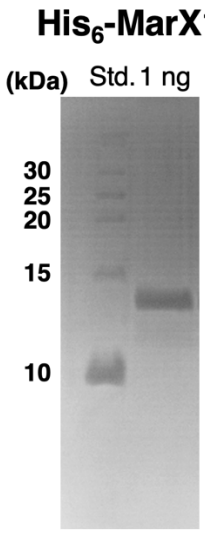

Figure SI-3.5: SDS-PAGE gel (18%) of purified MarX1. The bands are consistent with the predicted molecular weight of His_6-MarX1 (13.7 kDa). Protein was judged to be ~90% pure based on band intensities.

```
MarH1       -MTTGHSPVSGFSPRRRSLLIGGASAAALLPLGHAG-----T-AAAAEGGKAAQAEFDLD      53
Mcl40       MKTSGHTSASDLSLGRRSLLLGGSSAALMLALPH-------P-ANAGTSEEPPTFDFDLD      52
NapH1       MTTSGHTSFSDYSPRRRSMLLGGLGGAAALSAAGFTGMASAS-PRGSAGSKAAAIEFDLD      59
NapH4       ------------------------------------------------------------      0
NapH3       ---------------------------------------------VTTSAPAQQIPFDFD      15
MarH2       MTTSGSSSVPGFSPRRRSLLLGGGSAAALTALGHAGTAAA---EPGPAAEPPP--AFDLD      55
MarH3       -MTSGNSSSAGFSPARRSLLLGGASTAALATLGTGTAAA-AGQGTGPAAKPAAAAEFDFD      58
Mcl24       MTTSERSSVSDFSPRRRSLLIGSASAAALATLGSTGTAAAAGA-----ADEPPTVDFDFD      55

MarH1       KDNYIEWFQPE-DDGAGISPSSEIFGPMDVTVFLWINHLTGLGWFDAVAPYHETAVGVHS      112
Mcl40       TDNYIKWVKPATDEQASQSPLWESVGSMDVTVILWMSRVGNLAVFDAVAPYHETAVGVYS      112
NapH1       KDNYIKWAQPT-DENAGQSPTLAILGPMDVTVFLWINRVVWLAAFDALAPYHETAVGVYS      118
NapH4       ------------------------------------------------------------      0
NapH3       NGNFIRDLITT--HGGGGYPPADAMAPGDVSSYTWVTHLLQTSWFDALAPYHPTAVGVYS      73
MarH2       KGNFVRDLLTV--A-GDSSGETQDLGPADVTLIFWIQDVMQTAWFDALAPYHPTAVGVRT      112
MarH3       TGNFHRDLLST--AA---NPSEEPLGPMDATVLVYLTHLTMTAWFDALAPYHPTAVGRHS      113
Mcl24       NGNFIRDLIIT--RAGGVFPEEGVIGPMDASVYIWITSLFQLSWFDALAPYHPTAVGIHS      113

MarH1       RIPRRPSSESATNRNMNIACIYSQYQLVKQVIPSRV----KPMRDLLTSIGLDPDDDSMD      168
Mcl40       RIPRRPSSESATNRNMNIAILYTQLHTFERLLPLGLRGPAGSLRAMMVGLGLDPDNKSED      172
NapH1       QIPRRPSSESATNRNLNIAALHAQHGVWKRVLPQQV----DQLRELMTALGLDPSDETEN      174
NapH4       ---------------MNIACIHAQNAIWSRLLPPIV----AGLRELMVALGLDPDDKSED      41
NapH3       RIPRRPAEESATNRNKNIAGLYAMFQVVKAAFTERV----PVLRQALGALGLDPDDESQD      129
MarH2       RLPRRPAGESETNRNKNIAGLYATYHVVSVAYPERG----YILRGLLEAIGLDPDDESED      168
MarH3       RIPRRPASESNTNRNKNVAAFHAANVVFQSVFKERV----AAFRQLMTTLGLDPDDQSTD      169
Mcl24       RIARRPAGEAATNRNKNIAGLYAALRVLEGVFEERV----PVMRAGFTAAGLDPDDRSED      169

MarH1       PADPVGVGNIAGKSVFEALKNDGMNFLGHDGGRKYNPRPWADYTGYRPVNTAFDVVNPSR      228
Mcl40       LTTPVGIGNVAFKSVWNALKNDGMNVLGYEGGRKYNPLPWADYTGYEPVNTPFRLNNPSR      232
NapH1       LSSPVGIGNVAAKNAFNALKNDGMNFLGYE-GRKYNPRPWADYTGYEPVNTAFKVNNPSR      233
NapH4       VTTPVGIGNVAAKAVWNVLKNDGMNVLGHEGGRKYNPRPWADYTGYVPTNTAFKLNNPSR      101
NapH3       LSTAVGIGNTAGKAVAAARMGDGMNALGGK-DRTHNGQPYEDYTGYRPVNTADELVDPSR      188
MarH2       PATPAGIGNLAGKAAVEARRRDGMNFLGDE-GRRYHPQPFEDYTGYEPVNTAYKLVDPSK      227
MarH3       PTSPVGIGNLAARGVLKAKARDGMNLFGDE-GRKYHGQPYEDYTGFEPVNTAYKLVNPSK      228
Mcl24       PTTPIGIGNIAGKAVVRARANDGMNHLGNV-GRKYHGKPYEDYTGYQPVNSPYKLVNPSK      228

MarH1       WQPQLQAHNGRRVGGGPGDLGIWVAQHFVTPQMRMVKPHIYADPREFTVPPPKHVDHTRP      288
Mcl40       WQPQLHAHNGRRPGGGPGDLGIYVSQHFVTPQIALTKPHIFTDPAQFPLAAPKHSDHTRP      292
NapH1       WQPQLQAHNARRAGGGPGDLGIYVTQHFVTPQTARTKAHIFRDPSRFRIPRPEFSDHTNT      293
NapH4       WQPQLQAHNGRRAGGGPGDLGIYVTQHFVTPQIAVTLPHIFKDPTAFPLPRPDFTDHTDR      161
NapH3       WQPAVEPHR-RRTDGGPGDKGIFTAQRFATPQLGLVAPQTYRDPARFKLAAPDHLDHNDA      247
MarH2       WQPARTPHR-RRVGGGPGDKGIFTVQQFATPQLRLVEGHTFRDPGRFELPPPDHSDHTAP      286
MarH3       WQPARHPHR-RRVGGGPGDKGIFVVQHMVTPQMALVKPDTYRHPSQFPLAPPDHLDHTDP      287
Mcl24       WQPALHPHQ-RRVGGGPGDKGIWVIQAFVTPQLALVKPYTYRNPGQFTVPVPDHSTHTNV      287

MarH1       RDFKRSADEVLEASAALTDEQKAIAEVMDNKIWGIGHSALVIARKHDQNGELGVQGWAHF      348
Mcl40       RDYKRSVDEILEASASLNDERKALAEVMDNKLWGIGYTSTVIGRKYDENNEMGVFGWAAW      352
NapH1       RAYKRSVDEIIDASANLNDERKALAEIMENKLWGIGHSSIVIANKYDQNNEMGVHGWCHW      353
NapH4       RAYKRSVDEIIEASAALDDERKALAEIMENKLWGIGHSSIEIGLKNDQNNELGVHGWAQW      221
NapH3       GAYRQAVDEVLAASAGLTDEQKVKAEFFEHTPLSVTLSPRAAAMAH----DLDLDGWAQL      303
MarH2       GRYKRAVDEILRASAALTDEQKAKAEFFSNNYQGILLATRAAAIAH----DLDLDGWVHL      342
MarH3       RRYKRSVDEILEASATLDDEQKVKAEFFDNKFLGIGQSTKAAGIAH----DLELDDWVHL      343
Mcl24       RKYKQSVDQILEASATLTDEKKLMAEWFDNKLAGIALAPSAAALSH----DLDLDGWCHL      343

MarH1       ILEHLLATFDPLIAVWNEKTKYDAARPVTVIQHVYGKKKVTSWGGPGMGTVDDMPAGEWS      408
Mcl40       SLQHFLATFDALIAVWRNKRKYDTVRPVSAVRHVYGHSKVTAWGGAGMGTVNDIRATEWM      412
NapH1       MLAHVLATFEPLIAAWHHKTRFDAVRPVTAIRHVYGNRKIRAWGGVGMGTVD-IRASEWS      412
NapH4       MLQHILATFDTLIAAWGYKRKYEAVRPITAVRHVYGNRKIRAWGGVGMGTVDDIPANEWA      281
NapH3       FLVCSTARFDSLIAAWHHKRAYDTVRPFSAVRHVYGSKPVTAWGGPGKGTVESIPADEWT      363
MarH2       YMTSSVAQLDNLIASWHLKHAYDAVRPFSAVRHVYGRQKVRAWGGPGKGTV-ELRADEWA      401
MarH3       IYTSSLAQVEDLIAAWHYKVKYQAPRPFSAIRHVYGKKKVSAWGGPGIGTVHDMPADEWA      403
Mcl24       YAVTALARLDDLIAAWHWKTKFNSVRPFTAVHHVYGRKKISAWGGVGKGTVHDMPANEWS      403

MarH1       SYLPVGDHPEYPSGSTTLCSAASQCARRYFGSDELDWKFTFPAGSTRTEPGVVPAKDIEL      468
Mcl40       PYLPTGDHPEYPSGSTSLCAAGAQTARRYFNSEELDWTLEFNAGTSAVEPETTPAKNLQL      472
NapH1       SYLPVGDHPEYPSGSTSLCSATSQAARRYFDSDELDWTINYPAGSTVVEPGITPGKDLSI      472
NapH4       GYLPVGDHPEYPSGSTTVGSAASQAARRFFDSDDLNWEFDFEVGKSIVEPGITPVENVRV      341
NapH3       GYLPVGNHPEYPSGFTTLIAAQAQAARSFLGDDVLNWTHAFPAGSGQREPGAVPASDLEL      423
MarH2       GYLPVNDHPEYPSGSTALCAAMAQGARRFLGDDVLEWTYTFKAGSTQTEPGLVPARDIEL      461
MarH3       SFLPVGDHPDYPSGSTTLCAAEAQAARRFLGDDRLDWTWPIPAGWTLTEPGITPARDMEL      463
Mcl24       SYLPVGDHPEYISGSTTLCSAEAQAARRFLGDDVLDWTYSFPAGSGLTEPGLVPAKDTEL      463

MarH1       HFPTWTDFTQKCGASRVWGGVHFRKTVETSIAFGEQFGDMAHEFVQKHIKGEVED----      523
Mcl40       HFHTWAEFNKACAESRVWGGVHFRKTVQQSLIYGEQFGDLAHEFVNRHVKGNIKTDTRN      531
NapH1       HIPTWTDFTRTCATSRVWGGVHFQTTVDRTIDFGEQFGDLAHEFVQRHVKGDVKD----      527
NapH4       SFPTWTDFNKRCAYSRLDGGVHFKKTVERSMAFGEQFGDLAHDFIQRHVKGEGDG----      396
NapH3       TWATWTDFENDCATSRVWAGAHFTKTAETSLAFGTQFGDLAHTFVQRHINGDVKD----      478
MarH2       NYGTWTTFVRDAALSRVWAGVNFTKTAERSVEFGKQFGDLAHEFVQRHVSGEAED----      516
```

```
MarH3       HYGTWTEFVKDCGYSRLWAGVHFTTTVERSMEFGTQFGDLAYEFAQKYIKGDVED----       518
Mcl24       HWDTWTRFTRDCADSRVWGGVHFQTTVDRSIEWGAQFGDRAHQFLQRHIKGEVS-----       517
```

Figure SI-3.6: Multiple sequence alignment of VHPO homologues from *Streptomyces* spp. meroterpenoid gene clusters: NapH1, H3 and H4 from the napyradiomycin cluster in *Streptomyces* sp. CNQ-525; Mcl24 and 40 from the merochlorin cluster in *Streptomyces* sp. CNH-189; and MarH1, H2 and H3 from the putative marinone cluster in *Streptomyces* sp. CNQ-509. The key vanadate-coordinating histidine residue [His494 in NapH1 sequence – PDB 3W36] highlighted in red is mutated to an asparagine residue in MarH2. Sequence alignment was performed using Clustal Omega.[25]

marH1:

```
ATGACGACCGGACACTCTCCTGTCTCAGGCTTCTCCCCGCGGCGCAGGTCGCTGCTCATCGGCGGTGCCTCCGCCGCCGCGCTGCTCCCCCTG
GGTCACGCCGGCACGGCCGCCGCCGCCGAGGGCGGCAAGGCGGCCCAGGCAGAGTTCGACCTTGACAAGGACAACTACATCGAGTGGTTCCAG
CCCGAGGACGACGGCGCCGGGATCTCCCCCTCGTCGGAGATCTTCGGCCCGATGGACGTCACGGTGTTCCTCTGGATCAACCACCTGACGGGT
CTCGGGTGGTTCGACGCGGTGGCGCCCTACCATGAGACCGCGGTCGGTGTGCACTCCCGGATTCCCCGCCGTCCGTCCAGCGAGTCCGCCACC
AACCGGAACATGAACATCGCCTGTATCTACTCCCAGTACCAGTTGGTCAAGCAGGTGATCCCGAGCCGGGTCAAGCCCATGCGGGACCTGCTG
ACCAGCATCGGCCTGGACCCCGACGACGACTCGATGGATCCGGCCGACCCGGTCGGTGTCGGTAACATCGCCGGCAAGTCCGTCTTCGAGGCC
CTCAAGAACGACGGCATGAACTTCCTCGGTCACGACGGCGGCCGCAAGTACAACCCCAGGCCCTGGGCGGACTACACCGGCTACCGGCCCGTG
AACACCGCCTTCGACGTCGTCAACCCCTCGCGCTGGCAGCCGCAGCTCCAGGCCCACAACGGCCGCCGCGTCGGCGGCGGTCCCGGCGACCTG
GGCATCTGGGTGGCCCAGCACTTCGTCACCCCGCAGATGCGGATGGTGAAGCCCCACATCTACGCCGACCCGCGCGAGTTCACCGTCCCGCCG
CCCAAGCACGTCGACCACACCCGGCCCCGGGACTTCAAGCGCTCCGCGGACGAGGTCCTGGAGGCGTCGGCCGCGCTCACCGACGAGCAGAAG
GCCATCGCCGAGGTCATGGACAACAAGATCTGGGGAATCGGCCACTCGGCGCTGGTCATCGCGCGGAAGCACGACCAGAACGGCGAGCTGGGC
GTGCAGGGCTGGGCGCACTTCATCCTGGAGCACCTGCTGGCGACGTTCGACCCGCTGATCGCCGTCTGGAACGAGAAGACCAAGTACGACGCG
GCGCGGCCGGTCACGGTGATCCAGCACGTCTACGGCAAGAAGAAGGTGACCTCCTGGGGCGGCCCCGGCATGGGGACGGTCGACGACATGCCC
GCCGGGGAATGGTCCAGCTATCTCCCGGTGGGCGACCACCCGGAGTACCCGTCGGGCTCCACGACGCTGTGCTCCGCGGCGTCCCAGTGCGCG
CGGCGCTACTTCGGCTCCGACGAGCTGGACTGGAAGTTCACGTTCCCGGCAGGCTCGACGCGGACGGAGCCCGGCGTCGTCCCCGCGAAGGAC
ATCGAACTGCACTTCCCCACCTGGACCGACTTCACGCAGAAGTGCGGCGCCAGCCGCGTGTGGGGCGGGGTGCACTTCCGCAAGACGGTCGAG
ACGTCCATCGCCTTCGGGGAGCAGTTCGGCGACATGGCCCACGAGTTCGTGCAGAAGCACATCAAGGGTGAGGTCGAGGACTGA
```

marH2:

```
ATGACGACGTCCGGAAGCTCCTCCGTCCCCGGCTTCTCACCACGGCGCAGGTCGCTGCTGCTCGGCGGCGGCTCGGCCGCGGCCCTCACCGCC
CTGGGCCACGCGGGCACCGCCGCCGCCGAGCCGGGACCGGCGGCGGAGCCGCCGCCCGCCTTCGACCTCGACAAGGGCAACTTCGTCCGTGAC
CTGCTCACCGTGGCGGGCGACTCCAGCGGGGAGACGCAGGACCTCGGTCCCGCGGACGTCACCCTCATCTTCTGGATCCAGGACGTCATGCAG
ACCGCCTGGTTCGACGCCCTGGCGCCCTACCATCCGACCGCCGTCGGCGTGCGCACCCGGCTCCCCCGCCGCCCCGCCGGCGAGTCCGAGACC
AACAGGAACAAGAACATCGCCGGGCTGTACGCCACGTACCACGTGGTGAGCGTCGCCTACCCGGAGCGGGGCTACATCCTGCGGGGGCTGCTG
GAGGCGATCGGCCTCGACCCCGACGACGAGTCGGAGGACCCGGCCACCCCTGCGGGCATCGGCAATCTGGCCGGCAAGGCCGCCGTCGAGGCC
CGGCGGCGCGACGGCATGAACTTCCTCGGGGACGAGGGCCGGAGGTACCACCCCCAGCCCTTCGAGGACTACACCGGCTACGAGCCGGTGAAC
ACCGCCTACAAGCTGGTCGACCCGTCGAAGTGGCAGCCCGCCAGGACCCCGCACCGCCGCCGGGTGGGCGGCGGCCCGGGCGACAAGGGCATC
TTCACCGTCCAGCAGTTCGCCACCCCGCAGCTCCGGCTGGTCGAGGGCCACACCTTCCGGGACCCGGGCCGGTTCGAGCTGCCGCCGCCCGAC
CACAGCGACCACACCGCACCGGGCCGCTACAAGCGCGCCGTGGACGAGATCCTCCGCGCCTCCGCCGCGCTGACCGACGAGCAGAAGGCGAAG
GCGGAGTTCTTCAGCAACAACTACCAGGGCATCCTGCTGGCGACGAGGGCCGCGGCGATCGCCCACGACCTGGACCTGGACGGCTGGGTGCAC
CTCTACATGACCAGCTCGGTGGCCCAGCTCGACAACCTGATCGCCTCCTGGCACCTCAAGCACGCGTACGACGCCGTCCGGCCCTTCAGCGCG
GTCAGGCACGTGTACGGCAGGCAGAAGGTGCGCGCCTGGGGCGGTCCCGGCAAGGGGACGGTCGAACTCCGCGCCGACGAGTGGGCCGGCTAC
CTGCCGGTGAACGACCACCCCGAGTACCCGTCGGGATCCACCGCCCTGTGCGCCGCCATGGCGCAGGGGGCGCGGCGCTTCCTCGGTGACGAC
GTCCTGGAGTGGACGTACACCTTCAAAGCCGGCTCGACGCAGACGGAACCCGGGCTGGTCCCGGCCCGCGACATCGAGCTGAACTACGGCACC
TGGACCACCTTCGTCCGGGACGCCGCCCTGAGCCGGGTGTGGGCCGGCGTGAACTTCACGAAGACGGCCGAGAGGTCCGTGGAGTTCGGCAAG
CAGTTCGGCGACCTGGCCCACGAGTTCGTGCAGCGGCACGTCTCGGGCGAGGCCGAGGACTGA
```

marH3:

```
ATGACGTCCGGAAACTCCTCCTCCGCTGGCTTCTCCCCAGCTCGCAGGTCGCTGCTGCTCGGCGGCGCCTCGACCGCCGCGCTGGCGACCCTG
GGGACCGGCACCGCGGCCGCCGCCGGCCAGGGCACGGGACCGGCGGCGAAGCCGGCCGCCGCCGCCGAATTCGACTTCGACACCGGCAACTTC
CACCGGGACCTGCTCAGCACGGCGGCCAACCCGTCCGAGGAGCCGCTCGGCCCGATGGACGCGACGGTCCTCGTCTACCTCACCCATCTCACG
ATGACCGCGTGGTTCGACGCGCTGGCGCCCTACCACCCGACCGCCGTCGGCCGGCACAGCCGCATACCGCGCCGTCCCGCCAGCGAGTCGAAC
ACCAACCGGAACAAGAACGTCGCCGCGTTCCACGCCGCGAACGTGGTGTTCCAGTCCGTCTTCAAGGAGCGGGTGGCGGCCTTCCGGCAGCTC
ATGACCACGCTCGGCCTGGACCCCGACGACCAGTCGACGGATCCCACCAGCCCGGTGGGCATCGGCAACCTGGCCGCCAGGGGCGTCCTCAAG
GCCAAGGCGCGTGACGGCATGAACCTCTTCGGCGACGAGGGCCGGAAGTACCACGGGCAGCCCTACGAGGACTACACCGGCTTCGAGCCGGTG
AACACCGCCTACAAGCTGGTCAACCCGTCGAAGTGGCAGCCGGCCAGGCACCCGCACCGCCGCCGGGTGGGCGGCGGCCCGGGCGACAAGGGC
ATCTTCGTCGTCCAGCACATGGTCACCCCGCAGATGGCGCTGGTGAAGCCGGACACCTACCGGCACCCGAGCCAGTTCCCGCTGGCCCCGCCG
GACCACCTCGACCACACCGACCCGCGCCGCTACAAGCGCTCGGTGGACGAGATCCTGGAGGCGTCCGCCACGCTCGACGACGAGCAGAAGGTG
AAGGCCGAGTTCTTCGACAACAAGTTCCTGGGCATCGGCCAGTCGACGAAGGCCGCGGGGATAGCCCACGACCTGGAGCTGGACGACTGGGTC
CACCTGATCTACACGAGTTCGCTGGCACAGGTCGAGGATCTCATCGCGGCCTGGCACTATAAGGTCAAGTACCAGGCGCCGCGGCCGTTCTCC
GCCATCCGGCACGTGTACGGCAAGAAGAAGGTGTCCGCCTGGGGCGGGCCCGGCATCGGGACCGTGCACGACATGCCCGCCGACGAGTGGGCC
AGCTTCCTCCCCGTGGGCGACCACCCCGACTACCCGTCGGGATCCACGACGCTCTGCGCCGCCGAGGCGCAGGCCGCCCGGCGCTTCCTCGGC
GACGACCGCCTGGACTGGACCTGGCCCATCCCCGCCGGCTGGACGCTGACGGAGCCCGGGATCACCCCCGCCAGGGACATGGAGCTGCACTAC
GGCACCTGGACCGAGTTCGTGAAGGACTGCGGCTACAGCCGGCTCTGGGCCGGGGTGCACTTCACGACCACGGTCGAGCGGTCGATGGAGTTC
GGCACCCAGTTCGGCGACCTCGCGTACGAGTTCGCCCAGAAGTACATCAAGGGCGACGTGGAGGACTGA
```

Figure SI-3.7: *marH* gene sequences used in this study.

marO:

```
ATGACACAAGGAGCCACACTCGCGCGCATCCGCGACTACATGGTGGGCCCCACCCGGTTTATGACCCTCCTGTCCTGTTTCGAGCTCGGCATC
ATCGACGCACTGCGCGACAAGCCCGGCATGACCGCGGCCGACCTCGGCGCCGCGGTGGCACCAAGCCCGACGCCGTGGAGCAGCTTCTCTTCC
TGCTCATCAAGGAGGGCTTCGTCGCGCGCGACGAGGCGTCCGGCACGTACACCCTCGACGCGCTCGGCGAGGTTCCCGAGCGCGACCTGAAGC
GCGCGCTCACCTACATGAACATGATCAAGGTGGTGGCGCTCAGGCAGCTCTTCCACCTCACCGAGAGCGCGCGGACCGGCACGCTCGTCGGCC
TCAAGGAGTTCTACGGCGTCACCGAGGGCACCATGTACGACGCCGTGGCCGAGCACAAGGACCTCCGGGAGTCCTGGGGGACGTTGATGGACA
ACGTCACCGCCAACATCGACCCCTGGTTCTTCGGGAACGTCGACATCGCGGCGGGCGCCCAGGTGCTCGACCTCGCCGGGAACACGGGTCTCG
GGGCGATCCACGCCTACGAGTCGAAGGCCTCCCCCGGGCTCCGGGTGACGACGTTCGACCTGCCGGAGAAGGAGGAGGAGGCCCTGGAGAACT
TCCGGGCGCACGGCGTGGCGGAACACTGCTCGTTCATCGGCGGCAACGTCTTCGAGGAGATCCCGCAGGGCTTCGACGTCGTTCTCATCAAGC
ACTTCCTGGACATGTTCGACAAGGACGACGTGATCCGGATCCTCACCGGCGTCAACCGGTCGCTGCCGGTCGGCGGCGAGGTCAACGTGCTGG
TCCCGGTGTACCCCGAGAACCTCACGGACACCGACAACTACAACGTCGACTTCTTCCCGGCCTTCTTCATCGGCTGCACCATGGGCCAGGGCG
GCCCGCAGAAGCTGTCGGTCTACCGGAGCTGGCTGGAGGAGTGCGGGTTCGAGGTGACGAAGGCGATCACCAAGGACCCCGCCGAACTGCCGA
AGGACGTCATCCCGGTGCCGGCCCTCCTCTCCGCCACGAAGGTCCGGTGA
```

Figure SI-3.8: Putative methyl transferase *marO* gene sequences used in this study.

marX4:

```
ATGGAAGCCATCGAAGTTCCGGTTCTGATCGTGGGCGGCGGCGGTTGCGGCCTGTCCGCCTCCATCTTCTTGTCCGGCCAGGGTGTCGAGCAC
CTGCTGGTCGAGCGGCACACGGACACGTCGAGGCTGCCGCGCGCCCACTACCTCAACCAGCGCACCATGGACATCTTCCGCCAGCACGGTCTC
GTGGACTCCGTCCACGAACTGTCGGCGCCGCCCGAGGTGTTCGGCAGGGTGCGCTGGCAGACCTCCCTCGCCGGGGACGACCCGCTGGACGGG
CAGGTCATCTACGAGATGGACGCCTTCGGGGGCGGTGCCCTCACCGAGGTGTACGCGGAGCACGGCCCCGTCCTGCCCGCCAAGCTCCCGCAG
TTGCGGCTGGAGCCGATGCTGCGCCGCCGCGCCGAGCGGGACAATCCCGGCCGGGTGCTCTTCGGCCACGAGCTGACCACCTTCTCCGACAAG
GGCGACCGCGTCGTCGCCGAGATCCGCGACATCGCCACCGGCGAGACGACCACGGTCACCGCGCAGTACGTCATCGCCGCCGACGGCGGCCGC
ACCATCGGCGCCGAGCTGGGCGTGGAGATGCAGGGCGTGCCCAGCATGCTGAACGTCACCACCGCGTACCTCACCGCCGACCTCTCCCCGTGG
TGGCACGACGGCACGATCATCACCTGGTTCGTCAACCCCTTCCGCCCCGACCTCTCCAGCACGCTGATGGAGATGGGTCCCACCTGGGGCAAG
CACTGCGAGGAGTGGGCGCTGCACTTCAACCCCGGCGACGCCGACCGCGACGACCCGGAGGCGATGACAGCCCGGATCCGCGAGGTCCTCGGC
GTGCCGGACCTGGAGCTGACCCTGCACCGGATCAGCCAGTGGACCGTCGAGGGCGTGCTCGCCGACCGCTACCGCCAGGGTCGCGTCCTCATC
GTCGGCGACGCCGCGCACCGCCAGCCGCCCACCACCGGTCTCGGCCTCAACGGCGGCGTCCAGGACGTGCACAACCTGGCGTGGAAGCTGGCC
GCCGTGGTCGCCGGCCACGCCGACGACAGCCTCCTCGACTCCTACGAGACCGAGCGCCGCGCCGTCGGCAAGCGGAATGTCGACTGGGGCCTG
TCGACGTGGTTCCACCACAAGGTGGTGACCGAGGCCGCGATCGGGCTCGGCGCCCACATCCCGGTCGAGCGCCGGTCGGCGGTGTTCTCCGCC
TACTTCGACCCCTCCCCGGTCGGCACGGCCGTACGGGCCCGGGCCGCGGAGATCTTCCAGACCCACCGCTCCGAGTGCCAGGCGCACGACCTG
GAGGTGGGCTTCGCGTACGAGGACGGCGCGCTCGTCCCTGACGGCACCGCGCCCCCGGCCCGCGCGCCCCTCGGCAACACCTACCACCCCACC
ACCCGGCCCGGGCACATGCTCCCGCACGCCTGGATCGAGCGGGACGGCGAGCGCCTGTCCACCCACGATCTGGTCGGCCGCGGCGGCGGCTTC
GTGCTGATCGCAGGCCCCGAGGGGAAGGCGTGGTGCGACGCGGCGGCGGAGGCGGCCGAGAAGTTCTCGATCCCGCTCACGGCGGTGCGCATC
GGCGAGGGCGCCGAGTACGCCGCCGCGGACGGCCGGTGGGCGGCGGTCCGCGAGATCACCGACGAGGGCGCCATCCTGGTACGCCCGGACCAC
CACGTGGCCTGGCGGAGCACGTCCGCCGGAGCCGATCCGGCGGCCGCGCTCGCCGACGTGCTCTCGCGCGTCCTCGCCCACGGCGGCACCCGG
CACGGCTAG
```

Figure SI-3.9: Putative aromatic monooxygenase possibly FAD binding *marX4* gene sequences used in this study.

marX1:

```
ATGAGCGTCCGCATGTTCCGTGCCAAGATCAAGGAAGACAAGGTCGAGACCGCGGAGAAGGCTGCGAAGGAACTCTTCGCGGCGATCGAGGAA
GCGAAGCCCGAGGGCGTCCGCTATTCCTGGTGCAAACTCGCGGACGGGCGGACCCTCGTTCTCGTGGTGGATCTGGAGGATGACGAGAAGAAC
CCTCTTCTCACCATGCCGGCATTCCAGGAGACGATGAACGGCCTGAAGAACGAGTGGATCTCGGAGCCGCTGTCGGTCGAGCCGATGACGTCA
CTCGGCTCGTACCGCCTCTTCTACTGA
```

marX2:

```
ATGCGTAGTCTGAAGAGGTTCCGCATGCCGCTCGCCGTCGCGGCGGCGACGGCGCTCGCGGGTGTGGCAGCCGGTCCGTCGGGTCAGGTGGTC
GCGGCGGAGAAGGGTTCGGGCACGCTGTCCGGCGACGCCCCGGTCGAGGTCATCGCGAAGGGGCTGCACTCGCCCCGCGACCTGACCTGGACG
CCCGAGGGCCGGCTTCTCGTCTCCGAGGCGGGCGGCATCGAGCAGCTCTGCGACAACGCCGACATCATGACGGCGAAGTGCTTCAGCACCACG
GGCGCCATCACCGACGTCACCGACGGCAAGCCGAAGCGGATCGTCGAGGGCCTGGCCTCGAACGTGAACAACGCCGAGGTCGTCGGCCCGAAC
GCGATGGTCTACTCCGAGGGCAAGCTGCACGTCCTTCAGGCGGGCCACGGCATCGGGCTGCCGAAGTGGCTGCCCCGCGACCTGCGCACCACC
CTGAAGAACCAGTACGGCAGGGTGCTCCAGGTCACGGAGAAGAAGGTCAAGGCGGTCGCCAACCCCGGCGCGGCCGGCTACAAGTGGATGCAG
GAGAACCCGGACCTCGTCTCCGAGGACCCGACGTCCAACCCCGTCTCGCTCGCCGCGAAGCCGGGCGGCGGCTTCTACTACGTGGACGCGGCC
GCGAACATCCTCGGTGAGATCGACCGCCGGGGCAAGGTCAAGGTCCTGAAGTGGTTCCCGAAGGCCCCGAACGGCGCCGACGCCGTACCCACC
TGCGTCGACGTCGGCCCCGACGGCGCGGTGTACGCCGGGCAGCTCACCGGCTTCGGCAACACCGGCAACGCCGCGGCCAACATCTACCGGTAC
GACCCGAAGACCGGCGAGCTGAAGGTCTGGGAGAGCGGCTTCGCCACCATCTCCGGCTGCGGCTTCGGCGCCAACGGCGACTTCTACGTCACC
CAGTTCGACCGGACCGGCTTCCCGCCGCCCCGGTGACCCGCAGGGCGTCGTCGTCCAGATCGCCAAGGACGGCACCCGCACCGAGCTGGGCGCG
GGCAAGCTCTTCGCCCCGCAGGGCTTCCTCGCGGGCCCCGACGGCTCCATCTACGTCACCAACAACACCGTGTGGTACCCGGTCGGCACCACC
AACCGCTGGGACCAGGGCGAGGTCGTCAAGATCGGCTGA
```

marX2 minus signal peptide:

```
GAGAAGGGTTCGGGCACGCTGTCCGGCGACGCCCCGGTCGAGGTCATCGCGAAGGGGCTGCACTCGCCCCGCGACCTGACCTGGACGCCCGAG
GGCCGGCTTCTCGTCTCCGAGGCGGGCGGCATCGAGCAGCTCTGCGACAACGCCGACATCATGACGGCGAAGTGCTTCAGCACCACGGGCGCC
ATCACCGACGTCACCGACGGCAAGCCGAAGCGGATCGTCGAGGGCCTGGCCTCGAACGTGAACAACGCCGAGGTCGTCGGCCCGAACGCGATG
GTCTACTCCGAGGGCAAGCTGCACGTCCTTCAGGCGGGCCACGGCATCGGGCTGCCGAAGTGGCTGCCCCGCGACCTGCGCACCACCCTGAAG
AACCAGTACGGCAGGGTGCTCCAGGTCACGGAGAAGAAGGTCAAGGCGGTCGCCAACCCCGGCGCGGCCGGCTACAAGTGGATGCAGGAGAAC
CCGGACCTCGTCTCCGAGGACCCGACGTCCAACCCCGTCTCGCTCGCCGCGAAGCCGGGCGGCGGCTTCTACTACGTGGACGCGGCCGCGAAC
ATCCTCGGTGAGATCGACCGCCGGGGCAAGGTCAAGGTCCTGAAGTGGTTCCCGAAGGCCCCGAACGGCGCCGACGCCGTACCCACCTGCGTC
GACGTCGGCCCCGACGGCGCGGTGTACGCCGGGCAGCTCACCGGCTTCGGCAACACCGGCAACGCCGCGGCCAACATCTACCGGTACGACCCG
AAGACCGGCGAGCTGAAGGTCTGGGAGAGCGGCTTCGCCACCATCTCCGGCTGCGGCTTCGGCGCCAACGGCGACTTCTACGTCACCCAGTTC
GACCGGACCGGCTTCCCGCCGCCCGGTGACCCGCAGGGCGTCGTCGTCCAGATCGCCAAGGACGGCACCCGCACCGAGCTGGGCGCGGGCAAG
CTCTTCGCCCCGCAGGGCTTCCTCGCGGGCCCCGACGGCTCCATCTACGTCACCAACAACACCGTGTGGTACCCGGTCGGCACCACCAACCGC
TGGGACCAGGGCGAGGTCGTCAAGATCGGCTGA
```

marX3:

```
ATGCGACGTCTCGCACGATGTCGGATGCTGCTCGCCGCGGCAGCGGCGACAACGCTCGCCGGTGTGGCGGCCGGATCGTCCGGACCCGTGGCC
GCCGCCGACCACGGCCGGGGCTCGGGCACGCTCGGCAAGGACGCCGAGGTCGAGGTGATCGCGGAGGGTCTGCACTCGCCGCGCTCCCTGACC
TGGGGCCCGGGGGGCCGGCTGCTGGTCTCCGAGACCGGCACGCCGCCGCTGACGGCGCCGTCCGAGTGCAACATGGTCTCGGAAGAGATCGTC
TTCGAGATGAAGTGCTTCGGCCACACCGGTTCCGTCGCCGACATCACGAACGGCACGCCGAAGCGGATCGTGAAGAACCTGCCCTCGGCGCTG
AACCTCCAGGACATGATCGGCCCGAACGGGCTGGCCTACAGCCAGGGCCGCCTGTACACGCTGCAGGCGGGCTCGCCGCAGGCCCTCCCGACC
GACGCGTGGCTCTCCGACGGCCTGCGGAACAAGCTCAAGCCGTACGTCGGCACCCTGCTCGACGTCACCAACCCGAAGAAGCCGCGGGTGGCC
GCCCGGCCGGGTGCGGCCGACTACGAGTACATCAAGGAGAACCCGGACCCGACGCCCGACTTCGATGTCACGAACCCGTACTCGCTCACGCCC
AGGAAGGGCGGCGGCTTCTACTACGTGGACGCCGCGGCGAACGTGCTCGGCGAGATCGACCGGTGGGGCAACGTCGAGATCCTCACCGGCTTC
CCGCCCAGCCAGGCGGGCTCCGACGCCGTGCCCACCTGCGTCGCCCAGGGCCCGGACCGCGCGGTGTACGTCGGCGAGCTGACCGGCCACGGC
AACACCGGCGAGGAGGGCGCCAAGGCCGCCAAGGTCTACCGCTACGAGCCGTGGAGCGGTGACCTGGAGGTCTGGCAGCGGGGCTTCAGCGCC
ATCTCGGGCTGCGGCTTCGGCAAGAACGGCGACTTCTACGTCACGCAGTTCACCTCGACCGGCTTCCTGCCGTCGCCCGACGACGACGGCGGC
AGCGTCATCCAGATCGGCCGCGACGGCACCCGTACGGAGCTGGGCAAGGGCAAGCTGTTCTTCCCGCACGGCTTCCTCGCGGGCCGGGACGGC
TCGATCTACGTGGCCAACAAGAGCCTGTGGTGGCCCCCGGGCACCACAGGCGACTGGGACAAGGGAGAGGTCATCAAGATCGGCTGA
```

marX3 minus signal peptide:

```
GACCACGGCCGGGGCTCGGGCACGCTCGGCAAGGACGCCGAGGTCGAGGTGATCGCGGAGGGTCTGCACTCGCCGCGCTCCCTGACCTGGGGC
CCGGGGGGCCGGCTGCTGGTCTCCGAGACCGGCACGCCGCCGCTGACGGCGCCGTCCGAGTGCAACATGGTCTCGGAAGAGATCGTCTTCGAG
ATGAAGTGCTTCGGCCACACCGGTTCCGTCGCCGACATCACGAACGGCACGCCGAAGCGGATCGTGAAGAACCTGCCCTCGGCGCTGAACCTC
CAGGACATGATCGGCCCGAACGGGCTGGCCTACAGCCAGGGCCGCCTGTACACGCTGCAGGCGGGCTCGCCGCAGGCCCTCCCGACCGACGCG
TGGCTCTCCGACGGCCTGCGGAACAAGCTCAAGCCGTACGTCGGCACCCTGCTCGACGTCACCAACCCGAAGAAGCCGCGGGTGGCCGCCCGG
CCGGGTGCGGCCGACTACGAGTACATCAAGGAGAACCCGGACCCGACGCCCGACTTCGATGTCACGAACCCGTACTCGCTCACGCCCAGGAAG
GGCGGCGGCTTCTACTACGTGGACGCCGCGGCGAACGTGCTCGGCGAGATCGACCGGTGGGGCAACGTCGAGATCCTCACCGGCTTCCCGCCC
AGCCAGGCGGGCTCCGACGCCGTGCCCACCTGCGTCGCCCAGGGCCCGGACCGCGCGGTGTACGTCGGCGAGCTGACCGGCCACGGCAACACC
GGCGAGGAGGGCGCCAAGGCCGCCAAGGTCTACCGCTACGAGCCGTGGAGCGGTGACCTGGAGGTCTGGCAGCGGGGCTTCAGCGCCATCTCG
GGCTGCGGCTTCGGCAAGAACGGCGACTTCTACGTCACGCAGTTCACCTCGACCGGCTTCCTGCCGTCGCCCGACGACGACGGCGGCAGCGTC
ATCCAGATCGGCCGCGACGGCACCCGTACGGAGCTGGGCAAGGGCAAGCTGTTCTTCCCGCACGGCTTCCTCGCGGGCCGGGACGGCTCGATC
TACGTGGCCAACAAGAGCCTGTGGTGGCCCCCGGGCACCACAGGCGACTGGGACAAGGGAGAGGTCATCAAGATCGGCTGA
```

Figure SI-3.10: Hypothetical genes *marX1*, *marX2* and *marX3* gene sequences used in this study. Sequences for *marX2* and *marX3* have been given with and without signal peptide sequence.

General VCPO activity assay procedure:

To a 1 mL solution of 50 mM buffer solution (MES-NaOH, pH 6.0 or HEPES-NaOH, pH 8.0), 100 mM KCl, 100 μM sodium orthovanadate, 1 mM hydrogen peroxide (1 equivalent), and 20 μM MarH enzyme(s), a DMSO solution of 1 mM substrate (final concentration) was added and incubated at 20 °C. Aliquots (50 μL) were removed at 1, 3 and 18 h intervals, quenched with 50 μL of acetonitrile, centrifuged for 2 minutes at 13000 x *g* to pellet proteins, and the clarified supernatant was analysed by RP-HPLC-MS in negative ionization mode using the following method: 10 - 100% B (20 min), 100% B (4 min), 100 - 10% B (3 min), 10% B (3 min), where A = 0.1% aqueous formic acid, and B = 0.1% formic acid in acetonitrile (flow rate: 0.75 mL/min; column: Agilent Eclipse XDB-C18 5 μm, 4.6 x 150 mm; LC: Agilent Technologies 1200 series system with a diode-array detector; MS: Bruker Amazon SL ESI-Ion Trap mass spectrometer; data processing: Bruker Compass Data Analysis 4.2 SR2). VCPO assay analytes showing comparable retention times and *m/z* to synthetic standards are highlighted in grey boxes (*m/z* values ± 0.2 Da of synthetic standards: **3.14a** – 343.2; **3.14b** – 411.2; **3.16a** – 377.1; **3.16b** – 445.2; **3.20a** – 411.1; **3.20b** – 479.1).

Activity of MarH1 on pre-marinone (3.12b) at pH 6.0:

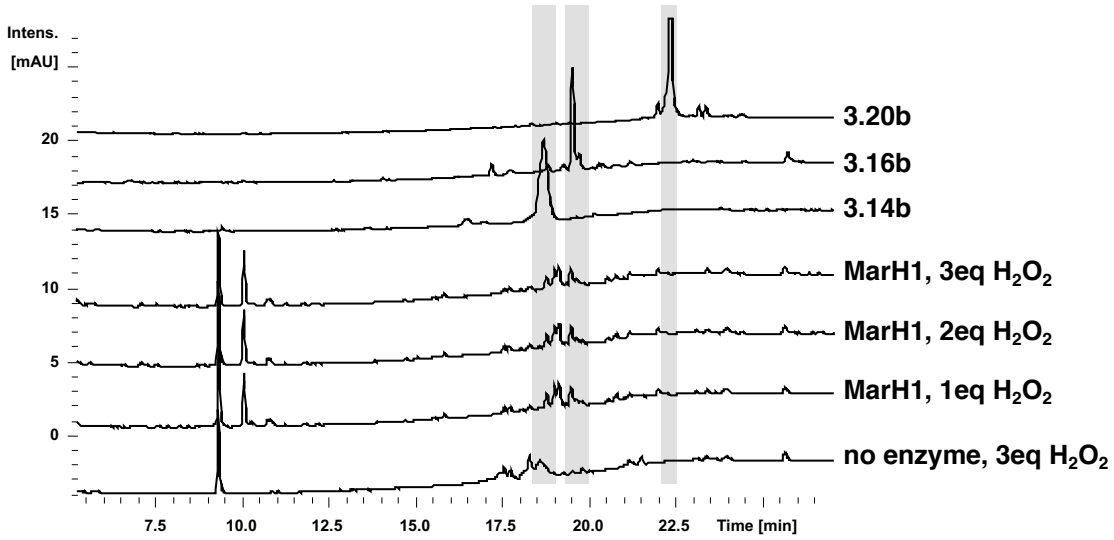

Figure SI-3.11: RP-HPLC-MS analysis (λ = 300 nm) of *in vitro* MarH1 incubation with **3.12b** in the presence of variable equivalents of hydrogen peroxide (pH 6.0, 18 h), and comparison to synthetic standards **3.14b**, **3.16b**, and **3.20b**.

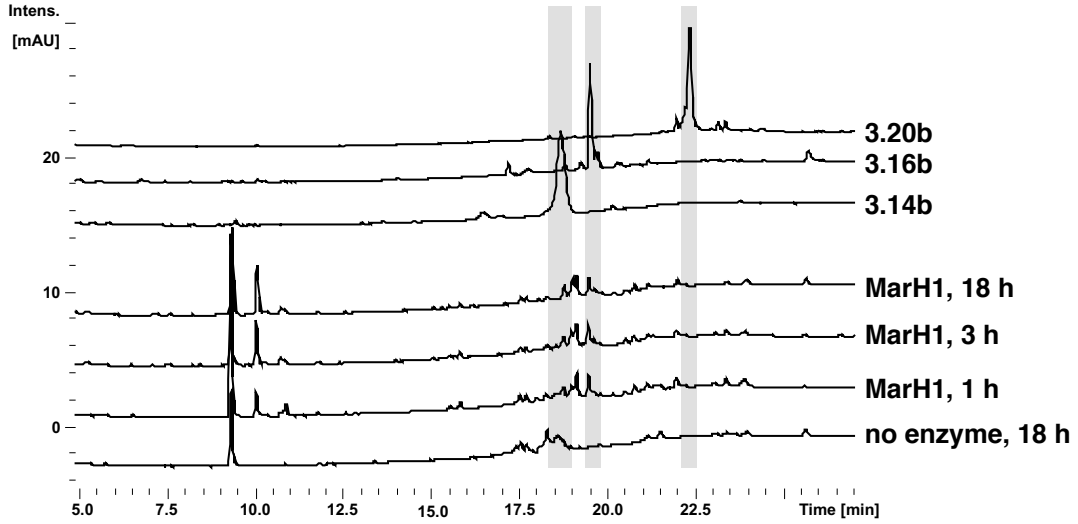

Figure SI-3.12: RP-HPLC-MS analysis (λ = 300 nm) of *in vitro* MarH1 incubation with **3.12b** over time (pH 6.0, 1 equiv. hydrogen peroxide), and comparison to synthetic standards **3.14b**, **3.16b**, and **3.20b**.

Activity of MarH3 on pre-marinone (3.12b) at pH 6.0:

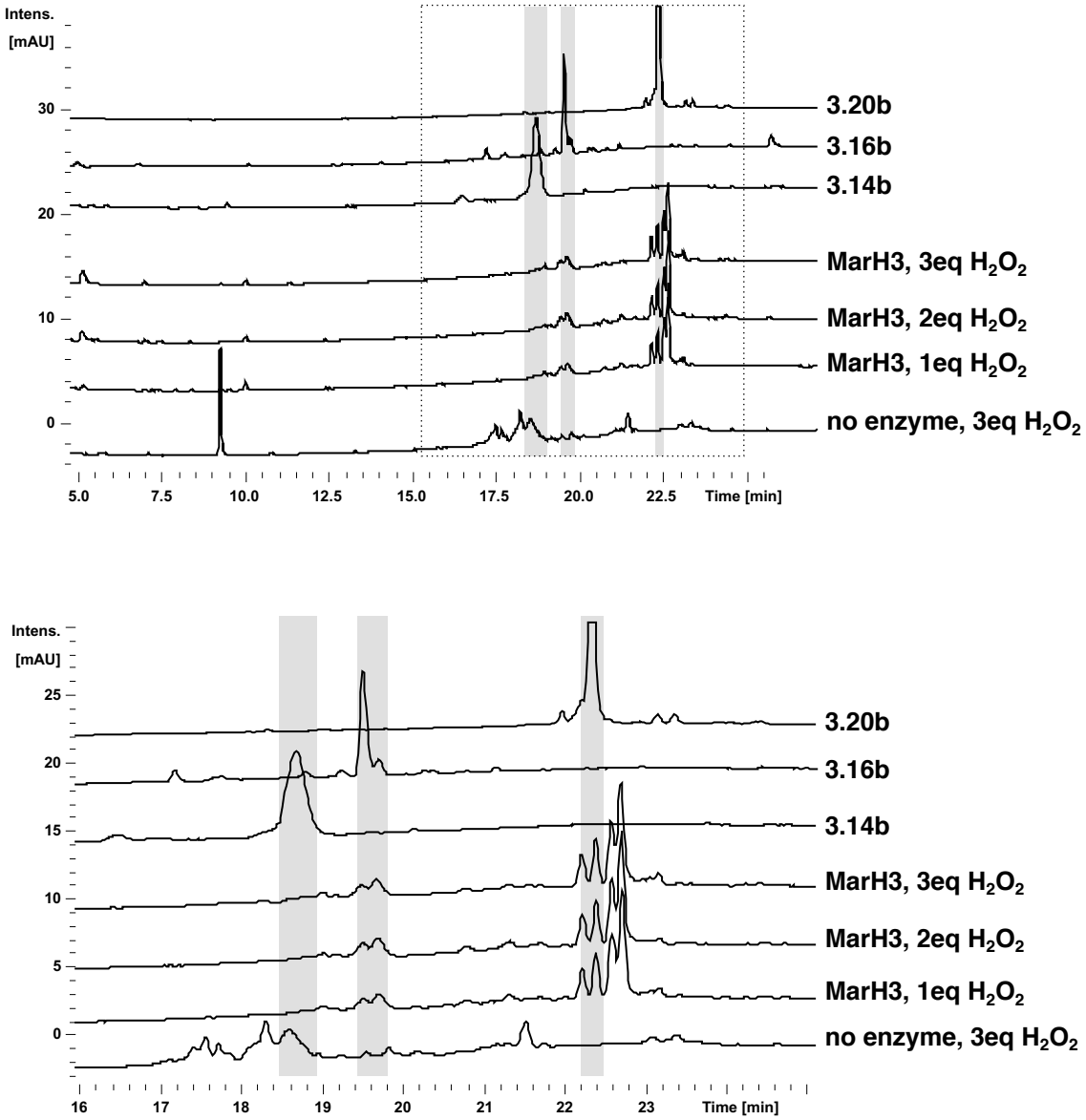

Figure SI-3.13: RP-HPLC-MS analysis (λ = 300 nm) of *in vitro* MarH3 incubation with **3.12b** in the presence of variable equivalents of hydrogen peroxide (pH 6.0, 18 h), and comparison to synthetic standards **3.14b**, **3.16b**, and **3.20b**.

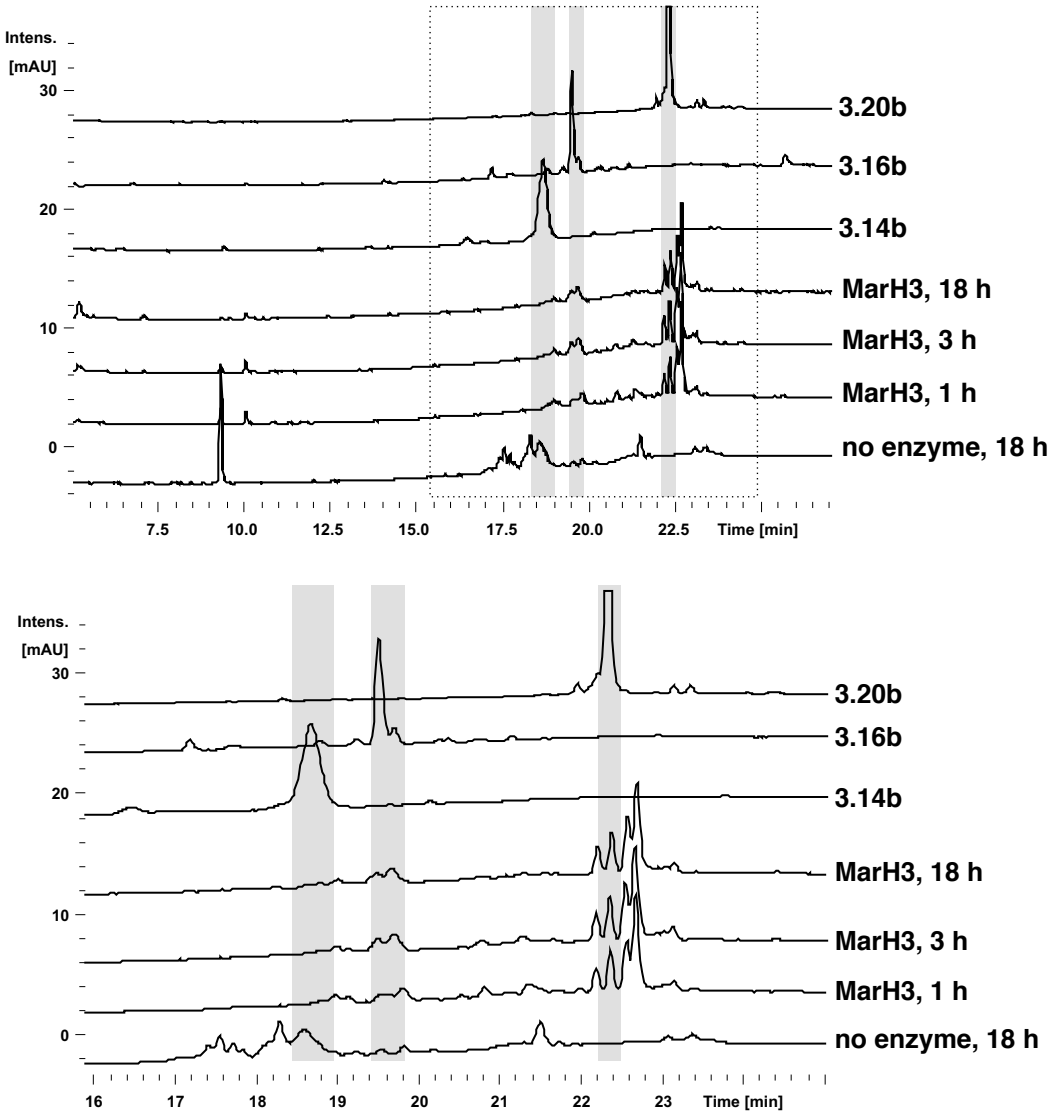

Figure SI-3.14: RP-HPLC-MS analysis (λ = 300 nm) of *in vitro* MarH3 incubation with **3.12b** over time (pH 6.0, 3 equiv. hydrogen peroxide), and comparison to synthetic standards **3.14b**, **3.16b**, and **3.20b**.

Sequential activities of MarH1, then MarH3 on pre-marinone (3.12b) at pH 6.0

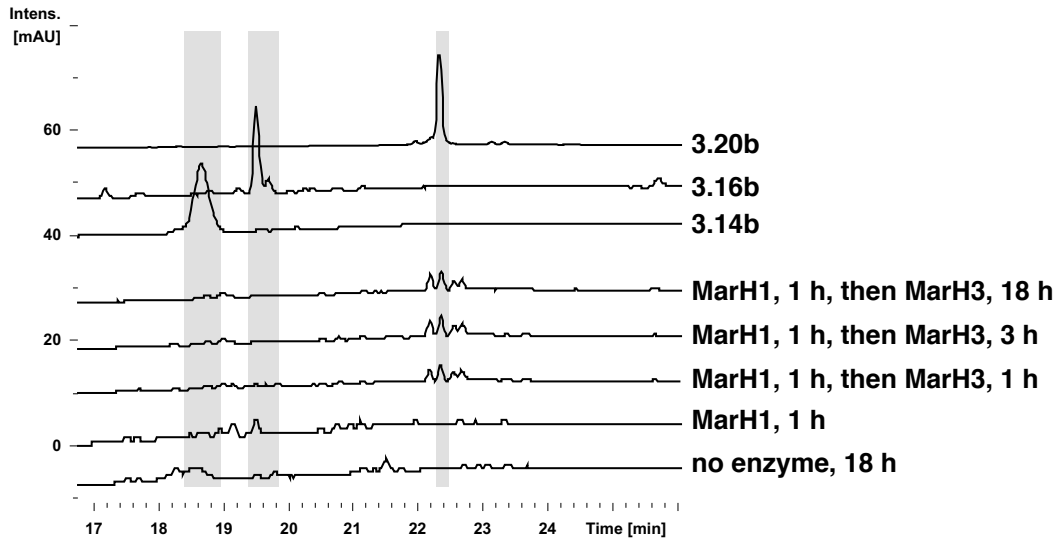

Figure SI-3.15: RP-HPLC-MS analysis (λ = 300 nm) of *in vitro* incubation of **3.12b** with MarH1 (pH 6.0, 2 equiv. hydrogen peroxide, 1 h) followed by MarH3 (1 additional equiv. hydrogen peroxide, variable time), and comparison to synthetic standards **3.14b**, **3.16b**, and **3.20b**.

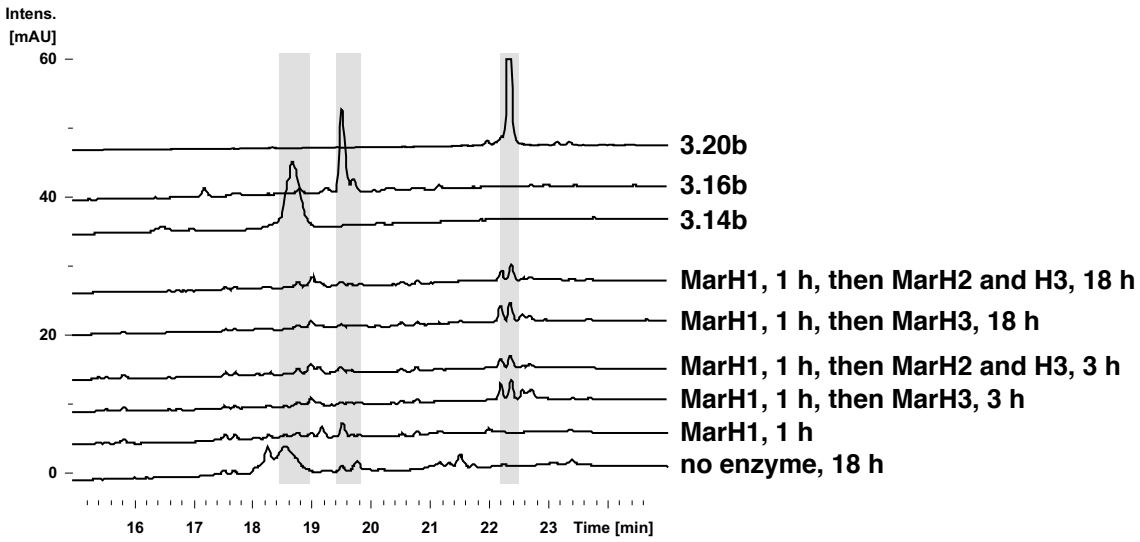

Figure SI-3.16: RP-HPLC-MS analysis (λ = 300 nm) of *in vitro* incubation of **3.12b** with MarH1 (pH 6.0, 2 equiv. hydrogen peroxide, 18 h) followed by MarH3 with or without MarH2 (1 additional equiv. hydrogen peroxide, variable time), and comparison to synthetic standards **3.14b**, **3.16b**, and **3.20b**.

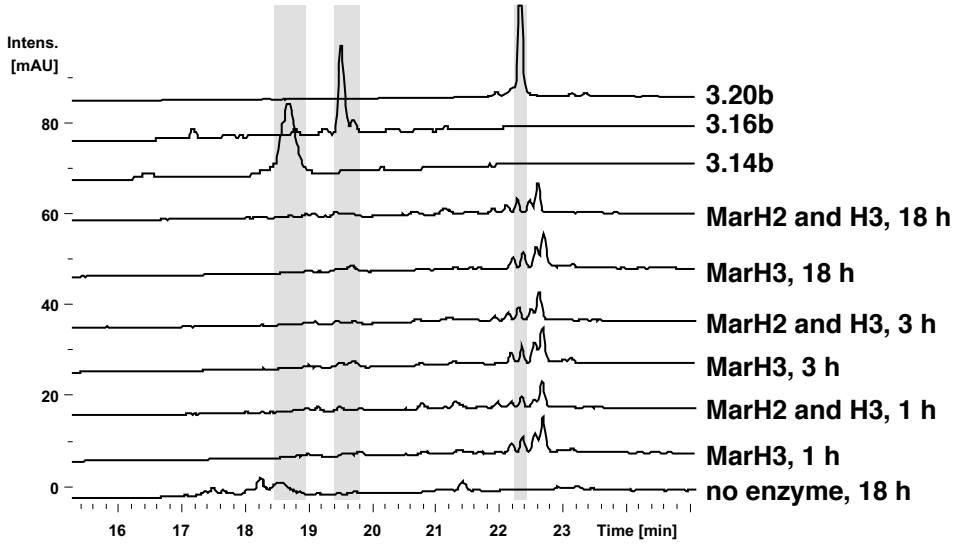

Figure SI-3.17: RP-HPLC-MS analysis (λ = 300 nm) of *in vitro* incubation of **3.12b** with MarH3 over time (pH 6.0, 3 equiv. hydrogen peroxide) with or without MarH2, and comparison to synthetic standards **3.14b**, **3.16b**, and **3.20b**.

General *O*-methyltransferase MarO activity assay procedure:

To a 1 mL solution of 50 mM buffer solution (HEPES-NaOH, pH 8.0), 100 mM KCl, 1mM *S*-adenosyl methionine (SAM), and 50μM MarO enzyme, a DMSO solution of 1 mM substrate (final concentration) was added and incubated at 20 °C. Aliquots (50 μL) were removed at 30 min, 1 h, 3 h and 18 h intervals, quenched with 50 μL of methanol, centrifuged for 2 minutes at 13000 x *g* to pellet proteins, and the clarified supernatant was analysed by RP-HPLC-MS in negative ionization mode using the following method: 10 - 100% B (20 min), 100% B (4 min), 100 - 10% B (3 min), 10% B (3 min), where A = 0.1% aqueous formic acid, and B = 0.1% formic acid in acetonitrile (flow rate: 0.75 mL/min; column: Agilent Eclipse XDB-C18 5 μm, 4.6 x 150 mm; LC: Agilent Technologies 1200 series system with a diode-array detector; MS: Bruker Amazon SL ESI-Ion Trap mass spectrometer; data processing: Bruker Compass Data Analysis 4.2 SR2). *O*-Methyltransferase assay analytes showing comparable retention times

and *m/z* to synthetic standards are highlighted in grey boxes (*m/z* values ± 0.2 Da of synthetic standards: **3.21b** – 444.2; **3.21a** – 376.1; **3.23b** – 410.2; **3.23a** – 342.2).

Denaturation/Renaturation of MarO to remove SAM from the enzyme active site:

Following expression and purification as outlined above, MarO was obtained with concentration of 5.95 mg/mL in buffer solution. A volume of 5.04 mL of protein solution was diluted in 20 mL buffer A (50 mM Tris-HCl (pH 8.0), 0.5 M NaCl, and 25 mM imidazole) to give a final protein concentration of 1.5 mg/mL. Solution was placed in dialysis tubing (14 kDa cutoff) and dialysed against denaturation buffer (20 mM Tris-NaOH (pH 8.0) 300mM NaCl and 8 M urea) at 4 ºC for 16 h. The protein was then refolded using sequential buffer exchange steps. The protein was next dialysed against 20 mM Tris-NaOH (pH 8.0) 300mM NaCl and 5 M urea for 2 h at 4 ºC. Buffer was then exchanged every 2 h, decreasing urea concentration from 5 M to 2 M, 0.5 M and finally 0M. Dialysis against 20 mM Tris-NaOH (pH 8.0) 300mM NaCl was left for 16 h at 4ºC. The dialysed protein was concentrated to 3.5 mL using an Amicon Ultra 30 kDa cutoff concentrator (EMD Millipore) by centrifugation at (4000 x *g*, 4 °C) and further purified by size exclusion chromatography using Supedex 200 column (16 cm × 60 cm, GE Healthcare) and buffer: 25 mM Tris (pH 8.0), 200 mM NaCl, 10% glycerol. Enzyme was concentrated using an Amicon Ultra 30 kDa cutoff concentrator (EMD Millipore) by centrifugation at (4000 x *g*, 4 °C) to 3.71 mg/mL, aliquoted, frozen on dry ice and stored at –80 °C until needed.

Upscale *O*-methyltransferase MarO assay procedure:

To a 1 mL solution of 50 mM buffer solution (HEPES-NaOH, pH 8.0), 100 mM KCl, 100μM MarO enzyme, a DMSO solution of 1.12 mM substrate (final concentration) was added and incubated at 20 °C. A total of 20 x 1 mL reactions were prepared following this method. Reactions were left at room temperature for 30 min, and reaction progress confirmed through LC-MS as outlined above. All reactions were combined and acidified with 1M HCl to pH 3. EtOAc (10 mL) was added and the resulting emulsion centrifuged for 10 minutes at 5000 x g. Organic phase was decanted and concentrated *in vacuo*. Residue was diluted with Brine (30 mL) and extracted with EtOAc (3 x 20 mL). Combined organics were dried over $MgSO_4$, filtered and concentrated *in vacuo*. Crude extract was purified by semi-prep HPLC, followed by flash chromatography on SiO_2 (9:1 → 6:1 hexane/EtOAc) to give **3.23b** as an orange solid. NMR spectra were recorded on a Bruker Avance III spectrometer (600 MHz) using a 1.7 mm inverse detection triple resonance (H-C/N/D) cryoprobe in acetone-d_6.

Enzymatic Product **3.23b***:*

^{1}H NMR (600 MHz, acetone-d_6): δ 11.52 (s, 1H), 7.09 (d, *J* = 2.4 Hz, 1H), 6.54 (d, *J* = 2.3 Hz, 1H), 5.22 – 5.17 (m, 1H), 5.06 (t, *J* = 7.0 Hz, 1H), 5.00 (t, *J* = 7.2 Hz, 1H), 3.24 (d, *J* = 7.4 Hz, 2H), 2.09 – 2.01 (m, 2H), 2.01 – 1.93 (m, 4H), 1.90 – 1.84 (m, 2H), 1.78 (s, 3H), 1.61 (s, 3H), 1.54 (s, 3H), 1.52 (s, 3H).

Synthetic Standard **3.23b***:*

^{1}H NMR (600 MHz, acetone-d_6): δ 11.51 (s, 1H), 7.09 (d, *J* = 2.4 Hz, 1H), 6.53 (d, *J* = 2.4 Hz, 1H), 5.19 (t, *J* = 7.5 Hz, 1H), 5.05 (t, *J* = 6.5 Hz, 1H), 5.00 (t, *J* = 7.0 Hz, 1H), 3.23 (d, *J* = 7.4 Hz, 2H), 2.09 – 2.04 (m, 2H), 2.01 – 1.93 (m, 4H), 1.90 – 1.84 (m, 2H), 1.78 (s, 3H), 1.61 (s, 3H), 1.54 (s, 3H), 1.52 (s, 3H).

MarX4 activity assay procedure:

Assay setup 1: Three component oxidation of hydroxyquinone substrate **3.23b**

To a 250 μL solution of 50 mM buffer solution (HEPES-NaOH, pH 8.0), 100 mM NaCl, 1 μM FAD, 2.4 mM $NADP^+$, 5.0 μM PtdH, 7.5 μM SsuE, 10 mM Na_3PO_3, and 7.5 μM MarO enzyme, a DMSO solution of 250 μM substrate (final concentration) was added and incubated at 20 °C.

Assay setup 2: Two component oxidation of hydroxyquinone substrate **3.23b**

To a 250 μL solution of 50 mM buffer solution (HEPES-NaOH, pH 8.0), 100 mM NaCl, 1 μM FAD, 2.5 mM NADPH, 7.5 μM SsuE, and 7.5 μM MarO enzyme, a DMSO solution of 250 μM substrate (final concentration) was added and incubated at 20 °C.

Assay setup 3: Three component bromination of debromomarinone **3.07**

To a 250 μL solution of 50 mM buffer solution (HEPES-NaOH, pH 8.0), 100 mM NaCl, 100 mM KBr, 1 μM FAD, 2.4 mM $NADP^+$, 5.0 μM PtdH, 7.5 μM SsuE, 10 mM Na_3PO_3, and 7.5 μM MarO enzyme, a DMSO solution of 250 μM substrate (final concentration) was added and incubated at 20 °C.

Assay setup 4: Two component bromination of debromomarinone **3.07**

To a 250 μL solution of 50 mM buffer solution (HEPES-NaOH, pH 8.0), 100 mM NaCl, 100 mM KBr, 1 μM FAD, 2.5 mM NADPH, 7.5 μM SsuE, and 7.5 μM MarO enzyme, a DMSO solution of 250 μM substrate (final concentration) was added and incubated at 20 °C.

General analysis procedure for MarX4 activity assays:

Aliquots (50 μL) were removed at 30 min, 1 h, 3 h and 18 h intervals, quenched with 50 μL of 0.1% formic acid in methanol, centrifuged for 2 minutes at 13000 x *g* to pellet proteins, and the clarified supernatant was analysed by RP-HPLC-MS in negative ionization mode using the following method: 10 - 100% B (20 min), 100% B (4 min), 100 - 10% B (3 min), 10% B (3 min), where A = 0.1% aqueous formic acid, and B = 0.1% formic acid in acetonitrile (flow rate: 0.75 mL/min; column: Agilent Eclipse XDB-C18 5 μm, 4.6 x 150 mm; LC: Agilent Technologies 1200 series system with a diode-array detector; MS: Bruker Amazon SL ESI-Ion Trap mass spectrometer; data processing: Bruker Compass Data Analysis 4.2 SR2). MarX4 assay analytes showed only starting materials with comparable retention times and *m/z* to synthetic standards.

General MarX1, MarX2, MarX3 activity assay procedure:

To a 250 μL solution of 50 mM buffer solution (HEPES-NaOH, pH 8.0), 100 mM KCl, 25% v/v crude lysate of MarX enzyme(s) and a DMSO solution of 1 mM substrate **3.23b** (final concentration) was added and incubated at 20 °C. Aliquots (50 μL) were removed at 1, 3 and 18 h intervals, quenched with 50 μL of acetonitrile, centrifuged for 2 minutes at 13000 x *g* to pellet proteins, and the clarified supernatant was analysed by RP-HPLC-MS in negative ionization mode using the following method: 10 - 100% B (20 min), 100% B (4 min), 100 - 10% B (3 min), 10% B (3 min), where A = 0.1% aqueous formic acid, and B = 0.1% formic acid in acetonitrile (flow rate: 0.75 mL/min; column: Agilent Eclipse XDB-C18 5 μm, 4.6 x 150 mm; LC: Agilent Technologies 1200 series system with a diode-array detector; MS: Bruker Amazon SL ESI-Ion Trap mass spectrometer; data processing: Bruker Compass Data Analysis 4.2 SR2).

3.5 References

(1) Osbourn, A. *Trends Genet.* **2010**, *26*, 449.
(2) Mouncey, N. J.; Otani, H.; Udwary, D.; Yoshikuni, Y. *J. Ind. Microbiol. Biotechnol.* **2019**, *46*, 273.
(3) Jensen, P. R. *Trends Microbiol.* **2016**, *24*, 968.
(4) Medema, M. H.; Blin, K.; Cimermancic, P.; De Jager, V.; Zakrzewski, P.; Fischbach, M. A.; Weber, T.; Takano, E.; Breitling, R. *Nucleic Acids Res.* **2011**, *39*, 339.
(5) Weber, T.; Blin, K.; Duddela, S.; Krug, D.; Kim, H. U.; Bruccoleri, R.; Lee, S. Y.; Fischbach, M. A.; Müller, R.; Wohlleben, W.; Breitling, R.; Takano, E.; Medema, M. H. *Nucleic Acids Res.* **2015**, *43*, W237.
(6) Altschul, S. F.; Gish, W.; Miller, W.; Myers, E. W.; Lipman, D. J. *J. Mol. Biol.* **1990**, *215*, 403.
(7) Corr, C.; Challis, G. L. *Compr. Nat. Prod. II Chem. Biol.* **2010**, *2*, 429.
(8) Li, J.; Amatuni, A.; Renata, H. *Curr. Opin. Chem. Biol.* **2020**, *55*, 111.
(9) Miles, Z. D.; Diethelm, S.; Pepper, H. P.; Huang, D. M.; George, J. H.; Moore, B. S. *Nat. Chem.* **2017**, *9*, 1235.
(10) McKinnie, S. M. K.; Miles, Z. D.; Jordan, P. A.; Awakawa, T.; Pepper, H. P.; Murray, L. A. M.; George, J. H.; Moore, B. S. *J. Am. Chem. Soc.* **2018**, *140*, 17840.
(11) Rückert, C.; Leipoldt, F.; Zeyhle, P.; Fenical, W.; Jensen, P. R.; Kalinowski, J.; Heide, L.; Kaysser, L. *J. Biotechnol.* **2015**, *216*, 140.
(12) Pepper, H. P.; George, J. H. *Angew. Chem. Int. Ed.* **2013**, *52*, 12170.
(13) Pepper, H. P.; George, J. H. *Angew. Chem. Int. Ed.* **2013**, *52*, 12170.
(14) Viviani, F.; Gaudry, M.; Marquet, A. *J. Chem. Soc. Perkin Trans. 1* **1990**, 1255.
(15) Ghosh, A. K.; Wang, Y.; Kim, J. T. *J. Org. Chem.* **2001**, *66*, 8973.
(16) Monti, H.; Leandri, G.; Klos-Ringuet, M.; Corriol, C. *Synth. Commun.* **1983**, *13*, 1021.
(17) Leipoldt, F.; Zeyhle, P.; Kulik, A.; Kalinowski, J.; Heide, L.; Kaysser, L. *PLoS One* **2015**, *10*, 1.
(18) Winter, J. M.; Moore, B. S. *J. Biol. Chem.* **2009**, *284*, 18577.
(19) Kaysser, L.; Bernhardt, P.; Nam, S. J.; Loesgen, S.; Ruby, J. G.; Skewes-Cox, P.; Jensen, P. R.; Fenical, W.; Moore, B. S. *J. Am. Chem. Soc.* **2012**, *134*, 11988.
(20) Bernhardt, P.; Okino, T.; Winter, J. M.; Miyanaga, A.; Moore, B. S. *J. Am. Chem. Soc.* **2011**, *133*, 4268.
(21) Moore, B. S. *Synlett* **2018**, *29*, 401.
(22) Morris, D. R.; Hager, L. P. *J. Biol. Chem.* **1966**, *241*, 1763.
(23) Wever, R.; Krenn, B. E.; Renirie, R. *Marine Vanadium-Dependent Haloperoxidases, Their Isolation, Characterization, and Application*, 1st ed.; Elsevier Inc., 2018; Vol. 605.
(24) McKinnie, S. M. K.; Miles, Z. D.; Moore, B. S. *Methods Enzymol.* **2018**, *604*, 405.
(25) Sievers, F.; Wilm, A.; Dineen, D.; Gibson, T. J.; Karplus, K.; Li, W.; Lopez, R.; McWilliam, H.; Remmert, M.; Söding, J.; Thompson, J. D.; Higgins, D. G. *Mol. Syst. Biol.* **2011**, *7*.
(26) Struck, A. W.; Thompson, M. L.; Wong, L. S.; Micklefield, J. *ChemBioChem* **2012**, *13*, 2642.

(27) Ohashi, M.; Liu, F.; Hai, Y.; Chen, M.; Tang, M. cheng; Yang, Z.; Sato, M.; Watanabe, K.; Houk, K. N.; Tang, Y. *Nature* **2017**, *549*, 502.
(28) Jin, W. B.; Wu, S.; Jian, X. H.; Yuan, H.; Tang, G. L. *Nat. Commun.* **2018**, *9*.
(29) Ohashi, M.; Jamieson, C. S.; Cai, Y.; Tan, D.; Kanayama, D.; Tang, M. C.; Anthony, S. M.; Chari, J. V.; Barber, J. S.; Picazo, E.; Kakule, T. B.; Cao, S.; Garg, N. K.; Zhou, J.; Houk, K. N.; Tang, Y. *Nature* **2020**, *586*, 64.
(30) Agarwal, V.; Miles, Z. D.; Winter, J. M.; Eustáquio, A. S.; El Gamal, A. A.; Moore, B. S. *Chem. Rev.* **2017**, *117*, 5619.
(31) Fontecave, M.; Atta, M.; Mulliez, E. *Trends Biochem. Sci.* **2004**, *29*, 243.
(32) Coward, J. K.; Slisz, E. P. *J. Med. Chem.* **1973**, *16*, 460.
(33) Bauer, N. J.; Kreuzman, A. J.; Dotzlaf, J. E.; Yeh, W. K. *J. Biol. Chem.* **1988**, *263*, 15619.
(34) Zhang, J.; Zheng, Y. G. *ACS Chem. Biol.* **2016**, *11*, 583.
(35) Taura, F.; Morimoto, S.; Shoyama, Y. *J. Am. Chem. Soc.* **1995**, *117*, 9766.
(36) Shoyama, Y. Y.; Tamada, T.; Kurihara, K.; Takeuchi, A.; Taura, F.; Arai, S.; Blaber, M.; Shoyama, Y. Y.; Morimoto, S.; Kuroki, R. *J. Mol. Biol.* **2012**, *423*, 96.
(37) Bennett-Lovsey, R. M.; Herbert, A. D.; Sternberg, M. J. E.; Kelley, L. A. *Proteins* **2008**, *70*, 611.
(38) Tian, Z.; Sun, P.; Yan, Y.; Wu, Z.; Zheng, Q.; Zhou, S.; Zhang, H.; Yu, F.; Jia, X.; Chen, D.; Mándi, A.; Kurtán, T.; Liu, W. *Nat. Chem. Biol.* **2015**, *11*, 259.
(39) Sciara, G.; Kendrew, S. G.; Miele, A. E.; Marsh, N. G.; Federici, L.; Malatesta, F.; Schimperna, G.; Savino, C.; Vallone, B. *EMBO J.* **2003**, *22*, 205.
(40) Balskus, E. P.; Walsh, C. T. *J. Am. Chem. Soc.* **2008**, *130*, 15260.
(41) Balskus, E. P.; Walsh, C. T. *J. Am. Chem. Soc.* **2009**, *131*, 14648.
(42) Ferreira, D.; Garcia-Pichel, F. *Front. Microbiol.* **2016**, *7*, 1.
(43) Almagro Armenteros, J. J.; Tsirigos, K. D.; Sønderby, C. K.; Petersen, T. N.; Winther, O.; Brunak, S.; von Heijne, G.; Nielsen, H. *Nat. Biotechnol.* **2019**, *37*, 420.
(44) Stocking, E. M.; Williams, R. M. *Angew. Chem. Int. Ed.* **2003**, *42*, 3078.
(45) Oikawa, H.; Tokiwano, T. *Nat. Prod. Rep.* **2004**, *21*, 321.
(46) Klas, K.; Tsukamoto, S.; Sherman, D. H.; Williams, R. M. *J. Org. Chem.* **2015**, *80*, 11672.
(47) Minami, A.; Oikawa, H. *J. Antibiot.* **2016**, *69*, 500.
(48) Jamieson, C. S.; Ohashi, M.; Liu, F.; Tang, Y.; Houk, K. N. *Nat. Prod. Rep.* **2019**, *36*, 698.
(49) Gao, L.; Su, C.; Du, X.; Wang, R.; Chen, S.; Zhou, Y.; Liu, C.; Liu, X.; Tian, R.; Zhang, L.; Xie, K.; Chen, S.; Guo, Q.; Guo, L.; Hano, Y.; Shimazaki, M.; Minami, A.; Oikawa, H.; Huang, N.; Houk, K. N.; Huang, L.; Dai, J.; Lei, X. *Nat. Chem.* **2020**, *12*, 620.
(50) Eichhorn, E.; Van Der Ploeg, J. R.; Leisinger, T. *J. Biol. Chem.* **1999**, *274*, 26639.
(51) El Gamal, A.; Agarwal, V.; Diethelm, S.; Rahman, I.; Schorn, M. A.; Sneed, J. M.; Louie, G. V.; Whalen, K. E.; Mincer, T. J.; Noel, J. P.; Paul, V. J.; Moore, B. S. *Proc. Natl. Acad. Sci. U. S. A.* **2016**, *113*, 3797.
(52) Luhavaya, H.; Sigrist, R.; Chekan, J. R.; McKinnie, S. M. K.; Moore, B. S. *Angew. Chem. Int. Ed.* **2019**, *58*, 8394.

(53) Agarwal, V.; El Gamal, A. A.; Yamanaka, K.; Poth, D.; Kersten, R. D.; Schorn, M.; Allen, E. E.; Moore, B. S. *Nat. Chem. Biol.* **2014**, *10*, 640.
(54) Gibson, D. G.; Young, L.; Chuang, R. Y.; Venter, J. C.; Hutchison, C. A.; Smith, H. O. *Nat. Methods* **2009**, *6*, 343.
(55) Gibson, D. G. *Methods Enzymol.* **2011**, *498*, 349.

3.6 Appendix

3.6.1 NMR Spectra

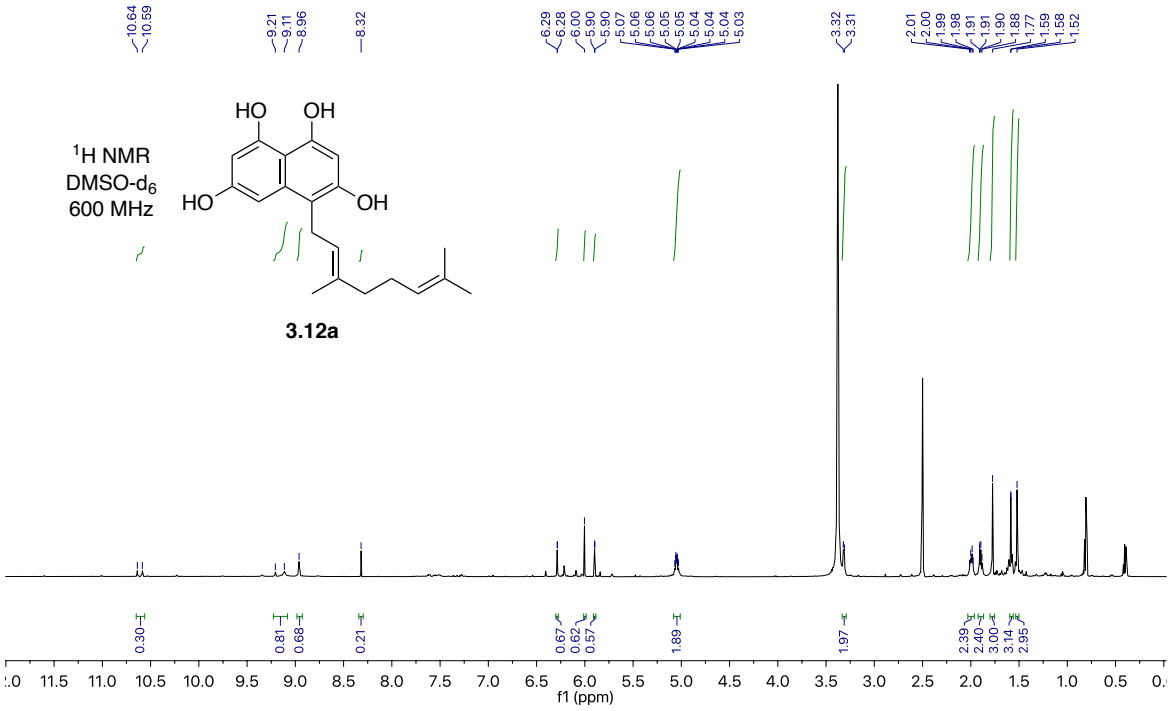

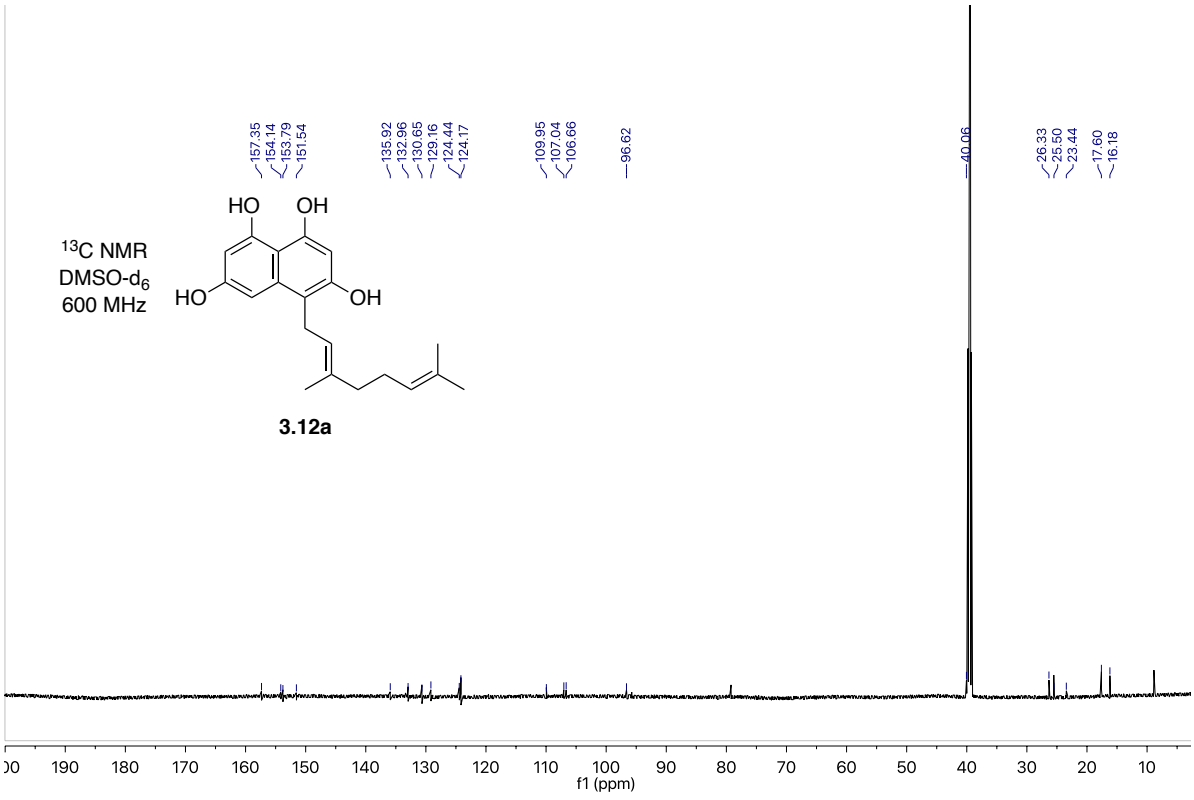

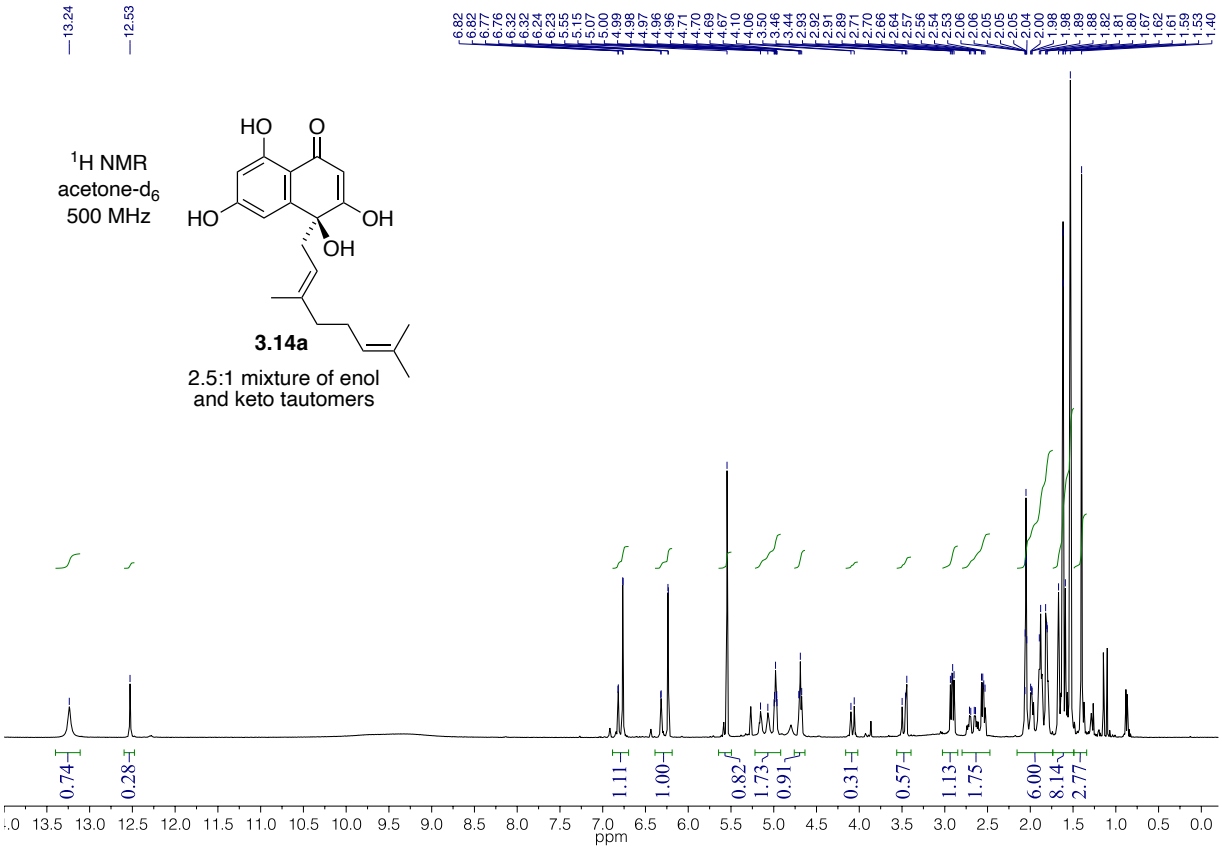
^{1}H NMR
acetone-d$_6$
500 MHz
HO
O
HO
OH
OH
3.14a
2.5:1 mixture of enol
and keto tautomers
ppm

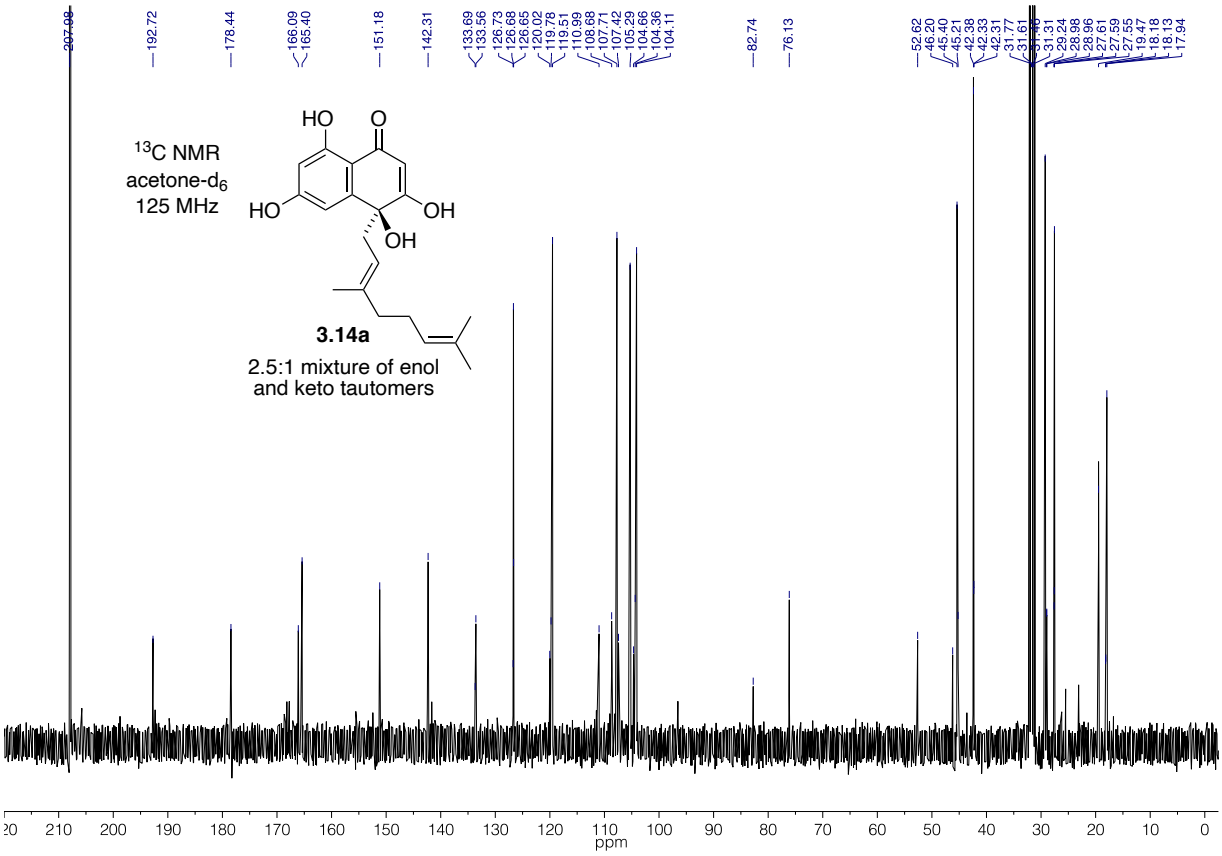
^{13}C NMR
acetone-d$_6$
125 MHz
HO
O
HO
OH
OH
3.14a
2.5:1 mixture of enol
and keto tautomers
ppm

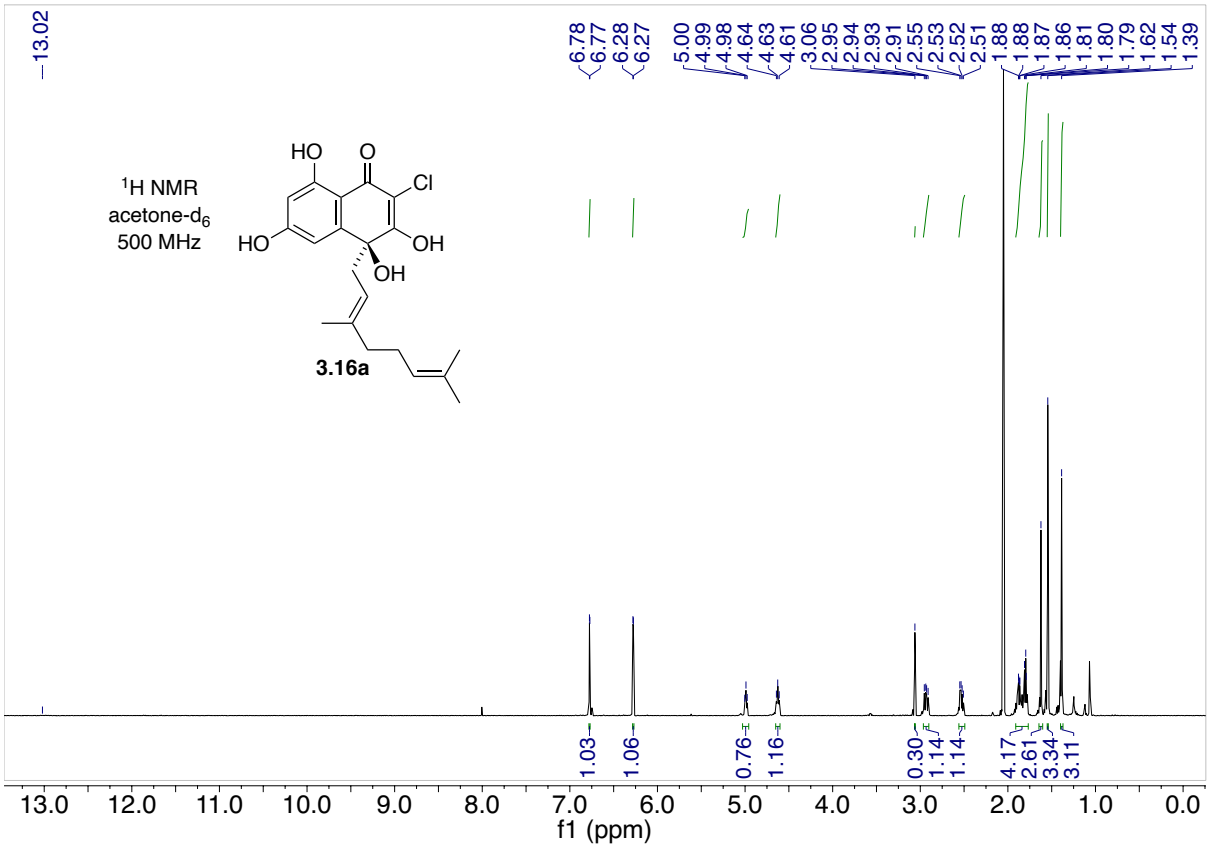
13.02
6.78
6.77
6.28
6.27
5.00
4.99
4.98
4.64
4.63
4.61
3.06
2.95
2.94
2.93
2.91
2.55
2.53
2.52
2.51
1.88
1.87
1.86
1.81
1.80
1.79
1.62
1.54
1.39
1H NMR
acetone-d6
500 MHz
HO
O
Cl
HO
OH
OH
3.16a
1.03
1.06
0.76
1.16
0.30
1.14
1.14
4.17
2.61
3.34
3.11
13.0 12.0 11.0 10.0 9.0 8.0 7.0 6.0 5.0 4.0 3.0 2.0 1.0 0.0
f1 (ppm)

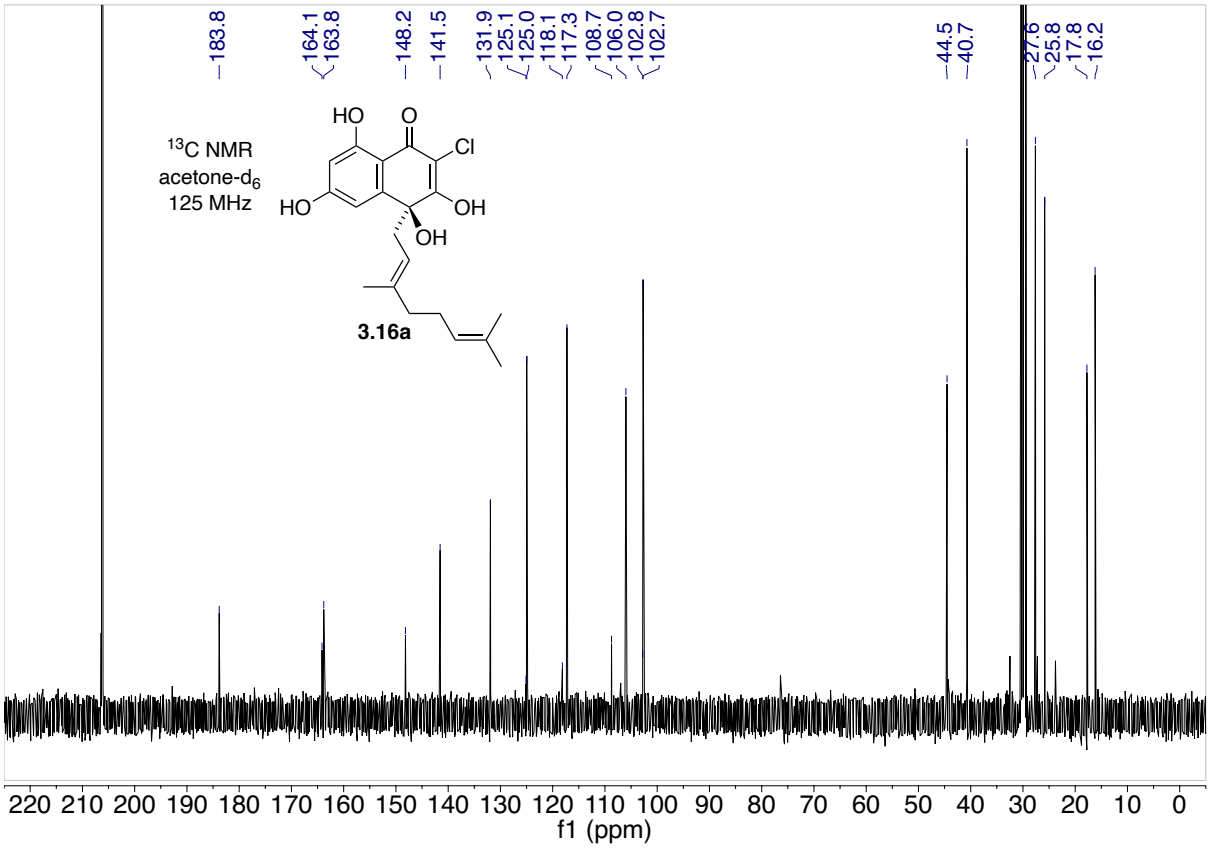
183.8
164.1
163.8
148.2
141.5
131.9
125.1
125.0
118.1
117.3
108.7
106.0
102.8
102.7
44.5
40.7
27.6
25.8
17.8
16.2
13C NMR
acetone-d6
125 MHz
HO
O
Cl
HO
OH
OH
3.16a
220 210 200 190 180 170 160 150 140 130 120 110 100 90 80 70 60 50 40 30 20 10 0
f1 (ppm)

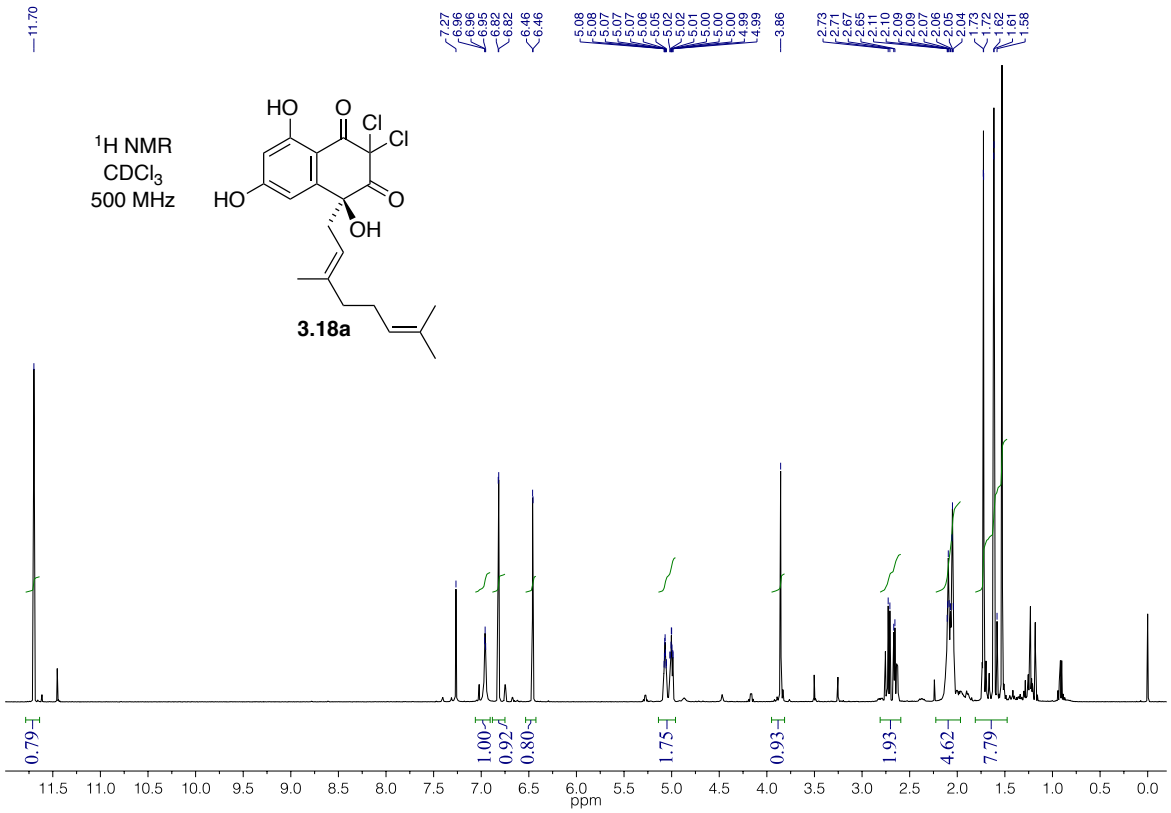
^{1}H NMR
$CDCl_3$
500 MHz
HO
O
Cl
Cl
HO
O
OH
3.18a
11.70
7.27
6.96
6.96
6.95
6.82
6.82
6.46
6.46
5.08
5.08
5.07
5.07
5.07
5.06
5.05
5.02
5.02
5.01
5.00
5.00
4.99
4.99
3.86
2.73
2.71
2.67
2.65
2.11
2.10
2.09
2.09
2.07
2.06
2.05
2.04
1.73
1.72
1.62
1.61
1.58
0.79
1.00
0.92
0.80
1.75
0.93
1.93
4.62
7.79
ppm

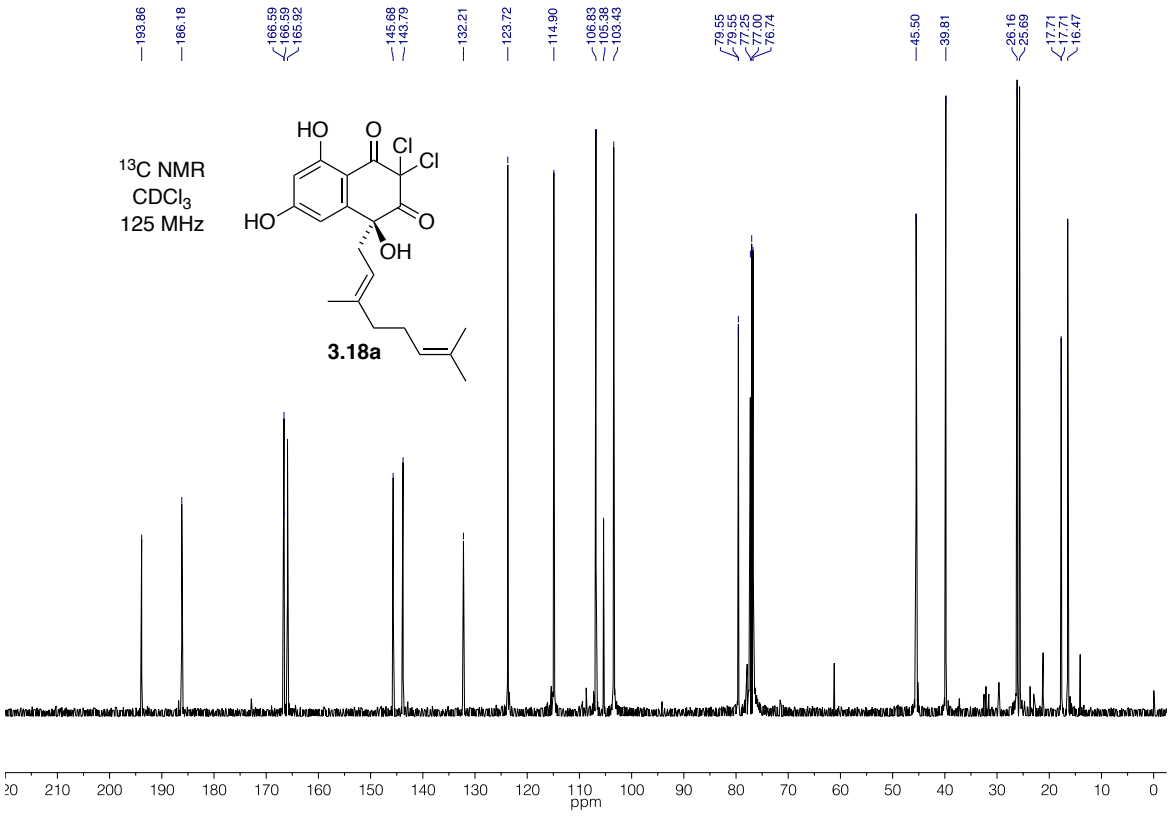
^{13}C NMR
$CDCl_3$
125 MHz
HO
O
Cl
Cl
HO
O
OH
3.18a
193.86
186.18
166.59
166.59
165.92
145.68
143.79
132.21
123.72
114.90
106.83
105.38
103.43
79.55
79.55
77.55
77.00
76.74
45.50
39.81
26.16
25.89
17.71
17.71
16.47
ppm

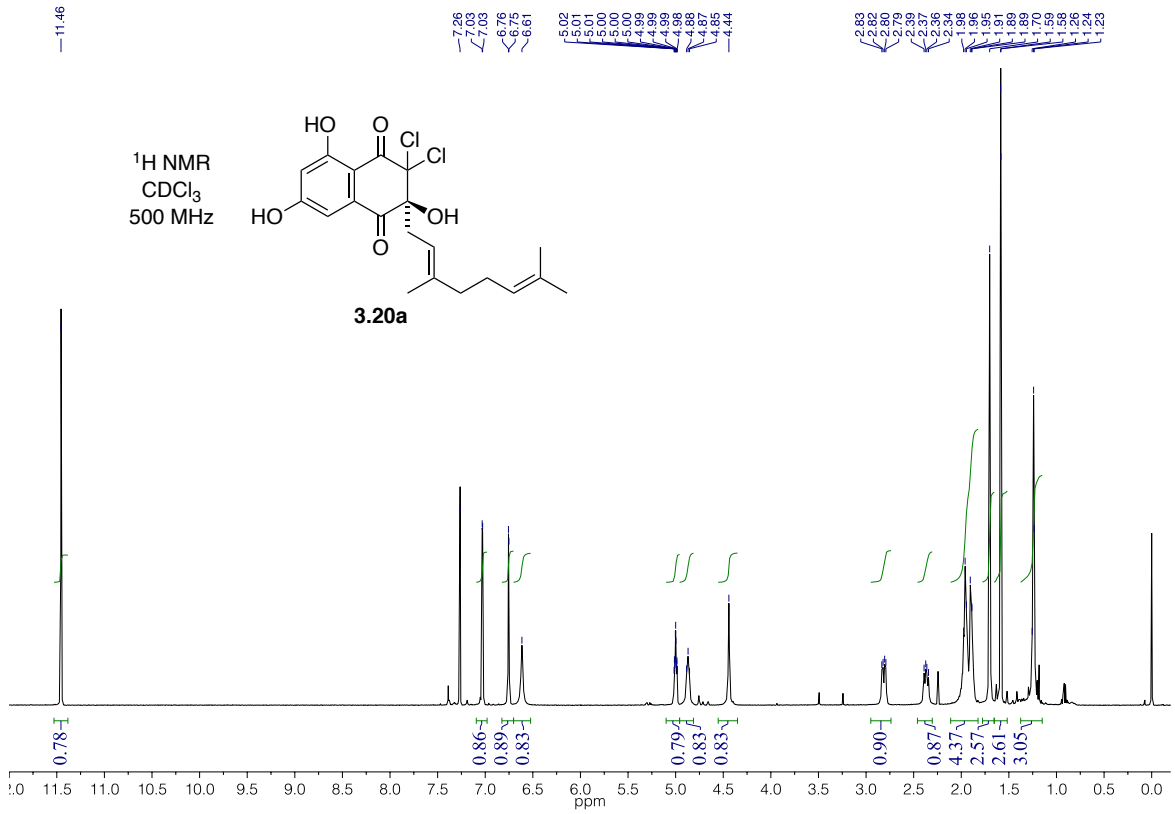
^{1}H NMR
$CDCl_3$
500 MHz
HO
O
Cl
Cl
HO
OH
O
3.20a
ppm

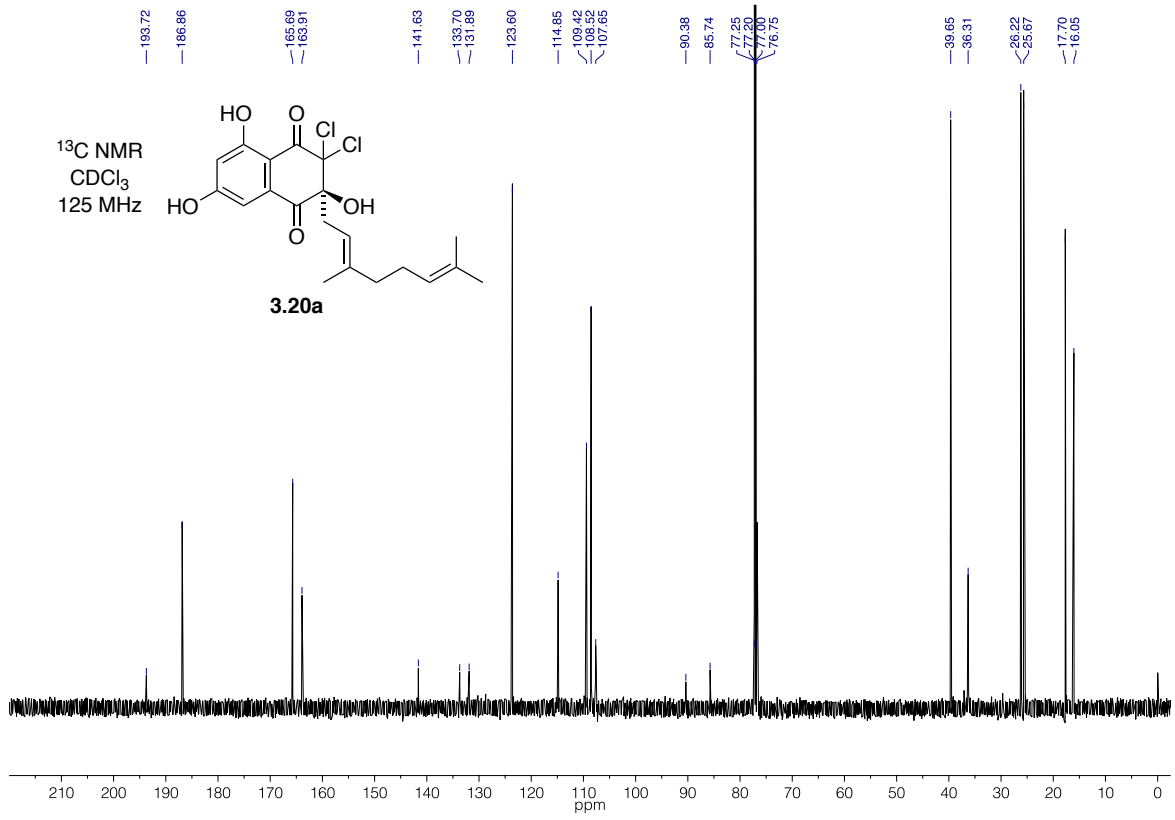
^{13}C NMR
$CDCl_3$
125 MHz
HO
O
Cl
Cl
HO
OH
O
3.20a
ppm

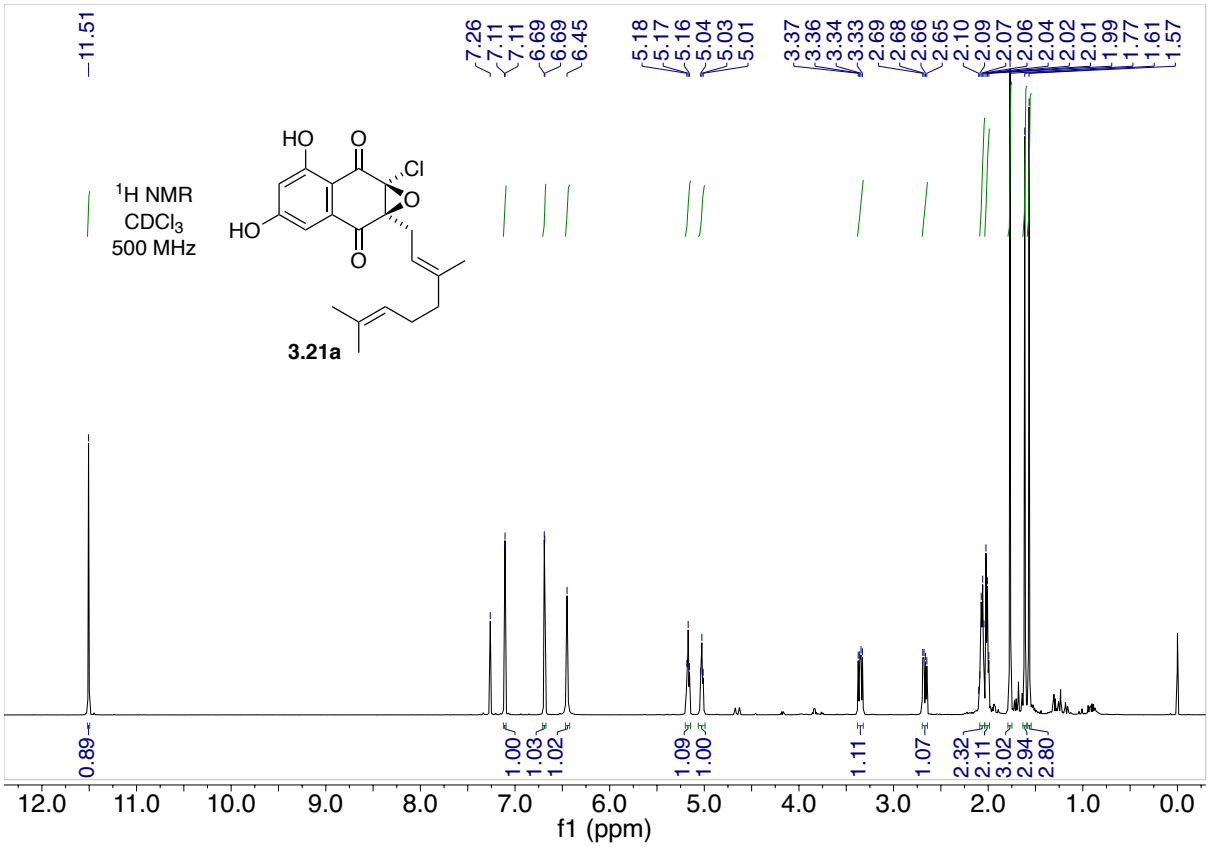
11.51
7.26
7.11
7.11
6.69
6.69
6.45
5.18
5.17
5.16
5.04
5.03
5.01
3.37
3.36
3.34
3.33
2.69
2.68
2.66
2.65
2.10
2.09
2.07
2.06
2.04
2.02
2.01
1.99
1.77
1.61
1.57
1H NMR
CDCl3
500 MHz
HO
O
Cl
O
HO
O
3.21a
0.89
1.00
1.03
1.02
1.09
1.00
1.11
1.07
2.32
2.11
3.02
2.94
2.80
12.0
11.0
10.0
9.0
8.0
7.0
6.0
5.0
4.0
3.0
2.0
1.0
0.0
f1 (ppm)

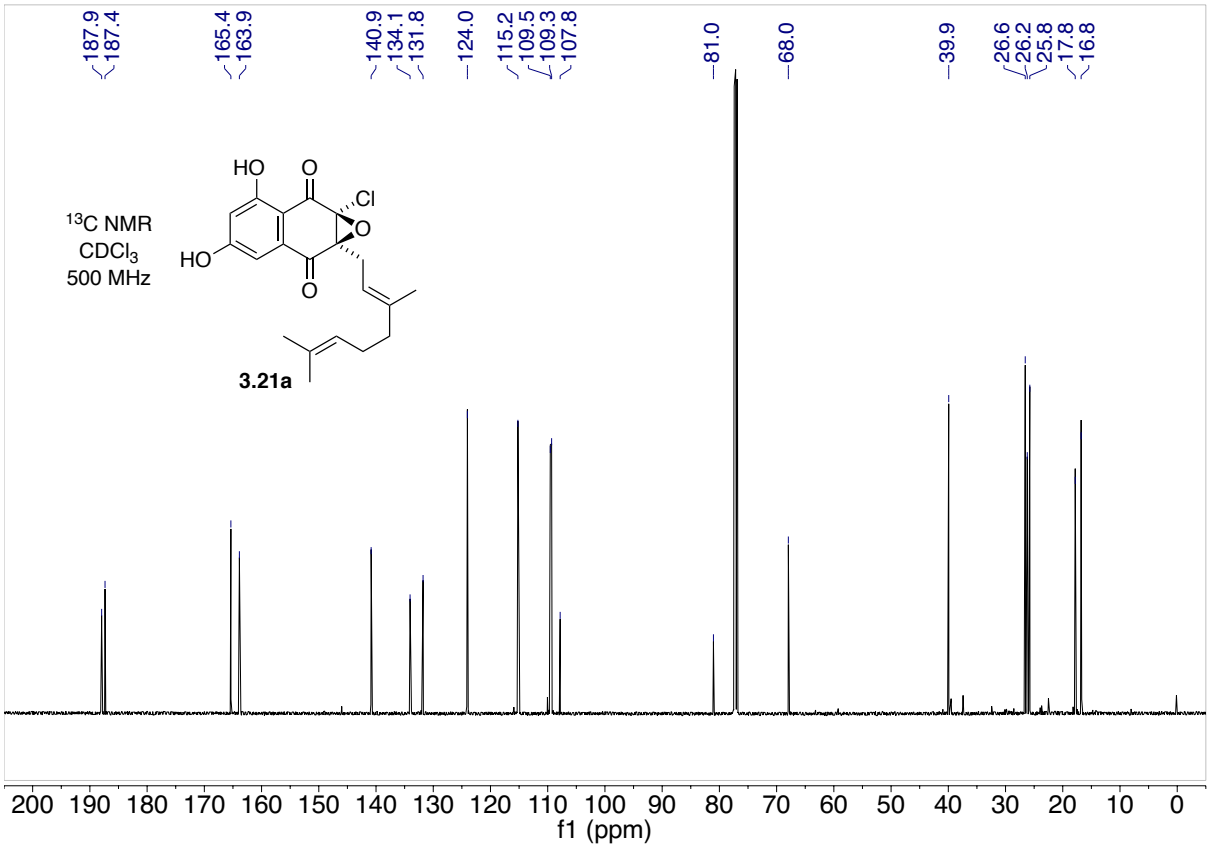
187.9
187.4
165.4
163.9
140.9
134.1
131.8
124.0
115.2
109.5
109.3
107.8
81.0
68.0
39.9
26.6
26.2
25.8
17.8
16.8
13C NMR
CDCl3
500 MHz
HO
O
Cl
O
HO
O
3.21a
200
190
180
170
160
150
140
130
120
110
100
90
80
70
60
50
40
30
20
10
0
f1 (ppm)

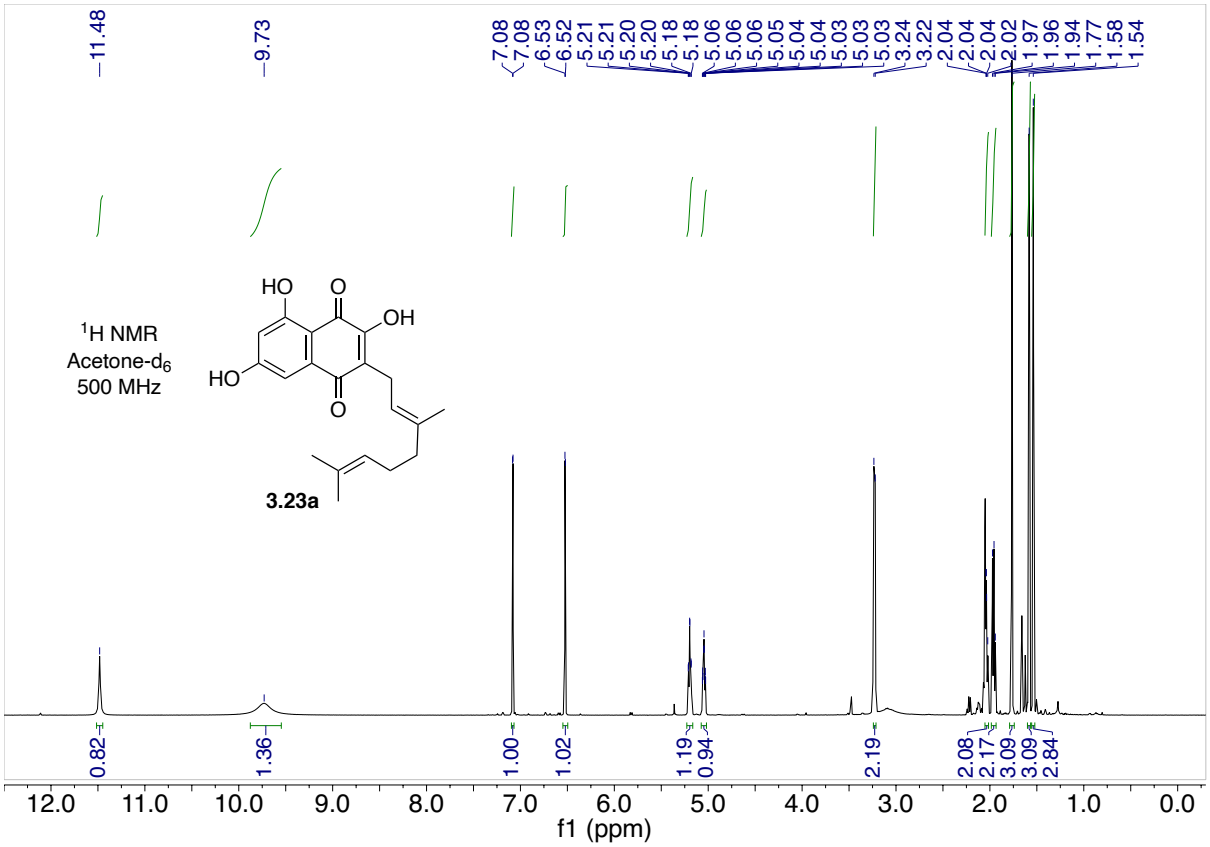
11.48
9.73
7.08
7.08
6.53
6.52
5.21
5.21
5.20
5.20
5.18
5.18
5.06
5.06
5.06
5.05
5.04
5.04
5.03
5.03
3.24
3.22
2.04
2.04
2.04
2.02
1.97
1.96
1.94
1.77
1.58
1.54
^{1}H NMR
Acetone-d$_6$
500 MHz
HO
O
OH
HO
O
3.23a
0.82
1.36
1.00
1.02
1.19
0.94
2.19
2.08
2.17
3.09
3.09
2.84
12.0
11.0
10.0
9.0
8.0
7.0
6.0
5.0
4.0
3.0
2.0
1.0
0.0
f1 (ppm)

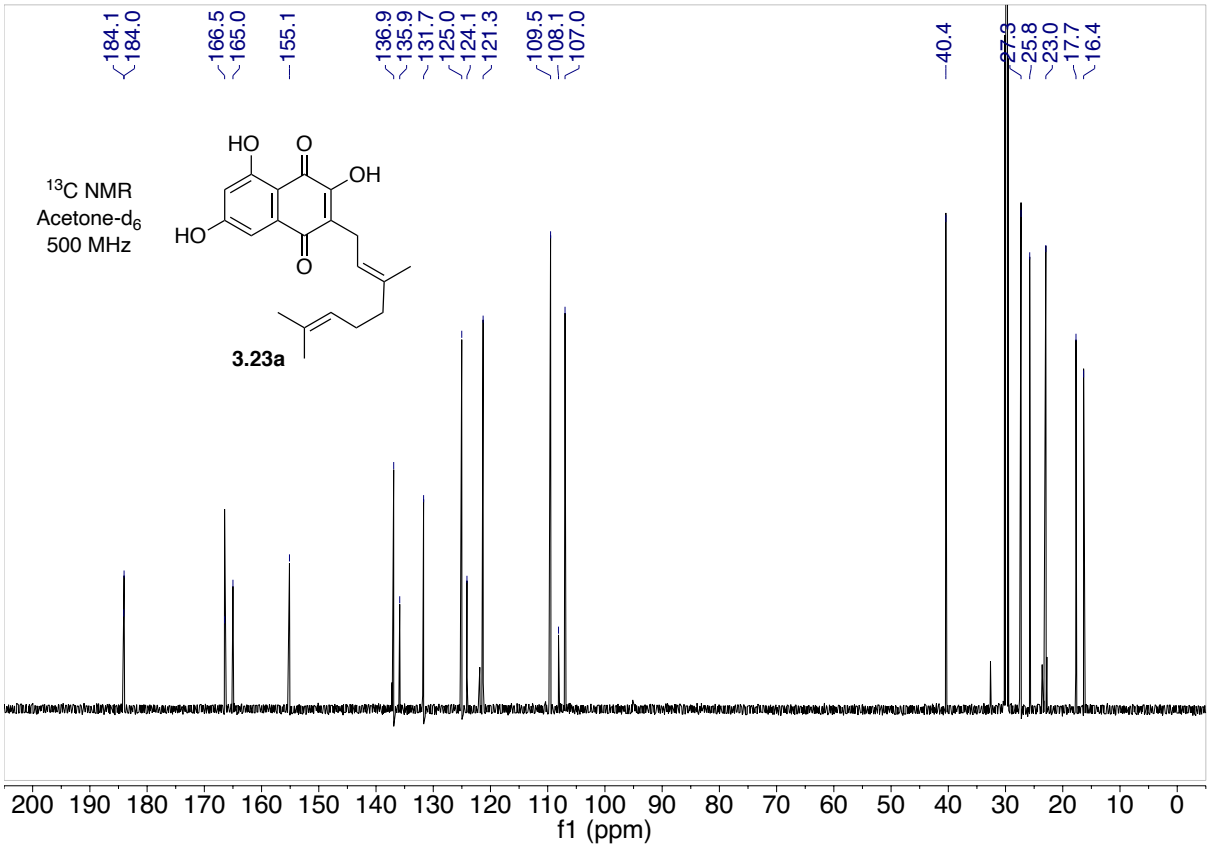
184.1
184.0
166.5
165.0
155.1
136.9
135.9
131.7
125.0
124.1
121.3
109.5
108.1
107.0
40.4
27.3
25.8
23.0
17.7
16.4
^{13}C NMR
Acetone-d$_6$
500 MHz
HO
O
OH
HO
O
3.23a
200
190
180
170
160
150
140
130
120
110
100
90
80
70
60
50
40
30
20
10
0
f1 (ppm)

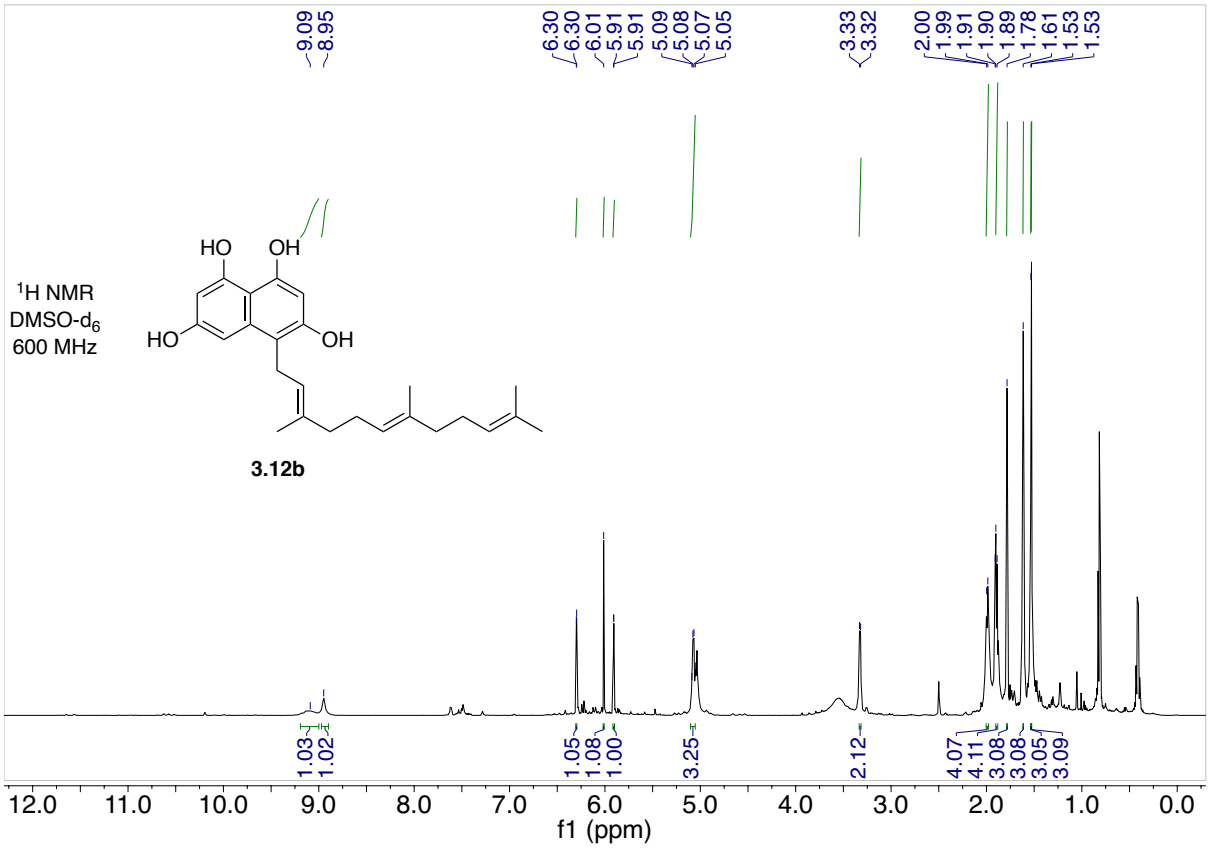
9.09
8.95
6.30
6.30
6.01
5.91
5.91
5.09
5.08
5.07
5.05
3.33
3.32
2.00
1.99
1.91
1.90
1.89
1.78
1.61
1.53
1.53
HO
OH
HO
OH
1H NMR
DMSO-d6
600 MHz
3.12b
1.03
1.02
1.05
1.08
1.00
3.25
2.12
4.07
4.11
3.08
3.08
3.05
3.09
12.0
11.0
10.0
9.0
8.0
7.0
6.0
5.0
4.0
3.0
2.0
1.0
0.0
f1 (ppm)

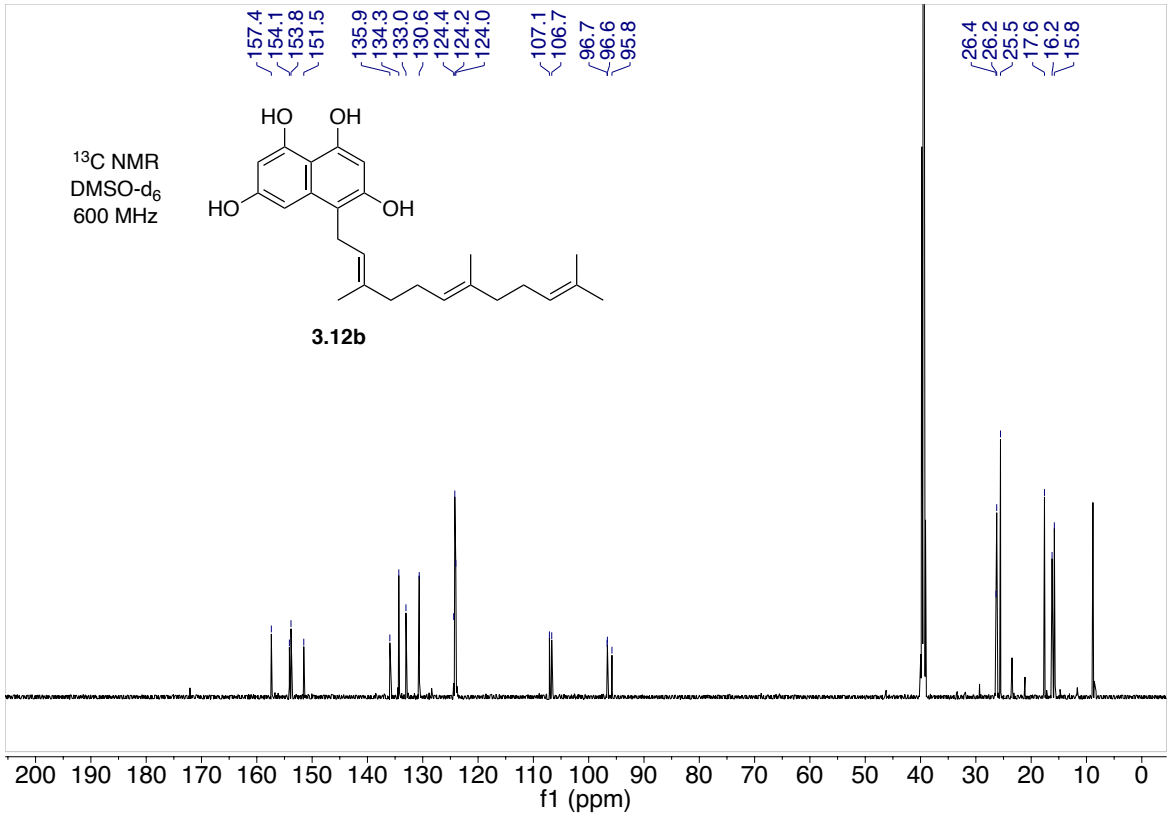
157.4
154.1
153.8
151.5
135.9
134.3
133.0
130.6
124.4
124.2
124.0
107.1
106.7
96.7
96.6
95.8
26.4
26.2
25.5
17.6
16.2
15.8
HO
OH
HO
OH
13C NMR
DMSO-d6
600 MHz
3.12b
200
190
180
170
160
150
140
130
120
110
100
90
80
70
60
50
40
30
20
10
0
f1 (ppm)

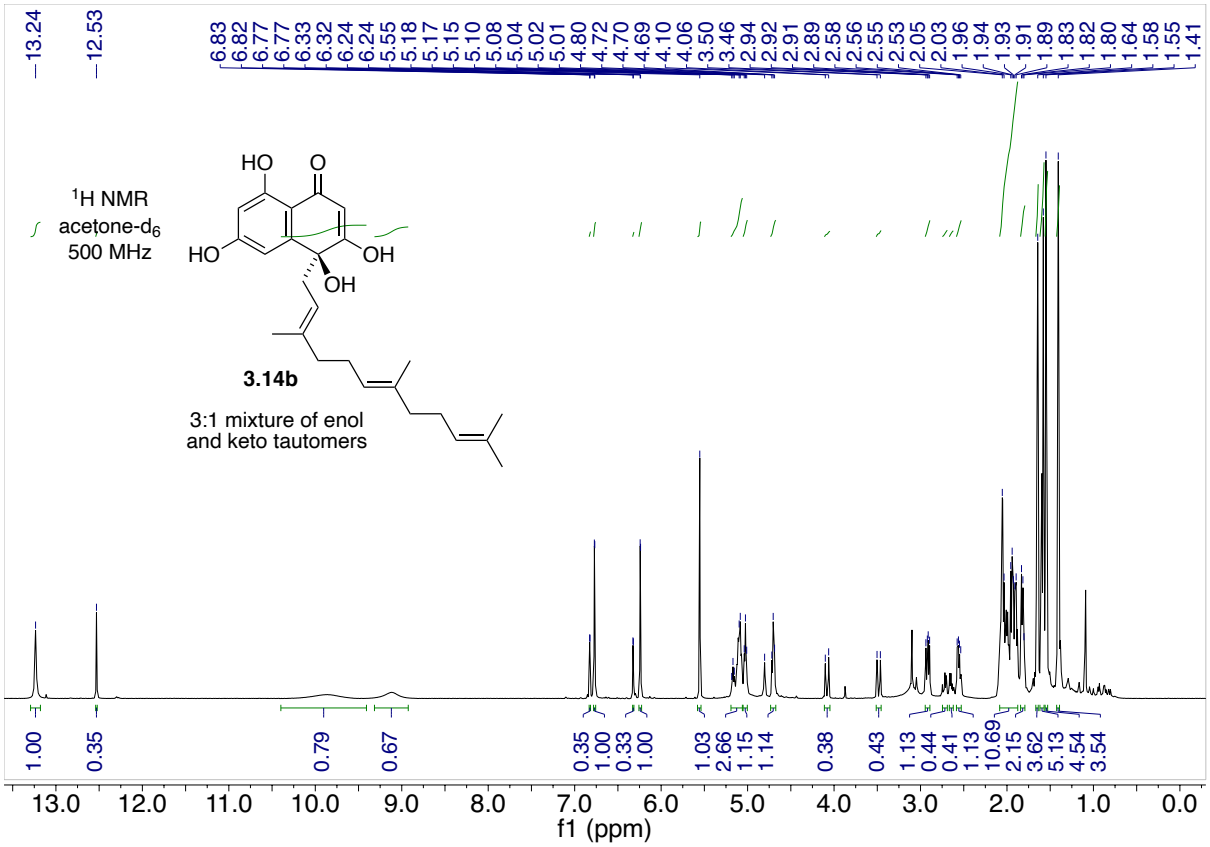
^{1}H NMR
acetone-d$_6$
500 MHz
HO
O
HO
OH
OH
3.14b
3:1 mixture of enol
and keto tautomers
f1 (ppm)

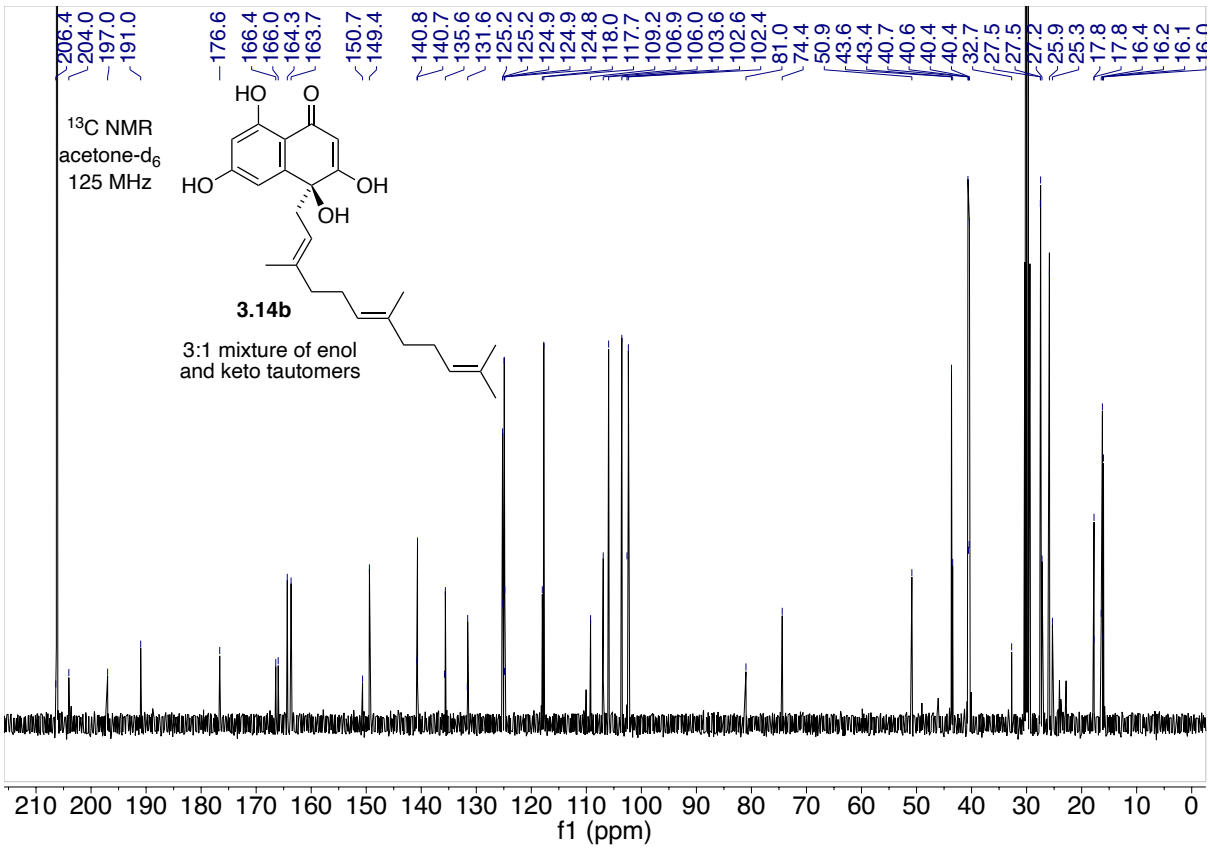
^{13}C NMR
acetone-d$_6$
125 MHz
HO
O
HO
OH
OH
3.14b
3:1 mixture of enol
and keto tautomers
f1 (ppm)

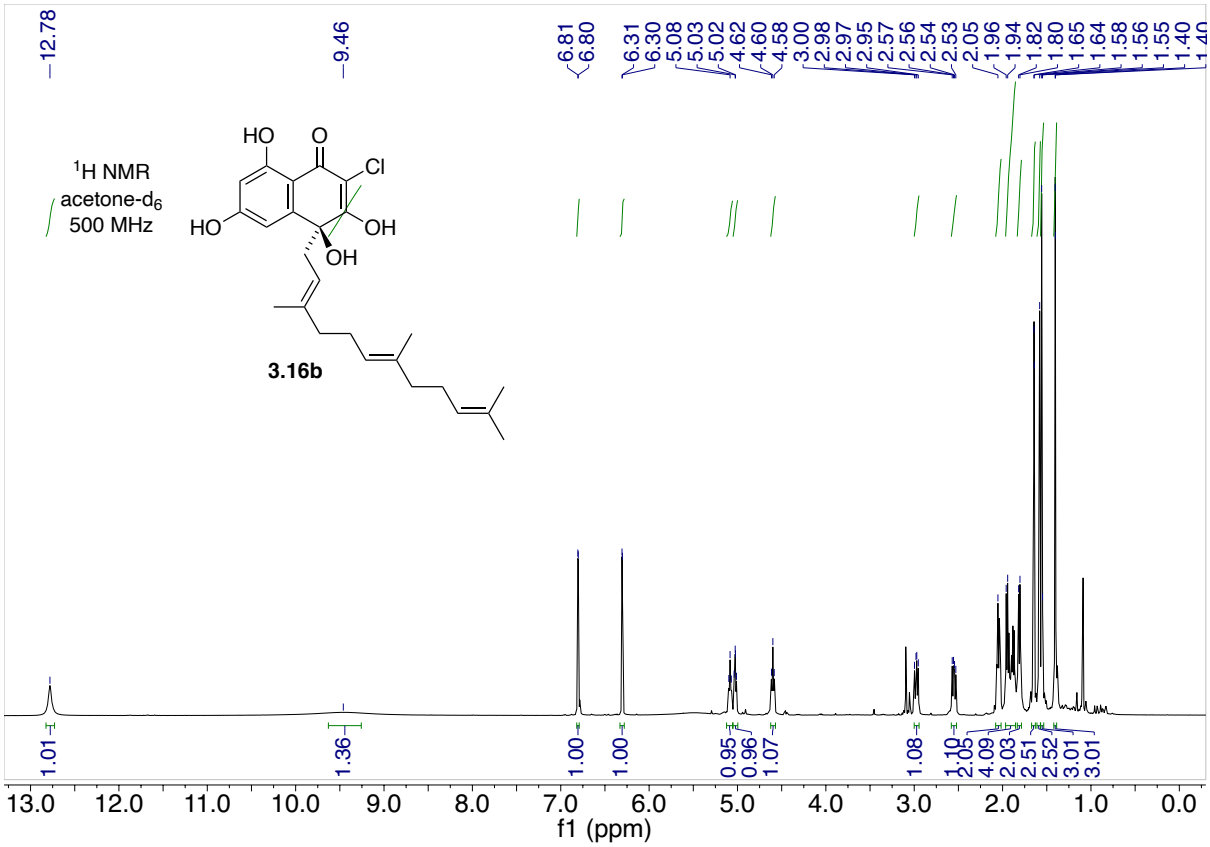
12.78
9.46
6.81
6.80
6.31
6.30
5.08
5.03
5.02
4.62
4.60
4.58
3.00
2.98
2.97
2.95
2.57
2.56
2.54
2.53
2.05
1.96
1.94
1.82
1.80
1.65
1.64
1.58
1.56
1.55
1.40
1H NMR
acetone-d6
500 MHz
HO
O
Cl
HO
OH
OH
3.16b
1.01
1.36
1.00
1.00
0.95
0.96
1.07
1.08
1.10
2.05
4.09
2.03
2.51
2.52
3.01
3.01
13.0
12.0
11.0
10.0
9.0
8.0
7.0
6.0
5.0
4.0
3.0
2.0
1.0
0.0
f1 (ppm)

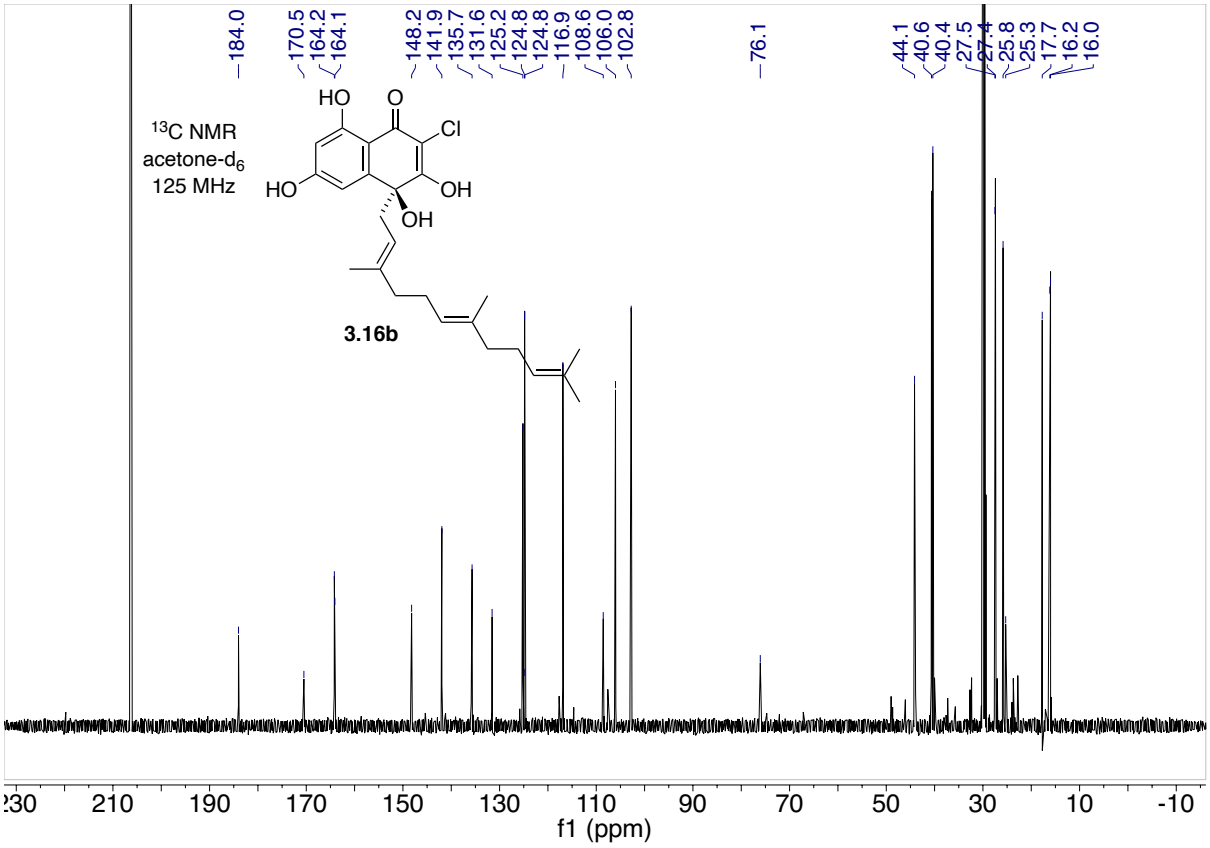
184.0
170.5
164.2
164.1
148.2
141.9
135.7
131.6
125.2
124.8
124.8
116.9
108.6
106.0
102.8
76.1
44.1
40.6
40.4
27.5
27.4
25.8
25.3
17.7
16.2
16.0
13C NMR
acetone-d6
125 MHz
HO
O
Cl
HO
OH
OH
3.16b
230
210
190
170
150
130
110
90
70
50
30
10
-10
f1 (ppm)

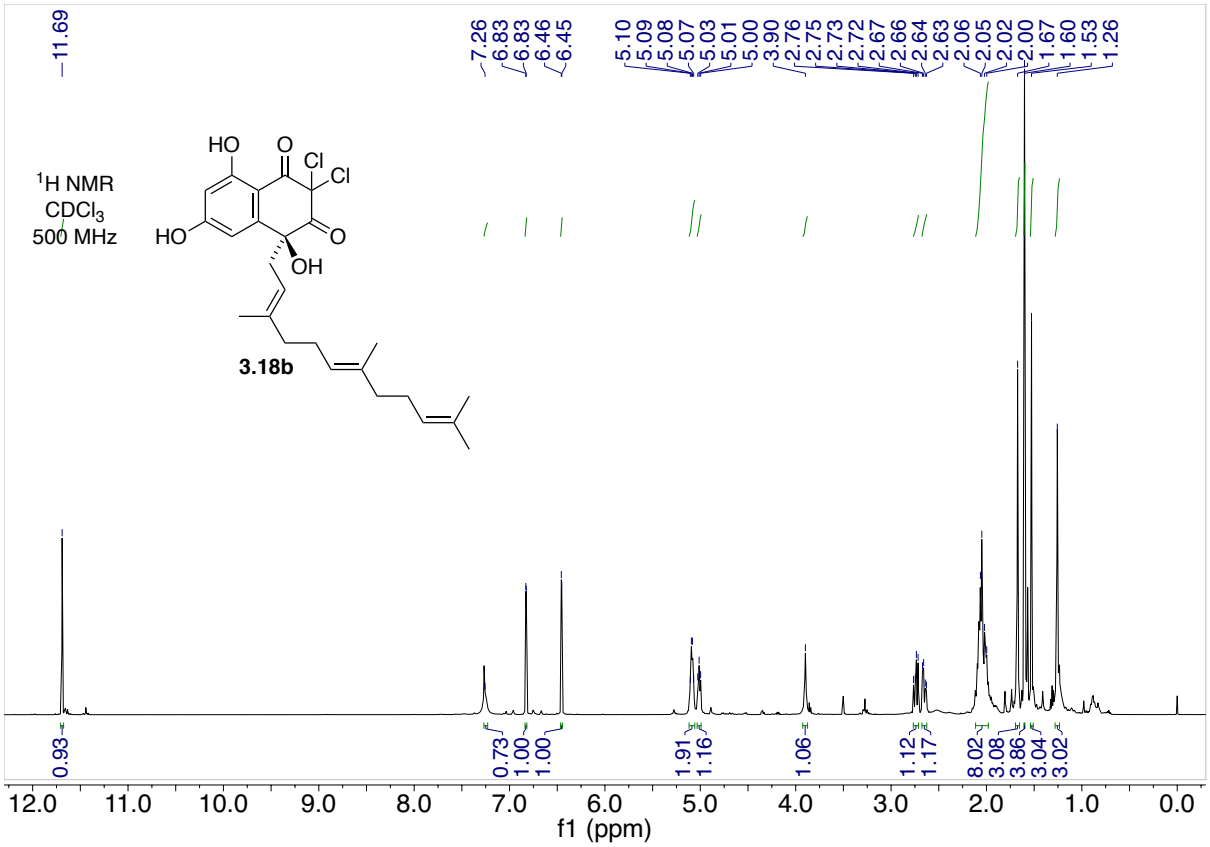
11.69
7.26
6.83
6.83
6.46
6.45
5.10
5.09
5.08
5.07
5.03
5.01
5.00
3.90
2.76
2.75
2.73
2.72
2.67
2.66
2.64
2.63
2.06
2.05
2.02
2.00
1.67
1.60
1.53
1.26
1H NMR
CDCl3
500 MHz
HO
O
Cl
Cl
HO
O
OH
3.18b
0.93
0.73
1.00
1.00
1.91
1.16
1.06
1.12
1.17
8.02
3.08
3.86
3.04
3.02
12.0
11.0
10.0
9.0
8.0
7.0
6.0
5.0
4.0
3.0
2.0
1.0
0.0
f1 (ppm)

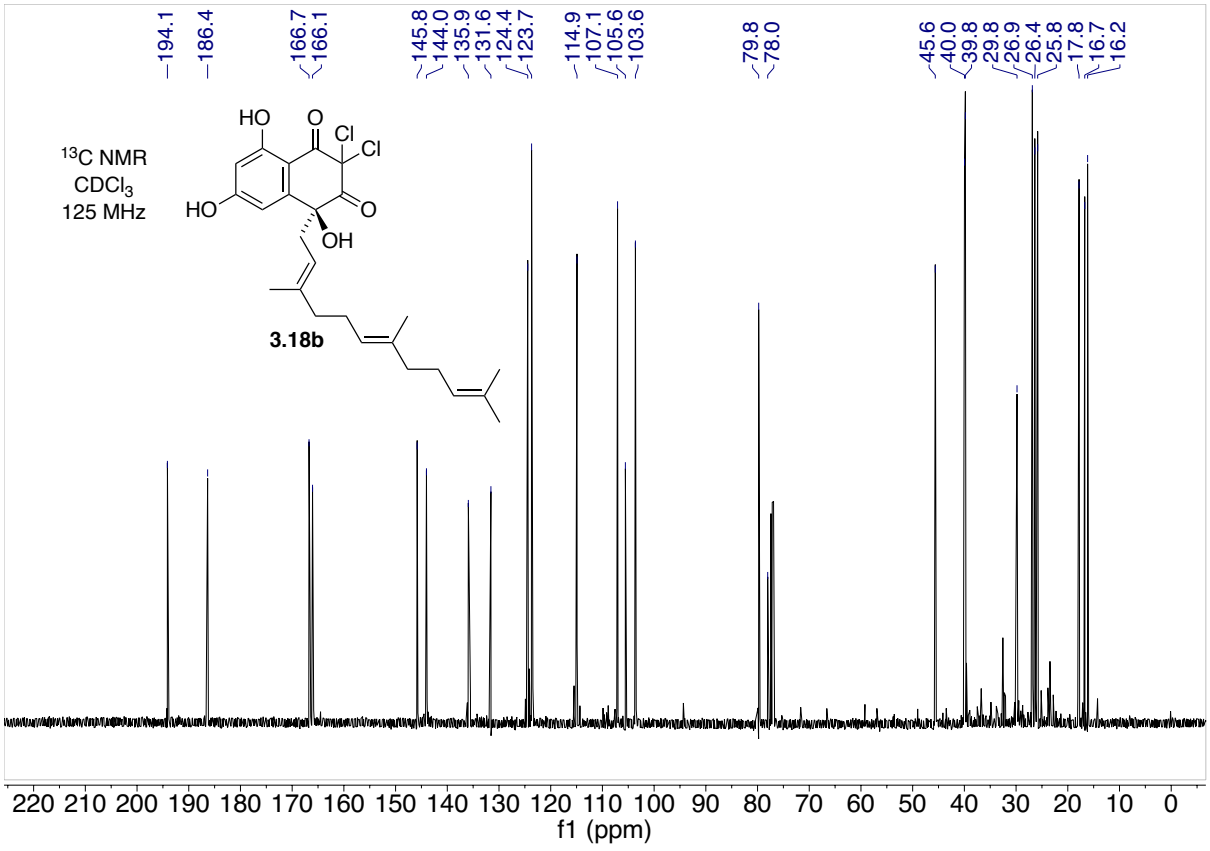
194.1
186.4
166.7
166.1
145.8
144.0
135.9
131.6
124.4
123.7
114.9
107.1
105.6
103.6
79.8
78.0
45.6
40.0
39.8
29.8
26.9
26.4
25.8
17.8
16.7
16.2
13C NMR
CDCl3
125 MHz
HO
O
Cl
Cl
HO
O
OH
3.18b
220 210 200 190 180 170 160 150 140 130 120 110 100 90 80 70 60 50 40 30 20 10 0
f1 (ppm)

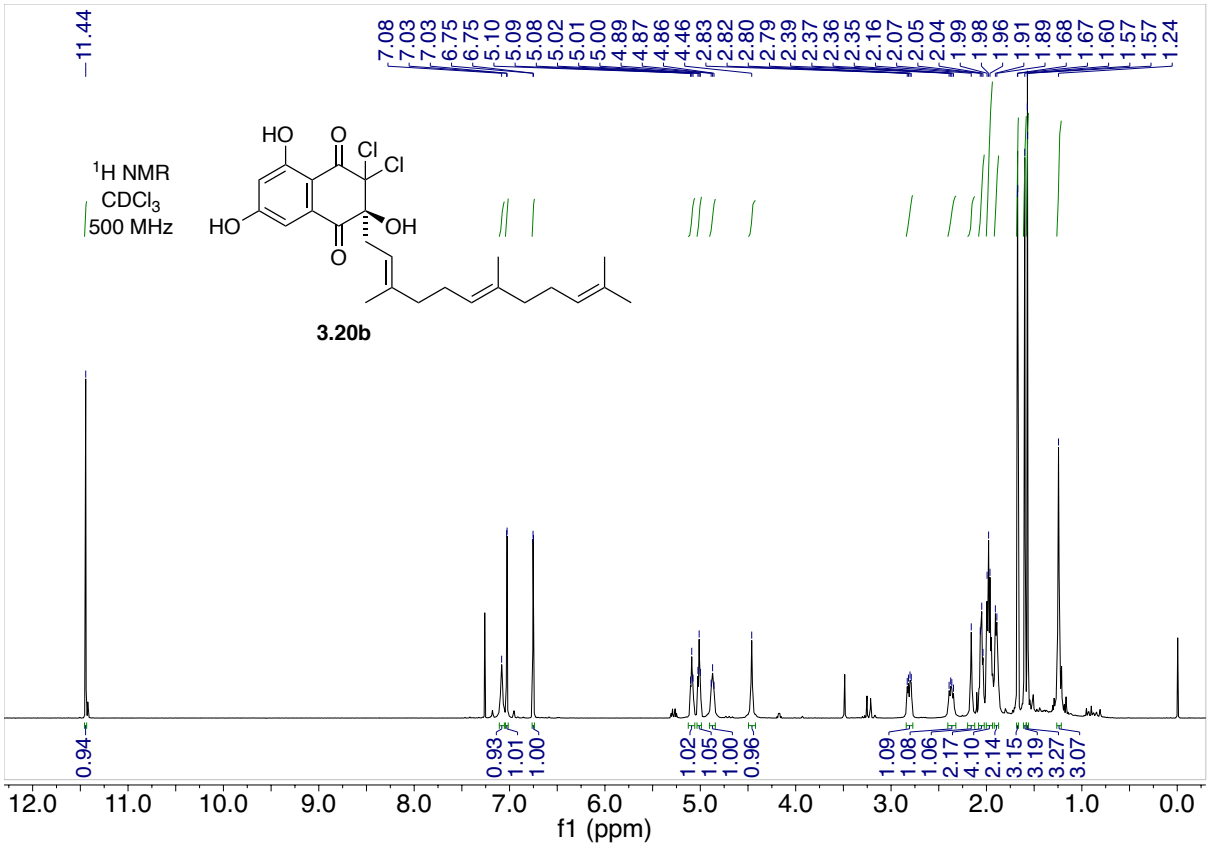
11.44
7.08
7.03
7.03
6.75
6.75
5.10
5.09
5.08
5.02
5.01
5.00
4.89
4.87
4.86
4.46
2.83
2.82
2.80
2.79
2.39
2.37
2.36
2.35
2.16
2.07
2.05
2.04
1.99
1.98
1.96
1.91
1.89
1.68
1.67
1.60
1.57
1.57
1.24
1H NMR
CDCl3
500 MHz
HO
O
Cl
Cl
HO
OH
O
3.20b
0.94
0.93
1.01
1.00
1.02
1.05
1.00
0.96
1.09
1.08
1.06
2.17
4.10
2.14
3.15
3.19
3.27
3.07
12.0
11.0
10.0
9.0
8.0
7.0
6.0
5.0
4.0
3.0
2.0
1.0
0.0
f1 (ppm)

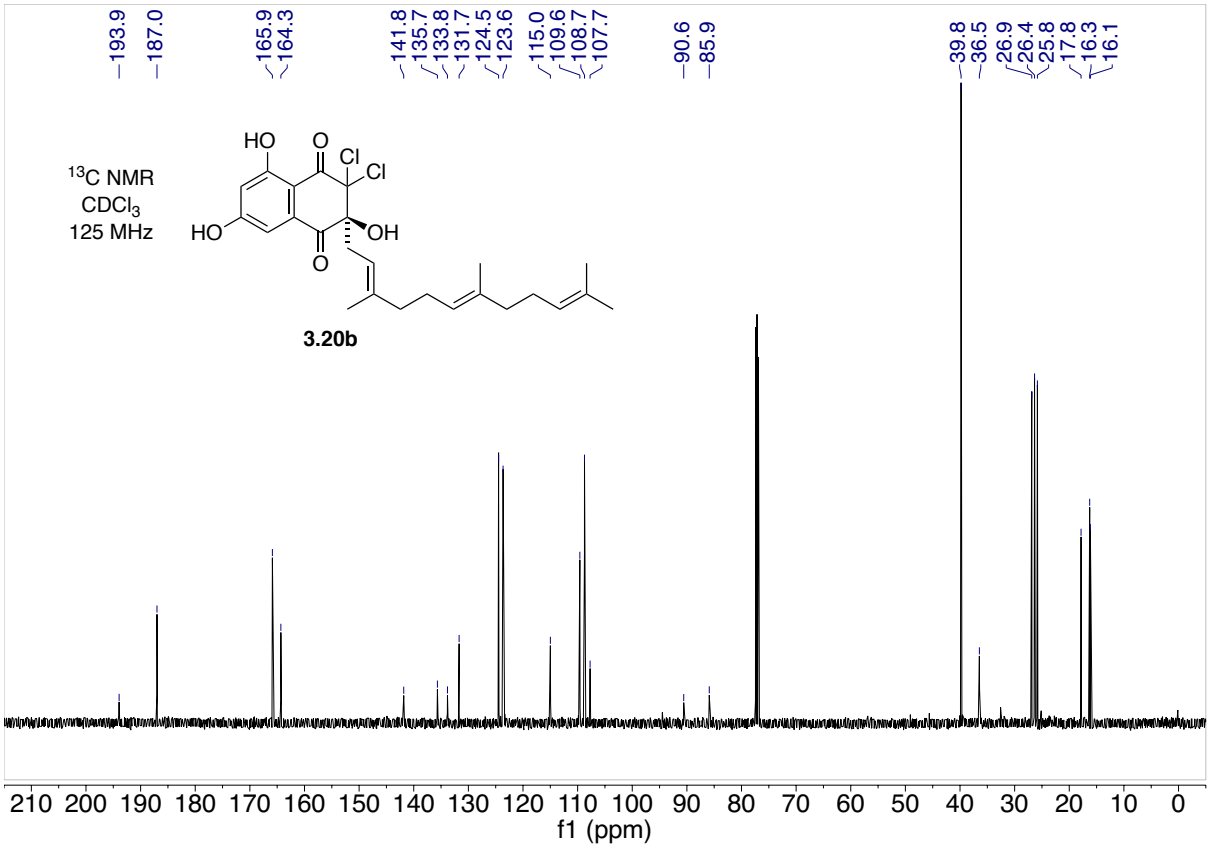
193.9
187.0
165.9
164.3
141.8
135.7
133.8
131.7
124.5
123.6
115.0
109.6
108.7
107.7
90.6
85.9
39.8
36.5
26.9
26.4
25.8
17.8
16.3
16.1
13C NMR
CDCl3
125 MHz
HO
O
Cl
Cl
HO
OH
O
3.20b
210 200 190 180 170 160 150 140 130 120 110 100 90 80 70 60 50 40 30 20 10 0
f1 (ppm)

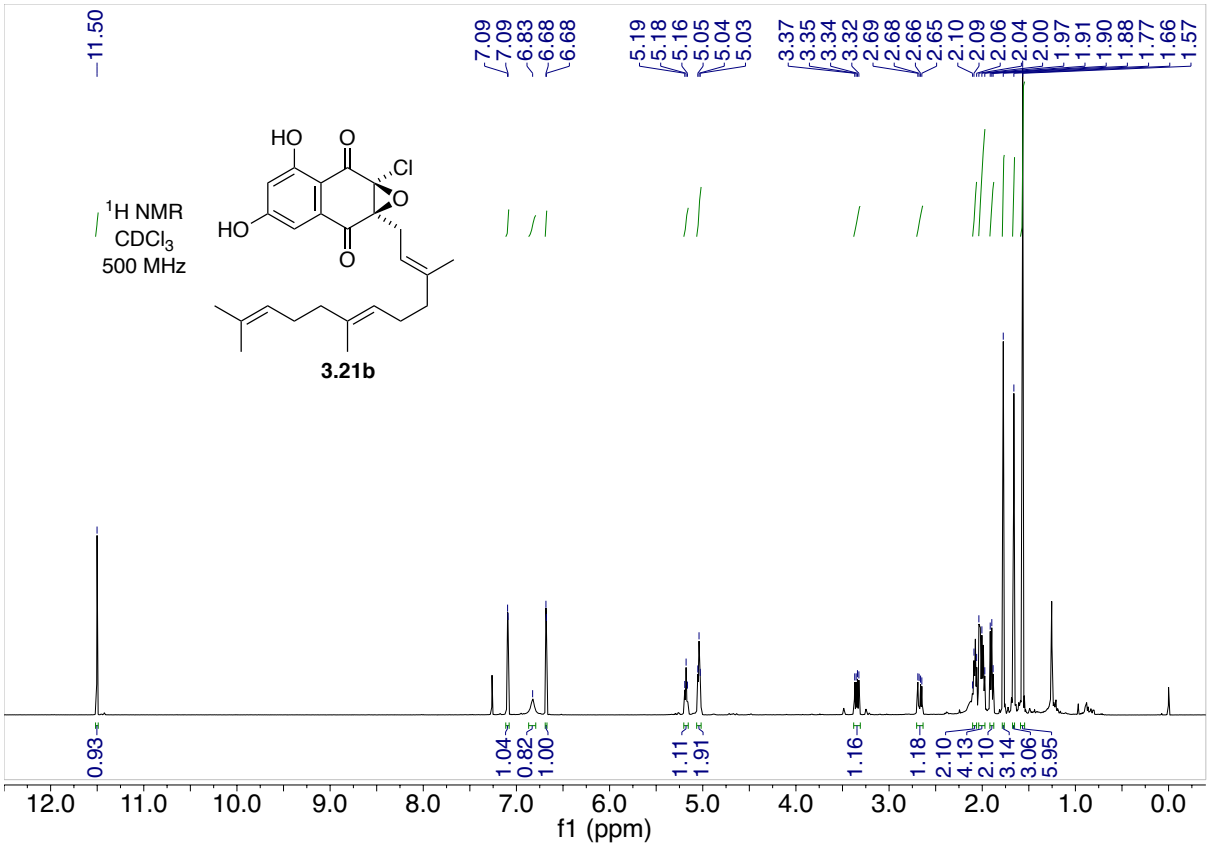
11.50
7.09
7.09
6.83
6.68
6.68
5.19
5.18
5.16
5.05
5.04
5.03
3.37
3.35
3.34
3.32
2.69
2.68
2.66
2.65
2.10
2.09
2.06
2.04
2.00
1.97
1.91
1.90
1.88
1.77
1.66
1.57
HO
O
Cl
O
HO
O
1H NMR
CDCl3
500 MHz
3.21b
0.93
1.04
0.82
1.00
1.11
1.91
1.16
1.18
2.10
4.13
2.10
3.14
3.06
5.95
12.0
11.0
10.0
9.0
8.0
7.0
6.0
5.0
4.0
3.0
2.0
1.0
0.0
f1 (ppm)

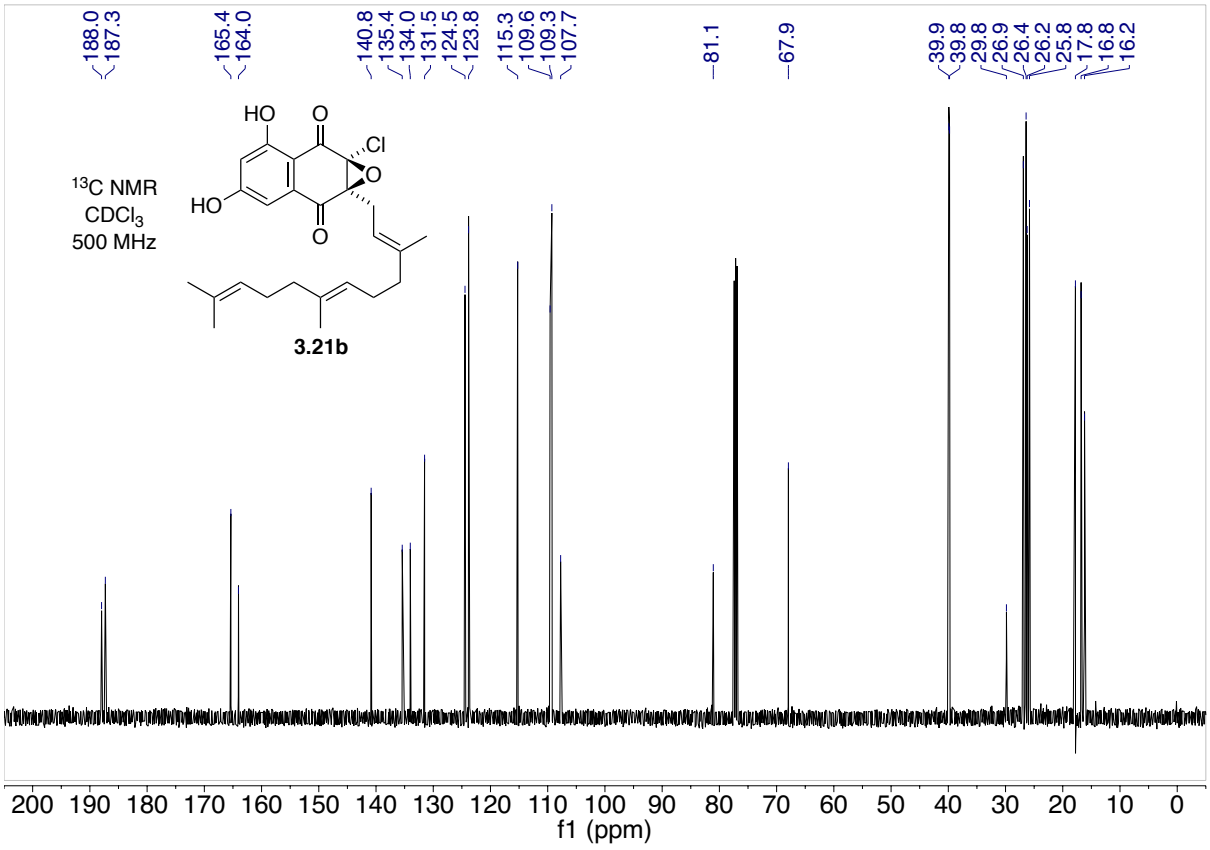
188.0
187.3
165.4
164.0
140.8
135.4
134.0
131.5
124.5
123.8
115.3
109.6
109.3
107.7
81.1
67.9
39.9
39.8
29.8
26.9
26.4
26.2
25.8
17.8
16.8
16.2
HO
O
Cl
O
HO
O
13C NMR
CDCl3
500 MHz
3.21b
200
190
180
170
160
150
140
130
120
110
100
90
80
70
60
50
40
30
20
10
0
f1 (ppm)

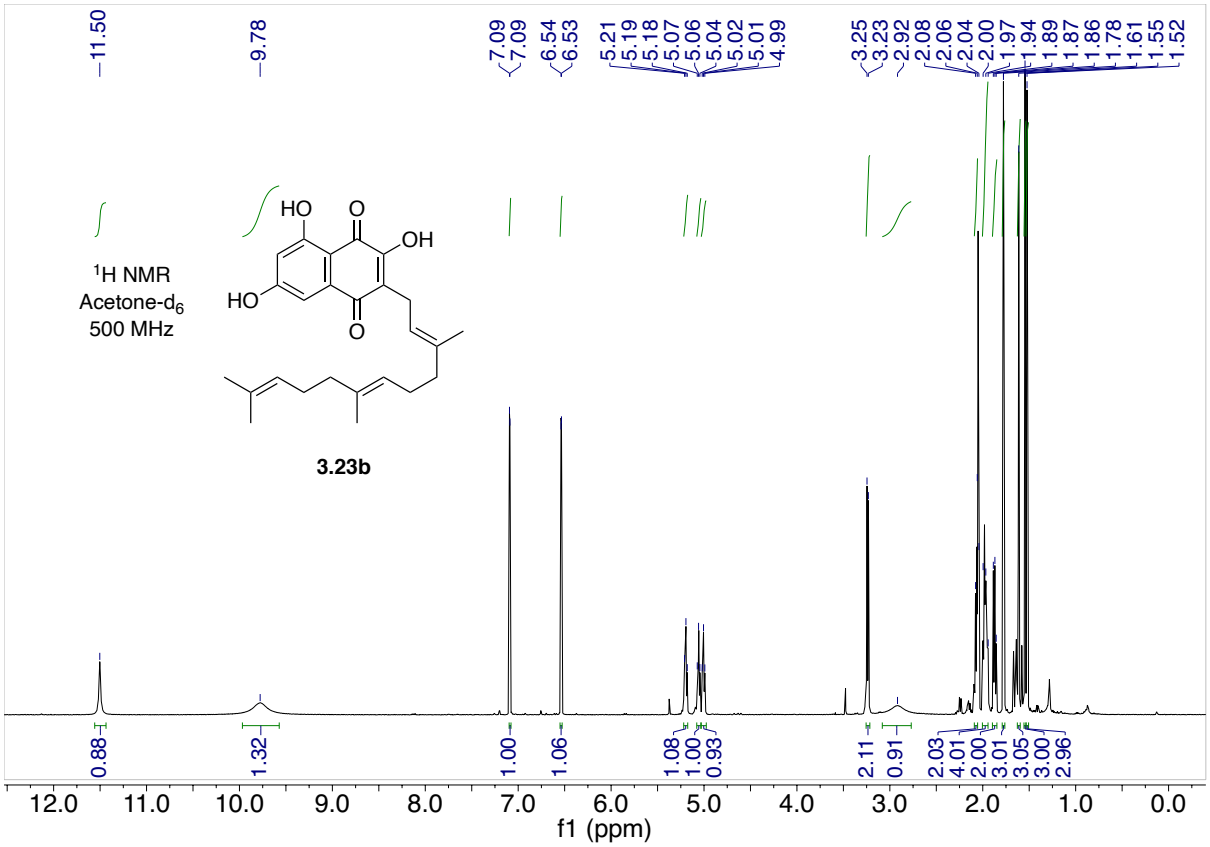
11.50
9.78
7.09
7.09
6.54
6.53
5.21
5.19
5.18
5.07
5.06
5.04
5.02
5.01
4.99
3.25
3.23
2.92
2.08
2.06
2.04
2.00
1.97
1.94
1.89
1.87
1.86
1.78
1.61
1.55
1.52
HO
O
OH
HO
O
1H NMR
Acetone-d6
500 MHz
3.23b
0.88
1.32
1.00
1.06
1.08
1.00
0.93
2.11
0.91
2.03
4.01
2.00
3.01
3.05
3.00
2.96
12.0
11.0
10.0
9.0
8.0
7.0
6.0
5.0
4.0
3.0
2.0
1.0
0.0
f1 (ppm)

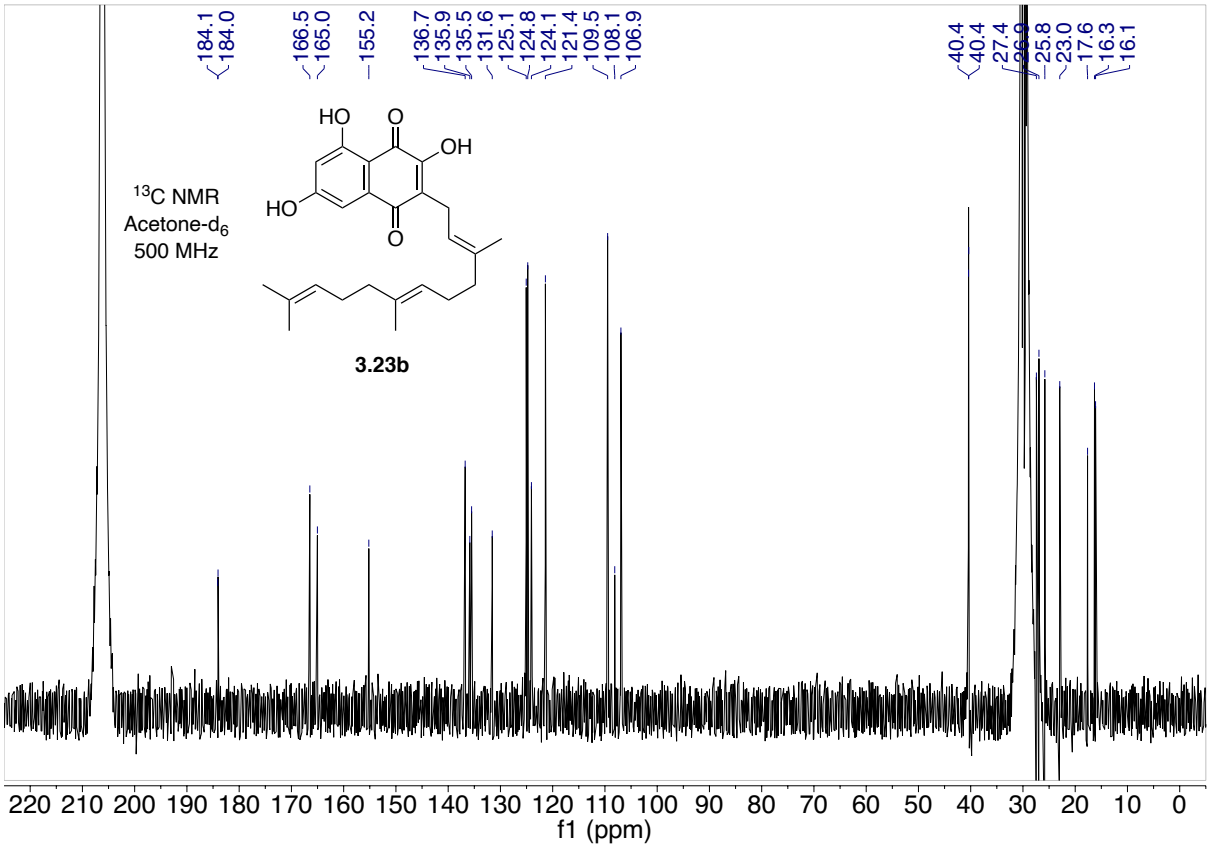
184.1
184.0
166.5
165.0
155.2
136.7
135.9
135.5
131.6
125.1
124.8
124.1
121.4
109.5
108.1
106.9
40.4
40.4
27.4
26.0
25.8
23.0
17.6
16.3
16.1
HO
O
OH
HO
O
13C NMR
Acetone-d6
500 MHz
3.23b
220 210 200 190 180 170 160 150 140 130 120 110 100 90 80 70 60 50 40 30 20 10 0
f1 (ppm)

Assay NMR spectra

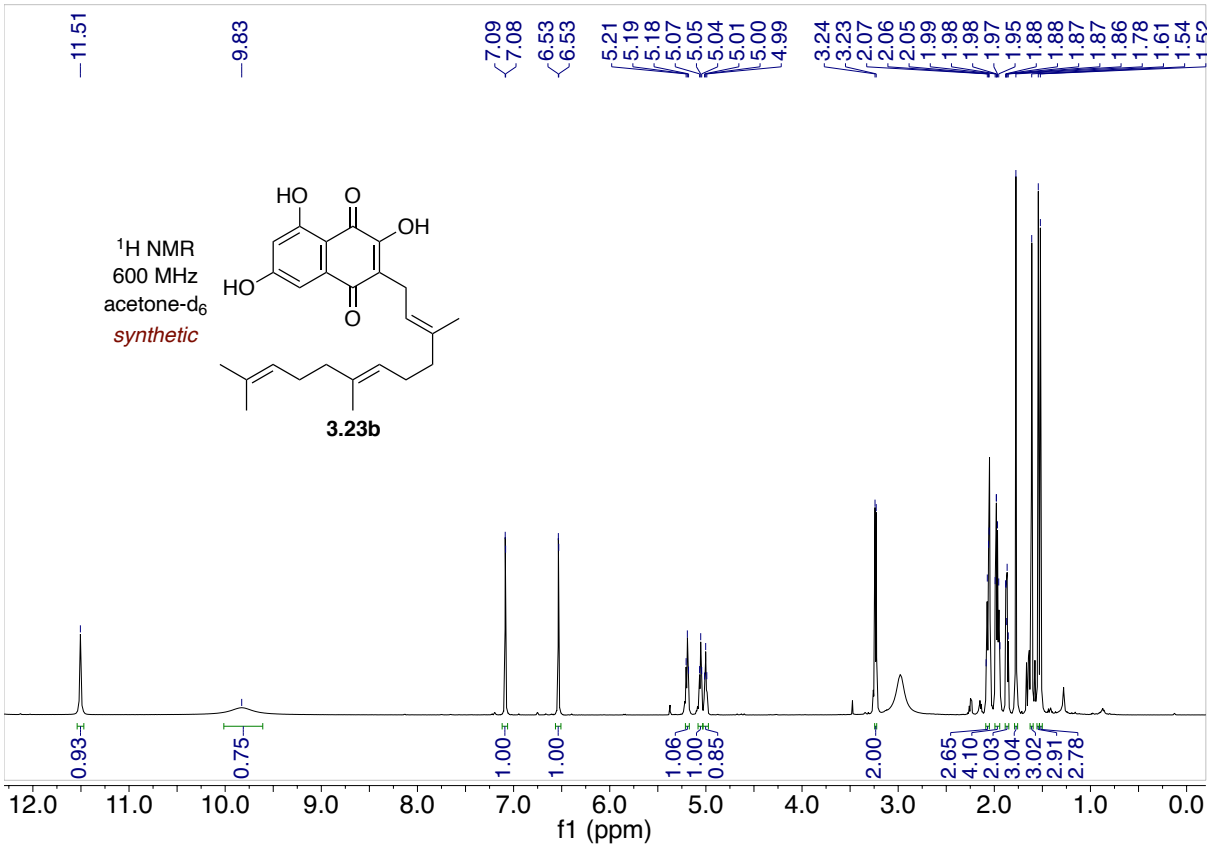

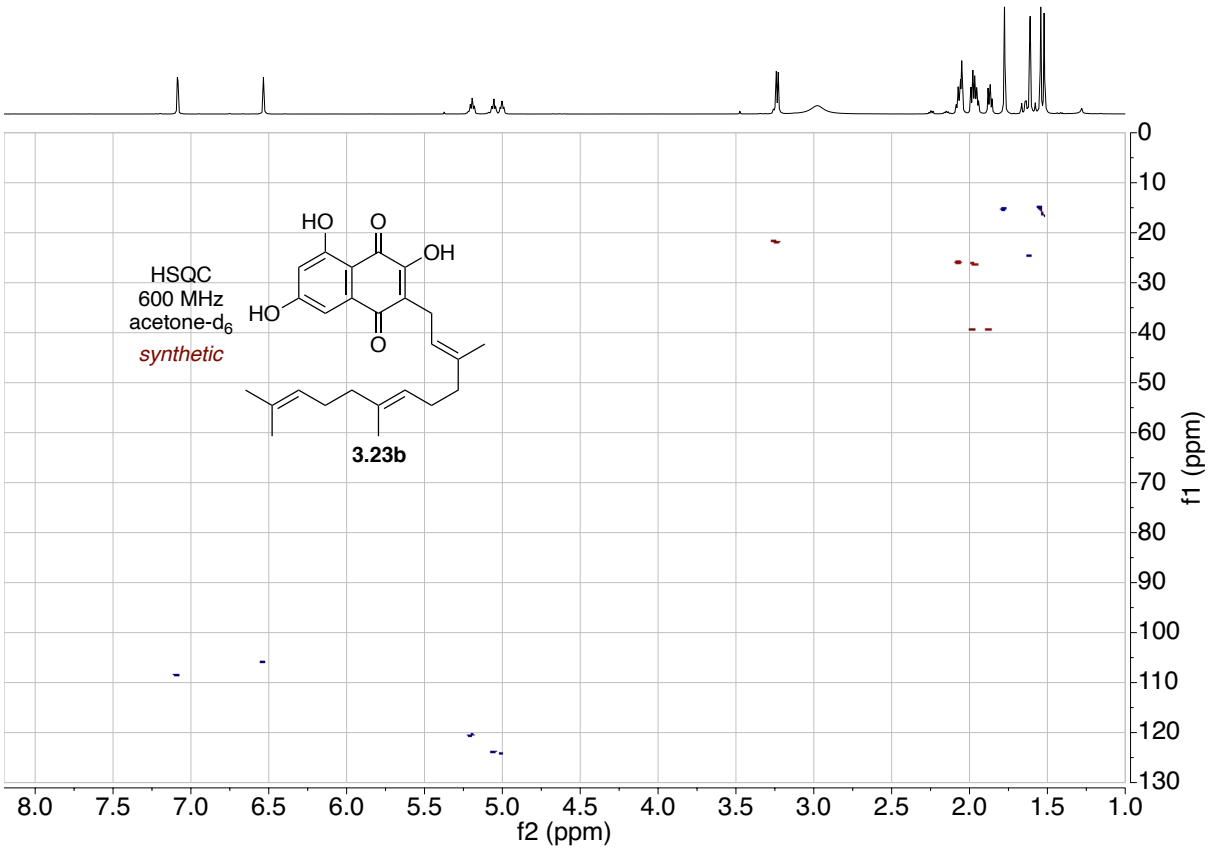

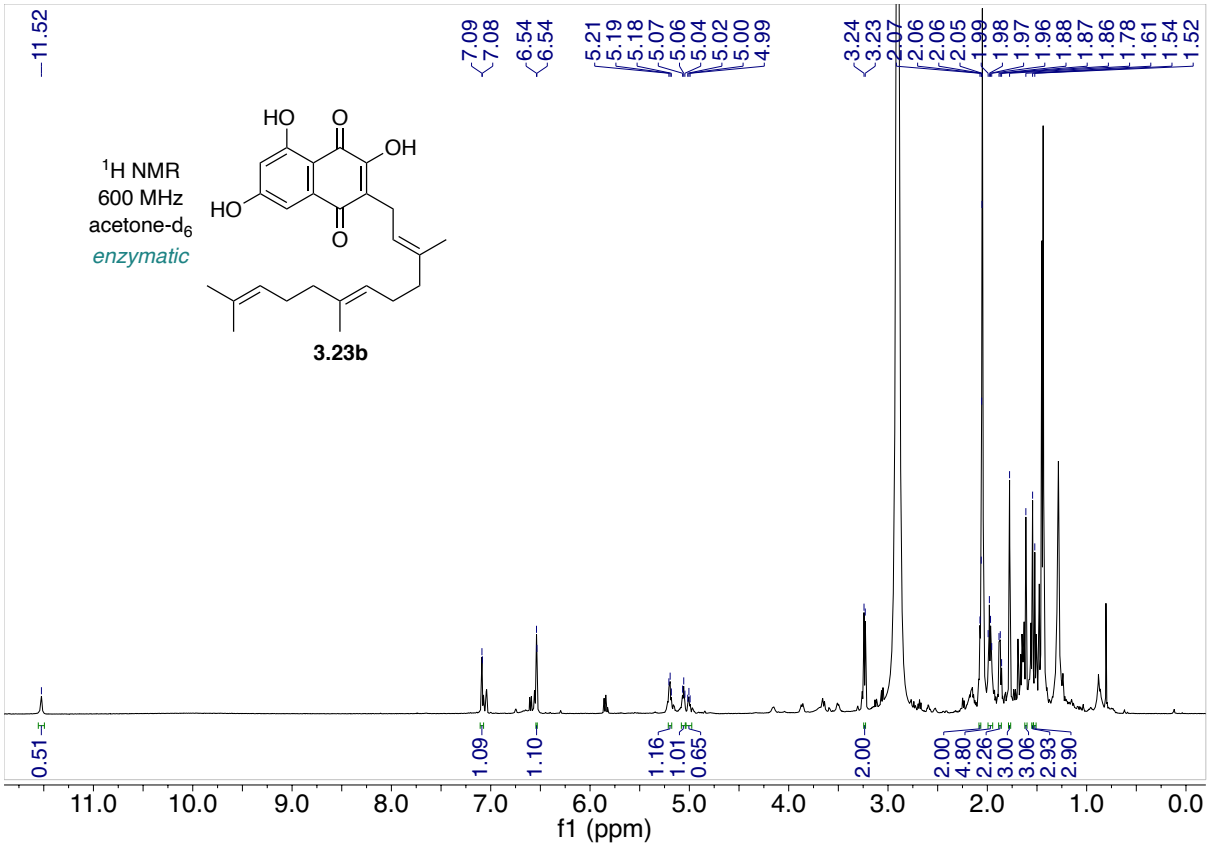
11.52
7.09
7.08
6.54
6.54
5.21
5.19
5.18
5.07
5.06
5.04
5.02
5.00
4.99
3.24
3.23
2.07
2.06
2.06
2.05
1.99
1.98
1.97
1.96
1.88
1.87
1.86
1.78
1.61
1.54
1.52
HO
O
OH
HO
O
1H NMR
600 MHz
acetone-d6
enzymatic
3.23b
0.51
1.09
1.10
1.16
1.01
0.65
2.00
2.00
4.80
2.26
3.00
3.06
2.93
2.90
11.0
10.0
9.0
8.0
7.0
6.0
5.0
4.0
3.0
2.0
1.0
0.0
f1 (ppm)

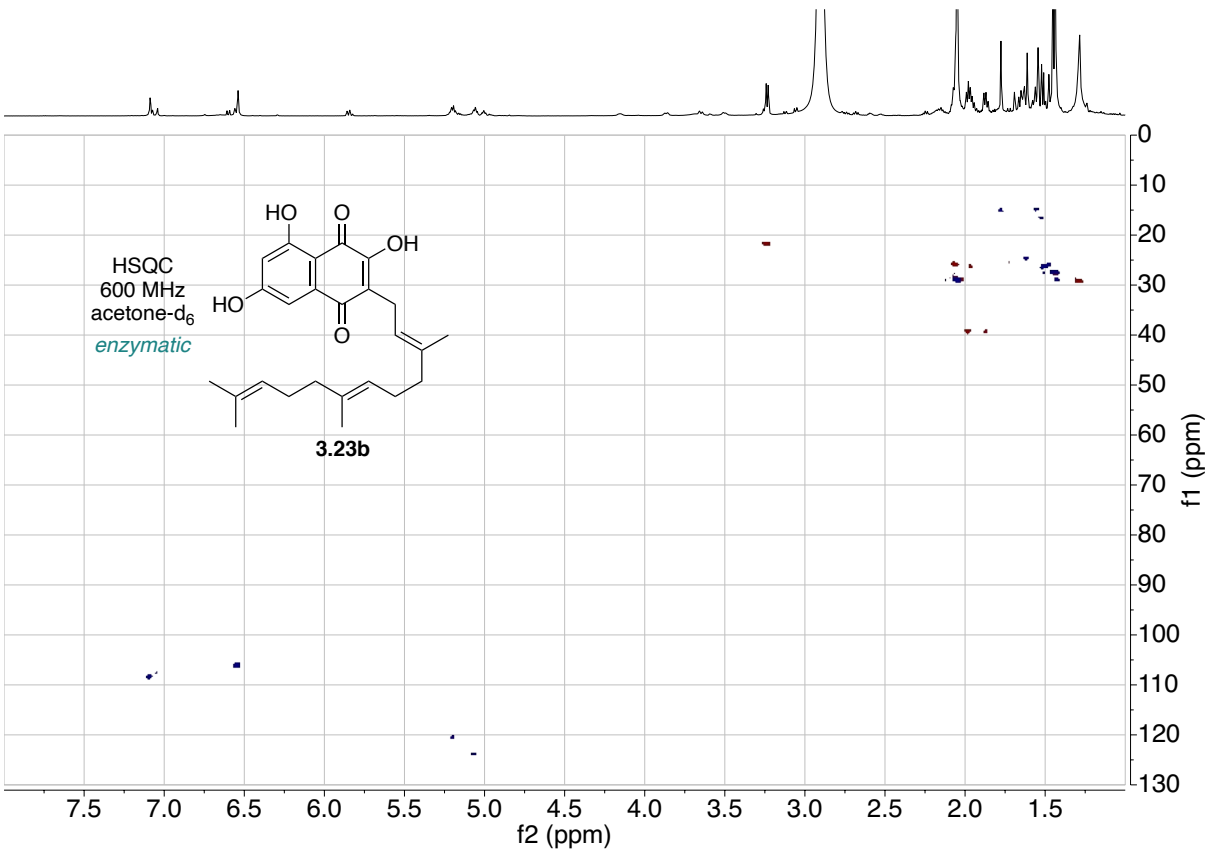
HO
O
OH
HO
O
HSQC
600 MHz
acetone-d6
enzymatic
3.23b
0
10
20
30
40
50
60
70
80
90
100
110
120
130
f1 (ppm)
7.5
7.0
6.5
6.0
5.5
5.0
4.5
4.0
3.5
3.0
2.5
2.0
1.5
f2 (ppm)

CHAPTER 4

Total Synthesis of Naphterpin and Marinone Natural Products

Carbon atoms of naphterpin and marinone natural products are numbered throughout this chapter as follows:

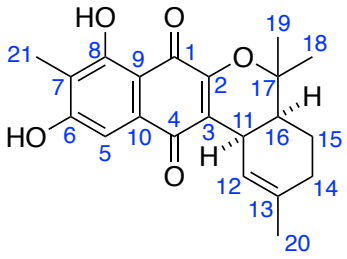

naphterpin

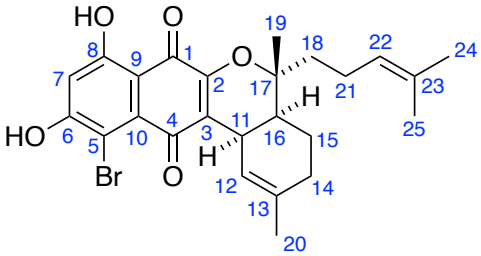

marinone

Parts of this chapter have been published as follows:

Murray, L. A. M.; Fallon, T.; Sumby, C. J.; George, J. H. *Org. Lett.* **2019**, *21*, 8312.

4.1 Introduction

4.1.1 Diels-Alder Reactions in Total Synthesis of Natural Products

The Diels-Alder reaction is a powerful reaction in synthetic organic chemistry. This concerted [4+2] cycloaddition between a diene and a dienophile results in the stereospecific formation of a six-membered ring, containing two new carbon-carbon bonds (Scheme 4.01).[1] In the case that a heteroatom is involved, this is known as a hetero-Diels-Alder reaction.

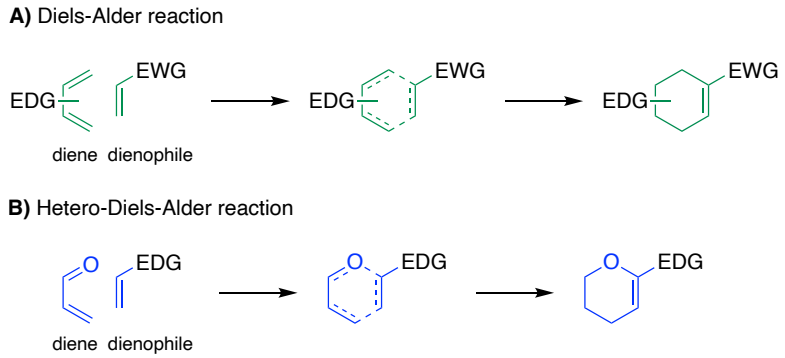

Scheme 4.01: **A)** General example of a Diels-Alder reaction. **B)** General example of a hetero-Diels-Alder reaction. EDG = electron donating group; EWG = electron withdrawing group.

Diels-Alder reactions are known for their ability to rapidly build molecular complexity and are therefore commonly employed in natural product synthesis.[2,3] In 2001 Nicolaou and co-workers reported their total synthesis of the structurally complex diterpenoid colombiasin A, employing both an intermolecular and an intramolecular Diels-Alder reaction.[4] This synthesis began with an intermolecular Diels-Alder between diene (**4.01**) and quinone (**4.02**) to form the bicyclic intermediate **4.03**. Further functionalisation of this intermediate furnished sulfone **4.04**. Treatment of **4.04** at high temperatures unveiled the intermediate diene **4.05**, which could then undergo an impressive intramolecular Diels-Alder reaction, forming two adjacent stereogenic quaternary carbons to give **4.06**. With the tetracyclic framework established, **4.06**

was subjected to a final sequence of deoxygenation and deprotection to form the natural product colombiasin A (**4.07**).

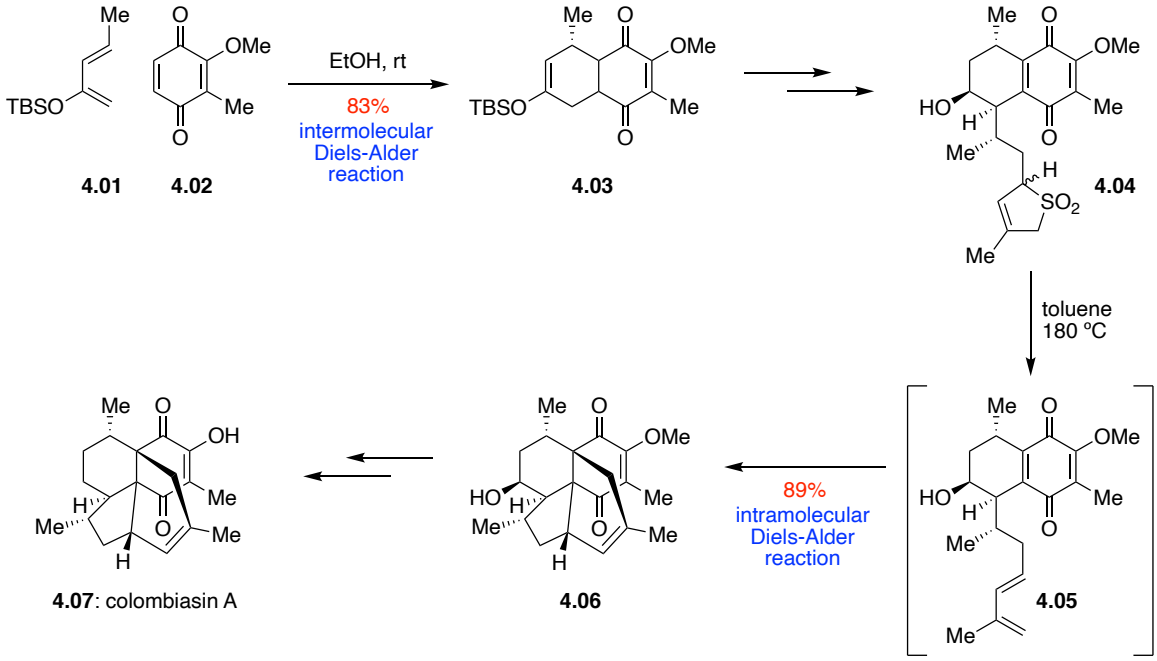

Scheme 4.02: Nicolaou's total synthesis of colombiasin A (**4.07**).[4]

The Diels-Alder reaction continues to play a crucial role in the assembly of complex molecular structures, including biologically active natural products.

4.1.2 Intramolecular Diels-Alder Reactions in Meroterpenoid Synthesis

Intramolecular Diels-Alder reactions can also be employed in both the synthesis and biosynthesis of meroterpenoid natural products.[3] Many of these natural products contain an electron-rich polyketide-derived core, furnished with a terpene derived sidechain. This sidechain is commonly cyclised through an intramolecular Diels-Alder reaction to form complex cyclic frameworks.

More recently, this approach has been applied by Zhao and co-workers in their biomimetic total synthesis of meroterpenoid natural product cochlearol T (**4.08**) (Scheme 4.03).[5] Firstly commercially available geranylacetone (**4.09**) as a mixture of *E*/*Z*-isomers and 5-methoxysalicylaldehyde (**4.10**) were subjected to a Lewis acid promoted Mukaiyama aldol reaction, followed by reduction of the intermediate ketone with $NaBH_4$ to form triol **4.11**. Subsequent reflux of **4.11** in toluene in the presence of silica gel catalysed the desired intramolecular hetero-Diels-Alder reaction, forming tricyclic intermediate **4.12**, which was then immediately oxidised to ketone **4.13** using PCC. Intermediate cyclohexanone **4.13** was then exposed to a palladium nanoparticle catalysed aerobic dehydrogenation to form phenol **4.14**, which after demethylation afforded the natural product cochlearol T (**4.08**).

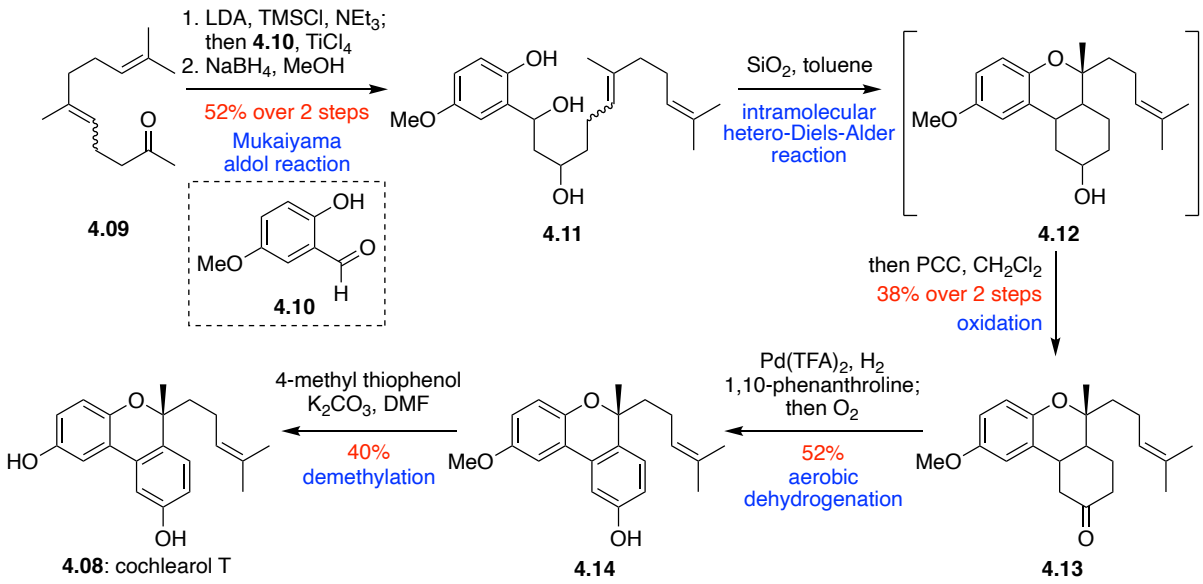

Scheme 4.03: Zhao's total synthesis of cochlearol T (**4.08**).[5]

A similar intramolecular hetero-Diels-Alder reaction is proposed to occur enzymatically in the biosynthesis of Δ^1-tetrahydrocannabinolic acid (THCA, **4.15**) (Scheme 4.04).[6] Enzyme-catalysed oxidation of cannabigerolic acid (**4.16**) in the presence of enzyme-FAD generates intermediate *ortho*-quinone methide **4.17**. This intermediate **4.17** can then undergo an intramolecular hetero-Diels-Alder reaction to afford THCA (**4.15**).

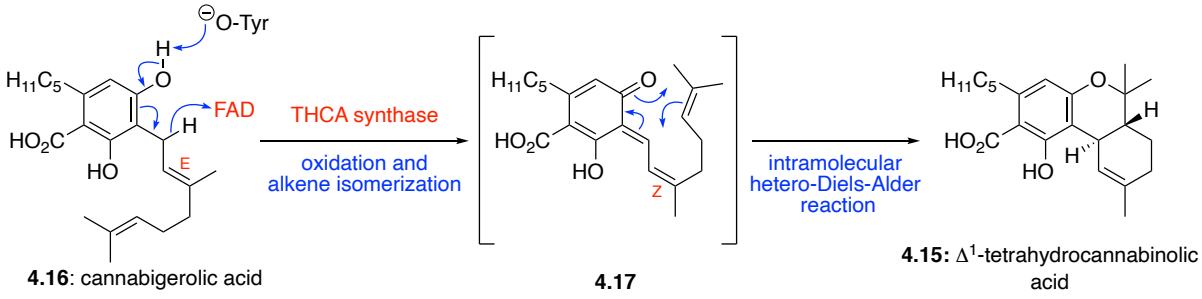

Scheme 4.04: Proposed catalytic mechanism of Δ^1-tetrahydrocannabinolic acid (**4.15**) synthesis.[6]

4.1.3 Project Aims

The objective of this project was to create a shorter synthetic route to access our previously synthesised natural products 7-demethylnaphterpin and debromomarinone as well as a collection of other natural products from the naphterpin and marinone families.

Our previous biomimetic syntheses to access the naphterpins and the marinones followed our biosynthetic proposal, in which the THN ring system was oxidised *via* a series of cryptic chlorination events, catalysed by vanadium-dependent chloroperoxidases (VCPOs), despite the absence of chlorine in these natural products.[7] The success of this synthesis gave us access to each proposed biosynthetic intermediate for chemoenzymatic studies. So far, the use of these biosynthetic intermediates has deciphered the reactivity of two VHPO enzymes from the putative marinone gene cluster, that chlorinate and dearomatize prenylated THN derivatives.

Although successful, the complexity of the biosynthetic pathway meant that our biomimetic syntheses were 15 steps from commercially available (3,5-dimethoxyphenyl) acetic acid, and 10 steps from THN derivative **4.18** (Scheme 4.05). This synthetic strategy was therefore too long and too linear to synthesise sufficient material in order to access the further oxidized or brominated members of the naphterpin/marinone families. To combat this, we envisaged a shorter non-biomimetic synthesis of 7-demethylnaphterpin (**4.19**), in which the naphthoquinone ring could be introduced as the final step. No longer constrained by the use of the THN building block, we predicted a significant decrease in step count, and consequently, an increase in overall yield.

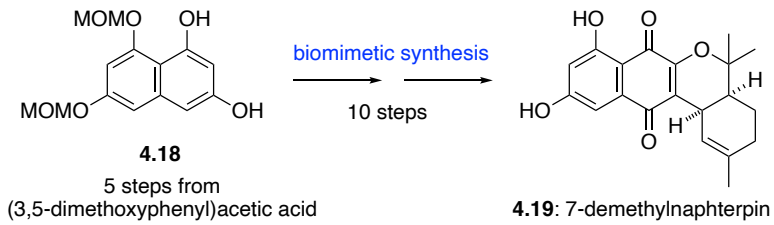

Scheme 4.05: Previous biomimetic synthesis of 7-demethylnaphterpin (**4.19**).[7]

A related synthesis was published by Tapia and co-workers[8] (Scheme 4.06) in their study toward the naphterpins (however naphterpin was never successfully synthesised). This study began with MOM protection of commercially available 2,5-dimethoxyphenol (**4.20**) to give protected phenol **4.21**. Subsequent *ortho*-lithiation of **4.21** with *n*-BuLi and addition of citral (**4.22**) gave secondary alcohol **4.23**. Treatment of **4.23** with 6M HCl in THF initiated the cascade of MOM deprotection, *ortho*-quinone methide formation, alkene isomerisation and an intramolecular hetero-Diels-Alder reaction to give the tricyclic scaffold **4.24**. Oxidative demethylation with Ag_2O then gave quinone **4.25**. Finally, an intermolecular Diels-Alder

reaction with Brassard diene **4.26** and acid catalysed oxidation gave benzo[*b*]naphtho[2,3-*b*]pyran-7,12-dione **4.27**.

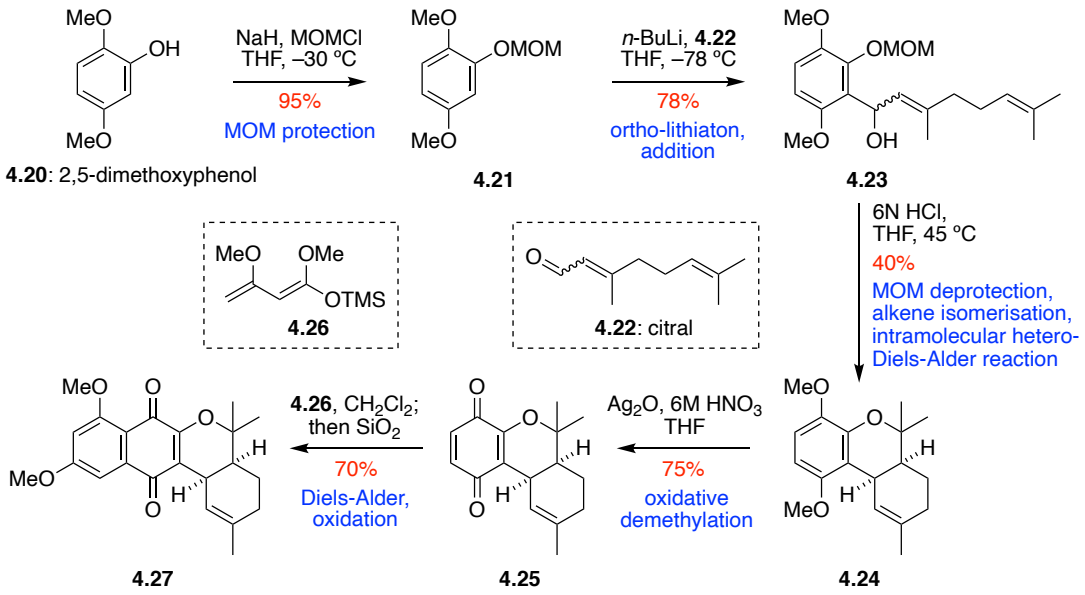

Scheme 4.06: Tapia's total synthesis of benzo[*b*]naphtho[2,3-*b*]pyran-7,12-dione (**4.27**).[9]

We envisaged that employing a similar synthetic strategy with a modification of the Brassard diene **4.26** could give us access to 7-demethylnaphterpin **4.19** and other members from the naphterpin family. We also predicted that an alteration of the sidechain length would allow us to access members from the marinone family of natural products. This shortened synthesis had the potential for us to access substantial quantities of these natural products, allowing us to investigate the synthesis of oxidized and brominated members of the naphterpin and marinone families.

4.2 Results and Discussion

4.2.1 Initial Retrosynthesis of 7-Demethylnaphterpin and Naphterpin

Building on the methodology developed by Tapia *et al.*,[8] we devised a simpler non-biomimetic retrosynthetic analysis of the naphterpins (Scheme 4.07). Firstly, we envisaged that the aromatic ring of naphterpin (**4.28**) and 7-demethylnaphterpin (**4.19**) could be installed through an intermolecular Diels−Alder reaction (and aerobic oxidation) by disconnection to simple Brassard dienes **4.29**/**4.30** and quinone **4.25**. A similar intermolecular Diels−Alder reaction was used in Nakata's total synthesis of the napyradiomycin A80915G.[10] Quinone **4.25** could be generated through oxidation of **4.24**. The *cis*-fused cyclohexane and pyran rings of **4.24** could be formed through an intramolecular Diels-Alder reaction of a reactive enone **4.31**, which would be unveiled *via* oxidation (and alkene isomerization) of alcohol **4.32**. Finally, intermediate **4.23** could be formed through an addition of citral **4.22** to a protected form of commercially available 2,5-dimethoxyphenol **4.33**.

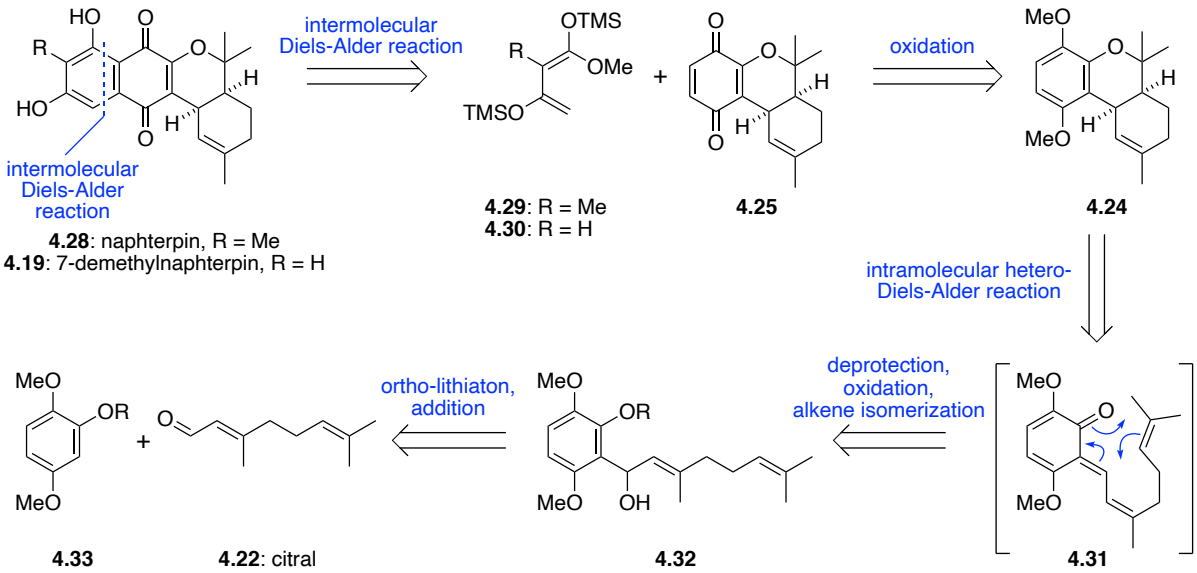

Scheme 4.07: Retrosynthetic analysis of naphterpin **4.28** and 7-demethylnaphterpin **4.19**.

The success of this synthetic route would significantly shorten our biomimetic synthesis and therefore allow divergent access to other naphterpin family members.

4.2.2 Investigation into the Total Synthesis of 7-Demethylnaphterpin

This synthesis began with a Dakin oxidation of commercially available 2,5-dimethoxybenzaldehyde (**4.34**), producing 2,5-dimethoxyphenol (**4.20**) (Scheme 4.08). Although commercially available, **4.20** was synthesised due to high cost and poor availability from commercial suppliers. Treatment of **4.20** with MOMCl in the presence of *i*-Pr_2NEt gave the protected phenol **4.21** in excellent yields.[11]

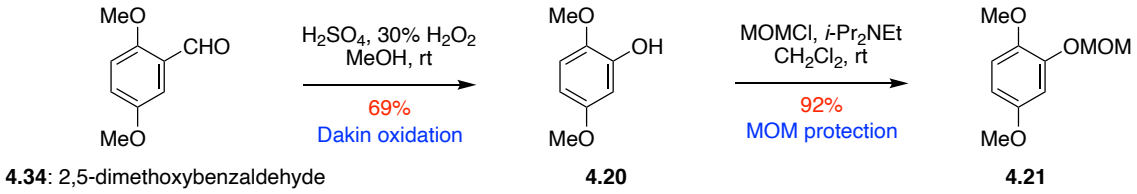

4.34: 2,5-dimethoxybenzaldehyde **4.20** **4.21**

Scheme 4.08: Dakin oxidation and MOM protection of 2,5-dimethoxybenzaldehyde (**4.34**).

Next, we focused on the aromatic substitution of our protected phenol intermediate **4.21** (Scheme 4.09). Tapia[9] had reported good yields for *ortho*-metalation using *n*-BuLi, followed by addition of citral (**4.22**) to give desired intermediate **4.23**. A similar regioselective metalation and substitution strategy was employed by Zhang *et al.*[12] in their synthesis of rossinone B. Frustratingly, early attempts using these conditions were unsuccessful in our hands.

We suspected the lack of success resulted from an issue with the *ortho*-lithiation step. Alkyl lithium reagents often exist as aggregates in solution. The addition of amine additives disperses these aggregates, accelerating reactivity due to increased basicity. Tetramethylethylenediamine

(TMEDA) is a bidentate amine ligand, commonly employed in these reactions for this purpose. *Ortho*-lithiation of protected phenol **4.21** with *n*-Buli at 0 ºC in the presence of TMEDA, followed by addition of citral (**4.22**) gave the desired secondary alcohol **4.23** in a 2:1 mixture of *E*/*Z* isomers (Scheme 4.09).

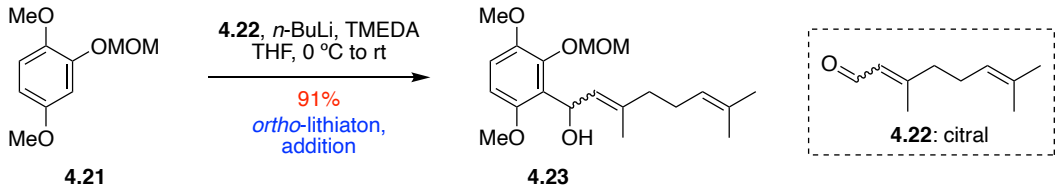

Scheme 4.09: *Ortho*-lithiation and addition of citral (**4.22**) to protected phenol **4.23**.

With alcohol **4.23** in hand, Tapia's acid catalysed cascade of MOM deprotection, alkene isomerisation and intramolecular hetero-Diels-Alder reaction was attempted. A similar cascade was used Snider's synthesis of the bisabosquals.[13,14] Treatment of **4.23** with HCl in THF at 45 ºC (Scheme 4.10) showed consumption of starting material after 2 hours. TLC analysis showed the formation of two new products, very close together on the TLC plate, and with higher R_f values than the starting material. We predicted that this may be the case if we were to observe both *cis* and *trans* fused rings. Separation of these two compounds by flash chromatography proved difficult and ^{1}H NMR analysis of the compounds showed complex mixtures. Despite repeating this reaction multiple times, the outcome was unchanged. Due to the poor yield and inseparable impurities, it was decided that these reaction conditions were not viable. From our previous success with $SnCl_4$ in the biomimetic synthesis of 7-demethylnaphterpin (**4.19**), we decided to investigate whether this Lewis acid could catalyse the desired deprotection and cyclisation. Unfortunately, treatment of **4.23** with $SnCl_4$ in EtOH at reflux or at room temperature did not change the outcome of this reaction, again resulting in an inseperable complex mixture.

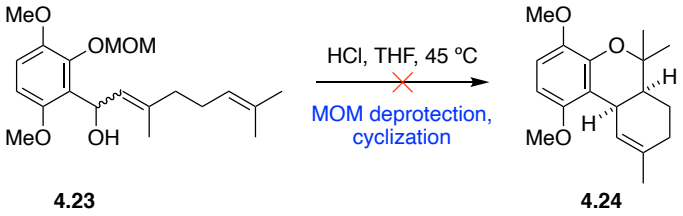

4.23 **4.24**

Scheme 4.10: Attempted conditions for MOM deprotection and cyclisation of **4.23**.

4.2.3 Revised Retrosynthesis of Naphterpins

It was clear that our initial retrosynthetic analysis as previously presented contained issues in both yield, reliability and purity. Despite resolving our initial issues, lack of success in the crucial cyclisation to give **4.24** and the potential stereoselectivity issues at the *cis*-fused ring junction steered us towards a new retrosynthetic analysis (Scheme 4.11).

We proposed that the *cis*-fused cyclohexane and pyran rings of **4.28**/**4.19** could be formed through a similar intramolecular hetero-Diels-Alder reaction. In this synthesis, this would be accomplished through the reactive enones **4.35**/**4.36**, which could be unveiled *via* a late-stage retro-6π-electrocyclization (and alkene isomerization) of naphthoquinones **4.37**/**4.38**. This sequence was established in our previous biomimetic synthesis.[7] Disconnection of naphthoquinones **4.37**/**4.38** to simple Brassad dienes **4.29**/**4.30** and quinone **4.39** *via* an intermolecular Diels−Alder reaction (and aerobic oxidation) would then allow for a divergent synthesis. There are many excellent examples in total synthesis of quinones such as **4.39** used as dienophiles in Diels-Alder reactions.[2,15]

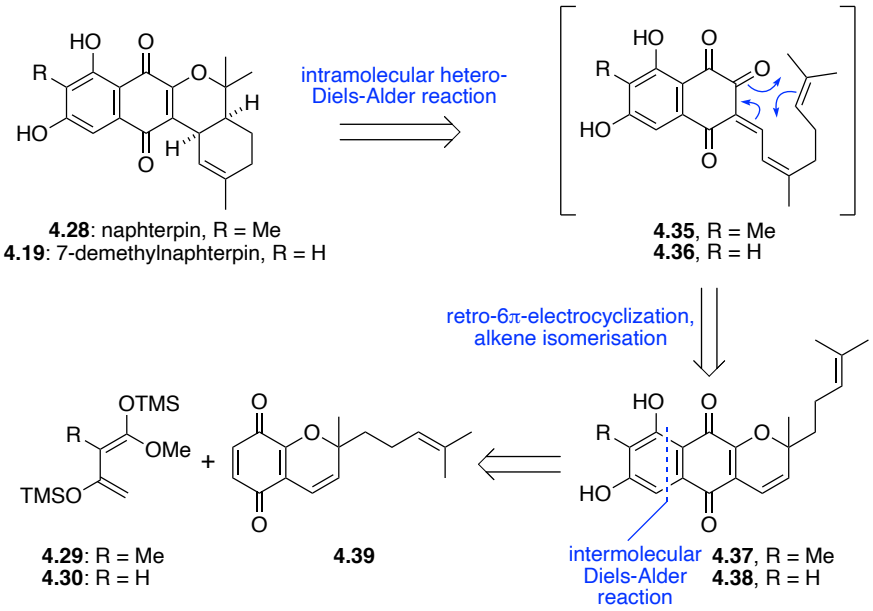

Scheme 4.11: Second generation retrosynthetic analysis of naphterpin (**4.28**) and 7-demethylnaphterpin (**4.19**).

We proposed that quinone **4.39** could be formed through oxidative demethylation of **4.40**. We then envisaged that dimethoxybenzopyran **4.40** could be synthesised through a chromenylation of simple starting material, 2,5-dimethoxyphenol (**4.20**) with the naturally abundant terpenoid, citral (**4.22**).

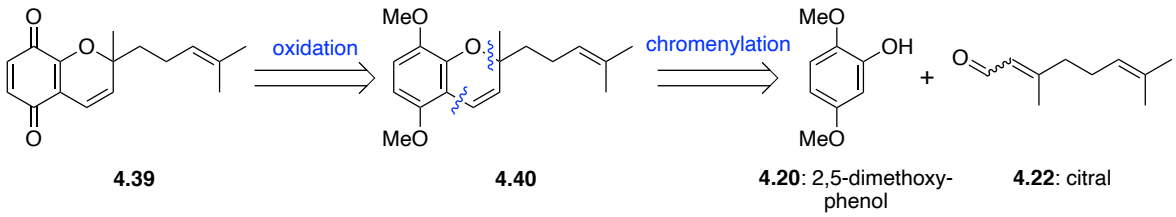

Scheme 4.12: Retrosynthetic analysis of quinone **4.39**.

4.2.4 Quinone Synthesis

This synthetic approach began with a Knoevenagel condensation between **4.20** and **4.22** to give **4.41**. Subsequent elimination of **4.41** gave *o*-quinone methide **4.42**, followed by a 6π-electrocyclization to give chromene **4.40** (Scheme 4.13).

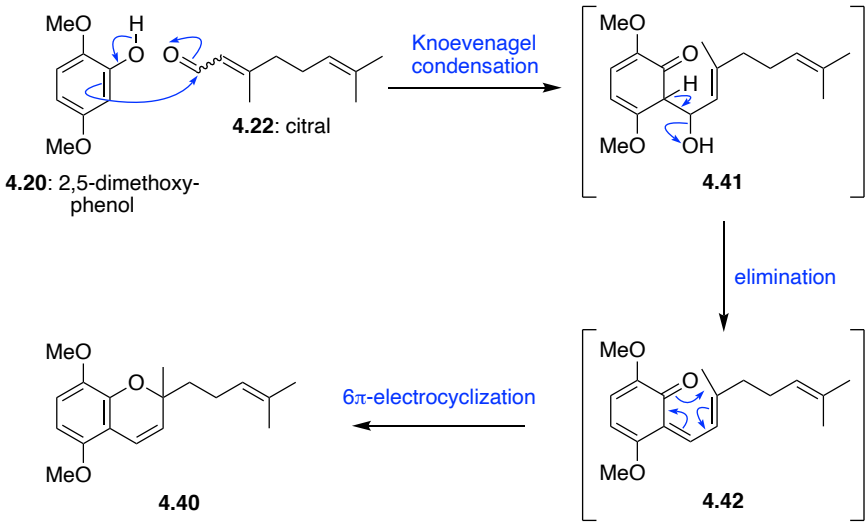

Scheme 4.13: Synthesis of chromene **4.40**.

Despite similar chromenylations performed on 3,5-dimethoxyphenol substrates,[16] to the best of our knowledge, no reactions of this kind were reported on 2,5-dimethoxyphenol (**4.20**). The conditions screened are outlined in Table 4.01. Firstly, ethylenediaminediacetic acid (*EDDA*) catalysed reaction conditions reported by Wang and co-workers were attempted (entry 1).[17,18] No reaction was observed when phenol **4.20** was subjected to these conditions, even at high temperatures and extended reaction times. Attempts to perform the reaction using pyridine,[19] $CaCl_2$ in the presence of NEt_3[20] (entry 3) or $Ti(O\textit{i}\text{-}Pr)_4$[21] (entry 4) all resulted in no reaction. Finally, following literature conditions of $PhB(OH)_2$ in the presence of AcOH,[22–24] the desired chromene was synthesised in 9% yield (entry 5). TLC analysis showed the production of multiple side products. As this was the first step in what we hoped would be a scalable synthesis, the poor yield of this reaction meant this sequence would not be viable.

Table 4.01: Attempted optimization conditions for chromenylation of **4.20**.

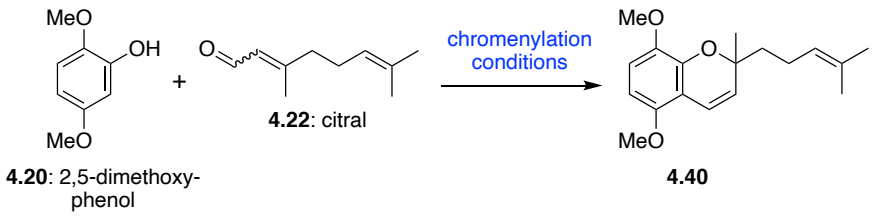

Entry	Base/Acid	Solvent	Temperature	Time	Result
1	EDDA	PhMe	110 ºC	30 h	no reaction
2	pyridine	-	115 ºC	6 h	no reaction
3	$CaCl_2$, NEt_3	EtOH	78 ºC	7 h	no reaction
4	Ti(O*i*-Pr)$_4$	PhMe	0 ºC → rt	24 h	no reaction
5	$PhB(OH)_2$, AcOH	PhMe	110 ºC	14 h	**4.40** (9%)

Hoping to still access quinone **4.39**, we reconsidered our retrosynthetic analysis (Scheme 4.14). Substituting our intermediate chromene **4.40** for phenol **4.43**, would still enable a three-step synthesis from commercially available and extremely cheap compounds, resorcinol (**4.44**) and **4.22**.

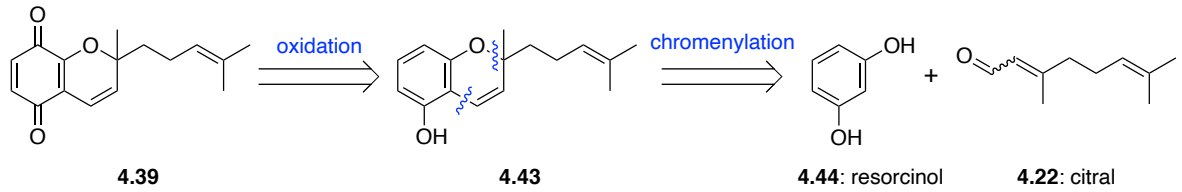

Scheme 4.14: Revised retrosynthetic analysis of quinone **4.39**.

Chromenylation of **4.44** was initially attempted using our previously successful conditions of $PhB(OH)_2$ and AcOH, affording the desired chromene **4.43** in 14% yield. Despite an improvement in yield from our previous route, a further literature search showed that EDDA, ethylenediamine and *R,R*-(–)-1,2-diaminocyclohexane (**4.45**) had been used with more success for the chromenylation of **4.44**.[25] While EDDA did increase the yield of this reaction to 20%,

ethylenediame and *R,R*-(–)-1,2-diaminocyclohexane (**4.45**) (Scheme 4.15) gave 27% and 29% yield, respectively. Despite the low yield, we could obtain enough **4.43** from this reaction to continue the synthesis. As **4.44** and **4.22** are both inexpensive and readily commercially available, the low yield of this reaction could be compensated for by its scalability.

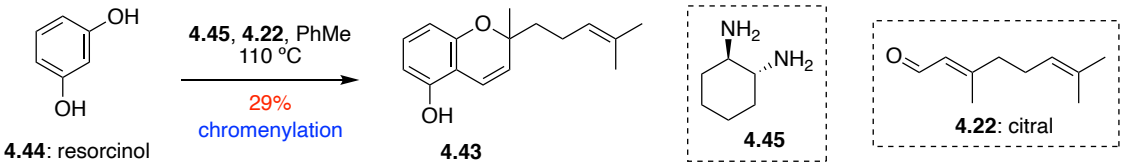

Scheme 4.15: Chromenylation of resorcinol (**4.44**).

With chromene **4.43** in hand, we investigated the oxidation to quinone **4.39** (Table 4.02). Consulting the literature, there are numerous reagents capable of oxidising phenols to quinones.[26] One reagent that is known to readily oxidise phenols to quinones is Frémy's salt (potassium nitrosodisulphonate).[27] Although originally prepared by Frémy[28] in 1845 as the disodium salt, the more effective potassium salt was later prepared by Raschig[29] and is now the favoured and commercially available reagent. As the salt decomposes in aqueous solutions at pH > 10, the reaction is commonly performed in aqueous acetone or alcohol, buffered with phosphate or acetate. Exposure of phenol **4.43** to Frémy's salt following literature conditions of 5% KH_2PO_4 buffer and acetone resulted in no reaction, despite multiple attempts varying temperature and time (entries 1-4).[30] Modifying the buffer to 5% NaOAc also gave no reaction (entries 5 and 6). Attempts to perform the reaction with $PhI(OCOCF_3)_2$ resulted in almost immediate degradation of the starting material (entries 7-9).[31,32] Finally, treatment with $PhI(OAc)_2$ under similar conditions to Claudio[33] and Tapia[34] gave the desired quinone **4.39** in varying yields (entries 10-20). Upon optimisation, it was discovered that halogenated solvents such as $(CF_3)_2CHOH$ and $CHCl_3$, led to degradation of the product if used as reaction solvents or during workup. An increase in yield was also observed when running the reaction in aqueous

THF over aqueous MeCN. Despite many attempts at optimising this reaction and work-up, the outcome was found to be unreliable. Our best yield of 73% (entry 17) was never reproducible under the same conditions, and consequently the yield commonly ranged between 10-30%.

Table 4.02: Attempted optimization conditions for oxidation of **4.43**.

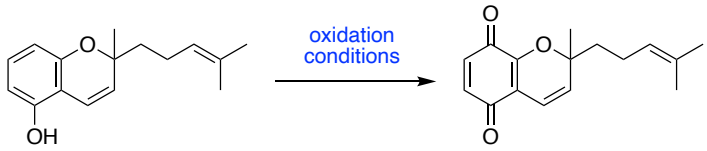

4.43 **4.39**

Entry	Reagent	Solvent	Temperature	Time	Result
1	Frémy's salt[a]	5% KH_2PO_4 buffer/ acetone	0 ºC to rt	2 h	no reaction
2	Frémy's salt[a]	5% KH_2PO_4 buffer/ acetone	rt	3 h	no reaction
3	Frémy's salt[a]	5% KH_2PO_4 buffer/ acetone	rt	20 h	no reaction
4	Frémy's salt[a]	5% KH_2PO_4 buffer/ acetone	60 ºC	20 h	no reaction
5	Frémy's salt[b]	5% NaOAc buffer/ acetone	0 ºC to rt	16 h	no reaction
6	Frémy's salt[c]	5% NaOAc buffer/ acetone	0 ºC to rt	16 h	no reaction
7	$PhI(OCOCF_3)_2$[a]	1:1 MeCN:H_2O	0 ºC	1 h	degradation
8	$PhI(OCOCF_3)_2$[a]	2:1 MeCN:H_2O	0 ºC	5 min	degradation
9	$PhI(OCOCF_3)_2$[a]	2:1 THF:H_2O	0 ºC	5 min	degradation
10	$PhI(OAc)_2$[a]	Et_2O	0 ºC to rt	16 h	no reaction
11	$PhI(OAc)_2$[a]	$CHCl_3$	0 ºC to rt	16 h	degradation
12	$PhI(OAc)_2$[a]	2:1 $(CF_3)_2CHOH$:H_2O	0 ºC	5 min	degradation
13	$PhI(OAc)_2$[a]	1:1 MeCN: H_2O	0 ºC to rt	16 h	**4.39** (15 %)
14	$PhI(OAc)_2$[a]	1:1 MeCN: H_2O	0 ºC	1 h	**4.39** (40 %)
15	$PhI(OAc)_2$[a]	2:1 MeCN: H_2O	0 ºC	5 min	**4.39** (12 %)
16	$PhI(OAc)_2$[a]	2:1 THF: H_2O	0 ºC	20 min	**4.39** (31 %)
17	$PhI(OAc)_2$[a]	2:1 THF: H_2O	-5 ºC to rt	30 min	**4.39** (73 %)
18	$PhI(OAc)_2$[a]	2:1 THF: H_2O	-5 ºC to rt	20 min	**4.39** (48 %)
19	$PhI(OAc)_2$[a]	2:1 THF: H_2O	-5 ºC to rt	40 min	**4.39** (21 %)
20	$PhI(OAc)_2$[a]	2:1 THF: H_2O	-5 ºC to rt	30 min	**4.39** (32 %)

[a] 2 equivalents were used, [b] 3 equivalents were used, [c] 5 equivalents were used.

Our new synthetic route toward naphterpin was beginning to prove more difficult than anticipated, demonstrating low yields and unreliable procedures. At this stage we decided it was once again worth re-evaluating our synthesis of quinone **4.39**. In this retrosynthesis, we

proposed the same chromene intermediate **4.40** as shown in Scheme 4.12, however this time it would be accessed through a two-step procedure. Chromene **4.40** would be synthesised through a thermally-induced cyclisation of propargyl ether **4.46**, which in turn would be synthesised through a Cu-catalysed alkylation of **4.20** with alkyne **4.47**.[35]

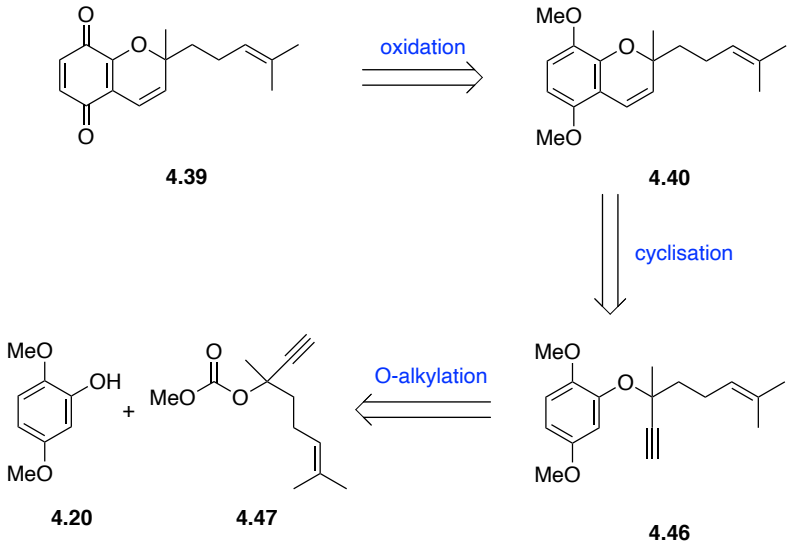

Scheme 4.16: Revised retrosynthetic analysis of quinone **4.38**.

Propargylic carbonate **4.47** was first synthesised in one step from commercially available 6-methyl-5-hept-2-one (**4.48**) (Scheme 4.17).[36] Treatment with Grignard reagent ethynylmagnesium bromide (**4.49**), followed by methyl chloroformate (**4.50**) gave propargylic carbonate (**4.47**) in very good yield.

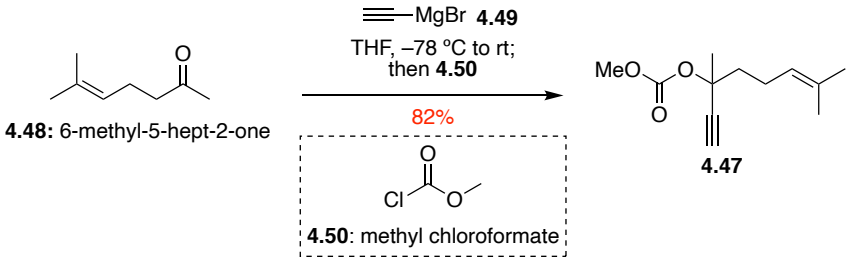

Scheme 4.17: Propargylic carbonate synthesis.[36]

Propargylic carbonate (**4.47**) was coupled with 2,5-dimethoxyphenol (**4.20**), in the presence of DBU and copper(II) chloride[35] to give **4.46**.[37]

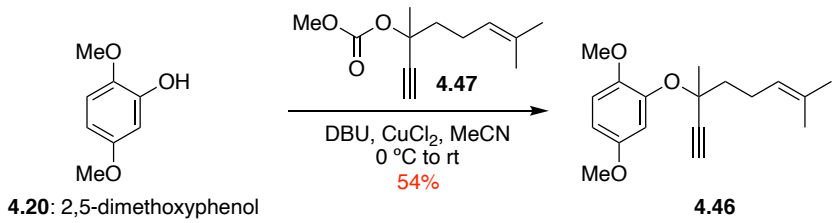

Scheme 4.18: Coupling of propargylic carbonate **4.47** with 2,5-dimethoxy phenol (**4.20**).[37]

Refluxing **4.46** in xylene thermally induced the desired cyclisation to give chromene **4.40**. This cyclisation followed a sequence of aromatic Claisen rearrangement to give *o*-allenyl phenol **4.51**, followed by tautomerisation to **4.52**. A 1,5-hydrogen shift gave *o*-quinone methide **4.42**, which underwent a final oxa-6π-electrocyclisation to give chromene **4.40** in excellent yields.[38]

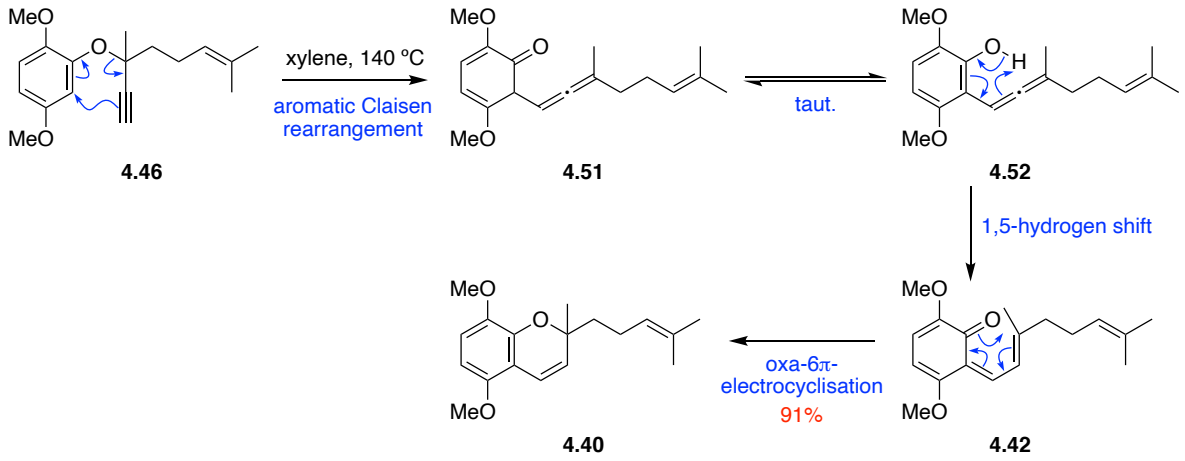

Scheme 4.19: Thermally induced Claisen rearrangement, 1,5-hydrogen shift and oxa-6π-electrocyclisation of **4.46**.

This new method consistently gave chromene **4.40** in ~50% yield over two steps. With a reliable and moderate yielding synthesis of **4.40**, we investigated oxidation conditions to form quinone **4.39**.

Early attempts following Tapia's[39] conditions of AgO in the presence of HNO_3 gave low and inconsistent yields, therefore several different oxidising agents were screened. Our previously successful conditions of $PhI(OAc)_2$ in 2:1 MeCN:H_2O led to degradation. Following literature procedure, attempted oxidation with CAN also led to degradation.[33] Nicolaou and co-workers performed a similar transformation using $PhI(OCOCF_3)_2$ in their synthesis of 1-*O*-methyllateriflorone.[40] Treatment of **4.40** with $PhI(OCOCF_3)_2$ furnished quinone **4.39**, consistently giving over 50% yield (Scheme 4.20).

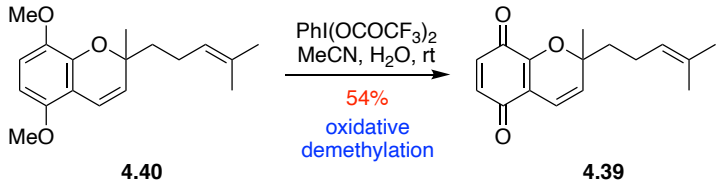

4.40 **4.39**

Scheme 4.20: Oxidation of chromene **4.40** to quinone **4.39**.

4.2.5 Synthesis of 7-demethylnaphterpin

With a reliable synthesis of quinone **4.39**, we finally had substantial quantities to begin investigating the intermolecular Diels-Alder reaction. A similar intermolecular Diels−Alder reaction was implemented by Nakata and co-workers in their total synthesis of napyradiomycin A80915G.[10] In this case, Nakata screened a series of Brassard[41] dienes to identify the most successful diene for the reaction (Scheme 4.21). Under these conditions, it was found that reaction with diene **4.55** was successful, while reaction with all other dienes resulted in decomposition. Tapia took a similar approach is his synthetic study, implementing diene **4.26** to give a dimethoxy protected analogue of 7-demethylnaphterpin.[9]

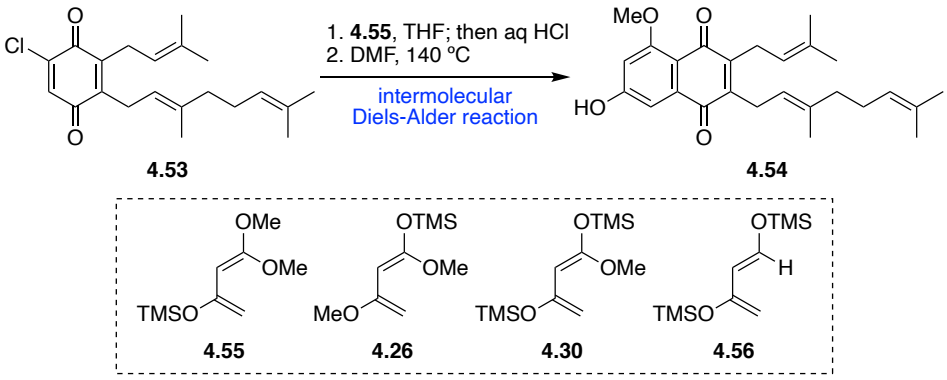

Scheme 4.21: Intermolecular Diels-Alder reaction from Nakata's total synthesis of A80915G.[10]

While producing the correct naphthoquinone scaffold, these examples of intermolecular Diels-Alder reactions yielded either mono- or di-methoxy protected phenols. In our case, we were cautious to generate a methoxy protected phenol, due to previous difficulties with deprotection on similar scaffolds. Encouragingly, consultation of the literature revealed that an intermolecular Diels-Alder reaction between diene **4.30** and quinone **4.57** gave the deprotected naphthoquinone **4.58** in good yield (Scheme 4.22).[42]

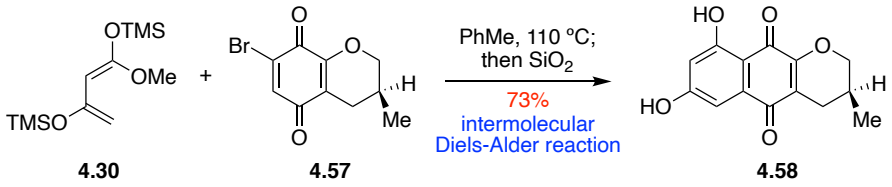

Scheme 4.22: Intermolecular Diels-Alder reaction on quinone **4.57**.[42]

Following the literature synthesis by Brassard[41] and more recently reported by Brimble,[43] diene **4.30** was synthesised in two steps from methyl acetoacetate **4.59** (Scheme 4.23). Methyl acetoacetate **4.59** was treated with NEt_3 and TMSCl to give silyl ether **4.60**, which was then purified by distillation. A second silyl protection was achieved in the presence of LDA to afford

diene **4.30**. Diene **4.30** was found to be unstable at elevated temperatures and was therefore used without further purification in this synthesis.

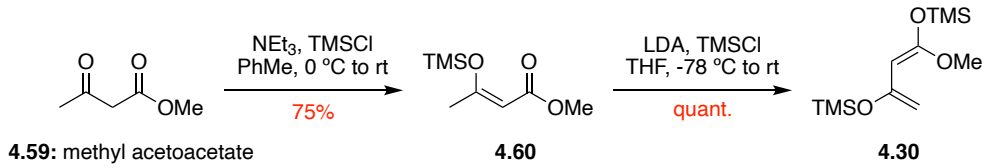

Scheme 4.23: Synthesis of Brassard Diene **4.30**.[41]

With diene **4.30** in hand, we could now investigate our key intermolecular Diels-Alder reaction. A regioselective intermolecular Diels-Alder reaction occurred spontaneously upon addition of diene **4.30** to quinone **4.39** in CH_2Cl_2 at room temperature, giving **4.61**. Subsequent aromatisation gave intermediate hydroquinone **4.62**, which underwent spontaneous aerobic oxidation to afford naphthoquinones **4.63** and **4.38** (Scheme 4.24). Initial TLC analysis showed the formation of only one new product, which after flash chromatography and NMR analysis was revealed to be C-8 hydroxy naphthoquinone **4.38**. Despite having synthesised **4.38**, the low yield raised questions as to the outcome of the remaining material. Significantly increasing the TLC solvent polarity revealed a baseline spot, which after purification by flash chromatography and NMR analysis was revealed to be the C-8 methoxy naphthoquinone **4.63**. Despite attempts to favour production of the C-8 hydroxy naphthoquinone **4.38**, the methoxy protected analogue **4.63** was always the major product under the reaction conditions.

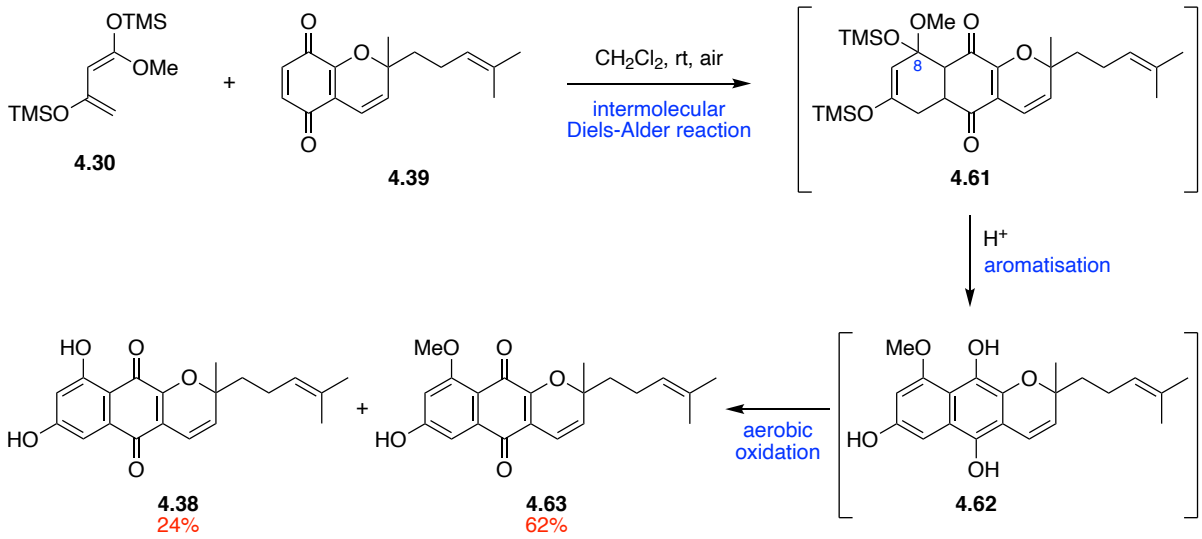

Scheme 4.24: Intermolecular Diels-Alder reaction.

With **4.38** and **4.63** in hand, we first investigated if the deprotected naphthoquinone **4.38** could undergo the same sequence of retro-6π-electrocyclization, alkene isomerisation and intramolecular hetero-Diels-Alder reaction as established for our biomimetic synthesis. Under our previous conditions of catalytic $SnCl_4$ in EtOH at 80 ºC, we were able to afford 7-demethylnaphterpin (**4.19**) in moderate yields.

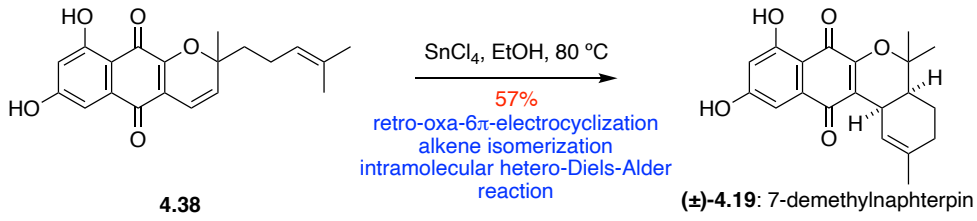

Scheme 4.25: Retro-6π-electrocyclization, alkene isomerisation and intramolecular hetero-Diels-Alder reaction to form 7-demethylnaphterpin (**4.19**).

With the successful synthesis of 7-demethylnaphterpin from **4.19**, we were now determined to employ a similar transformation to convert protected naphthoquinone **4.63** to the natural product **4.19** (Scheme 4.26). The cleavage of aromatic methyl ethers is known to be a difficult

transformation, often requiring the use of strong Lewis acids.[44] As both the methyl ether deprotection and rearrangement had the potential to be Lewis acid catalysed, we anticipated that this reaction could be achieved in one-pot.

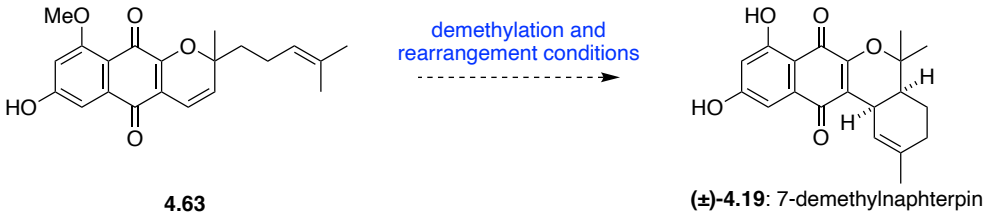

Scheme 4.26: Demethylation of rearrangement of **4.63**.

Attempted reaction conditions for the demethylation and rearragement of **4.63** are outlined in Table 4.03. Given our previous success using $SnCl_4$, we once again employed this reagent. Treatment of **4.63** with $SnCl_4$ at 80 ºC in EtOH resulted in a complex mixture of products (entry 1). Rearrangement to the naphterpin scaffold appeared to occur to some extent under these conditions, however no sign of methyl deprotection had occured. A similar result was observed using $AlCl_3$ (entry 2).

With a lack of success cleaving the aryl methyl ether, we decided to try the more conventional reaction conditions of BBr_3, despite the possibility of side reactions at the alkenes. Predictably, treatment of **4.63** with BBr_3 at room temperature in CH_2Cl_2 resulted in degradation of the starting material after 10 minutes, likely due to undesired side reactions (entry 3). Next we considered Krapcho[45,46] demethylation conditions, involving the use of LiCl in polar aprotic solvent at high temperatures. These conditions were successful for cleaving the aryl methyl ether in our synthesis of merochlorin A,[47] however on substrate **4.63**, these reaction conditions led to decomposition (entry 4).

Table 4.03: Attempted demethylation and rearrangement conditions trailed on **4.63**.

Entry	Reagent	Solvent	Temperature	Time	Result
1	$SnCl_4$	EtOH	80 ºC	1 h	Some rearrangement, no demethylation
2	$AlCl_3$	CH_2Cl_2	0 ºC to rt	25 min	Some rearrangement, no demethylation
3	BBr3	CH_2Cl_2	rt	10 min	decomposition
4	LiCl	DMF	135 ºC	3 h	decomposition
5	MgI_2	DCE	70 ºC	1 h	**4.19** (4%)
6	MgI_2	MeCN	80 ºC	1 h	**4.19** (37%)
7	MgI_2	MeCN	80 ºC	20 min	**4.19** (40%)
8	$MgBr_2{\cdot}OEt_2$	MeCN	80 ºC	4 h	**4.19** (56%)
9	$MgBr_2{\cdot}OEt_2$	MeCN	80 ºC	16 h	**4.19** (45%)
10	$MgBr_2$	MeCN	80 ºC	14 h	**4.19** (59%)

At this stage we decided to investigate Merlic's demethylation conditions using MgI_2 (entries 5-7).[48] These reaction conditions were also employed by Snyder and co-workers as part of their final deprotection steps in the synthesis of napyradiomycin A1.[49] Fortunately, treatment of **4.63** with MgI_2 in DCE at 70 ºC for 1 h gave the desired Lewis-acid-catalysed rearrangement and demethylation product **4.19**, albeit in very poor yield (entry 5). Optimisation of solvent, temperature and time was able to increase this yield to 40% using MgI_2 (entry 7). Further optimisation, exchanging MgI_2 for $MgBr_2$ saw a further increase in yield, giving 7-demethylnaphterpin (**4.19**) in 59% yield (entry 10) (Scheme 4.27).

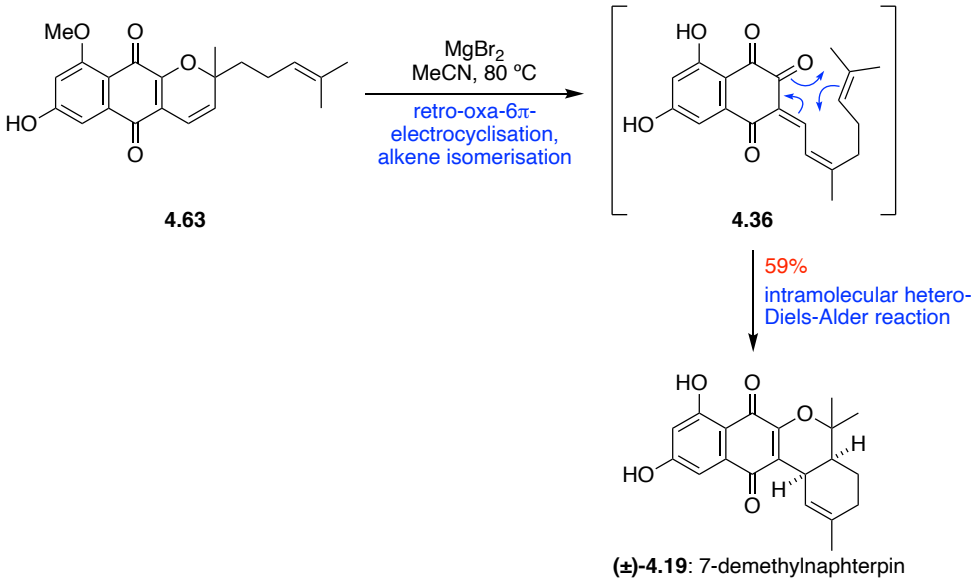

Scheme 4.27: Demethylation and rearrangement with $MgBr_2$.

The ^{1}H and ^{13}C NMR data was found to match perfectly with that of the isolation chemists, alongside the data from our biomimetic synthesis.

At this stage we were interested if late stage oxidation would allow us access to members of the naphthgeranine family, such as **4.64**-**4.67** depicted in Scheme 4.28. Attempted allylic oxidation of **4.19** with SeO_2 in the presence of *t*-BuOOH gave complex mixtures that could not be separated by flash chromatography. To date, we have been unable to successfully access members of the naphthgeranine family *via* allylic oxidations.

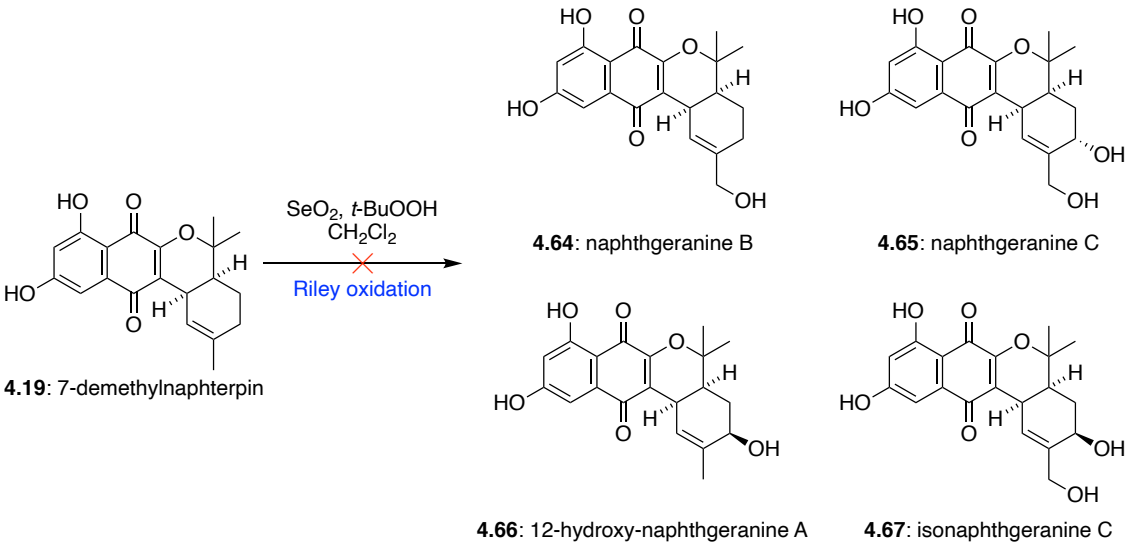

Scheme 4.28: Attempted Riley oxidation of 7-demethylnaphterpin (**4.19**).

4.2.6 Synthesis of Naphterpin

Our newly developed concise synthetic route to 7-demethylnaphterpin (**4.19**), required only five linear steps from commercially available 2,5-dimethoxyphenol (**4.20**). We believed the modular nature of this synthesis, along with the introduction of the late stage intramolecular Diels-Alder reaction, would allow for divergent access to naphterpin (**4.28**) and further oxidised members of the naphterpin family.

With this in mind we set out to complete the first ever synthesis of naphterpin (**4.28**). Following previous literature syntheses, methylated Brassard diene (**4.29**) was synthesised in 3 steps from commercially available methyl acetoacetate (**4.59**) (Scheme 4.29).[50,51] Methylation was performed in neat **4.59**, with the addition of MeI in the presence of K_2CO_3 to give methyl 2-methylacetoacetate (**4.68**). Treatment with TMSCl gave silyl ether **4.69**, followed by a second silylation to give Brassard diene **4.29**. Diene **4.29** was found to be unstable at room temperature and was used immediately without further purification.

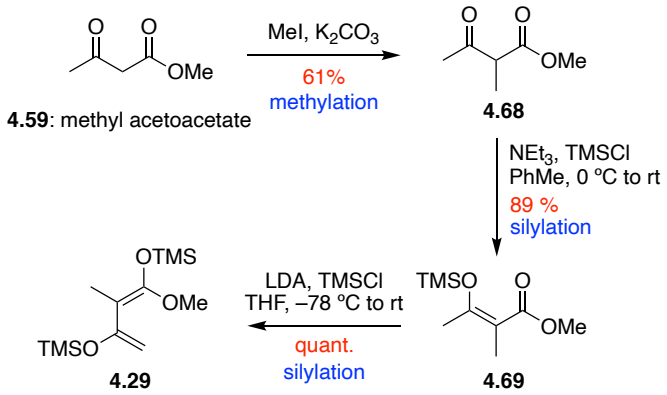

Scheme 4.29: Synthesis of methylated diene **4.29**.[50,51]

With diene **4.29** in hand, we could now attempt the regioselective intermolecular Diels-Alder reaction (Scheme 4.30). Addition of diene **4.29** to quinone **4.39** at room temperature resulted in the formation of two new products by TLC analysis, both with similar R_f values. Upon separation through flash chromatography, NMR analysis of the major and more polar product identified it as the C-8 methoxy intermediate **4.70**. The less polar spot was found to contain the C-8 hydroxy intermediate as part of a complex mixture. Further purification of this mixture was not possible by conventional flash chromatography.

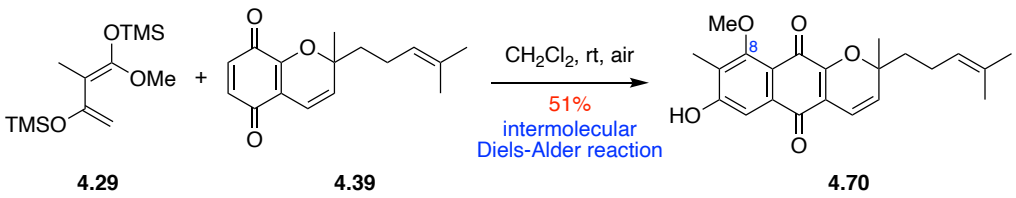

Scheme 4.30: Regioselective intermolecular Diels-Alder reaction.

Under our previously optimised conditions, heating **4.70** with $MgBr_2$ in MeCN induced the desired cascade of retro-6π-electrocyclization, alkene isomerization and intramolecular Diels−Alder reaction to afford naphterpin (**4.28**) (Scheme 4.31). As desired, the C-8 methyl ether was cleaved under the reaction conditions.

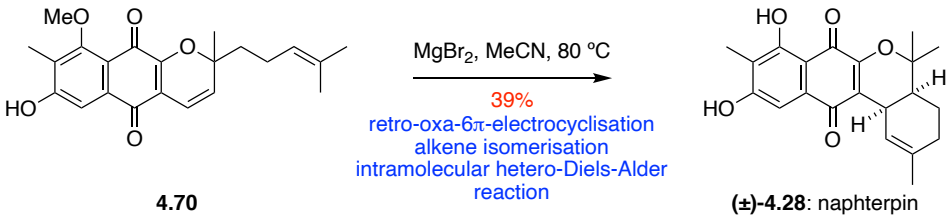

Scheme 4.31: Retro-6π-electrocyclization, alkene isomerization and intramolecular Diels−Alder reaction to afford naphterpin (**4.28**).

A comparison of the NMR data for both the natural[52] and synthetic **4.28** was found to match (Table 4.04), confirming the successful synthesis. This was the first reported synthesis of naphterpin (**4.28**), achieved in 5 steps from commercially available **4.20**.

Table 4.04: ^{1}H and ^{13}C NMR data of natural[52] and synthetic naphterpin (**4.28**) in $CDCl_3$.

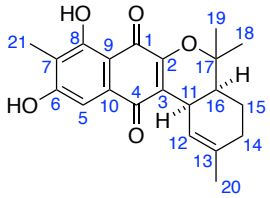

4.28: naphterpin

Position	Natural **4.28**, ^{1}H NMR	Synthetic **4.28**, ^{1}H NMR, 500 MHz	Natural **4.28**, ^{13}C NMR	Synthetic **4.28**, ^{13}C NMR, 125 MHz
1			183.1	183.5
2			153.5	153.2
3			123.3	123.7
4			184.8	184.2
5	7.31	7.18 (s, 1H)	108.4	108.5
6			161.5	160.7
7			117.2	116.8
8			162.6	162.5
9			107.9	107.9
10			131.4	131.8
11	3.47	3.49 (br s)	31.1	31.3
12	6.01	6.06 (d, J = 5.2 Hz, 1H)	120.0	120.3
13			136.1	136.2
14	1.95	2.08 – 1.91 (m, 3H)	29.6	29.8
15	1.25, 1.95	2.08 – 1.91 (m, 3H), 1.34 – 1.27 (m, 1H)	20.4	20.5
16	1.75	1.77 (ddd, J = 12.1, 6.2, 2.8 Hz, 1H)	39.7	39.9
17			80.8	80.7
18	1.51	1.56 (s, 3H),	25.6	25.8
19	1.34	1.34 (s, 3H)	25.1	25.2
20	1.64	1.68 (s, 3H)	23.5	23.7
21	2.15	2.18 (s, 3H)	7.8	7.9
6-OH	8.25	6.46 (1H, s)		
8-OH	12.20	12.29 (s, 1H)		

4.2.7 Synthesis of Naphterpin B and C

With an established 5 step synthesis to naphterpin (**4.28**), we now had access to enough material to investigate some of the more complex, oxidised naphterpin natural products. We envisaged epoxidation of naphterpin (**4.28**) on the $\Delta^{12,13}$-alkene, followed by ring opening would give naphterpin B (**4.71**) and/or C (**4.72**), dependent on the stereoselectivity of the epoxidation. A similar epoxidation on a *cis*-fused meroterpenoid ring system was employed in Snider's synthetic studies toward the bisabosquals, and found to occur with complete exo selectivity.[13,14]

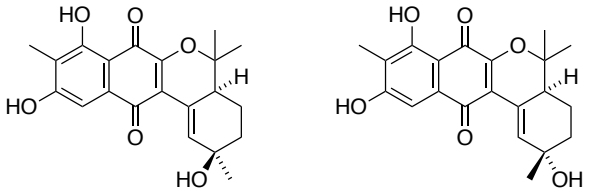

Figure 4.01: Structure of naphterpin B (**4.71**) and C (**4.72**).

The epoxidation of naphterpin (**4.28**) with *m*-CPBA gave a separable 3:1 mixture of endo epoxide **4.73** and exo epoxide **4.74** (Scheme 4.32). The major diastereomer **4.73** resulted from electrophilic attack on the concave face of the $\Delta^{12,13}$ alkene of **4.28**. A similar ratio of endo and exo epoxide products were observed by Brase *et al.* in the epoxidation of an analogous meroterpenoid system.[53]

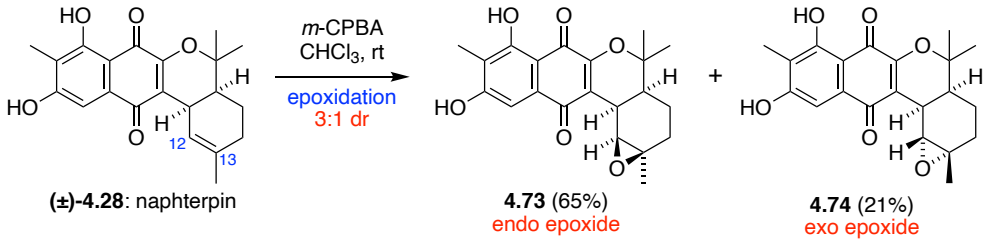

Scheme 4.32: Epoxidation of naphterpin (**4.28**).

To unambiguously assign the major diastereoisomer **4.73**, single-crystal X-ray crystallography was used to confirm the relative configuration (Figure 4.02). Crystals were acquired through vapour diffusion of pentane into $CHCl_3$.

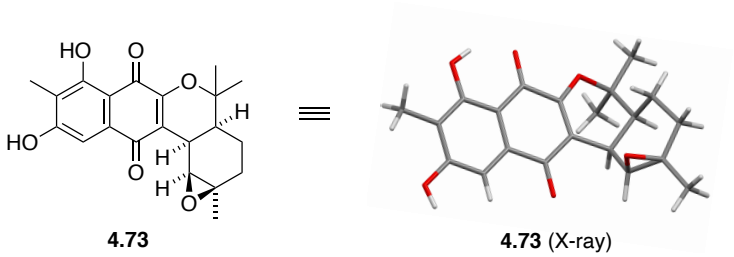

Figure 4.02: X-ray crystal structure of endo epoxide **4.73**.

The minor diastereoisomer **4.74** was confirmed using nuclear Overhauser effect (NOE) data and a comparison of key ^{3}J coupling constants with computational predictions (Figure 4.03). This computational work was perfomed by Dr Thomas Fallon at the University of Adelaide (see Supporting Information, section 4.4.3 for a full presentation of molecular modelling and NMR predictions).

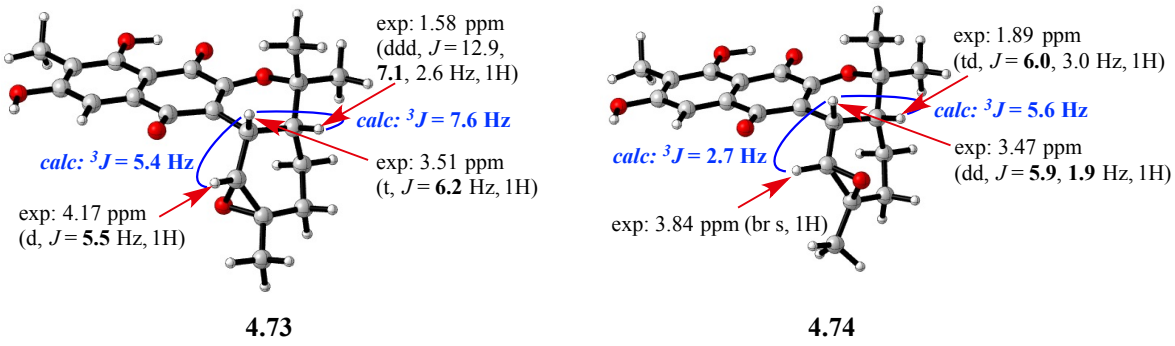

Figure 4.03: Comparison of selected ^{1}H spin-spin coupling constants of compounds **4.73** (left) and **4.74** (right) with experimental data.

With both epoxides successfully synthesised and characterised, both **4.73** and **4.74** were treated with lithium diisopropylamide (LDA). The subsequent ring opening gave naphterpin B (**4.71**)

and naphterpin C (**4.72**), respectively (Scheme 4.33/4.34). This reaction was presumed to proceed through an E1cB mechanism, involving an intermediate *o*-quinone methide enolate, with the retention of the stereochemistry at C-13 (Scheme 4.33). Seto originally assigned the relative configuration of naphterpin C *via* a rotating frame Overhauser enhancement spectroscopy (ROESY) correlation between Me-20 and Me-18.[54]

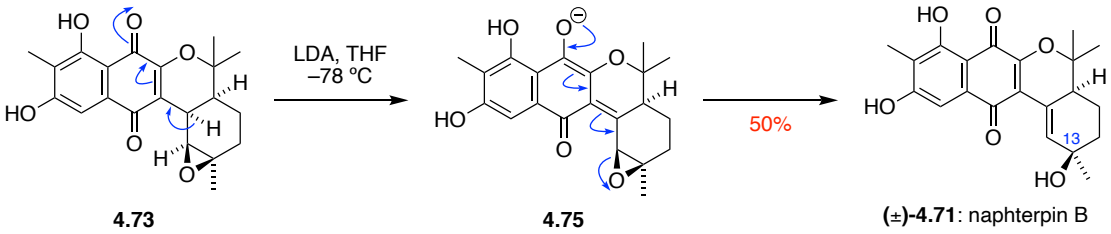

Scheme 4.33: Epoxide ring opening with LDA to give naphterpin B (**4.71**)

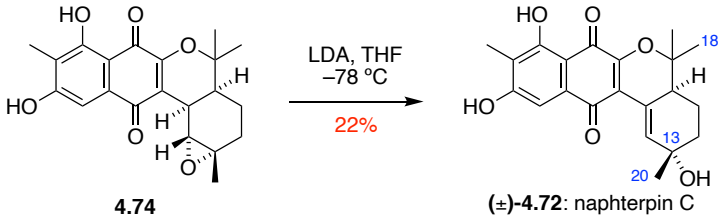

Scheme 4.34: Epoxide ring opening with LDA to give naphterpin C (**4.72**)

Both **4.71** and **4.72** were found to be extremely susceptible to elimination in the presence of acid. Consequently, all $CHCl_3$ and $CDCl_3$ used in isolation and spectroscopy was first treated with K_2CO_3. ^1H and ^{13}C NMR data in $CDCl_3$ for the synthetic naphterpin B (**4.71**) was found to be an excellent match to the natural naphterpin B (**4.71**) as displayed in Table 4.05. Unfortunately, due to instability issues in $CDCl_3$, 1D and 2D NMR experiments of naphterpin C (**4.72**) could not be obtained to a satisfactory standard. As a result, the data of **4.72** was collected in both acetone and DMSO, and a comparison of synthetic naphterpin C (**4.72**) in DMSO to natural naphterpin C in $CDCl_3$ is displayed in Table 4.06.

Table 4.05: ^{1}H and ^{13}C NMR data of natural[54] and synthetic naphterpin B (**4.71**) in $CDCl_3$.

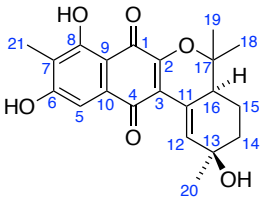

4.71: naphterpin B

Position	Natural **4.71**, ^{1}H NMR	Synthetic **4.71**, ^{1}H NMR, 600 MHz	Natural **4.71**, ^{13}C NMR	Synthetic **4.71**, ^{13}C NMR, 150 MHz
1			182.4	182.5
2			154.5	154.5
3			127.0	127.1
4			183.3	183.4
5	7.16	7.20	108.5	108.5
6			161.8	161.6
7			117.0	117.0
8			162.2	162.3
9			107.9	108.0
10			131.4	131.6
11			116.1	116.2
12	7.46	7.46	135.3	135.5
13			68.5	68.4
14	1.61, 1.95	1.64 – 1.58 (m), 1.98 – 1.92 (m)	35.7	35.8
15	1.61, 1.80	1.64 – 1.58 (m), 1.83 – 1.79 (m)	20.1	20.2
16	2.30	2.35 – 2.28 (m)	42.4	42.4
17			82.4	82.4
18	1.12	1.16 (s)	19.3	19.5
19	1.56	1.57 (s)	26.7	26.7
20	1.52	1.49 (s)	30.7	30.7
21	2.12	2.12 (s)	7.7	7.8
6-OH	N. D.	8.17 (s)		
8-OH	12.2	12.24 (s)		

Table 4.06: ^{1}H and ^{13}C NMR data of natural[54] and synthetic naphterpin C (**4.72**) in $CDCl_3$ and DMSO-d_6, respectively.

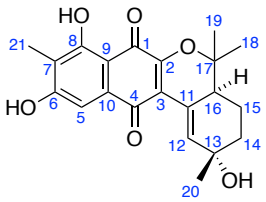

4.72: naphterpin C

Position	Natural **4.72**, ^{1}H NMR	Synthetic **4.72**, ^{1}H NMR, 600 MHz	Natural **4.72**, ^{13}C NMR	Synthetic **4.72**, ^{13}C NMR, 150 MHz
1			181.2	182.1
2			154.2	153.1
3			125.5	122.9
4			183.9	182.6
5	7.10	7.07	107.8	107.4
6			162.3	161.1
7			117.2	115.9
8			162.4	162.9
9			107.3	107.0
10			131.4	131.4
11			115.5	115.4
12	7.23	7.31	137.0	140.0
13			71.6	68.0
14	2.00, 2.08	1.78 – 1.73 (m) 1.66 – 1.60 (m)	37.0	36.7
15	1.24, 2.00	1.88 – 1.83 (m) 1.31 – 1.26 (m)	22.5	22.1
16	2.54	2.35 (ddd, J = 11.1, 6.0, 2.0 Hz, 1H)	41.8	41.9
17			82.2	81.5
18	1.08	1.09 (s)	19.4	19.1
19	1.57	1.45 (s)	27.3	26.0
20	1.36	1.22 (s)	26.2	28.9
21	2.08	2.01 (s)	7.8	7.8
6-OH	N. D.	4.80 (s)		
8-OH	12.0	12.30 (s)		

4.2.8 Synthesis of Marinone Natural Products

After successfully synthesising multiple members of the naphterpin family, we were now interested in extending this synthesis to members of the marinone family. The most achievable target was the simplest member of the marinone family, debromomarinone (**4.76**) (Figure 4.04). Theoretically, this could be achieved by simply substituting the prenyl propargylic carbonate (**4.47**) with a geranyl propargylic carbonate.[55]

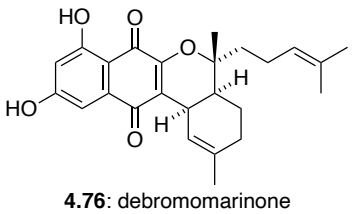

4.76: debromomarinone

Figure 4.04: Structure of debromomarinone (**4.76**).

In order to successfully synthesise the longer propargylic carbonate, we first needed to synthesise (*E*)-geranylacetone (**4.09**), available in two steps from geranyl bromide (**4.77**) (Scheme 4.35).[56] Alkylation of ethyl acetoacetate (**4.78**) with geranyl bromide (**4.77**) gave acetate **4.79**. The crude mixture then underwent saponification with KOH in MeOH, followed by decarboxylation to give (*E*)-geranylacetone (**4.09**) in 65% yield over two steps.

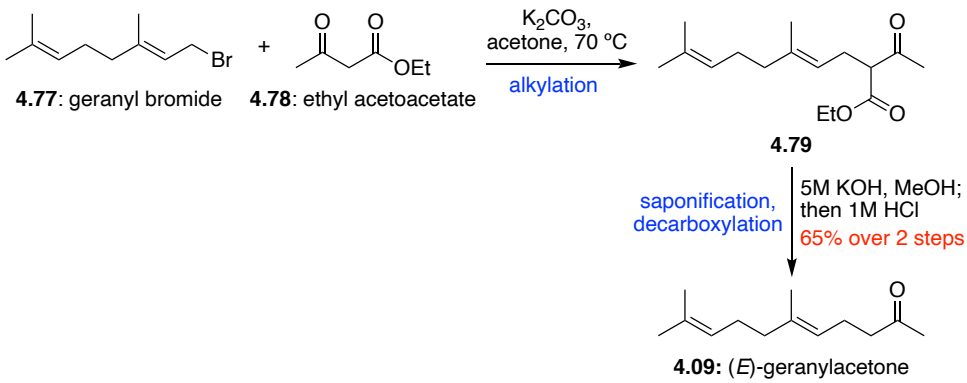

4.77: geranyl bromide **4.78**: ethyl acetoacetate

4.09: (*E*)-geranylacetone

Scheme 4.35: Synthesis of (*E*)-geranylacetone (**4.09**).

With **4.09** now in hand, we could synthesise the desired geranyl propargylic carbonate **4.80** in one step. Treatment of **4.09** with ethynylmagnesium bromide **4.49** followed by methyl chlorofomate **4.50** gave **4.80** in excellent yields (Scheme 4.36).

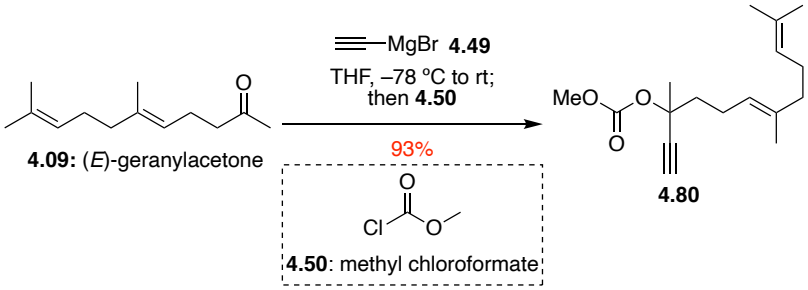

Scheme 4.36: Synthesis of propargylic carbonate **4.80**.[56]

After successfully synthesising the desired carbonate **4.80**, we could now follow our previously established synthesis, coupling **4.20** with **4.80** (Scheme 4.37). Despite a slightly lower yield than observed with the prenyl propargylic carbonate (**4.47**), the reaction proceeded as expected giving propargyl ether **4.81**.

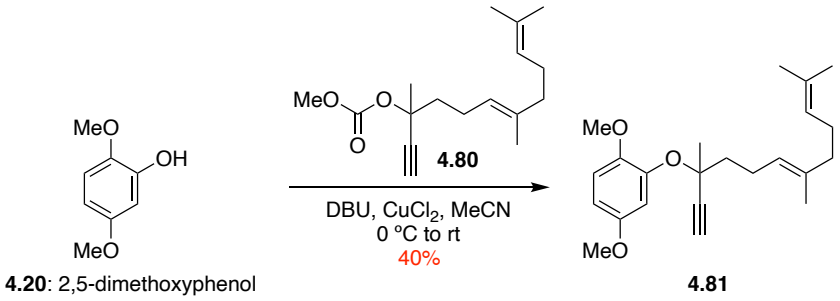

Scheme 4.37: Propargyl ether synthesis.

Heating **4.81** in toluene catalysed the desired thermal aromatic Claisen rearrangement, giving chromene **4.82** in very good yields. Subsequent oxidative demethylation with $PhI(OCOCF_3)_2$ afforded quinone **4.83**, which then underwent a facile intermolecular Diels-Alder reaction with

diene **4.30** to give the naphthoquinone **4.84**. The formation of the C-8 hydroxy naphthoquinone product was also observed from this reaction in 14% yield.

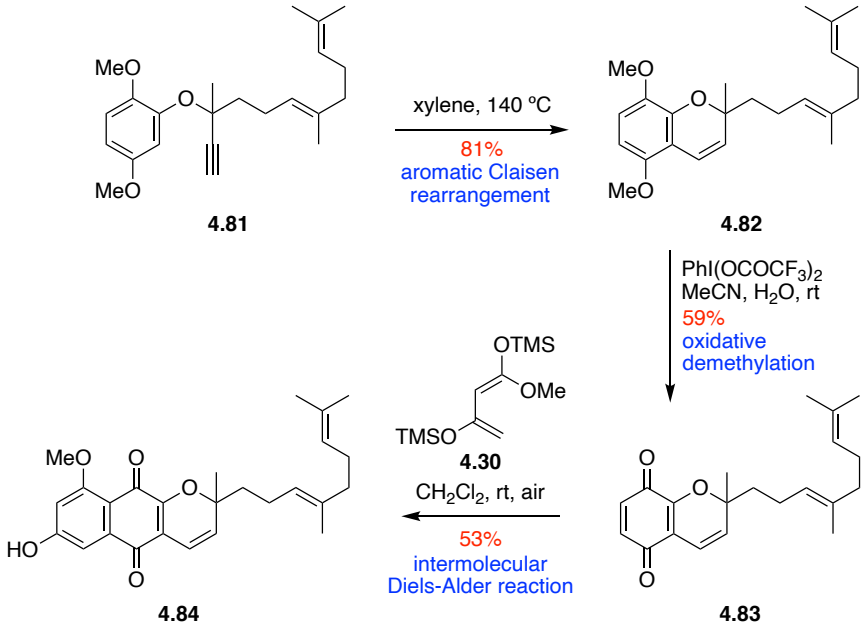

Scheme 4.38: Cyclisation, oxidation and intermolecular Diels-Alder reaction to form **4.84**.

Finally, naphthoquinone **4.84** was subjected to our previous $MgBr_2$ conditions, catalysing our well established cascade of retro-oxa-6π-electrocyclization and the intramolecular hetero-Diels−Alder reaction to afford the natural product debromomarinone (**4.76**) (Scheme 4.39). The ^{1}H and ^{13}C NMR data for **4.76** was found to match that of the isolation chemists, alongside the data from our previous biomimetic synthesis.

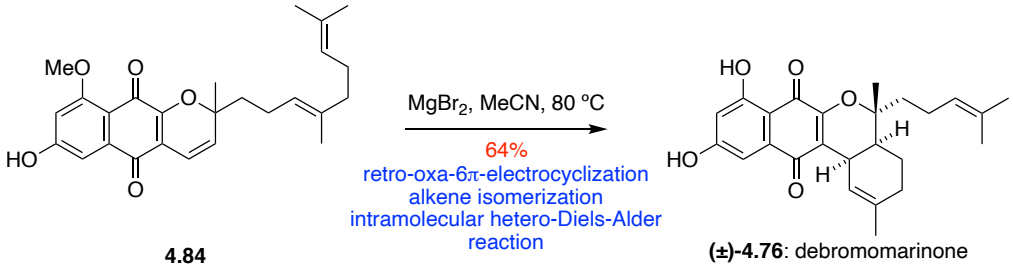

Scheme 4.39: Synthesis of debromomarinone (**4.76**).

With access to significant quantities of debromomarinone (**4.76**), late stage bromination could be attempted to complete the first total synthesis of marinone (**4.85**) and/or isomarinone (**4.86**) (Scheme 4.40).

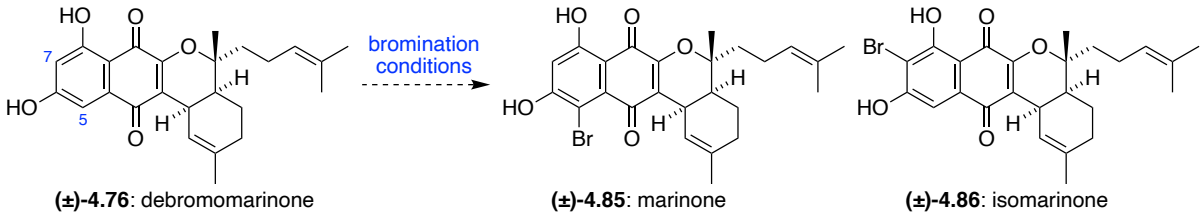

Scheme 4.40: Potential bromination of debromomarinone (**4.86**).

Treatment of debromomarinone (**4.76**) with 1.5 equivalents of *N*-bromosuccinimide (NBS) in CH_2Cl_2 at 0 °C was found to exclusively brominate **4.76** at the C-7 position to afford isomarinone (**4.86**) in 38% yield (Scheme 4.41). Interestingly, no bromination was observed at C-5, and therefore no marinone (**4.85**) was formed during this reaction.

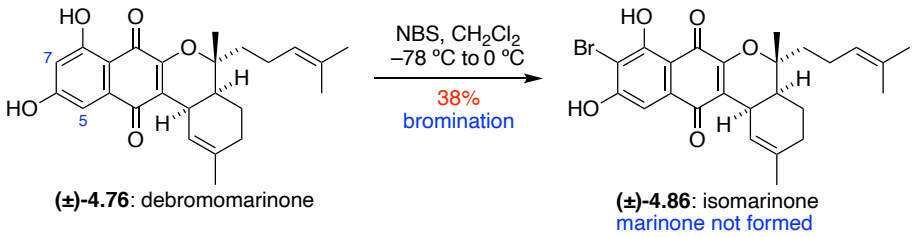

Scheme 4.41: Bromination of debromomarinone (**4.76**) to give isomarinone (**4.86**).

^{1}H and ^{13}C NMR data for our synthetic isomarinone (**4.86**) was found to be an excellent match with that obtained by Fenical[57] of natural isomarinone (**4.86**) (Table 4.07).

Table 4.07: ^{1}H and ^{13}C NMR data of natural[57] and synthetic isomarinone (**4.86**) in DMSO-d_6.

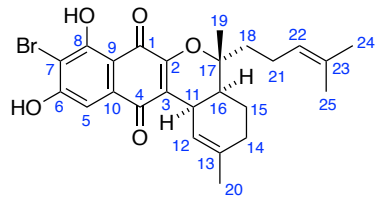

4.86: isomarinone

Position	Natural **4.86**, ^{1}H NMR, 300 MHz	Synthetic **4.86**, ^{1}H NMR, 600 MHz	Natural **4.86**, ^{13}C NMR, 75 MHz	Synthetic **4.86**, ^{13}C NMR, 150 MHz
1			182.0	182.1
2			152.3	152.3
3			123.1	123.1
4			182.4	182.5
5	7.09 (s, 1H)	7.08 (s, 1H)	107.4	107.4
6			161.8	161.9
7			101.7	101.8
8			159.6	159.7
9			107.0	107.1
10			132.1	132.1
11	3.35 (m, 1H)	3.36 - 3.34 (m, 1H)	30.3	30.4
12	5.95 (d, J = 5.0 Hz, 1H)	5.95 (d, J = 5.0 Hz, 1H)	120.1	120.1
13			135.3	135.4
14	1.84 (m, 2H)	2.04 – 1.84 (m, 2H)	29.1	29.2
15	1.87 (m, 1H), 1.18 (m, 1H)	1.93 – 1.84 (m 1H), 1.22 – 1.14 (m 1H)	19.7	19.7
16	1.86 (m, 1H)	1.93 – 1.84 (m, 1H)	36.6	36.6
17			82.4	82.4
18	1.54 (m, 2H)	1.59 – 1.54 (m, 2H)	35.9	36.0
19	1.43 (s, 3H)	1.42 (s, 3H)	21.6	21.6
20	1.61 (s, 3H)	1.61 (s, 3H)	23.3	23.4
21	1.94 (m, 2H)	2.04 – 1.84 (m, 2H)	22.0	22.0
22	5.04 (bt, J = 6.8 Hz, 1H)	5.03 (bt, J = 6.5 Hz, 1H)	123.8	123.8
23			131.1	131.1
24	1.55 (s, 3H)	1.55 (s, 3H)	25.3	25.3
25	1.50 (s, 3H)	1.49 (s, 3H)	17.3	17.3
6-OH	12.11 (s, 1H)	12.09 (s, 1H)		
8-OH	12.54 (s, 1H)	12.54 (s, 1H)		

The original assignment of the isomarinone bromination pattern was confirmed by Heteronuclear multiple bond correlation (HMBC) correlations. In order to confirm the C-7 substitution, we again confirmed the HMBC correlations as shown in Figures 4.04 and 4.05. As observed in Figure 4.05, diagnostic ^{3}J HMBC correlations can be seen between the C-8 hydroxyl proton and the C-1 carbonyl, as well as ^{4}J HMBC correlations between the C-11 proton and the C-4 carbonyl, further confirming the synthesis of isomarinone (**4.86**).

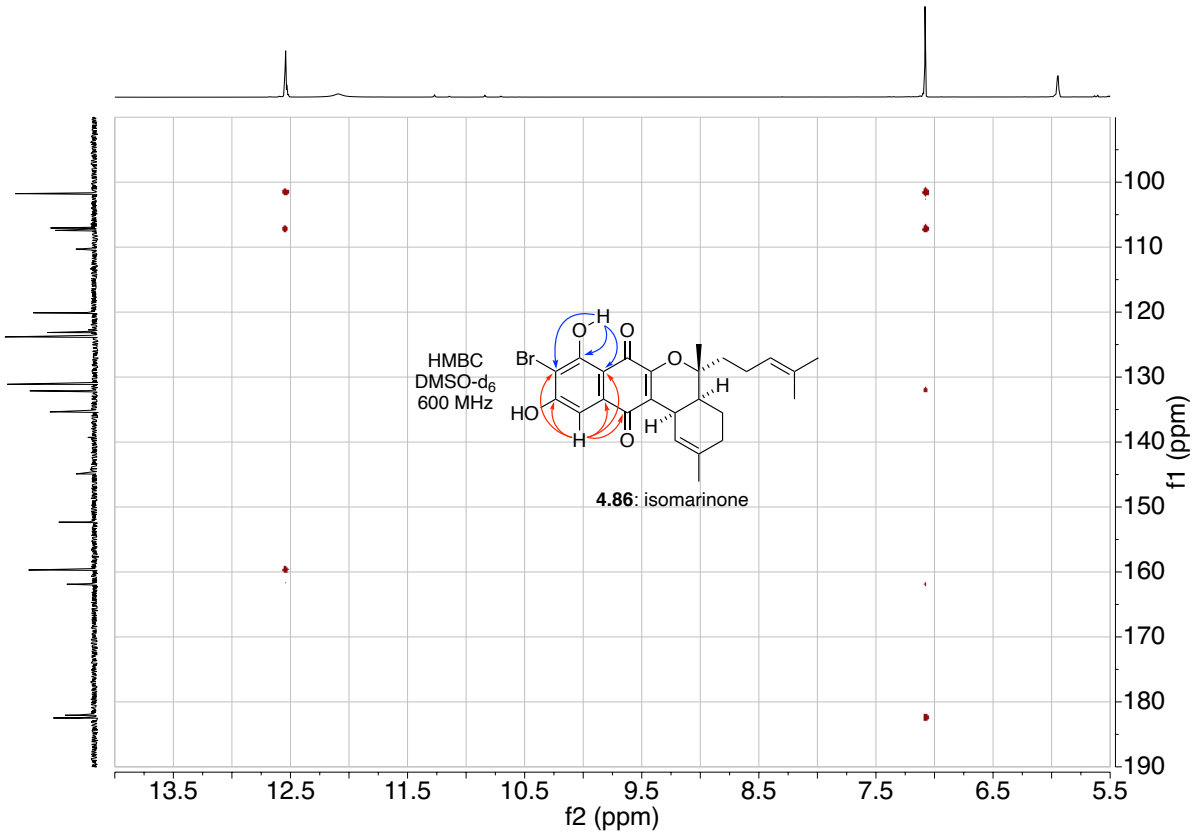

Figure 4.04: HMBC spectrum of isomarinone (**4.86**).

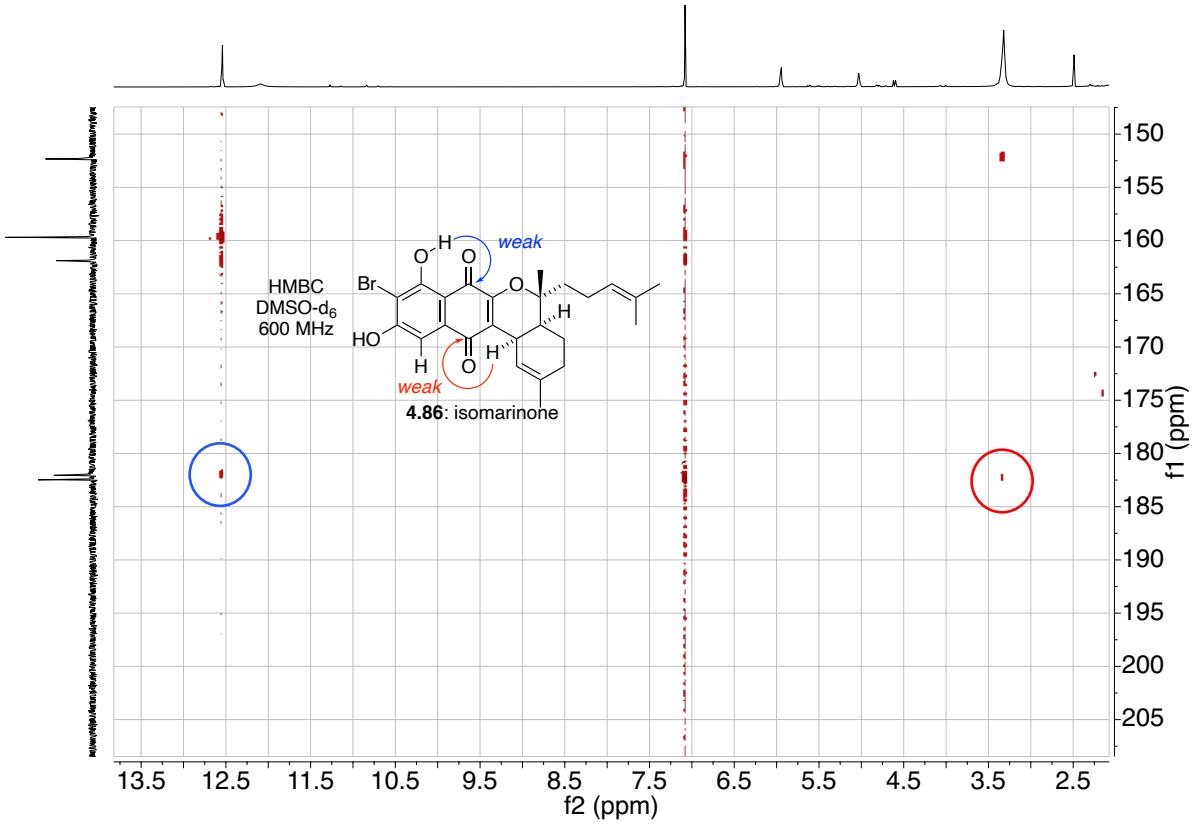

Figure 4.05: HMBC spectrum of isomarinone (**4.86**).

Despite the regioselectivity of this reaction in the flask, it is possible that in nature this reaction occurs under the control of a vanadium-dependent haloperoxidase enzyme. Therefore, marinone (**4.85**) may be formed through an enzyme-controlled selective C-5 bromination of **4.76**. It is also possible that this bromination may occur at an earlier stage in the biosynthetic pathway.

4.2.9 Studies Towards the Synthesis of the Azamerone Phthalazinone Ring

Following our success in accessing members of the naphterpin and marinone families, our curiosity to investigate the biosynthesis of novel meroterpenoid natural products continued. We were particularly interested in a structurally unique natural product from the napyradiomycin family, azamerone (**4.87**), originally isolated from *Streptomyces* sp. CNQ-766.[58] Possessing a phthalazinone ring system, **4.87** is the first example of its kind in a natural product and raises many questions about its unusual biosynthesis. Despite being a member of the napyradiomycin family, its biological activity was found to be quite modest, showing only weak *in vitro* cytotoxicity against murine splenocyte T-cells and macrophages.

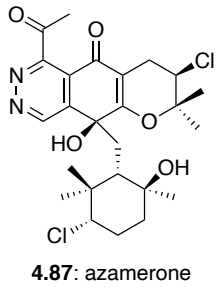

4.87: azamerone

Figure 4.06: Azamerone (**4.87**).

Azamerone (**4.87**) was isolated alongside the diazoketo-functionalised napyradiomycins SF2415A3 (**4.89**) and A80915D (**4.90**), suggesting a common biogenetic pathway (Scheme 4.42). Further feeding experiments with [1,2-$^{13}C_2$]acetate on *Streptomyces* sp. CNQ-766 showed that the bicyclic phthalazinone unit of **4.87** is derived from a symmetrical THN building block, analogous to that of other members of the napyradiomycin family.[59] The C-8 methyl of **4.87** was the only carbon atom not enriched by [1,2-$^{13}C_2$]acetate, however the C-8 methyl was enriched by L-[methyl-^{13}C]methionine (Scheme 4.42). The origin of the diazo group of **4.89**, and the pyridazine of **4.87** was investigated using [^{15}N]nitrite labelling studies, which showed selective incorporation of ^{15}N at the distal diazo nitrogen atom of **4.89**, and at

N-2 of **4.87**. These results suggested that the napyradiomycin diazo group is installed in a stepwise manner *via* nucleophilic attack of an aminonaphthoquinone **4.88** on nitrous acid, strongly implying that **4.89** and **4.90** are the biosynthetic precursors of **4.87**. Finally, feeding studies of biosynthetically prepared and labelled [2-^{15}N, 9-^{13}C]-SF2415A3 (**4.89**) into *Streptomyces* sp. CNQ-766 culture was able to confirm the biosynthetic link between azamerone (**4.87**) and the napyradiomycins. NMR and HPLC-MS analysis of the resultant azamerone (**4.87**) clearly showed ^{13}C enrichment at C-8 and ^{15}N enrichment at *N*-2, thus demonstrating that the pyridazine ring of **4.87** is derived from the diazo group of **4.89**. The mechanism for the conversion of **4.90** to **4.87** is currently unclear. It has been proposed to involve oxidative cleavage of the diazonaphthoquinone ring system of A80915D (**4.90**), followed by a 1,2-shift of the monoterpene unit from C-4 to C-3. The pyridazine ring system is then proposed to form by cyclisation of an intermediate diketone such as **4.91**, followed by aromatisation *via* dehydration and decarboxylation steps to give **4.87**. The uncertainty around both the chemistry and biosynthetic precedent of the final oxidative cleavage and cyclisation steps in the azamerone biosynthesis is something we wished to investigate in more detail.

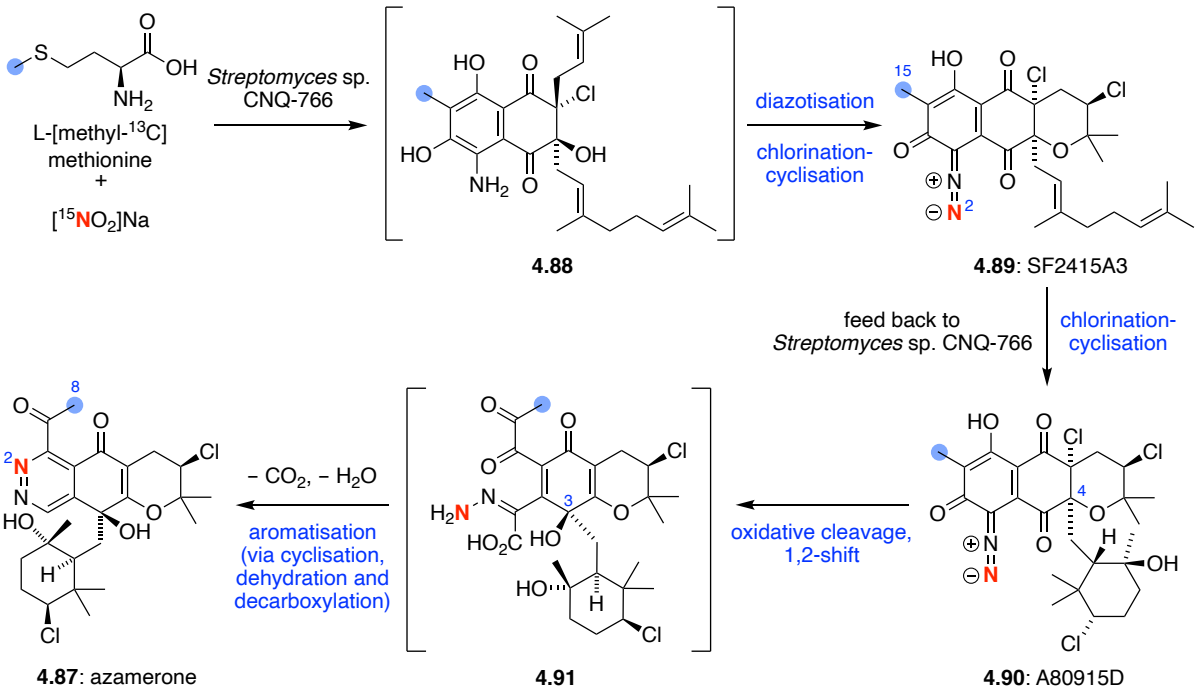

Scheme 4.42: Key labelling studies in the biosynthesis of azamerone (**4.87**).

The first and only total synthesis of azamerone (**4.87**) to date was reported by Burns and co-workers in 2019.[60] This synthesis employed an enantioselective, convergent approach uniting boronic hemiester and quinone diazide coupling partners (Scheme 4.43). The boronic hemiester building block was prepared from geranyl acetate (**4.92**) in four steps. Chlorocyclisation of **4.92** employing Snyder's two-step methodology gave racemic chlorocycle **4.93**. Further resolution of **4.93** using chiral derivatisation with (*S*)-α-methoxyphenylacetic acid gave diastereomeric esters that were separable by flash chromatography. Following ester hydrolysis, **4.93** was obtained in 90% *ee*. Dehydration of **4.93** formed exocyclic alkene **4.94**, which after hydroboration afforded the enantioenriched stable boronic hemiester **4.95**. The quinone diazide building block was synthesised from prenylquinone **4.96** using an enantioselective choroetherification. This reaction was catalysed by a chiral titanium complex derived from ligand **4.97**, affording chloropyran **4.98** in 40% yield and 84% *ee*. Despite the modest stereoselectivity and efficiency of this chloroetherification

reaction, it is to date the closest synthetic equivalent of the NapH4-catalysed chloronium-initiated prenyl cyclisation involved in the biosynthesis of most napyradiomycin natural products. The Burns group methodology therefore has good potential for future applications in the total synthesis of more common members of the napyradiomycin family. *Ortho*-quinone **4.98** was then isomerised to a more stable *para*-quinone under acidic conditions, followed by chlorination and conversion to azide **4.99**. Pd-catalysed coupling of azide **4.99** and boronic hemiester **4.95** gave phenol **4.100**, forming the key C5-C1' bond. Dechlorination, TBS-protection and oxidative dearomatisation of **4.100** then gave *para*-quinol **4.101**, which underwent a spectacular [4+2]-cycloaddition/oxidation cascade with tetrazine **4.102**, catalysed by the bisboron complex **4.103**. Subsequent silyl deprotection under acidic conditions gave (–)-azamerone (**4.86**).

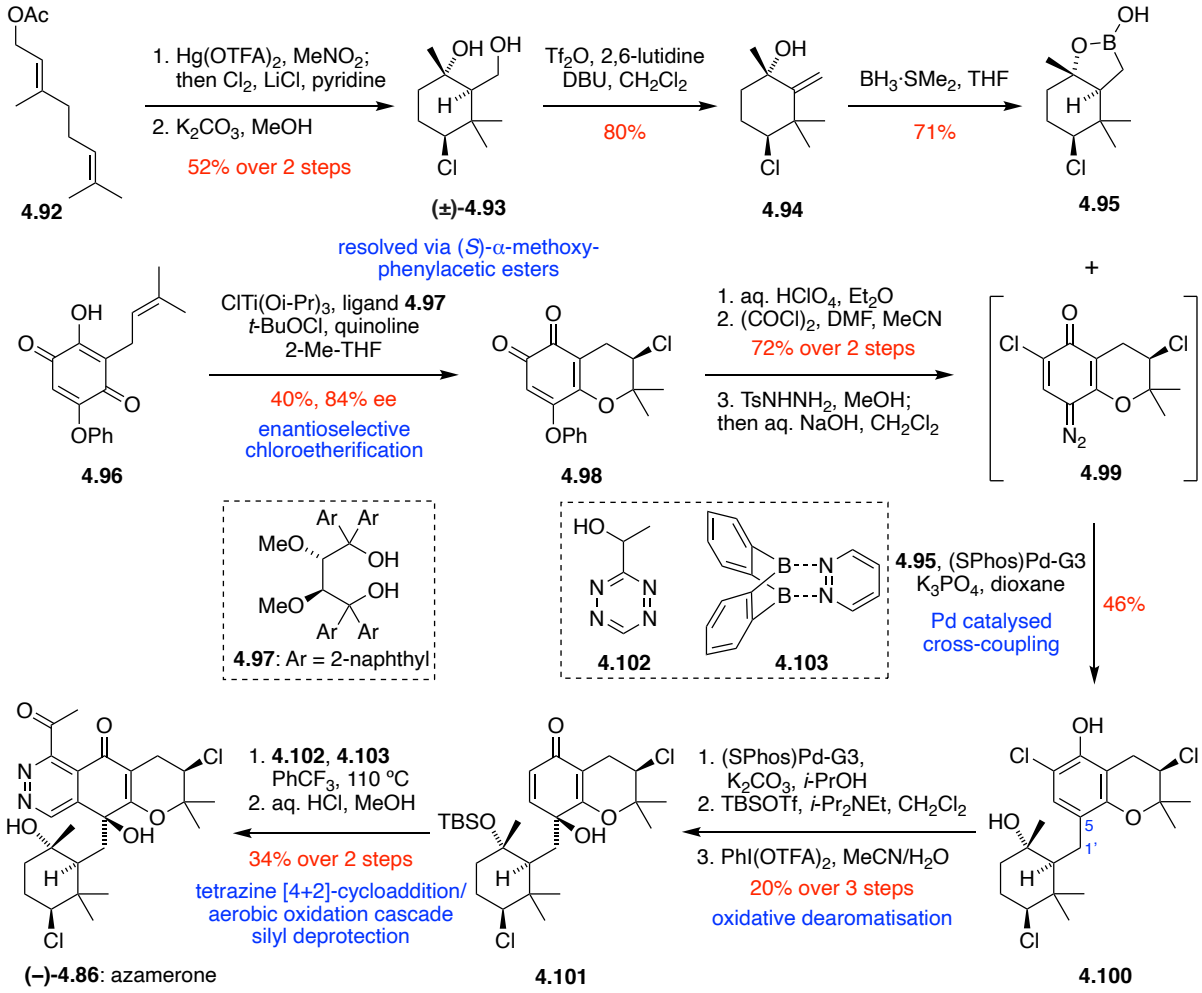

Scheme 4.43: Burns's total synthesis of (–)-azamerone (**4.86**).[60]

In the same year, Gademann[61] and co-workers also published a synthetic approach towards azamerone (**4.86**). This synthesis produced two advanced coupling partners, with the potential to form the azamerone scaffold.

The publication of these two synthetic approaches further indicated the growing interest in the unique structure of this natural product, however the synthesis of **4.86** is yet to be investigated through a biomimetic route. Without access to large quantities of biosynthetic intermediates such as **4.89** or **4.90**, we proposed the use of naphterpin (**4.28**) as a synthetic model system (Scheme 4.44). Although different in the overall scaffold, we envisaged the methylated

naphthoquinone ring of naphterpin (**4.28**) (after diazotisation to **4.104**) would be a great model system for investigation into the proposed oxidative cleavage in azamerone biosynthesis.

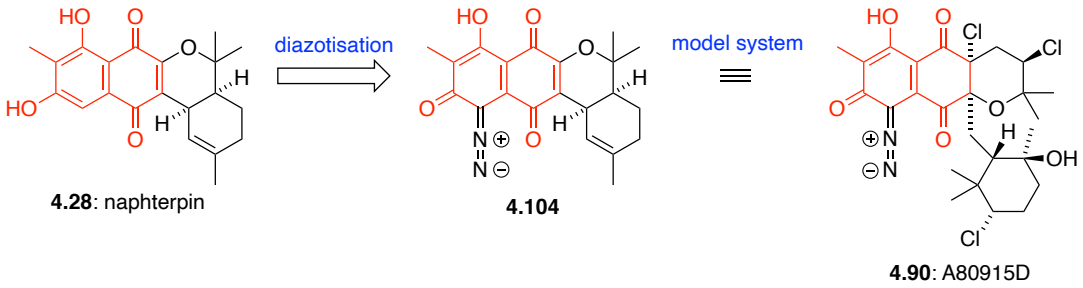

Scheme 4.44: Proposed diazotisation of naphterpin to give **4.104** as a model system of A80915D (**4.90**).

Retrosynthetically, we proposed that the diazotised naphterpin system could be formed in two steps from naphterpin (**4.28**) (Scheme 4.45). Firstly, regioselective amination at C-5 would give aniline (**4.105**), which could then be converted to diazo compound **4.104** under standard diazotisation conditions.

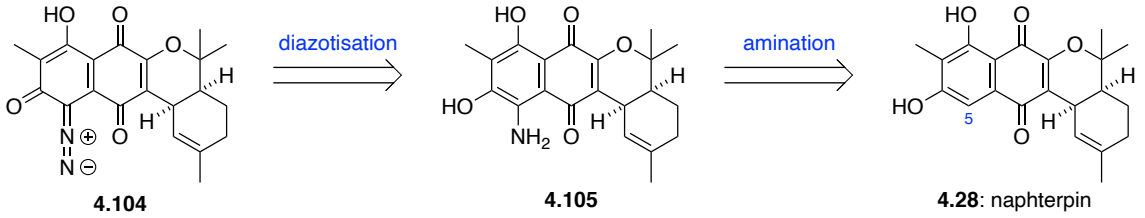

Scheme 4.45: Retrosynthetic analysis of diazonaphterpin (**4.104**) from naphterpin (**4.28**).

With our previously synthesised naphterpin (**4.28**) in hand, we began screening amination conditions. A similar amination had been achieved on the commercially available natural product, emodin (**4.106**) (Scheme 4.46).[62] This synthesis applied an oxidative amination in which substitution of the C-4 hydrogen was achieved using $PhI(OAc)_2$ and the desired amine.

From these studies it was discovered that secondary amines such as piperidine could give the intermediate tertiary amine **4.107**, followed by conversion to 4-amino-emodin (**4.108**) at high temperatures and extended reaction times.

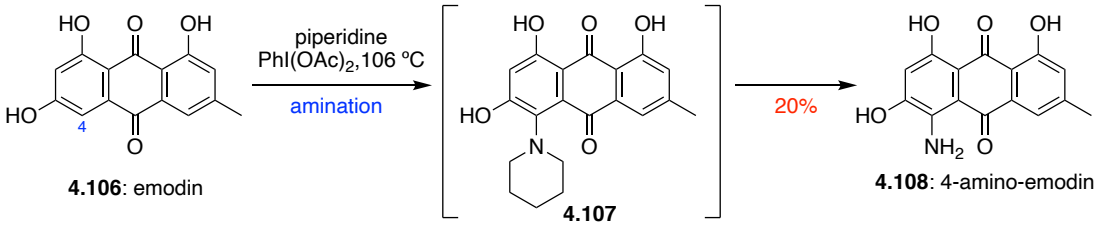

Scheme 4.46: Amination of emodin (**4.106**).[62]

Despite structural similarities between naphterpin (**4.28**) and emodin (**4.106**), attempts to aminate naphterpin under these reaction conditions resulted in no reaction at low temperatures, followed by decomposition at high temperatures. Efforts to oxidatively aminate naphterpin with alternative amines such as allylamine and dimethylamine gave analogous results. Literature precedent suggested amination of naphthoquinones was achievable utilising *O*-alkylhydroxylamines as an alkylating agent in the presence of base NEt_3.[63] Treatment of naphterpin (**4.28**) with *O*-benzylhydroxylamine in the presence of either NEt_3 or K_2CO_3 resulted in decomposition. A similar amination of a naphthoquinone core was reported by Kimpe using NH_4OAc in the presence of acetic acid,[64] however treatment of naphterpin under these conditions resulted in no formation of the desired product, even at high temperatures and extended reaction times.

With no success aminating naphterpin (**4.28**), we decided to investigate the use of the natural product emodin (**4.106**) as a model system. Emodin contains a similar naphthoquinone core to that of naphterpin, but is also commercially available with literature precedent for such an amination (Scheme 4.46). Treatment of emodin (**4.106**) with literature conditions of $PhI(OAc)_2$

in piperidine at reflux for 10 hours gave 4-amino-emodin (**4.108**), in low yields and poor purity. Despite multiple attempts, yields ranged from 4-16% with varying purity. Due to high polarity and poor solubility, **4.108** was difficult to purify by column chromatography. Further attempts to convert 4-amino-emodin (**4.108**) to the desired diazo intermediate (**4.109**) under standard conditions of $NaNO_2$ in the presence of HCl resulted in degradation.

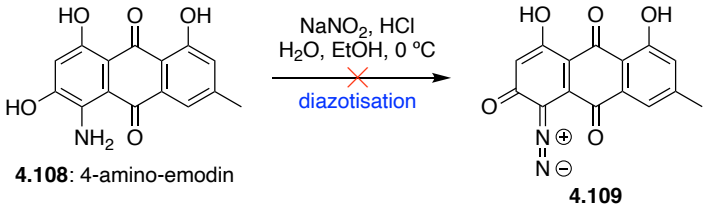

Scheme 4.47: Attempted diazotisation of 4-amino-emodin (**4.108**).

As a result, emodin was not found to be a suitable model system, and we returned our studies to the naphterpin system. Further consultation of the literature revealed a reported amination of naphthoquinone **4.110**, using $HNMe_2$ in EtOH, giving the correct substitution desired for our naphterpin system (Scheme 4.48).[65] We propose that such an amination could occur through a redox driven nucleophilic aromatic substitution mechanism. Attack of secondary amine $HNMe_2$ on phenol **4.110** would form the transient intermediate **4.111**, which following proton transfer would afford **4.112**. Subsequent aromatisation would give hydroquinone **4.113**, which after aerobic oxidation would furnish the observed naphthoquinone structure **4.114**.

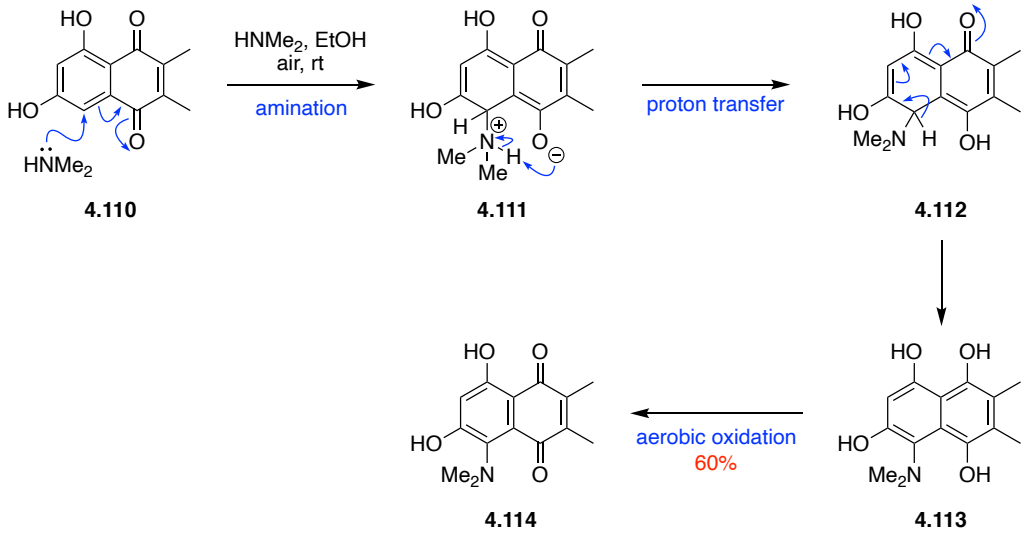

Scheme 4.48: Amination of **4.110**.[65]

Although the free amine was desired for our synthesis, we decided to investigate these amination conditions with the primary amine, methylamine. Treatment of naphterpin (**4.28**) with $MeNH_2$ in EtOH at rt gave **4.115** in a 60% yield (Scheme 4.49). We propose that this reaction would occur following the same mechanism as outlined in Scheme 4.48.

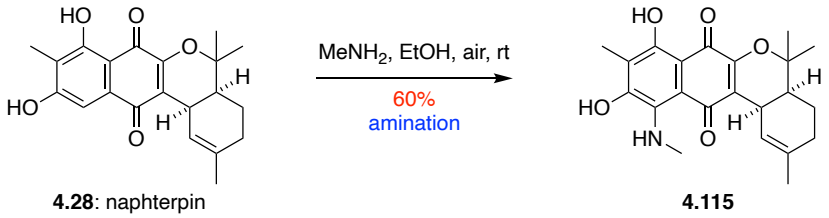

Scheme 4.49: Amination of naphterpin (**4.28**) with methylamine.

After successful amination with a primary amine, we embarked on the same amination using ammonia as the nitrogen source. Addition of a 30% ammonia solution to naphterpin (**4.28**) in EtOH at room temperature resulted in a new minor product after 36 h. Isolation and ^1H NMR analysis confirmed the desired aniline (**4.105**) was formed, however in extremely poor yield.

Multiple attempts to repeat this reaction resulted in only starting material, even at extended reaction times.

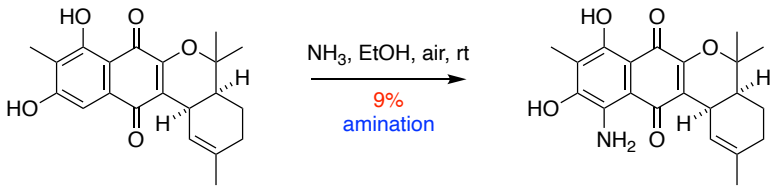

4.28: naphterpin **4.105**

Scheme 4.50: Amination of naphterpin (**4.28**) with ammonia.

Due to the low yields and poor reproducibility of this reaction, we decided to revisit the use of a primary amine. Considering our success with methylamine, we now focused on choosing a small, reactive amine with the potential for future deprotection. Cleavage of allylic C-N bonds can be achieved by many methods,[66] although Pd catalysts are commonly used.[67] Great success has also been observed in literature employing DDQ[68] or Grubbs' carbene.[69,70] With this in mind, we decided to choose the simplest allylic amine for our amination step, allylamine, envisaging future deprotection. The reaction between naphterpin (**4.28**) and allylamine was sluggish at room temperature, leaving mainly starting material. Leaving the reaction for 16-20 hours showed the formation of a more polar spot by TLC analysis. Attempted isolation of this spot gave a complex mixture by NMR analysis, therefore characterisation was inconclusive. Following optimisation of this reaction, we found that heating the reaction to 80 ºC with the addition of K_2CO_3 gave a better conversion to the previously isolated spot. NMR analysis of the product showed the absence of the C-5 hydrogen, however no allyl peaks were observed. Consequently, the structure was determined by ^{1}H, ^{13}C and 2D NMR analysis, HRMS and IR to be the free amine **4.105**. Similar to that observed in Eger's amination of emodin, after amination the allyl group was found to be cleaved under the reaction conditions.[62] Several

further conditions were screened in an attempt to optimise this reaction further, however the best results were still observed using K_2CO_3 in EtOH at 80 ºC for 16 h (Scheme 4.51).

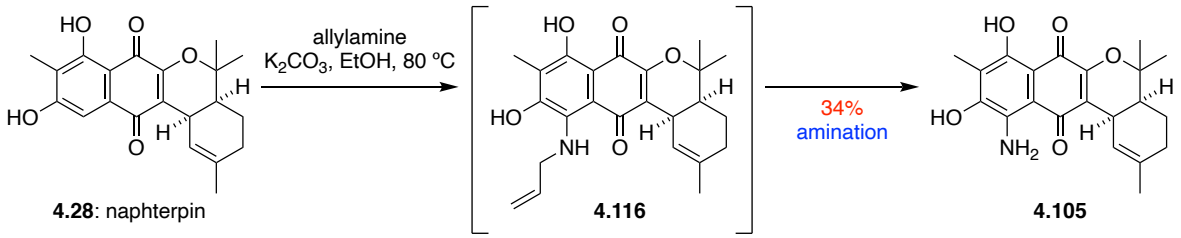

Scheme 4.51: Amination of naphterpin (**4.28**) with allylamine.

Following successful amination, we next attempted acid catalysed diazotisation of **4.105** under standard conditions employing $NaNO_2$ in the presence of HCl (Scheme 4.52).[71] After 30 min, total conversion of the starting material to a single, less polar, product was observed. After isolation, the ^{1}H NMR spectra was slightly shifted from that observed for **4.105**, however further analysis was required to confirm the synthesis of the diazo compound **4.104**. Thankfully, HRMS confirmed the correct mass, while the IR spectrum showed a diagnostic diazo stretch at 2152 cm^{-1}. This stretch is consistent with that observed in diazo containing napyradiomycin natural product SF2415A1, which was reported to have a diazo stretch at 2155 cm^{-1}.[72]

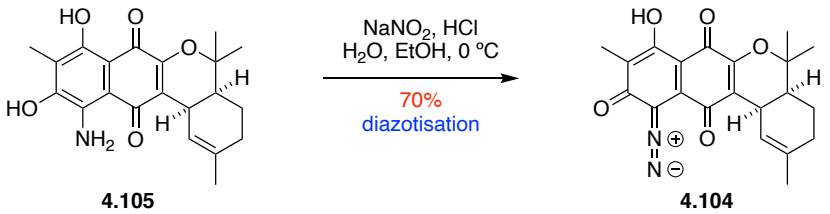

Scheme 4.52: Diazotisation of **4.105**.

With diazo compound **4.104** in hand, we could now begin to investigate oxidation conditions, mimicking that of our proposed azamerone biosynthesis. In order to form the correct left-hand portion of the azamerone scaffold on the naphterpin diazo system, we envisaged a biosynthetic proposal such as that outlined in Scheme 4.53. Mechanistically, we propose oxidation at the C-7 carbon, giving the 1,3-diketone **4.117**. Subsequent nucleophilic attack at the C-6 carbonyl would afford anion **4.118**, followed by cleavage of the C6-C7 bond to give **4.119**. Attack from the newly formed enolate species of **4.120** onto the terminal diazo nitrogen would form **4.121**, followed by protonation to give **4.122**, containing the left hand side of the previously proposed biosynthetic precursor. Subsequent decarboxylation and dehydration would afford **4.123**, containing the pyridazine ring system of azamerone.

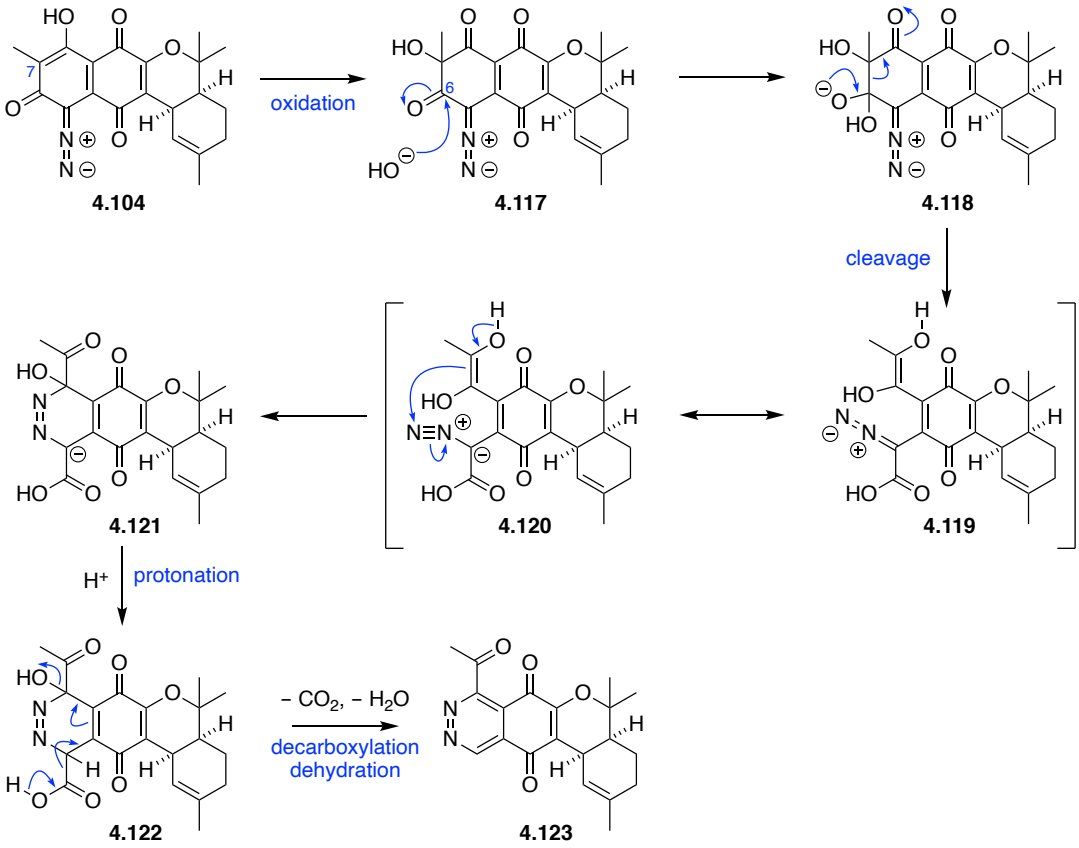

Scheme 4.53: Proposed mechanism for formation of the phthalazinone ring system.

Alternatively, we propose that from the same oxidised intermediate **4.120**, an 8π-electrocyclsation could occur, forming an intermediate 7-membered ring **4.124**. Tautomerisation would give intermediate **4.125**, which is prime to undergo a 1,2-shift, resulting in a ring contraction to form intermediate **4.126**. Tautomerisation to **4.122**, followed by successive decarboxylation and dehydration would afford **4.123**.

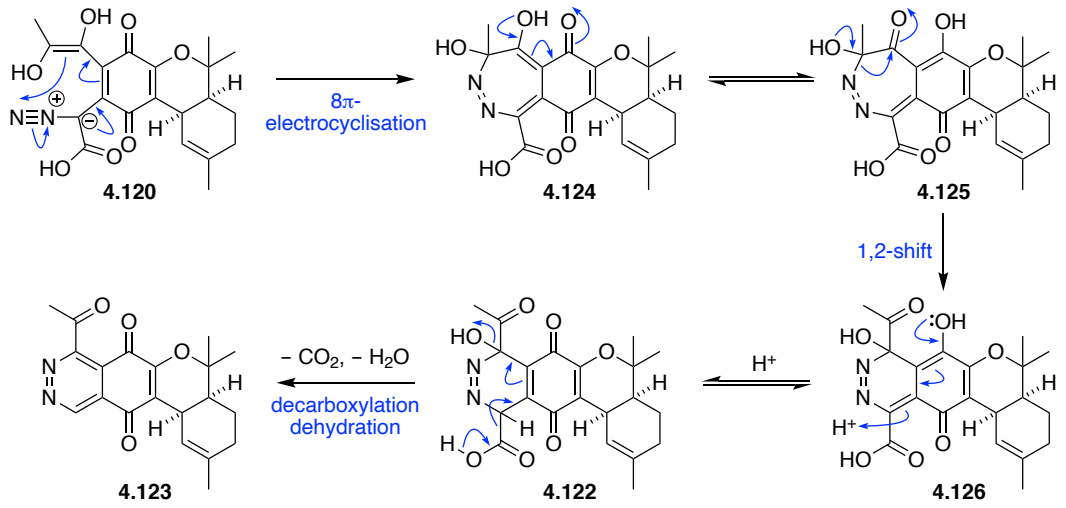

Scheme 4.54: Alternative mechanism for formation of the phthalazinone ring system.

With these proposed mechanisms in mind, we decided to screen a range of oxidants on our newly synthesised diazo naphterpin (**4.104**). Previous biosynthetic proposals have suggested a Baeyer-Villiger-type oxidation of a diazonaphthoquinone intermediate in the biosynthesis of azamerone.[59] Consequently, we decided to try standard Baeyer-Villiger conditions of *m*-CPBA in CH_2Cl_2 for our first oxidation attempt. Treatment of **4.104** with *m*-CPBA at –5 ºC resulted in endo epoxidation at the $\Delta^{12,13}$ alkene, to give **4.127** (Scheme 4.55). Despite the reaction taking place at –5 ºC instead of room temperature, this result mimicked that observed in the synthesis of naphterpin B (**4.71**) (Scheme 4.32). Treatment of the isolated epoxide **4.127** with a further equivalent of *m*-CPBA resulted in no reaction, even at extended reaction times.

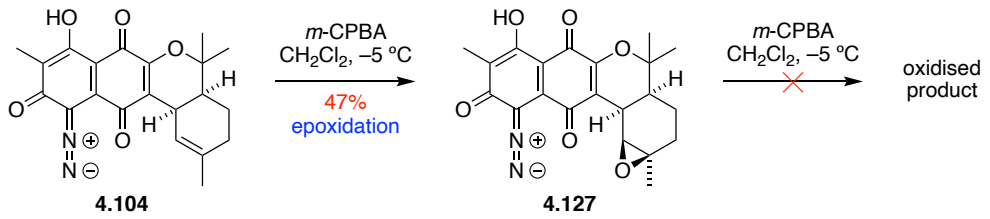

Scheme 4.55: Oxidation of **4.104** with *m*-CPBA.

Following this attempt, further oxidants were screened. Treatment with $Pb(OAc)_4$ resulted in no reaction at rt in $CHCl_3$ or THF. Davis' oxaziridine in the presence of NaHMDS resulted in decomposition of the starting material. $PhI(OAc)_2$ in THF/H_2O resulted in the formation of a new spot by TLC analysis. ^1H NMR of the isolated product showed the absence of the C-8 hydroxy group, however the IR spectrum showed the absence of the diazo peak. As vanadium dependent chloroperoxidases are prevalent in napyradiomycin biosynthesis, we decided to investigate the use of NCS as a chemical equivalent. Treatment of **4.104** with NCS in THF resulted in the formation of two new spots by TLC after 10 min at –78 ºC. These spots were isolated individually by column chromatography, both in approximately 50% yield from the starting material, however upon NMR analysis they were found to interconvert to the same mixture of products. Again, absence of the C-8 hydroxy in the ^1H NMR suggested C-7 chlorination, giving a potential mixture of two epimers (**4.128**). IR analysis showed retention of the diazo functional group, while HRMS found a mass consistent with that of **4.128**.

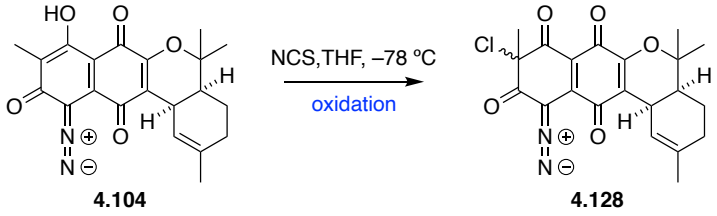

Scheme 4.56: Oxidation of **4.104** with NCS.

Confident of our tentative assignment of **4.128**, we propose a radical mechanism for the interconversion of these individually isolated epimers (Scheme 4.57). In the presence of light, homolytic cleavage of the C-Cl bond could occur, forming tertiary radical **4.129**. Recombination with the free chlorine atom could then occur from either face of the molecule, resulting in a mixture of both epimers.

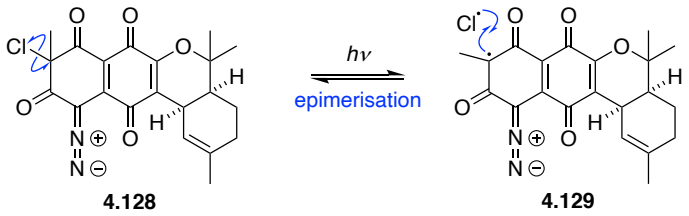

Scheme 4.57: Radical epimerisation of **4.128**.

This mechanism is similar to that observed in our earlier biomimetic synthesis of 7-demethylnaphterpin (Scheme 4.58). Homolytic cleavage of the di-chlorinated 1,3 diketone **4.130** resulted in an analogous tertiary radial **4.131**, which in this case underwent a cascade of 6-*endo*-trig, 5-*exo*-trig to give secondary radical **4.132**. Subsequent chlorine atom abstraction gave the observed side product **4.133**.

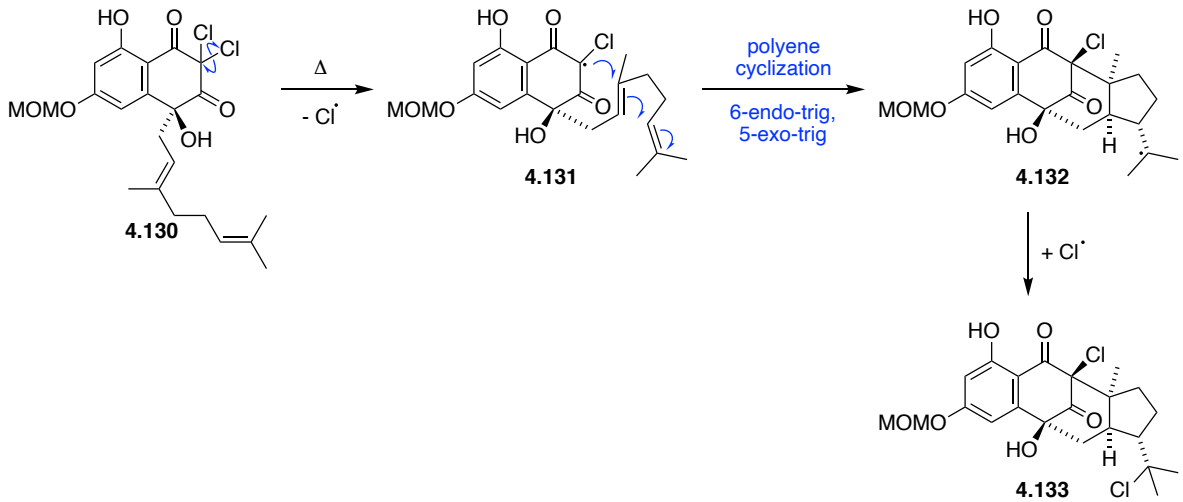

Scheme 4.58: Radical cyclisation and chlorine atom transfer mechanism.

Despite what seemed to be an inevitable interconversion of epimers, we decided to take the mixture through to our next reaction. As proposed in our earlier mechanism, we suggested nucleophilic attack from a hydroxide ion to the C-6 carbonyl. A similar mechanism was proposed by Namboothiri and co-workers in their synthesis of pyrazole rings from chalcones and α-diazo-β-ketoesters (Scheme 4.59).[73] In this mechanism, base catalysed deacylation of α-diazo-β-ketoesters **4.134** occurs through attack of the ethoxide ion, resulting in diazo anion **4.135**, which then undergoes deacylation to **4.136**. 1,3-Dipole intermediate **4.138** can then undergo a [3+2] annulation with chalcone **4.137** to afford pyrazole ketoester **4.139**. Subsequent protonation of the cyclised intermediate **4.139** affords pyrazolidine **4.140**, which can then undergo aromatisation though aerial oxidation to form **4.141**. Subsequent tautomerisation gave the trisubstituted pyrazole ketoester **4.142**.

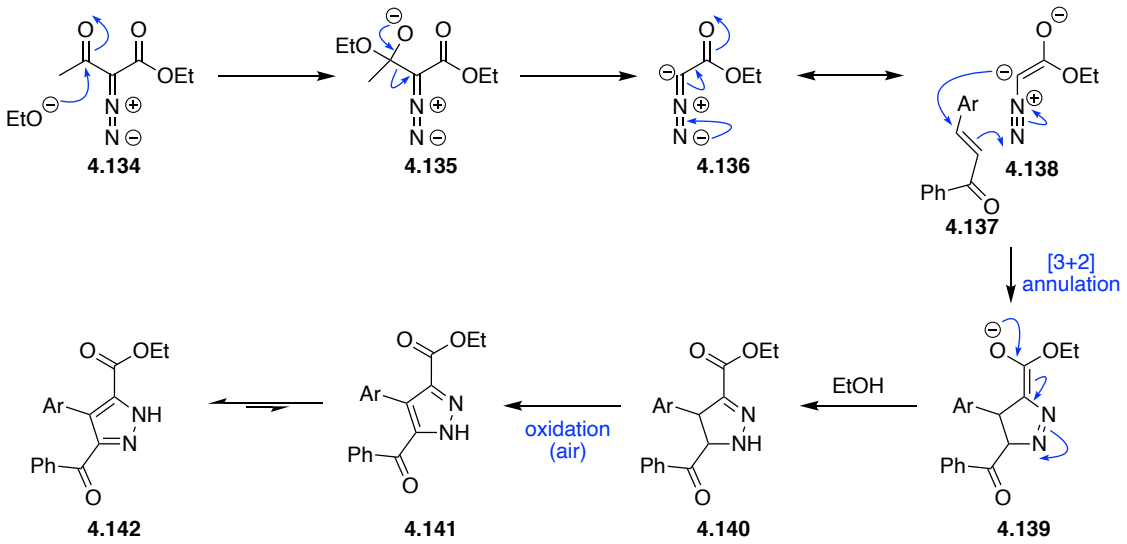

Scheme 4.59: Proposed mechanism to form pyrazole ketoester **4.142**.[73]

In an intramolecular sense, we hoped to catalyse a similar cascade to form our desired pyridazine ring system. Although we were yet to form our desired C-7 hydroxyl diazo naphterpin intermediate **4.117**, we were able to form what we proposed as the C-7 chloro-

intermediate **4.128**. Treatment of **4.128** with NaOH in EtOH at 0 ºC (Scheme 4.60) showed complete conversion to two new compounds by TLC after 10 minutes. Interestingly, NMR analysis showed these two compounds to be diazo naphterpin compound **4.104** and naphterpin **4.28**, with no sign of nucleophilic attack at C-6.

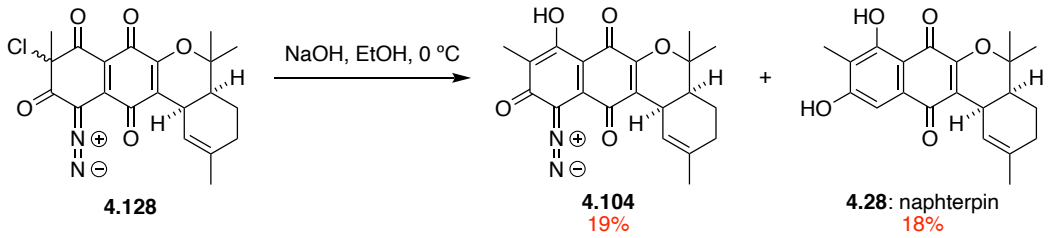

Scheme 4.60: Treatment of **4.128** under basic conditions.

Further investigations into the oxidation of the diazo naphterpin intermediate **4.104** are currently underway. Successful formation of the pyridazine ring on the naphterpin model system would give great insight into the final oxidative rearrangement involved in the biosynthesis of azamerone (**4.87**).

4.3 Conclusions

A concise and modular strategy was developed for the synthesis of the naphterpin and marinone families of natural products from 2,5-dimethoxyphenol (**4.20**) (Scheme 4.61).

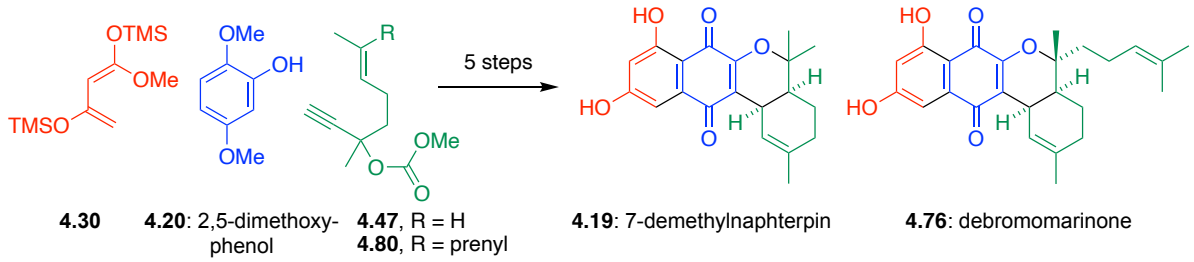

Scheme 4.61: Summary of the modular strategy used in the synthesis of members from the naphterpin and marinone families of natural products

Utilising a plethora of pericyclic reactions, we were able to complete these total syntheses in the absence of protecting group strategies, enabling an efficient synthesis of six meroterpenoid natural products as outlined in Figure 4.07. The total syntheses of both 7-demethylnaphterpin (**4.19**) and debromomarinone (**4.76**) were significantly shortened from 14 steps in our biomimetic syntheses, to just 5 steps in our non-biomimetic syntheses, no longer focused on the synthesis of biosynthetic intermediates. This synthesis produced 7-demethylnaphterpin (**4.19**) and debromomarinone (**4.76**) in 10% and 6% yields, respectively, compared to 0.4% and 0.1% yields in our previous syntheses. This modular approach allowed the first synthesis of naphterpin (**4.28**) to be achieved in 5 steps, and 5% overall yield. Late-stage oxidation and bromination reactions were also investigated, resulting in the first total syntheses of naphterpin B (**4.71**), naphterpin C (**4.72**) and isomarinone (**4.86**).

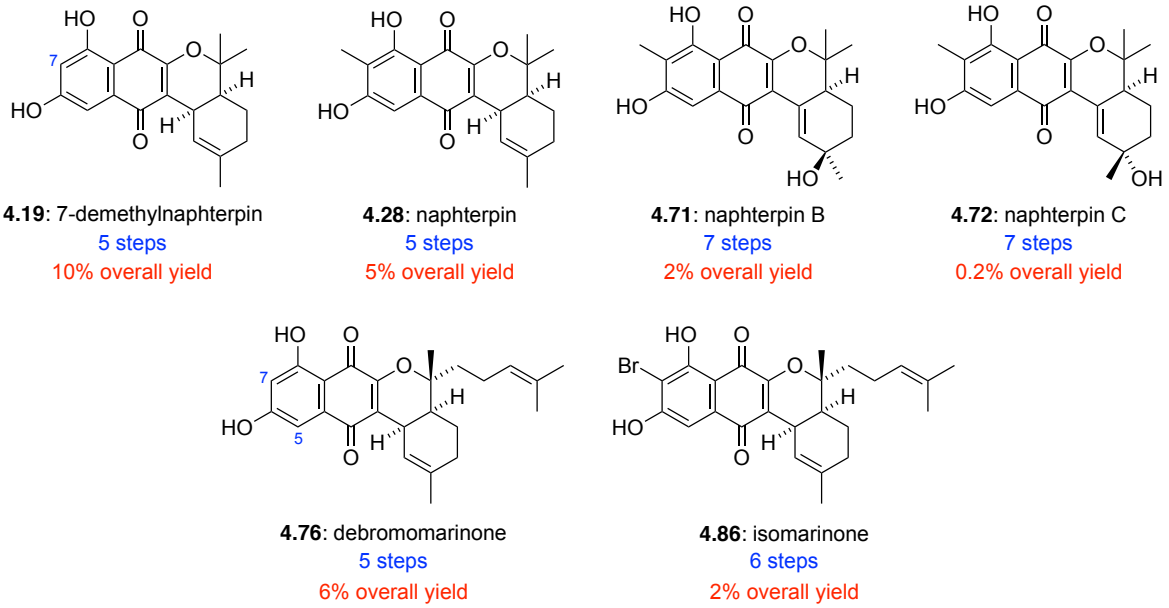

Figure 4.07: Synthesised members of the naphterpin and marinone families of natural products.

The robust nature of this modular approach lends itself to the synthesis of more members within these meroterpenoid families (Scheme 4.62). Further oxidation of 7-demethylnaphterpin (**4.19**) (also isolated as naphthgeranine A) would allow access to other oxidised members of the naphthgeranine family such as naphthgeranine B (**4.64**) and naphthgeranine C (**4.65**). Alongside the already synthesised naphterpin B (**4.71**) and C (**4.72**), additional oxidations of naphterpin could allow access to naphterpin D (**4.143**) and E (**4.144**). Bromination at the C-5 position of debromomarinone (**4.76**) would enable the synthesis of marinone (**4.85**). Additionally, oxidation at the C-13 position of **4.76** would give hydroxydebromomarinone (**4.145**).

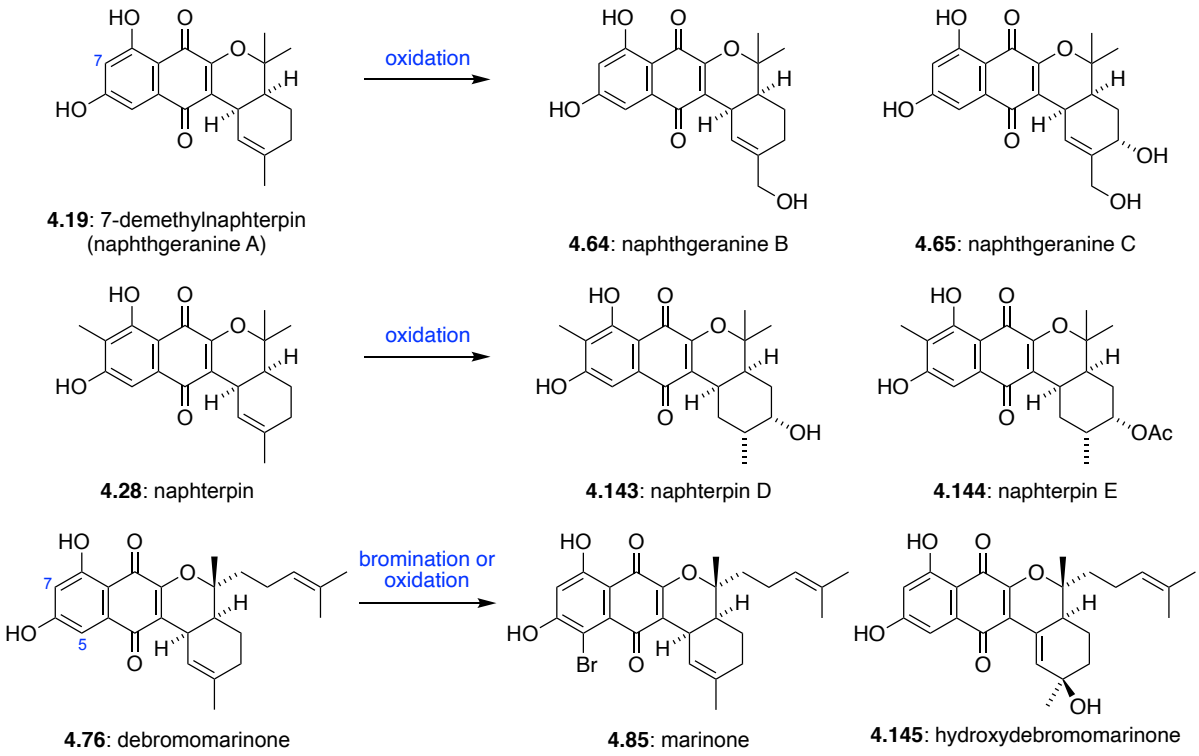

Scheme 4.62: Future oxidation and bromination reactions to access more members of the naphthgeranine, naphterpin and marinone families of natural products.

The successful synthesis of naphterpin (**4.28**) provided a model study scaffold to investigate the biosynthesis of the phthalazinone meroterpenoid natural product, azamerone (**4.87**). Successful amination and diazotisation of the naphthoquinone core enabled us to begin our exploration into the biosynthesis of the unique pyridazine ring (Scheme 4.63).

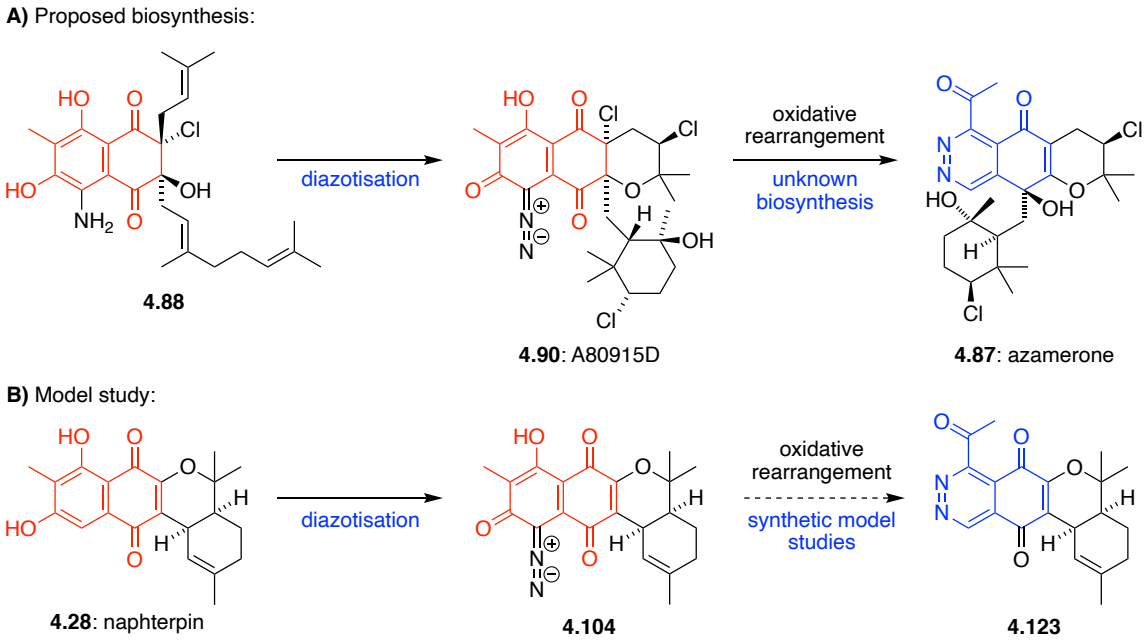

Scheme 4.63: **A)** Proposed biosynthesis of azamerone (**4.87**) from intermediate **4.88**, through known natural product intermediate A80915D (**4.90**). **B)** Model study to investigate the biosynthesis of azamerone analogue **4.123**, starting from synthetic naphterpin (**4.28**).

Synthetic studies allowed for the successful amination and diazotisation of naphterpin (**4.28**) to give diazo intermediate (**4.104**). Further oxidative rearrangement studies are required to determine the oxidative rearrangement involved in the pyridazine ring formation. Success of these studies would give exciting insight into the biosynthesis of the unique meroterpenoid natural product, azamerone (**4.87**).

4.4 Supporting Information

4.4.1 General Methods

All chemicals used were purchased from commercial suppliers and used as received. All reactions were performed under an inert atmosphere of N_2. All organic extracts were dried over anhydrous sodium sulfate. Thin layer chromatography was performed using aluminium sheets coated with silica gel F_{254}. Visualization was aided by viewing under a UV lamp and staining with ceric ammonium molybdate followed by heating. All R_f values were measured to the nearest 0.05. Flash column chromatography was performed using 40-63 micron grade silica gel. Infrared spectra were recorded using an FT-IR spectrometer as the neat compounds. High field NMR spectra were recorded using a 500 MHz spectrometer (^{1}H at 500 MHz, ^{13}C at 125 MHz) or a 600 MHz spectrometer (^{1}H at 600 MHz, ^{13}C at 150 MHz) as indicated. The solvent used for spectra was $CDCl_3$ unless otherwise specified. ^{1}H chemical shifts are reported in ppm on the δ-scale relative to $CDCl_3$ (δ 7.26). and ^{13}C NMR are reported in ppm relative to $CDCl_3$ (δ 77.16). Multiplicities are reported as (br) broad, (s) singlet, (d) doublet, (t) triplet, (q) quartet, (quin) quintet, (sext) sextet, (hept) heptet and (m) multiplet. All *J*-values were rounded to the nearest 0.1 Hz. ESI high-resolution mass spectra were recorded on an ESI-TOF mass spectrometer.

4.4.2 Experimental Procedures

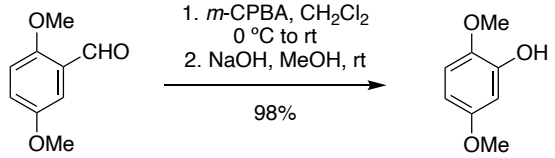

4.34: 2,5-dimethoxybenzaldehyde **4.20**: 2,5-dimethoxyphenol

A solution of 2,5-dimethoxybenzaldehyde (**4.34**) (5.00 g, 30.1 mmol) in CH_2Cl_2 (10 mL) was added dropwise over 15 minutes to a solution of *m*-CPBA (7.00 g, 31.6 mmol) in CH_2Cl_2 (40 mL) at 0 °C. The mixture was then warmed to room temperature and stirred for 16 h. The reaction mixture was quenched with saturated $NaHCO_3$ solution (100 mL). The organic layer was separated, and washed with saturated $NaHCO_3$ solution (4 × 100 mL) and saturated $Na_2S_2O_3$ solution (100 mL). The organic layer was then dried over anhydrous $MgSO_4$, filtered and concentrated *in vacuo*. The resulting yellow residue was dissolved in MeOH and stirred with 10% NaOH (60 mL) for 3 h. The mixture was acidified to pH 1 with 6 M hydrochloric acid and extracted with dichloromethane (3 × 50 mL). The combined organic layers were dried over anhydrous $MgSO_4$, filtered and concentrated *in vacuo*. The residue was purified by flash chromatography (petrol/EtOAc 2:1) to yield **4.20** (4.56 g, 98%) as a yellow oil. Data for **4.20** matched that previously obtained in the literature.[74]

Data for 4.20:

R_f = 0.30 (CH_2Cl_2)

IR (neat): cm^{-1} 3429, 3001, 2938, 2837, 1597, 1506, 1465, 1440, 1282 cm^{-1}.

^{1}H NMR (500 MHz, $CDCl_3$): 6.76 (d, *J* = 8.8 Hz, 1H), 6.56 (d, *J* = 2.9 Hz, 1H), 6.37 (dd, *J* = 8.8, 2.9 Hz, 1H), 5.76 (s, 1H), 3.82 (s, 3H), 3.73 (s, 3H).

^{13}C NMR (125 MHz, $CDCl_3$): δ 154.7, 146.6, 141.1, 111.7, 104.4, 101.9, 56.7, 55.7.

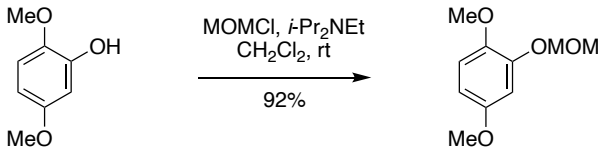

4.20: 2,5-dimethoxyphenol **4.21**

To a solution of 2,5-dimethoxyphenol (**4.20**) (533 mg, 3.46 mmol) in CH_2Cl_2 (30 mL) at room temperature was added MOMCl (0.4 mL, 5.19 mmol) and *i*-Pr_2NEt (1.21 mL, 6.92 mmol). The reaction was stirred at room temperature for 16 h. The reaction mixture was quenched with saturated NH_4Cl solution (30 mL) and extracted with CH_2Cl_2 (3 × 30 mL). The combined organic extracts were washed with brine (100 mL), dried over $MgSO_4$, filtered and concentrated *in vacuo*. The residue was purified by flash chromatography on SiO_2 (neat CH_2Cl_2) to give **4.21** (631 mg, 92%) as a colourless oil.

Data for 4.21:

R_f = 0.75 (20:1, CH_2Cl_2 /MeOH)

IR (neat): 2953, 2834, 1612, 1596, 1465, 1452, 1226 cm^{-1}.

^{1}H NMR (600 MHz, $CDCl_3$): δ 6.82 – 6.80 (m, 2H), 6.49 (dd, *J* = 8.8, 2.9 Hz, 1H), 5.22 (s, 2H), 3.83 (s, 3H), 3.76 (s, 3H), 3.51 (s, 3H).

^{13}C NMR (150 MHz, $CDCl_3$): δ 154.2, 147.4, 144.3, 112.8, 105.8, 104.6, 95.6, 56.7, 56.2, 55.8.

HRMS (ESI): calculated for $C_{10}H_{15}O_4$ 199.0965 $[M+H]^+$, found 199.0935.

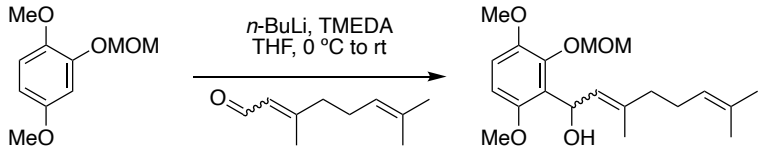

To a solution of **4.21** (634 mg, 3.20 mmol) in THF (60 mL) at 0 ºC was added TMEDA (2.38 mL, 15.98 mmol) and *n*-BuLi (2M in cyclohexane, 8.00 mL, 15.98 mmol). The reaction was stirred at 0 ºC for 45 min prior to the addition of citral (**4.22**) (1.09 mL, 6.39 mmol). The reaction was stirred at 0 ºC for 3 h. The reaction mixture was warmed to room temperature, quenched with saturated NH_4Cl solution (60 mL) and extracted with EtOAc (3 × 50 mL). The combined organic extracts were dried over $MgSO_4$, filtered and concentrated *in vacuo*. The residue was purified by flash chromatography on SiO_2 (10:1 → 4:1, petrol/EtOAc gradient elution) to give **4.23** (844 mg, 91%) as a pale yellow oil.

Data for 4.23:

R_f = 0.10 (4:1, petrol/EtOAc)

IR (neat): 2964, 2837, 1487, 1465, 1256, 1067 cm^{-1}.

^{1}H NMR (600 MHz, $CDCl_3$): δ 6.75 (d, *J* = 9.0 Hz, 1H), 6.61 (d, *J* = 9.0 Hz, 1H), 5.91 – 5.85 (m, 1H), 5.73 – 5.69 (m, 1H), 5.16 – 5.11 (m, 2H), 5.09 – 5.03 (m, 1H), 3.83 (s, 3H), 3.79 (s, 3H), 3.61 (s, 3H), 2.10 – 2.03 (m, 2H), 2.01 – 1.96 (m, 2H), 1.80 (s, 3H), 1.63 (s, 3H), 1.55 (s, 3H).

^{13}C NMR (150 MHz, $CDCl_3$): δ 151.7, 146.8, 144.0, 138.1, 131.5, 127.5, 126.8, 124.2, 111.0, 106.5, 99.5, 64.7, 57.9, 56.3, 56.0, 39.7, 26.5, 25.7, 17.7, 16.6.

HRMS (ESI): calculated for $C_{20}H_{31}O_5$ 351.2166 $[M+H]^+$, found 351.2112.

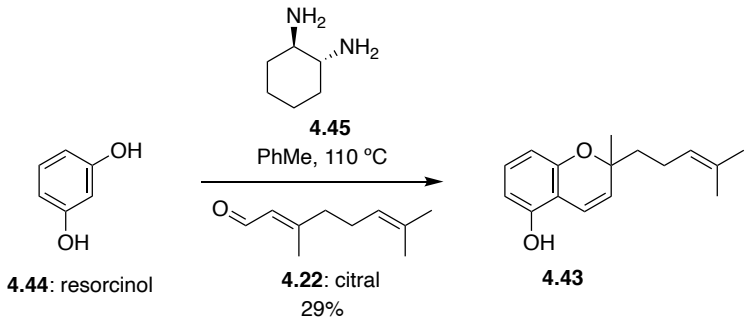

To a solution of resorcinol (**4.44**) (5.00 g, 45.4 mmol) in PhMe (100 mL) was added *R,R*-(–)-1,2-diaminocyclohexane (**4.45**) (518 mg, 4.54 mmol) and citral (**4.22**) (9.32 mL, 54.49 mmol). The reaction was stirred at 110 ºC for 3 h using a Dean-Stark apparatus. The reaction mixture was concentrated *in vacuo*. The residue was purified by flash chromatography on SiO_2 (20:1 → 9:1, petrol/EtOAc gradient elution) to give **4.43** (3.25 g, 29%) as a red oil.

Data for 4.43:

R_f = 0.60 (3:2, petrol/EtOAc)

IR (neat): 3389, 2969, 2924, 1614, 1583, 1505, 1461, 1376, 1291, 1265, 1152 cm^{-1}.

^{1}H NMR (500 MHz, $CDCl_3$): δ 6.94 (t, *J* = 8.1 Hz, 1H), 6.68 (d, *J* = 10.0 Hz, 1H), 6.42 (d, *J* = 8.1 Hz, 1H), 6.29 (d, *J* = 8.1 Hz, 1H), 5.57 (d, *J* = 10.0 Hz, 1H), 5.12 (t, *J* = 6.8 Hz, 1H), 2.20 – 2.09 (m, 2H), 1.77 (ddd, *J* = 13.7, 10.4, 6.3 Hz, 1H), 1.72 – 1.65 (m, 1H), 1.69 (s, 3H), 1.60 (s, 3H), 1.41 (s, 3H).

^{13}C NMR (125 MHz, $CDCl_3$): δ 154.4, 151.4, 131.8, 129.0, 128.4, 124.3, 116.9, 109.6, 109.3, 107.7, 78.4, 41.2, 26.4, 25.8, 22.8, 17.7.

HRMS (ESI): calculated for $C_{16}H_{21}O_2$ 245.1536 $[M+H]^+$, found 245.1551.

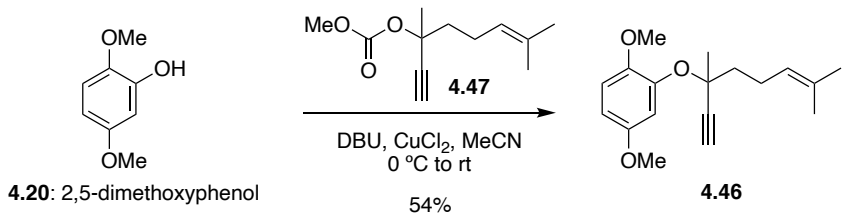

To a solution of **4.20** (250 mg, 1.62 mmol) in MeCN (50 mL) at 0 °C was added DBU (0.32 mL, 2.11 mmol) dropwise, $CuCl_2$ (2 mg, 0.016 mmol) and **4.47**[36,37] (410 mg, 1.95 mmol). The reaction mixture was stirred at 0 °C for 8 h prior to being warmed to rt and stirred for a further 16 h. The mixture was quenched with saturated NH_4Cl solution (50 mL) and extracted with EtOAc (3 × 40 mL). The combined organic extracts were washed with saturated brine (100 mL), dried over anhydrous $MgSO_4$, filtered and concentrated *in vacuo*. The residue was purified by flash chromatography on SiO_2 (9:1 → 4:1, petrol/EtOAc gradient elution) to give **4.46** (252 mg, 54%) as a colourless oil.

Data for 4.46:

R_f = 0.55 (4:1 petrol/EtOAc)

IR (neat): 3284, 2934, 2834, 1609, 1589, 1503, 1442, 1260 cm^{-1}.

^{1}H NMR (500 MHz, $CDCl_3$): δ 7.10 (d, *J* = 3.0 Hz, 1H), 6.81 (d, *J* = 8.8 Hz, 1H), 6.56 (dd, *J* = 8.9, 3.0 Hz, 1H), 5.16 (t, *J* = 7.2, 1H), 3.77 (s, 3H), 3.76 (s, 3H), 2.57 (s, 1H), 2.38 – 2.22 (m, 2H), 1.99 (ddd, *J* = 13.4, 11.4, 5.2 Hz, 1H), 1.87 (ddd, *J* = 13.4, 11.7, 5.3 Hz, 1H), 1.69 (s, 3H), 1.64 (s, 3H), 1.58 (s, 3H).

^{13}C NMR (125 MHz, $CDCl_3$): δ 153.7, 147.4, 145.8, 132.1, 123.9, 113.6, 110.3, 107.9, 85.6, 77.1, 74.9, 56.9, 55.8, 42.5, 26.7, 25.8, 23.4, 17.8.

HRMS (ESI): calculated for $C_{18}H_{24}NaO_3$ 311.1623 $[M+Na]^+$, found 311.1623.

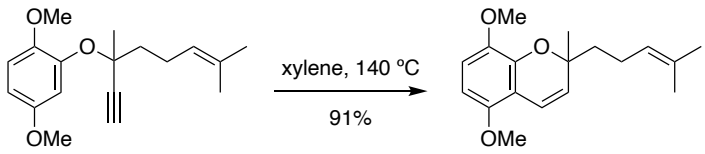

4.46 **4.40**

A solution of **4.46** (4.30 g, 14.91 mmol) in xylene (300 mL) was stirred at 140 ºC for 3 h. The mixture was cooled to room temperature and concentrated *in vacuo*. The residue was purified by flash chromatography on SiO_2 (9:1, petrol/EtOAc) to give **4.40** (3.90 g, 91%) as a yellow oil.

Data for 4.40:

R_f = 0.55 (4:1 petrol/EtOAc)

IR (neat): 2967, 2836, 1491, 1464, 1439, 1386 cm^{-1}.

^{1}H NMR (500 MHz, $CDCl_3$): δ 6.69 (t, *J* = 9.5 Hz, 2H), 6.29 (d, *J* = 8.8 Hz, 1H), 5.55 (d, *J* = 10.1 Hz, 1H), 5.09 (t, *J* = 7.1 Hz, 1H), 3.80 (s, 3H), 3.77 (s, 3H), 2.12 (q, *J* = 7.9 Hz, 2H), 1.86 – 1.77 (m, 1H), 1.71 – 1.63 (overlapping m, 1H), 1.65 (s, 3H), 1.56 (s, 3H), 1.43 (s, 3H).

^{13}C NMR (125 MHz, $CDCl_3$): δ 149.8, 143.4, 143.1, 131.7, 128.4, 124.3, 117.6, 113.1, 111.9, 101.7, 78.4, 57.3, 56.0, 40.9, 26.3, 25.8, 22.9, 17.7.

HRMS (ESI): calculated for $C_{18}H_{24}NaO_3$ 311.1623 $[M+Na]^+$, found 311.1623.

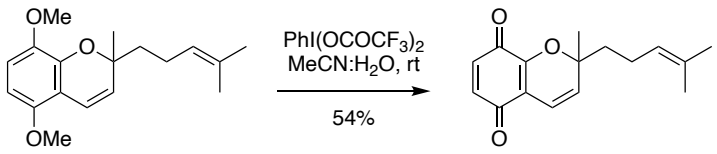

4.40 **4.39**

To a solution of **4.40** (2.09 g, 7.25 mmol) in MeCN:H_2O (120 mL, 2:1 v/v) at room temperature was added $PhI(OCOCF_3)_2$ (6.86 g, 15.9 mmol). The reaction mixture was stirred at room temperature for 5 min. The mixture was quenched with saturated $NaHCO_3$ solution (50 mL) and extracted with EtOAc (3 × 100 mL). The combined organic extracts were washed with H_2O (100 mL) and saturated brine (100 mL), dried over anhydrous $MgSO_4$, filtered and concentrated *in vacuo*. The residue was purified by flash chromatography on SiO_2 (20:1 → 9:1, petrol/EtOAc gradient elution) to give **4.39** (1.01 g, 54%) as a dark red oil.

Data for 4.39:

R_f = 0.40 (4:1 petrol/EtOAc)

IR (neat): cm^{-1} 2971, 2926, 1673, 1646, 1608, 1575, 1448, 1413, 1376, 1335, 1312 cm^{-1}.

^{1}H NMR (500 MHz, $CDCl_3$): δ 6.63 (s, 2H), 6.47 (d, *J* = 10.0 Hz, 1H), 5.58 (d, *J* = 10.1 Hz, 1H), 5.07 (t, *J* = 7.1 Hz, 1H), 2.09 (m, 2H), 1.96 – 1.87 (m, 1H), 1.69 – 1.62 (overlapping m, 1H), 1.65 (s, 3H), 1.56 (s, 3H), 1.48 (s, 3H).

^{13}C NMR (125 MHz, $CDCl_3$): δ 184.4, 181.6, 150.9, 135.9, 134.7, 132.4, 129.3, 123.5, 115.7, 115.4, 83.3, 41.6, 27.6, 25.7, 22.7, 17.8.

HRMS (ESI): calculated for $C_{16}H_{19}O_3$ 259.1334 $[M+H]^+$, found 259.1331.

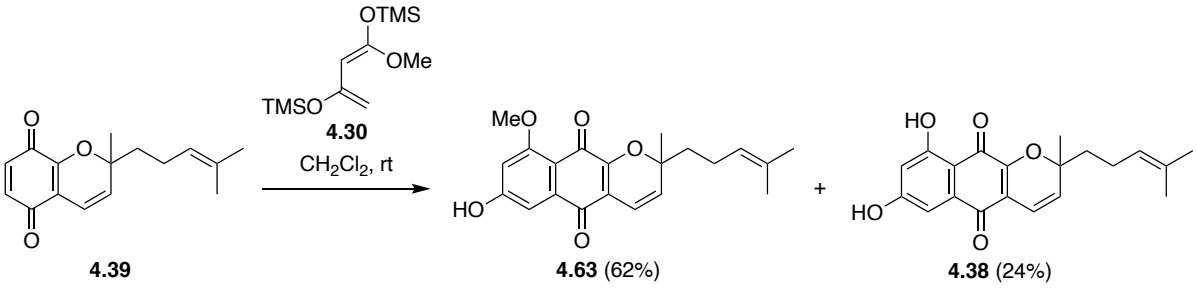

To a solution of **4.39** (132 mg, 0.51 mmol) in CH_2Cl_2 (5 mL) at room temperature was added **4.30**[43] (182 mg, 0.66 mmol). The reaction mixture was stirred at room temperature for 2 h. The mixture was quenched with 1M HCl (10 mL) and stirred at room temperature for 1 h. The mixture was extracted with EtOAc (3 × 5 mL). The combined organic extracts were washed with saturated brine (20 mL), dried over anhydrous $MgSO_4$, filtered and concentrated *in vacuo*. The residue was purified by flash chromatography on SiO_2 (20:1 → 9:1, petrol/EtOAc gradient elution) to give **4.63** (112 mg, 62%) as a red solid and **4.38** (41 mg, 24%) as a red oil.

Data for 4.63:

R_f = 0.10 (3:2 petrol/EtOAc)

IR (neat): cm^{-1} 3237, 2932, 1640, 1584, 1438, 1415, 1347, 1216 cm^{-1}.

^{1}H NMR (500 MHz, $CDCl_3$): δ 7.41 (d, *J* = 2.4 Hz, 1H), 6.76 (d, *J* = 2.4 Hz, 1H), 6.59 (d, *J* = 10.1 Hz, 1H), 5.57 (d, *J* = 10.1 Hz, 1H), 5.04 (t, *J* = 6.3 Hz, 1H), 3.93 (s, 3H), 2.16 – 2.01 (m, 2H), 1.95 – 1.85 (m, 1H), 1.70 – 1.62 (m, 1H), 1.62 (s, 3H), 1.53 (s, 3H), 1.48 (s, 3H).

^{13}C NMR (125 MHz, $CDCl_3$): δ 182.1, 177.7, 163.8, 163.1, 154.6, 135.9, 132.4, 128.5, 123.6, 115.8, 115.4, 112.6, 108.0, 103.9, 83.7, 56.5, 41.7, 27.6, 25.7, 22.8, 17.8.

HRMS (ESI): calculated for $C_{21}H_{23}O_5$ 355.1545 $[M+H]^+$, found 355.1541.

Data for 4.38:

R_f = 0.50 (3:2 petrol/EtOAc)

IR (neat): cm^{-1} 3287, 2969, 2925, 2855, 1614, 1575, 1452, 1400, 1317, 1225 cm^{-1}.

^{1}H NMR (500 MHz, $CDCl_3$): δ 12.01 (s, 1H), 7.26 (d, *J* = 2.2 Hz, 1H), 6.62 (d, *J* = 10.1 Hz, 1H), 6.60 (d, *J* = 2.2 Hz, 1H), 5.63 (d, *J* = 10.1 Hz, 1H), 5.07 (t, *J* = 7.0 Hz, 1H), 2.10 (q, *J* = 7.6 Hz, 2H), 1.97 – 1.90 (m, 1H), 1.70 – 1.65 (m, 1H), 1.63 (s, 3H), 1.55 (s, 3H), 1.51 (s, 3H).

^{13}C NMR (125 MHz, $CDCl_3$): δ 182.6, 181.5, 164.8, 164.1, 153.8, 133.7, 132.6, 129.5, 123.5, 117.5, 115.8, 109.4, 109.2, 108.0, 84.0, 41.8, 27.8, 25.7, 22.8, 17.8.

HRMS (ESI): calculated for $C_{20}H_{21}O_5$ 341.1389 $[M+H]^+$, found 341.1387.

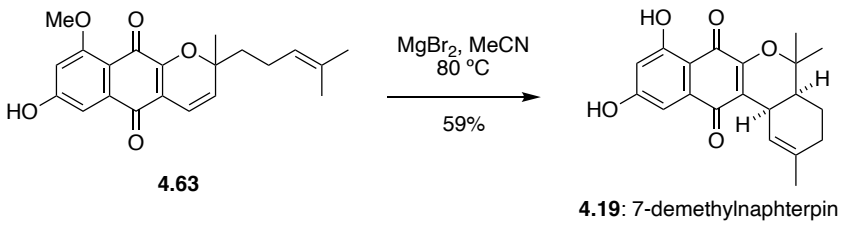

To a solution of **4.63** (35 mg, 0.10 mmol) in MeCN (4 mL) at room temperature was added $MgBr_2$ (91 mg, 0.50 mmol). The reaction was stirred at 80 ºC for 14 h. The mixture was cooled to room temperature, quenched with 1 M HCl (10 mL) and extracted with EtOAc (3 × 10 mL). The combined organic extracts were washed with saturated brine (30 mL), dried over anhydrous $MgSO_4$, filtered and concentrated *in vacuo*. The residue was purified by flash chromatography on SiO_2 (9:1 → 4:1, petrol/EtOAc gradient elution) to give **4.19** (20 mg, 59%) as an orange solid.

Data for 4.19:

R_f = 0.60 (1:1, petrol/EtOAc)

Mp = 255 - 257 °C

IR (neat): 3344, 2921, 1625, 1600, 1572, 1458, 1335, 1285, 1220, 1159, 1126 cm^{-1}.

^{1}H NMR (500 MHz, $CDCl_3$): δ 11.91 (s, 1H), 7.19 (d, *J* = 2.3 Hz, 1H), 6.89 (s, 1H), 6.56 (d, *J* = 2.4 Hz, 1H), 6.03 (d, *J* = 3.8 Hz, 1H), 3.49 (t, *J* = 5.9 Hz, 1H), 1.99 (dd, *J* = 20.7, 6.8 Hz, 2H), 1.93 (dd, *J* = 5.6, 2.2 Hz, 1H), 1.77 (ddd, *J* = 12.1, 6.2, 2.8 Hz, 1H), 1.67 (s, 3H), 1.55 (s, 3H), 1.34 (s, 3H), 1.33 – 1.28 (m, 1H).

^{13}C NMR (125 MHz, $CDCl_3$): δ 184.1, 183.2, 164.6, 153.4, 136.3, 135.0, 123.9, 120.1, 108.9, 108.8, 107.4, 80.9, 39.9, 31.3, 29.9, 29.8, 25.8, 25.2, 23.7, 20.5.

HRMS (ESI): calculated for $C_{20}H_{21}O_5$ 341.1389 $[M+H]^+$, found 341.1388.

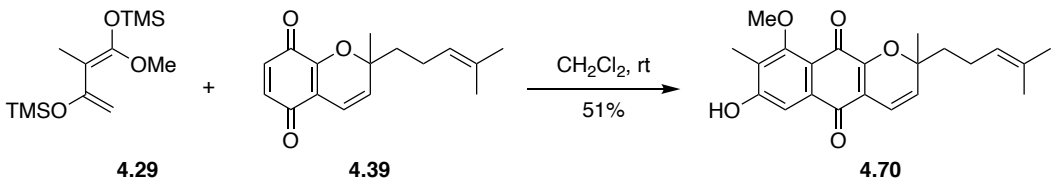

4.29 **4.39** **4.70**

To a solution of **4.39** (916 mg, 3.55 mmol) in CH_2Cl_2 (20 mL) at room temperature was added **4.29**[51] (1.27 g, 4.61 mmol). The reaction mixture was stirred at room temperature for 2 h. A second portion of **4.29** (681 mg, 2.48 mmol) was then added and the reaction was stirred at room temperature for a further 30 min. The mixture was quenched with 1M HCl (20 mL) and stirred at room temperature for 30 min. The mixture was extracted with EtOAc (3 × 40 mL). The combined organic extracts were washed with saturated brine (150 mL), dried over anhydrous $MgSO_4$, filtered and concentrated *in vacuo*. The residue was purified by flash chromatography on SiO_2 (20:1 → 9:1, petrol/EtOAc gradient elution) to give **4.70** (667 mg, 51%) as a dark orange solid.

Data for 4.70:

R_f = 0.20 (4:1 petrol/EtOAc)

Mp = 132 - 134 °C

IR (neat): 1362, 2928, 1625, 1573, 1436, 1332, 1281, 1248 cm^{-1}.

^{1}H NMR (500 MHz, $CDCl_3$): δ 8.65 (s, 1H), 7.72 (s, 1H), 6.60 (d, *J* = 10.1 Hz, 1H), 5.60 (d, *J* = 10.1 Hz, 1H), 5.05 (t, *J* = 7.0 Hz, 1H), 3.89 (s, 3H), 2.25 (s, 3H), 2.15 – 2.07 (m, 2H), 1.96 – 1.89 (m, 1H), 1.72 – 1.64 (m, 1H), 1.62 (s, 3H), 1.54 (s, 3H), 1.50 (s, 3H).

^{13}C NMR (125 MHz, $CDCl_3$): δ 182.6, 177.8, 161.4, 161.2, 154.3, 132.5, 132.4, 128.7, 125.8, 123.5, 116.8, 115.7, 115.5, 110.6, 83.8, 61.3, 41.7, 27.7, 25.7, 22.8, 17.8, 9.0.

HRMS (ESI): calculated for $C_{22}H_{25}O_5$ 369.1702 $[M+H]^+$, found 369.1700.

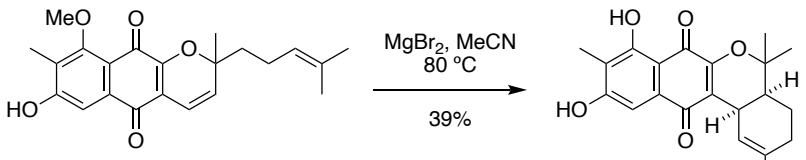

4.70 **4.28**: naphterpin

To a solution of **4.70** (500 mg, 1.36 mmol) in MeCN (40 mL) at room temperature was added $MgBr_2$ (1.25 g, 6.79 mmol). The reaction was stirred at 80 ºC for 16 h. The mixture was cooled to room temperature, quenched with 1 M HCl (50 mL) and extracted with EtOAc (3 × 50 mL). The combined organic extracts were washed with saturated brine (100 mL), dried over anhydrous $MgSO_4$, filtered and concentrated *in vacuo*. The residue was purified by flash chromatography on SiO_2 (9:1 → 4:1, petrol/EtOAc gradient elution) to give crude **4.28** as a brown oil. Trituration from CH_2Cl_2 gave pure **4.28** (190 mg, 39%) as an orange amorphous solid.

Data for 4.28:

R_f = 0.60 (1:1 petrol/EtOAc)

IR (neat): 1362, 2928, 1625, 1573, 1436, 1332, 1281, 1248 cm^{-1}.

^{1}H NMR (500 MHz, $CDCl_3$): δ 12.29 (s, 1H), 7.18 (s, 1H), 6.45 (s, 1H), 6.06 (d, *J* = 5.2 Hz, 1H), 3.51 – 3.46 (m, 1H), 2.18 (s, 3H), 2.08 – 1.91 (m, 3H), 1.77 (ddd, *J* = 12.1, 6.2, 2.8 Hz, 1H), 1.68 (s, 3H), 1.56 (s, 3H), 1.34 (s, 3H), 1.34 – 1.27 (m, 1H).

^{13}C NMR (125 MHz, $CDCl_3$): δ 184.2, 183.5, 162.5, 160.7, 153.2, 136.2, 131.8, 123.7, 120.3, 116.8, 108.5, 107.9, 80.7, 39.9, 31.3, 29.8, 25.8, 25.2, 23.7, 20.5, 7.9.

HRMS (ESI): calculated for $C_{21}H_{23}O_5$ 355.1545 $[M+H]^+$, found 355.1543.

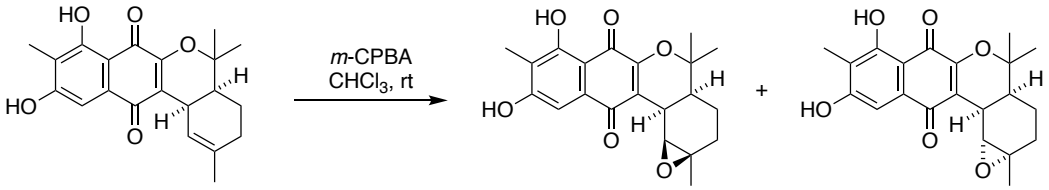

4.28: naphterpin **4.73** (65%) **4.74** (21%)

To a solution of **4.28** (75 mg, 0.21 mmol) in $CHCl_3$ (8 mL) at room temperature was added *m*-CPBA (77%, 57 mg, 0.26 mmol). The reaction was stirred at room temperature for 1 h. The mixture was diluted with saturated $NaHCO_3$ solution (15 mL) and extracted with $CHCl_3$ (3 × 10 mL). The combined organic extracts were washed with saturated $Na_2S_2O_3$ solution (40 mL) and saturated brine (40 mL), dried over anhydrous $MgSO_4$, filtered and concentrated *in vacuo*. The residue was purified by flash chromatography on SiO_2 (4:1 → 1:1, petrol/EtOAc gradient elution) to give **4.73** (51 mg, 65%) as a fine yellow powder and **4.74** (16 mg, 21%) as a fine orange powder.

Data for 4.73:

R_f = 0.30 (1:1 petrol/EtOAc)

IR (neat): 3276, 2963, 2924, 2854, 1633, 1591, 1434, 1377, 1325, 1289 cm^{-1}.

^{1}H NMR (600 MHz, $CDCl_3$): δ 12.16 (s, 1H), 8.42 (s, 1H), 6.89 (s, 1H), 4.17 (d, *J* = 5.5 Hz, 1H), 3.51 (t, *J* = 6.2 Hz, 1H), 2.18 – 2.14 (m, 1H), 1.95 (s, 3H), 1.78 (ddd, *J* = 14.9, 12.9, 5.0 Hz, 1H), 1.69 – 1.63 (m, 1H), 1.58 (ddd, *J* = 12.9, 7.1, 2.6 Hz, 1H), 1.53 (s, 3H), 1.45 (s, 3H), 1.33 – 1.27 (m, 1H), 1.30 (s, 3H).

^{13}C NMR (150 MHz, $CDCl_3$): δ 183.9, 182.4, 162.5, 161.7, 155.0, 130.9, 120.0, 117.3, 108.5, 107.8, 79.6, 62.2, 62.1, 39.2, 30.2, 30.1, 26.2, 24.7, 22.9, 17.5, 7.7.

HRMS (ESI): calculated for $C_{21}H_{23}O_6$ 371.1495 $[M+H]^+$, found 371.1492.

Data for 4.74:

R_f = 0.20 (1:1 petrol/EtOAc)

IR (neat): 3346, 2940, 1629, 1587, 1564, 1435, 1330, 1249 cm^{-1}.

^{1}H NMR (600 MHz, $CDCl_3$): δ 12.22 (s, 1H), 7.61 (s, 1H), 7.22 (s, 1H), 3.84 (s, 1H), 3.47 (dd, *J* = 5.9, 1.9 Hz, 1H), 2.16 (s, 3H), 1.99 – 1.92 (m, 1H), 1.89 (td, *J* = 6.0, 3.0 Hz, 1H), 1.86 – 1.79 (m, 1H), 1.76 – 1.70 (m, 1H), 1.46 (s, 3H), 1.41 (s, 3H), 1.34 – 1.26 (overlapping m, 1H), 1.30 (s, 3H).

^{13}C NMR (150 MHz, $CDCl_3$): δ 184.2, 182.7, 162.8, 161.6, 155.7, 131.4, 119.8, 117.4, 108.4, 108.3, 81.4, 61.3, 59.2, 36.3, 32.0, 27.1, 25.8, 25.1, 23.8, 19.1, 8.0.

HRMS (ESI): calculated for $C_{21}H_{23}O_6$ 371.1495 $[M+H]^+$, found 371.1492.

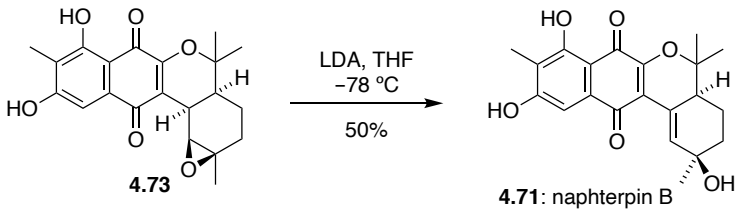

To a solution of diisopropylamine (0.05 mL, 0.38 mmol) in THF (2 mL) at 0 ºC was added *n*-BuLi (1.6 M in cyclohexane, 0.24 mL, 0.38 mmol). The reaction was cooled to −78 ºC and a solution of **4.73** (14 mg, 0.04 mmol) in THF (1 mL) was added dropwise to the reaction. The reaction was stirred at −78 ºC for 1.5 h. The mixture was quenched with saturated NH_4Cl solution (5 mL) and extracted with EtOAc (3 × 5 mL). The combined organic extracts were washed with saturated brine (15 mL), dried over anhydrous $MgSO_4$, filtered and concentrated *in vacuo*. The residue was purified by flash chromatography on SiO_2 (4:1 → 1:1, petrol/EtOAc gradient elution) to give **4.71** (7 mg, 50%) as a fine red-orange powder.

Data for 4.71:

R_f = 0.20 (1:1 petrol/EtOAc)

IR (neat): 3371, 2971, 1622, 1559, 1437, 1325, 1248 cm^{-1}.

^{1}H NMR (600 MHz, $CDCl_3$): δ 12.24 (s, 1H), 8.17 (s, 1H), 7.46 (s, 1H), 7.20 (s, 1H), 2.35 – 2.28 (m, 1H), 2.12 (s, 3H), 1.98 – 1.92 (m, 1H), 1.83 – 1.79 (m, 1H), 1.64 – 1.58 (m, 2H), 1.57 (s, 3H), 1.49 (s, 3H), 1.16 (s, 3H).

^{13}C NMR (150 MHz, $CDCl_3$): δ 183.4, 182.5, 162.3, 161.6, 154.5, 135.5, 131.6, 127.1, 117.0, 116.3, 108.5, 108.0, 82.3, 68.4, 42.5, 35.8, 30.7, 26.7, 20.2, 19.5, 7.8.

HRMS (ESI): calculated for $C_{21}H_{21}O_6$ 369.1338 $[M–H]^–$, found 369.1339.

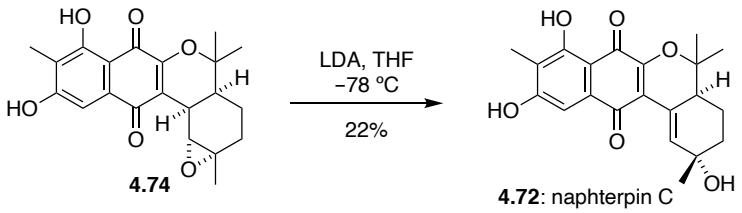

To a solution of diisopropylamine (0.09 mL, 0.61 mmol) in THF (3 mL) at 0 ºC was added *n*-BuLi (2.5 M in hexanes, 0.24 mL, 0.61 mmol). The reaction was stirred at 0 ºC for 5 min prior to being cooled to −78 ºC. A solution of **4.74** (45 mg, 0.12 mmol) in THF (2 mL) was added dropwise to the reaction. The reaction was stirred at −78 ºC for 2 h. The mixture was quenched with saturated NH_4Cl solution (10 mL) and extracted with EtOAc (3 × 10 mL). The combined organic extracts were washed with saturated brine (30 mL), dried over anhydrous $MgSO_4$, filtered and concentrated *in vacuo*. The residue was purified by flash chromatography on SiO_2 (4:1 → 1:1, petrol/EtOAc gradient elution) to give **4.72** (10 mg, 22%) as a fine orange powder.

Data for 4.72:

R_f = 0.20 (1:1 petrol/EtOAc)

IR (neat): 3451, 2925, 1633, 1597, 1436, 1325, 1288, 1247, 1076 cm^{-1}.

^{1}H-NMR (600 MHz, acetone-d_6): δ 12.43 (s, 1H), 7.45 (t, *J* = 1.8 Hz, 1H), 7.15 (s, 1H), 2.42 (ddd, *J* = 11.1, 5.9, 2.1 Hz, 1H), 2.11 (s, 3H), 2.01 – 1.93 (m, 1H), 1.89 (dtd, *J* = 12.6, 4.2, 3.8, 1.5 Hz, 1H), 1.76 (td, *J* = 13.4, 12.9, 3.4 Hz, 1H), 1.51 (s, 3H), 1.43 – 1.36 (m, 1H), 1.32 (s, 3H), 1.18 (s, 3H).

^{13}C-NMR (150 MHz, acetone-d_6): δ 183.8, 183.4, 163.4, 162.7, 162.4, 154.4, 140.9, 133.0, 124.6, 117.3, 116.9, 116.8, 108.1, 108.0, 82.2, 43.4, 37.9, 26.6, 23.7, 19.6, 7.9.

^{1}H-NMR (600 MHz, DMSO-d_6): δ 12.30 (s, 1H), 7.31 (t, *J* = 1.7 Hz, 1H), 7.07 (s, 1H), 4.80 (s, 1H), 2.35 (ddd, *J* = 11.1, 6.0, 2.0 Hz, 1H), 2.01 (s, 3H), 1.88 – 1.83 (m, 1H), 1.78 – 1.73 (m, 1H), 1.66 – 1.60 (m, 1H), 1.45 (s, 3H), 1.31 – 1.26 (m, 1H), 1.22 (s, 3H), 1.09 (s, 3H).

^{13}C-NMR (150 MHz, DMSO-d_6): δ 182.6, 182.1, 162.9, 161.1, 153.1, 140.0, 131.4, 122.9, 115.9, 115.4, 107.4, 107.0, 81.5, 68.0, 41.9, 36.7, 28.9, 26.0, 22.1, 19.1, 7.8.

HRMS (ESI): calculated for $C_{21}H_{21}O_6$ 369.1344 $[M-H]^-$, found 369.1338.

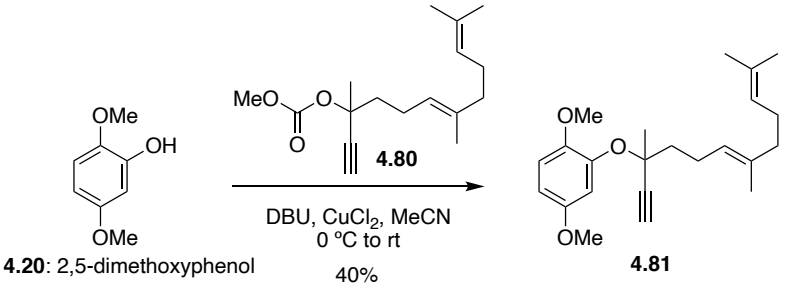

To a solution of **4.20** (2.07 g, 13.4 mmol) in MeCN (200 mL) at 0 °C was added DBU (2.17 mL, 17.5 mmol) dropwise $CuCl_2$ (18 mg, 0.013 mmol) and **4.80**[36,37] (4.48 g, 16.1 mmol). The reaction mixture was stirred at 0 °C for 8 h prior to being warmed to rt and stirred for a further 16 h. The mixture was quenched with saturated NH_4Cl solution (200 mL) and extracted with EtOAc (3 × 150 mL). The combined organic extracts were washed with saturated brine (300 mL), dried over anhydrous $MgSO_4$, filtered and concentrated *in vacuo*. The residue was purified by flash chromatography on SiO_2 (20:1, petrol/EtOAc gradient elution) to give **4.81** (1.89 g, 40%) as a pale yellow oil.

Data for 4.81:

R_f = 0.55 (4:1, petrol/EtOAc)

IR (neat): 3286, 2932, 1504, 1443, 1260, 1223 cm^{-1}.

^{1}H NMR (600 MHz, $CDCl_3$): δ 7.10 (d, *J* = 3.0 Hz, 1H), 6.81 (d, *J* = 8.8 Hz, 1H), 6.56 (dd, *J* = 8.8f, 3.0 Hz, 1H), 5.17 (tq, *J* = 7.1, 1.3 Hz, 1H), 5.10 (t, *J* = 6.9 Hz, 1H), 3.77 (s, 3H), 3.76 (s, 3H), 2.58 (s, 1H), 2.39 – 2.23 (m, 2H), 2.10 – 2.04 (m, 2H), 2.01 – 1.96 (m, 3H), 1.88 (ddd, *J* = 13.5, 11.8, 5.1 Hz, 1H), 1.68 (s, 3H), 1.63 (s, 3H), 1.60 (s, 3H), 1.58 (s, 3H).

^{13}C NMR (150 MHz, $CDCl_3$): δ 153.6, 147.4, 145.7, 135.7, 131.5, 124.5, 123.7, 113.5, 110.3, 107.8, 85.5, 77.1, 75.0, 56.9, 55.8, 42.5, 39.8, 26.8, 26.7, 25.8, 23.3, 17.8, 16.1.

HRMS (ESI): calculated for $C_{23}H_{33}O_3$ 357.2430 $[M+H]^+$, found 357.2416.

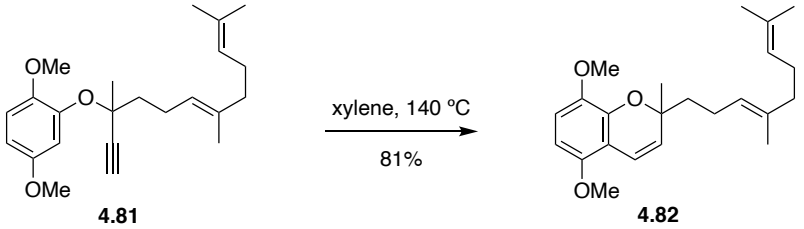

4.81 **4.82**

A solution of **4.81** (200 mg, 0.56 mmol) in xylene (15 mL) was stirred at 140 ºC for 2 h. The mixture was cooled to room temperature and concentrated *in vacuo*. The residue was purified by flash chromatography on SiO_2 (20:1, petrol/EtOAc) to give **4.82** (162 g, 81%) as a yellow oil.

Data for 4.82:

R_f = 0.50 (4:1, petrol/EtOAc)

IR (neat): 2967, 2925, 2836, 1491, 1463, 1439, 1385 cm^{-1}.

^{1}H NMR (600 MHz, $CDCl_3$): δ 6.69 (dd, *J* = 12.4, 9.5 Hz, 2H), 6.30 (d, *J* = 8.9 Hz, 1H), 5.56 (d, *J* = 10.1 Hz, 1H), 5.10 (tq, *J* = 7.1, 1.3 Hz, 1H), 5.07 (t, *J* = 7.0 Hz, 1H), 3.81 (s, 3H), 3.78 (s, 3H), 2.16 – 2.11 (m, 2H), 2.06 – 2.01 (m, 2H), 1.96 – 1.92 (m, 2H), 1.86 – 1.80 (m, 1H), 1.71 – 1.63 (overlapping m, 1H), 1.67 (s, 3H), 1.58 (s, 3H), 1.56 (s, 3H), 1.44 (s, 3H).

^{13}C NMR (150 MHz, $CDCl_3$): δ 149.7, 143.3, 143.1, 135.3, 131.4, 128.4, 124.5, 124.2, 117.6, 113.0, 111.8, 101.6, 78.5, 57.2, 56.0, 40.8, 39.8, 26.8, 26.3, 25.8, 22.8, 17.8, 16.0.

HRMS (ESI): calculated for $C_{23}H_{33}O_3$ 357.2430 $[M+H]^+$, found 357.2408.

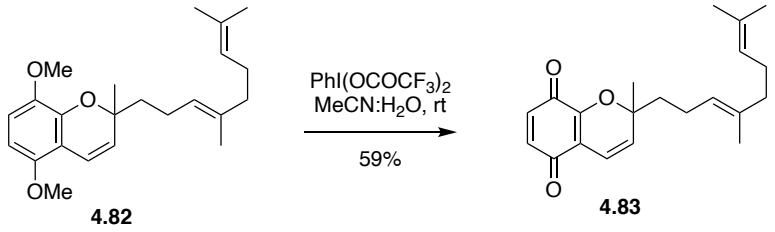

4.82 **4.83**

To a solution of **4.82** (1.32 g, 3.70 mmol) in MeCN:H_2O (90 mL, 2:1 v/v) at room temperature was added $PhI(OCOCF_3)_2$ (3.50 g, 8.15 mmol). The reaction mixture was stirred at room temperature for 5 min. The mixture was quenched with saturated $NaHCO_3$ solution (100 mL) and extracted with Et_2O (3 × 80 mL). The combined organic extracts were washed with H_2O (200 mL) and saturated brine (200 mL), dried over anhydrous $MgSO_4$, filtered and concentrated *in vacuo*. The residue was purified by flash chromatography on SiO_2 (20:1 → 9:1, petrol/EtOAc gradient elution) to give **4.83** (707 mg, 59%) as a dark red oil.

Data for 4.83:

R_f = 0.45 (4:1, petrol/EtOAc)

IR (neat): 2970, 2917, 1674, 1647, 1575, 1447, 1413, 1335 cm^{-1}.

^{1}H NMR (600 MHz, $CDCl_3$): δ 6.64 (s, 2H), 6.47 (d, *J* = 10.1 Hz, 1H), 5.59 (d, *J* = 10.1 Hz, 1H), 5.12 – 5.04 (m, 2H), 2.14 – 2.06 (m, 2H), 2.07 – 2.00 (m, 2H), 1.97 – 1.88 (m, 3H), 1.71 – 1.63 (overlapping m, 1H), 1.67 (s, 3H), 1.59 (s, 3H), 1.56 (s, 3H), 1.48 (s, 3H).

^{13}C NMR (150 MHz, $CDCl_3$): δ 184.4, 181.6, 150.9, 136.1, 136.0, 134.7, 131.5, 129.3, 124.3, 123.3, 115.8, 115.4, 83.3, 41.6, 39.7, 27.6, 26.7, 25.8, 22.6, 17.8, 16.1.

HRMS (ESI): calculated for $C_{21}H_{27}O_3$ 327.1960 $[M+H]^+$, found 327.1948.

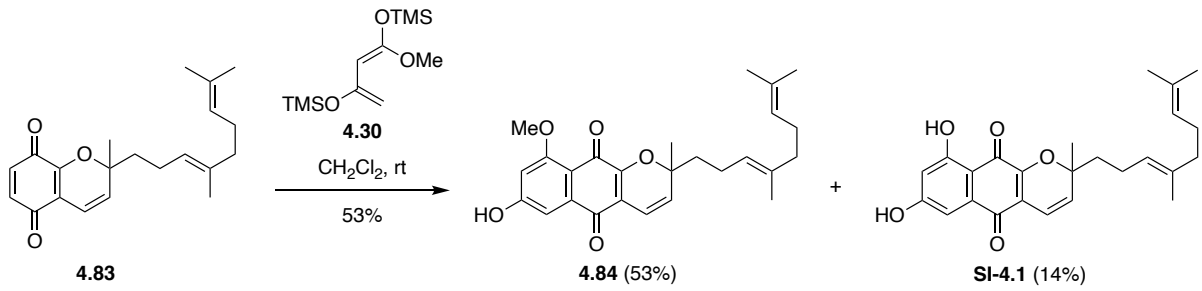

To a solution of **4.83** (597 mg, 1.83 mmol) in CH_2Cl_2 (12 mL) at room temperature was added **4.30** (619 mg, 2.38 mmol). The reaction mixture was stirred at room temperature for 20 min. The mixture was quenched with 1M HCl (10 mL) and stirred at room temperature for 1 h. The mixture was extracted with EtOAc (3 × 30 mL). The combined organic extracts were washed with saturated brine (100 mL), dried over anhydrous $MgSO_4$, filtered and concentrated *in vacuo*. The residue was purified by flash chromatography on SiO_2 (9:1 → 1:1, petrol/EtOAc gradient elution) to give **4.84** (408 mg, 53 %) as an amorphous red solid and **SI-4.1** (106 mg, 14 %) as a red oil.

Data for 4.84:

R_f = 0.10 (4:1, petrol/EtOAc)

IR (neat): 3252, 2970, 2925, 1628, 1597, 1568, 1439, 1349, 1222 cm^{-1}.

^{1}H NMR (600 MHz, $CDCl_3$): δ 7.45 (br s, 1H), 7.38 (d, *J* = 2.3 Hz, 1H), 6.72 (d, *J* = 2.4 Hz, 1H), 6.60 (d, *J* = 10.0 Hz, 1H), 5.58 (d, *J* = 10.0 Hz, 1H), 5.11 – 5.03 (m, 2H), 3.95 (s, 3H), 2.17 – 2.06 (m, 2H), 2.05 – 1.99 (m, 2H), 1.96 – 1.89 (m, 3H), 1.71 – 1.67 (m, 1H), 1.66 (s, 3H), 1.58 (s, 3H), 1.55 (s, 3H), 1.48 (s, 3H).

^{13}C NMR (150 MHz, $CDCl_3$): δ 182.1, 177.7, 164.0, 163.1, 154.6, 136.0, 135.8, 131.5, 128.6, 124.4, 123.3, 115.7, 115.4, 112.4, 108.1, 103.9, 83.7, 56.4, 41.7, 39.7, 27.6, 26.7, 25.8, 22.6, 17.8, 16.1.

HRMS (ESI): calculated for $C_{26}H_{29}O_5$ 421.2015 $[M–H]^–$, found 421.2014.

Data for SI-4.1:

R_f = 0.30 (4:1, petrol/EtOAc)

IR (neat): 3312, 2969, 2924, 1617, 1577, 1453, 1399, 1318, 1226 cm^{-1}.

^{1}H NMR (600 MHz, $CDCl_3$): δ 12.04 (s, 1H), 7.23 (d, *J* = 2.4 Hz, 1H), 6.83 (s, 1H), 6.63 (d, *J* = 10.1 Hz, 1H), 6.59 (d, *J* = 2.5 Hz, 1H), 5.65 (d, *J* = 10.1 Hz, 1H), 5.09 (t, *J* = 7.0 Hz, 1H), 5.06 (t, *J* = 6.9 Hz, 1H), 2.17 – 2.09 (m, 2H), 2.06 – 1.99 (m, 2H), 1.98 – 1.91 (m, 3H), 1.74 – 1.68 (m, 1H), 1.67 (s, 3H), 1.58 (s, 3H), 1.56 (s, 3H), 1.52 (s, 3H).

^{13}C NMR (150 MHz, $CDCl_3$): δ 182.7, 181.3, 164.7, 163.5, 153.6, 136.2, 133.8, 131.6, 129.6, 124.3, 123.2, 117.6, 115.8, 109.4, 109.0, 107.9, 83.9, 41.7, 39.7, 27.7, 26.7, 25.8, 22.7, 17.8, 16.2.

HRMS (ESI): calculated for $C_{25}H_{29}O_5$ 409.2015 $[M+H]^+$, found 409.2007.

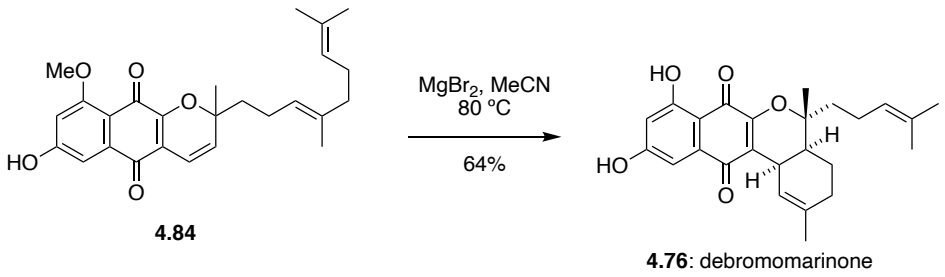

To a solution of **4.84** (212 mg, 0.50 mmol) in MeCN (20 mL) at room temperature was added $MgBr_2$ (462 mg, 2.51 mmol). The reaction was stirred at 80 ºC for 14 h. The mixture was cooled to room temperature, quenched with 1 M HCl (50 mL) and extracted with EtOAc (3 × 30 mL). The combined organic extracts were washed with saturated brine (90 mL), dried over anhydrous $MgSO_4$, filtered and concentrated *in vacuo*. The residue was purified by flash chromatography on SiO_2 (8:1, petrol/EtOAc) to give **4.76** (130 mg, 64 %) as an amorphous orange solid.

Data for 4.76:

R_f = 0.30 (3:1, petrol/EtOAc)

IR (neat): 3300, 2969, 2929, 1630, 1583, 1324, 1221, 1160, 1007, 769 cm^{-1}.

^{1}H NMR (500 MHz, $CDCl_3$): δ 11.90 (s, 1H), 7.22 (d, *J* = 2.3 Hz, 1H), 6.57 (d, *J* = 2.3 Hz, 1H), 6.03 (d, *J* = 4.3 Hz, 1H), 5.02 (t, *J* = 7.0 Hz, 1H), 3.45 (d, *J* = 6.0 Hz, 1H), 2.10 – 1.85 (m, 6H), 1.71 – 1.64 (m, 2H), 1.67 (s, 3H), 1.62 (s, 3H), 1.56 (s, 3H), 1.52 (s, 3H), 1.38 – 1.30 (m, 1H).

^{13}C NMR (125 MHz, $CDCl_3$): δ 184.3, 183.0, 164.6, 163.9, 153.4, 136.4, 134.9, 132.7, 124.1, 123.3, 120.1, 109.0, 108.7, 107.5, 83.3, 37.5, 36.9, 31.0, 29.9, 25.7, 23.7, 22.8, 22.4, 20.4, 17.8.

HRMS (ESI): calculated for $C_{25}H_{29}O_5$ 409.2015 $[M+H]^+$, found 409.2009.

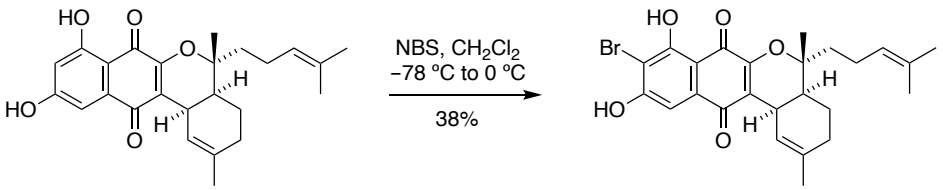

4.76: debromomarinone

4.86: isomarinone

To a solution of **4.76** (32 mg, 0.08 mmol) in CH_2Cl_2 (2 mL) at −78 ºC was added NBS (21 mg, 0.12 mmol). The reaction mixture was stirred at −78 ºC for 1 h, prior to being warmed to 0 ºC and stirred for a further 1.5 h. The mixture was warmed to room temperature, quenched with saturated $Na_2S_2O_3$ solution (10 mL) and extracted with CH_2Cl_2 (3 × 7 mL). The combined organic extracts were washed with saturated brine (20 mL), dried over anhydrous $MgSO_4$, filtered and concentrated *in vacuo*. The residue was purified by flash chromatography on SiO_2 (8:1, petrol/EtOAc gradient elution) to give **4.86** (15 mg, 38 %) as an amorphous orange solid.

Data for 4.86:

R_f = 0.25 (3:1, petrol/EtOAc)

IR (neat): 2959, 2923, 1635, 1588, 1430, 1377, 1329, 1280 cm^{-1}.

^{1}H NMR (600 MHz, $CDCl_3$): δ 12.72 (s, 1H), 7.28 (s, 1H), 6.51 (s, 1H), 6.05 (d, *J* = 4.1 Hz, 1H), 5.02 (t, *J* = 7.0 Hz, 1H), 3.49 – 3.45 (m, 1H), 2.08 – 1.97 (m, 4H), 1.96 – 1.92 (m, 1H), 1.89 (ddd, *J* = 12.1, 6.1, 3.0 Hz, 1H), 1.68 (s, 3H), 1.67 – 1.64 (overlapping m, 2H), 1.63 (s, 3H), 1.56 (s, 3H), 1.55 (s, 3H), 1.35 – 1.28 (m, 1H).

^{13}C NMR (150 MHz, $CDCl_3$): δ 183.3, 182.9, 160.0, 159.5, 152.7, 136.5, 133.3, 132.7, 124.9, 123.2, 120.0, 108.9, 107.8, 103.3, 83.3, 37.6, 36.8, 31.1, 29.9, 25.7, 23.7, 22.8, 22.4, 20.4, 17.8.

^{1}H NMR (600 MHz, DMSO-d_6): δ 12.54 (s, 1H), 12.09 (br s, 1H), 7.08 (s, 1H), 5.95 (d, J =5.0 Hz, 1H), 5.03 (t, *J* = 6.5 Hz, 1H), 3.36 - 3.34 (m, 1H), 2.04 – 1.84 (m, 6H), 1.61 (s, 3H), 1.59 – 1.54 (overlapping m, 2H), 1.55 (s, 3H), 1.49 (s, 3H), 1.42 (s, 3H), 1.22 – 1.14 (m, 1H).

^{13}C NMR (150 MHz, DMSO-d_6): δ 182.5, 182.1, 161.9, 159.7, 152.3, 135.4, 132.1, 131.1, 123.8, 123.1, 120.1, 107.4, 107.1, 101.8, 82.4, 36.6, 36.0, 30.4, 29.2, 25.3, 23.4, 22.0, 21.6, 19.7, 17.3.

HRMS (ESI): calculated for $C_{25}H_{28}BrO_5$ 487.1120 $[M+H]^+$, found 487.1098.

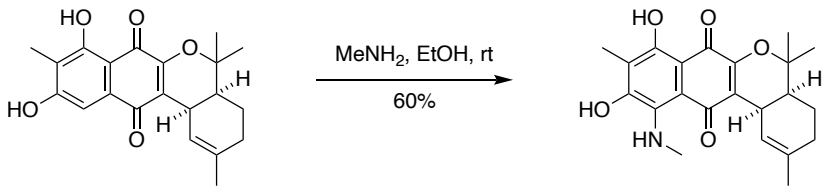

4.28: naphterpin **4.115**

To a solution of **4.28** (50 mg, 0.14 mmol) in EtOH (5 mL) was added $MeNH_2$ (40 mL, 0.30 mmol) at rt. The reaction was stirred at rt for 16 h. The mixture was acidified with 10% H_2SO_4 to pH 1 and extracted with EtOAc (3 × 15 mL). The combined organic extracts were washed sequentially with saturated $NaHCO_3$ solution (40 mL) and brine (40 mL), dried over $MgSO_4$, filtered and concentrated *in vacuo*. The residue was purified by flash chromatography on SiO_2 (2:1, petrol/EtOAc) to give **4.115** (32 mg, 60%) as a purple residue.

Data for 4.115:

R_f = 0.10 (2:1, petrol/EtOAc)

IR (neat): 2928, 2906, 1559, 1502, 1424, 1378, 1339 cm^{-1}.

^{1}H NMR (500 MHz, $CDCl_3$): δ 13.70 (s, 1H), 6.08 (d, *J* = 4.6 Hz, 1H), 3.49 (s, 1H), 2.85 (s, 3H), 2.17 (s, 3H), 2.03 – 1.91 (m, 3H), 1.77 (ddd, *J* = 11.8, 6.3, 2.8 Hz, 1H), 1.68 (s, 3H), 1.54 (s, 3H), 1.33 (s, 3H), 1.37 – 1.29 (m, 1H).

^{13}C NMR (125 MHz, $CDCl_3$): δ 185.8, 181.6, 161.7, 157.0, 152.3, 137.3, 136.0, 124.9, 120.6, 116.7, 116.4, 106.9, 80.1, 40.1, 35.3, 31.5, 29.8, 25.8, 25.1, 23.8, 20.7, 8.2.

HRMS (ESI): calculated for $C_{22}H_{26}NO_5$ 384.1805 $[M+H]^+$, found 384.1823.

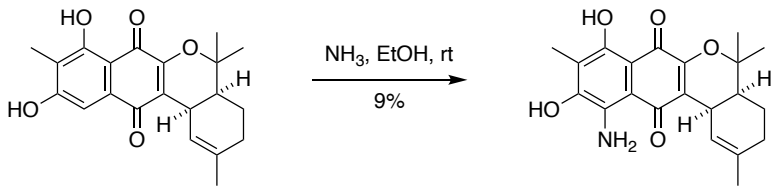

4.28: naphterpin **4.105**

To a solution of **4.28** (20 mg, 0.06 mmol) in EtOH (2.5 mL) was added a solution of NH_3 (30% in H_2O, 16.5 mL, 0.12 mmol) at rt. The reaction was stirred at rt for 36 h. The mixture was cooled to 0 ºC and acidified with 10% H_2SO_4 (20 mL) to pH 1. The mixture was extracted with EtOAc (3 × 10 mL). The combined organic extracts were washed sequentially with saturated $NaHCO_3$ solution (30 mL) and brine (30 mL), dried over $MgSO_4$, filtered and concentrated *in vacuo*. The residue was purified by flash chromatography on SiO_2 (2:1 → 3:7, petrol/EtOAc gradient elution) to give **4.105** (2 mg, 9%) as a magenta residue.

Data for 4.105:

R_f = 0.20 (1:1, petrol/EtOAc)

IR (neat): 3488, 3294, 3143, 2928, 1595, 1564, 1510, 1467, 1439, 1339, 1276 cm^{-1}.

^{1}H NMR (600 MHz, $CDCl_3$): δ 14.17 (s, 1H), 6.20 (d, *J* = 5.1 Hz, 1H), 3.55 – 3.51 (m, 1H), 2.18 (s, 3H), 2.04 – 1.90 (m, 3H), 1.77 (ddd, *J* = 11.8, 6.2, 2.8 Hz, 1H), 1.68 (s, 3H), 1.54 (s, 3H), 1.39 – 1.35 (m, 1H), 1.33 (s, 4H).

^{13}C NMR (150 MHz, $CDCl_3$): δ 184.9, 181.2, 159.6, 152.2, 150.9, 137.1, 135.7, 125.4, 121.1, 114.8, 106.9, 106.5, 79.7, 40.2, 31.8, 29.8, 25.8, 25.0, 23.8, 20.8, 8.0,

HRMS (ESI): calculated for $C_{21}H_{24}NO_5$ 370.1649 $[M+H]^+$, found 370.1671.

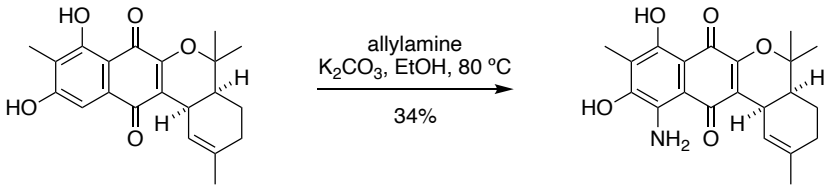

4.28: naphterpin **4.105**

To a solution of **4.28** (207 mg, 0.58 mmol) in EtOH (10 mL) at room temperature was added K_2CO_3 (805 mg, 5.83 mmol) and allylamine (5 mL). The reaction was stirred at 80 ºC for 16 h. The reaction mixture was quenched with 1M HCl (50 mL) and extracted with EtOAc (3 × 20 mL). The combined organic extracts were washed with brine (100 mL), dried over Na_2SO_4, filtered and concentrated *in vacuo*. The residue was purified by flash chromatography on SiO_2 (4:1 → 1:1, petrol/EtOAc gradient elution) to give **4.105** (81 mg, 34%) as a purple residue.

Data for 4.105:

R_f = 0.20 (1:1, petrol/EtOAc)

IR (neat): 3488, 3294, 3143, 2928, 1595, 1564, 1510, 1467, 1439, 1339, 1276 cm^{-1}.

^{1}H NMR (600 MHz, $CDCl_3$): δ 14.20 (s, 1H), 6.20 (d, *J* = 5.0 Hz, 1H), 3.55 – 3.51 (m, 1H), 2.17 (s, 3H), 2.04 – 1.90 (m, 3H), 1.77 (ddd, *J* = 11.7, 6.2, 2.8 Hz, 1H), 1.68 (s, 3H), 1.51 (s, 3H), 1.39 – 1.32 (m, 1H), 1.32 (s, 3H).

^{13}C NMR (150 MHz, $CDCl_3$): δ 184.8, 180.8, 160.1, 152.2, 151.4, 137.6, 135.7, 125.4, 121.1, 115.1, 106.8, 106.2, 79.7, 40.2, 31.8, 29.8, 25.7, 25.0, 23.8, 20.8, 8.1.

HRMS (ESI): calculated for $C_{21}H_{24}NO_5$ 370.1649 $[M+H]^+$, found 370.1648.

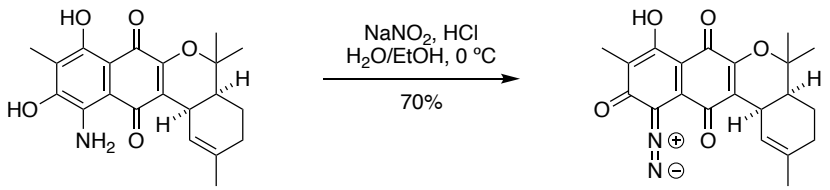

4.105 **4.104**

To a solution of **4.105** (43 mg, 0.12 mmol) in EtOH (2 mL) at 0 ºC was added 32% HCl (0.10 mL, 1.05 mmol). The reaction was stirred at 0 ºC for 5 min. A solution of $NaNO_2$ (22 mg, 0.32 mmol) in H_2O (0.5 mL) at 0 ºC was then added dropwise. The resulting mixture was stirred at 0 ºC for 30 min. The mixture was diluted with CH_2Cl_2 (10 mL), and a solution of K_2CO_3 (97 mg, 0.70 mmol) in H_2O (1 mL) was added at 0 ºC. The reaction was stirred vigorously at 0 ºC for 2 min. The organic phase was then separated, and the aqueous phase extracted with CH_2Cl_2 (2 × 10 mL). The combined organic extracts were washed with brine (30 mL), dried over Na_2SO_4, filtered and concentrated *in vacuo* (at 25 ºC). The residue was purified by flash chromatography on SiO_2 (2:1, petrol/EtOAc) to give **4.104** (16 mg, 77%) as a green/black residue.

Data for 4.104:

R_f = 0.55 (1:1, petrol/EtOAc)

IR (neat): 2928, 2152, 1642, 1583, 1521, 1431, 1389, 1368, 1333 cm^{-1}.

^{1}H NMR (600 MHz, $CDCl_3$): δ 11.34 (s, 1H), 6.00 (d, *J* = 5.1 Hz, 1H), 3.45 – 3.41 (m, 1H), 2.07 (s, 3H), 2.04 – 1.92 (m, 3H), 1.26 (ddd, *J* = 12.4, 6.1, 3.0 Hz, 1H), 1.69 (s, 3H), 1.56 (s, 3H), 1.34 (s, 3H), 1.31 – 1.21 (m, 1H).

^{13}C NMR (150 MHz, $CDCl_3$): δ 181.7, 180.9, 174.6, 161.0, 152.7, 137.0, 133.6, 121.2, 119.4, 119.3, 109.4, 81.9, 39.7, 31.0, 29.8, 25.7, 25.3, 23.7, 20.4, 8.7.

^{1}H NMR (600 MHz, C_6D_6): δ 11.59 (s, 1H), 6.23 – 6.19 (m, 1H), 3.13 – 3.10 (m, 1H), 2.39 (s, 3H), 1.68 (d, *J* = 6.6 Hz, 2H), 1.61 (s, 3H), 1.53 – 1.48 (m, 1H), 1.13 (s, 3H), 1.11 – 1.04 (m, 2H), 0.88 (s, 3H).

^{13}C NMR (150 MHz, C_6D_6): δ 181.4, 180.5, 174.0, 160.7, 152.6, 135.9, 133.5, 128.6, 120.4, 120.4, 118.5, 109.5, 80.8, 39.3, 31.0, 29.7, 25.3, 24.7, 23.6, 20.4, 8.9.

HRMS (ESI): calculated for $C_{21}H_{21}N_2O_5$ 381.1445 $[M+H]^+$, found 381.1449.

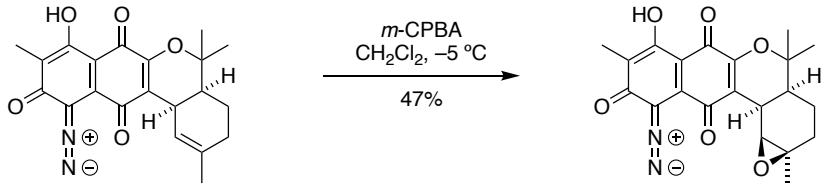

To a solution of **4.104** (24 mg, 0.06 mmol) in CH_2Cl_2 (2 mL) at –5 ºC was added *m*-CPBA (77%, 14 mg, 0.06 mmol). The reaction was stirred at –5 ºC for 1 h. The mixture was diluted with saturated $NaHCO_3$ solution (15 mL) and extracted with $CHCl_3$ (3 × 10 mL). The combined organic extracts were washed with saturated brine (25 mL), dried over anhydrous Na_2SO_4, filtered and concentrated *in vacuo*. The residue was purified by flash chromatography on SiO_2 (4:1 → 1:1, petrol/EtOAc gradient elution) to give **4.127** (11 mg, 47%) as a navy/black residue.

Data for 4.127:

R_f = 0.15 (1:1, petrol/EtOAc)

IR (neat): 2926, 2157, 1644, 1600, 1585, 1521, 1433, 1390, 1368, 1339 cm^{-1}.

^{1}H NMR (600 MHz, $CDCl_3$): δ 11.31 (s, 1H), 3.77 (d, *J* = 5.4 Hz, 1H), 3.40 (t, *J* = 6.1 Hz, 1H), 2.08 (s, 3H), 2.07 – 2.03 (m, 1H), 1.70 (ddd, *J* = 14.7, 12.7, 4.7 Hz, 1H), 1.59 – 1.54 (m, 2H), 1.52 (s, 3H), 1.36 (s, 3H), 1.32 (s, 3H), 1.20 – 1.12 (m, 1H).

^{13}C NMR (150 MHz, $CDCl_3$): δ 181.2, 180.9, 174.5, 161.0, 154.4, 133.3, 119.6, 118.5, 109.6, 82.8, 81.0, 59.9, 59.9, 39.1, 30.3, 30.2, 26.0, 25.0, 22.8, 17.5, 8.7.

HRMS (ESI): calculated for $C_{21}H_{21}N_2O_6$ 397.1394 $[M+H]^+$, found 397.1396.

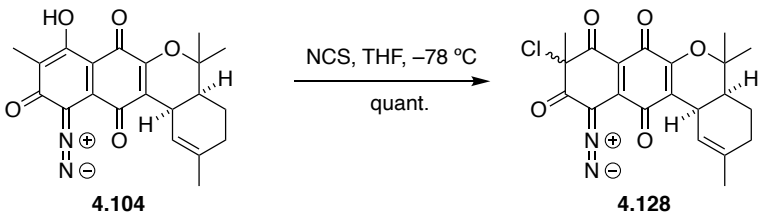

To a solution of **4.104** (26 mg, 0.07 mmol) in THF (1 mL) at –78 ºC was added NCS (11 mg, 0.08 mmol). The reaction was stirred at –78 ºC for 10 min. $Na_2S_2O_3.5H_2O$ (17.4 mg, 0.07 mmol) was added and the reaction mixture warmed to rt. The mixture was concentrated *in vacuo* (25 ºC). The residue was purified by flash chromatography on SiO_2 (9:1 → 4:1, petrol/EtOAc gradient elution) to give **4.128** (less polar epimer) (13.5 mg, 47%) and **4.128** (more polar epimer) (15.5 mg, 53%) as red residues.

4.128 ***mixture of epimers*****:**

R_f = 0.10, 0.20 (4:1, petrol/EtOAc)

IR (neat): 3423, 2930, 2136, 1716, 1674, 1549, 1429, 1363, 1328, 1280, 1130, 1073 cm^{-1}.

all peaks

^{1}H NMR (600 MHz, $CDCl_3$): δ 5.99 (d, *J* = 4.2 Hz, 1H), 5.94 (d, *J* = 4.8 Hz, 1H), 3.44 – 3.39 (m, 2H), 2.03 – 1.92 (m, 8H), 1.84 (s, 3H), 1.83 (s, 3H), 1.77 (ddd, *J* = 12.0, 5.9, 2.8 Hz, 2H), 1.71 (s, 3H), 1.68 (s, 3H), 1.56 (s, 6H), 1.35 (s, 3H), 1.32 (s, 3H).

all peaks

^{13}C NMR (150 MHz, $CDCl_3$): δ 185.1, 185.0, 184.2, 184.1, 182.1, 182.0, 174.7, 174.7, 153.4, 152.9, 140.8, 140.3, 137.1, 137.0, 120.5, 120.3, 119.2, 119.2, 116.0, 115.4, 82.1, 65.8, 65.3, 41.0, 39.7, 39.6, 30.9, 30.8, 29.9, 28.6, 25.7, 25.7, 25.4, 25.4, 24.0, 23.7, 23.6, 20.9, 20.3, 20.2, 19.0, 18.5.

HRMS (ESI): calculated for $C_{21}H_{20}ClN_2O_5$ 415.1055 $[M+H]^+$, found 415.1059.

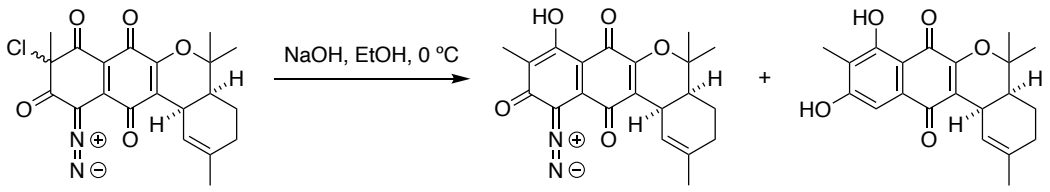

4.128

4.104
19%

4.28: naphterpin
18%

To a solution of **4.128** (12 mg, 0.03 mmol) in EtOH (1 mL) at –0 ºC was added NaOH (1.4 mg, 0.03 mmol). The reaction was stirred at rt for 10 min. The mixture was diluted with H_2O (5 mL) and brine (10 mL) and extracted with EtOAc (3 × 10 mL). The combined organic extracts were washed with saturated brine (25 mL), dried over anhydrous $MgSO_4$, filtered and concentrated *in vacuo*. The residue was purified by flash chromatography on SiO_2 (9:1 → 4:1, petrol/EtOAc gradient elution) to give naphterpin (**4.28**) (2 mg, 18%) and **4.104** (2 mg, 19%).

Data matched that given for naphterpin (**4.28**) and **4.104** above.

4.4.3 Molecular Modelling and NMR Calculations

Calculations of molecular geometries and energies were carried out with density functional theory (DFT) using Gaussian 16 (revision A.03).[75] Geometries optimisations, frequency analyses and single point energy calculations were run in the gas phase at the B3LYP/6-31G(d) level. Stable ground states were confirmed by the absence of imaginary vibrational frequencies. Calculations of NMR homonuclear ^{1}H spin–spin coupling constants were performed using the DU4 method.[76] Selected vicinal Fermi contact (FC) values were scaled according to J = 1.196*FC - 0.05.

^{13}C NMR chemical shift calculations for naphthgeranine C (**6**) and naphthoquinone C (**25**) were run using the GIAO method at the mPW1PW91/6-311+G(2d,p) level in methanol solvent using the SMD continuum solvent model.[77] Chemical shifts ($\boldsymbol{\delta}$) were calculated by scaling the isotropic magnetic shielding tensor values ($\boldsymbol{\sigma}$) according to $\boldsymbol{\delta}$ = (intercept - $\boldsymbol{\sigma}$)/(-slope), where slope = -1.0399, intercept = 186.5993.[78]

Comparison of selected ^{1}H spin-spin coupling constants of compounds **19** and **20** with experimental data:

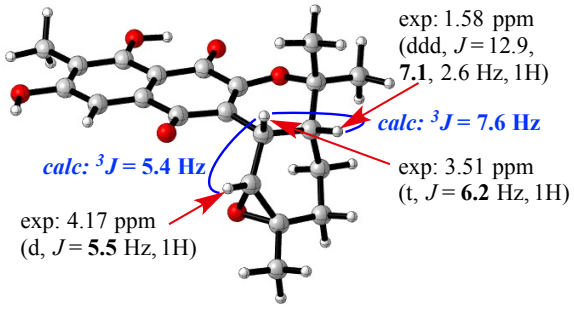

4.73

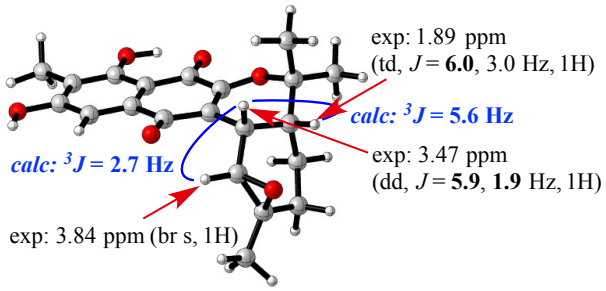

4.74

Molecular Structures and Energies

Epoxide 4.73

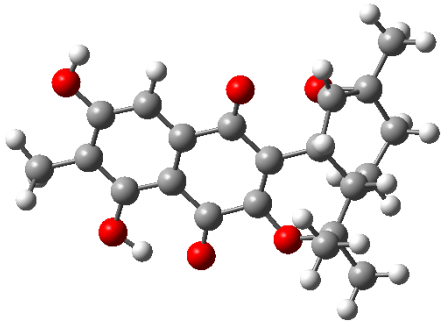

C 0.30505900 -1.16563800 0.09326300
O 1.16643000 -2.18025600 -0.07223200
C 2.46234100 -2.07147300 0.59901100
C 3.28730900 -3.20842800 -0.00621000
H 3.29803900 -3.15918400 -1.09688500
H 2.85608100 -4.17243300 0.28011300
H 4.31891800 -3.16852800 0.36013700
C 2.24378700 -2.33802800 2.09751300
H 1.58174200 -1.60152800 2.55957200
H 3.20316800 -2.31405600 2.62612200
H 1.79870100 -3.32787800 2.23640000
C 3.05413000 -0.66315300 0.34059300
H 3.97546400 -0.60050600 0.93741300
C 3.44398300 -0.41362500 -1.12917600
H 4.08108600 -1.22369000 -1.49528000
H 2.54865900 -0.39545200 -1.75938200
C 4.20595500 0.90716000 -1.27926000
H 5.18223200 0.83526700 -0.77739700
H 4.41433900 1.10536000 -2.33942300
C 3.44731200 2.08242100 -0.69558100
C 2.41083800 1.82992300 0.32426700
C 2.08193000 0.43237300 0.86674000
H 2.19756900 0.51325000 1.95655500
C 0.63682500 0.06345200 0.57357800
O 2.04619200 2.10176900 -1.04147000
C -1.08903300 -1.52759200 -0.33016400
C -0.42913400 1.02818700 0.89313700
C -1.82861100 0.70649400 0.47074900
C -4.49455000 0.13836200 -0.31665400
C -2.12994200 -0.53585600 -0.12753300
C -2.82627400 1.63967500 0.67775000
C -4.14723100 1.35367200 0.28169700
C -3.46768500 -0.80696000 -0.51473700
H -2.56927400 2.58690900 1.14444700
O -1.30322100 -2.64244200 -0.83383400
O -0.18784800 2.06518400 1.51213600
O -3.81015700 -1.97358600 -1.08124200
H -2.97971800 -2.51715500 -1.14109400
O -5.14128900 2.26584100 0.47378000
H -4.76419500 3.05842700 0.88690300
C -5.90168900 -0.18456800 -0.74291900
H -6.27573800 -1.06769700 -0.21158500
H -5.93705000 -0.42556200 -1.81155500
H -6.57293200 0.65263900 -0.54773400
H 2.15042800 2.63757600 1.00368300
C 4.13433600 3.42910500 -0.76204200
H 3.49544600 4.21066300 -0.34068400
H 4.35706200 3.69396600 -1.80285700
H 5.08115900 3.41452200 -0.20870400

Electronic Energy (EE) = -1264.8172 Hartree
Zero-point Energy Correction = 0.398147 Hartree

Epoxide 4.74

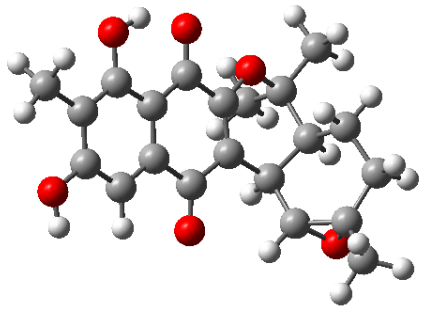

```
C 0.27343100 -1.16350300 0.10381400
O 1.10974300 -2.19841300 -0.03757700
C 2.44869900 -2.08178900 0.55057500
C 3.23567000 -3.22808600 -0.08688200
H 3.19876800 -3.18699900 -1.17720100
H 2.81276800 -4.18782700 0.22500300
H 4.28267200 -3.19085400 0.23267000
C 2.31759000 -2.32913900 2.06157900
H 1.65047200 -1.61076200 2.54405300
H 3.30055900 -2.25665100 2.53987800
H 1.91921800 -3.33238400 2.24038300
C 3.01203200 -0.67865600 0.22712300
H 3.98939100 -0.59451400 0.71614100
C 3.19760800 -0.44014600 -1.28547600
H 3.78123500 -1.25061000 -1.73149800
H 2.21537100 -0.46157900 -1.77370200
C 3.89379500 0.89126300 -1.60486100
H 4.97659700 0.80425700 -1.44364000
H 3.75634700 1.12094800 -2.66876900
C 3.40080000 2.05861700 -0.76236300
O 3.93252600 2.05981600 0.58513400
C 2.52786700 1.80837600 0.40165000
H 1.88520000 2.61070800 0.75157800
C 2.08563300 0.40968100 0.83430300
H 2.20687400 0.41235300 1.92772200
C 0.62798400 0.08557200 0.52884100
C 3.39889500 3.41833600 -1.42717200
H 3.10238100 4.19550100 -0.71678100
H 2.70636000 3.43734400 -2.27722600
H 4.40018100 3.66242700 -1.80348600
C -1.12925200 -1.52986600 -0.29585700
C -0.43632000 1.06206800 0.82626600
C -1.84433800 0.73004300 0.43603700
C -4.52556200 0.15157700 -0.29419300
C -2.16239400 -0.52870600 -0.11512000
C -2.83433600 1.67539400 0.62617300
C -4.16296800 1.38295500 0.26122500
C -3.50693900 -0.80577700 -0.47463700
H -2.56657400 2.63531500 1.05951100
O -1.35338700 -2.65854500 -0.76234200
O -0.19776900 2.12805500 1.39715500
O -3.86209400 -1.98890500 -0.99651000
H -3.03518700 -2.53841700 -1.04973500
O -5.14990400 2.30465800 0.44068400
H -4.76492800 3.10698000 0.82697600
C -5.94102100 -0.17619600 -0.68785500
H -6.34102000 -0.98653000 -0.06619900
H -5.98157400 -0.52879400 -1.72425600
H -6.58928000 0.69465200 -0.58278500
```

Electronic Energy (EE) = -1264.8158 Hartree
Zero-point Energy Correction = 0.398173 Hartree

4.4.4 Single Crystal X-ray Data

A single crystal of **4.73** was mounted in paratone-N oil on a Mitigen crystal mount and X-ray diffraction data were collected at 150(2) K on an Oxford X-calibur single crystal diffractometer using Mo Kα radiation. The data set was corrected for absorption using a multi-scan method, and the structures solved by direct methods using SHELXS-2008 and refined by full-matrix least squares on F2 by SHELXL-2015,[79–81] interfaced through the programs X-Seed[82] and Olex2 (Tables).[83] Unless otherwise stated, non-hydrogen atoms were refined anisotropically and hydrogen atoms were included as invariants at geometrically estimated positions. Full data for the structure determination has been deposited with the Cambridge Crystallographic Data Centre as CCDC 1946257. Copies of this information may be obtained free of charge from The Director, CCDC, 12 Union Street, Cambridge CB2 1EZ, U.K. (fax, +44-1223-336-033; e-mail, deposit@ccdc.cam.ac.uk). The table below provides the crystal data and structure refinement details for compound **4.73**.

Compound **4.73** crystallises in the triclinic space group *P*-1 with four complete molecules and four dichloroethane solvate molecules in the asymmetric unit; these comprise two crystallographically independent pairs of hydrogen bonded dimers of **4.73** in which each dimer comprises a pair of molecules of the same stereochemistry (the dimers of **4.73** within the asymmetric unit are enantiomers consistent with the compound being a racemic mixture). The figures below show a representation of the asymmetric unit and one selected molecule (thermal ellipsoids shown at the 50% probability level), a view of one of the hydrogen bonded dimers with the intramolecular and intermolecular hydrogen bonds shown and finally a packing diagram of the structure viewed down the *a*-axis.

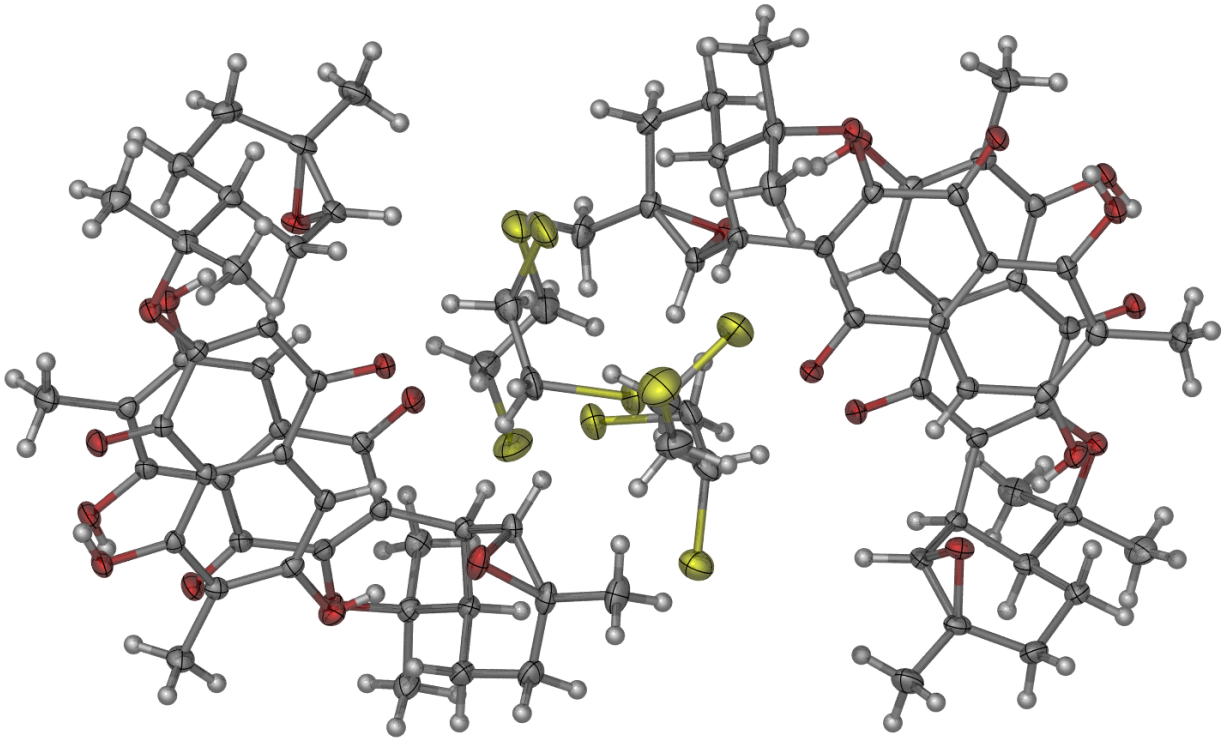

(a)

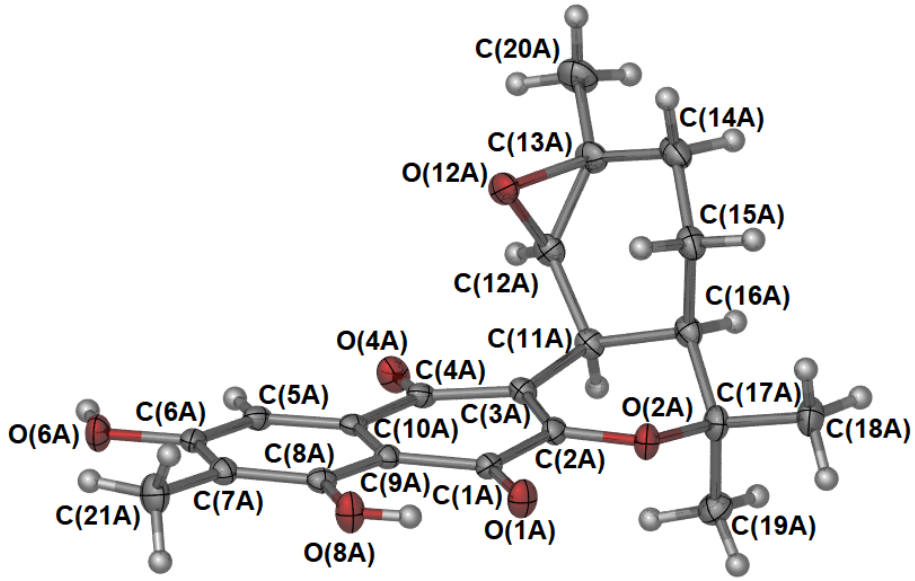

(b)

Figure SI-4.1: (a) A perspective view of the asymmetric unit of **4.73** with thermal ellipsoids shown at the 50% probability level. Carbon – grey; hydrogen – white; oxygen – red; chlorine – yellow. (b) One selected molecule of **4.73** is shown to more clearly represent the molecular structure.

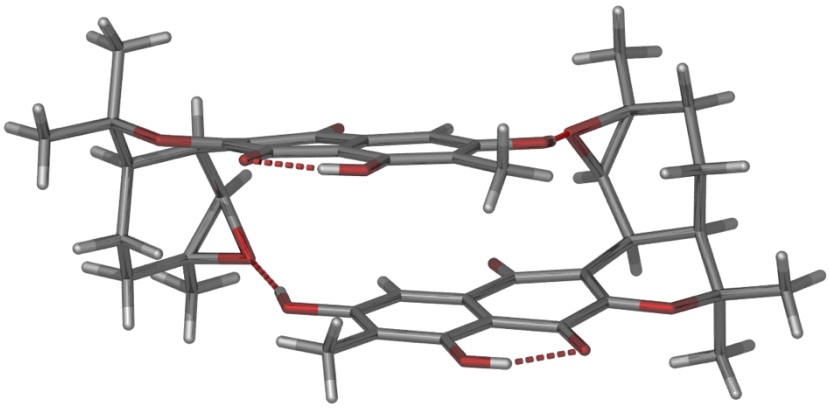

Figure SI-4.2: A perspective view of one of the hydrogen bonded dimers within the structure of **4.73**. The hydrogen bonds are shown with the dashed lines.

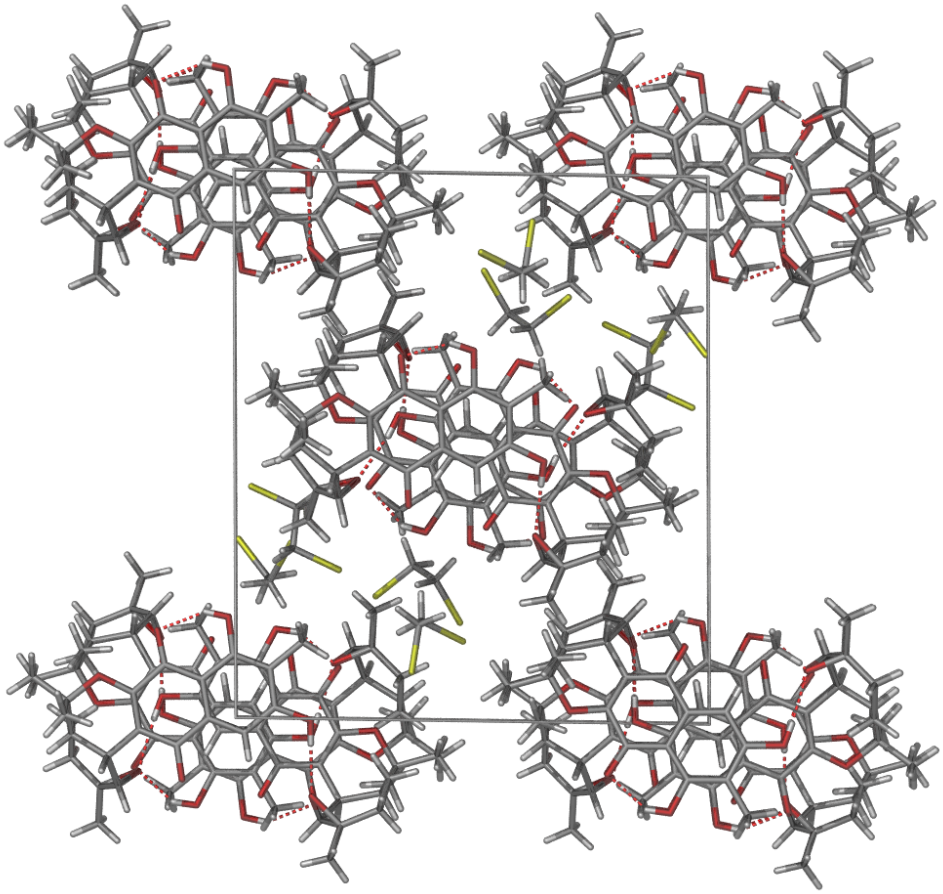

Figure SI-4.3: A view down the *a*-axis of the packing of compound **4.73.**

Table SI-4.1. Crystal data and structure refinement for **4.73**.

Identification code	LMX1
CCDC number	1946257
Empirical formula	$C_{92}H_{104}NO_{24}Cl_8$
Formula weight	1877.35
Temperature/K	150.1(2)
Crystal system	triclinic
Space group	P-1
a/Å	13.4564(3)
b/Å	17.9080(3)
c/Å	19.7291(3)
α/°	85.6940(10)
β/°	80.149(2)
γ/°	70.114(2)
Volume/Å^3	4404.13(15)
Z	2
ρ_{calc}g/cm^3	1.416
μ/mm^{-1}	0.333
F(000)	1968.0
Crystal size/mm^3	0.72 × 0.22 × 0.12
Radiation	MoKα (λ = 0.71073)
2θ range for data collection/°	6.698 to 58.926
Index ranges	$-18 \leq h \leq 18$, $-24 \leq k \leq 24$, $-27 \leq l \leq 25$
Reflections collected	97503
Independent reflections	21565 [R_{int} = 0.0435, R_{sigma} = 0.0395]
Data/restraints/parameters	21565/0/1141
Goodness-of-fit on F^2	1.018
Final R indexes [I>=2σ (I)]	R_1 = 0.0472, wR_2 = 0.1064
Final R indexes [all data]	R_1 = 0.0766, wR_2 = 0.1220
Largest diff. peak/hole / e Å^{-3}	0.65/-0.54

4.5 References

(1) Clayden, J.; Greeves, N.; Warren, S. G. *Organic Chemistry*; Oxford University Press: Oxford, 2012.

(2) Nicolaou, K. C.; Snyder, S. A.; Montagnon, T.; Vassilikogiannakis, G. *Angew. Chem. Int. Ed.* **2002**, *41*, 1668.

(3) Juhl, M.; Tanner, D. *Chem. Soc. Rev.* **2009**, *38*, 2983.

(4) Nicolaou, K. C.; Vassilikogiannakis, G.; Mägerlein, W.; Kranich, R. *Chem. - A Eur. J.* **2001**, *7*, 5359.

(5) Shao, H.; Gao, X.; Wang, Z. T.; Gao, Z.; Zhao, Y. M. *Angew. Chem. Int. Ed.* **2020**, *59*, 7419.

(6) Shoyama, Y. Y.; Tamada, T.; Kurihara, K.; Takeuchi, A.; Taura, F.; Arai, S.; Blaber, M.; Shoyama, Y. Y.; Morimoto, S.; Kuroki, R. *J. Mol. Biol.* **2012**, *423*, 96.

(7) Murray, L. A. M.; McKinnie, S. M. K.; Pepper, H. P.; Erni, R.; Miles, Z. D.; Cruickshank, M. C.; López-Pérez, B.; Moore, B. S.; George, J. H. *Angew. Chem. Int. Ed.* **2018**, *57*, 11009.

(8) Tapia, R. A.; Alegrı, L.; Valderrama, J. A.; Corte, M.; Lyon, C. B.; Rockefeller, A.; Cedex, L.; Alegría, L.; Valderrama, J. A.; Cortés, M.; Pautet, F.; Fillion, H. *Tetrahedron Lett.* **2001**, *42*, 887.

(9) Tapia, R. A.; Alegría, L.; Valderrama, J. A.; Cortés, M.; Pautet, F.; Fillion, H. *Tetrahedron Lett.* **2001**, *42*, 887.

(10) Takemura, S.; Hirayama, A.; Tokunaga, J.; Kawamura, F.; Inagaki, K.; Hashimoto, K.; Nakata, M. *Tetrahedron Lett.* **1999**, *40*, 7501.

(11) Capecchi, T.; De Koning, C. B.; Michael, J. P. *J. Chem. Soc. Perkin Trans. 1* **2000**, No. 16, 2681.

(12) Zhang, Z.; Chen, J.; Yang, Z.; Tang, Y. *Org. Lett.* **2010**, *12*, 5554.

(13) Snider, B. B.; Lobera, M. *Tetrahedron Lett.* **2004**, *45*, 5015.

(14) Zhou, J.; Lobera, M.; Neubert-Langille, B. J.; Snider, B. B. *Tetrahedron* **2007**, *63*, 10018.

(15) Nawrat, C. C.; Moody, C. J. *Angew. Chem. Int. Ed.* **2014**, *53*, 2056.

(16) Dimakos, V.; Singh, T.; Taylor, M. S. *Org. Biomol. Chem.* **2016**, *14*, 6703.

(17) Wang, X.; Lee, Y. R. *Tetrahedron* **2009**, *65*, 10125.

(18) Wang, X.; Lee, Y. R. *Tetrahedron* **2011**, *67*, 9179.

(19) Gembus, V.; Sala-Jung, N.; Uguen, D. *Bull. Chem. Soc. Jpn.* **2009**, *82*, 843.

(20) Kang, Y.; Mei, Y.; Du, Y.; Jin, Z. *Org. Lett.* **2003**, *5*, 4481.

(21) Hesse, R.; Gruner, K. K.; Kataeva, O.; Schmidt, A. W.; Knölker, H. J. *Chem. Eur. J.* **2013**, *19*, 14098.

(22) Chauder, B. A.; Lopes, C. C.; Lopes, R. S. C.; Silva, J. M. *Synthesis (Stuttg).* **1998**, 279.

(23) Pettigrew, J. D.; Cadieux, J. A.; So, S. S. S.; Wilson, P. D. *Org. Lett.* **2005**, *7*, 467.

(24) Schuster, C.; Julich-Gruner, K. K.; Schnitzler, H.; Hesse, R.; Jäger, A.; Schmidt, A. W.; Knölker, H. J. *J. Org. Chem.* **2015**, *80*, 5666.

(25) Katakawa, K.; Kainuma, M.; Suzuki, K.; Tanaka, S.; Kumamoto, T. *Tetrahedron* **2017**, *73*, 5063.

(26) Huang, Z.; Kwon, O.; Esguerra, K. V. N.; Lumb, J. P. *Tetrahedron* **2015**, *71*, 5871.
(27) Zimmer, H.; Lankin, D. C.; Horgan, S. W. *Chem. Rev.* **1971**, *71*, 229.
(28) Frémy, E. *Ann. Chim. Phys.* **1845**, *15*, 408.
(29) Raschig, F. *Schwefel and Stickstoff-Studien*; Verlag Chemie: Leipzig-Berlin, 1924.
(30) Cherkaoui, O.; Nebois, P.; Fillion, H.; Domard, M.; Fenet, B. *Tetrahedron* **1996**, *52*, 9499.
(31) Tan, Y.; Yang, X. Di; Liu, W. J.; Sun, X. W. *Tetrahedron Lett.* **2014**, *55*, 6105.
(32) Dong, S.; Frings, M.; Zhang, D.; Guo, Q.; Daniliuc, C. G.; Cheng, H.; Bolm, C. *Chem. - A Eur. J.* **2017**, *23*, 13888.
(33) Claudio, S. B.; Valderrama, J. A.; Tapia, R.; Farifia, F.; Paredes, M. C. *Synth. Commun.* **1992**, *22*, 955.
(34) Tapia, R. A.; Bau, A.; Salas, C. *Synth. Commun.* **2006**, *36*, 771.
(35) Godfrey, J. D.; Mueller, R. H.; Sedergran, T. C.; Soundararajan, N.; Colandrea, V. J. *Tetrahedron Lett.* **1994**, *35*, 6405.
(36) Tsuji, J.; Sugiura, T.; Minami, I. *Synthesis (Stuttg).* **1987**, *7*, 603.
(37) Gassner, C.; Hesse, R.; Schmidt, A. W.; Knölker, H. J. *Org. Biomol. Chem.* **2014**, *12*, 6490.
(38) Tisdale, E. J.; Chowdhury, C.; Vong, B. G.; Li, H.; Theodorakis, E. A. *Org. Lett.* **2002**, *4*, 909.
(39) Tapia, R. A.; Lizama, C.; López, C.; Valderrama, J. A. *Synth. Commun.* **2001**, *31*, 601.
(40) Nicolaou, K. C.; Sasmal, P. K.; Xu, H.; Namoto, K.; Ritzén, A. *Angew. Chem. Int. Ed.* **2003**, *42*, 4225.
(41) Savard, J.; Brassard, P. *Tetrahedron Lett.* **1979**, *20*, 4911.
(42) Donner, C. D.; Gill, M. *J. Chem. Soc. Perkin 1* **2002**, *2*, 938.
(43) Barker, D.; Brimble, M. A.; Do, P.; Turner, P. *Tetrahedron* **2003**, *59*, 2441.
(44) Wuts, P. G. M. *Greene's Protective Groups in Organic Synthesis*, 5th ed.; John Wiley & Sons, Inc., 2014.
(45) Krapcho, A. P.; Jahngen, Jr., E. G. E.; Lovey, A. J.; Short, F. W. *Tetrahedron Lett.* **1974**, *15*, 1091.
(46) Krapcho, A. P.; Weimaster, J. F.; Eldridge, J. M.; Jahngen, Jr., E. G. E.; Lovey, A. J.; Stephens, W. P. *J. Org. Chem.* **1978**, *43*, 138.
(47) Pepper, H. P.; George, J. H. *Angew. Chem. Int. Ed.* **2013**, *52*, 12170.
(48) Merlic, C. A.; Aldrich, C. C.; Albaneze-Walker, J.; Saghatelian, A. *J. Am. Chem. Soc.* **2000**, *122*, 3224.
(49) Snyder, S. A.; Tang, Z. Y.; Gupta, R. *J. Am. Chem. Soc.* **2009**, *131*, 5744.
(50) Courchesne, M.; Brassard, P. *J. Nat. Prod.* **1993**, *56*, 722.
(51) Nawrat, C. C.; Lewis, W.; Moody, C. J. *J. Org. Chem.* **2011**, *76*, 7872.
(52) Shin-ya, K.; Imai, S.; Furihata, K.; Hayakawa, Y.; Kato, Y.; Vanduyne, G. D.; Clardy, J.; Seto, H. *J. Antibiot.* **1990**, *21*, 444.
(53) Gläser, F.; Bröhmer, M. C.; Hurrle, T.; Nieger, M.; Bräse, S. *European J. Org. Chem.* **2015**, *2015*, 1516.
(54) Takagi, H.; Motohashi, K.; Miyamoto, T.; Shin-ya, K.; Furihata, K.; Seto, H. *J. Antibiot.* **2005**, *58*, 275.

(55) Tumma, N.; Jacolot, M.; Jean, M.; Chandrasekhar, S.; Van De Weghe, P. *Synlett* **2012**, *23*, 2919.
(56) Yu, J. S.; Kleckley, T. S.; Wiemer, D. F. *Org. Lett.* **2005**, *7*, 4803.
(57) Hardt, I. H.; Jensen, P. R.; Fenical, W. *Tetrahedron Lett.* **2000**, *41*, 2073.
(58) Cho, J. Y.; Kwon, H. C.; Williams, P. G.; Jensen, P. R.; Fenical, W. *Org. Lett.* **2006**, *8*, 2471.
(59) Winter, J. M.; Jansma, A. L.; Handel, T. M.; Moore, B. S. *Angew. Chem. Int. Ed.* **2009**, *48*, 767.
(60) Landry, M. L.; McKenna, G. M.; Burns, N. Z. *J. Am. Chem. Soc.* **2019**, *141*, 2867.
(61) Schnell, S. D.; Linden, A.; Gademann, K. *Org. Lett.* **2019**, *21*, 1144.
(62) Teich, L.; Daub, K. S.; Krügel, V.; Nissler, L.; Gebhardt, R.; Eger, K. *Bioorganic Med. Chem.* **2004**, *12*, 5961.
(63) Bittner, S.; Lempert, D. *Synthesis (Stuttg).* **1994**, *9*, 917.
(64) Jacobs, J.; Claessens, S.; Mavinga Mbala, B.; Huygen, K.; De Kimpe, N. *Tetrahedron* **2009**, *65*, 1193.
(65) Jonathan, H.; Crossleya, J.; Samuela, E. L. *Aust. J. Chem.* **1976**, *29*, 2247.
(66) Escoubet, S.; Gastaldi, S.; Bertrand, M. *European J. Org. Chem.* **2005**, No. 18, 3855.
(67) Garro-Helion, F.; Merzouk, A.; Guibé, F. *J. Org. Chem.* **1993**, *58*, 6109.
(68) Kumar, P.; Cherian, S. K.; Jain, R.; Show, K. *Tetrahedron Lett.* **2014**, *55*, 7172.
(69) Alcaide, B.; Almendros, P.; Alonso, J. M.; Aly, M. F. *Org. Lett.* **2001**, *3*, 3781.
(70) Alcaide, B.; Almendros, P.; Alonso, J. M. *Chem. - A Eur. J.* **2003**, *9*, 5793.
(71) Zhang, S. S.; Jiang, C. Y.; Wu, J. Q.; Liu, X. G.; Li, Q.; Huang, Z. S.; Li, D.; Wang, H. *Chem. Commun.* **2015**, *51*, 10240.
(72) Gomi, S.; Ohuchi, S.; Sasaki, T.; Itoh, J.; Sezake, M. *J. Antibiot.* **1987**, *40*, 740.
(73) Nair, D.; Pavashe, P.; Katiyar, S.; Namboothiri, I. N. N. *Tetrahedron Lett.* **2016**, *57*, 3146.
(74) Wriede, U.; Fernandez, M.; West, K. F.; Harcourt, D.; Moore, H. W. *J. Org. Chem.* **1987**, *52*, 4485.
(75) Frisch, M. J.; Trucks, G. W.; Schlegel, H. B.; Scuseria, G. E.; Robb, M. A.; Cheeseman, J. R.; Scalmani, G.; Barone, V.; Petersson, G. A.; Nakatsuji, H.; Li, X.; Caricato, M.; Marenich, A. V.; Bloino, J.; Janesko, B. G.; Gomperts, R.; Mennucci, B.; Hratch, D. J. Gaussian, Inc.: Wallingford CT 2016.
(76) Kutateladze, A. G.; Mukhina, O. A. *J. Org. Chem.* **2015**, *80*, 5218.
(77) Marenich, A. V.; Cramer, C. J.; Truhlar, D. G. *J. Phys. Chem. B* **2009**, *113*, 6378.
(78) Pierens, G. K. *J. Comput. Chem.* **2014**, *35*, 1388.
(79) Sheldrick, G. SHELXS-2014 and SHELXL-2014. Program for X-ray Crystal Structure Determination: Göttingen University, Göttingen, Germany 2014.
(80) Sheldrick, G. M. *Acta Crystallogr. Sect. A Found. Crystallogr.* **2008**, *64*, 112.
(81) Sheldrick, G. M. *Acta Crystallogr. Sect. C Struct. Chem.* **2015**, *71*, 3.
(82) Barbour, L. J. *J. Supramol. Chem.* **2001**, *1*, 189.
(83) Dolomanov, O. V.; Bourhis, L. J.; Gildea, R. J.; Howard, J. A. K.; Puschmann, H. *J. Appl. Crystallogr.* **2009**, *42*, 339.

4.6 Appendix

4.6.1 NMR Spectra

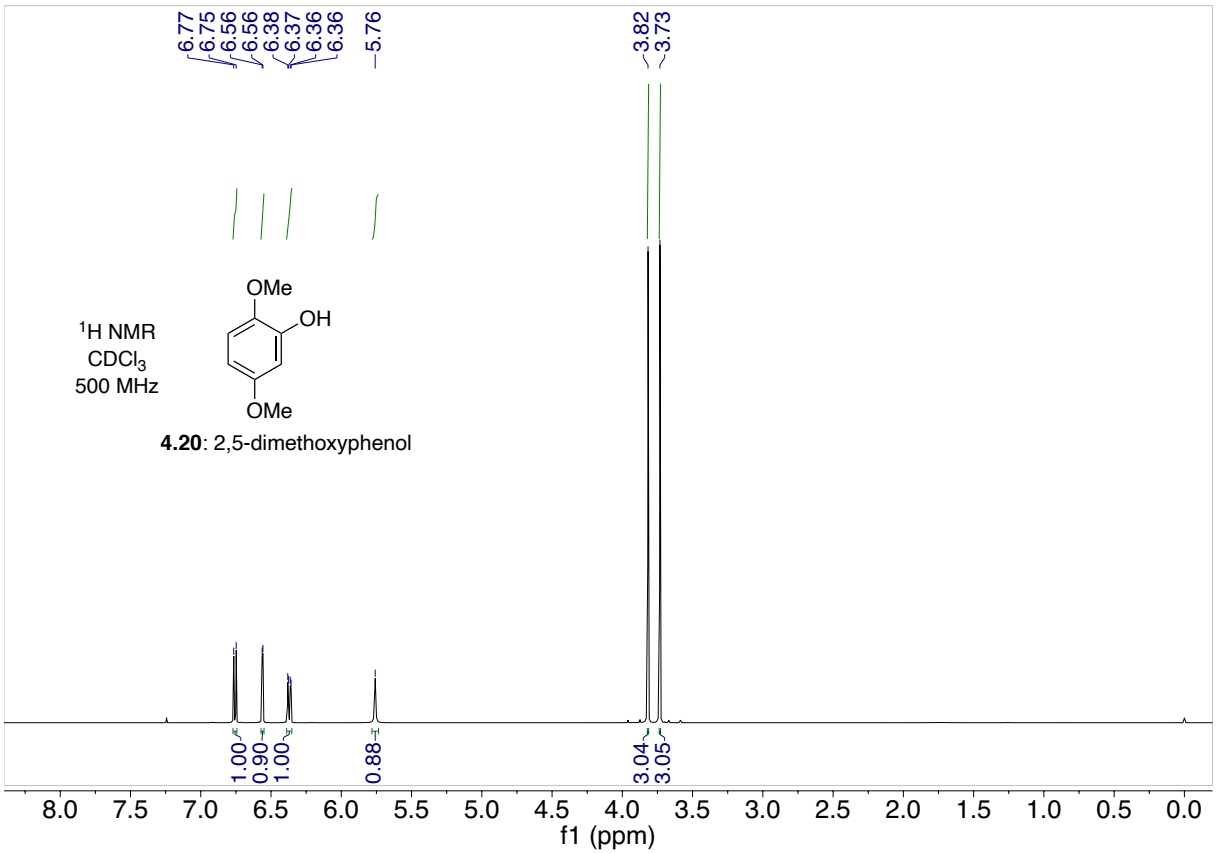

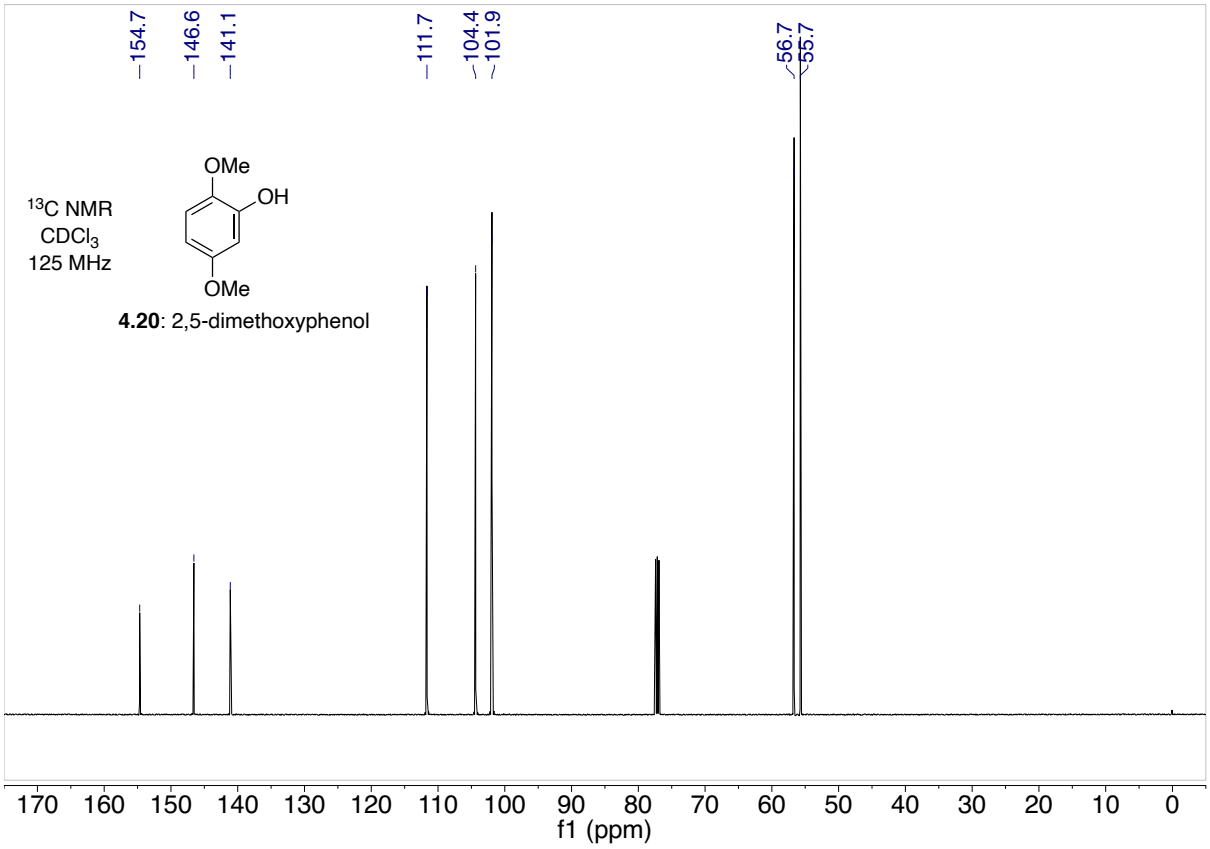

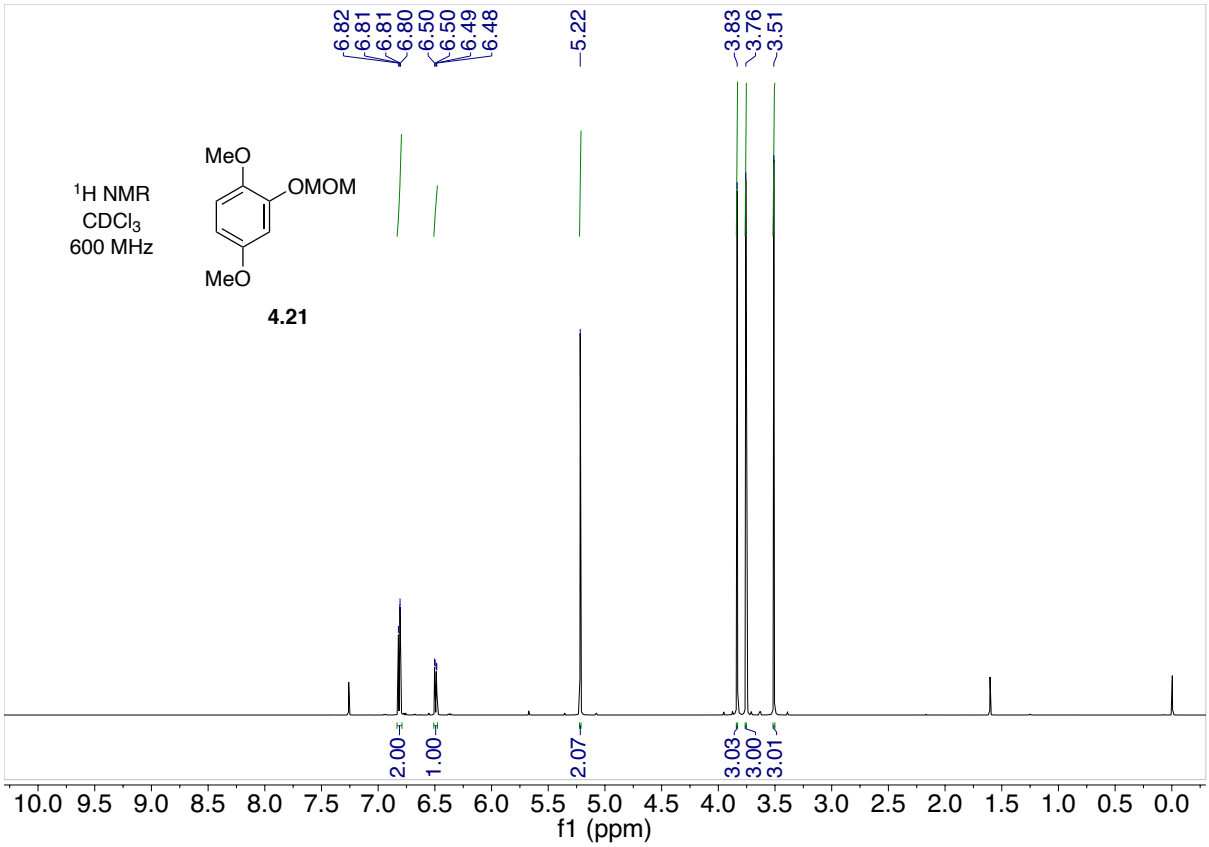
6.82
6.81
6.81
6.80
6.50
6.50
6.49
6.48
5.22
3.83
3.76
3.51
^{1}H NMR
$CDCl_3$
600 MHz
MeO
OMOM
MeO
4.21
2.00
1.00
2.07
3.03
3.00
3.01
10.0 9.5 9.0 8.5 8.0 7.5 7.0 6.5 6.0 5.5 5.0 4.5 4.0 3.5 3.0 2.5 2.0 1.5 1.0 0.5 0.0
f1 (ppm)

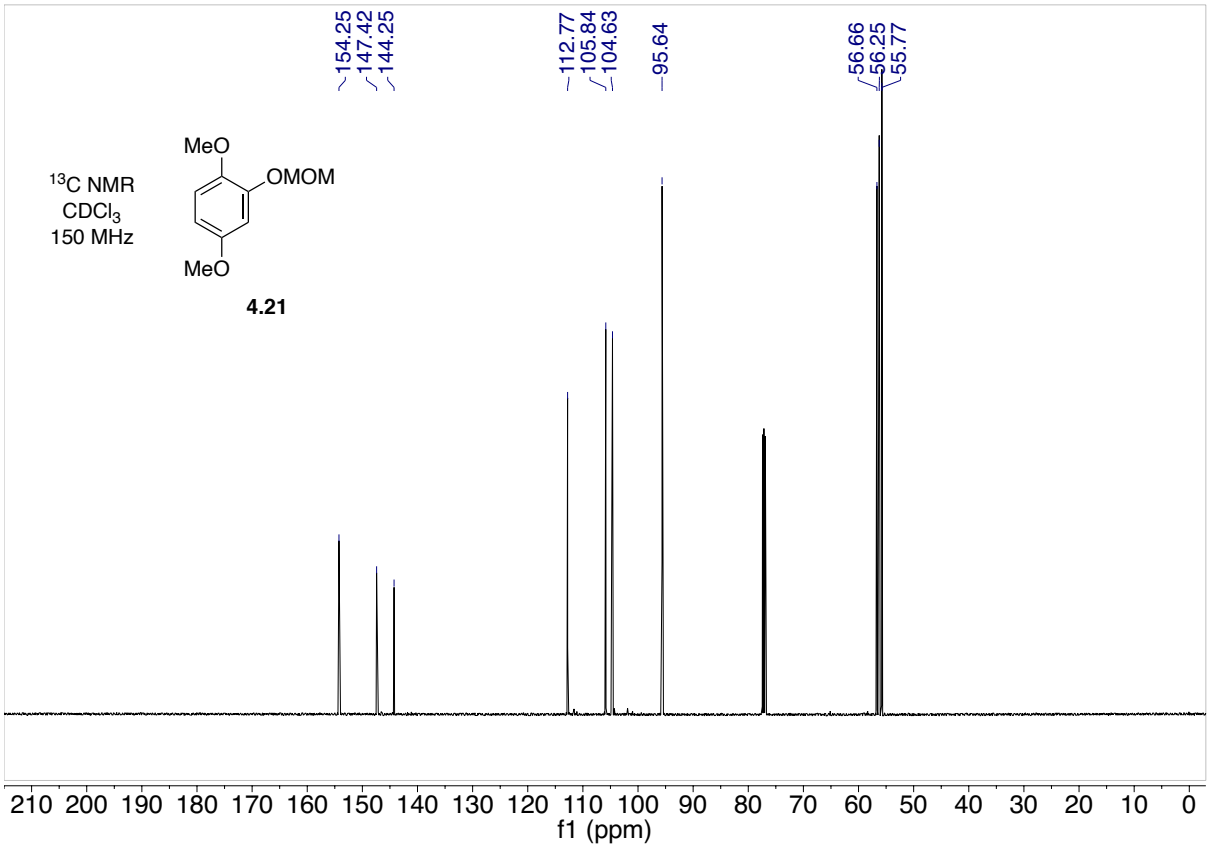
154.25
147.42
144.25
112.77
105.84
104.63
95.64
56.66
56.25
55.77
^{13}C NMR
$CDCl_3$
150 MHz
MeO
OMOM
MeO
4.21
210 200 190 180 170 160 150 140 130 120 110 100 90 80 70 60 50 40 30 20 10 0
f1 (ppm)

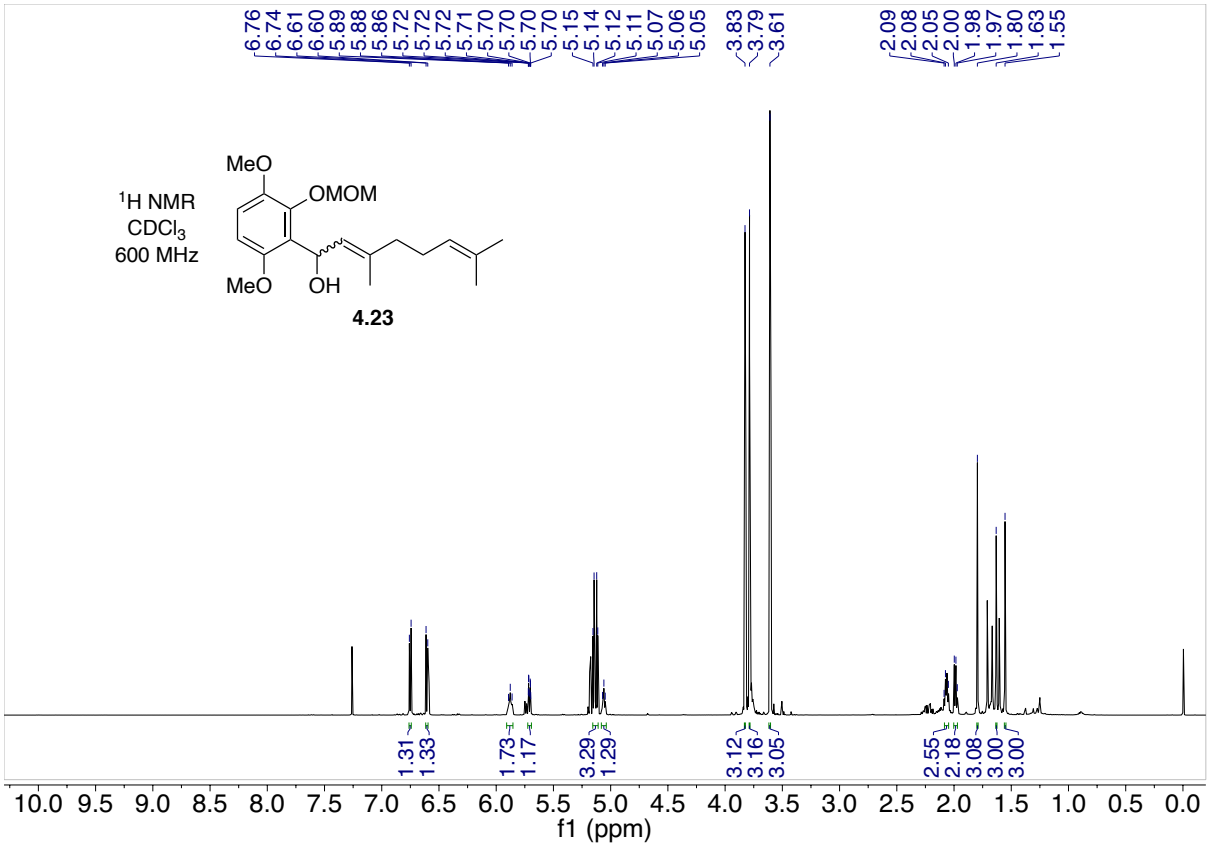
6.76
6.74
6.61
6.60
5.89
5.88
5.86
5.72
5.72
5.72
5.71
5.70
5.70
5.70
5.15
5.14
5.12
5.11
5.07
5.06
5.05
3.83
3.79
3.61
2.09
2.08
2.05
2.00
1.98
1.97
1.80
1.63
1.55
1H NMR
CDCl3
600 MHz
MeO
OMOM
MeO
OH
4.23
1.31
1.33
1.73
1.17
3.29
1.29
3.12
3.16
3.05
2.55
2.18
3.08
3.00
3.00
10.0 9.5 9.0 8.5 8.0 7.5 7.0 6.5 6.0 5.5 5.0 4.5 4.0 3.5 3.0 2.5 2.0 1.5 1.0 0.5 0.0
f1 (ppm)

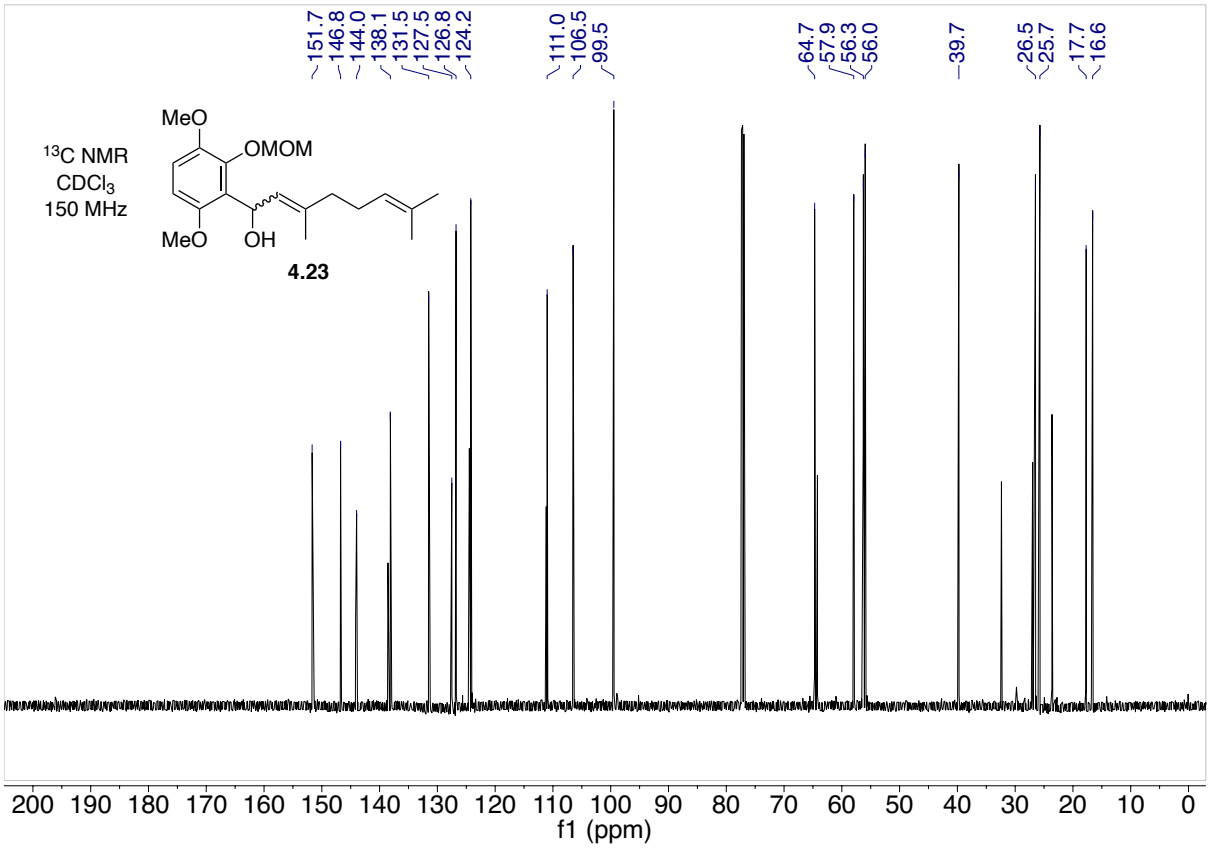
151.7
146.8
144.0
138.1
131.5
127.5
126.8
124.2
111.0
106.5
99.5
64.7
57.9
56.3
56.0
39.7
26.5
25.7
17.7
16.6
13C NMR
CDCl3
150 MHz
MeO
OMOM
MeO
OH
4.23
200 190 180 170 160 150 140 130 120 110 100 90 80 70 60 50 40 30 20 10 0
f1 (ppm)

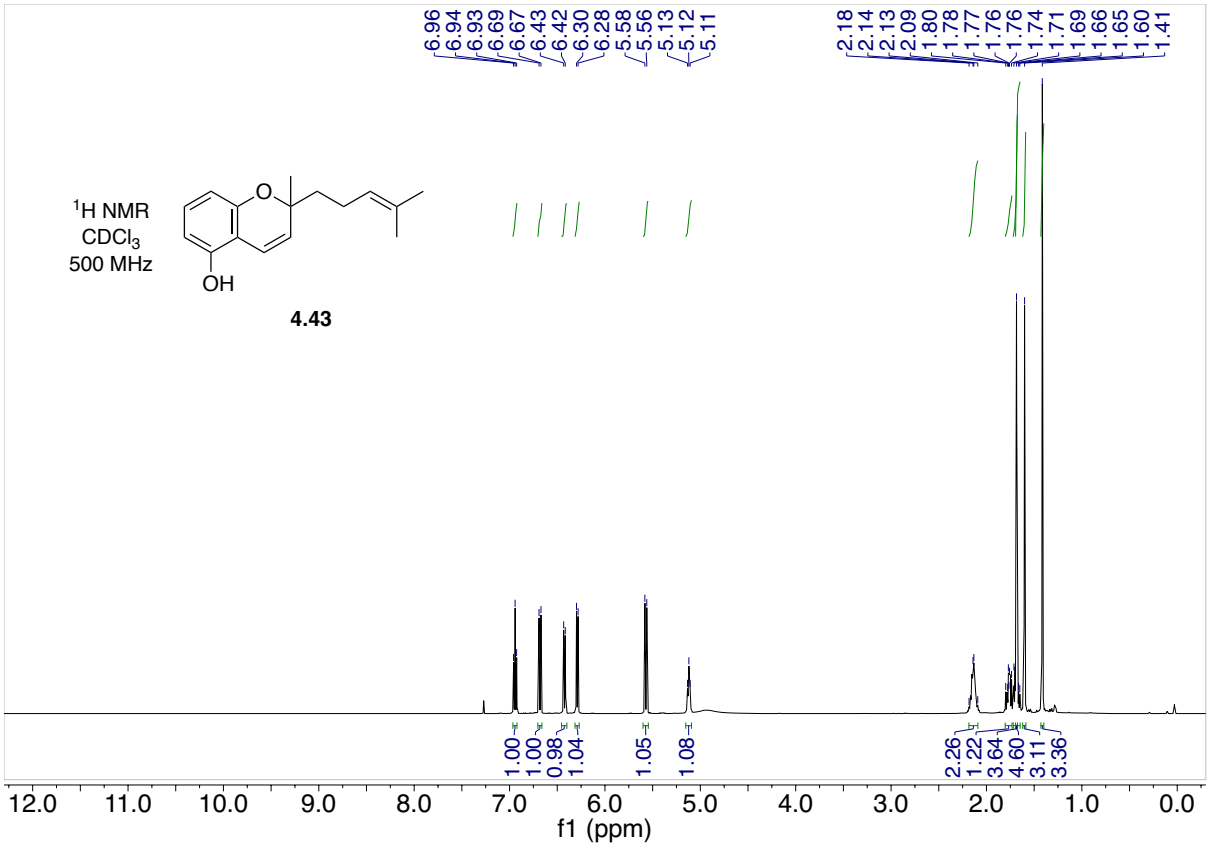
6.96
6.94
6.93
6.69
6.67
6.43
6.42
6.30
6.28
5.58
5.56
5.13
5.12
5.11
2.18
2.14
2.13
2.09
1.80
1.78
1.77
1.76
1.76
1.74
1.71
1.69
1.66
1.65
1.60
1.41
1H NMR
CDCl3
500 MHz
O
OH
4.43
1.00
1.00
0.98
1.04
1.05
1.08
2.26
1.22
3.64
4.60
3.11
3.36
12.0
11.0
10.0
9.0
8.0
7.0
6.0
5.0
4.0
3.0
2.0
1.0
0.0
f1 (ppm)

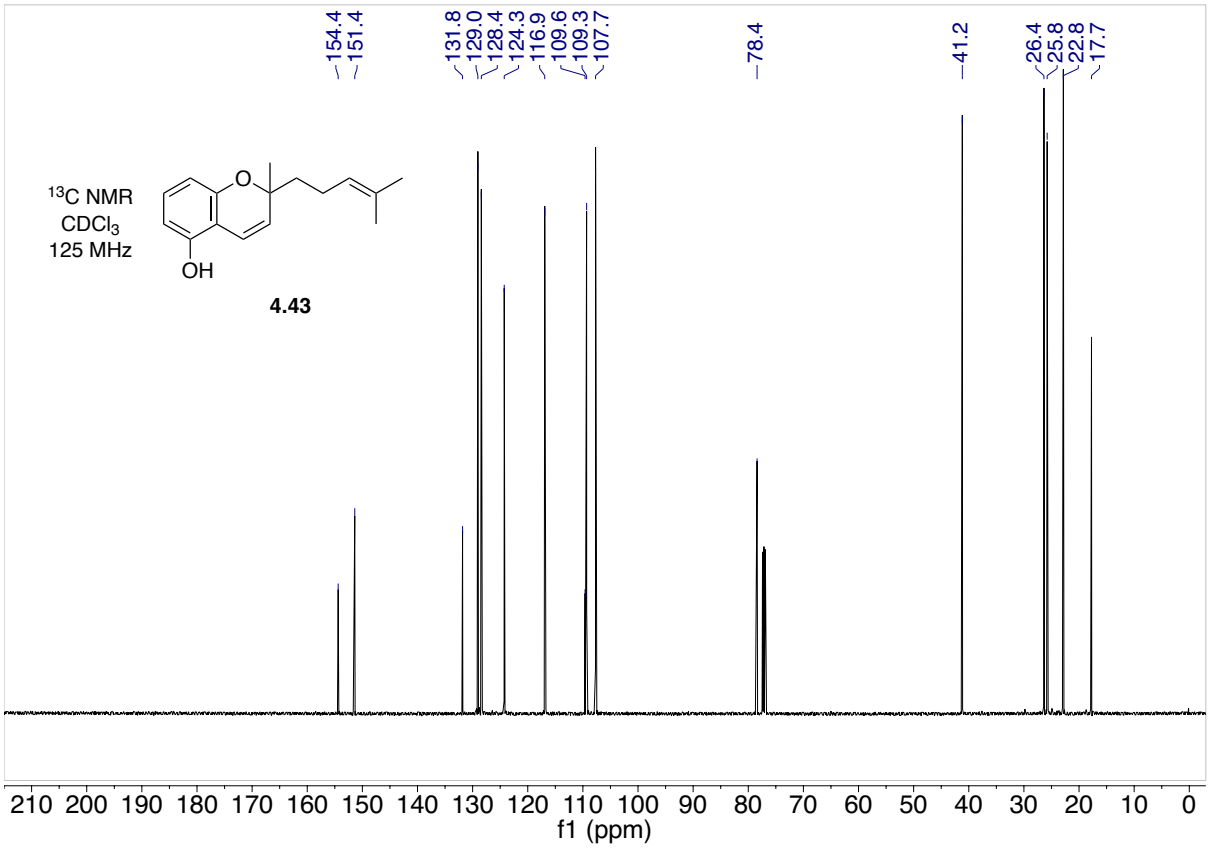
154.4
151.4
131.8
129.0
128.4
124.3
116.9
109.6
109.3
107.7
78.4
41.2
26.4
25.8
22.8
17.7
13C NMR
CDCl3
125 MHz
O
OH
4.43
210 200 190 180 170 160 150 140 130 120 110 100 90 80 70 60 50 40 30 20 10 0
f1 (ppm)

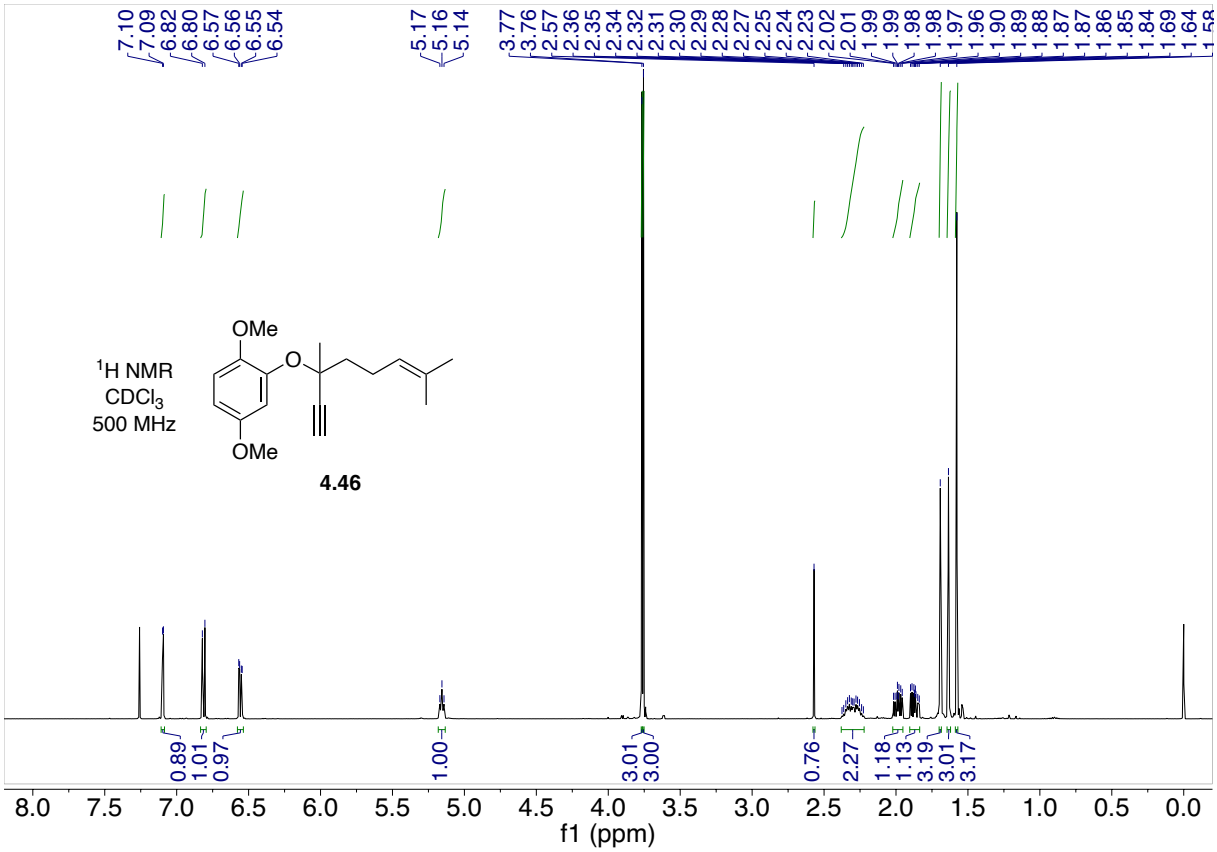
7.10
7.09
6.82
6.80
6.57
6.56
6.55
6.54
5.17
5.16
5.14
3.77
3.76
2.57
2.36
2.35
2.34
2.32
2.31
2.30
2.29
2.28
2.27
2.25
2.24
2.23
2.02
2.01
1.99
1.99
1.98
1.98
1.97
1.96
1.90
1.89
1.88
1.87
1.87
1.86
1.85
1.84
1.69
1.64
1.58
^{1}H NMR
$CDCl_3$
500 MHz
OMe
O
OMe
4.46
0.89
1.01
0.97
1.00
3.01
3.00
0.76
2.27
1.18
1.13
3.19
3.01
3.17
8.0
7.5
7.0
6.5
6.0
5.5
5.0
4.5
4.0
3.5
3.0
2.5
2.0
1.5
1.0
0.5
0.0
f1 (ppm)

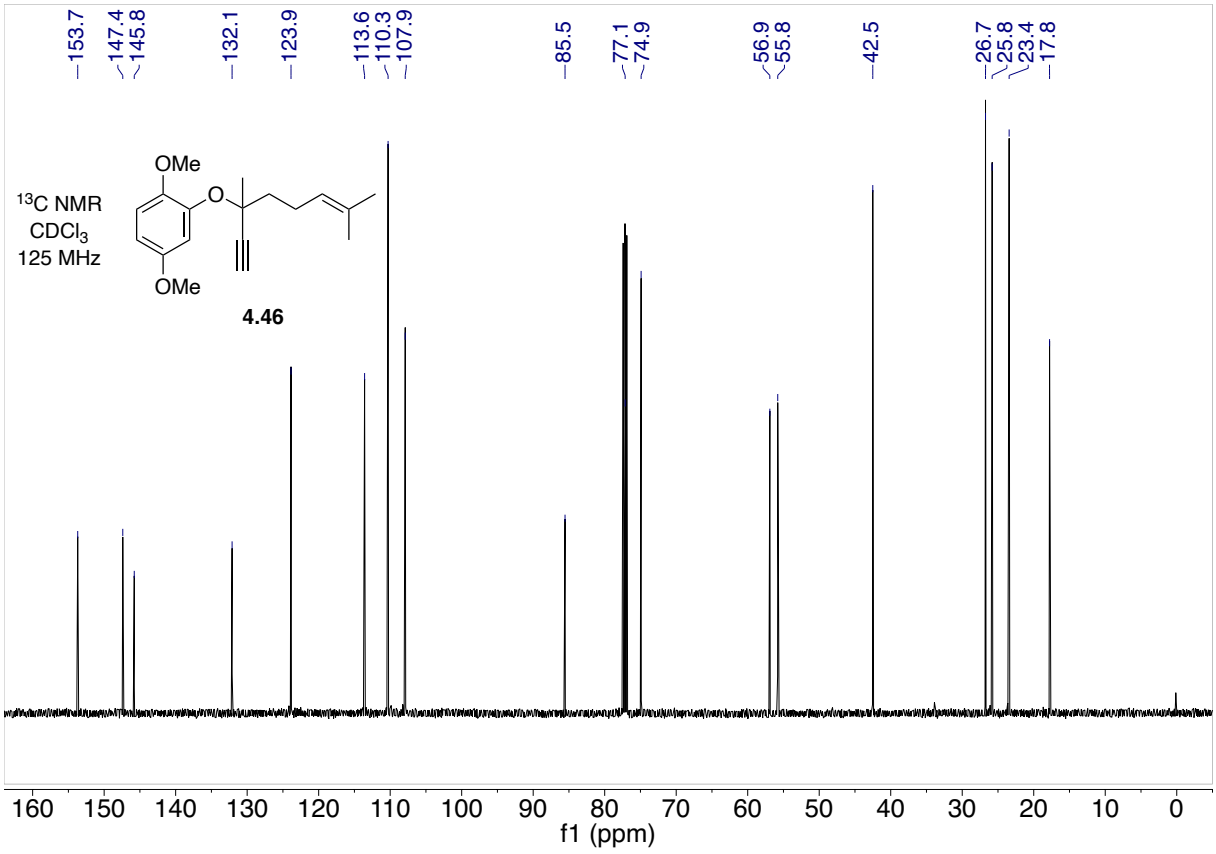
153.7
147.4
145.8
132.1
123.9
113.6
110.3
107.9
85.5
77.1
74.9
56.9
55.8
42.5
26.7
25.8
23.4
17.8
^{13}C NMR
$CDCl_3$
125 MHz
OMe
O
OMe
4.46
160
150
140
130
120
110
100
90
80
70
60
50
40
30
20
10
0
f1 (ppm)

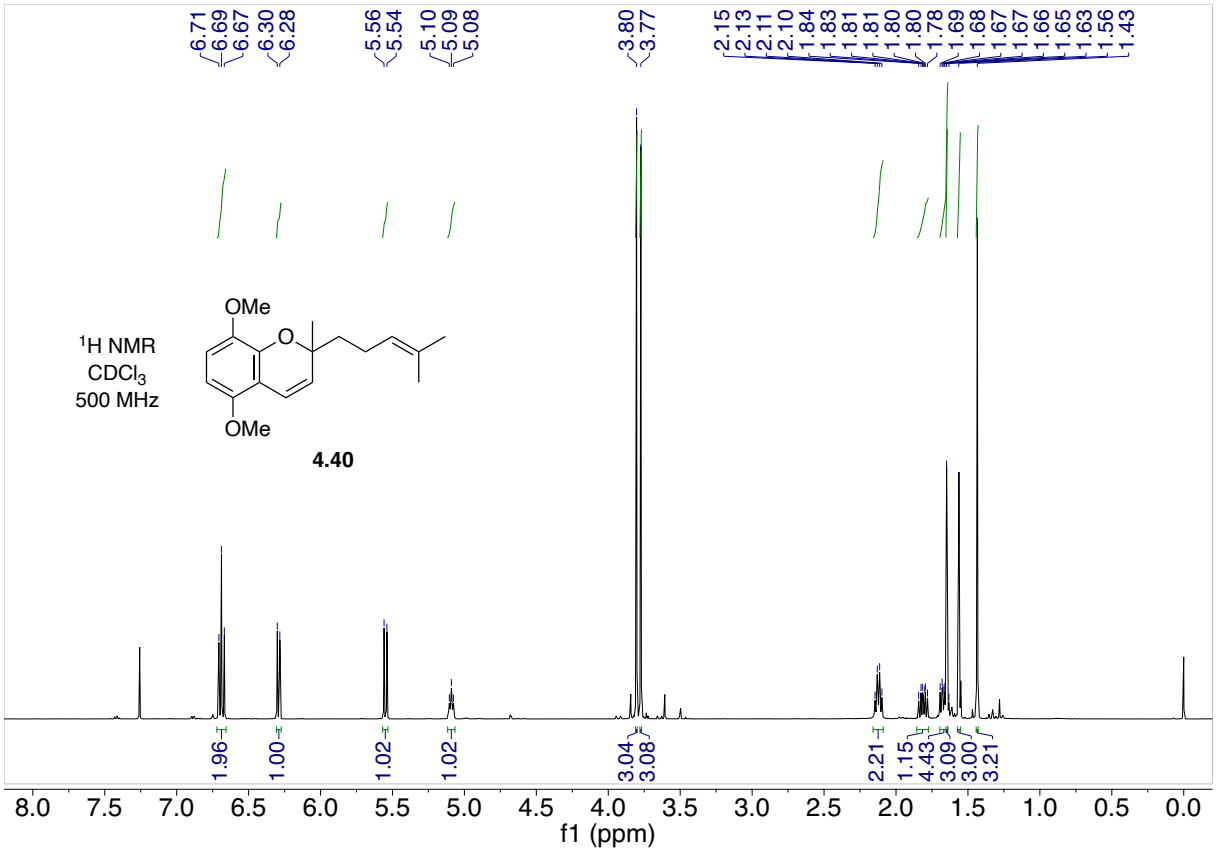
6.71
6.69
6.67
6.30
6.28
5.56
5.54
5.10
5.09
5.08
3.80
3.77
2.15
2.13
2.11
2.10
1.84
1.83
1.81
1.81
1.80
1.80
1.78
1.69
1.68
1.67
1.67
1.66
1.65
1.63
1.56
1.43
1H NMR
CDCl3
500 MHz
OMe
O
OMe
4.40
1.96
1.00
1.02
1.02
3.04
3.08
2.21
1.15
4.43
3.09
3.00
3.21
8.0 7.5 7.0 6.5 6.0 5.5 5.0 4.5 4.0 3.5 3.0 2.5 2.0 1.5 1.0 0.5 0.0
f1 (ppm)

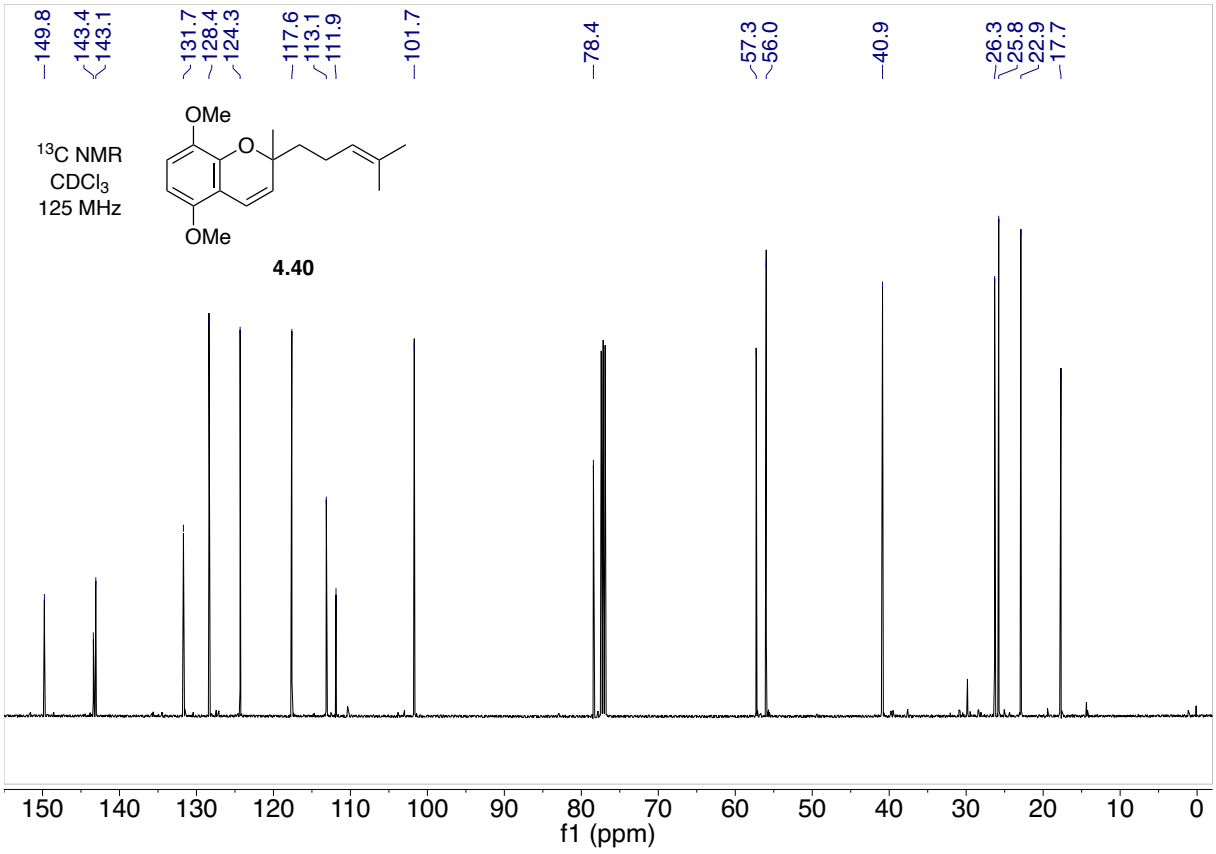
149.8
143.4
143.1
131.7
128.4
124.3
117.6
113.1
111.9
101.7
78.4
57.3
56.0
40.9
26.3
25.8
22.9
17.7
13C NMR
CDCl3
125 MHz
OMe
O
OMe
4.40
150 140 130 120 110 100 90 80 70 60 50 40 30 20 10 0
f1 (ppm)

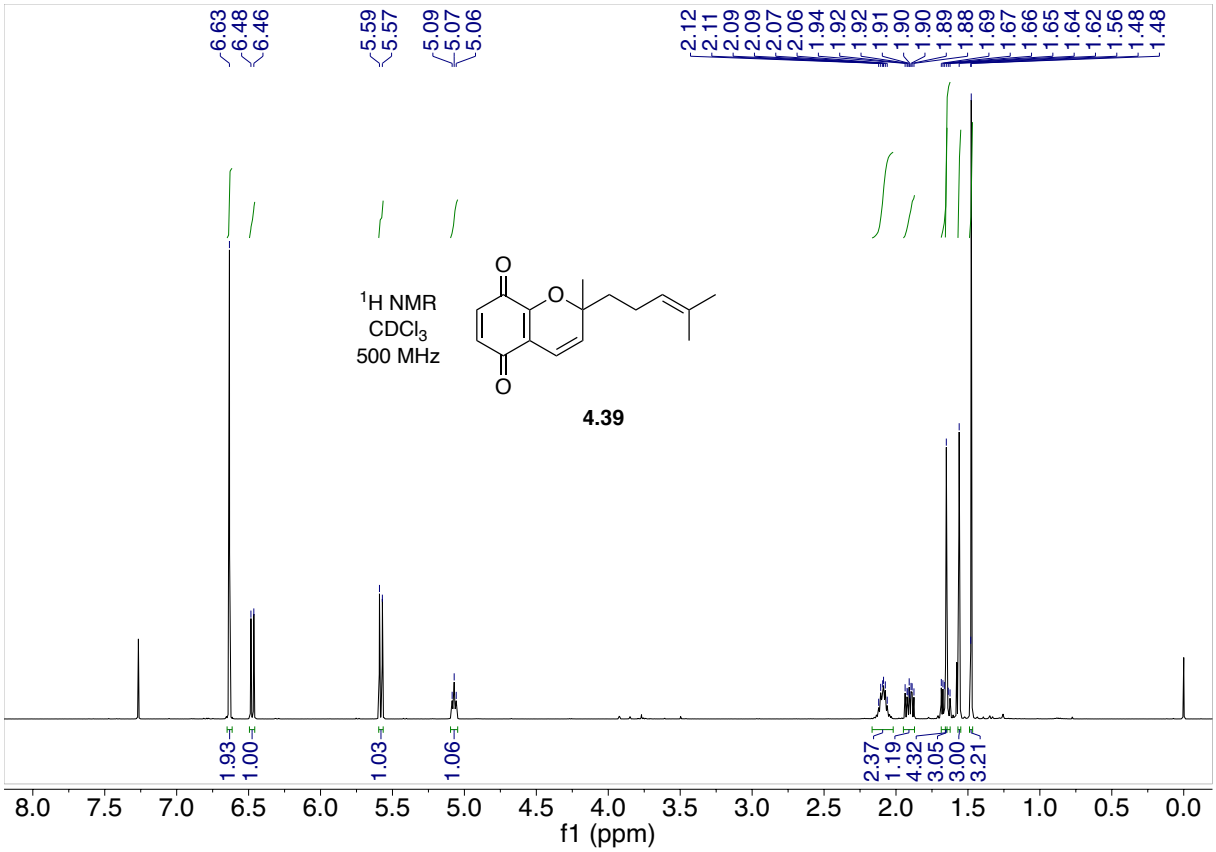
6.63
6.48
6.46
5.59
5.57
5.09
5.07
5.06
2.12
2.11
2.09
2.09
2.07
2.06
1.94
1.92
1.92
1.91
1.90
1.90
1.89
1.88
1.69
1.67
1.66
1.65
1.64
1.62
1.56
1.48
1.48
1H NMR
CDCl3
500 MHz
O
O
O
4.39
1.93
1.00
1.03
1.06
2.37
1.19
4.32
3.05
3.00
3.21
8.0 7.5 7.0 6.5 6.0 5.5 5.0 4.5 4.0 3.5 3.0 2.5 2.0 1.5 1.0 0.5 0.0
f1 (ppm)

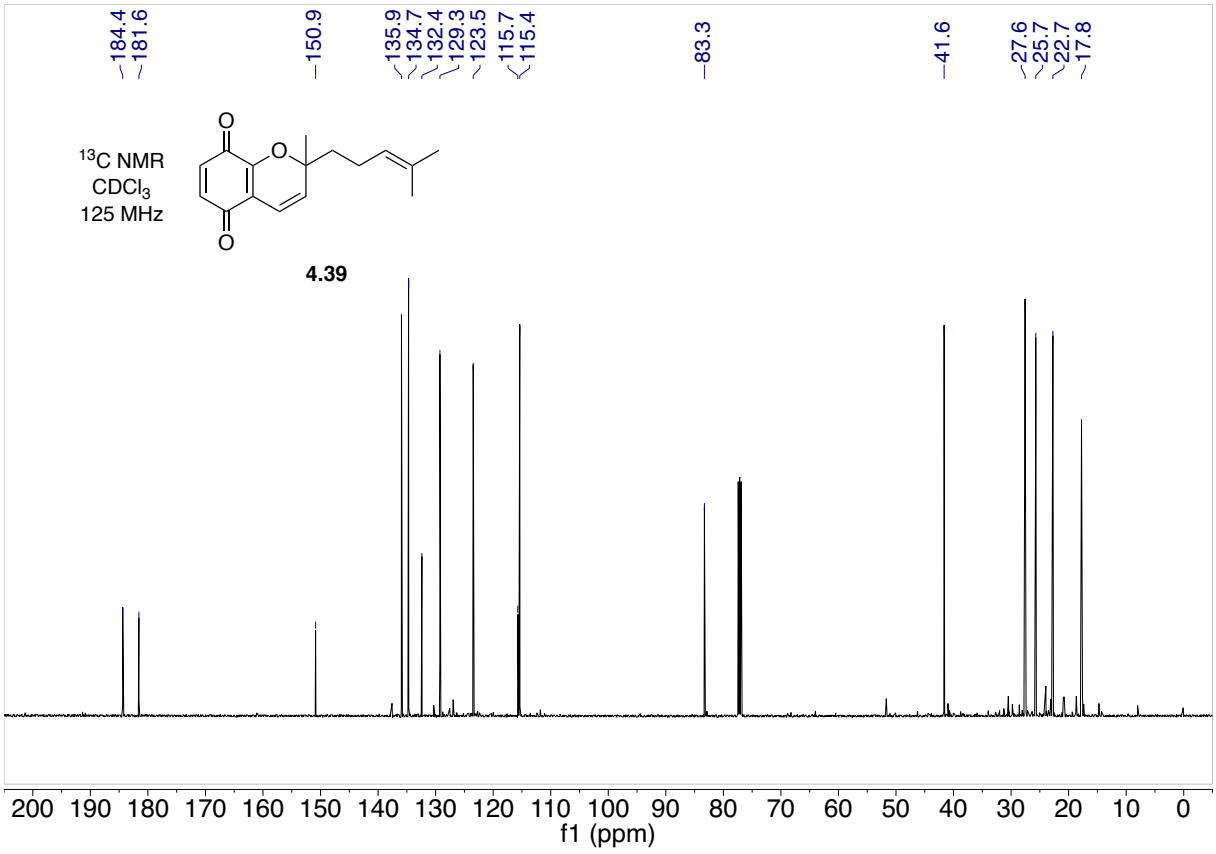
184.4
181.6
150.9
135.9
134.7
132.4
129.3
123.5
115.7
115.4
83.3
41.6
27.6
25.7
22.7
17.8
13C NMR
CDCl3
125 MHz
O
O
O
4.39
200 190 180 170 160 150 140 130 120 110 100 90 80 70 60 50 40 30 20 10 0
f1 (ppm)

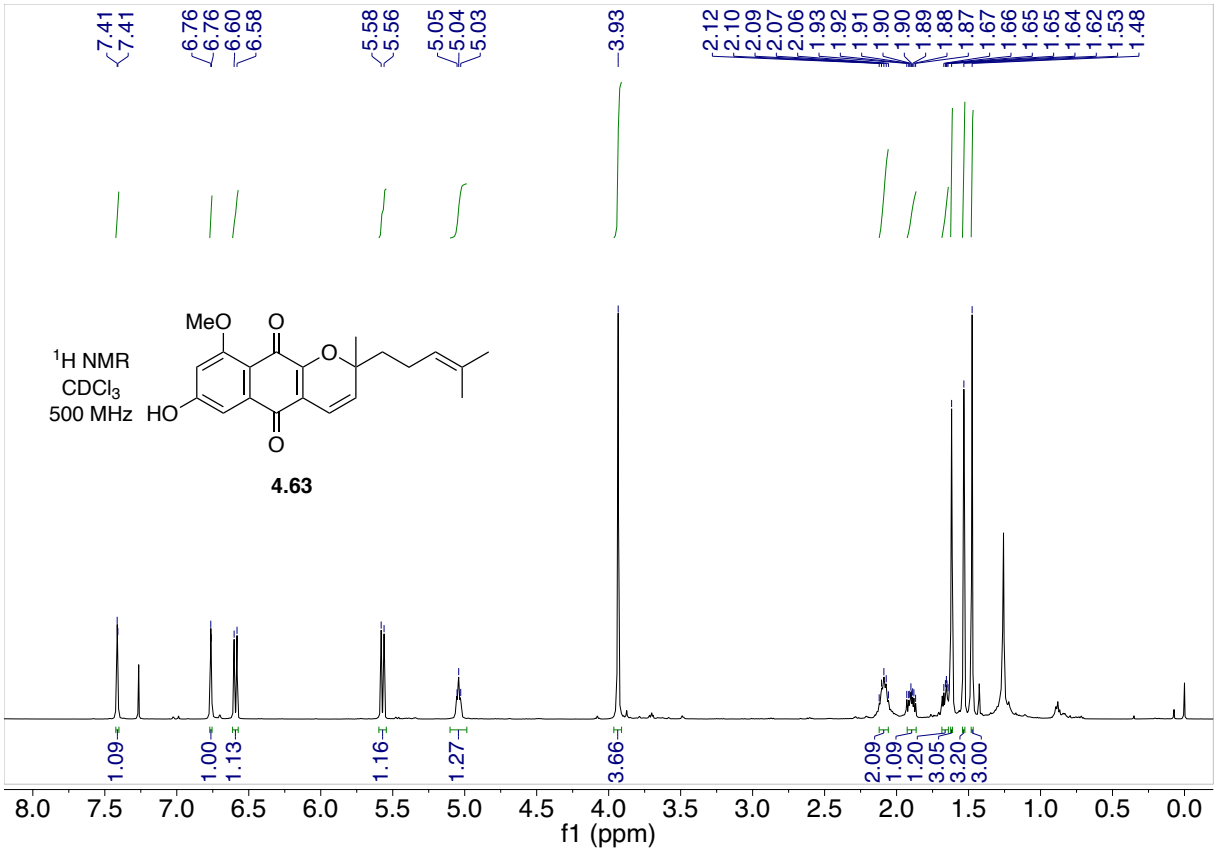
7.41
7.41
6.76
6.76
6.60
6.58
5.58
5.56
5.05
5.04
5.03
3.93
2.12
2.10
2.09
2.07
2.06
1.93
1.92
1.91
1.90
1.90
1.89
1.88
1.87
1.67
1.66
1.65
1.65
1.64
1.62
1.53
1.48
MeO
O
O
HO
O
1H NMR
CDCl3
500 MHz
4.63
1.09
1.00
1.13
1.16
1.27
3.66
2.09
1.09
1.20
3.05
3.20
3.00
8.0
7.5
7.0
6.5
6.0
5.5
5.0
4.5
4.0
3.5
3.0
2.5
2.0
1.5
1.0
0.5
0.0
f1 (ppm)

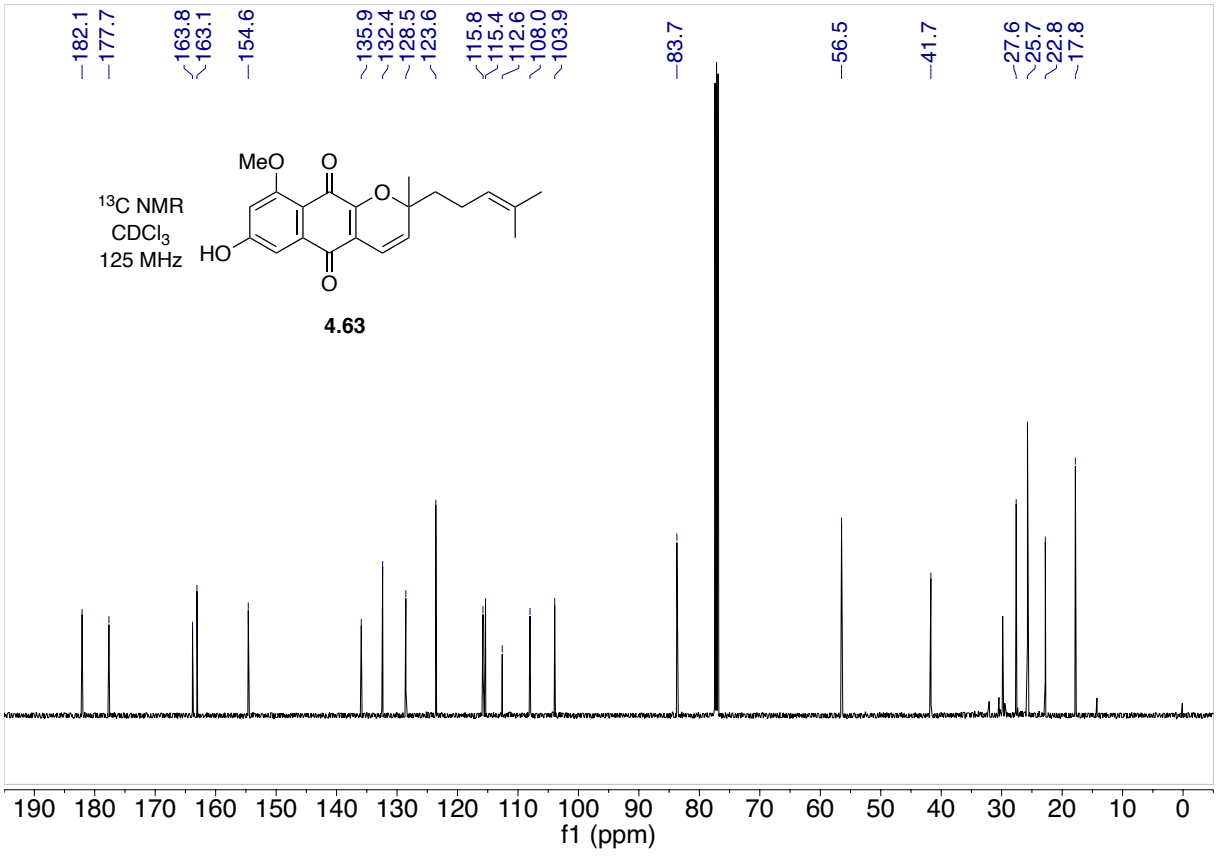
182.1
177.7
163.8
163.1
154.6
135.9
132.4
128.5
123.6
115.8
115.4
112.6
108.0
103.9
83.7
56.5
41.7
27.6
25.7
22.8
17.8
MeO
O
O
HO
O
13C NMR
CDCl3
125 MHz
4.63
190
180
170
160
150
140
130
120
110
100
90
80
70
60
50
40
30
20
10
0
f1 (ppm)

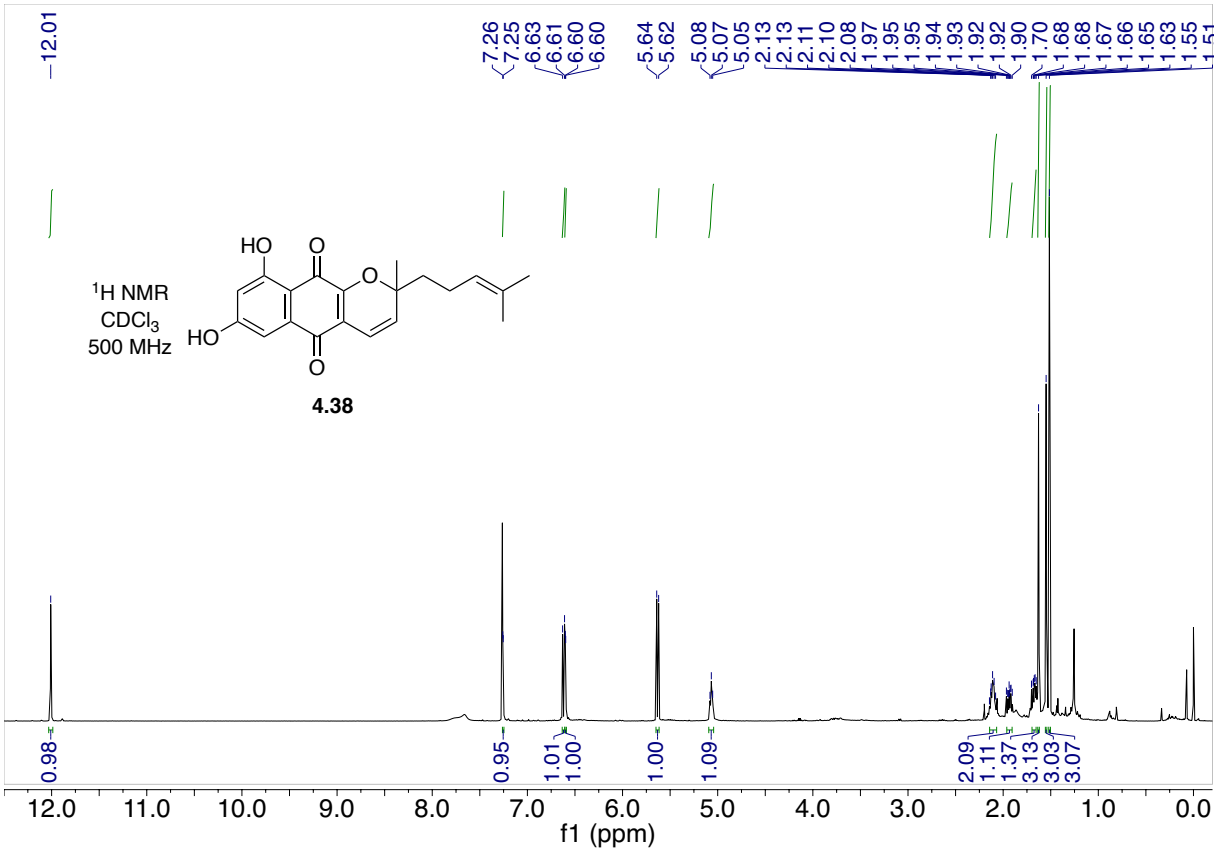
12.01
7.26
7.25
6.63
6.61
6.60
6.60
5.64
5.62
5.08
5.07
5.05
2.13
2.13
2.11
2.10
2.08
1.97
1.95
1.95
1.94
1.93
1.92
1.92
1.90
1.70
1.68
1.68
1.67
1.66
1.65
1.63
1.55
1.51
HO
O
O
HO
O
1H NMR
CDCl3
500 MHz
4.38
0.98
0.95
1.01
1.00
1.00
1.09
2.09
1.11
1.37
3.13
3.03
3.07
12.0
11.0
10.0
9.0
8.0
7.0
6.0
5.0
4.0
3.0
2.0
1.0
0.0
f1 (ppm)

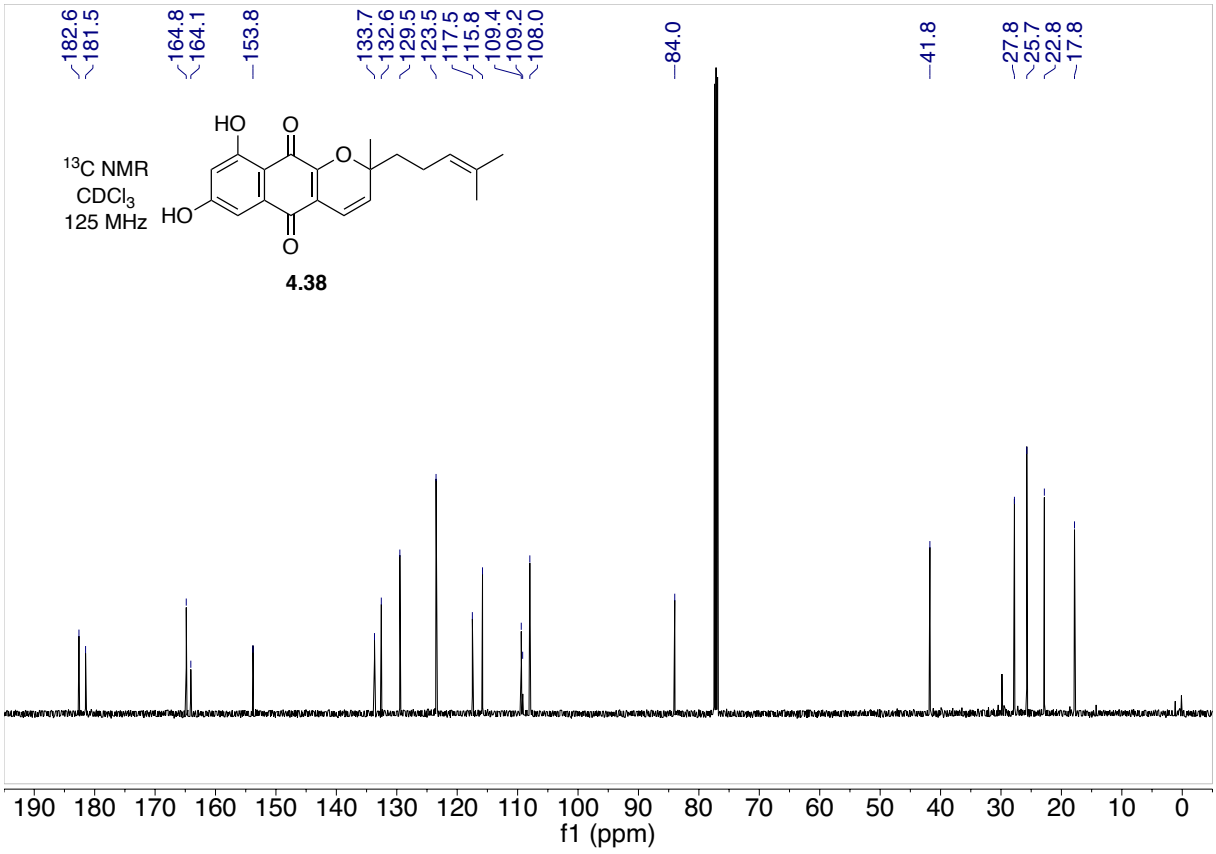
182.6
181.5
164.8
164.1
153.8
133.7
132.6
129.5
123.5
117.5
115.8
109.4
109.2
108.0
84.0
41.8
27.8
25.7
22.8
17.8
HO
O
O
HO
O
13C NMR
CDCl3
125 MHz
4.38
190
180
170
160
150
140
130
120
110
100
90
80
70
60
50
40
30
20
10
0
f1 (ppm)

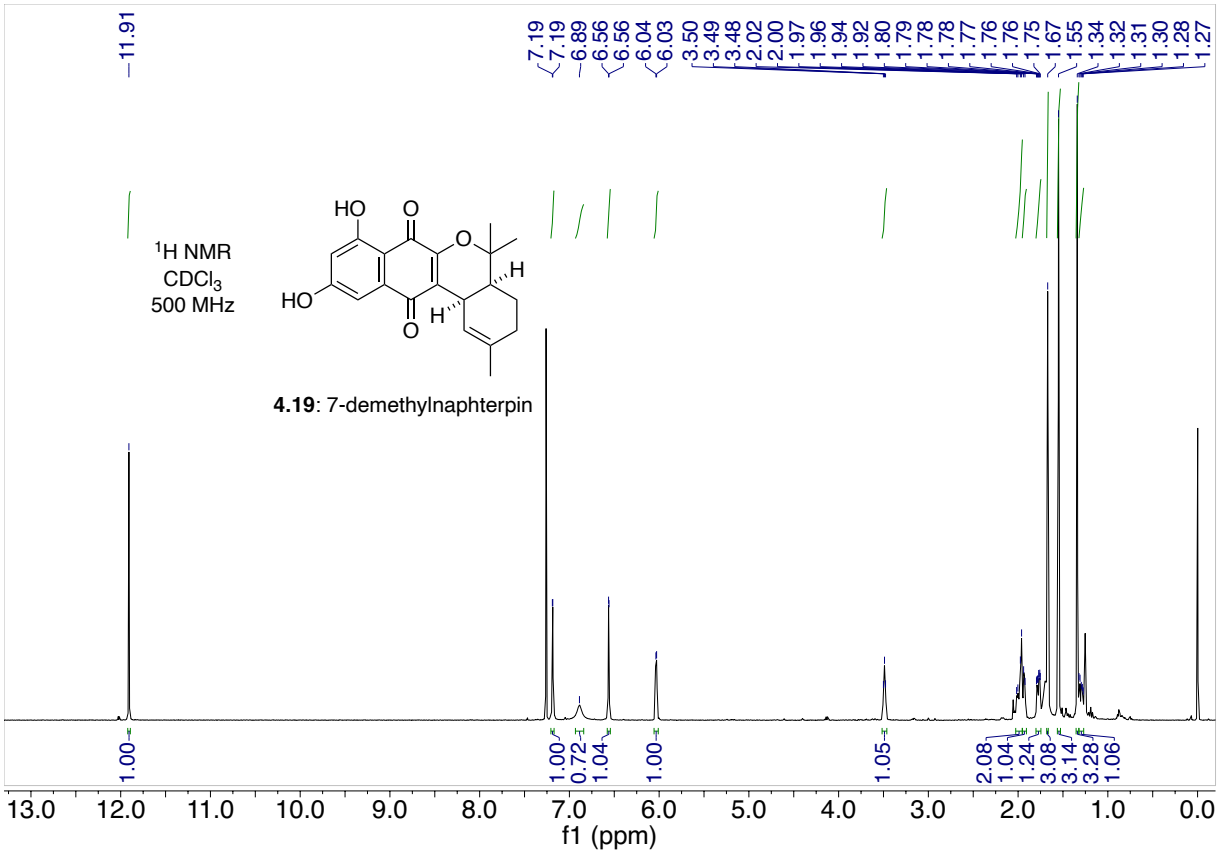
11.91
7.19
7.19
6.89
6.56
6.56
6.04
6.03
3.50
3.49
3.48
2.02
2.00
1.97
1.96
1.94
1.92
1.80
1.79
1.78
1.78
1.77
1.76
1.76
1.75
1.67
1.55
1.34
1.32
1.31
1.30
1.28
1.27
1H NMR
CDCl3
500 MHz
HO
O
O
H
HO
H
O
4.19: 7-demethylnaphterpin
1.00
1.00
0.72
1.04
1.00
1.05
2.08
1.04
1.24
3.08
3.14
3.28
1.06
13.0
12.0
11.0
10.0
9.0
8.0
7.0
6.0
5.0
4.0
3.0
2.0
1.0
0.0
f1 (ppm)

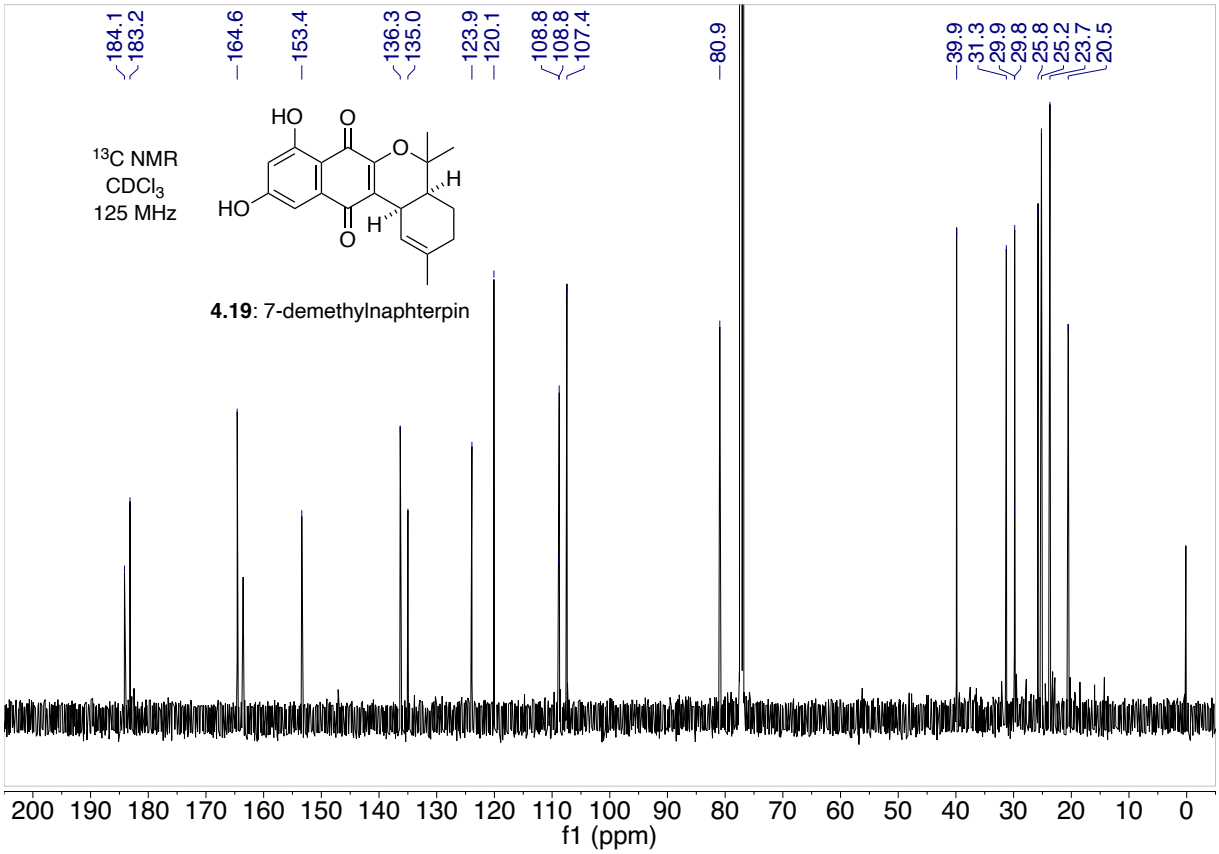
184.1
183.2
164.6
153.4
136.3
135.0
123.9
120.1
108.8
108.8
107.4
80.9
39.9
31.3
29.9
29.8
25.8
25.2
23.7
20.5
13C NMR
CDCl3
125 MHz
HO
O
O
H
HO
H
O
4.19: 7-demethylnaphterpin
200
190
180
170
160
150
140
130
120
110
100
90
80
70
60
50
40
30
20
10
0
f1 (ppm)

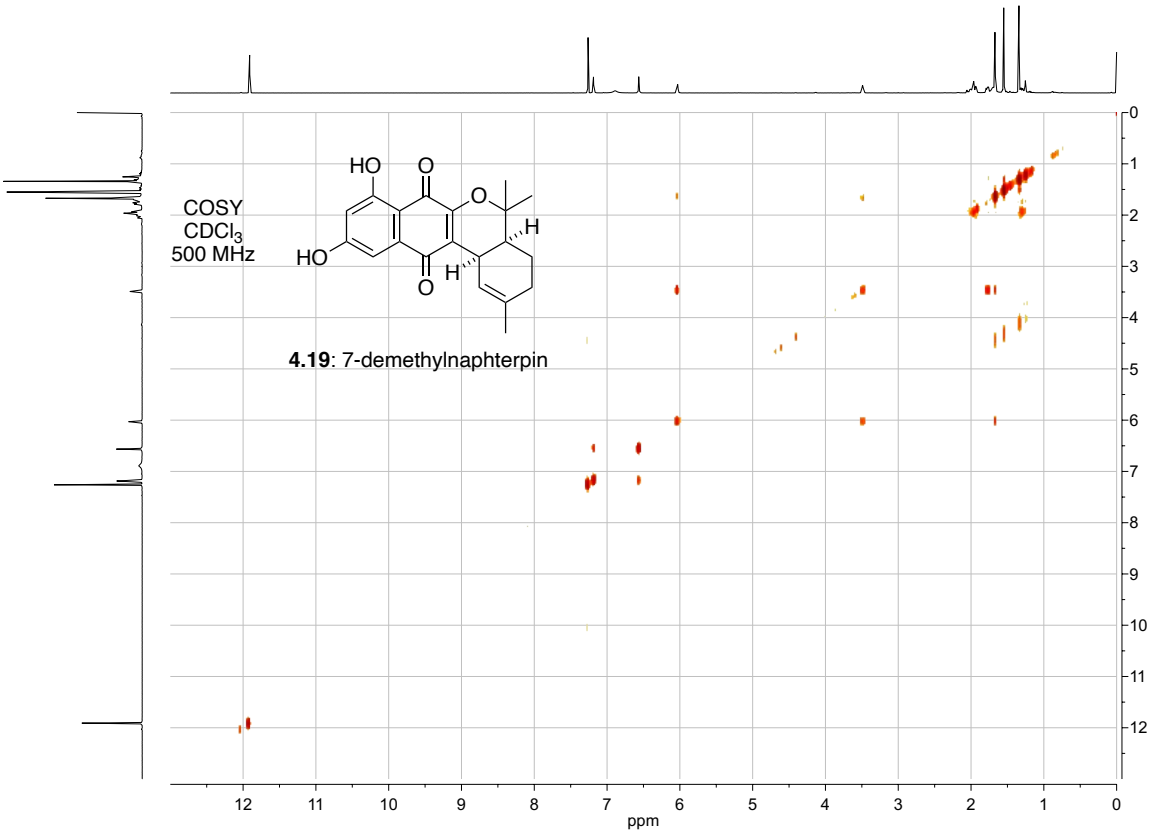
COSY
CDCl3
500 MHz
HO
O
O
H
HO
H
O
4.19: 7-demethylnaphterpin
ppm

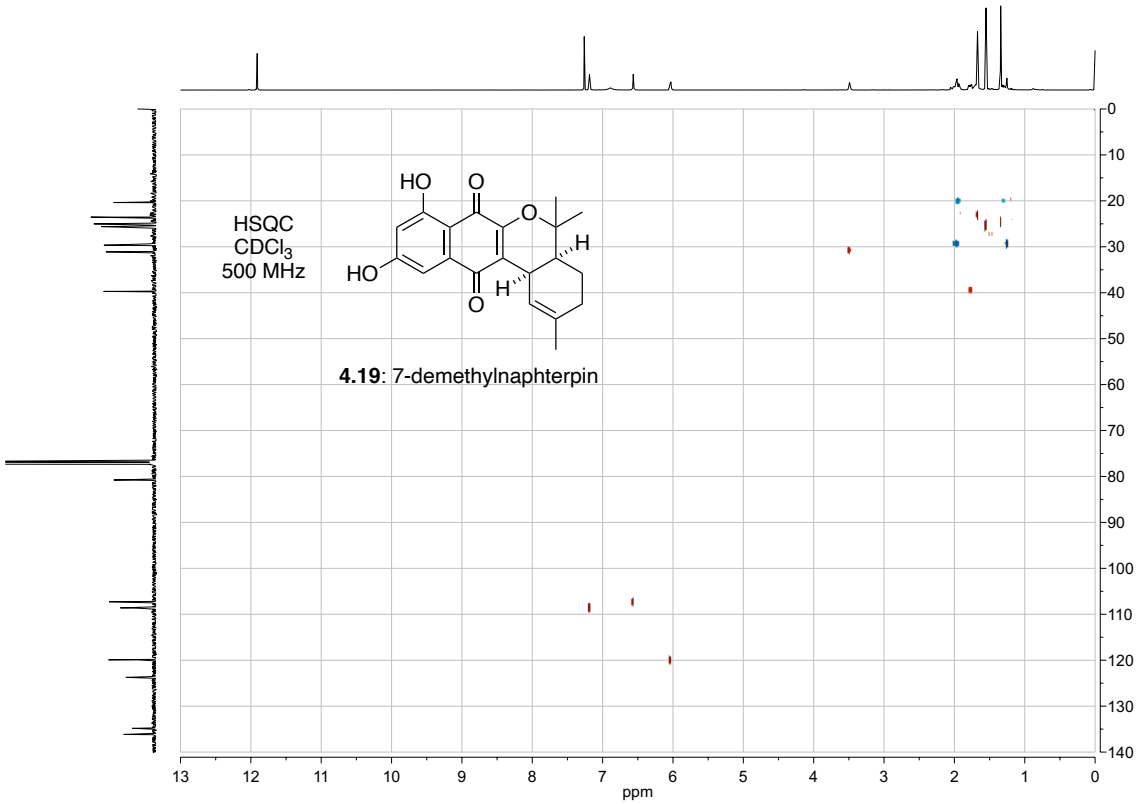
HSQC
CDCl3
500 MHz
HO
O
O
H
HO
H
O
4.19: 7-demethylnaphterpin
ppm

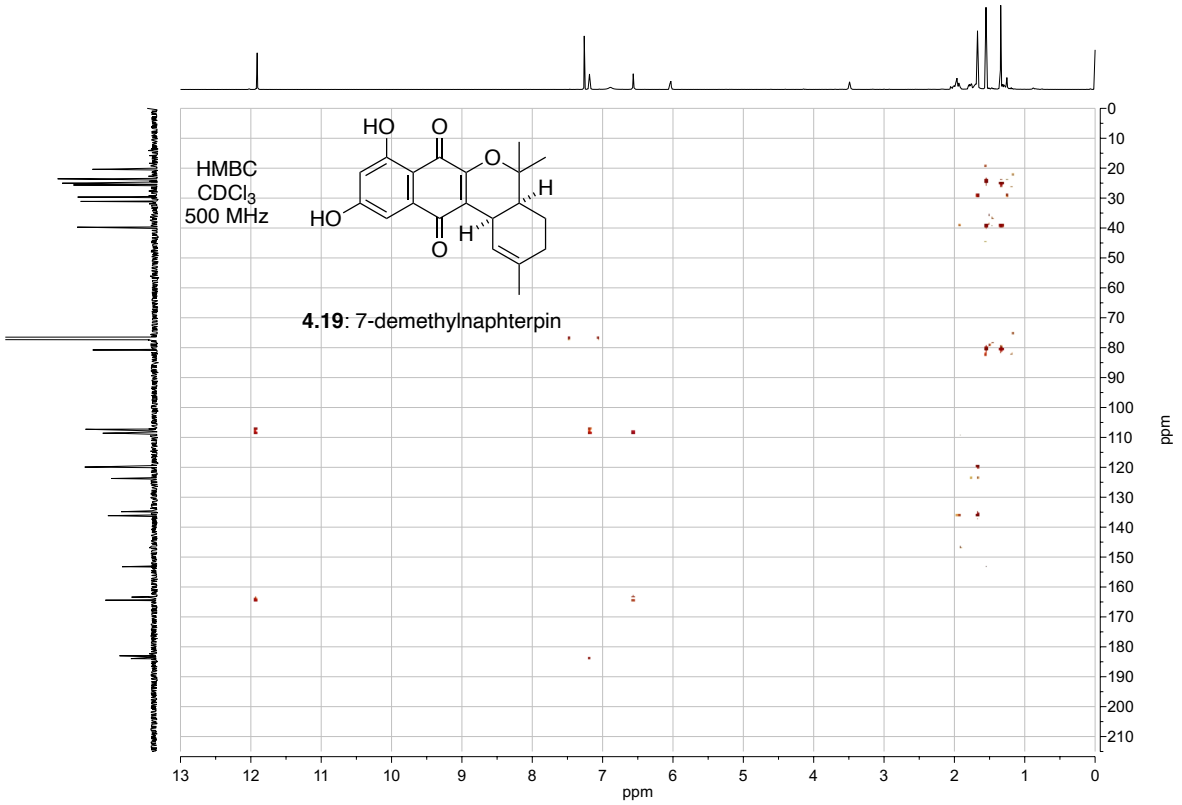
HMBC
CDCl3
500 MHz
HO
O
O
H
HO
H
O
4.19: 7-demethylnaphterpin
ppm
ppm

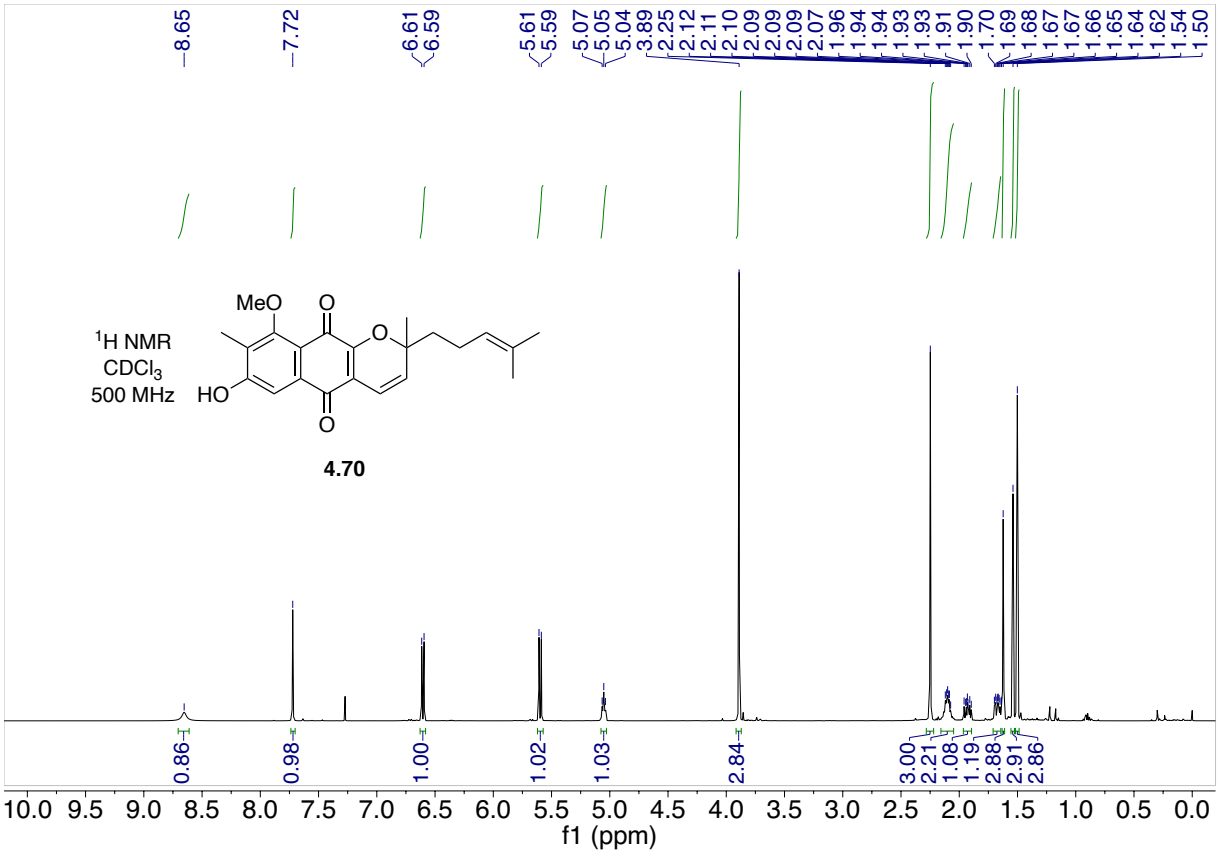
8.65
7.72
6.61
6.59
5.61
5.59
5.07
5.05
5.04
3.89
2.25
2.12
2.11
2.10
2.09
2.09
2.09
2.07
1.96
1.94
1.94
1.93
1.93
1.91
1.90
1.70
1.69
1.68
1.67
1.67
1.66
1.65
1.64
1.62
1.54
1.50
MeO
O
O
HO
O
1H NMR
CDCl3
500 MHz
4.70
0.86
0.98
1.00
1.02
1.03
2.84
3.00
2.21
1.08
1.19
2.88
2.91
2.86
10.0 9.5 9.0 8.5 8.0 7.5 7.0 6.5 6.0 5.5 5.0 4.5 4.0 3.5 3.0 2.5 2.0 1.5 1.0 0.5 0.0
f1 (ppm)

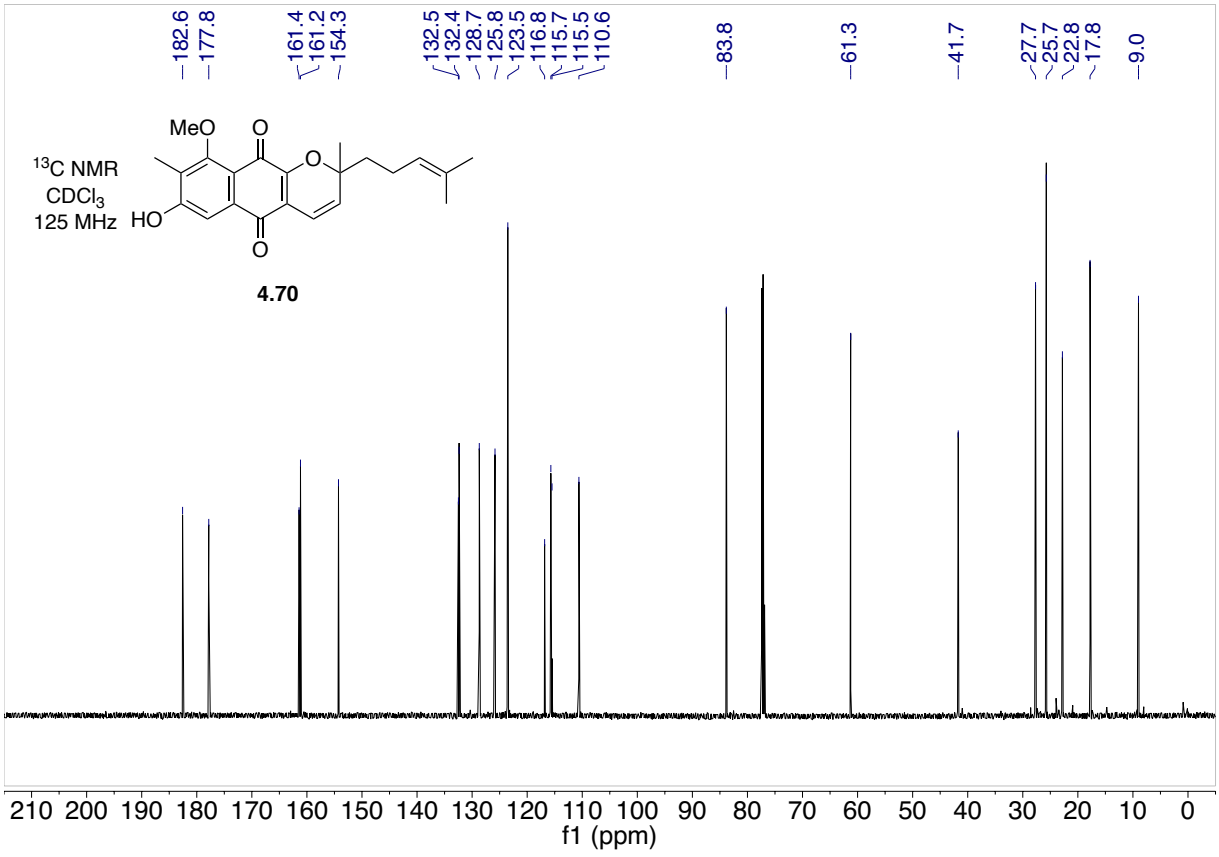
182.6
177.8
161.4
161.2
154.3
132.5
132.4
128.7
125.8
123.5
116.8
115.7
115.5
110.6
83.8
61.3
41.7
27.7
25.7
22.8
17.8
9.0
MeO
O
O
HO
O
13C NMR
CDCl3
125 MHz
4.70
210 200 190 180 170 160 150 140 130 120 110 100 90 80 70 60 50 40 30 20 10 0
f1 (ppm)

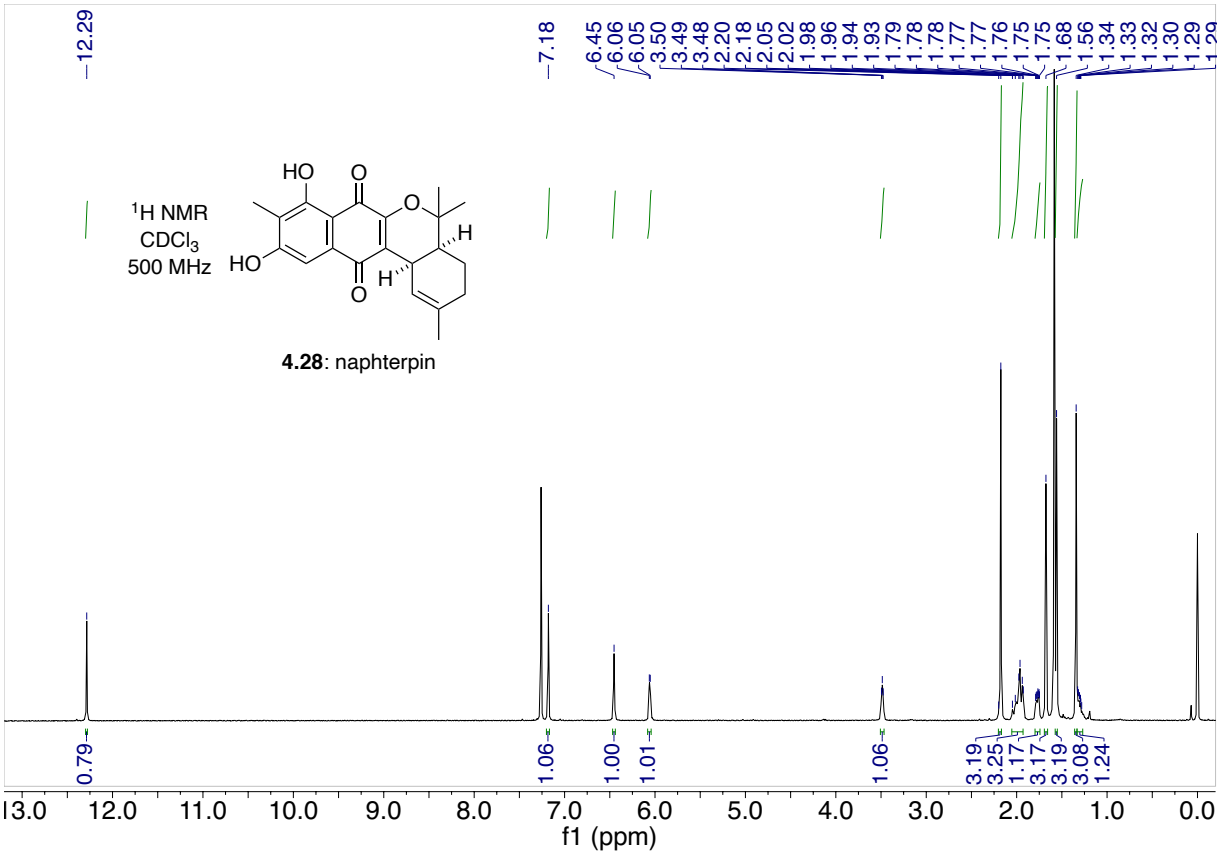
12.29
7.18
6.45
6.06
6.05
3.50
3.49
3.48
2.20
2.18
2.05
2.02
1.98
1.96
1.94
1.93
1.79
1.78
1.78
1.77
1.77
1.76
1.75
1.75
1.68
1.56
1.34
1.33
1.32
1.30
1.29
0.79
1.06
1.00
1.01
1.06
3.19
3.25
1.17
3.17
3.19
3.08
1.24
HO
O
O
H
HO
H
O
1H NMR
CDCl3
500 MHz
4.28: naphterpin
13.0
12.0
11.0
10.0
9.0
8.0
7.0
6.0
5.0
4.0
3.0
2.0
1.0
0.0
f1 (ppm)

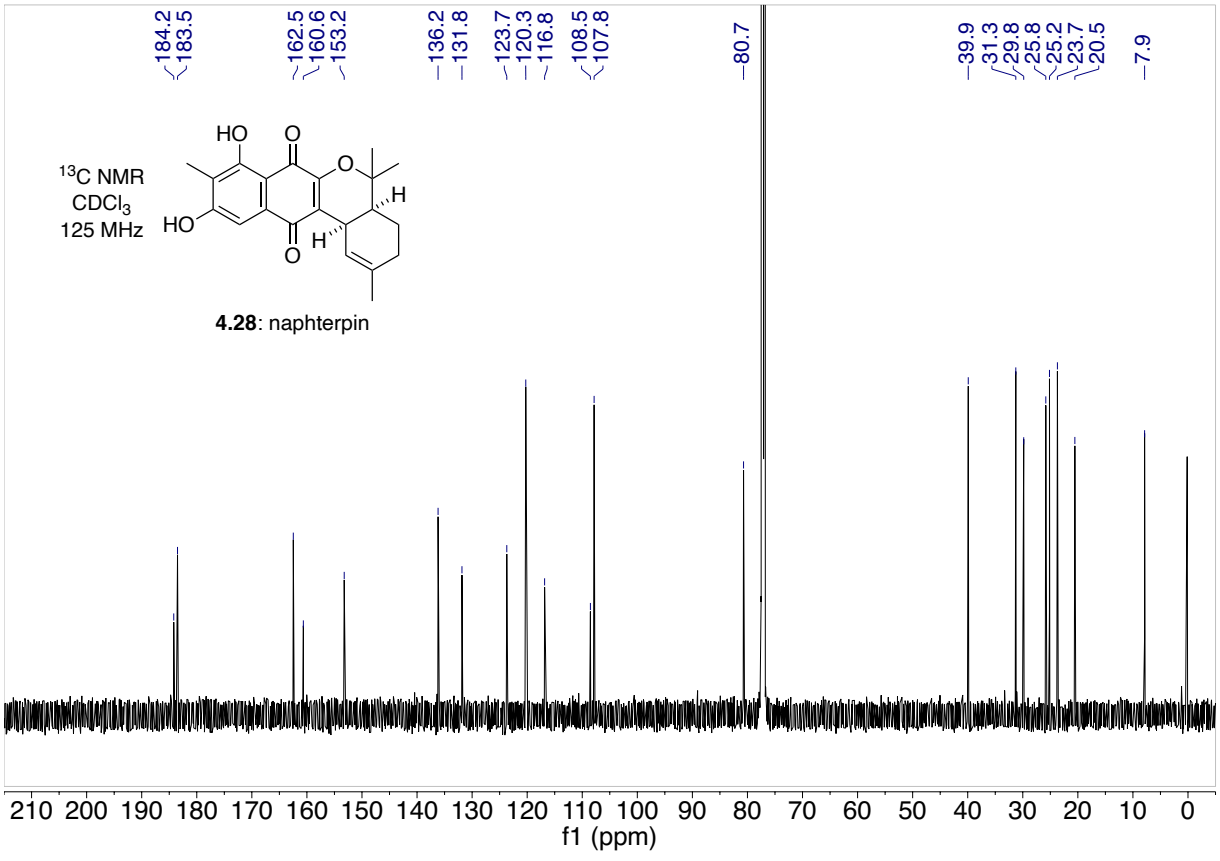
184.2
183.5
162.5
160.6
153.2
136.2
131.8
123.7
120.3
116.8
108.5
107.8
80.7
39.9
31.3
29.8
25.8
25.2
23.7
20.5
7.9
HO
O
O
H
HO
H
O
13C NMR
CDCl3
125 MHz
4.28: naphterpin
210
200
190
180
170
160
150
140
130
120
110
100
90
80
70
60
50
40
30
20
10
0
f1 (ppm)

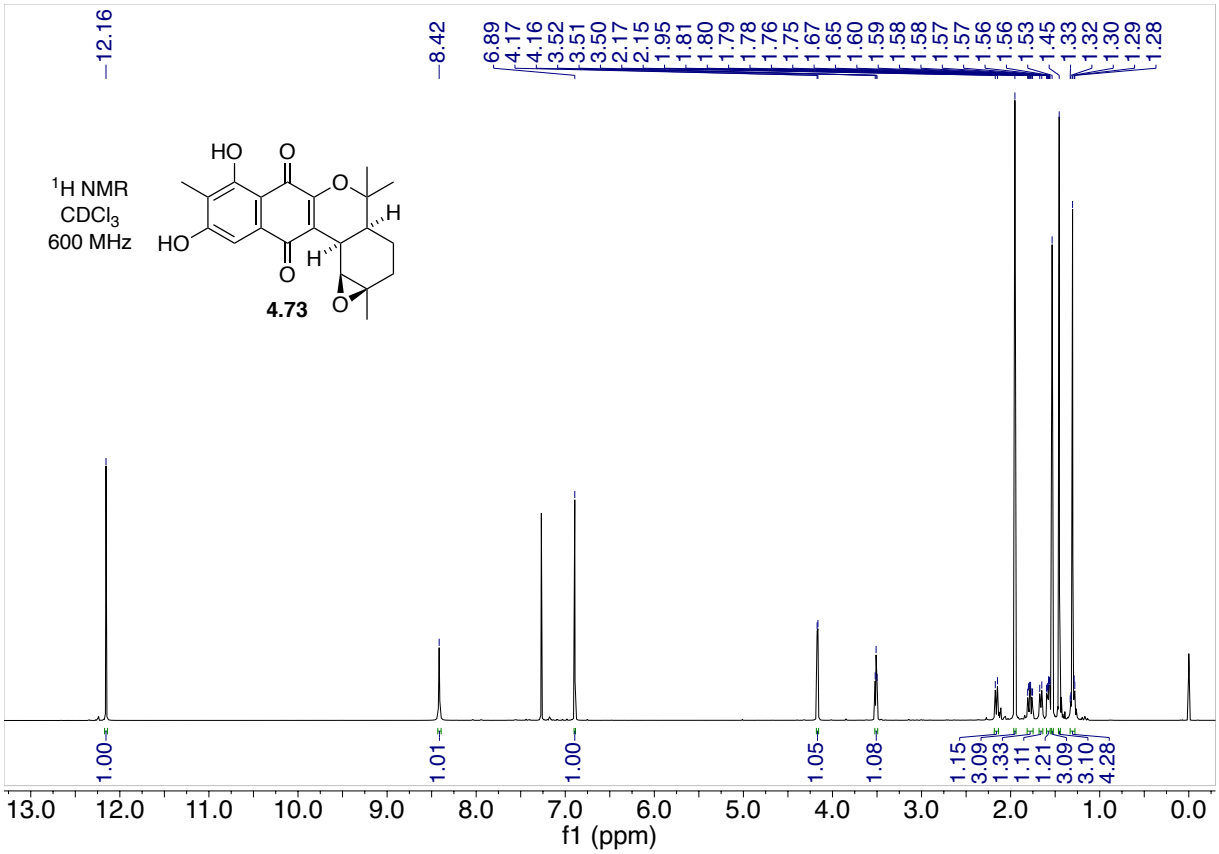
12.16
8.42
6.89
4.17
4.16
3.52
3.51
3.50
2.17
2.15
1.95
1.81
1.80
1.79
1.78
1.76
1.75
1.67
1.65
1.60
1.59
1.58
1.58
1.57
1.57
1.56
1.56
1.53
1.45
1.33
1.32
1.30
1.29
1.28
1H NMR
CDCl3
600 MHz
HO
O
O
H
HO
H
O
O
4.73
1.00
1.01
1.00
1.05
1.08
1.15
3.09
1.33
1.11
1.21
3.09
3.10
4.28
13.0
12.0
11.0
10.0
9.0
8.0
7.0
6.0
5.0
4.0
3.0
2.0
1.0
0.0
f1 (ppm)

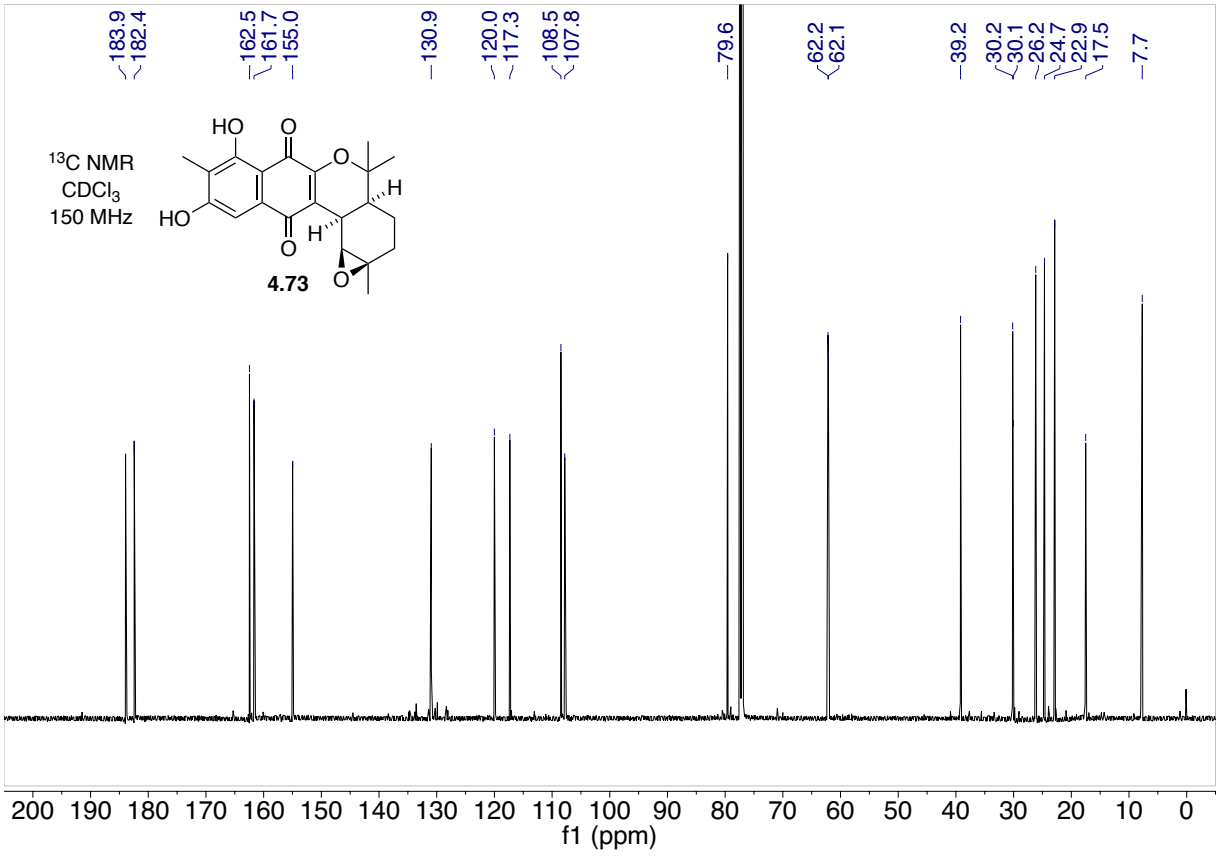
183.9
182.4
162.5
161.7
155.0
130.9
120.0
117.3
108.5
107.8
79.6
62.2
62.1
39.2
30.2
30.1
26.2
24.7
22.9
17.5
7.7
13C NMR
CDCl3
150 MHz
HO
O
O
H
HO
H
O
O
4.73
200
190
180
170
160
150
140
130
120
110
100
90
80
70
60
50
40
30
20
10
0
f1 (ppm)

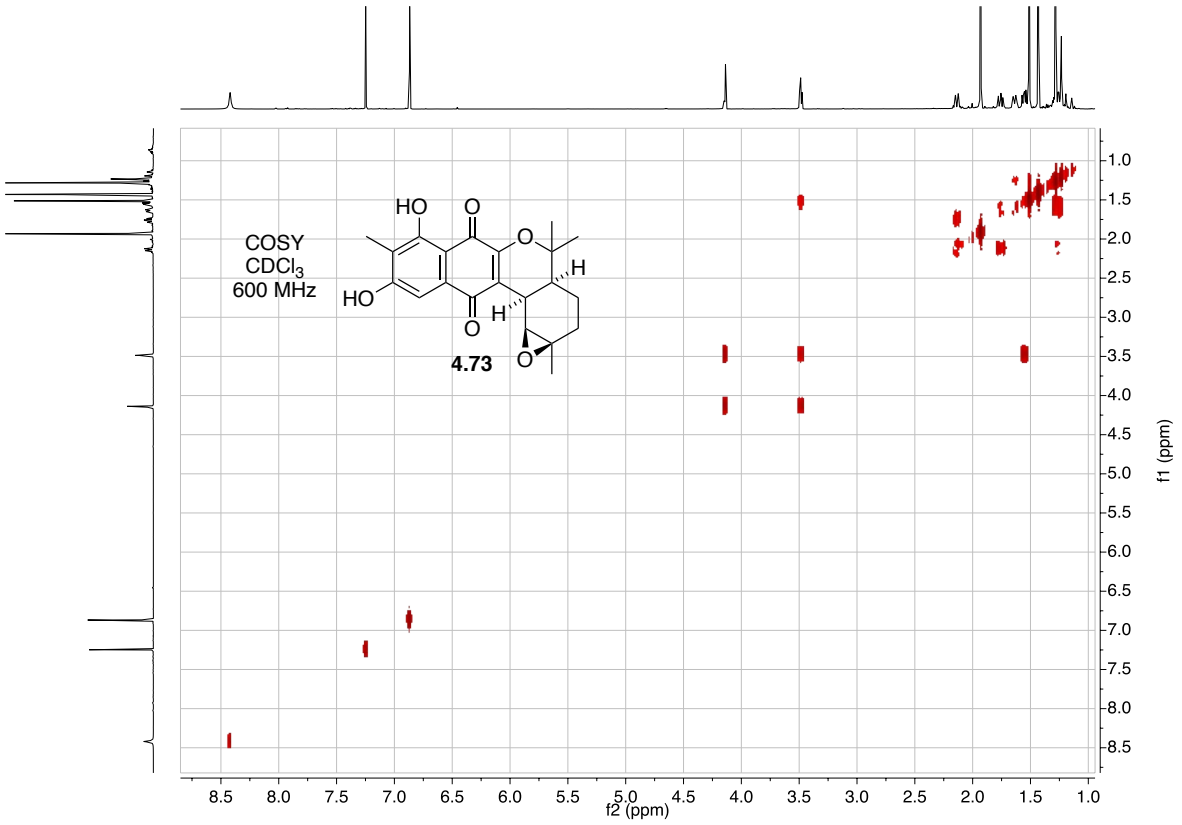
COSY
CDCl3
600 MHz
HO
O
O
H
HO
H
O
O
4.73
f2 (ppm)
f1 (ppm)

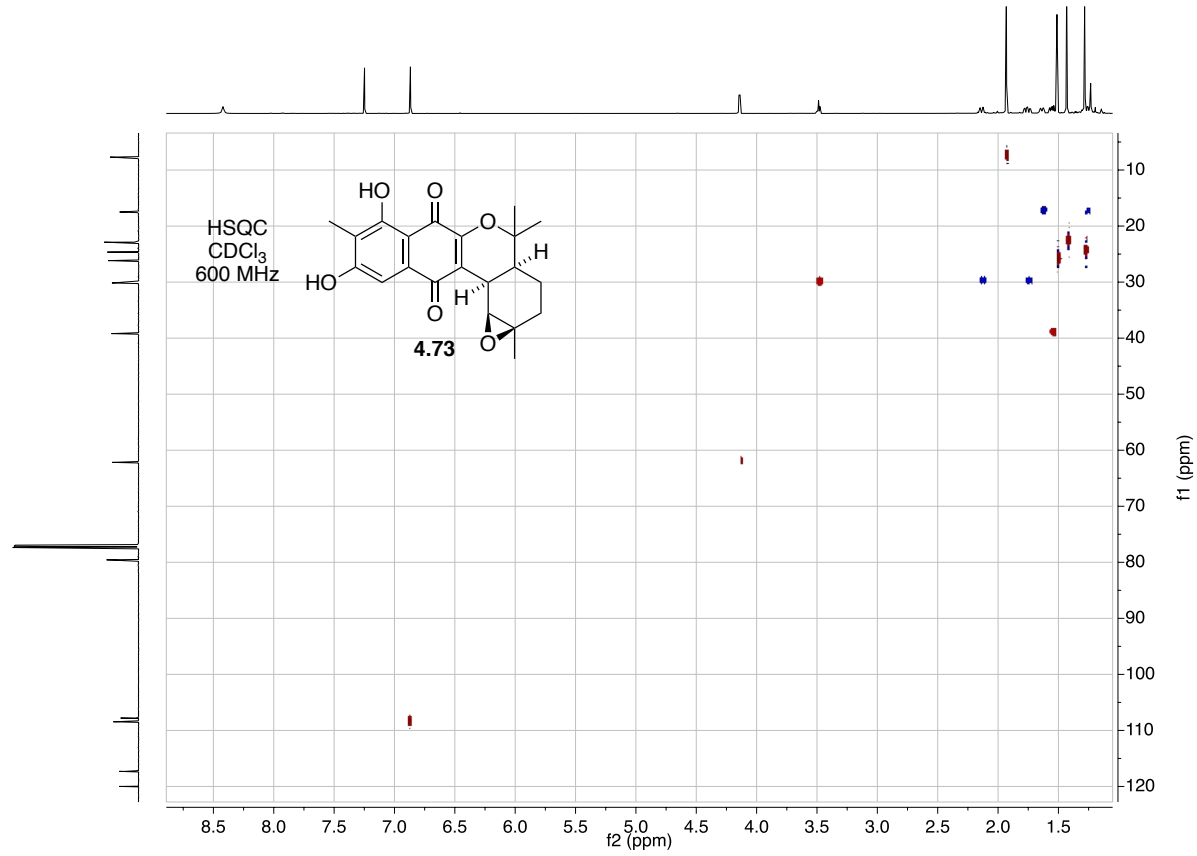
HSQC
CDCl3
600 MHz
HO
O
O
H
HO
H
O
O
4.73
f2 (ppm)
f1 (ppm)

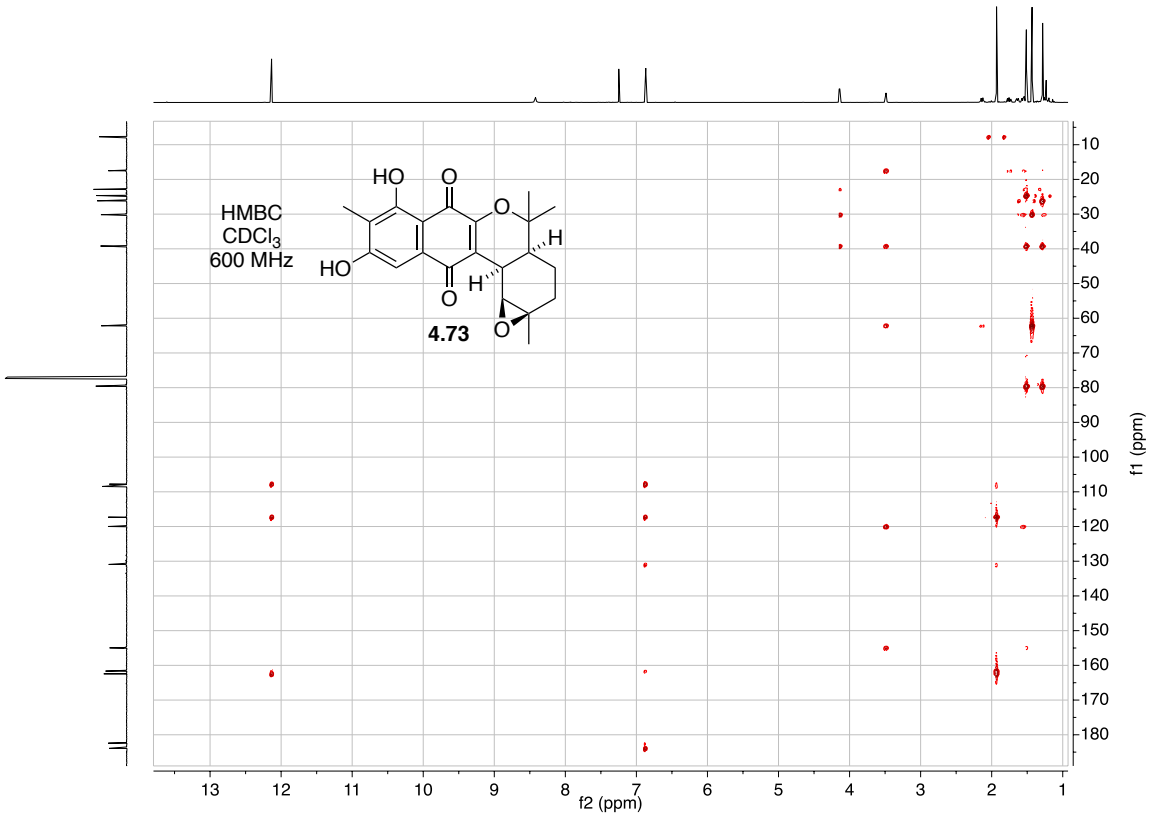
HMBC
CDCl3
600 MHz
HO
O
O
H
HO
H
O
O
4.73
f2 (ppm)
f1 (ppm)

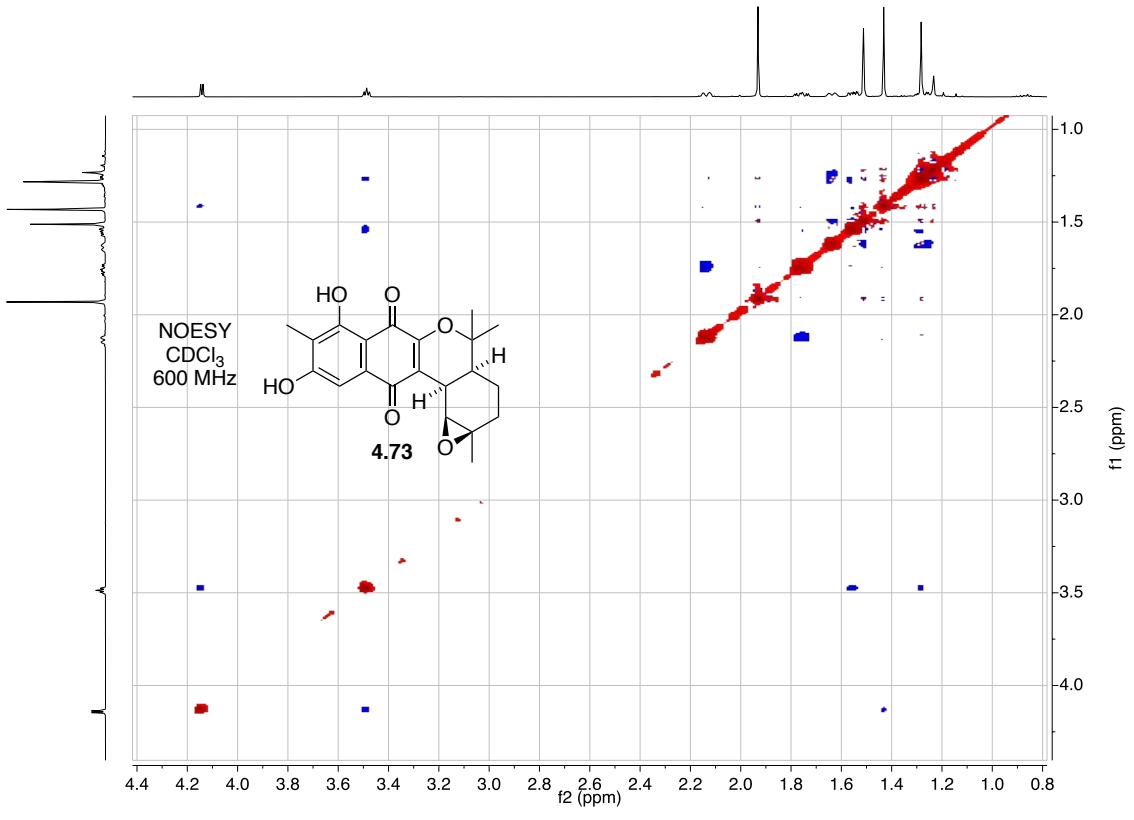
NOESY
CDCl3
600 MHz
HO
O
O
H
HO
H
O
O
4.73
f2 (ppm)
f1 (ppm)

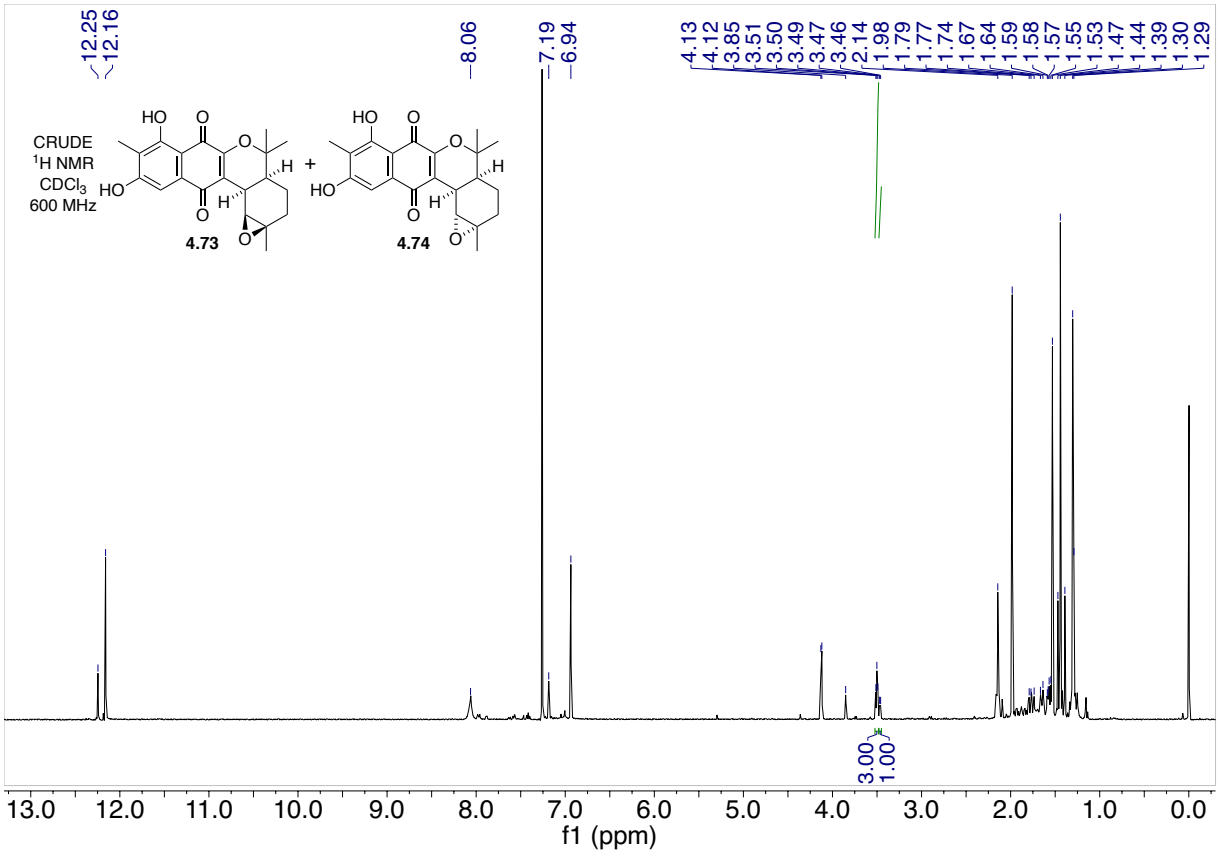
12.25
12.16
8.06
7.19
6.94
4.13
4.12
3.85
3.51
3.50
3.49
3.47
3.46
2.14
1.98
1.79
1.77
1.74
1.67
1.64
1.59
1.58
1.57
1.55
1.53
1.47
1.44
1.39
1.30
1.29
CRUDE
1H NMR
CDCl3
600 MHz
4.73
4.74
3.00
1.00
13.0
12.0
11.0
10.0
9.0
8.0
7.0
6.0
5.0
4.0
3.0
2.0
1.0
0.0
f1 (ppm)

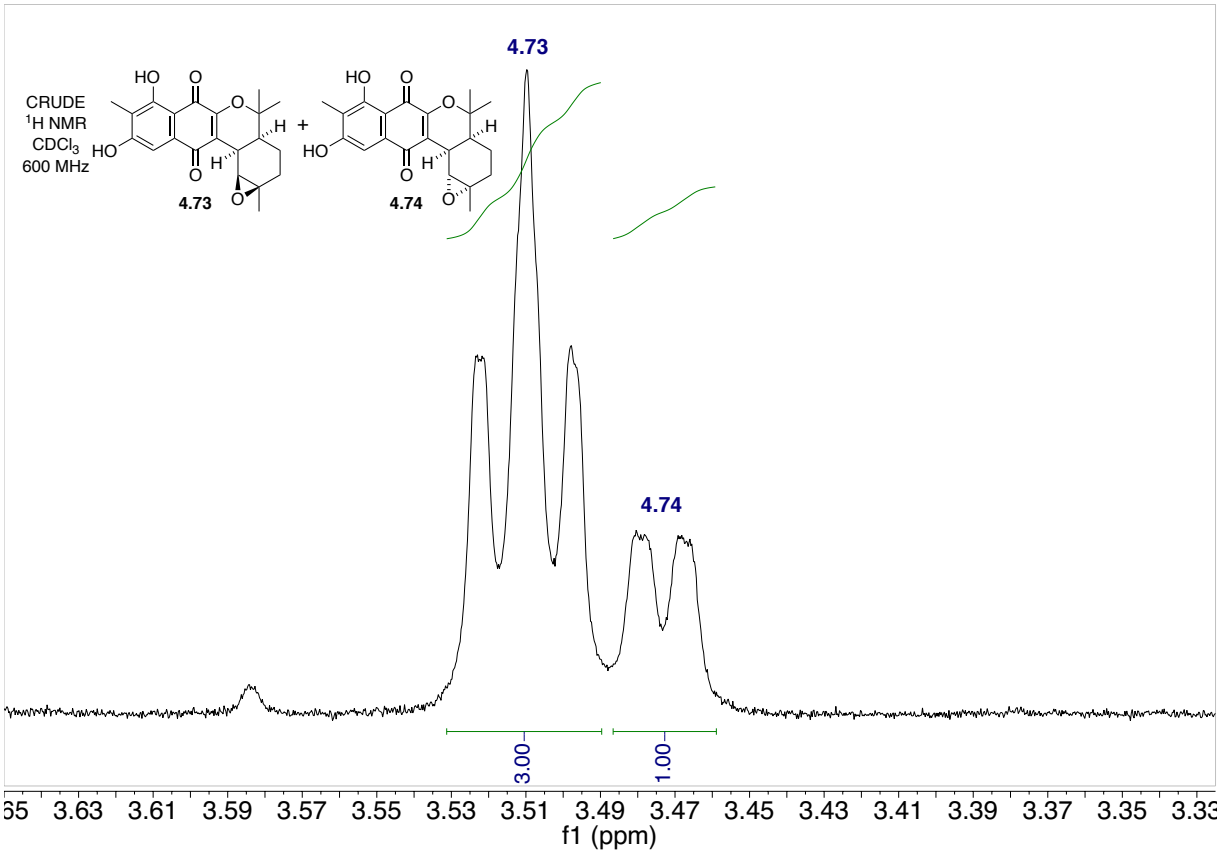
4.73
CRUDE
1H NMR
CDCl3
600 MHz
4.73
4.74
4.74
3.00
1.00
3.63
3.61
3.59
3.57
3.55
3.53
3.51
3.49
3.47
3.45
3.43
3.41
3.39
3.37
3.35
f1 (ppm)

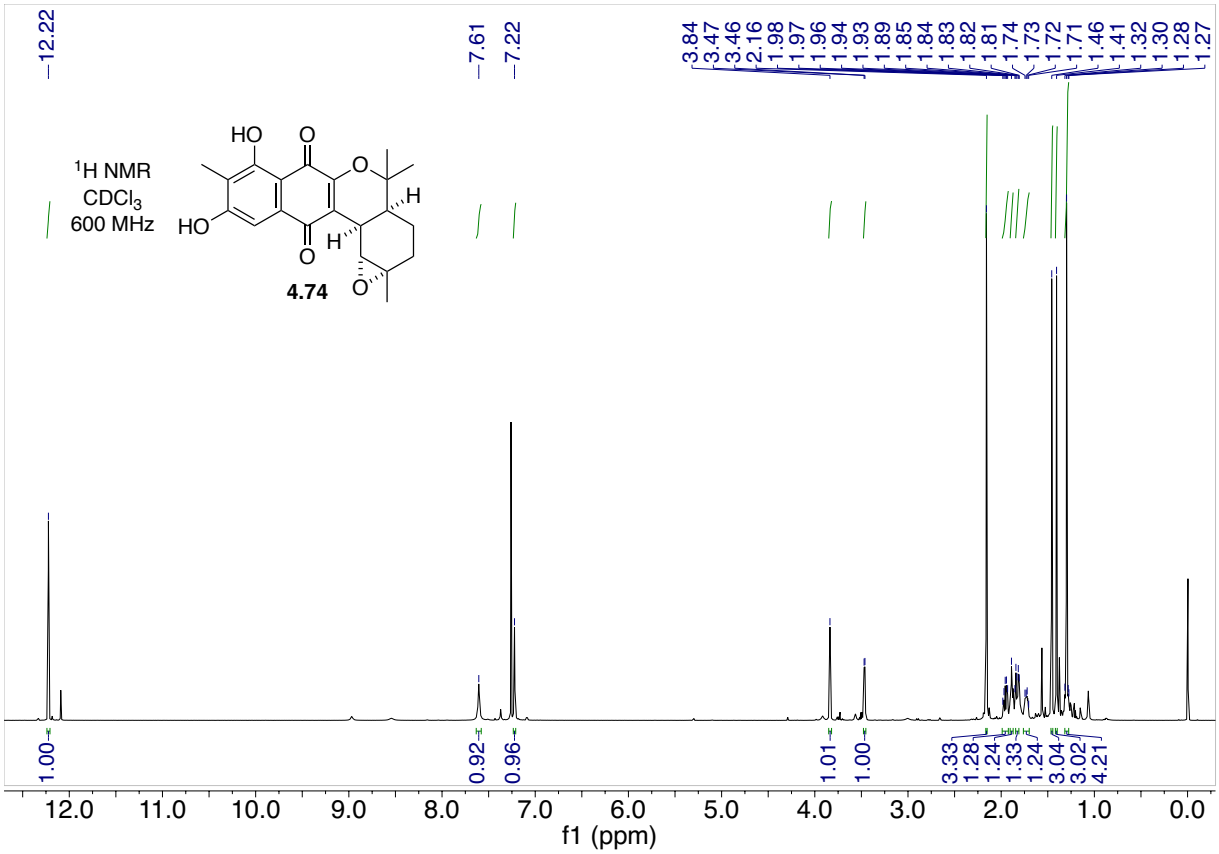
12.22
7.61
7.22
3.84
3.47
3.46
2.16
1.98
1.97
1.96
1.94
1.93
1.89
1.85
1.84
1.83
1.82
1.81
1.74
1.73
1.72
1.71
1.46
1.41
1.32
1.30
1.28
1.27
1H NMR
CDCl3
600 MHz
HO
O
O
H
HO
O
H
O
4.74
1.00
0.92
0.96
1.01
1.00
3.33
1.28
1.24
1.33
1.24
3.04
3.02
4.21
12.0
11.0
10.0
9.0
8.0
7.0
6.0
5.0
4.0
3.0
2.0
1.0
0.0
f1 (ppm)

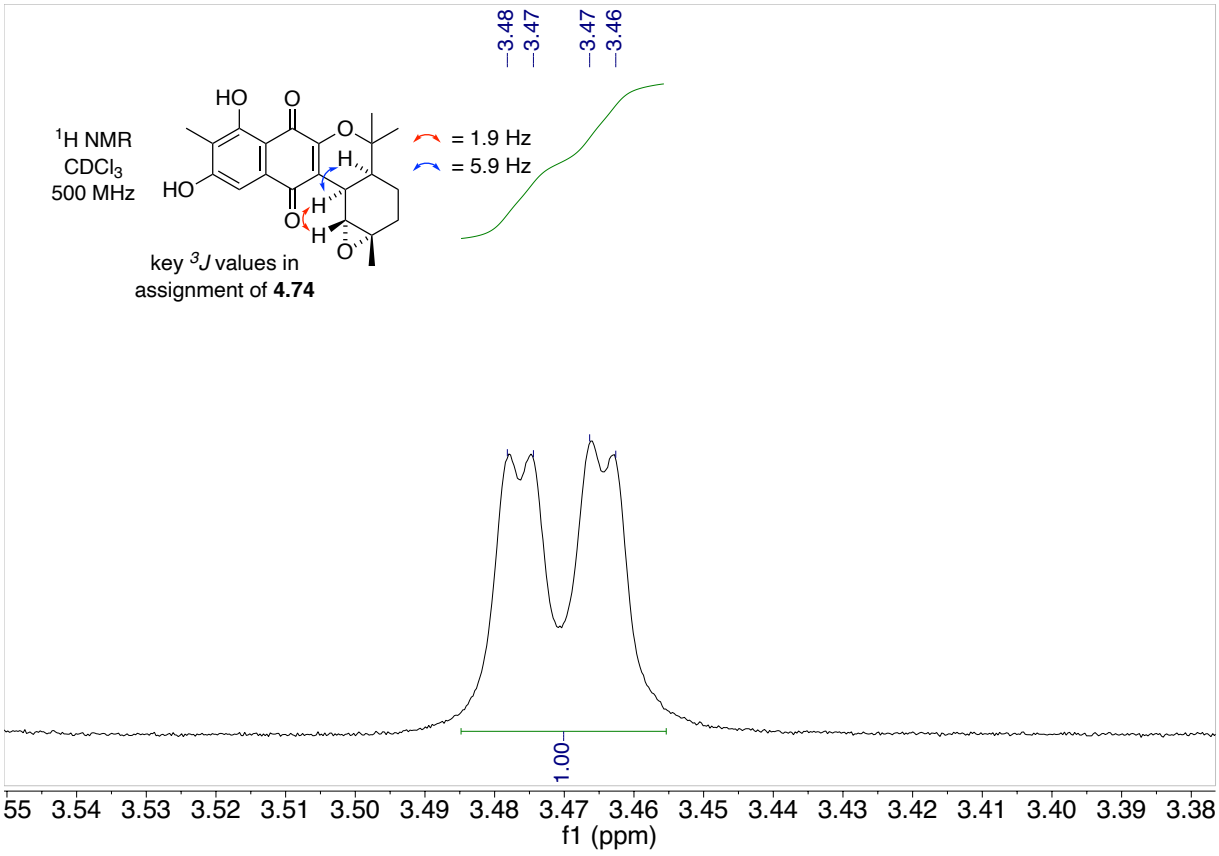
3.48
3.47
3.47
3.46
1H NMR
CDCl3
500 MHz
HO
O
O
H
HO
H
O
H
O
= 1.9 Hz
= 5.9 Hz
key 3J values in
assignment of 4.74
1.00
55
3.54
3.53
3.52
3.51
3.50
3.49
3.48
3.47
3.46
3.45
3.44
3.43
3.42
3.41
3.40
3.39
3.38
f1 (ppm)

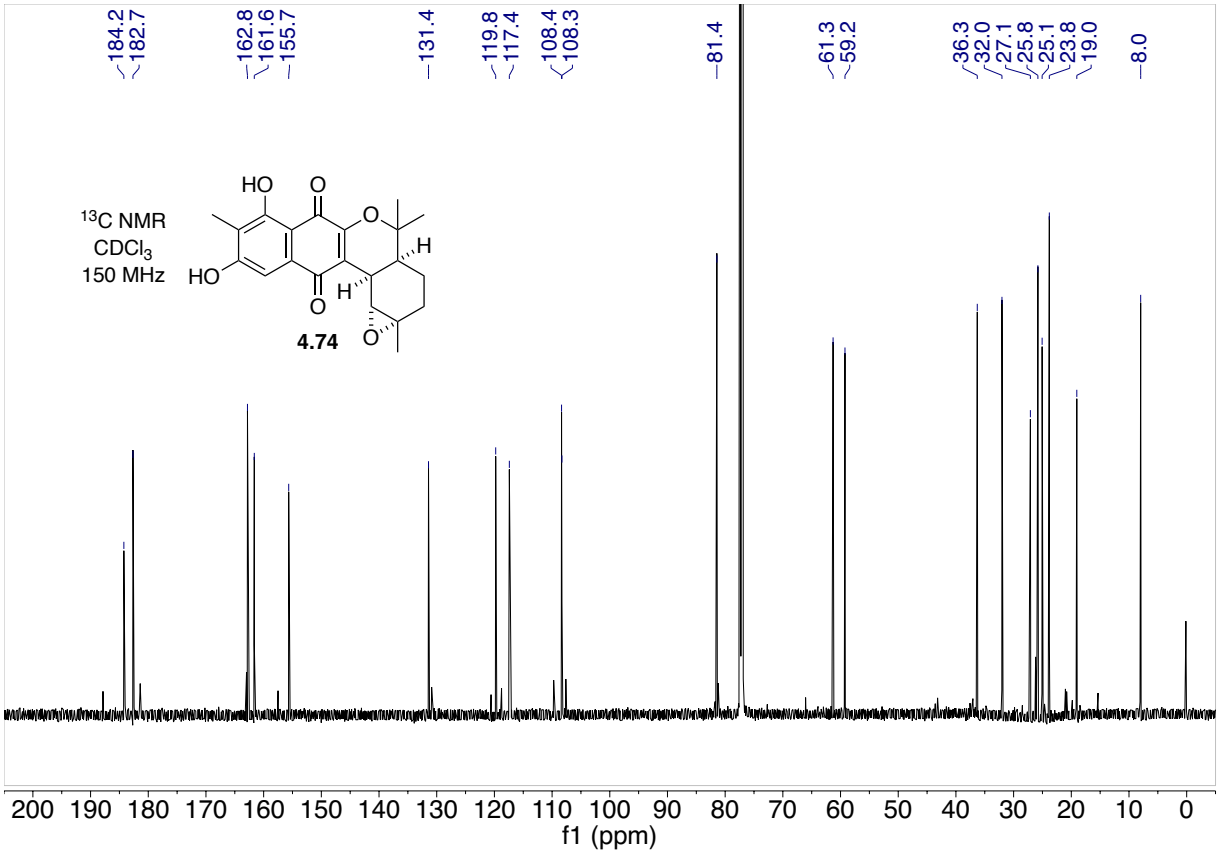
184.2
182.7
162.8
161.6
155.7
131.4
119.8
117.4
108.4
108.3
81.4
61.3
59.2
36.3
32.0
27.1
25.8
25.1
23.8
19.0
8.0
13C NMR
CDCl3
150 MHz
HO
O
O
H
HO
H
O
O
4.74
200 190 180 170 160 150 140 130 120 110 100 90 80 70 60 50 40 30 20 10 0
f1 (ppm)

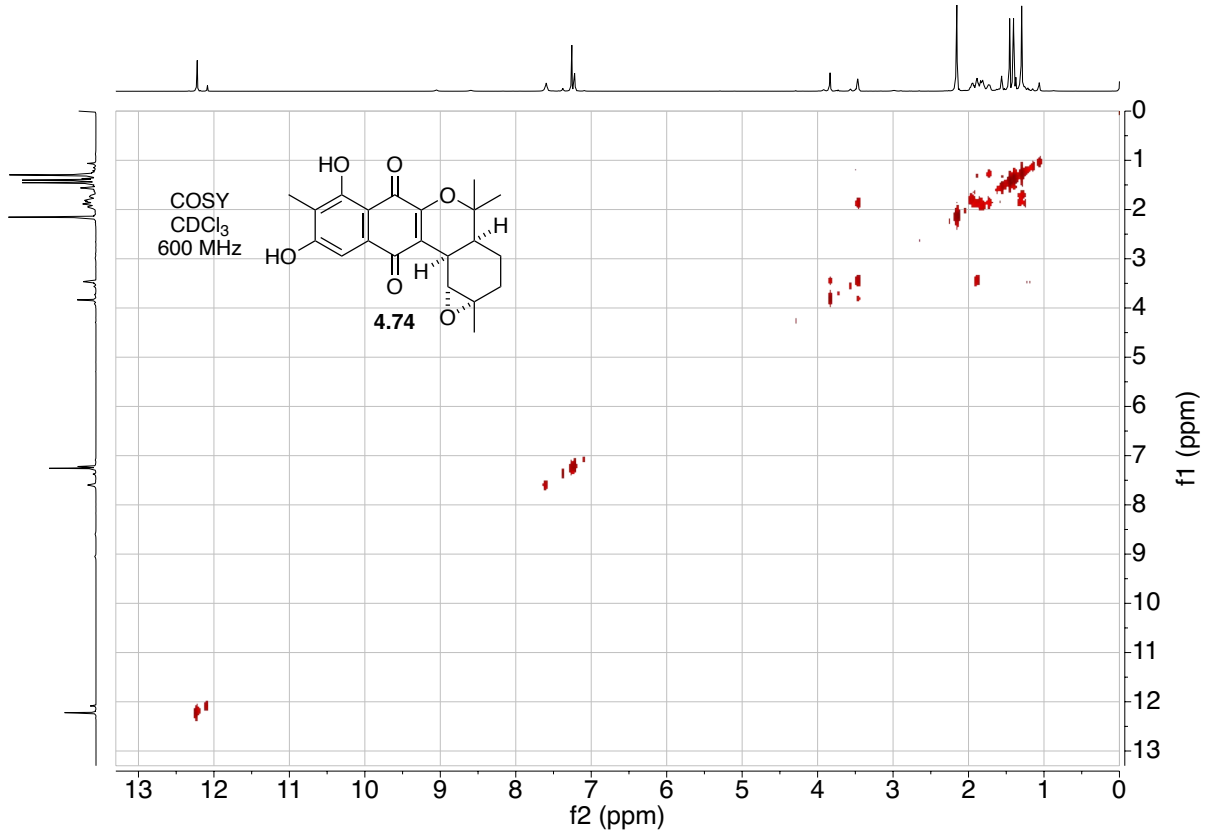
COSY
CDCl3
600 MHz
HO
O
O
H
HO
H
O
O
4.74
0 1 2 3 4 5 6 7 8 9 10 11 12 13
f1 (ppm)
13 12 11 10 9 8 7 6 5 4 3 2 1 0
f2 (ppm)

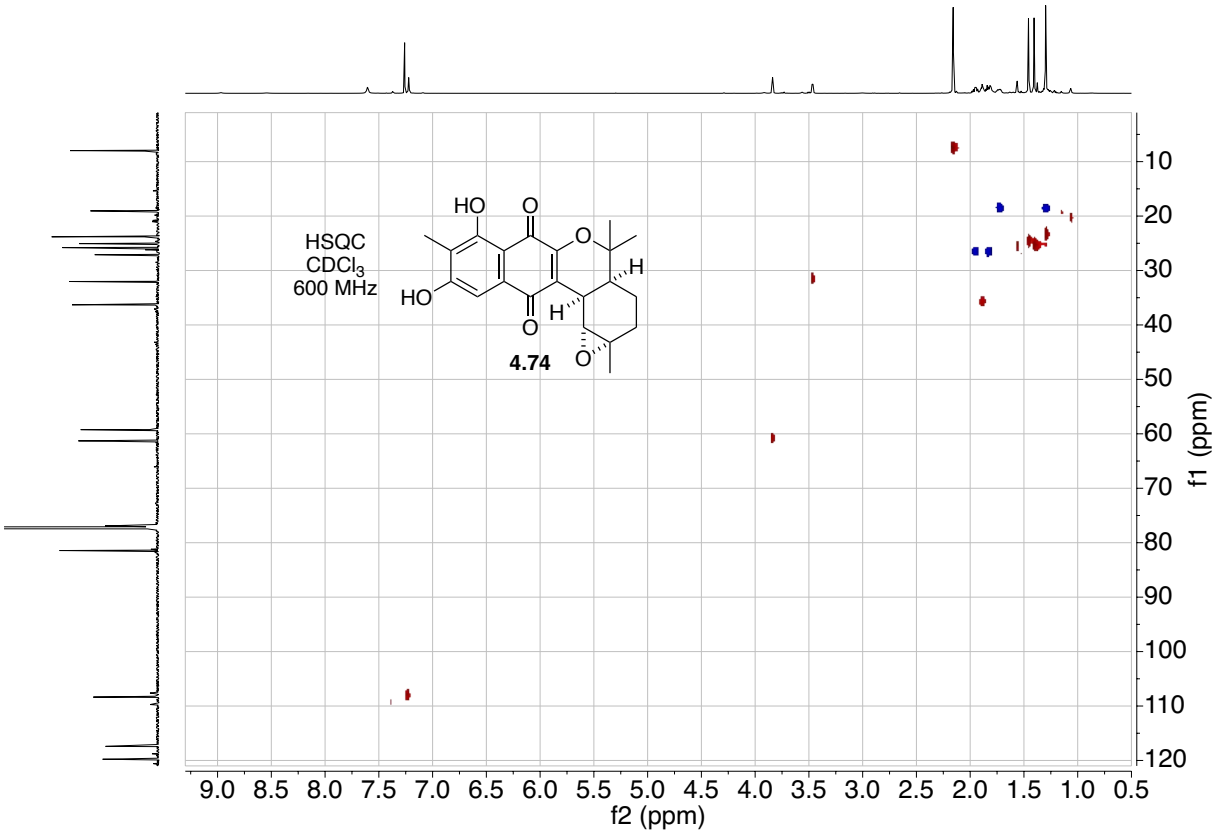
HSQC
CDCl3
600 MHz
HO
O
O
H
HO
H
O
O
4.74
f1 (ppm)
f2 (ppm)

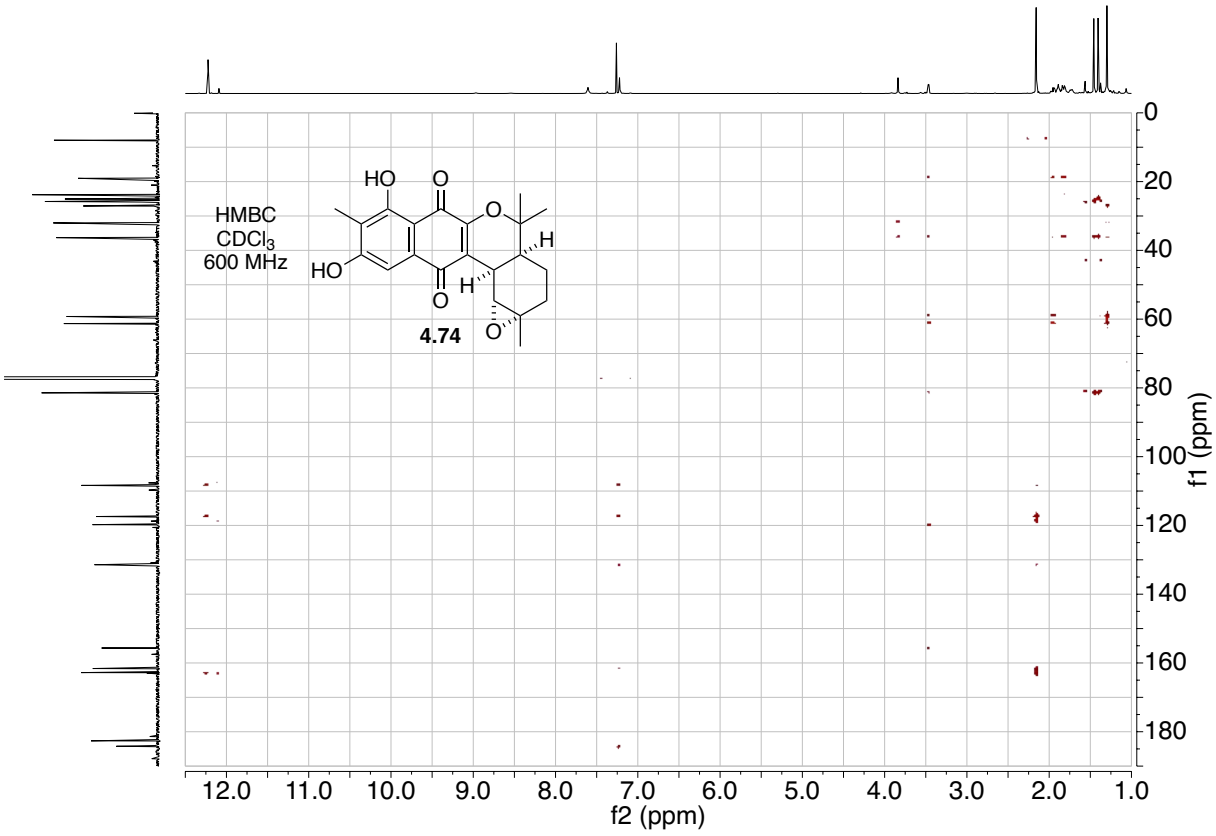
HMBC
CDCl3
600 MHz
HO
O
O
H
HO
H
O
O
4.74
f1 (ppm)
f2 (ppm)

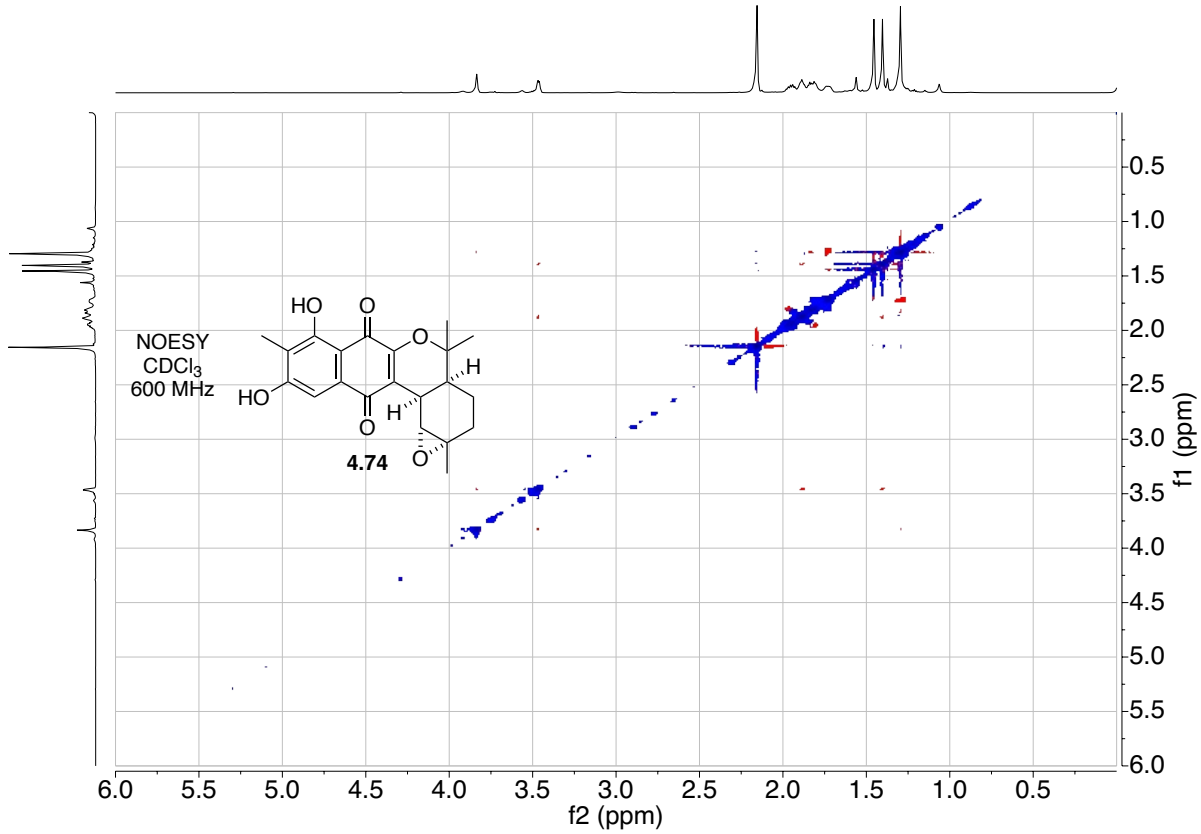
NOESY
CDCl3
600 MHz
HO
O
O
H
HO
H
O
O
4.74
f2 (ppm)
f1 (ppm)
6.0
5.5
5.0
4.5
4.0
3.5
3.0
2.5
2.0
1.5
1.0
0.5

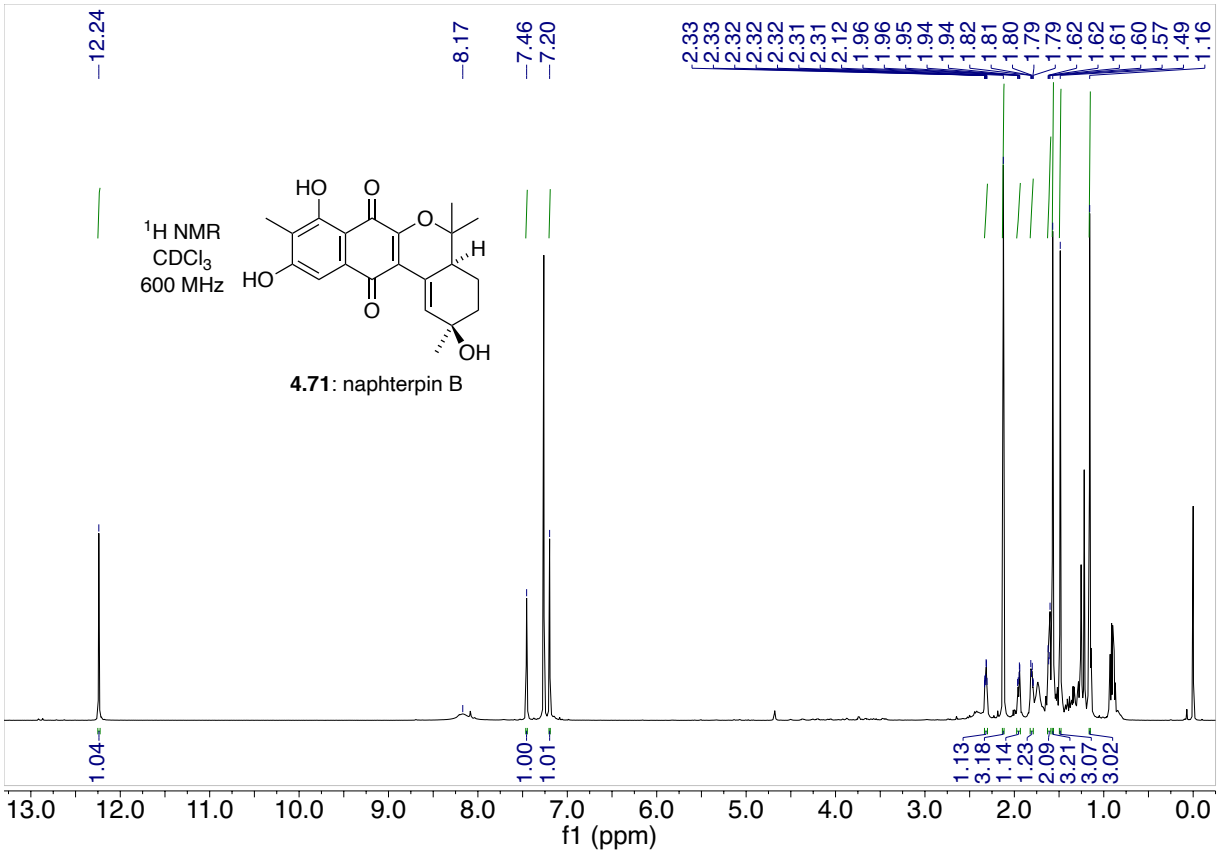
12.24
8.17
7.46
7.20
2.33
2.33
2.32
2.32
2.32
2.31
2.31
2.12
1.96
1.96
1.95
1.94
1.94
1.82
1.81
1.80
1.79
1.79
1.62
1.62
1.61
1.60
1.57
1.49
1.16
1H NMR
CDCl3
600 MHz
HO
O
O
H
HO
O
OH
4.71: naphterpin B
1.04
1.00
1.01
1.13
3.18
1.14
1.23
2.09
3.21
3.07
3.02
13.0
12.0
11.0
10.0
9.0
8.0
7.0
6.0
5.0
4.0
3.0
2.0
1.0
0.0
f1 (ppm)

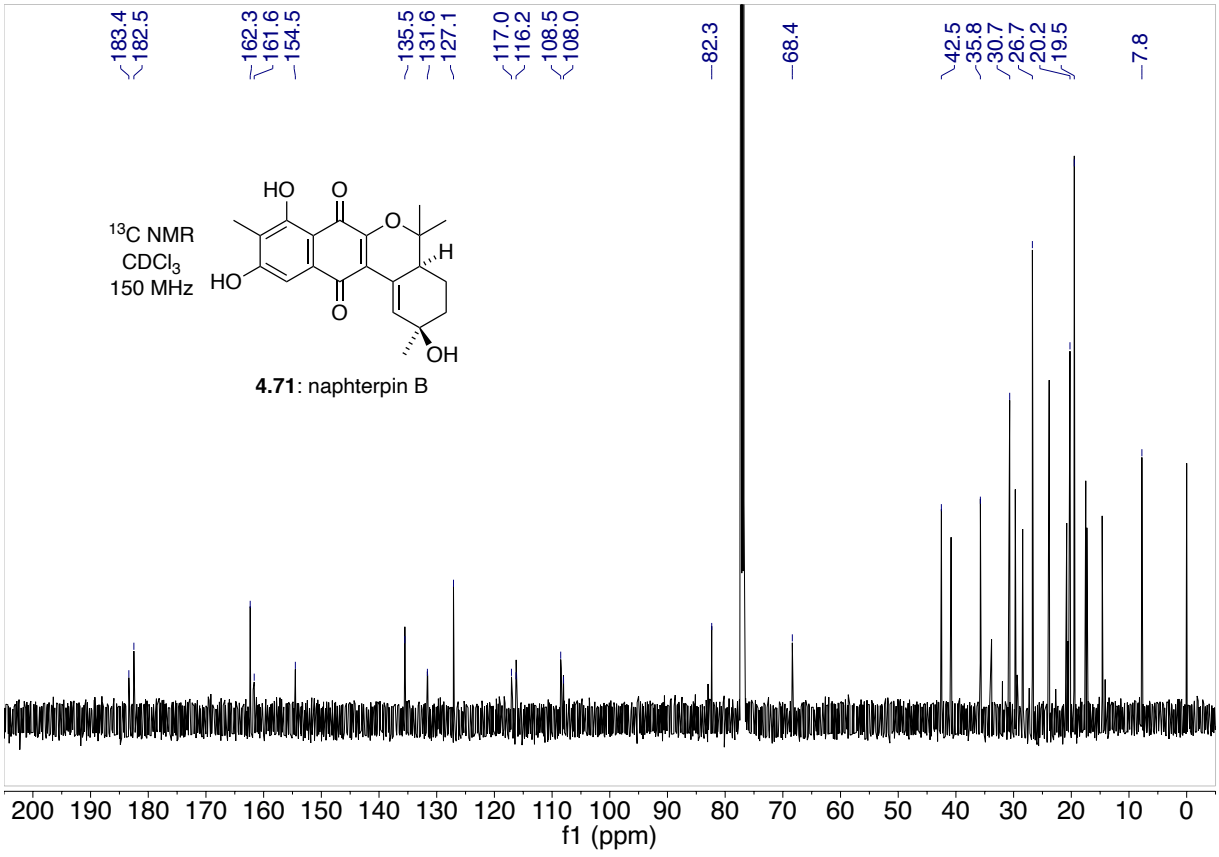
183.4
182.5
162.3
161.6
154.5
135.5
131.6
127.1
117.0
116.2
108.5
108.0
82.3
68.4
42.5
35.8
30.7
26.7
20.2
19.5
7.8
13C NMR
CDCl3
150 MHz
HO
O
O
H
HO
O
OH
4.71: naphterpin B
200
190
180
170
160
150
140
130
120
110
100
90
80
70
60
50
40
30
20
10
0
f1 (ppm)

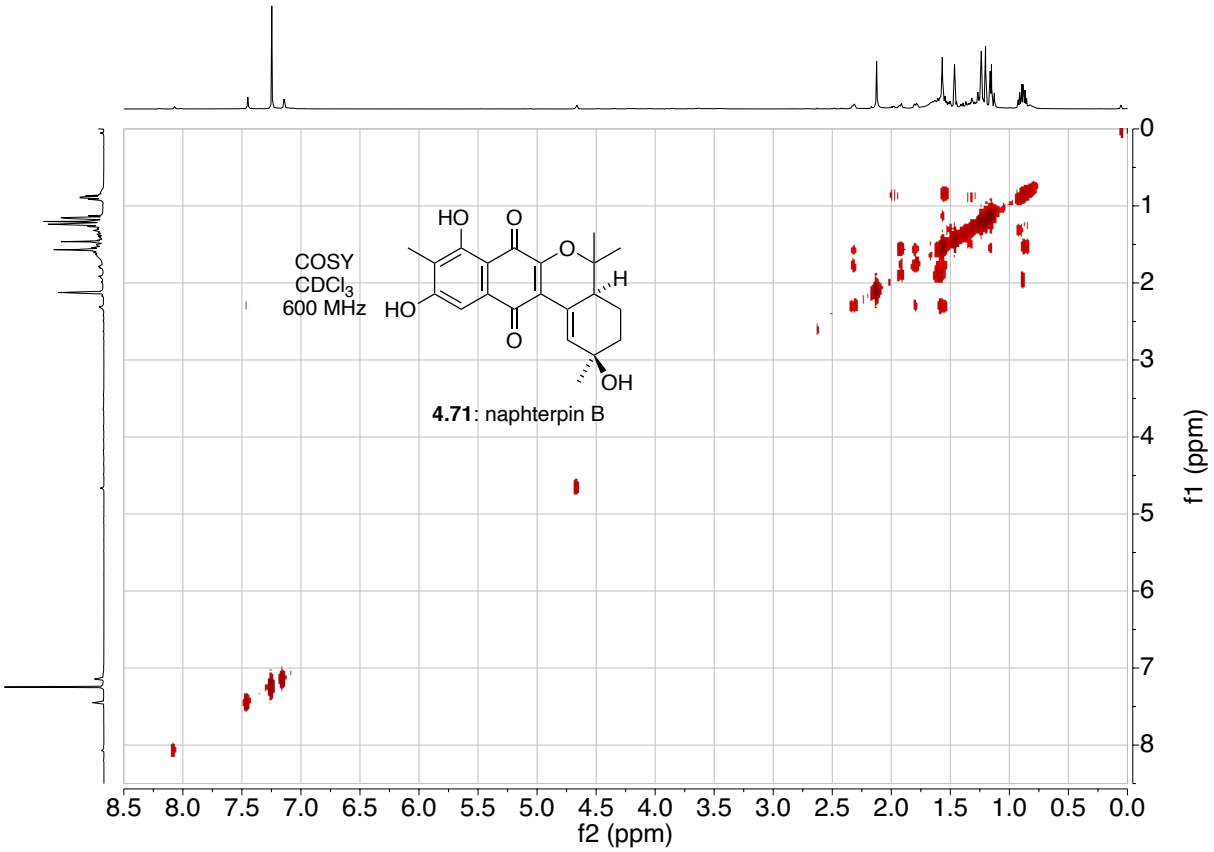
COSY
CDCl3
600 MHz
HO
O
O
H
HO
O
OH
4.71: naphterpin B
f2 (ppm)
f1 (ppm)

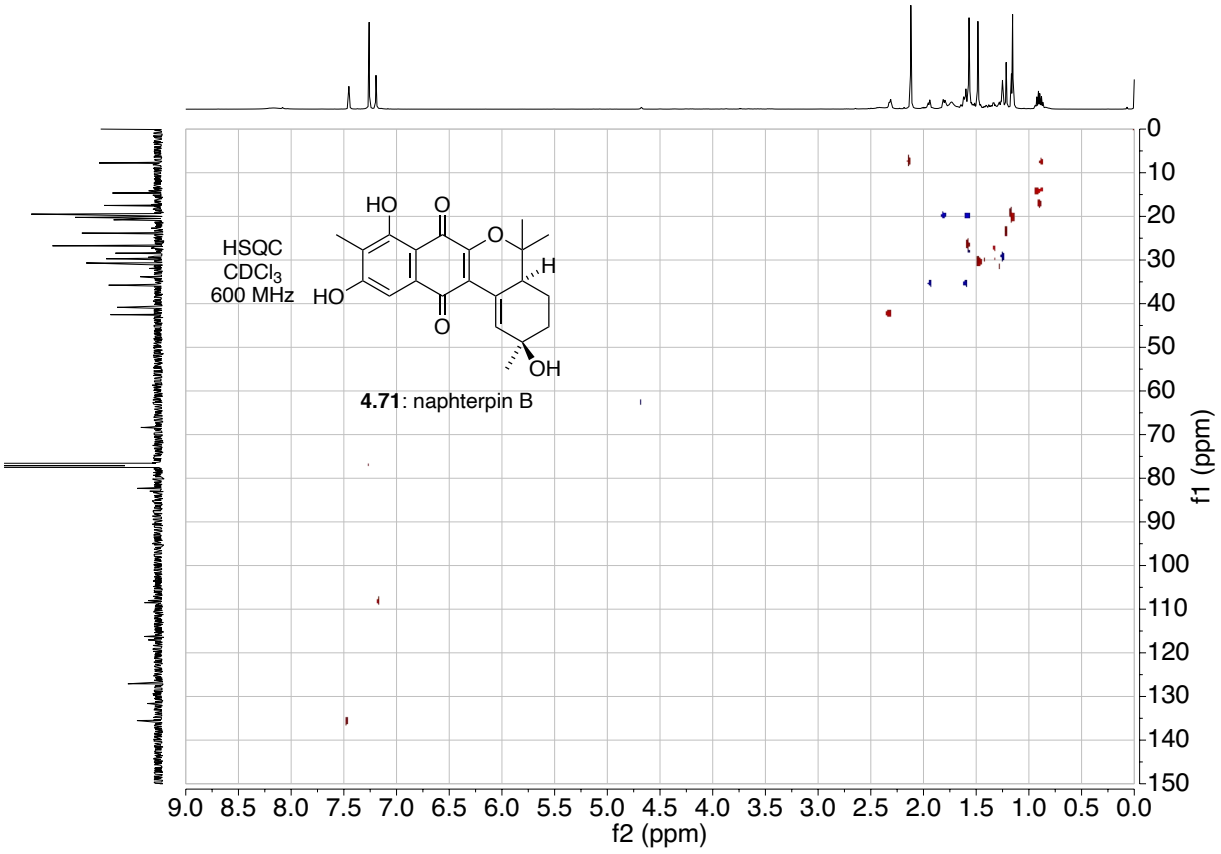
HSQC
CDCl3
600 MHz
HO
O
O
H
HO
O
OH
4.71: naphterpin B
f2 (ppm)
f1 (ppm)

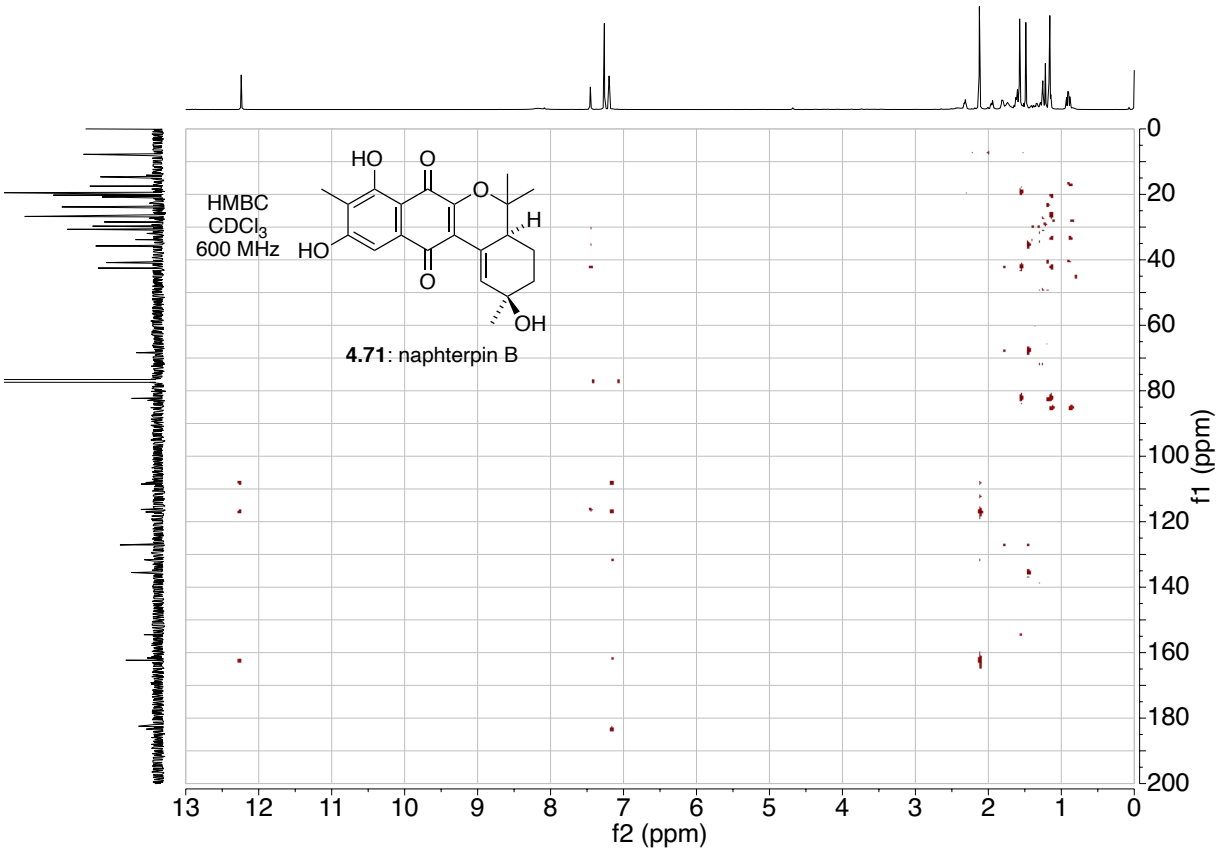
HMBC
CDCl3
600 MHz
HO
O
O
H
HO
O
OH
4.71: naphterpin B
f2 (ppm)
f1 (ppm)

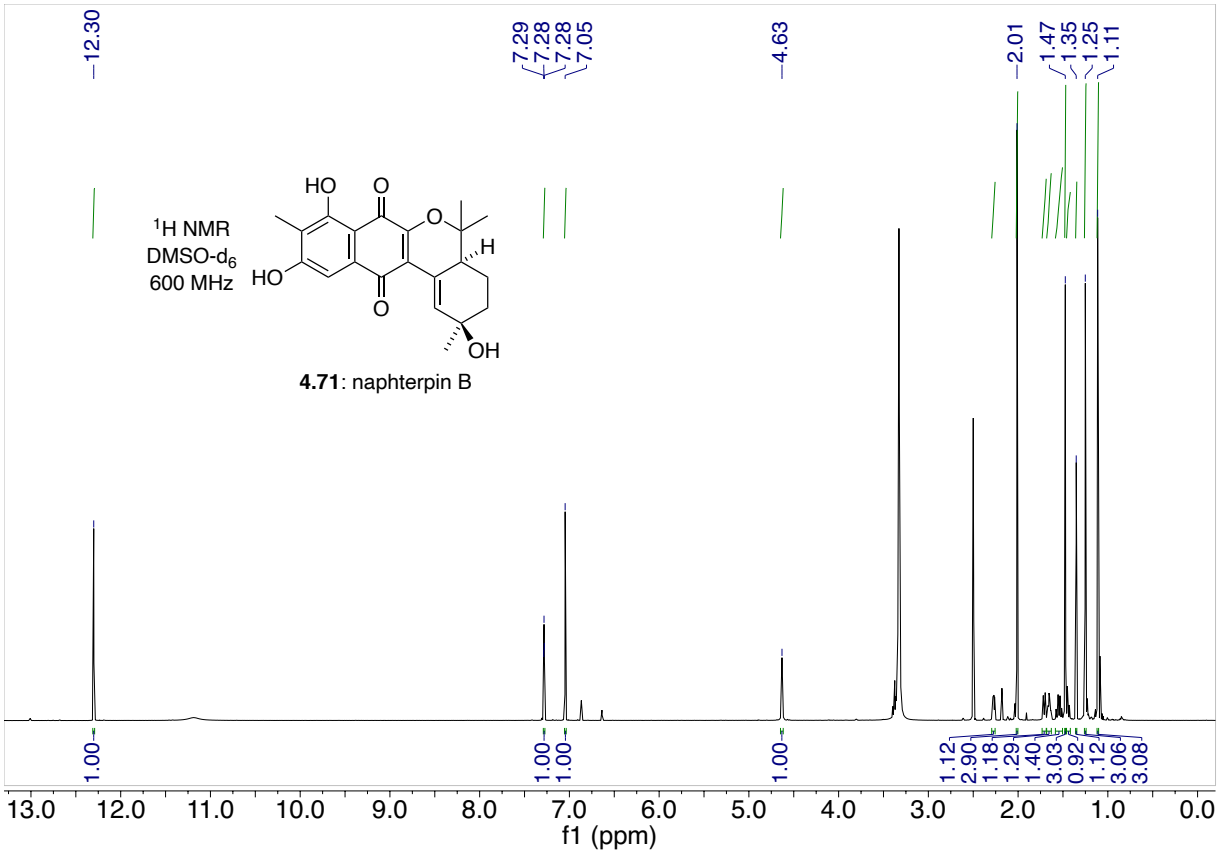

4.71: naphterpin B

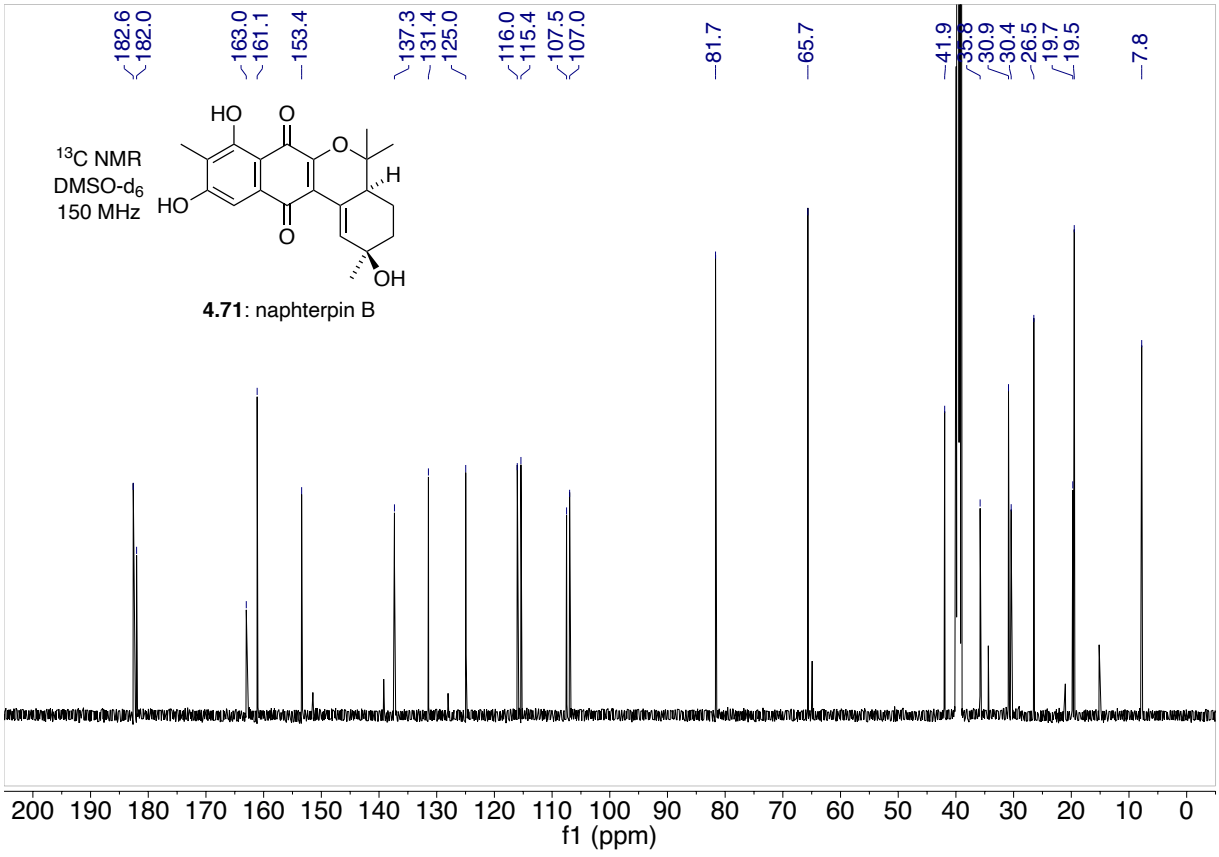

4.71: naphterpin B

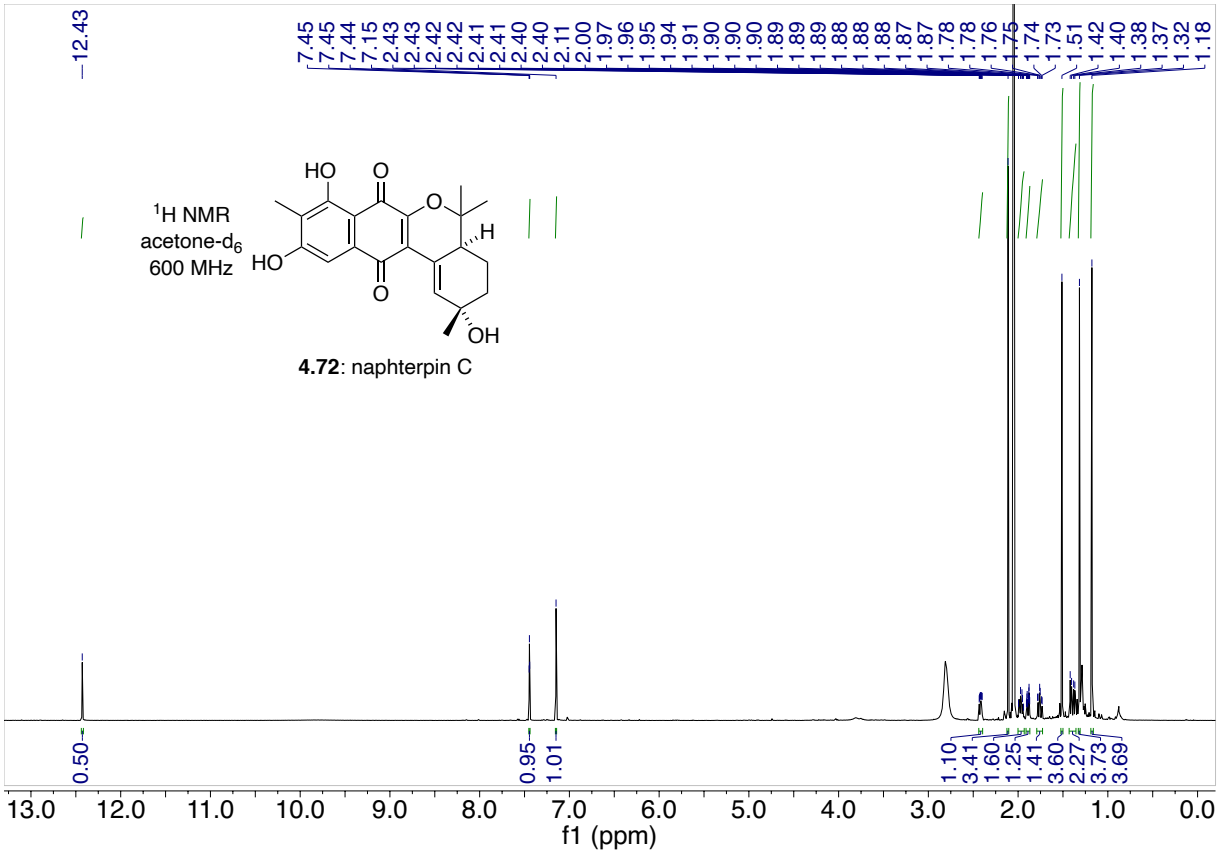

4.72: naphterpin C

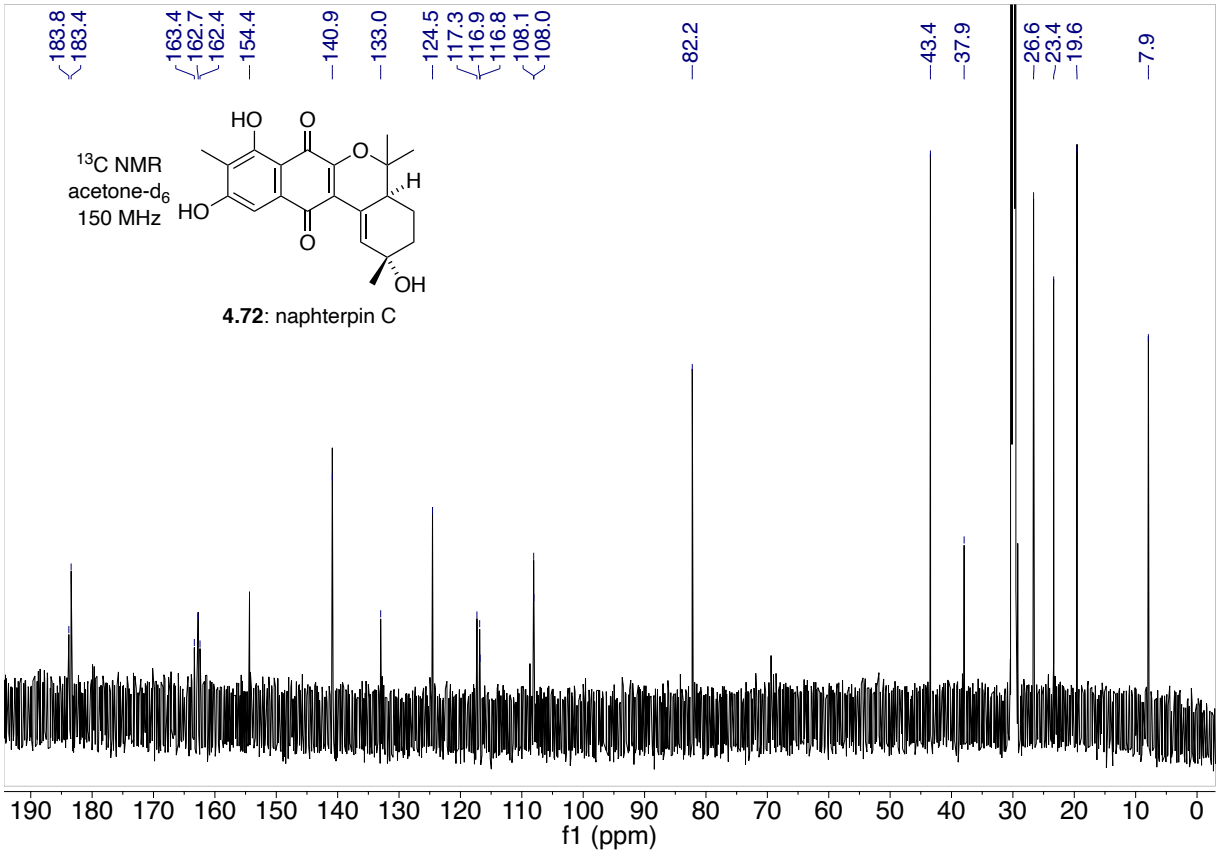

4.72: naphterpin C

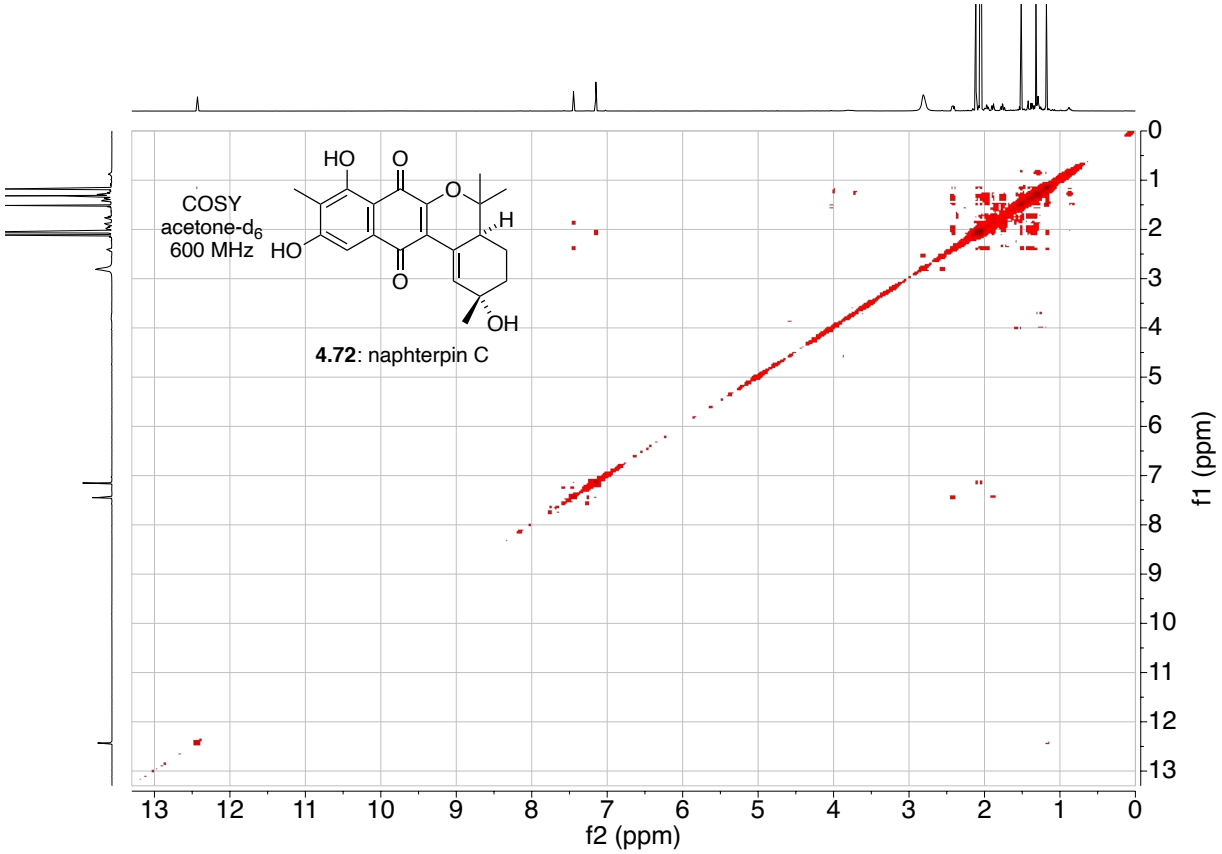
COSY
acetone-d6
600 MHz
HO
O
O
H
HO
O
OH
4.72: naphterpin C
f2 (ppm)
f1 (ppm)

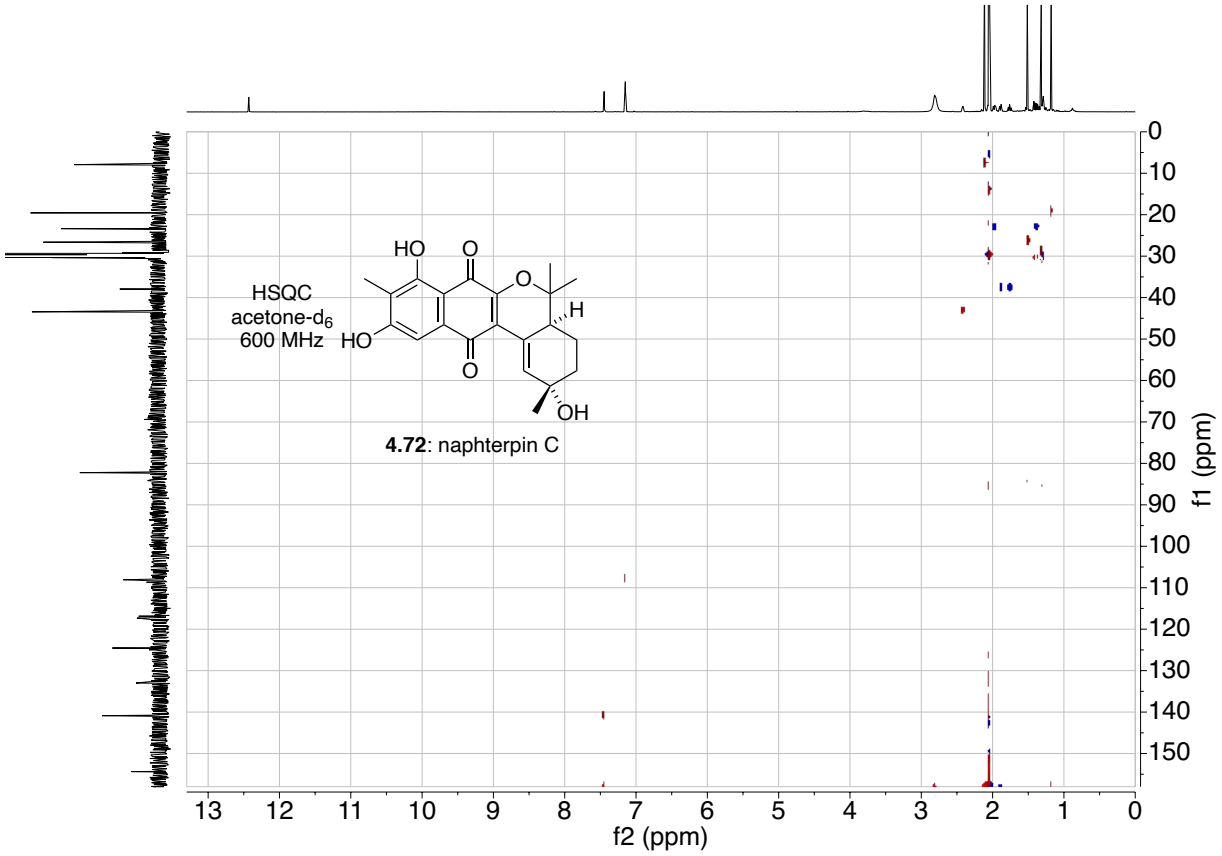
HSQC
acetone-d6
600 MHz
HO
O
O
H
HO
O
OH
4.72: naphterpin C
f2 (ppm)
f1 (ppm)

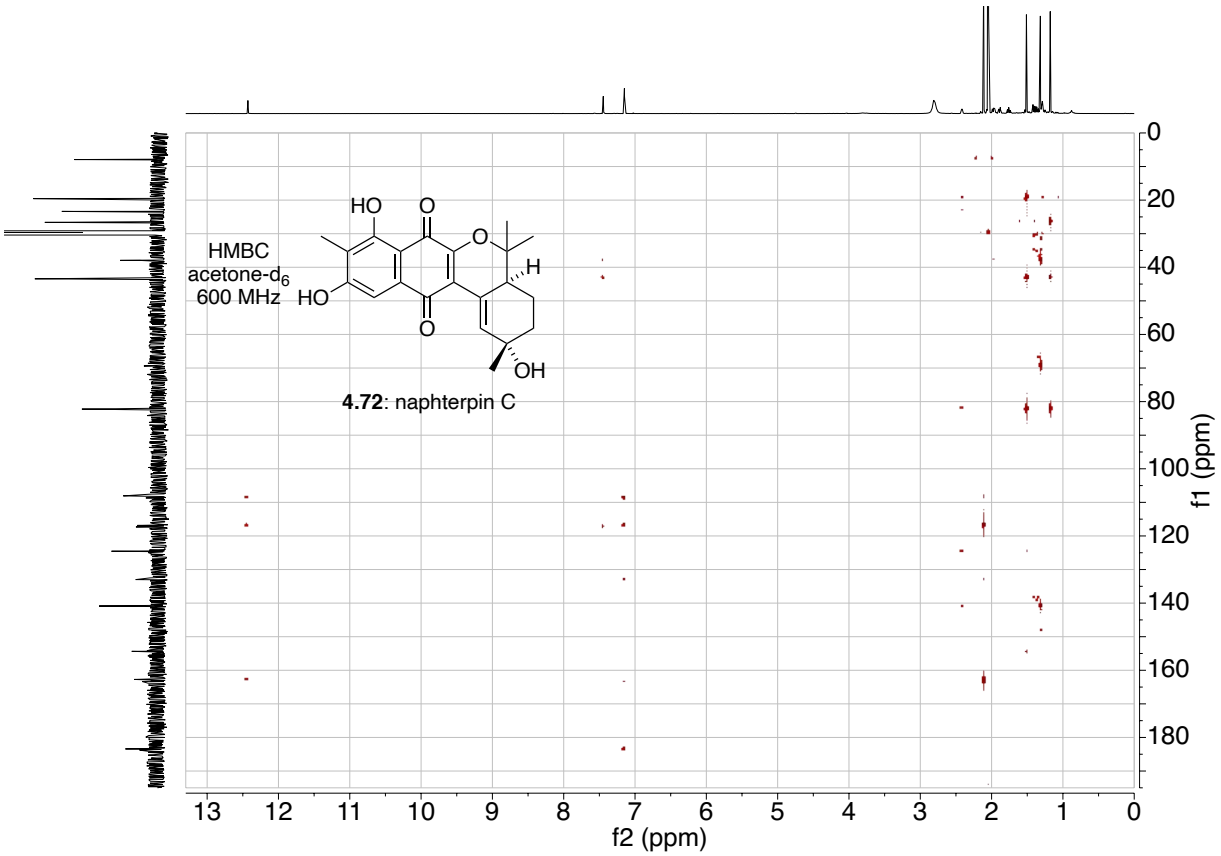
HMBC
acetone-d6
600 MHz
HO
O
O
H
HO
O
OH
4.72: naphterpin C
f2 (ppm)
f1 (ppm)

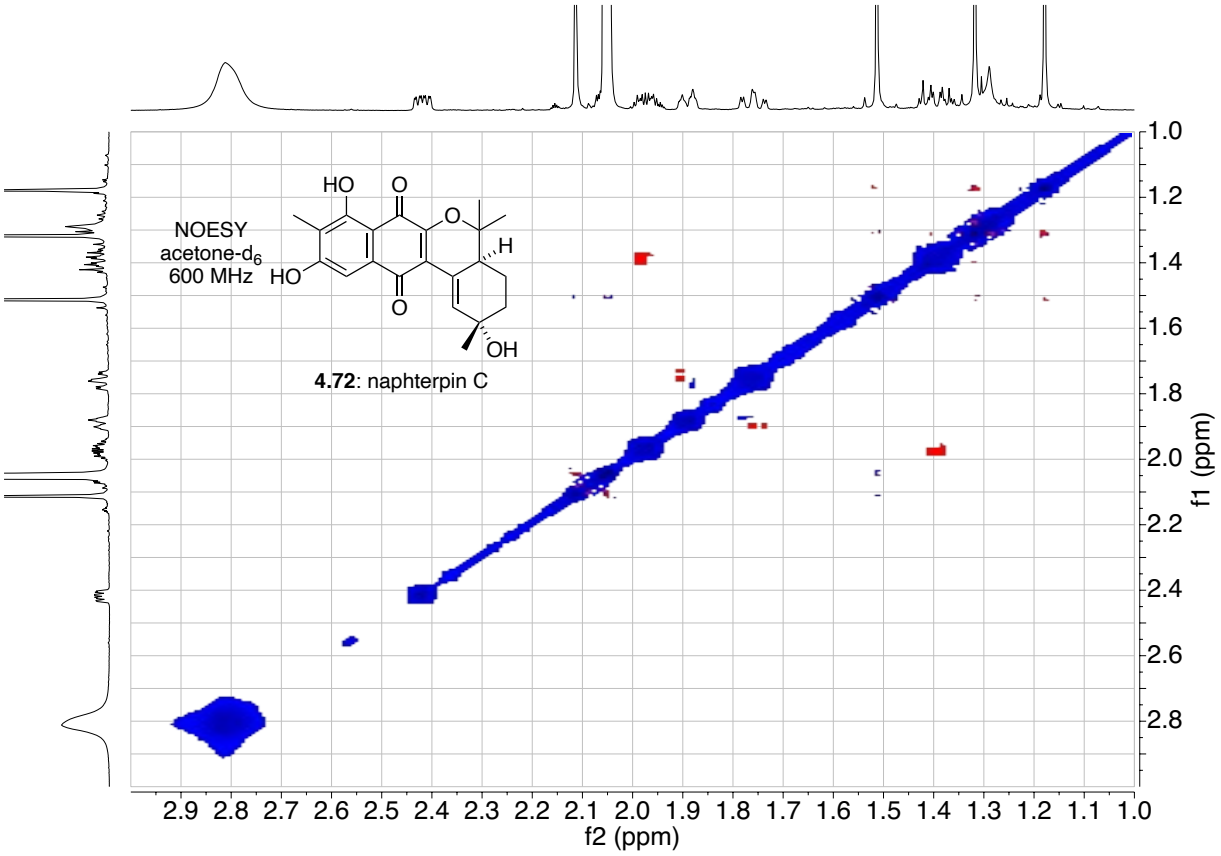
NOESY
acetone-d6
600 MHz
HO
O
O
H
HO
O
OH
4.72: naphterpin C
f2 (ppm)
f1 (ppm)

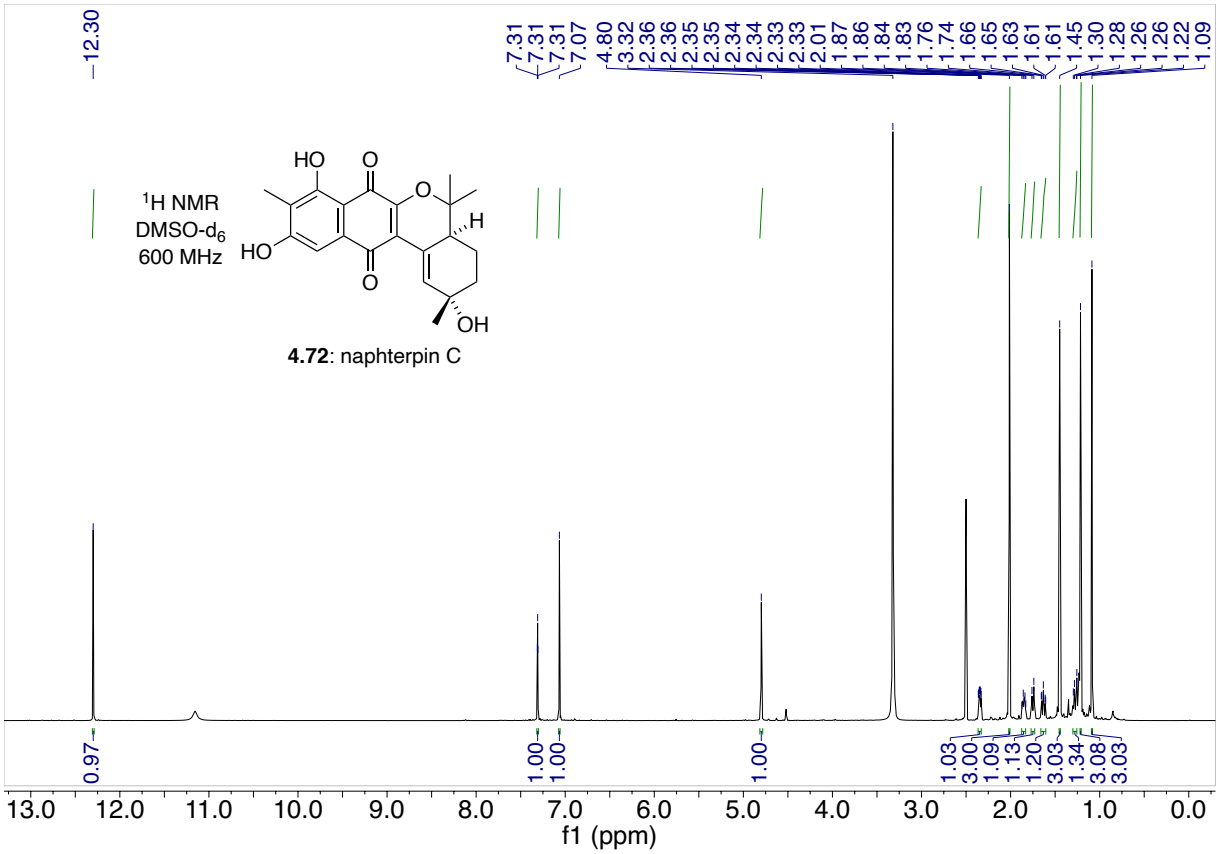

4.72: naphterpin C

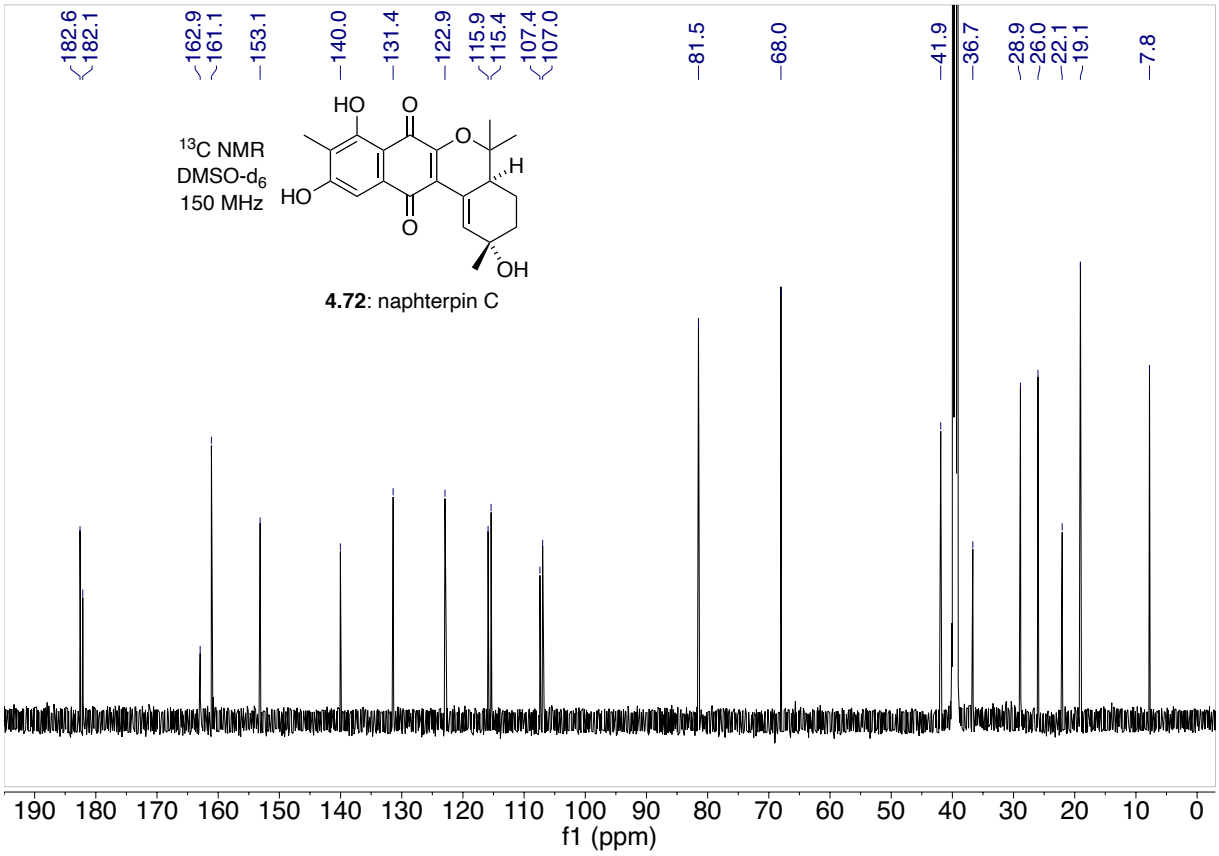

4.72: naphterpin C

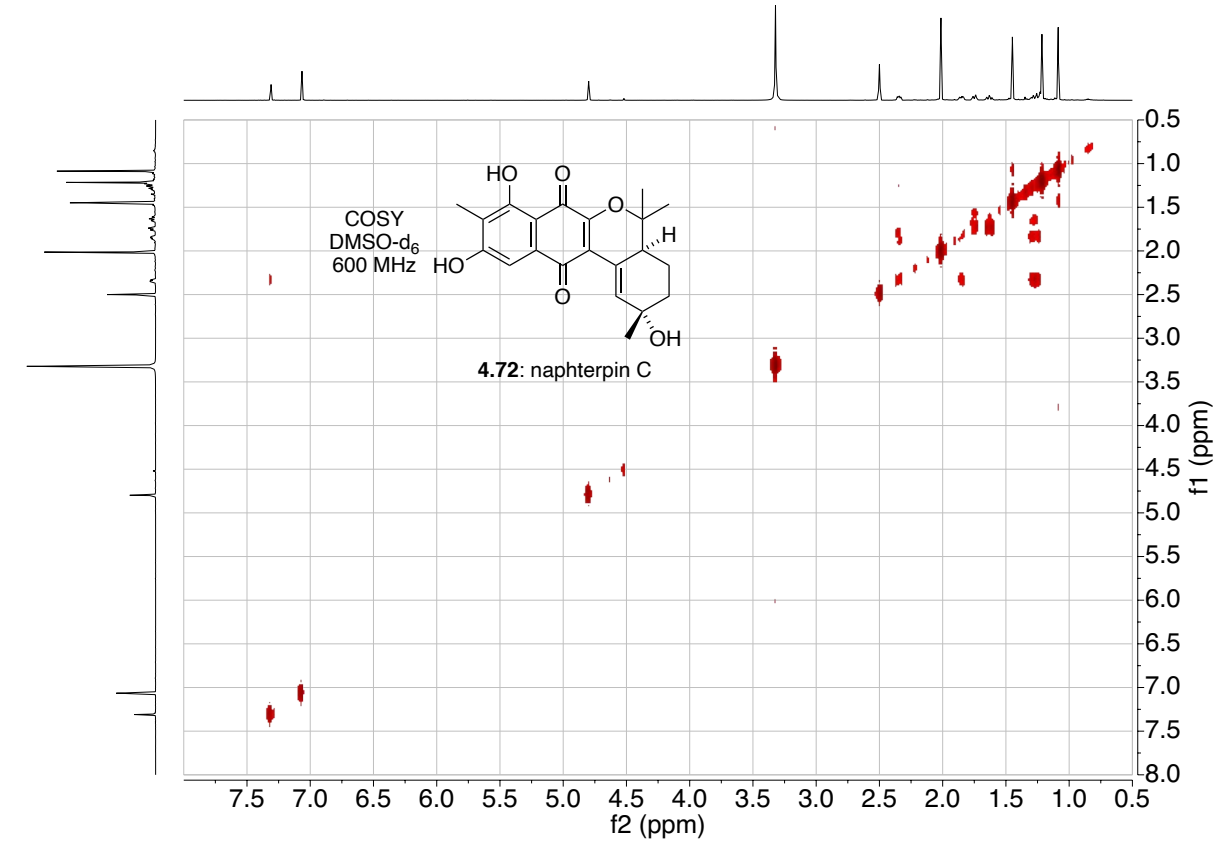
COSY
DMSO-d6
600 MHz
HO
O
O
H
HO
O
OH
4.72: naphterpin C
f2 (ppm)
f1 (ppm)

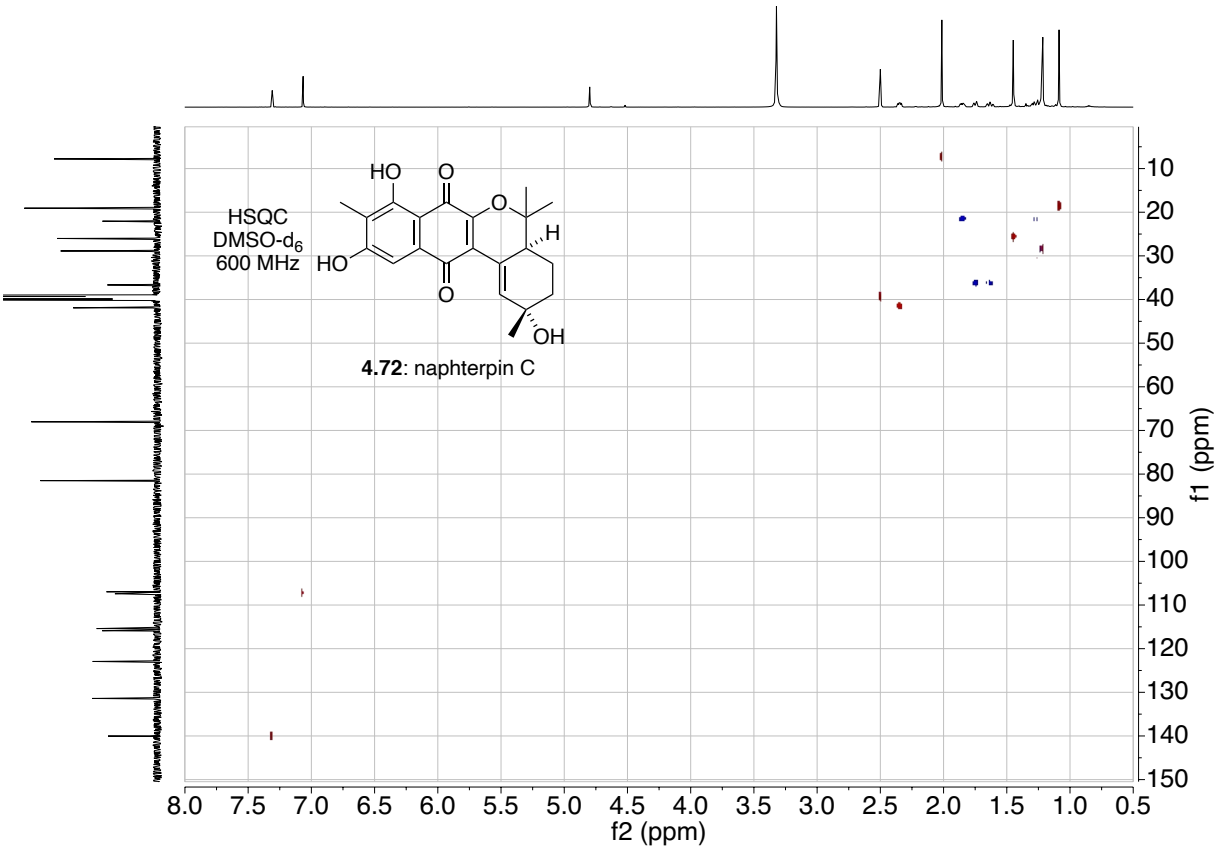
HSQC
DMSO-d6
600 MHz
HO
O
O
H
HO
O
OH
4.72: naphterpin C
f2 (ppm)
f1 (ppm)

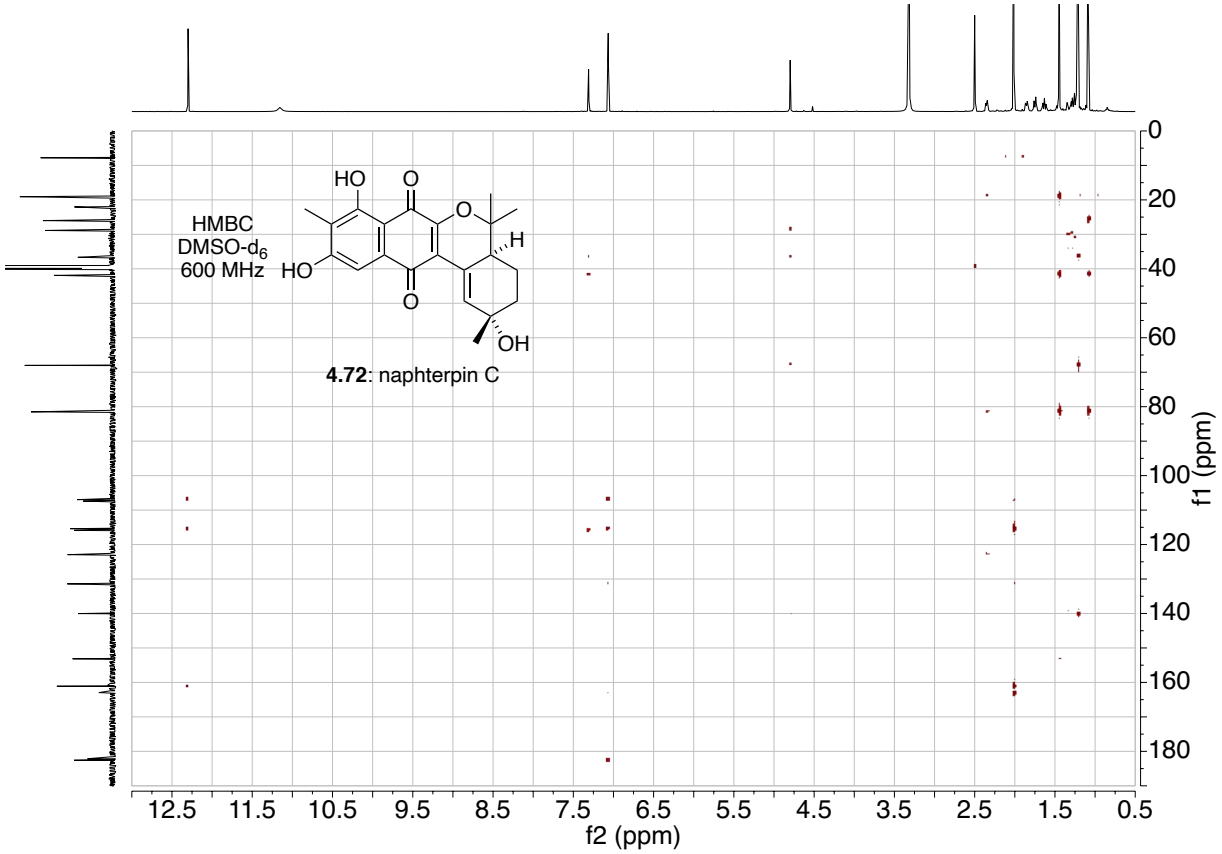
HMBC
DMSO-d6
600 MHz
HO
O
O
H
HO
O
OH
4.72: naphterpin C
f2 (ppm)
f1 (ppm)

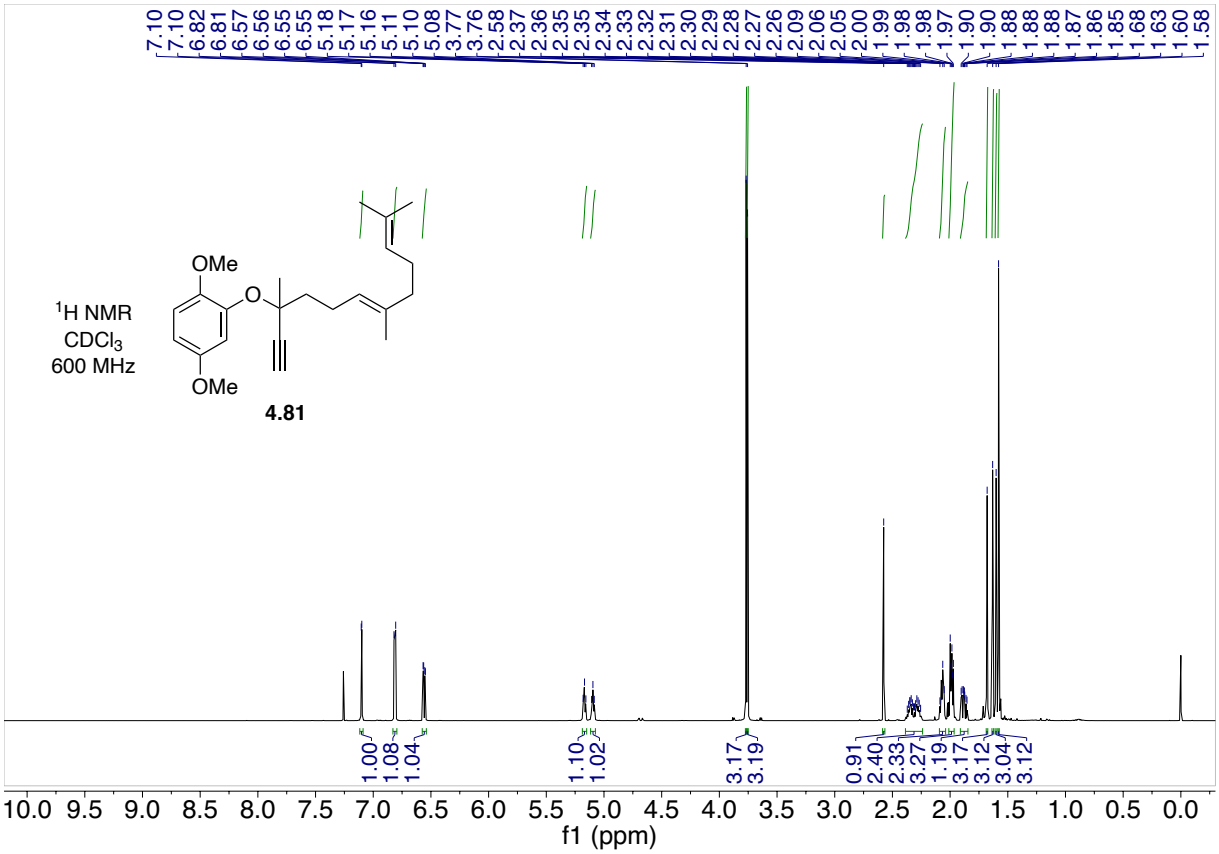
7.10 7.10 6.82 6.81 6.57 6.56 6.55 6.55 5.18 5.17 5.16 5.11 5.10 5.08 3.77 3.76 2.58 2.37 2.36 2.35 2.35 2.34 2.33 2.32 2.31 2.30 2.29 2.28 2.27 2.26 2.09 2.06 2.05 2.00 1.99 1.98 1.98 1.97 1.90 1.90 1.88 1.88 1.88 1.87 1.86 1.85 1.68 1.63 1.60 1.58
1H NMR
CDCl3
600 MHz
OMe
O
OMe
4.81
1.00 1.08 1.04 1.10 1.02 3.17 3.19 0.91 2.40 2.33 3.27 1.19 3.17 3.12 3.04 3.12
10.0 9.5 9.0 8.5 8.0 7.5 7.0 6.5 6.0 5.5 5.0 4.5 4.0 3.5 3.0 2.5 2.0 1.5 1.0 0.5 0.0
f1 (ppm)

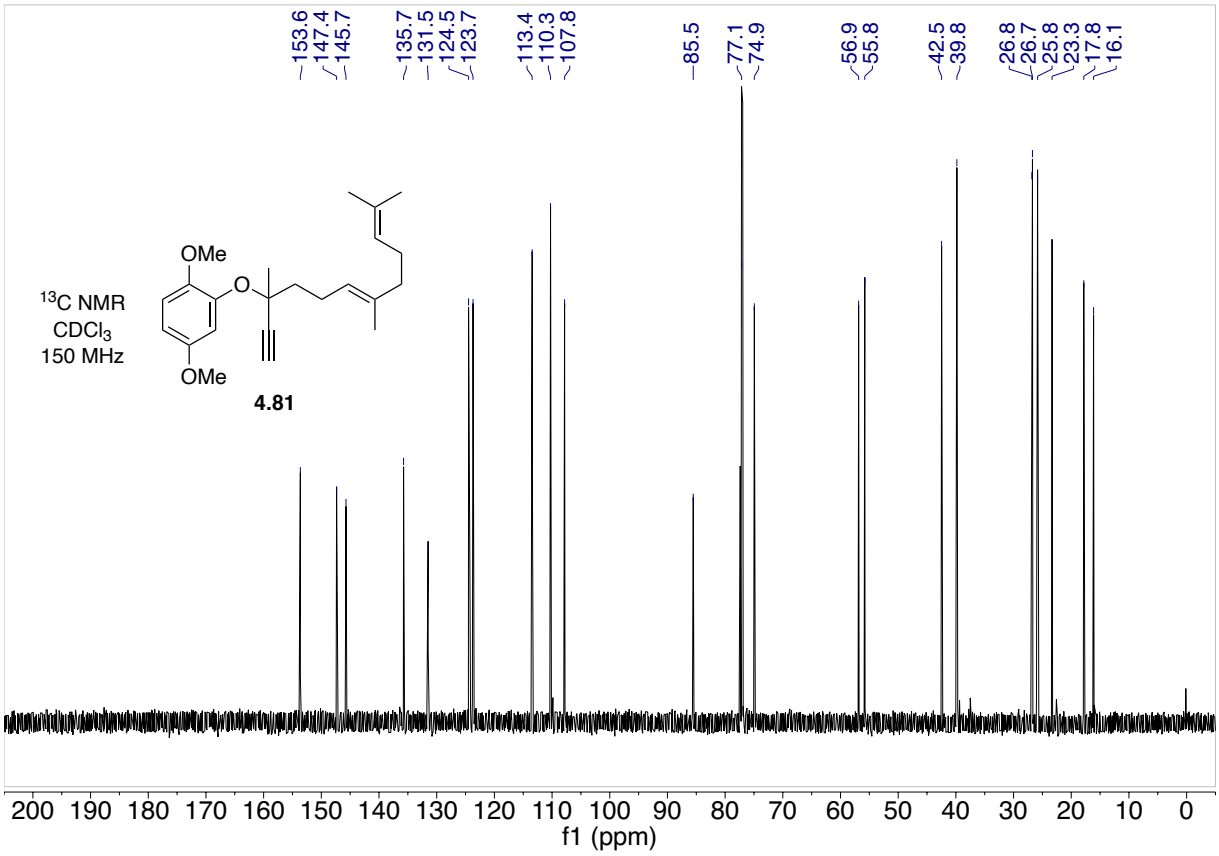
153.6 147.4 145.7 135.7 131.5 124.5 123.7 113.4 110.3 107.8 85.5 77.1 74.9 56.9 55.8 42.5 39.8 26.8 26.7 25.8 23.3 17.8 16.1
13C NMR
CDCl3
150 MHz
OMe
O
OMe
4.81
200 190 180 170 160 150 140 130 120 110 100 90 80 70 60 50 40 30 20 10 0
f1 (ppm)

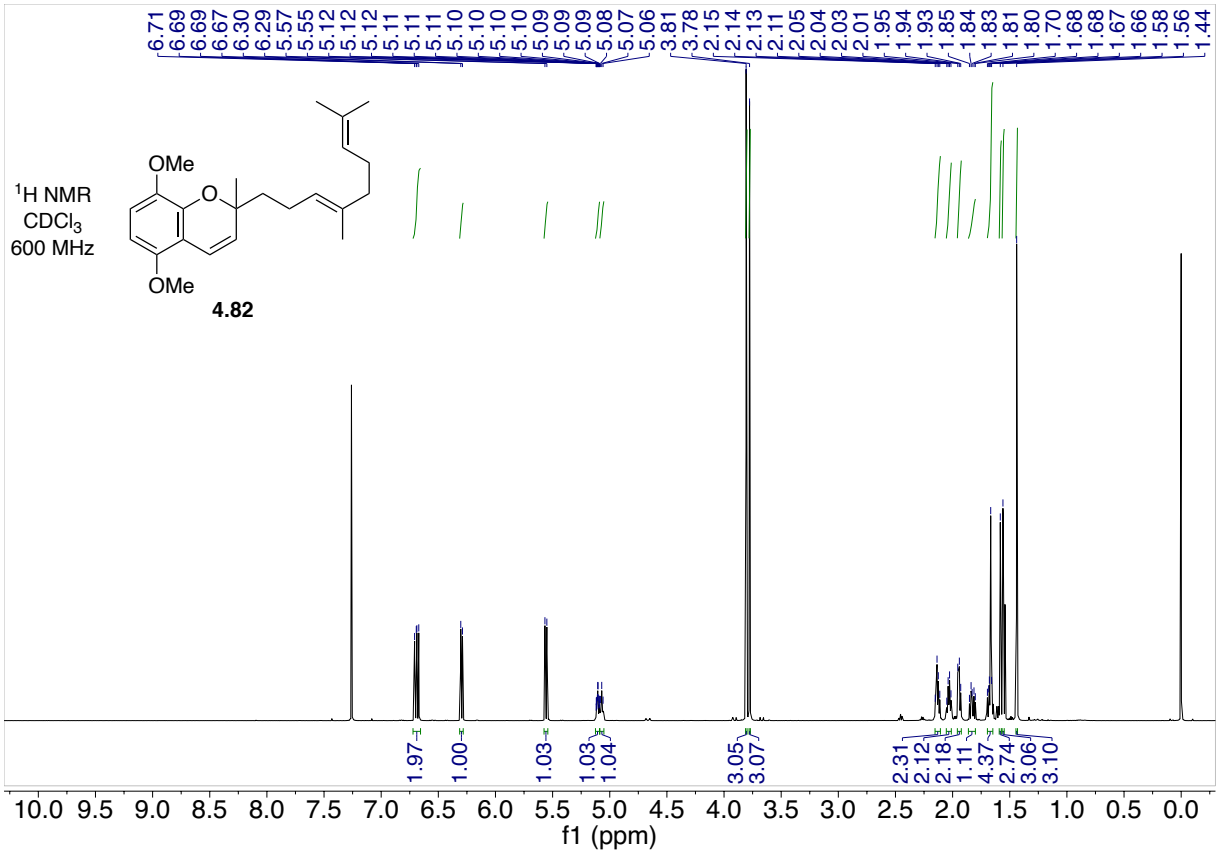
6.71 6.69 6.69 6.67 6.30 6.29 5.57 5.55 5.12 5.12 5.12 5.11 5.11 5.11 5.10 5.10 5.10 5.09 5.09 5.09 5.08 5.07 5.06
3.81 3.78 2.15 2.14 2.13 2.11 2.05 2.04 2.03 2.01 1.95 1.94 1.93 1.85 1.84 1.83 1.81 1.80 1.70 1.68 1.68 1.67 1.66 1.58 1.56 1.44
1H NMR
CDCl3
600 MHz
OMe
O
OMe
4.82
1.97 1.00 1.03 1.03 1.04 3.05 3.07 2.31 2.12 2.18 1.11 4.37 2.74 3.06 3.10
10.0 9.5 9.0 8.5 8.0 7.5 7.0 6.5 6.0 5.5 5.0 4.5 4.0 3.5 3.0 2.5 2.0 1.5 1.0 0.5 0.0
f1 (ppm)

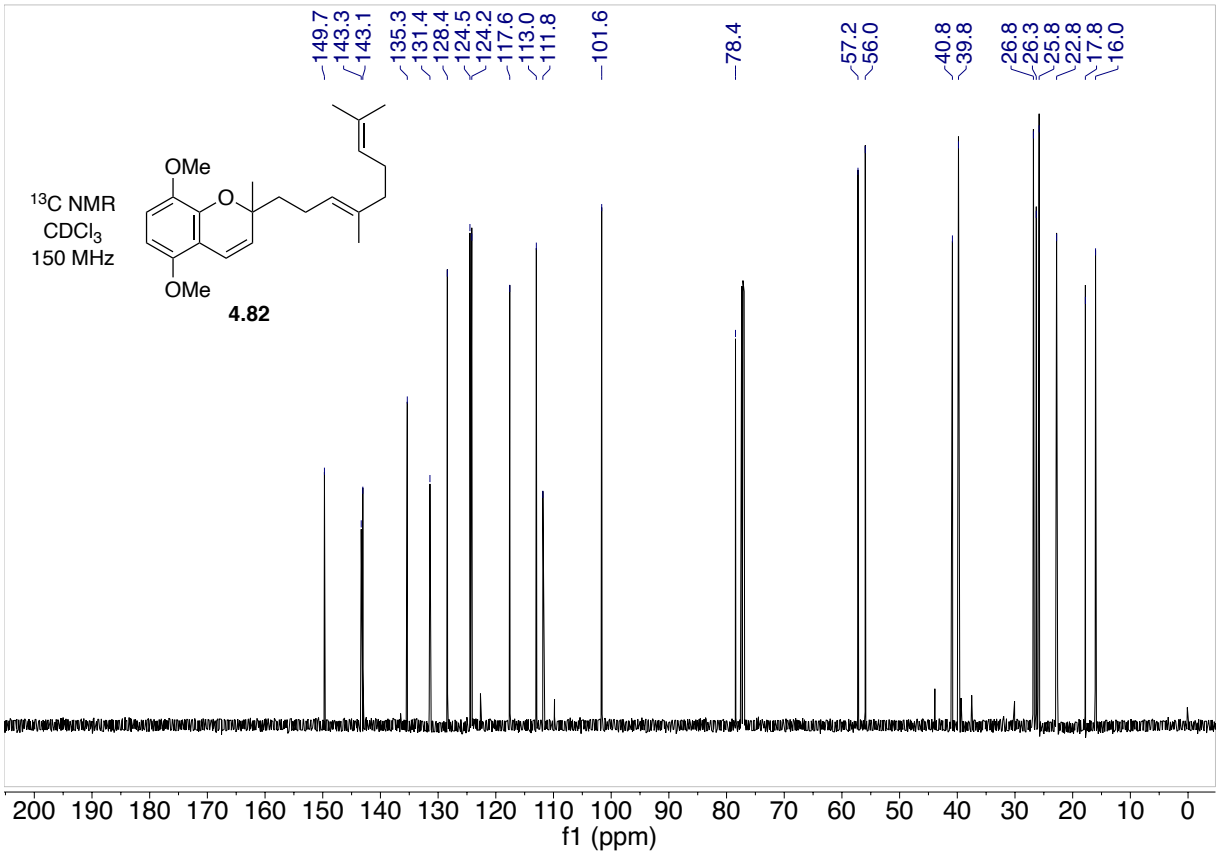
149.7 143.3 143.1 135.3 131.4 128.4 124.5 124.2 117.6 113.0 111.8 101.6 78.4 57.2 56.0 40.8 39.8 26.8 26.3 25.8 22.8 17.8 16.0
13C NMR
CDCl3
150 MHz
OMe
O
OMe
4.82
200 190 180 170 160 150 140 130 120 110 100 90 80 70 60 50 40 30 20 10 0
f1 (ppm)

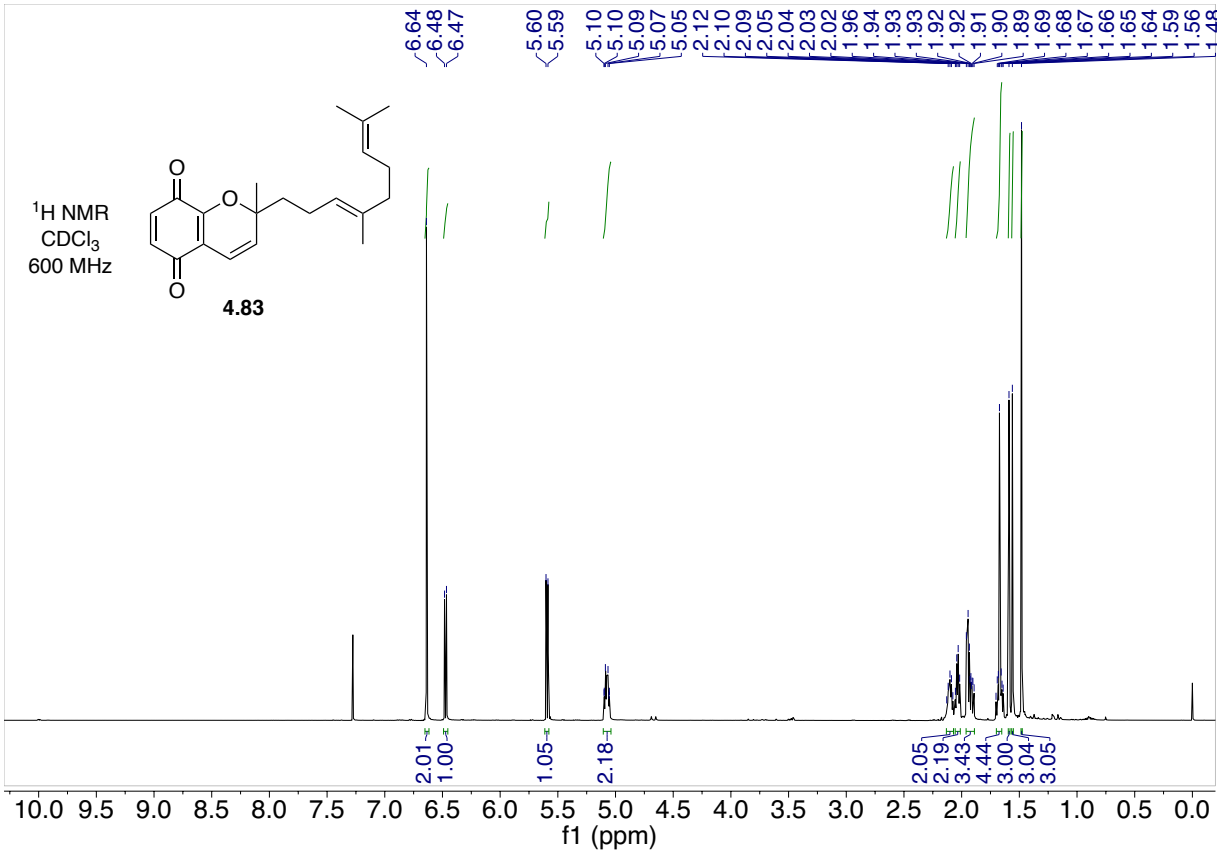
^{1}H NMR
$CDCl_3$
600 MHz
4.83
6.64
6.48
6.47
5.60
5.59
5.10
5.10
5.09
5.07
5.05
2.12
2.10
2.09
2.05
2.04
2.03
2.02
1.96
1.94
1.93
1.93
1.92
1.92
1.91
1.90
1.89
1.69
1.68
1.67
1.66
1.65
1.64
1.59
1.56
2.01
1.00
1.05
2.18
2.05
2.19
3.43
4.44
3.00
3.04
3.05
10.0 9.5 9.0 8.5 8.0 7.5 7.0 6.5 6.0 5.5 5.0 4.5 4.0 3.5 3.0 2.5 2.0 1.5 1.0 0.5 0.0
f1 (ppm)

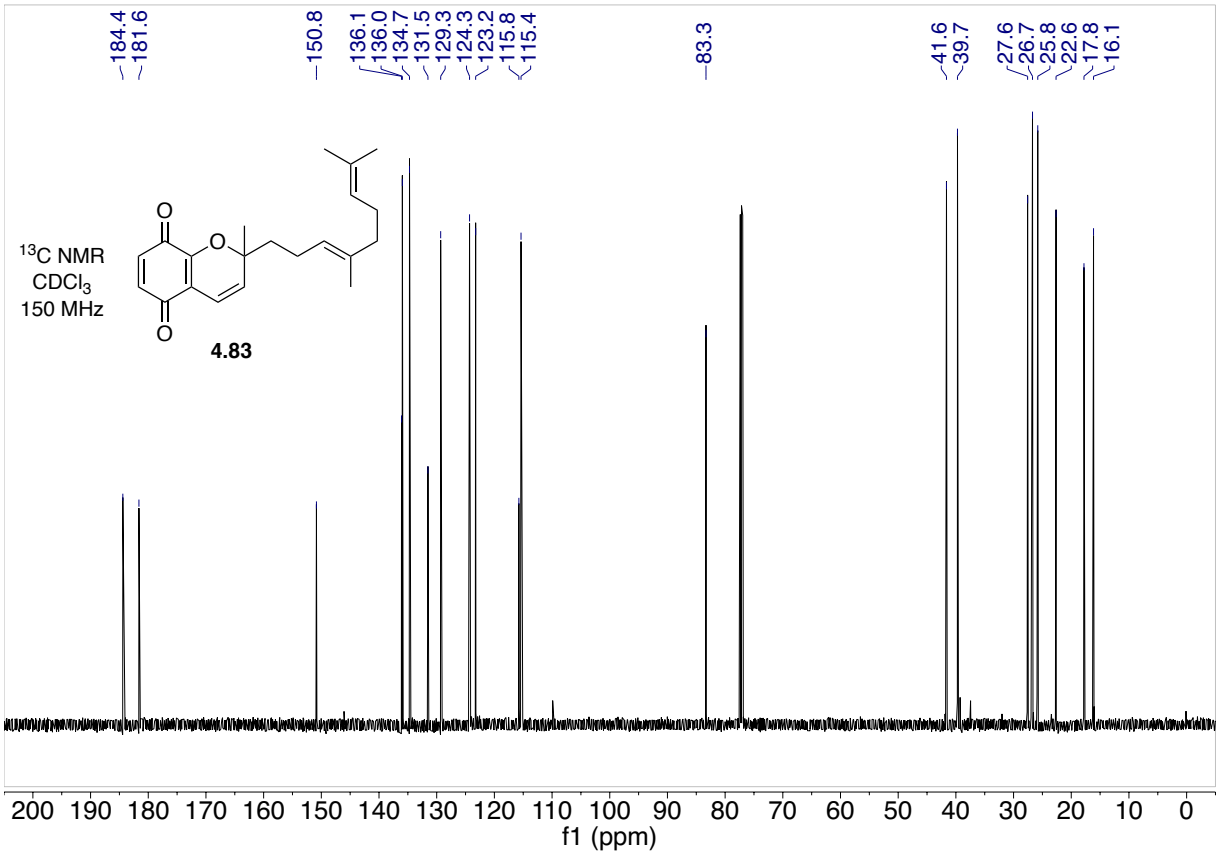
^{13}C NMR
$CDCl_3$
150 MHz
4.83
184.4
181.6
150.8
136.1
136.0
134.7
131.5
129.3
124.3
123.2
115.8
115.4
83.3
41.6
39.7
27.6
26.7
25.8
22.6
17.8
16.1
200 190 180 170 160 150 140 130 120 110 100 90 80 70 60 50 40 30 20 10 0
f1 (ppm)

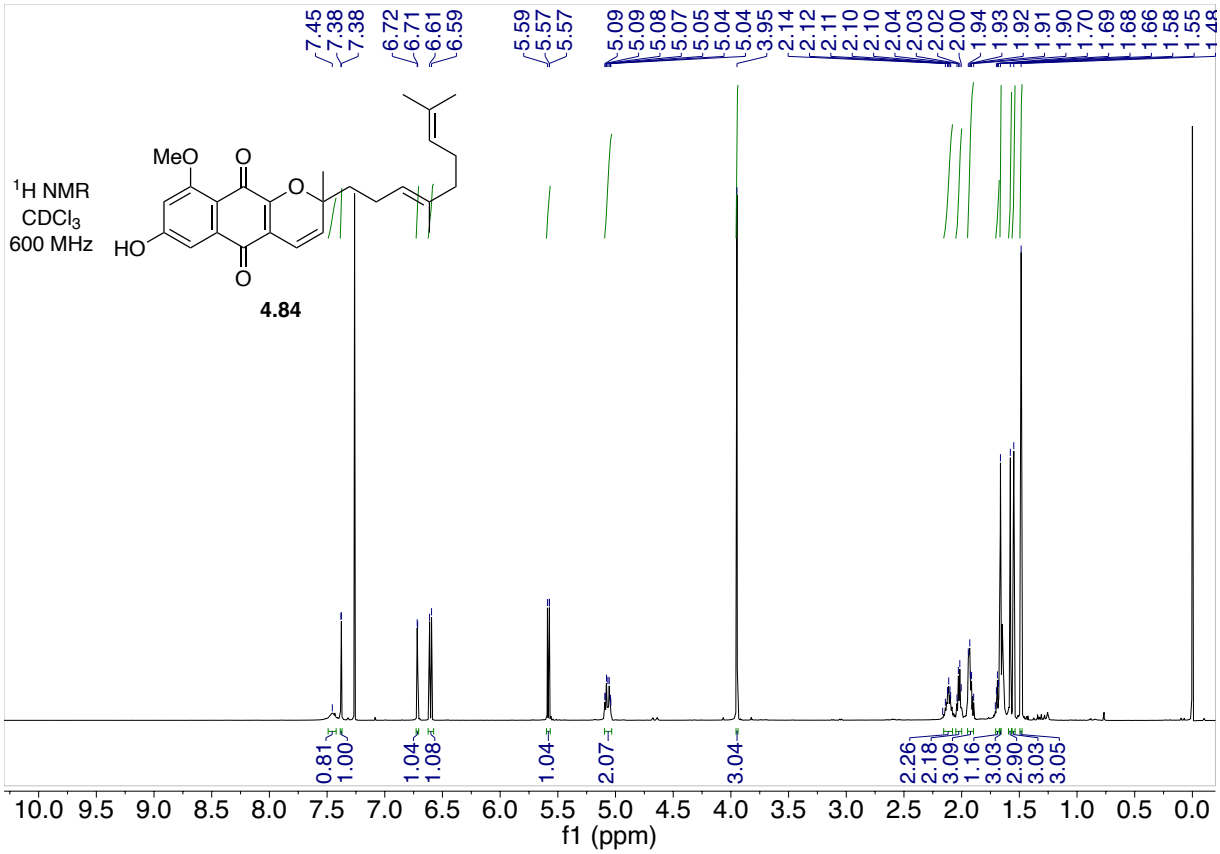
^{1}H NMR
$CDCl_3$
600 MHz
MeO
O
HO
O
O
4.84
7.45
7.38
7.38
6.72
6.71
6.61
6.59
5.59
5.57
5.57
5.09
5.09
5.08
5.07
5.05
5.04
5.04
3.95
2.14
2.12
2.11
2.10
2.10
2.04
2.03
2.02
2.00
1.94
1.93
1.92
1.91
1.90
1.70
1.69
1.68
1.66
1.58
1.55
0.81
1.00
1.04
1.08
1.04
2.07
3.04
2.26
2.18
3.09
1.16
3.03
2.90
3.03
3.05
10.0 9.5 9.0 8.5 8.0 7.5 7.0 6.5 6.0 5.5 5.0 4.5 4.0 3.5 3.0 2.5 2.0 1.5 1.0 0.5 0.0
f1 (ppm)

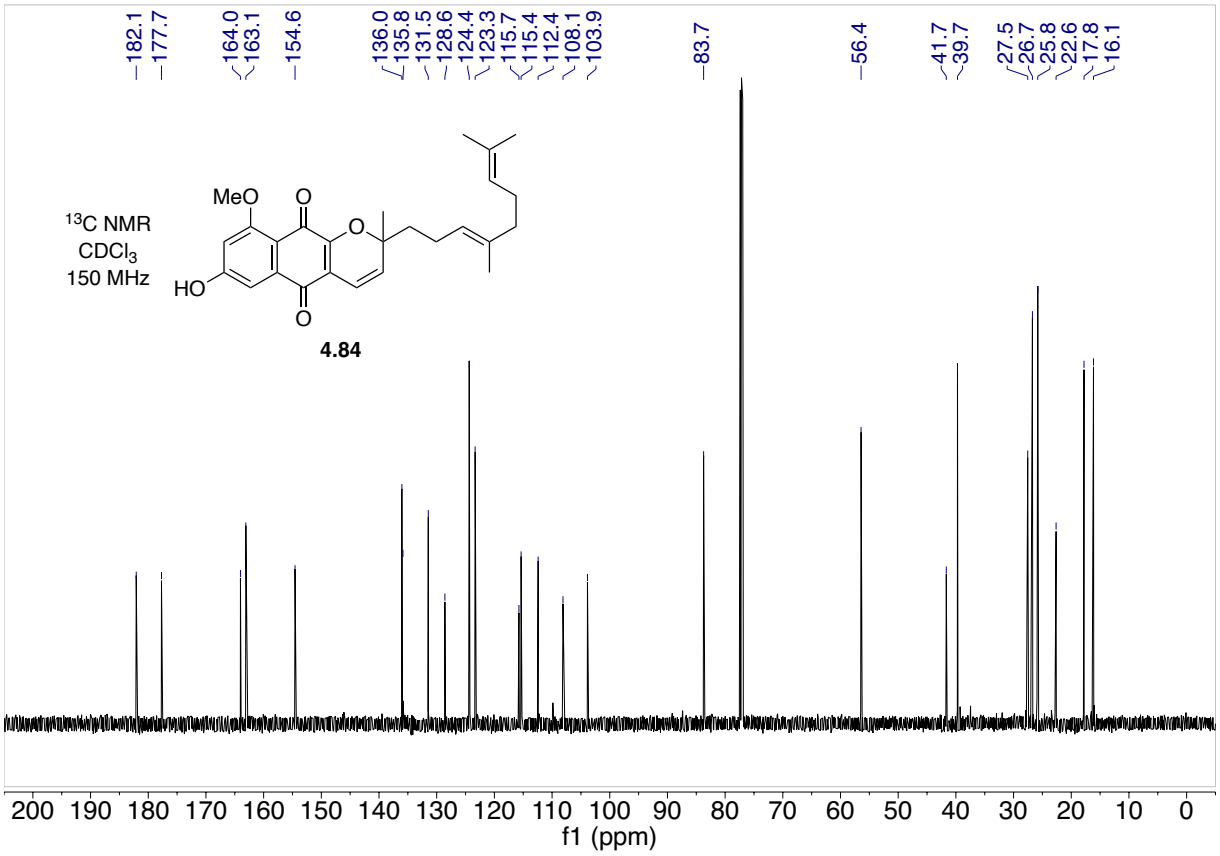
^{13}C NMR
$CDCl_3$
150 MHz
MeO
O
HO
O
O
4.84
182.1
177.7
164.0
163.1
154.6
136.0
135.8
131.5
128.6
124.4
123.3
115.7
115.4
112.4
108.1
103.9
83.7
56.4
41.7
39.7
27.5
26.7
25.8
22.6
17.8
16.1
200 190 180 170 160 150 140 130 120 110 100 90 80 70 60 50 40 30 20 10 0
f1 (ppm)

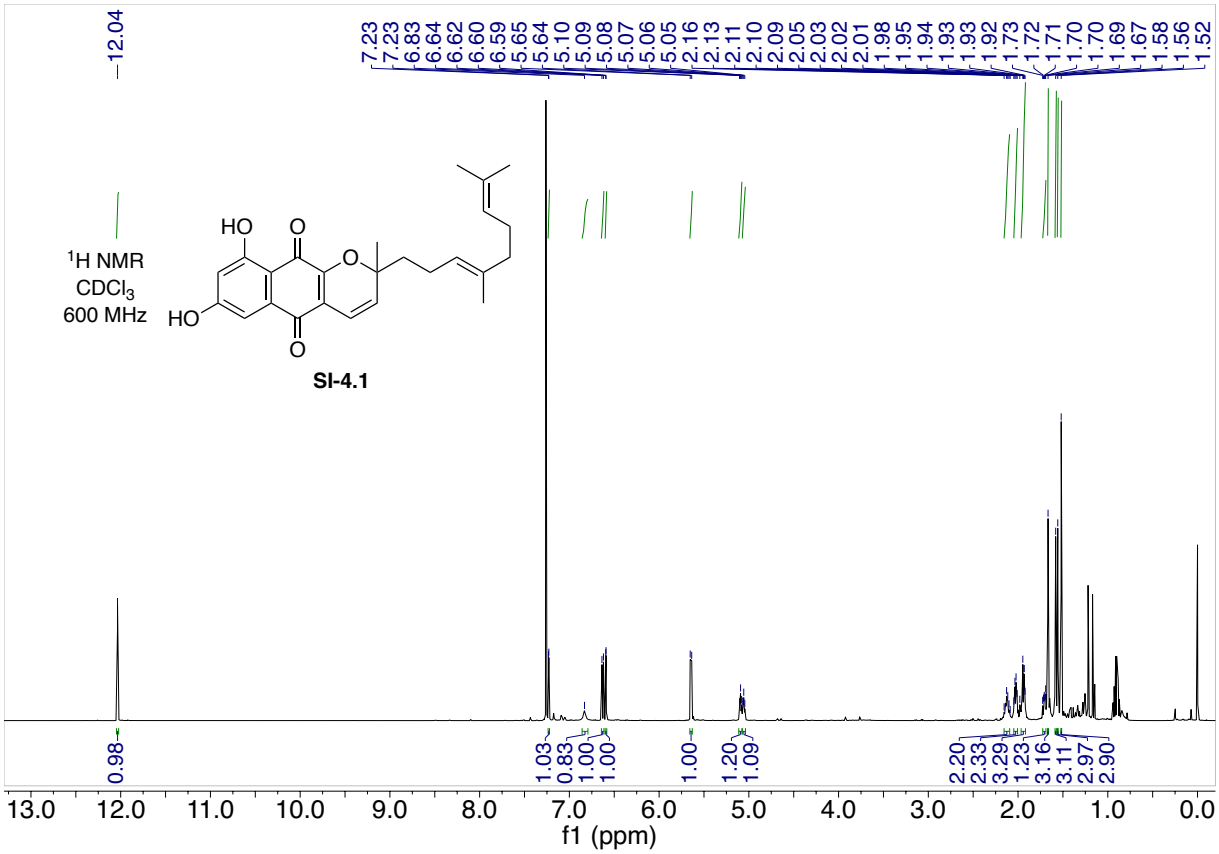
12.04
7.23
7.23
6.83
6.64
6.62
6.60
6.59
6.65
5.64
5.10
5.09
5.08
5.07
5.06
5.05
2.16
2.13
2.11
2.10
2.09
2.05
2.03
2.02
2.01
1.98
1.95
1.94
1.93
1.93
1.92
1.73
1.72
1.71
1.70
1.70
1.69
1.67
1.58
1.56
1.52
^{1}H NMR
$CDCl_3$
600 MHz
HO
O
O
HO
O
SI-4.1
0.98
1.03
0.83
1.00
1.00
1.00
1.20
1.09
2.20
2.33
3.29
1.23
3.16
3.11
2.97
2.90
13.0
12.0
11.0
10.0
9.0
8.0
7.0
6.0
5.0
4.0
3.0
2.0
1.0
0.0
f1 (ppm)

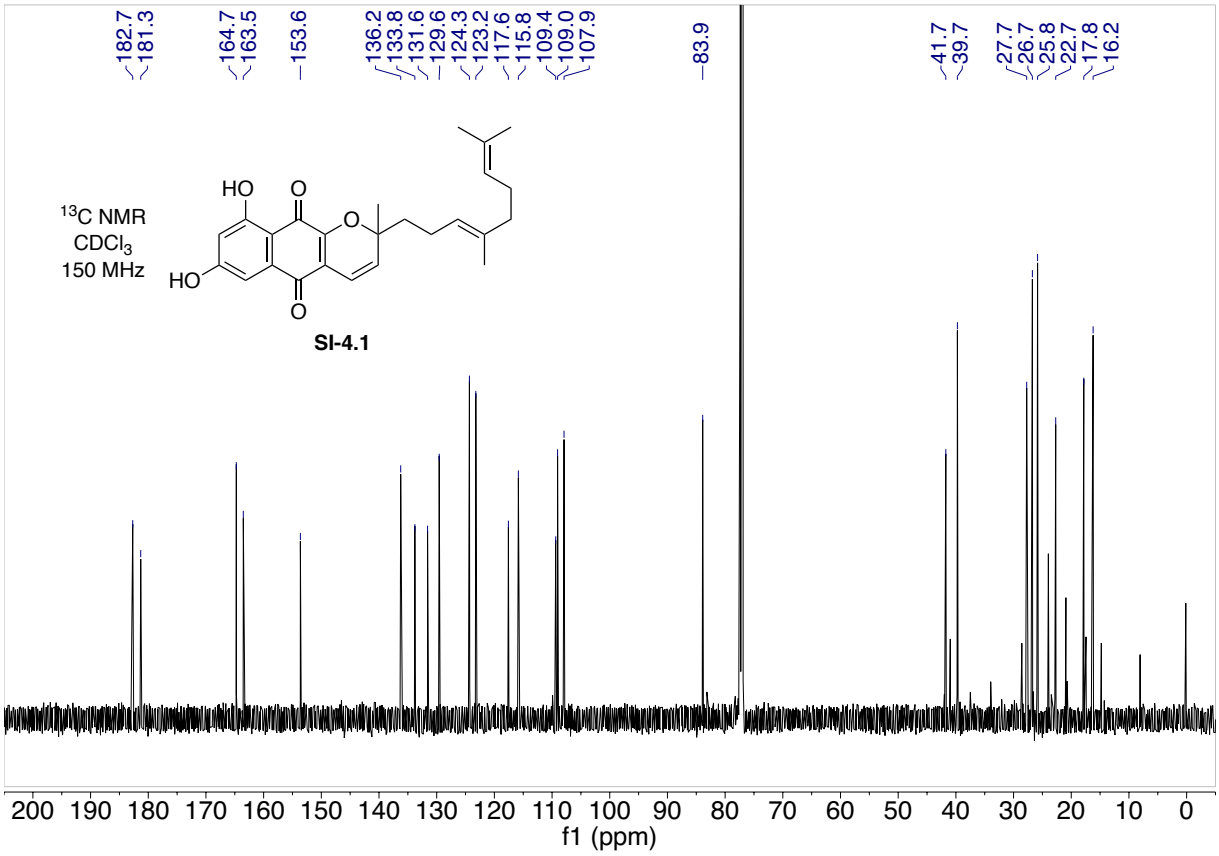
182.7
181.3
164.7
163.5
153.6
136.2
133.8
131.6
129.6
124.3
123.2
117.6
115.8
109.4
109.0
107.9
83.9
41.7
39.7
27.7
26.7
25.8
22.7
17.8
16.2
^{13}C NMR
$CDCl_3$
150 MHz
HO
O
O
HO
O
SI-4.1
200
190
180
170
160
150
140
130
120
110
100
90
80
70
60
50
40
30
20
10
0
f1 (ppm)

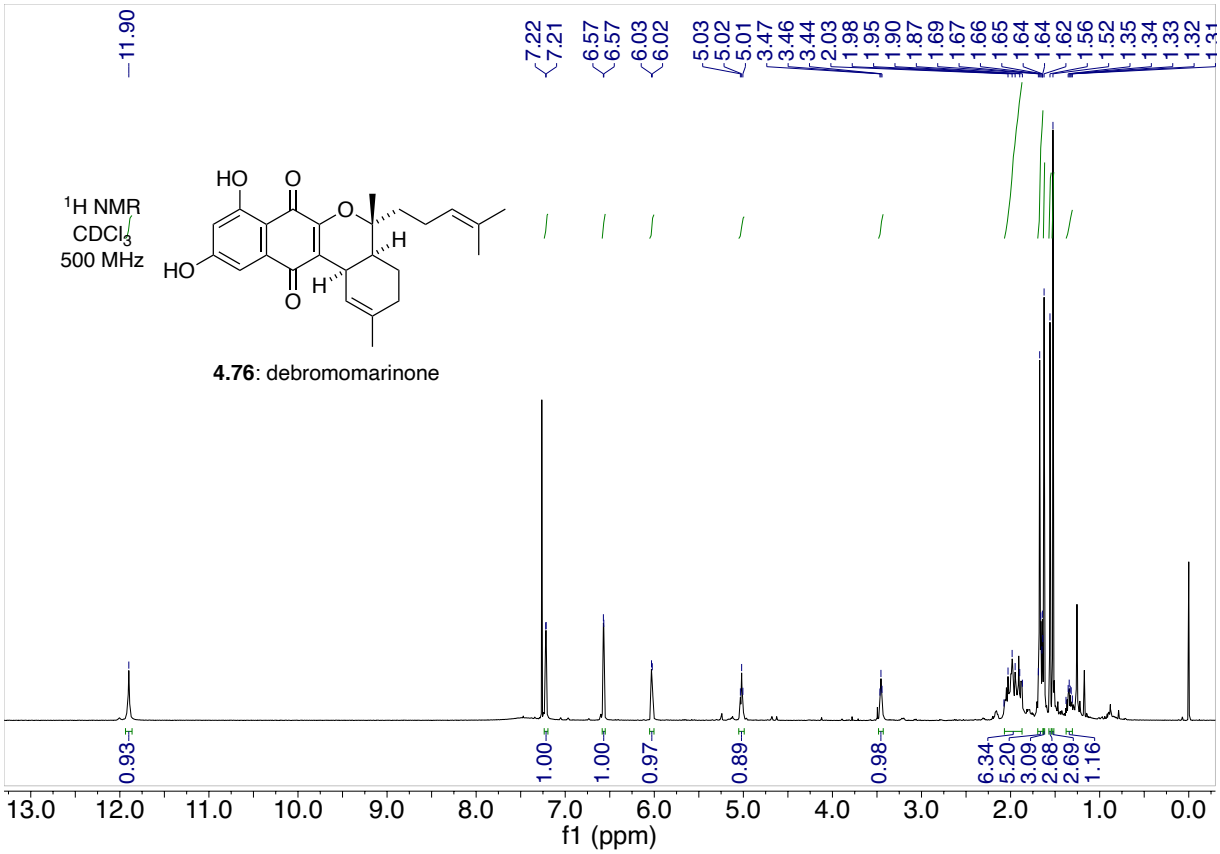

4.76: debromomarinone

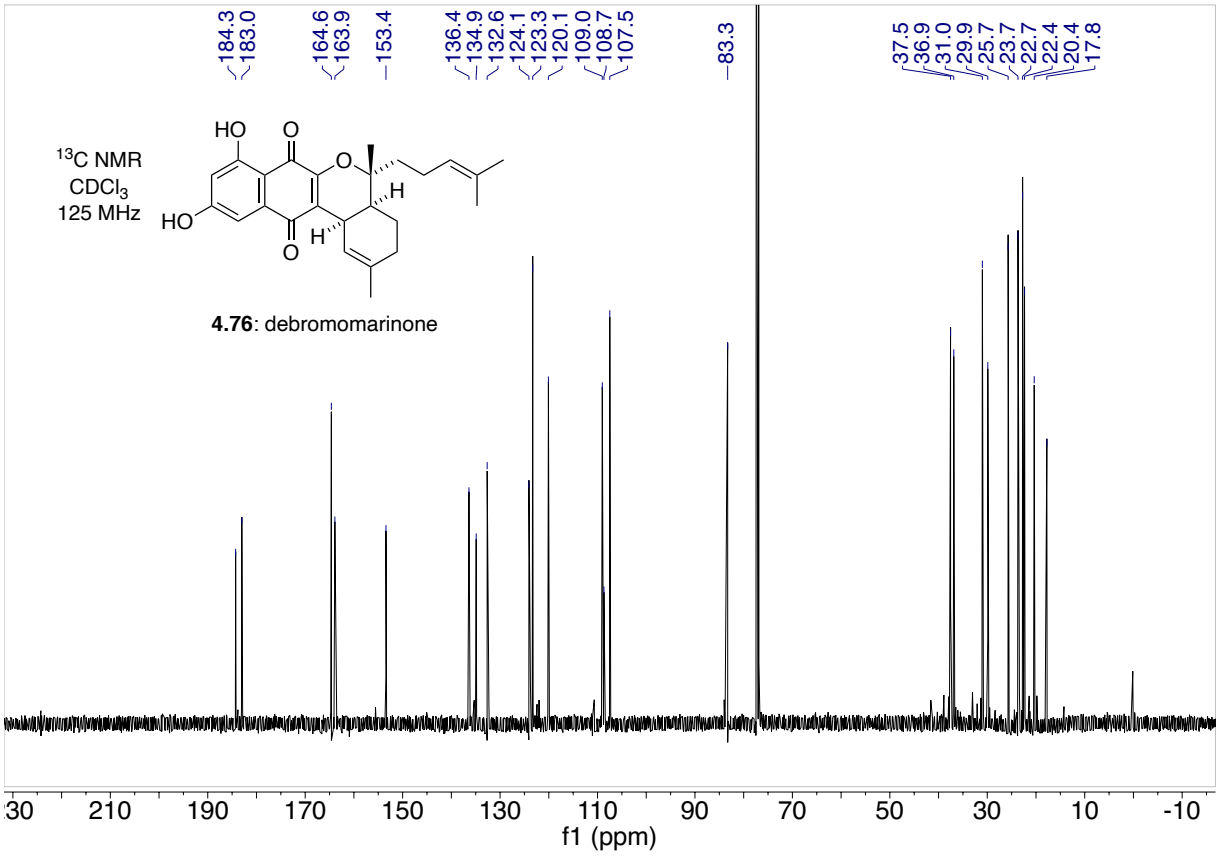

4.76: debromomarinone

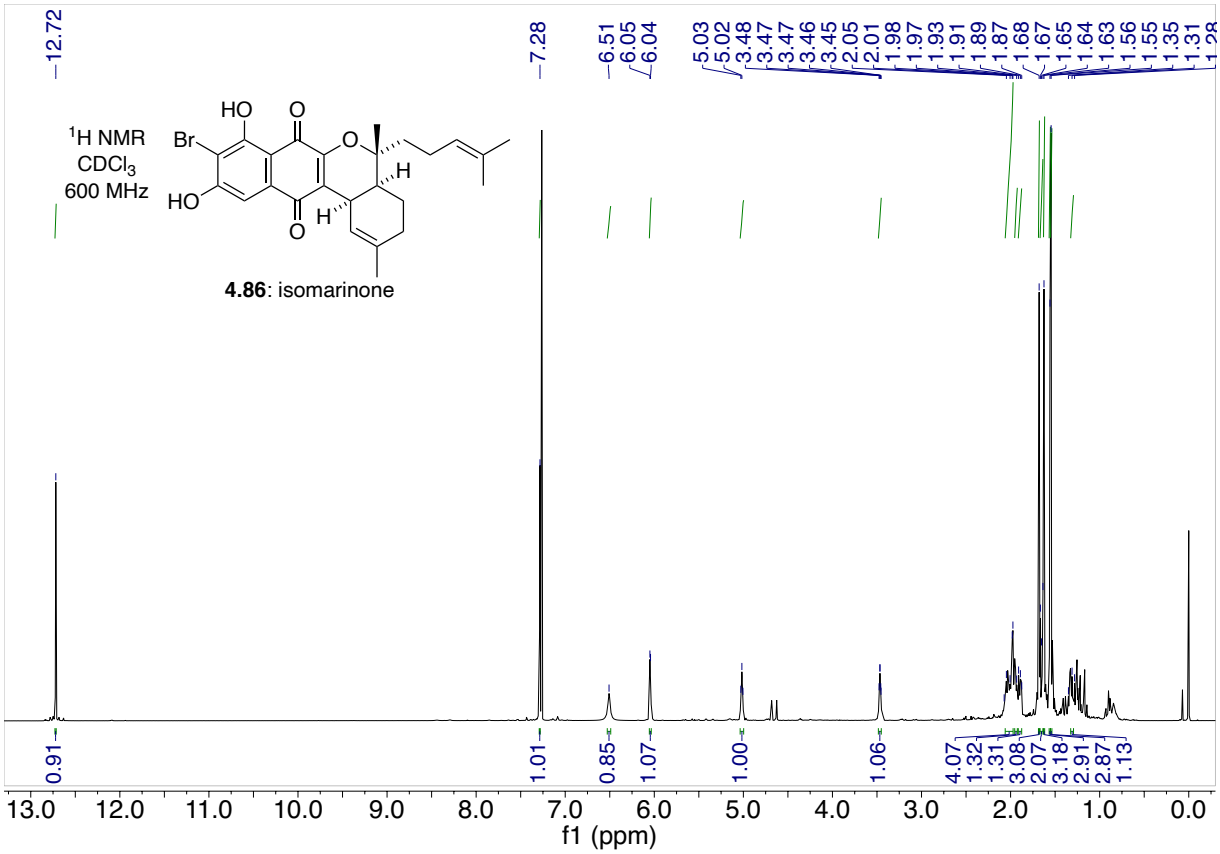
12.72
7.28
6.51
6.05
6.04
5.03
5.02
3.48
3.47
3.47
3.46
3.45
2.05
2.01
1.98
1.97
1.93
1.91
1.89
1.87
1.68
1.67
1.65
1.64
1.63
1.56
1.55
1.35
1.31
0.91
1.01
0.85
1.07
1.00
1.06
4.07
1.32
1.31
3.08
2.07
3.18
2.91
2.87
1.13
13.0
12.0
11.0
10.0
9.0
8.0
7.0
6.0
5.0
4.0
3.0
2.0
1.0
0.0
f1 (ppm)
1H NMR
CDCl3
600 MHz
HO
O
Br
O
H
HO
H
O
4.86: isomarinone

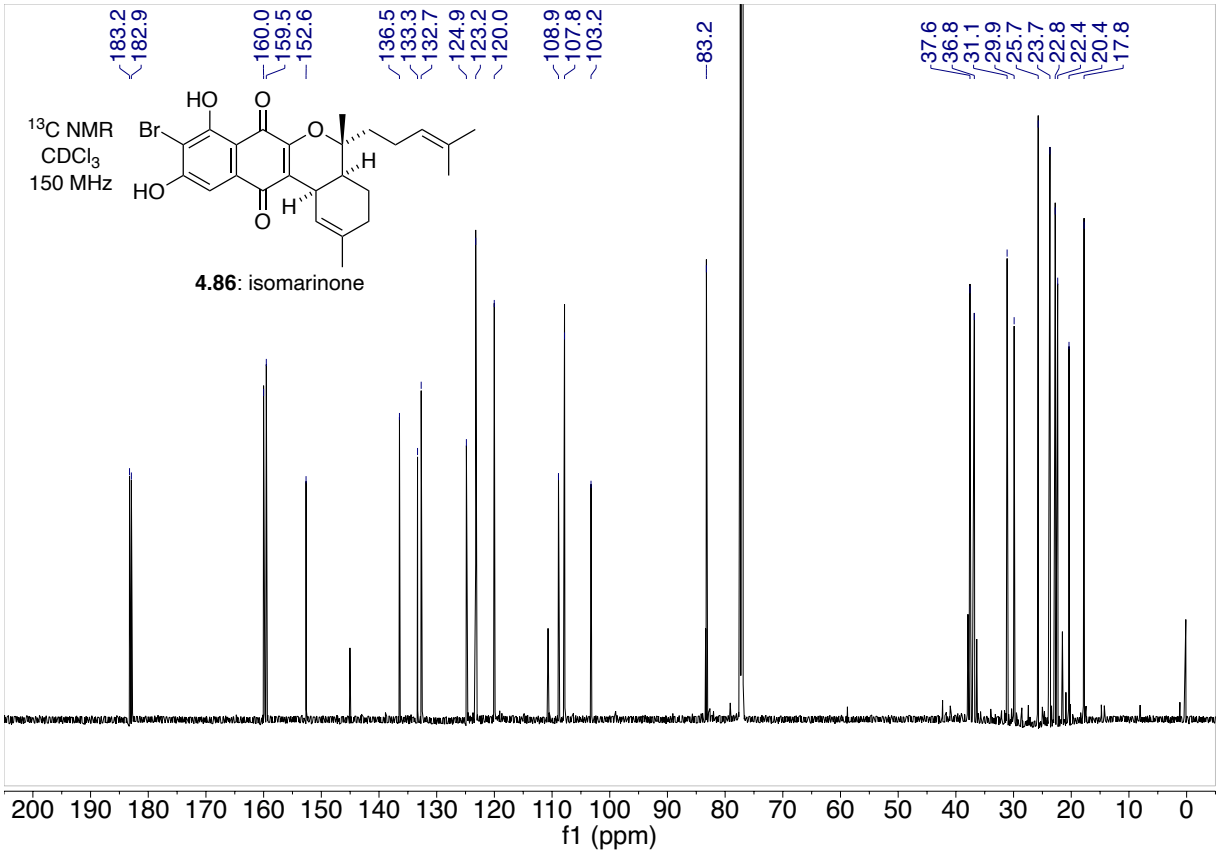
183.2
182.9
160.0
159.5
152.6
136.5
133.3
132.7
124.9
123.2
120.0
108.9
107.8
103.2
83.2
37.6
36.8
31.1
29.9
25.7
23.7
22.8
22.4
20.4
17.8
200
190
180
170
160
150
140
130
120
110
100
90
80
70
60
50
40
30
20
10
0
f1 (ppm)
13C NMR
CDCl3
150 MHz
HO
O
Br
O
H
HO
H
O
4.86: isomarinone

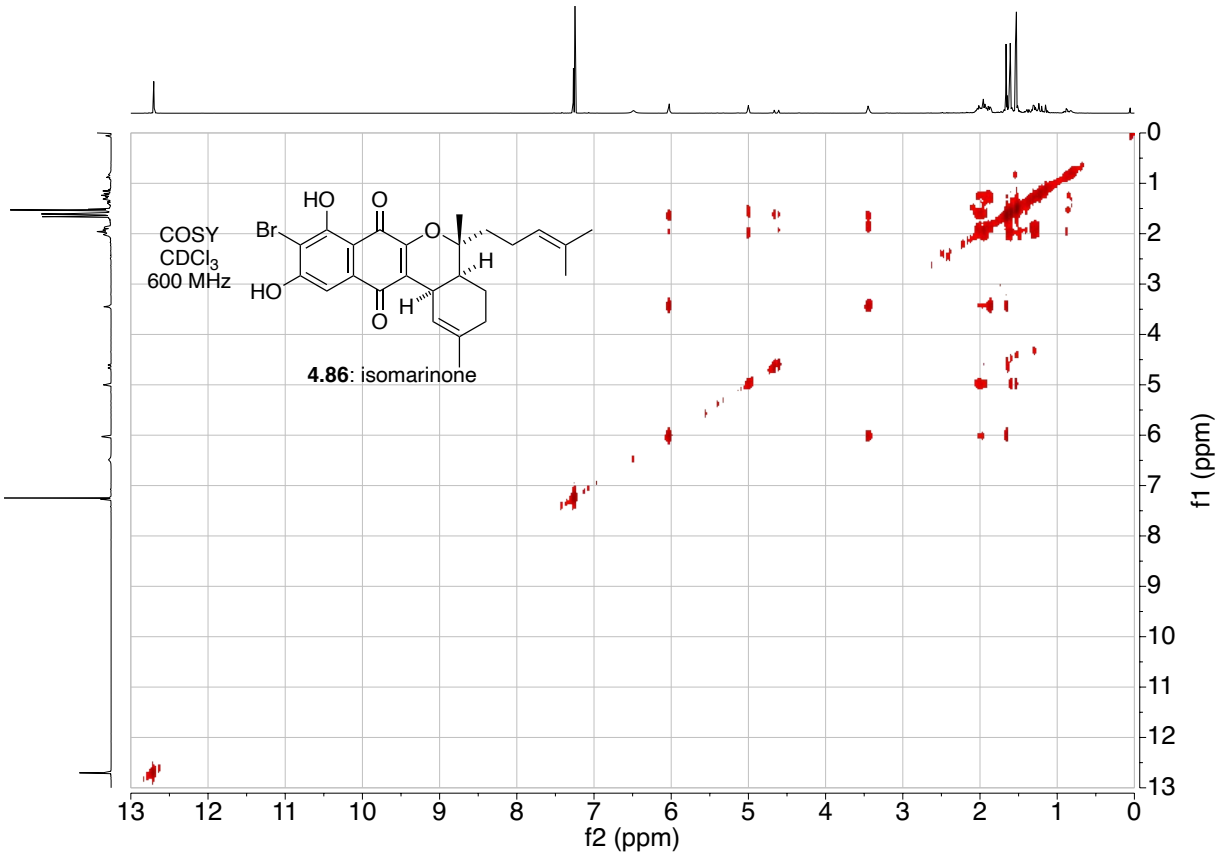
COSY
CDCl3
600 MHz
HO
O
Br
O
H
HO
H
O
4.86: isomarinone
f2 (ppm)
f1 (ppm)

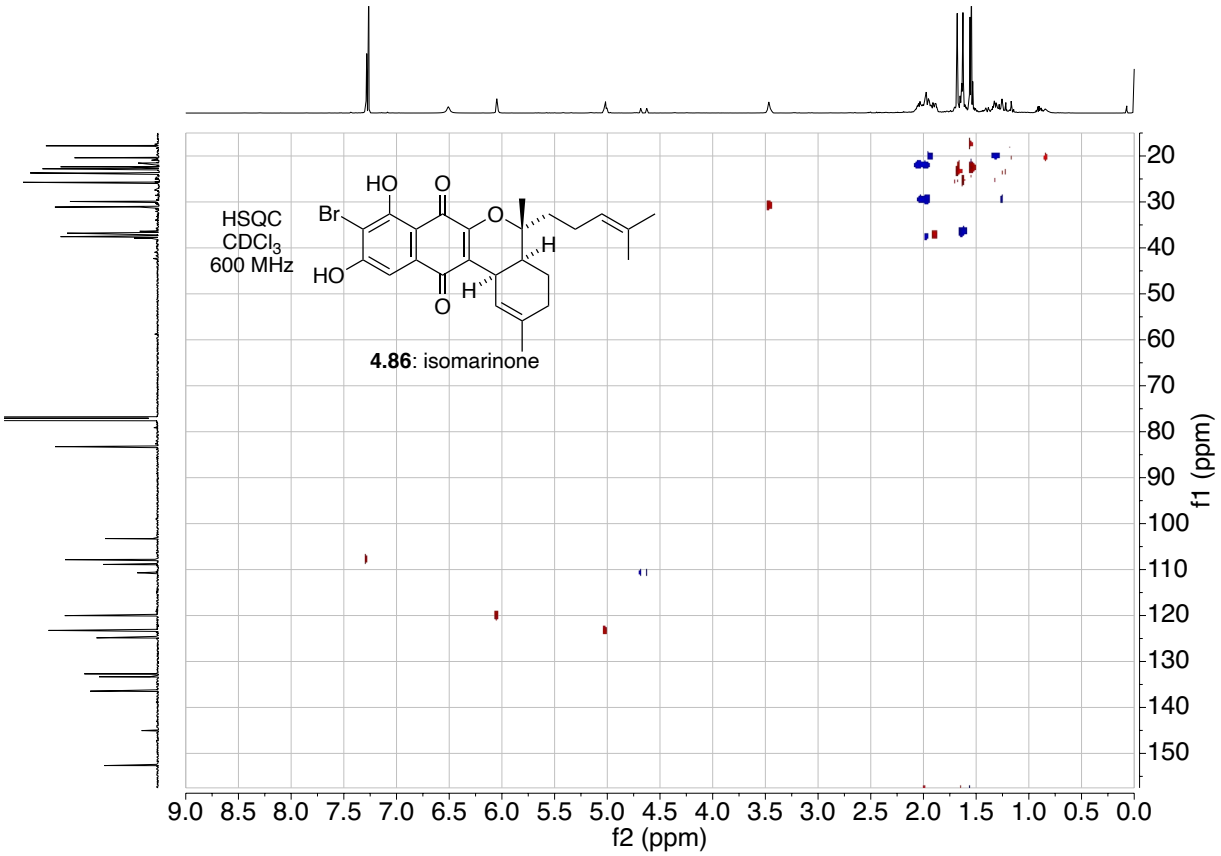
HSQC
CDCl3
600 MHz
HO
O
Br
O
H
HO
H
O
4.86: isomarinone
f2 (ppm)
f1 (ppm)

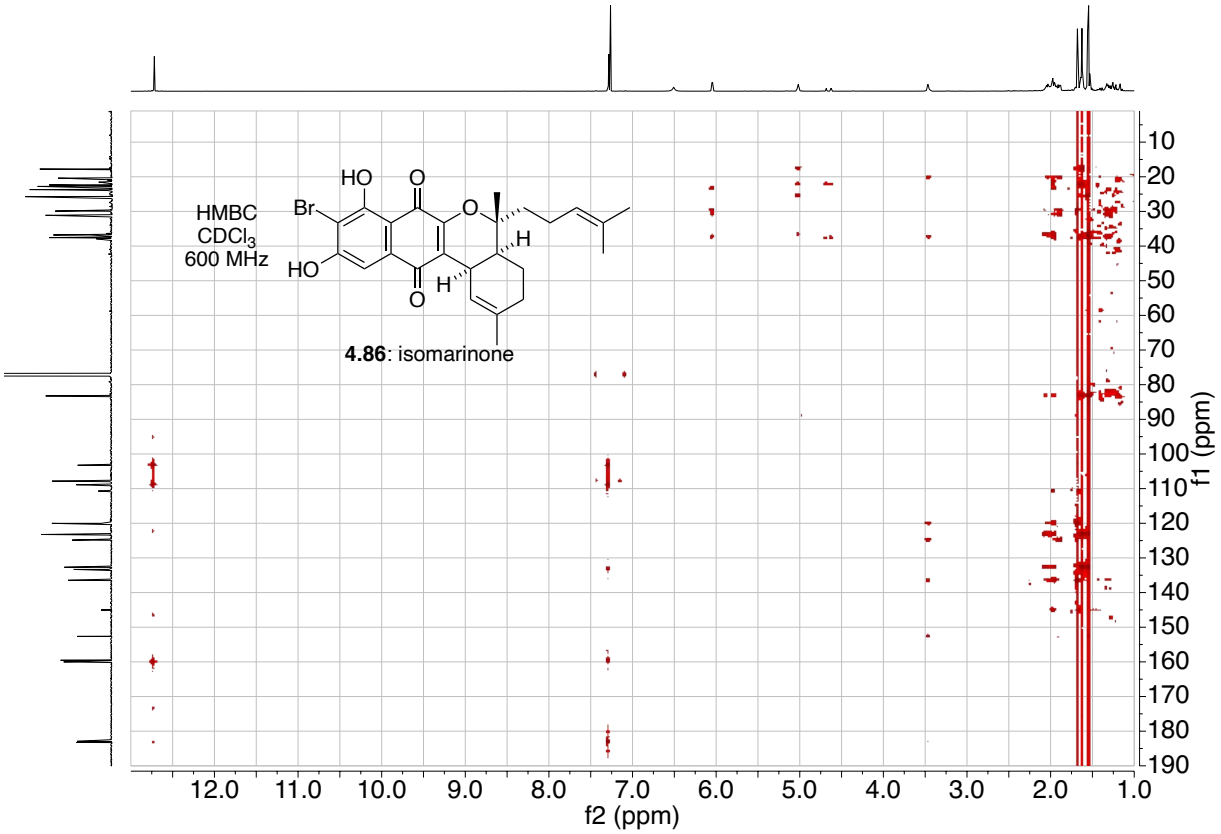
HMBC
CDCl3
600 MHz
HO
O
Br
O
H
HO
H
O
4.86: isomarinone
f2 (ppm)
f1 (ppm)

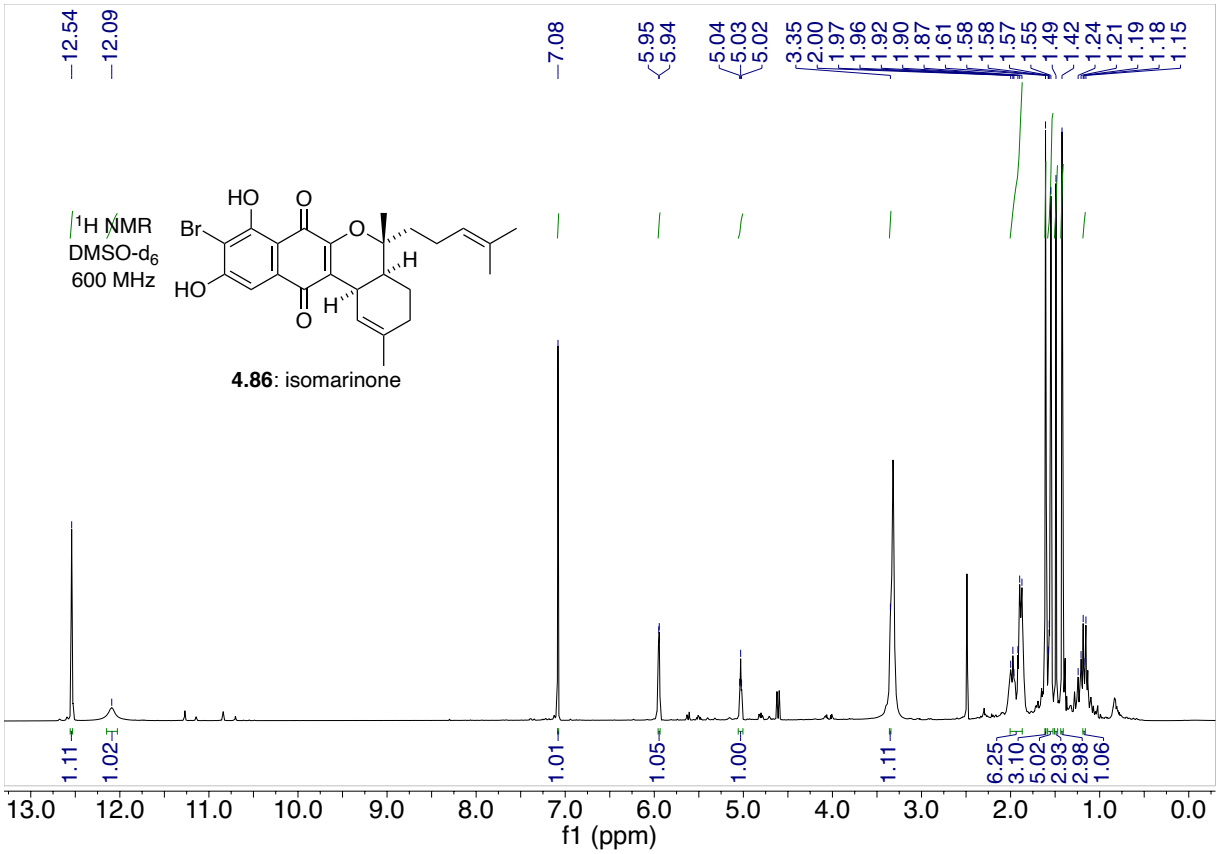
12.54
12.09
7.08
5.95
5.94
5.04
5.03
5.02
3.35
2.00
1.97
1.96
1.92
1.90
1.87
1.61
1.58
1.57
1.55
1.49
1.42
1.24
1.21
1.19
1.18
1.15
1H NMR
DMSO-d6
600 MHz
HO
O
Br
O
H
HO
H
O
4.86: isomarinone
1.11
1.02
1.01
1.05
1.00
1.11
6.25
3.10
5.02
2.93
2.98
1.06
13.0
12.0
11.0
10.0
9.0
8.0
7.0
6.0
5.0
4.0
3.0
2.0
1.0
0.0
f1 (ppm)

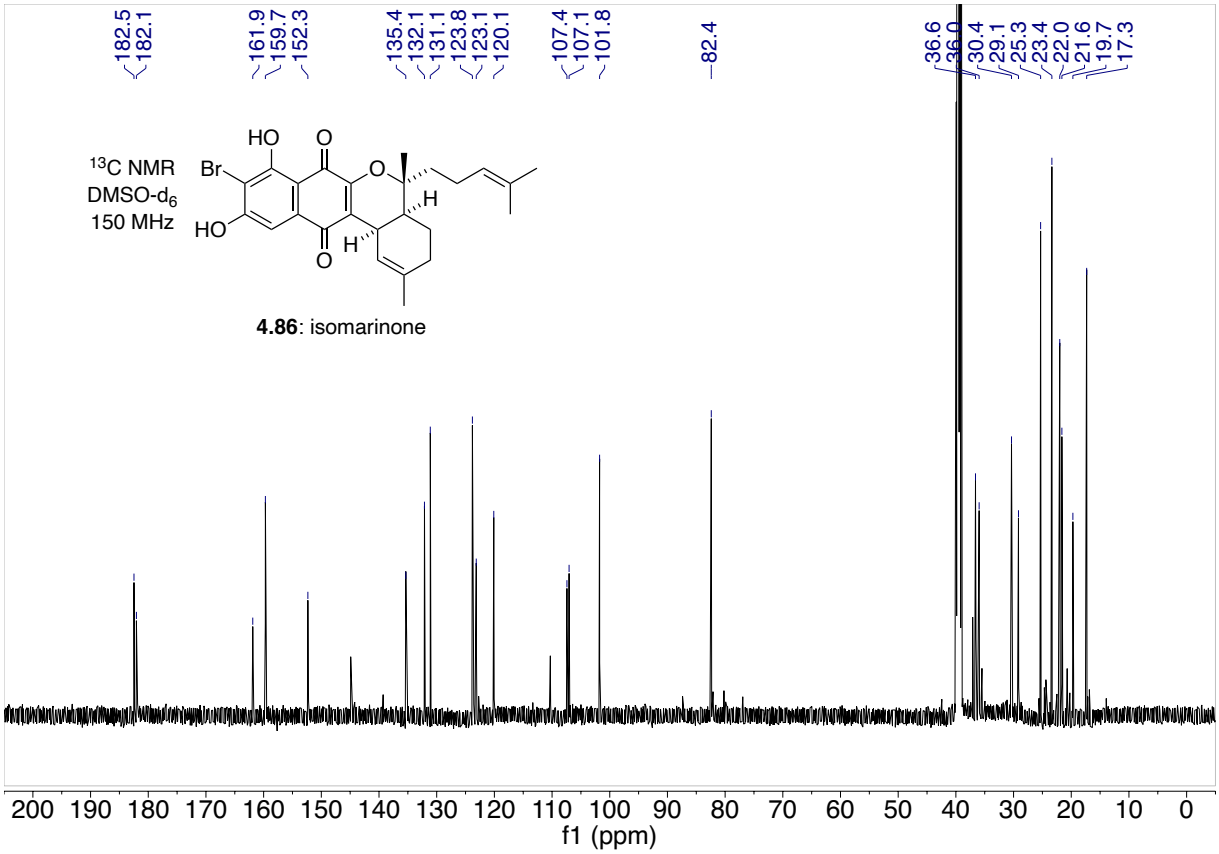
182.5
182.1
161.9
159.7
152.3
135.4
132.1
131.1
123.8
123.1
120.1
107.4
107.1
101.8
82.4
36.6
36.0
30.4
29.1
25.3
23.4
22.0
21.6
19.7
17.3
13C NMR
DMSO-d6
150 MHz
HO
O
Br
O
H
HO
H
O
4.86: isomarinone
200
190
180
170
160
150
140
130
120
110
100
90
80
70
60
50
40
30
20
10
0
f1 (ppm)

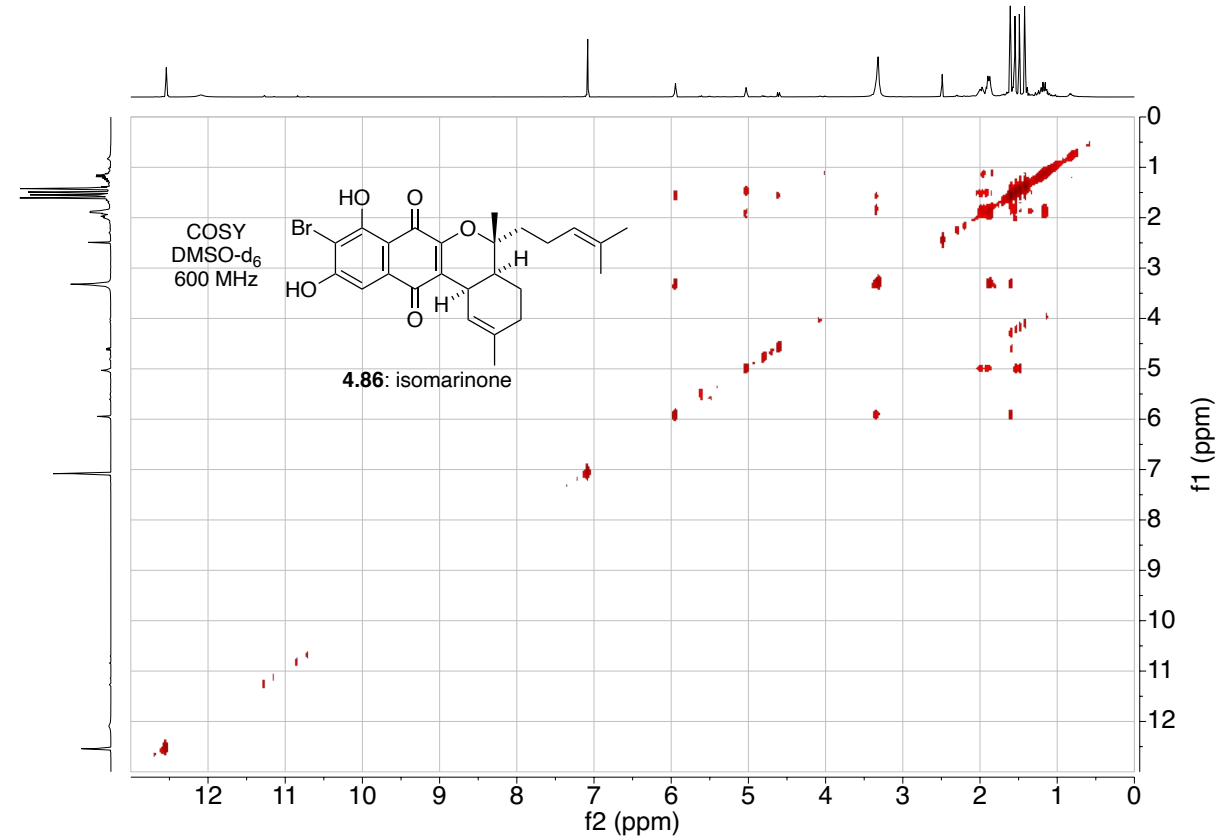
COSY
DMSO-d6
600 MHz
HO
O
Br
O
H
HO
H
O
4.86: isomarinone
f2 (ppm)
f1 (ppm)

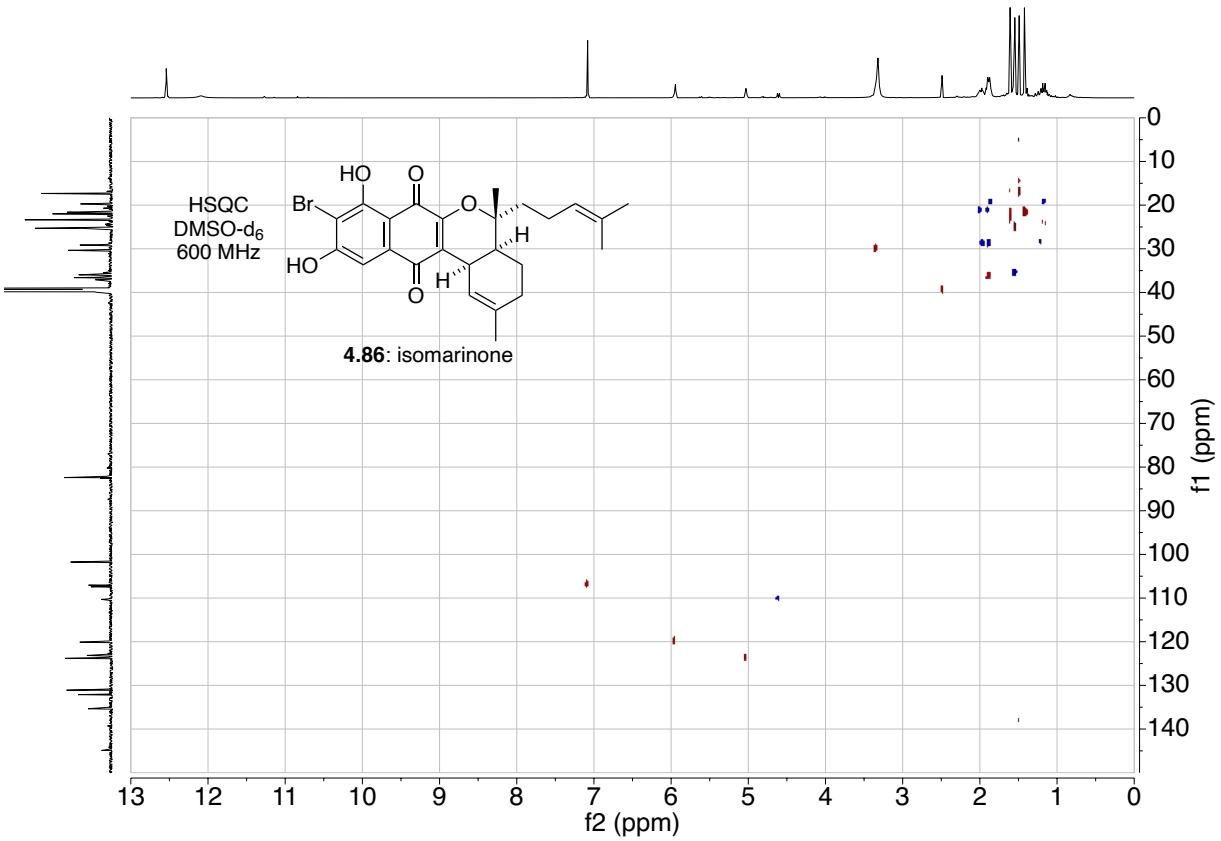
HSQC
DMSO-d6
600 MHz
HO
O
Br
O
H
HO
H
O
4.86: isomarinone
f2 (ppm)
f1 (ppm)

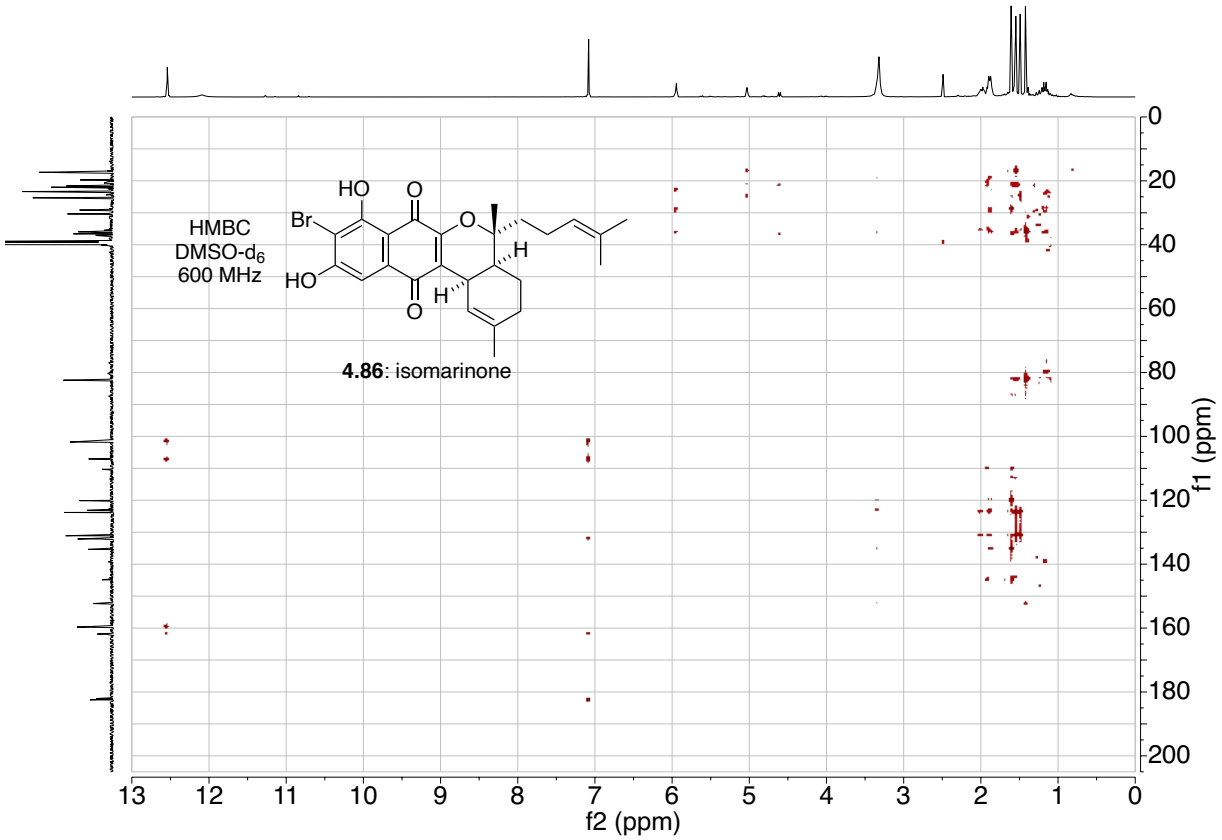
HMBC
DMSO-d6
600 MHz
HO
Br
HO
O
O
O
H
H
4.86: isomarinone
f2 (ppm)
f1 (ppm)

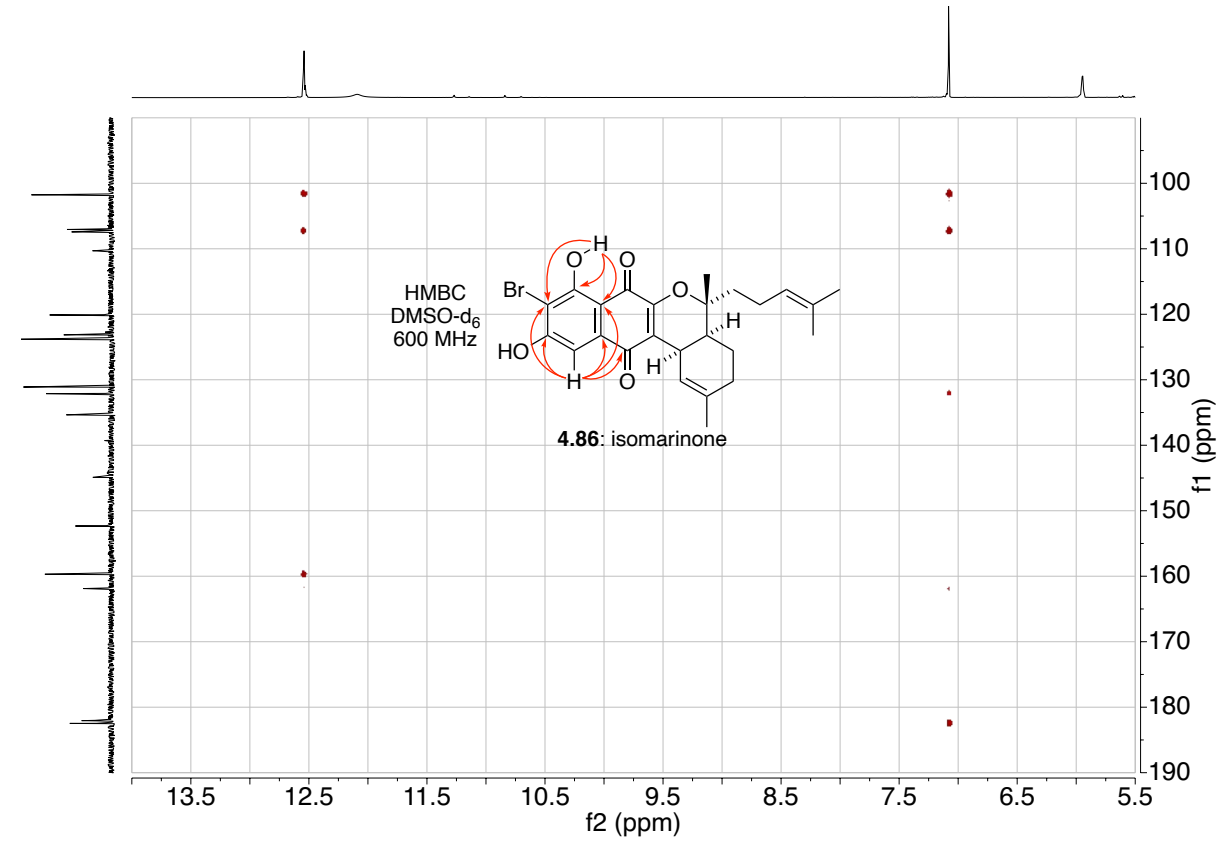
HMBC
DMSO-d6
600 MHz
H
O
O
Br
O
H
HO
H
H
O
4.86: isomarinone
f2 (ppm)
f1 (ppm)

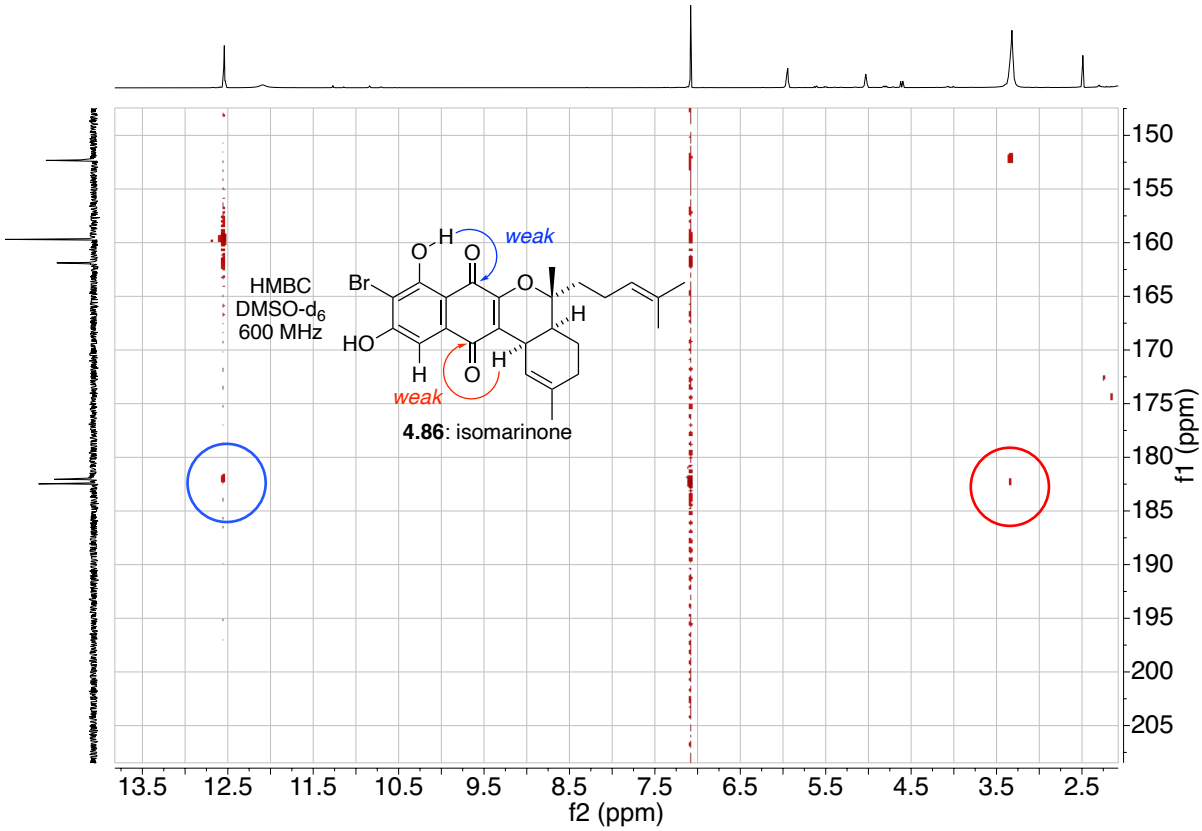
HMBC
DMSO-d6
600 MHz
Br
HO
O
H
O
O
O
H
H
O
H
weak
weak
4.86: isomarinone
13.5
12.5
11.5
10.5
9.5
8.5
7.5
6.5
5.5
4.5
3.5
2.5
f2 (ppm)
150
155
160
165
170
175
180
185
190
195
200
205
f1 (ppm)

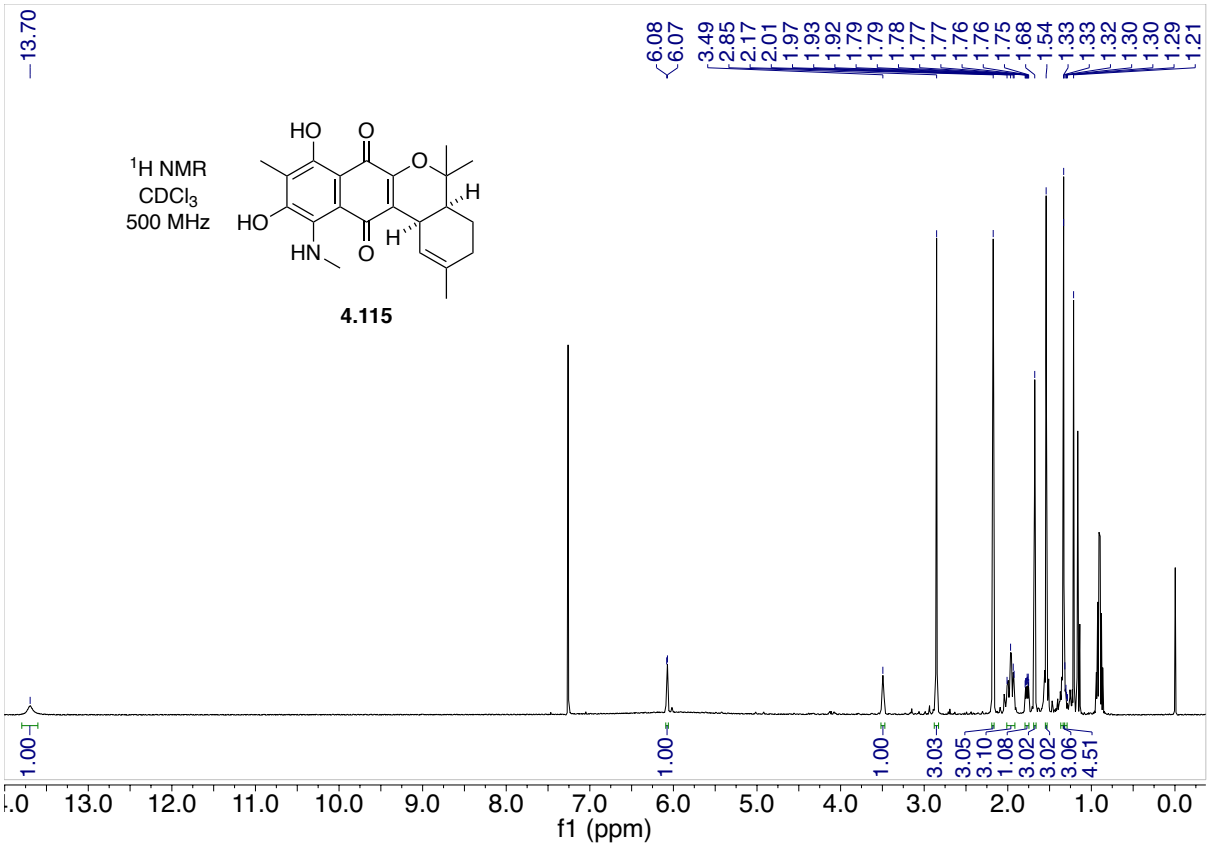
13.70
6.08
6.07
3.49
2.85
2.17
2.01
1.97
1.93
1.92
1.79
1.79
1.78
1.77
1.77
1.76
1.76
1.75
1.68
1.54
1.33
1.33
1.32
1.30
1.30
1.29
1.21
1H NMR
CDCl3
500 MHz
HO
O
O
H
HO
H
HN
O
4.115
1.00
1.00
1.00
3.03
3.05
3.10
1.08
3.02
3.02
3.06
4.51
13.0
12.0
11.0
10.0
9.0
8.0
7.0
6.0
5.0
4.0
3.0
2.0
1.0
0.0
f1 (ppm)

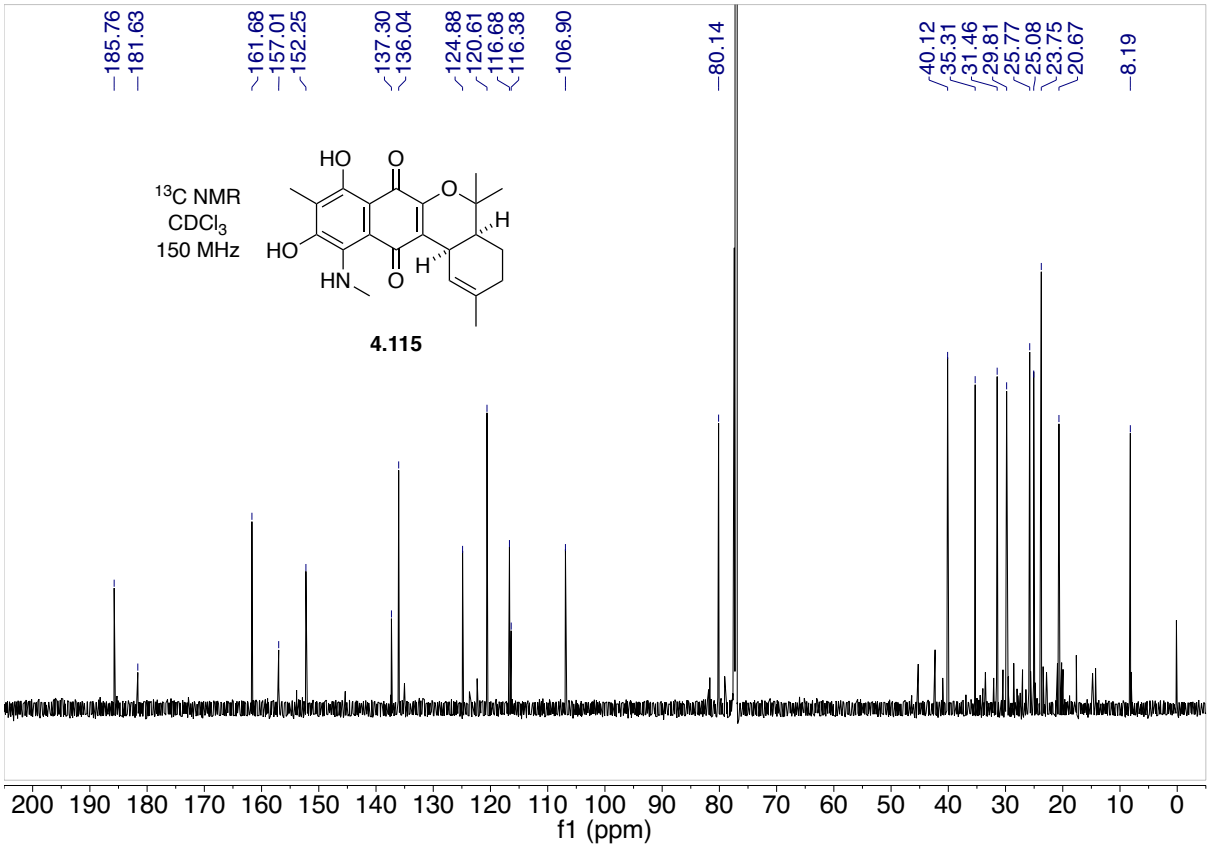
185.76
181.63
161.68
157.01
152.25
137.30
136.04
124.88
120.61
116.68
116.38
106.90
80.14
40.12
35.31
31.46
29.81
25.77
25.08
23.75
20.67
8.19
13C NMR
CDCl3
150 MHz
HO
O
O
H
HO
H
HN
O
4.115
200
190
180
170
160
150
140
130
120
110
100
90
80
70
60
50
40
30
20
10
0
f1 (ppm)

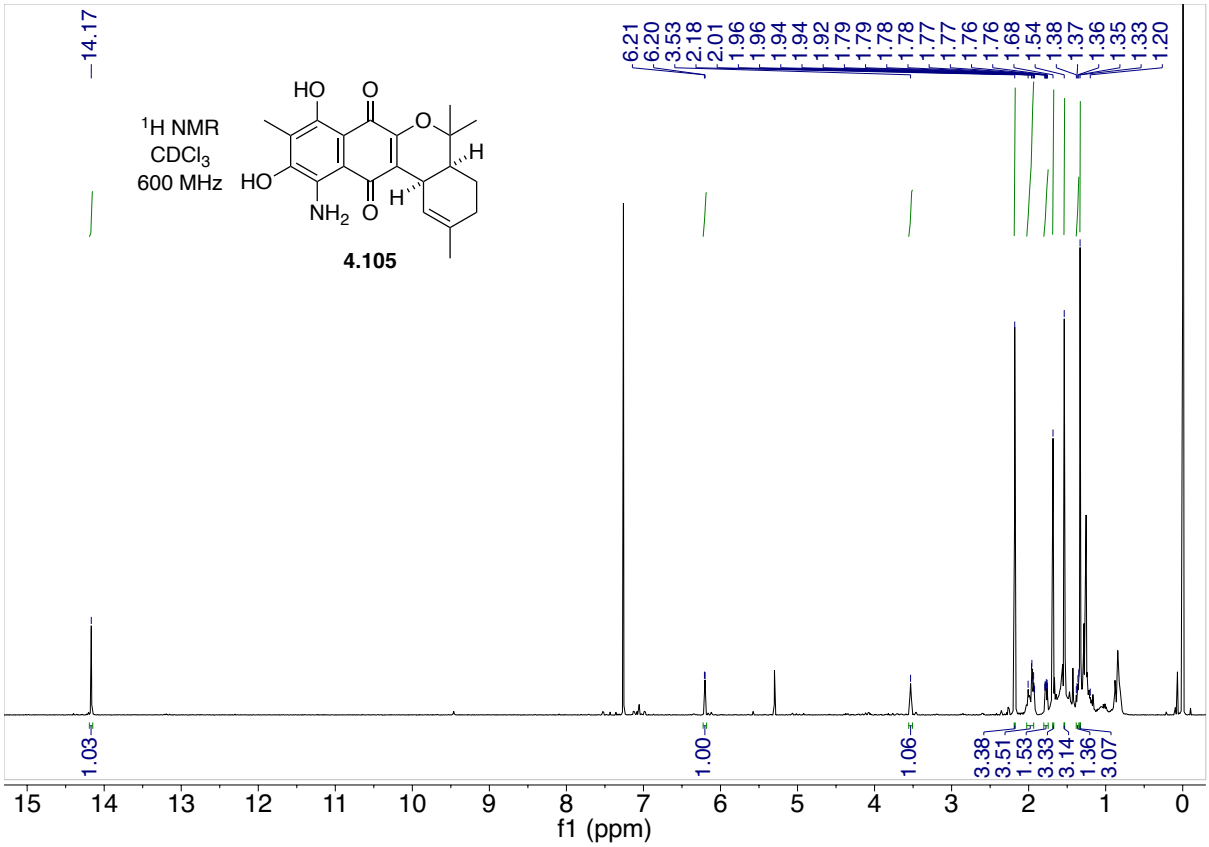
14.17
6.21
6.20
3.53
2.18
2.01
1.96
1.96
1.94
1.94
1.92
1.79
1.79
1.78
1.78
1.77
1.77
1.76
1.76
1.68
1.54
1.38
1.37
1.36
1.35
1.33
1.20
1H NMR
CDCl3
600 MHz
HO
O
O
H
HO
H
NH2
O
4.105
1.03
1.00
1.06
3.38
3.51
1.53
3.33
3.14
1.36
3.07
15 14 13 12 11 10 9 8 7 6 5 4 3 2 1 0
f1 (ppm)

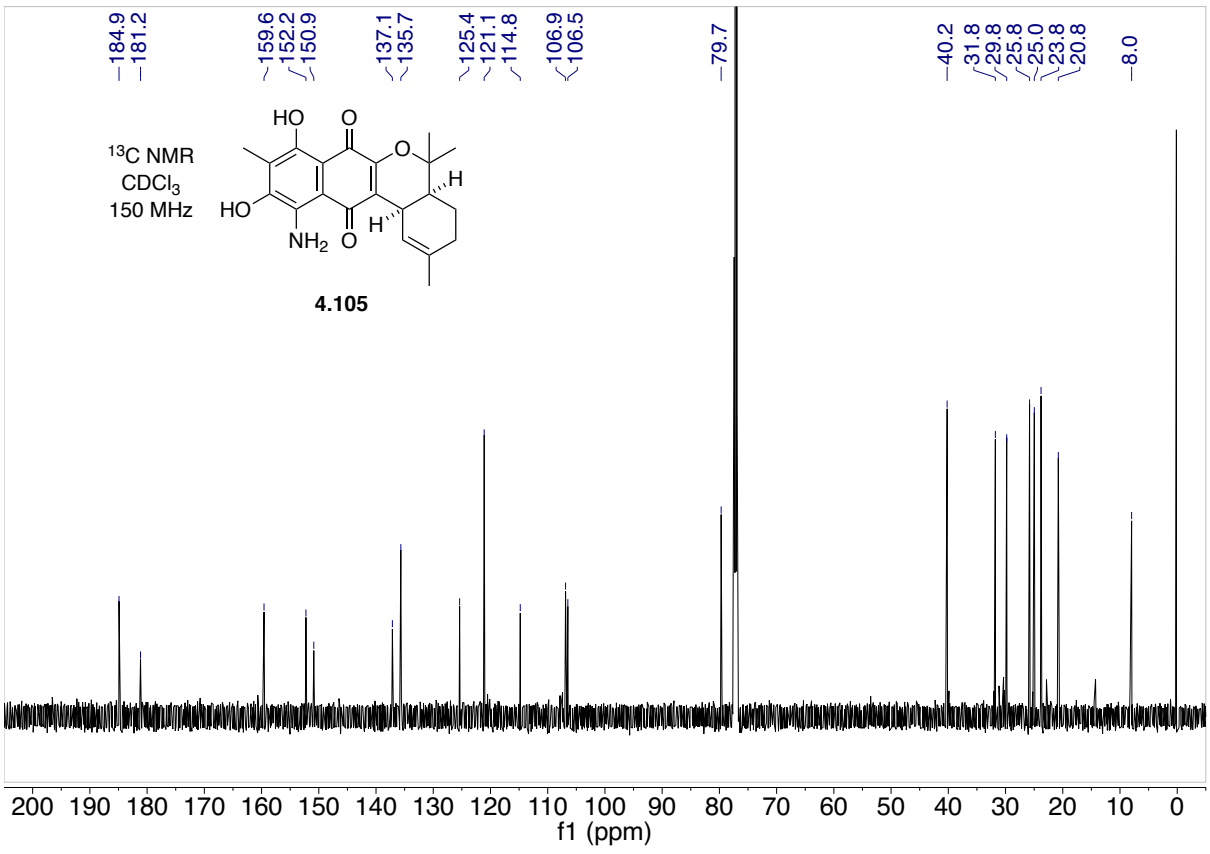
184.9
181.2
159.6
152.2
150.9
137.1
135.7
125.4
121.1
114.8
106.9
106.5
79.7
40.2
31.8
29.8
25.8
25.0
23.8
20.8
8.0
13C NMR
CDCl3
150 MHz
HO
O
O
H
HO
H
NH2
O
4.105
200 190 180 170 160 150 140 130 120 110 100 90 80 70 60 50 40 30 20 10 0
f1 (ppm)

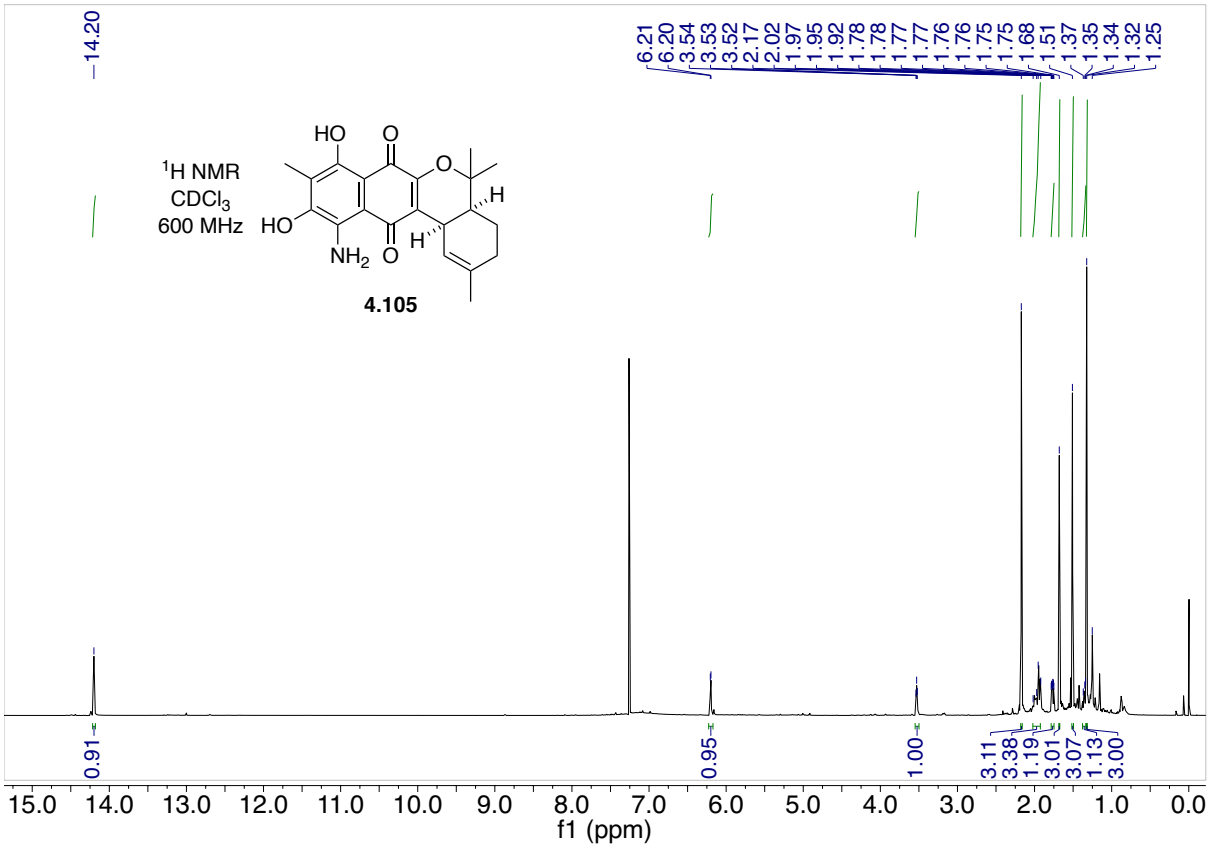
14.20
6.21
6.20
3.54
3.53
3.52
2.17
2.02
1.97
1.95
1.92
1.78
1.78
1.77
1.77
1.76
1.76
1.75
1.75
1.68
1.51
1.37
1.35
1.34
1.32
1.25
^{1}H NMR
$CDCl_3$
600 MHz
HO
O
O
H
HO
H
NH_2
O
4.105
0.91
0.95
1.00
3.11
3.38
1.19
3.01
3.07
1.13
3.00
15.0 14.0 13.0 12.0 11.0 10.0 9.0 8.0 7.0 6.0 5.0 4.0 3.0 2.0 1.0 0.0
f1 (ppm)

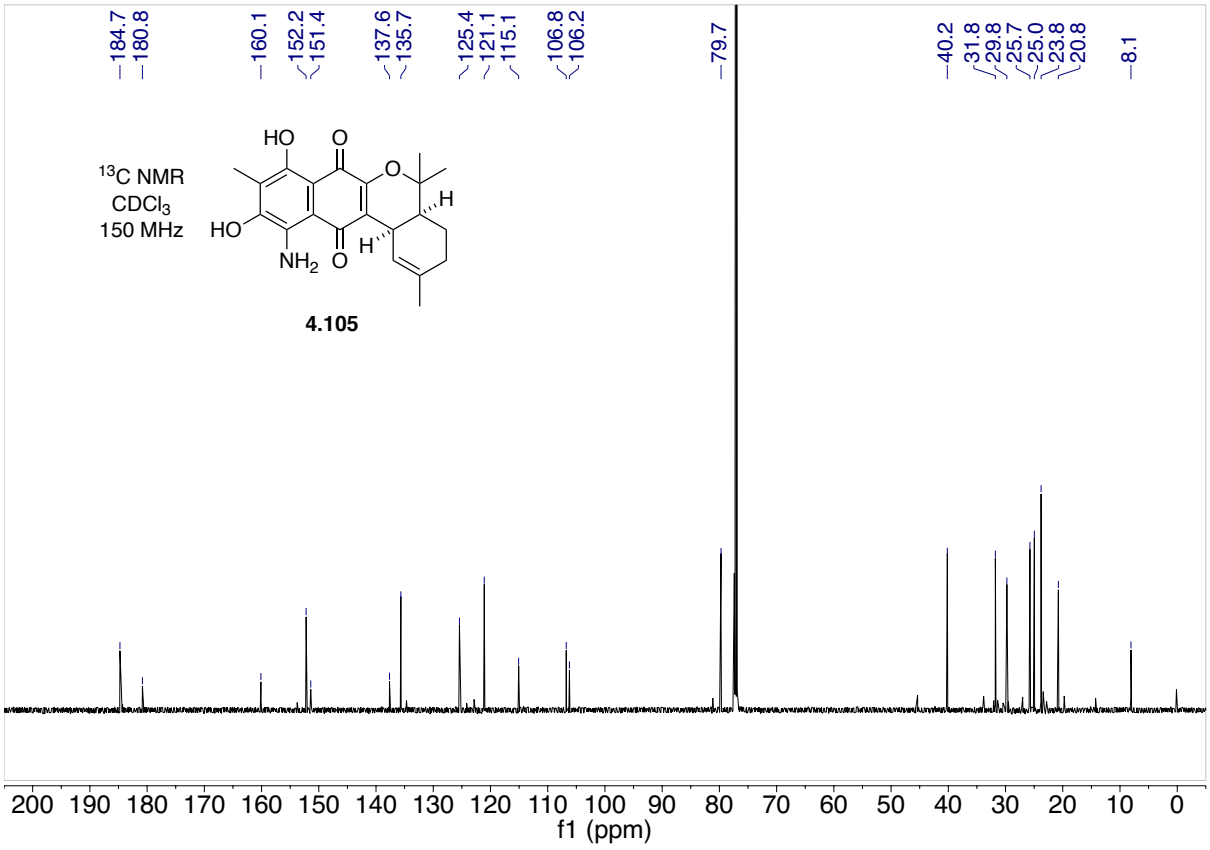
184.7
180.8
160.1
152.2
151.4
137.6
135.7
125.4
121.1
115.1
106.8
106.2
79.7
40.2
31.8
29.8
25.7
25.0
23.8
20.8
8.1
^{13}C NMR
$CDCl_3$
150 MHz
HO
O
O
H
HO
H
NH_2
O
4.105
200 190 180 170 160 150 140 130 120 110 100 90 80 70 60 50 40 30 20 10 0
f1 (ppm)

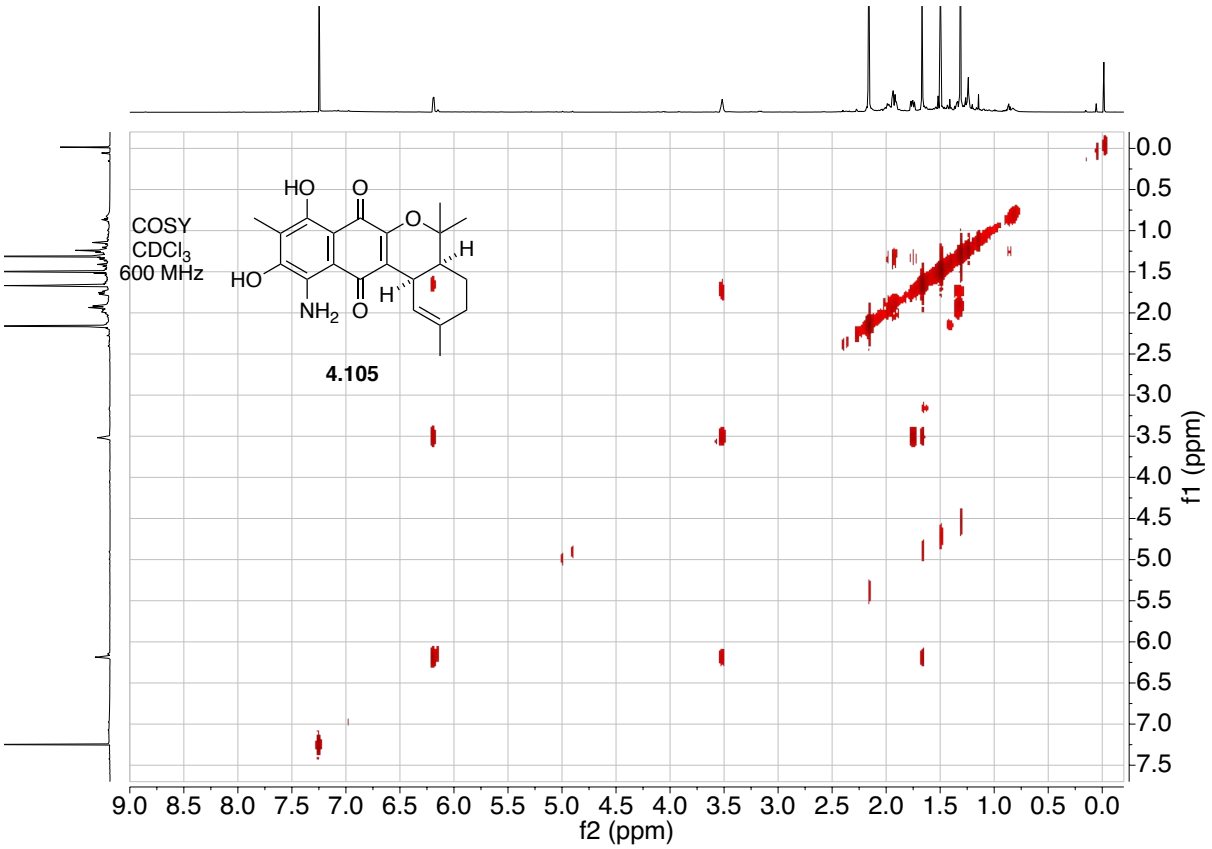
COSY
CDCl3
600 MHz
HO
O
O
H
HO
NH2
O
H
4.105
f2 (ppm)
f1 (ppm)

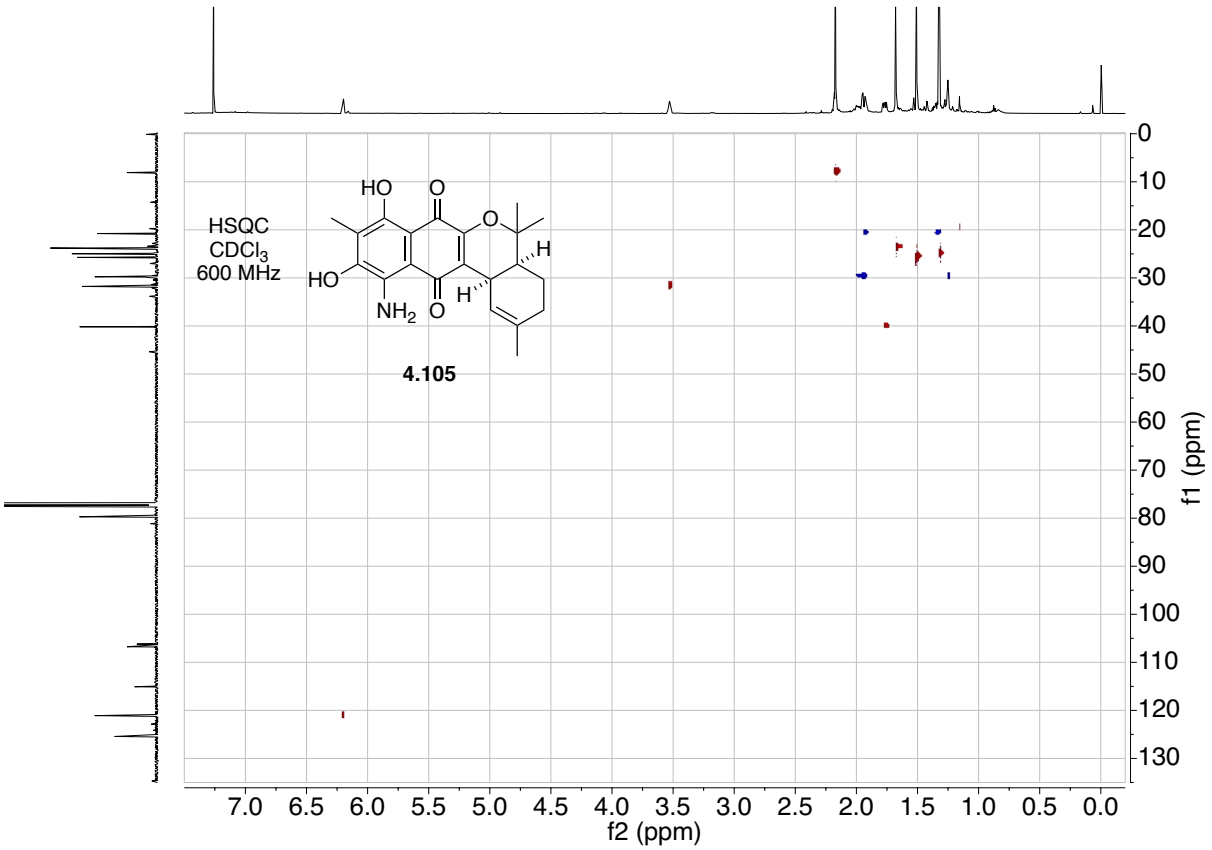
HSQC
CDCl3
600 MHz
HO
O
O
H
HO
NH2
O
H
4.105
f2 (ppm)
f1 (ppm)

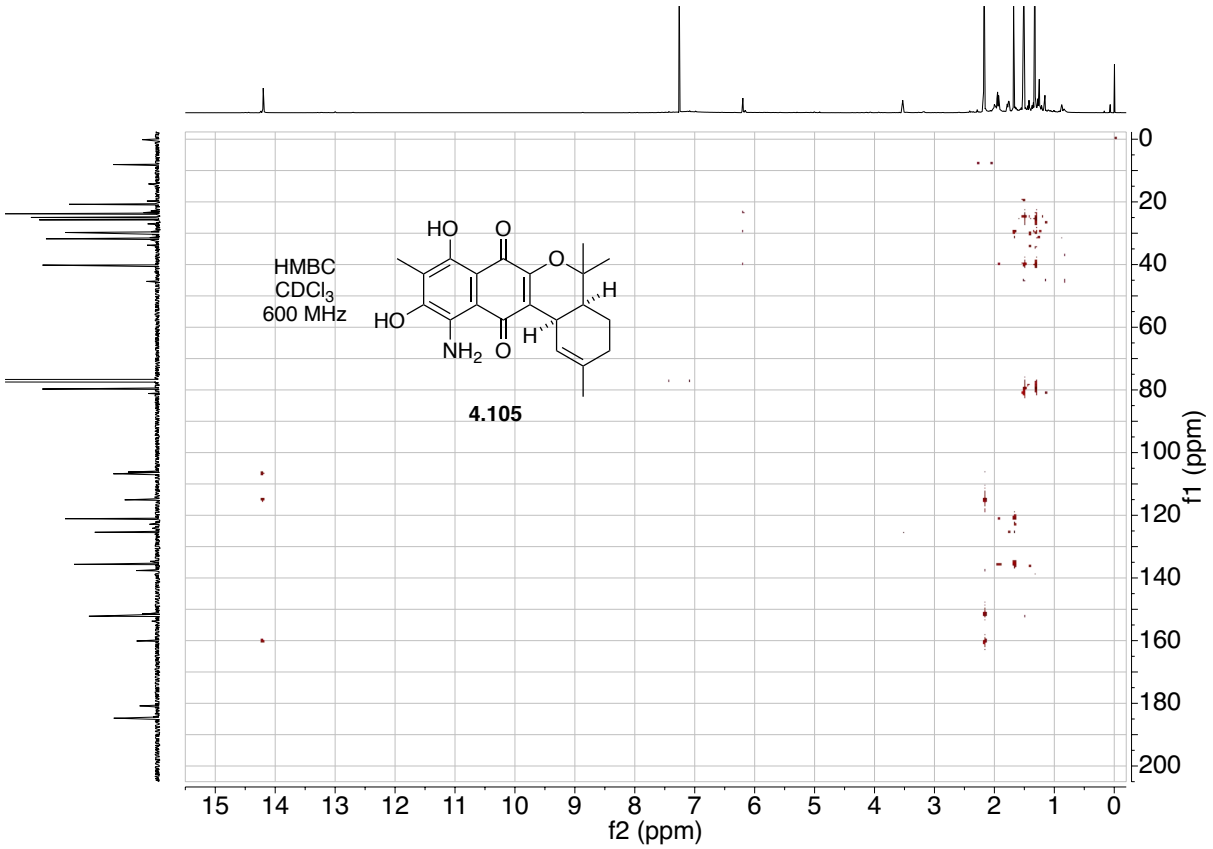
HMBC
CDCl3
600 MHz
HO
O
O
H
HO
H
NH2
O
4.105
f2 (ppm)
f1 (ppm)

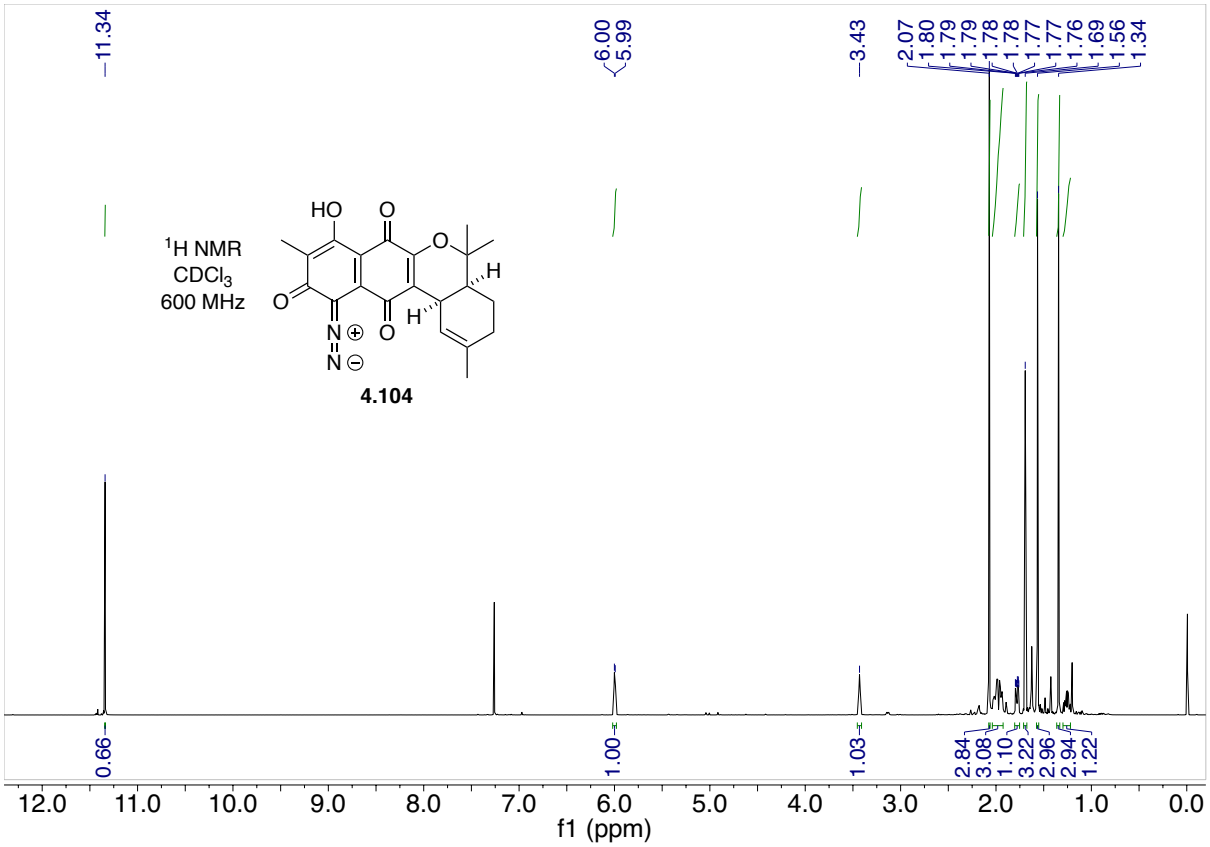
11.34
6.00
5.99
3.43
2.07
1.80
1.79
1.79
1.78
1.78
1.77
1.77
1.76
1.69
1.56
1.34
^{1}H NMR
$CDCl_3$
600 MHz
HO
O
O
O
H
H
O
N
N
4.104
0.66
1.00
1.03
2.84
3.08
1.10
3.22
2.96
2.94
1.22
12.0
11.0
10.0
9.0
8.0
7.0
6.0
5.0
4.0
3.0
2.0
1.0
0.0
f1 (ppm)

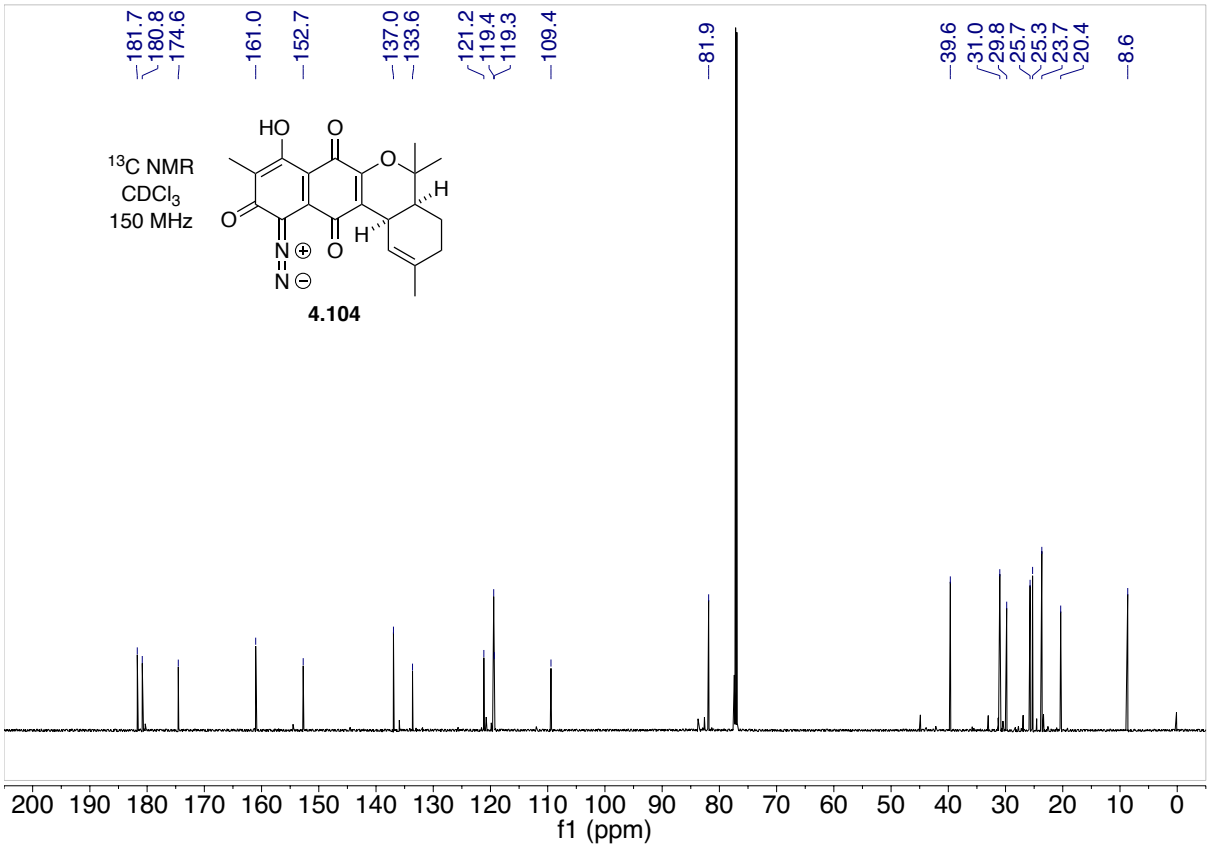
181.7
180.8
174.6
161.0
152.7
137.0
133.6
121.2
119.4
119.3
109.4
81.9
39.6
31.0
29.8
25.7
25.3
23.7
20.4
8.6
^{13}C NMR
$CDCl_3$
150 MHz
HO
O
O
O
H
H
O
N
N
4.104
200
190
180
170
160
150
140
130
120
110
100
90
80
70
60
50
40
30
20
10
0
f1 (ppm)

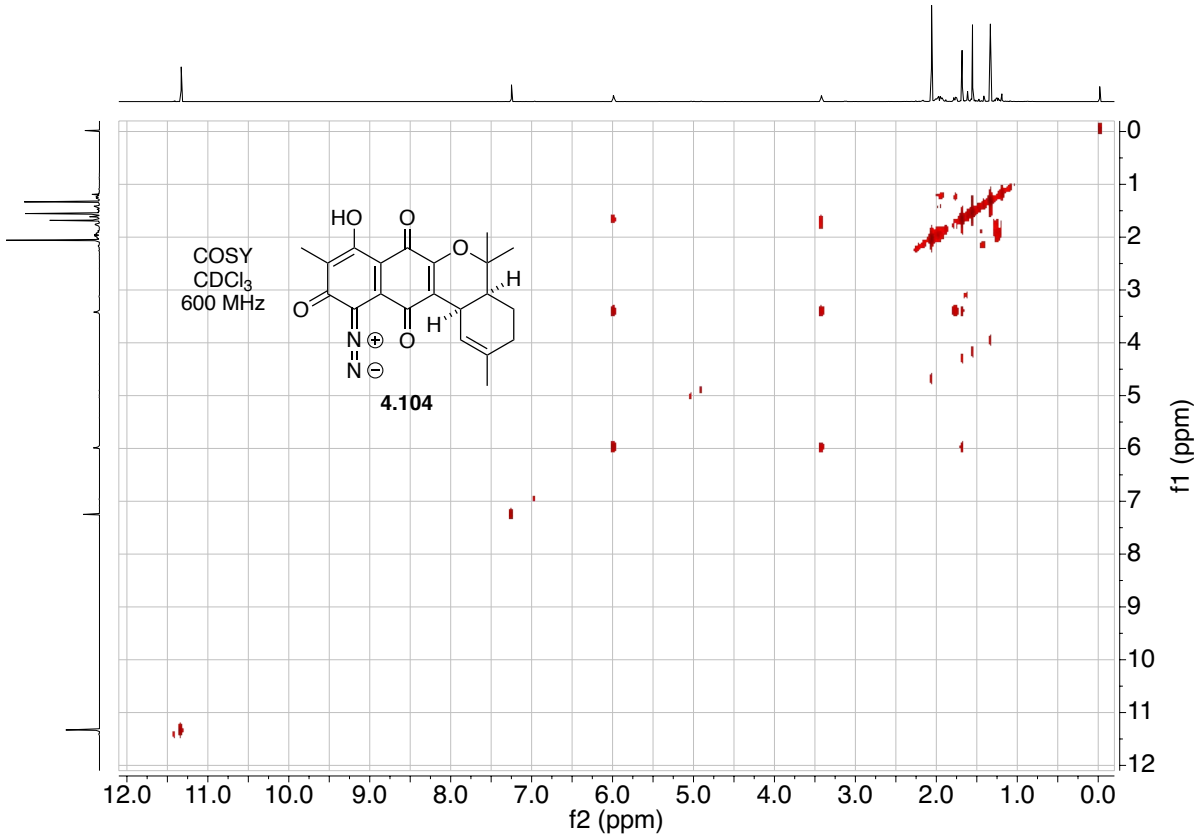
COSY
CDCl3
600 MHz
HO
O
O
H
O
H
N
N
4.104
f2 (ppm)
f1 (ppm)

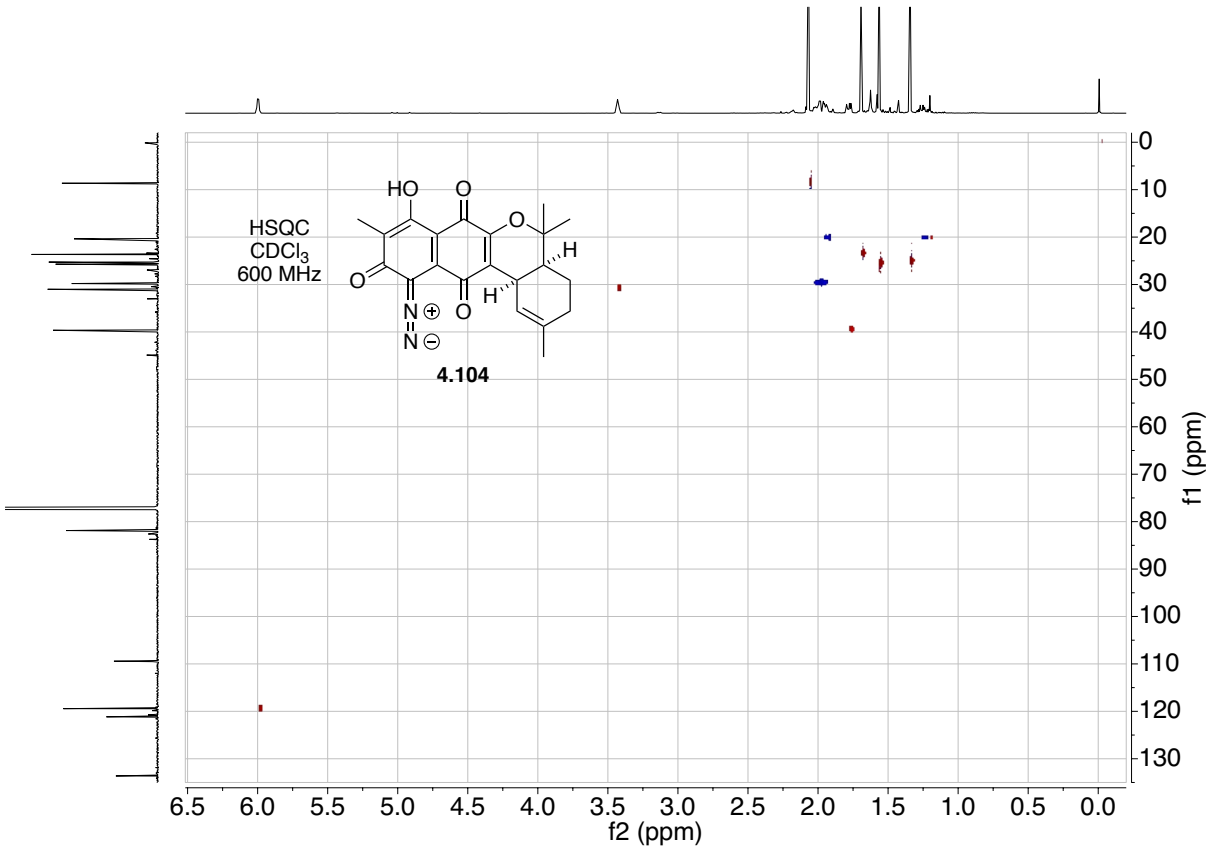
HSQC
CDCl3
600 MHz
HO
O
O
H
O
H
N
N
4.104
f2 (ppm)
f1 (ppm)

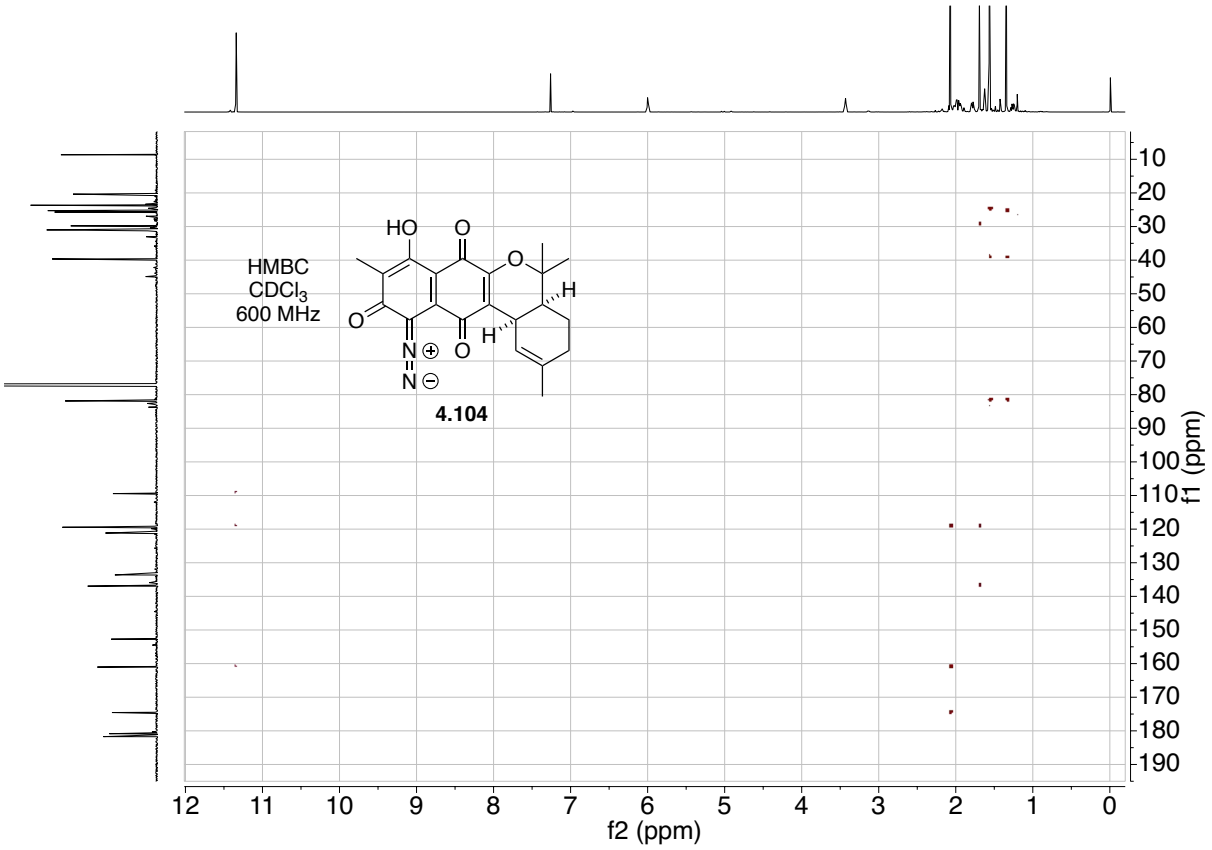
HMBC
CDCl3
600 MHz
HO
O
O
O
H
O
H
N
O
N
4.104
f2 (ppm)
f1 (ppm)

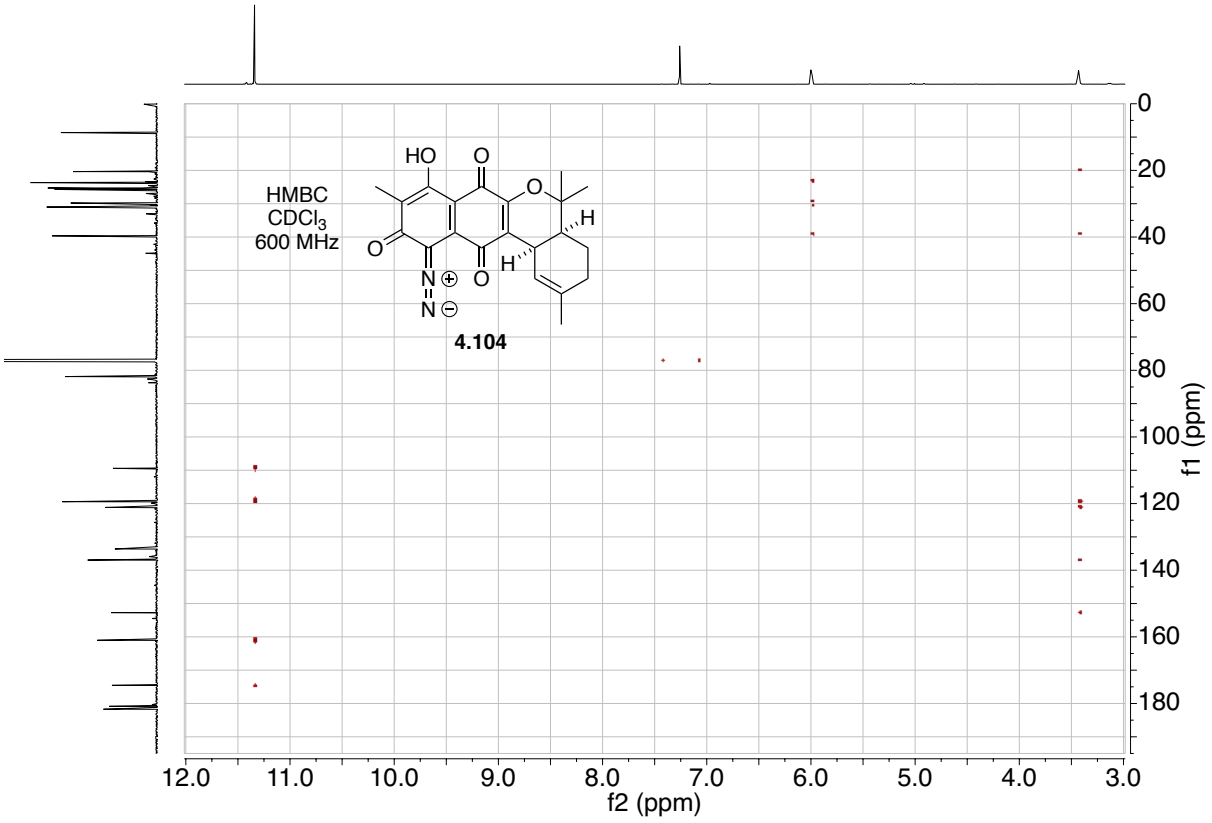
HMBC
CDCl3
600 MHz
HO
O
O
O
H
O
H
N
O
N
4.104
f2 (ppm)
f1 (ppm)

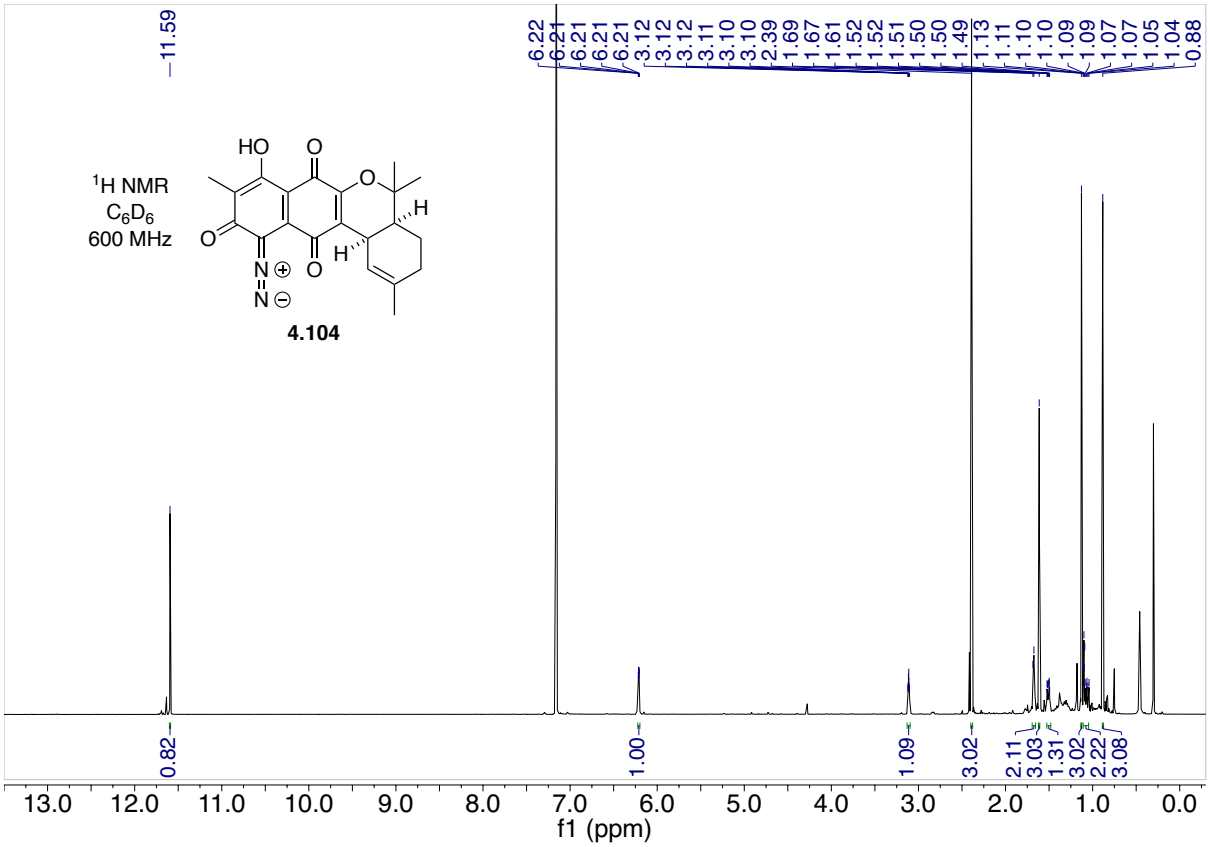
11.59
6.22
6.21
6.21
6.21
3.12
3.12
3.12
3.11
3.10
3.10
2.39
1.69
1.67
1.61
1.52
1.52
1.51
1.50
1.50
1.49
1.13
1.11
1.10
1.10
1.09
1.09
1.07
1.07
1.05
1.04
0.88
1H NMR
C6D6
600 MHz
HO
O
O
O
O
H
H
N
N
4.104
0.82
1.00
1.09
3.02
2.11
3.03
1.31
3.02
2.22
3.08
13.0 12.0 11.0 10.0 9.0 8.0 7.0 6.0 5.0 4.0 3.0 2.0 1.0 0.0
f1 (ppm)

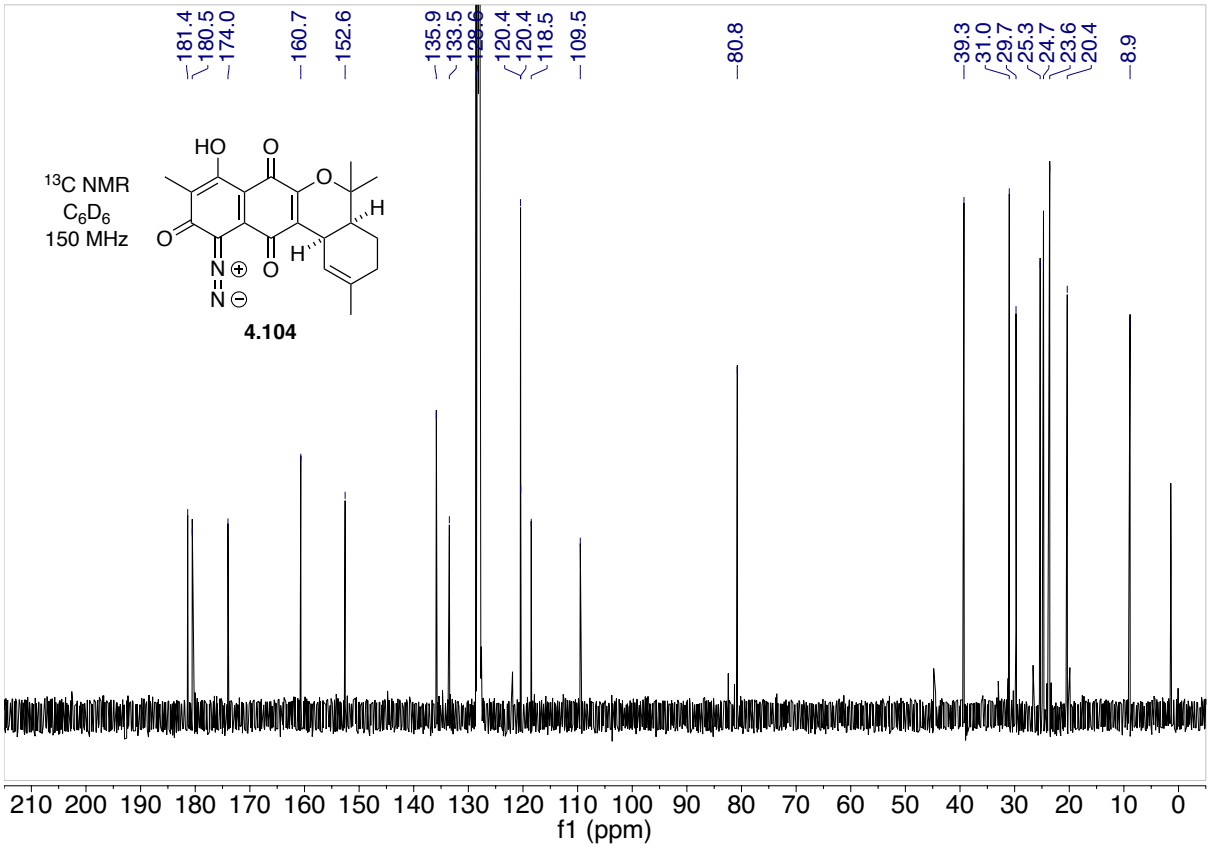
181.4
180.5
174.0
160.7
152.6
135.9
133.5
129.6
120.4
120.4
118.5
109.5
80.8
39.3
31.0
29.7
25.3
24.7
23.6
20.4
8.9
13C NMR
C6D6
150 MHz
HO
O
O
O
O
H
H
N
N
4.104
210 200 190 180 170 160 150 140 130 120 110 100 90 80 70 60 50 40 30 20 10 0
f1 (ppm)

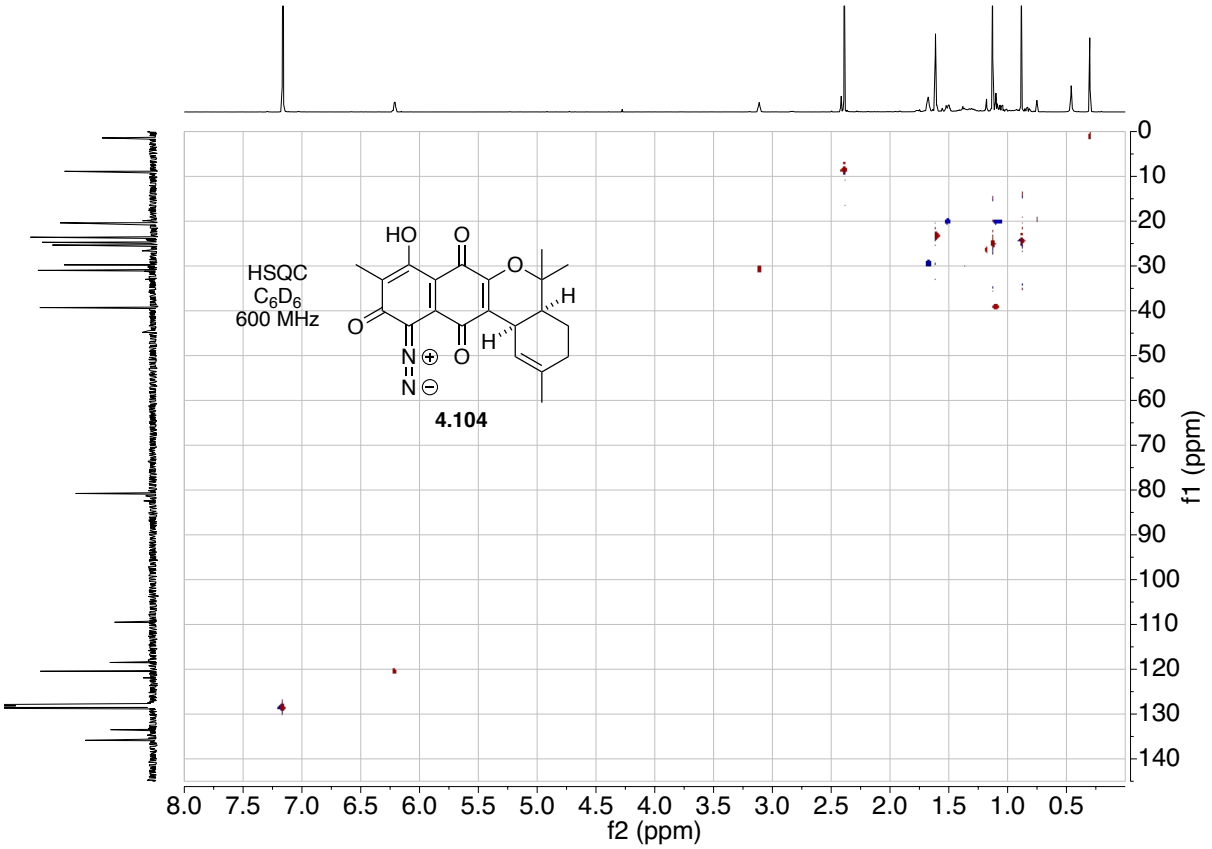
HSQC
C6D6
600 MHz
HO
O
O
O
H
O
H
N
N
4.104
f2 (ppm)
f1 (ppm)

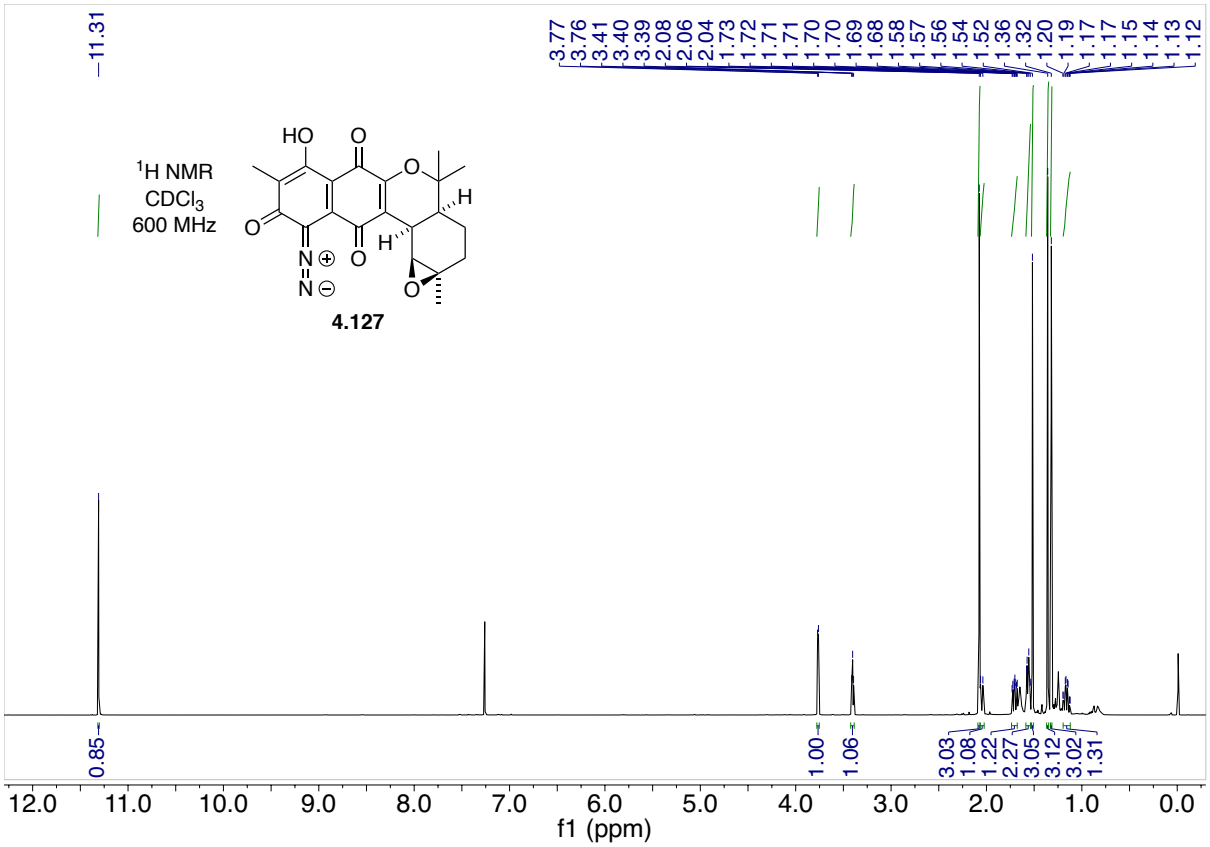
11.31
3.77
3.76
3.41
3.40
3.39
2.08
2.06
2.04
1.73
1.72
1.71
1.71
1.70
1.70
1.69
1.68
1.58
1.57
1.56
1.54
1.52
1.36
1.32
1.20
1.19
1.17
1.17
1.15
1.14
1.13
1.12
^{1}H NMR
$CDCl_3$
600 MHz
HO
O
O
O
O
H
H
N
N
O
4.127
0.85
1.00
1.06
3.03
1.08
1.22
2.27
3.05
3.12
3.02
1.31
12.0
11.0
10.0
9.0
8.0
7.0
6.0
5.0
4.0
3.0
2.0
1.0
0.0
f1 (ppm)

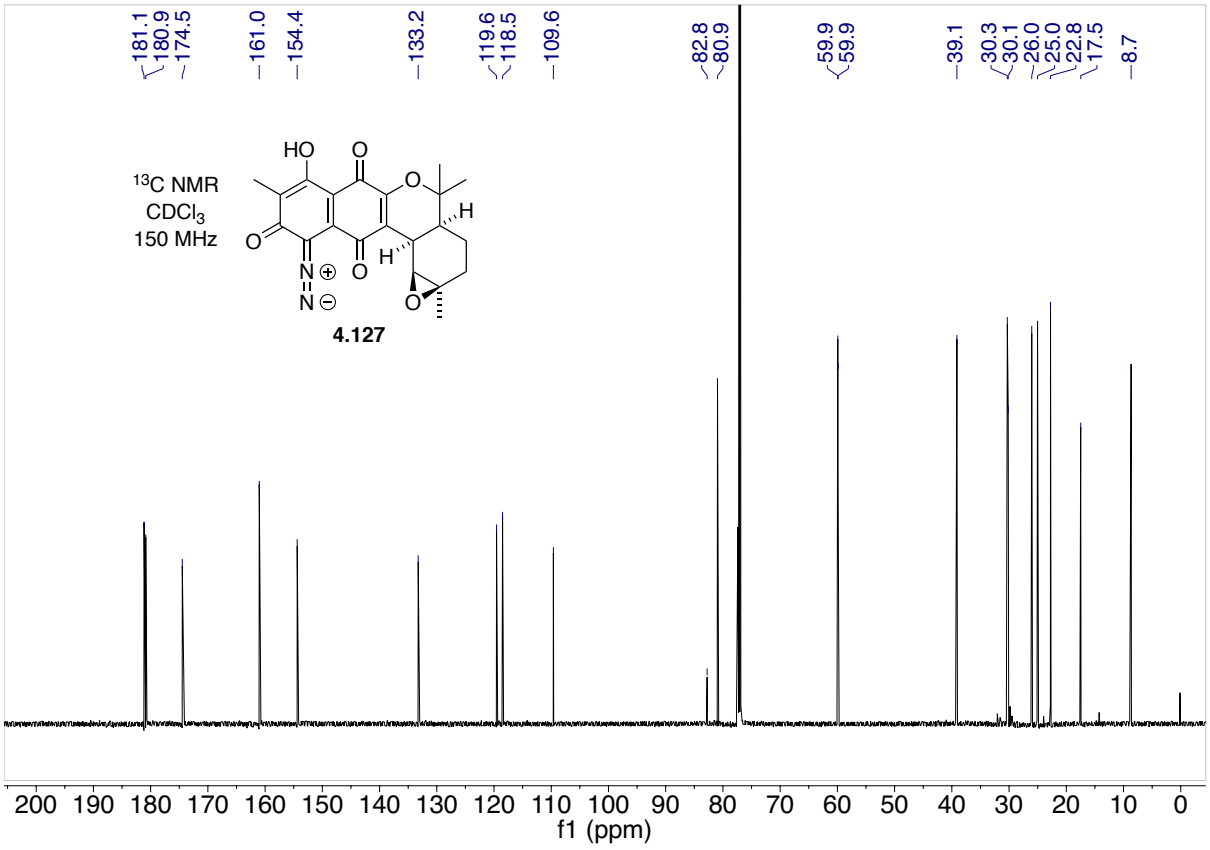
181.1
180.9
174.5
161.0
154.4
133.2
119.6
118.5
109.6
82.8
80.9
59.9
59.9
39.1
30.3
30.1
26.0
25.0
22.8
17.5
8.7
^{13}C NMR
$CDCl_3$
150 MHz
HO
O
O
O
O
H
H
N
N
O
4.127
200
190
180
170
160
150
140
130
120
110
100
90
80
70
60
50
40
30
20
10
0
f1 (ppm)

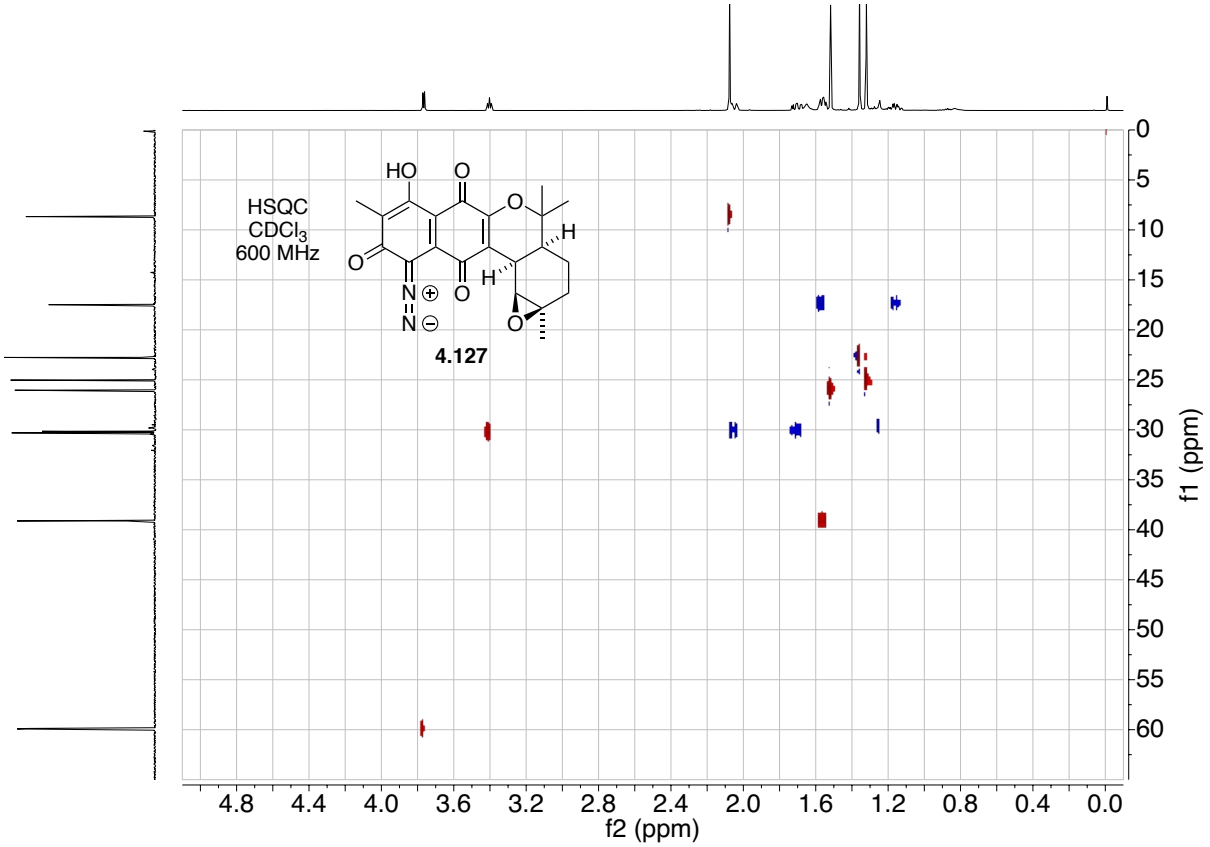
HSQC
CDCl3
600 MHz
HO
O
O
O
H
O
N
N
O
H
O
4.127
f1 (ppm)
f2 (ppm)
0
5
10
15
20
25
30
35
40
45
50
55
60
4.8
4.4
4.0
3.6
3.2
2.8
2.4
2.0
1.6
1.2
0.8
0.4
0.0

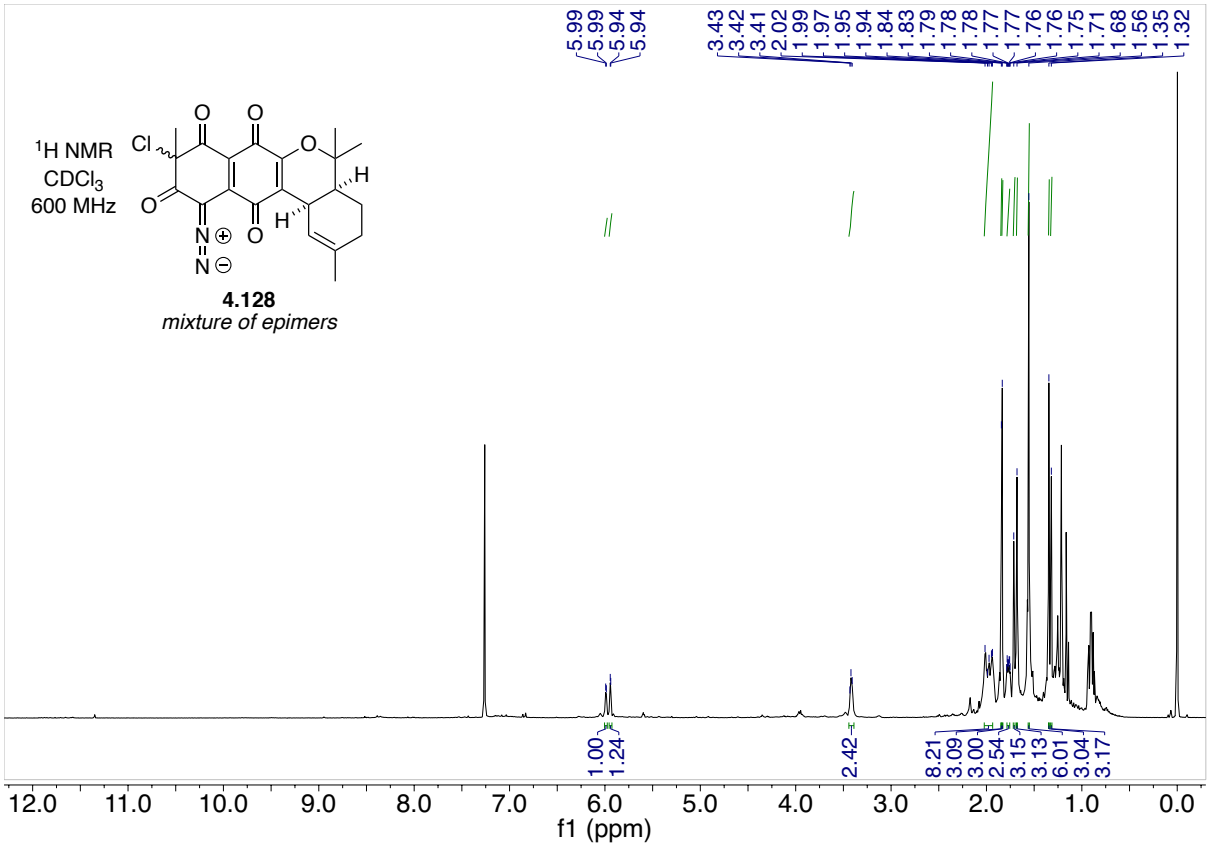

4.128
mixture of epimers

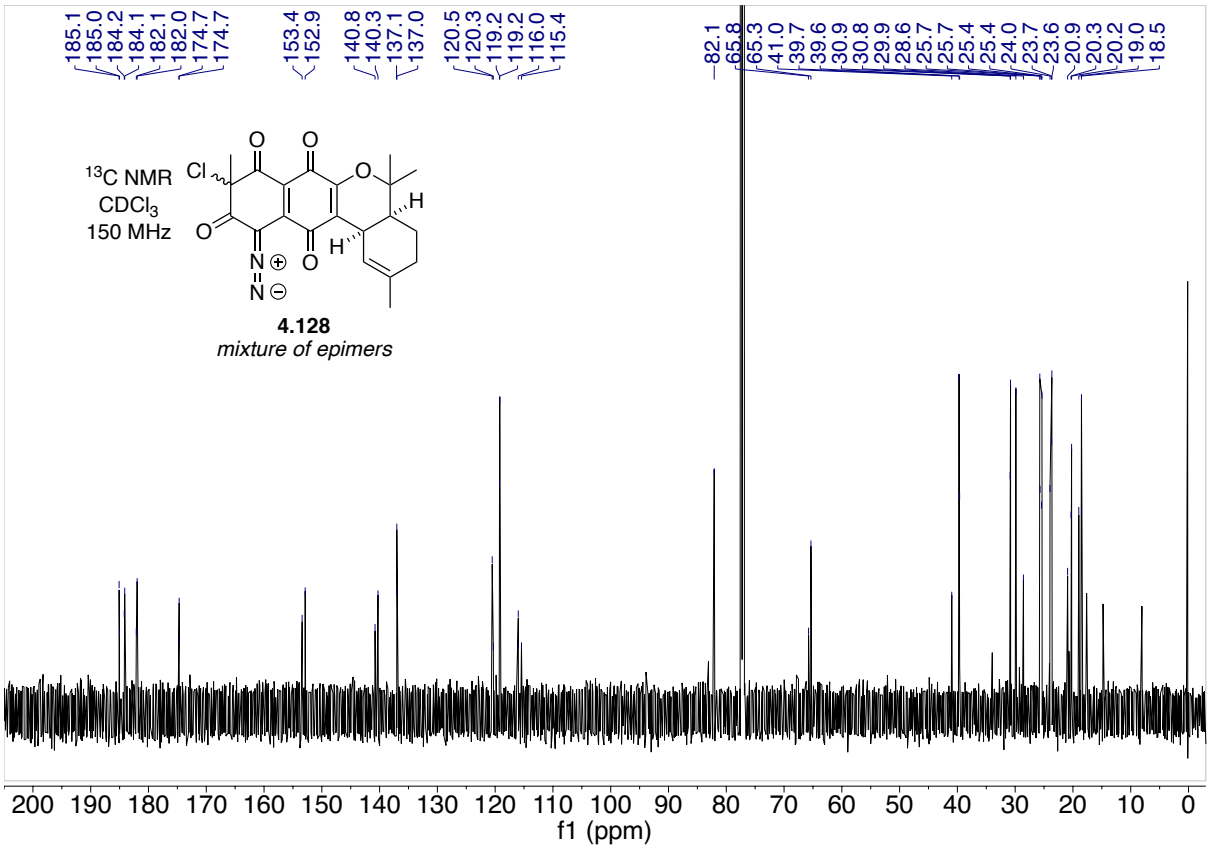

4.128
mixture of epimers

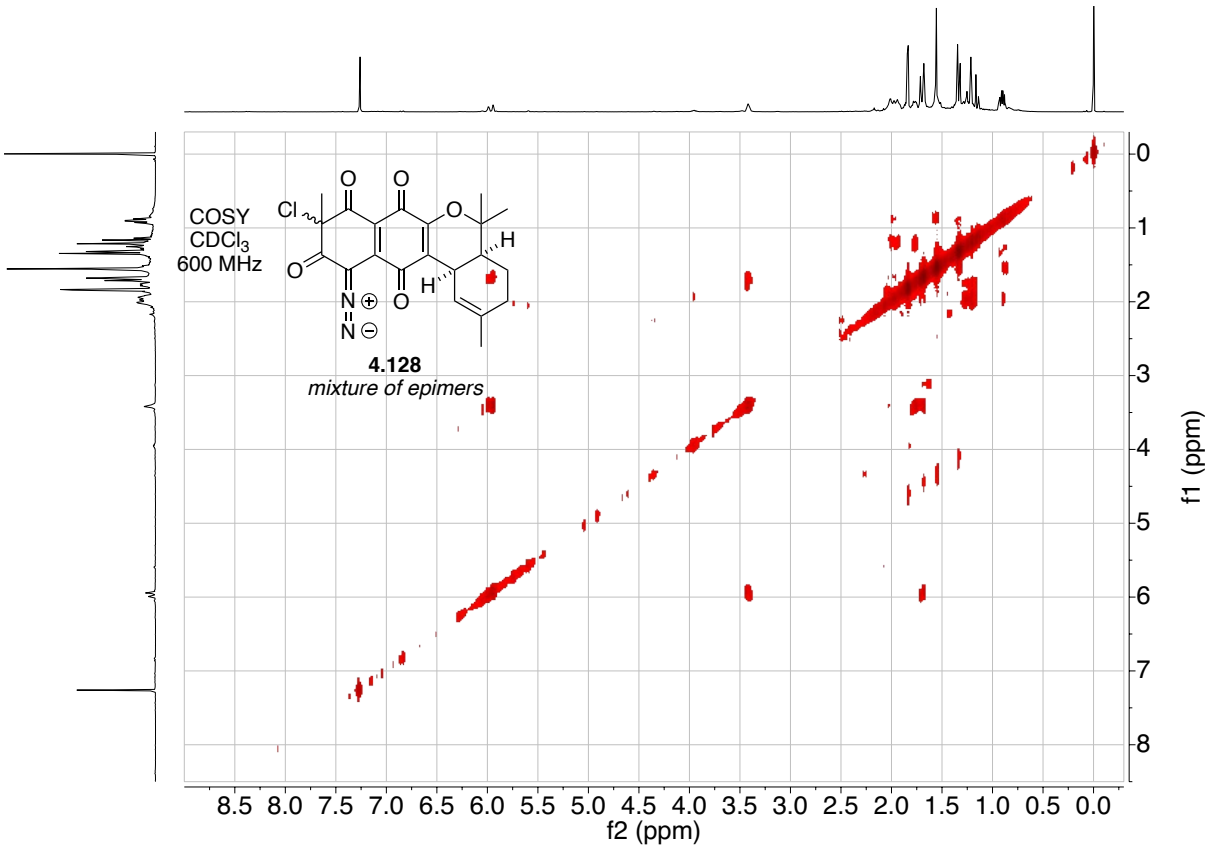
COSY
CDCl3
600 MHz
4.128
mixture of epimers
f2 (ppm)
f1 (ppm)

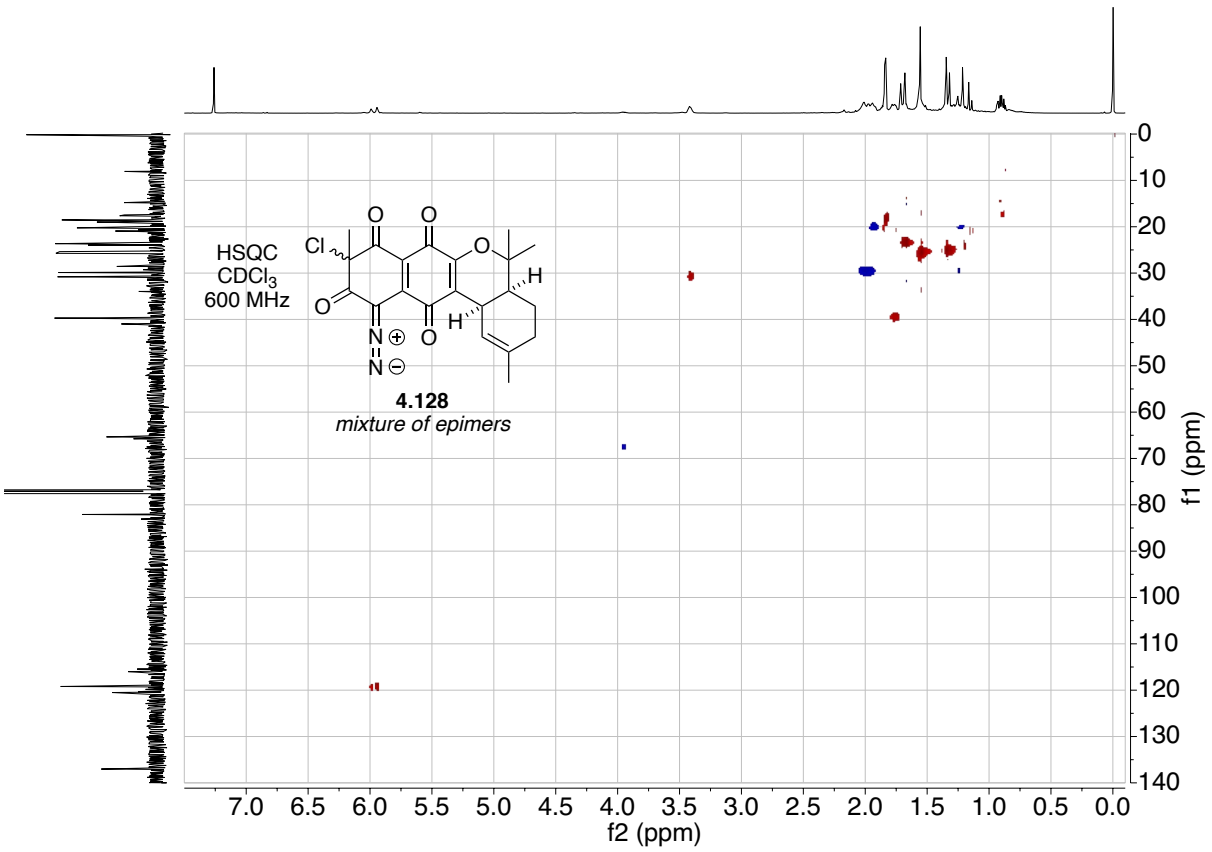
HSQC
CDCl3
600 MHz
4.128
mixture of epimers
f2 (ppm)
f1 (ppm)

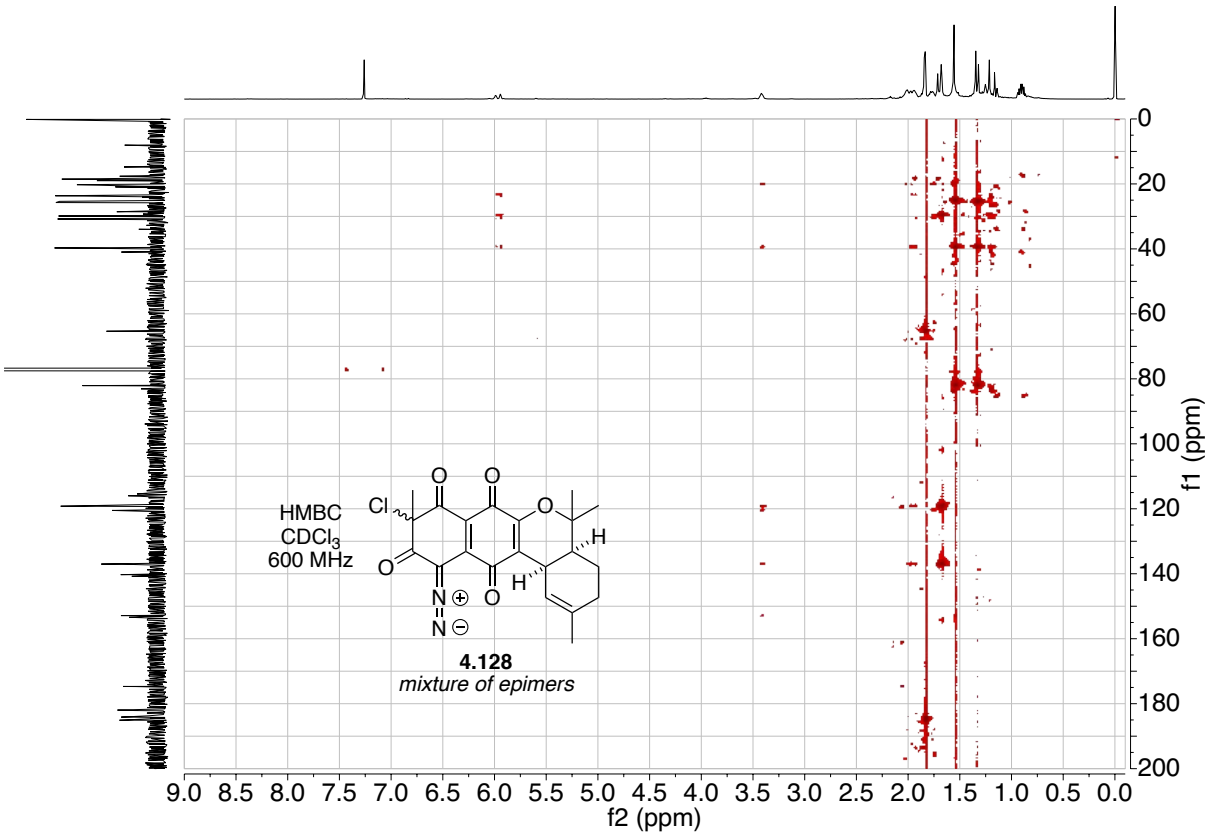
HMBC
CDCl3
600 MHz
4.128
mixture of epimers
f2 (ppm)
f1 (ppm)

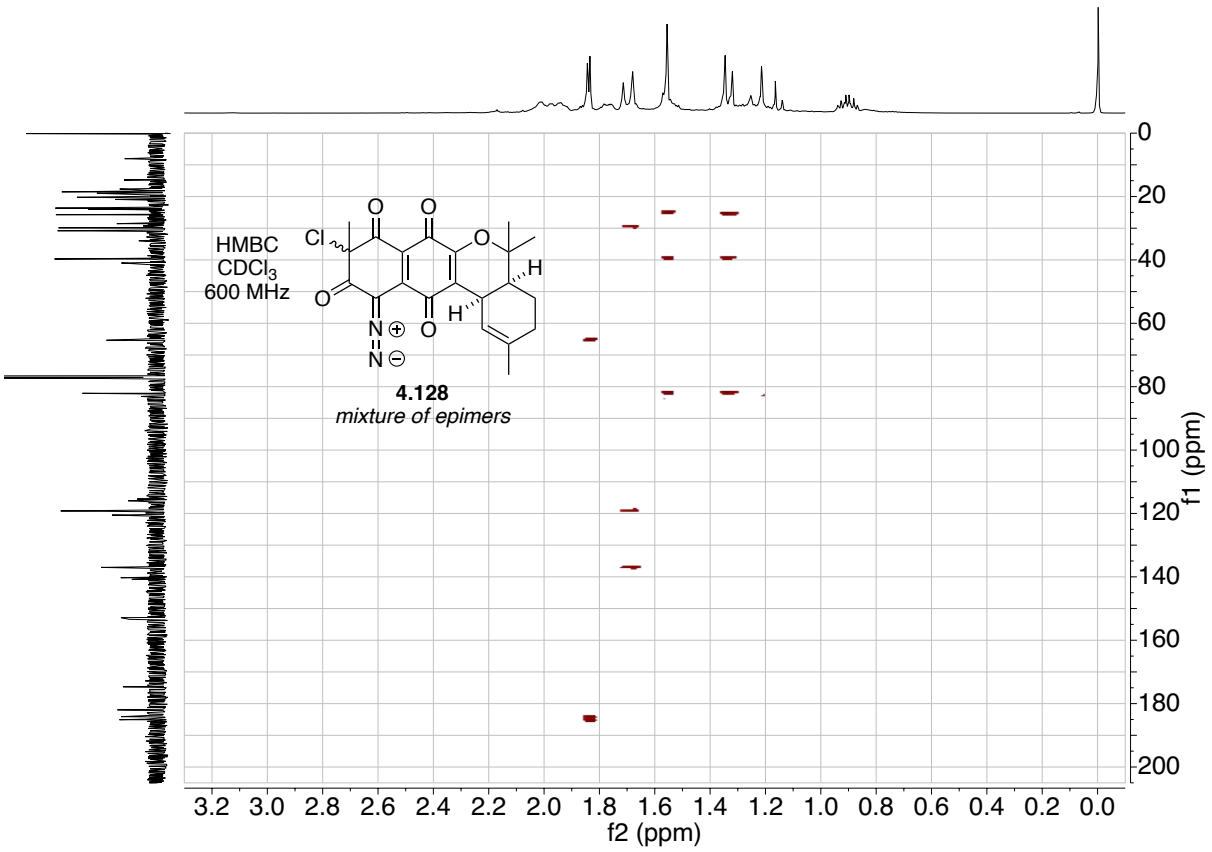
HMBC
CDCl3
600 MHz
4.128
mixture of epimers
f2 (ppm)
f1 (ppm)

4.6.2 IR spectra

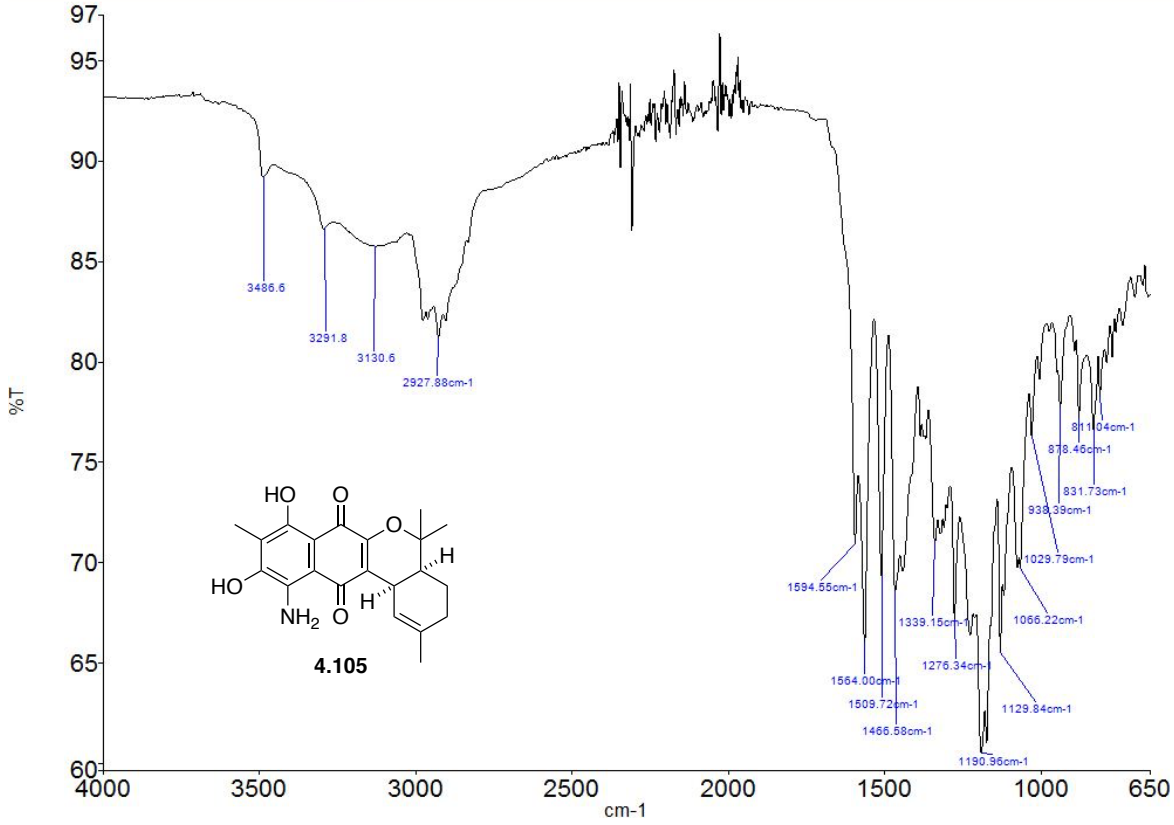

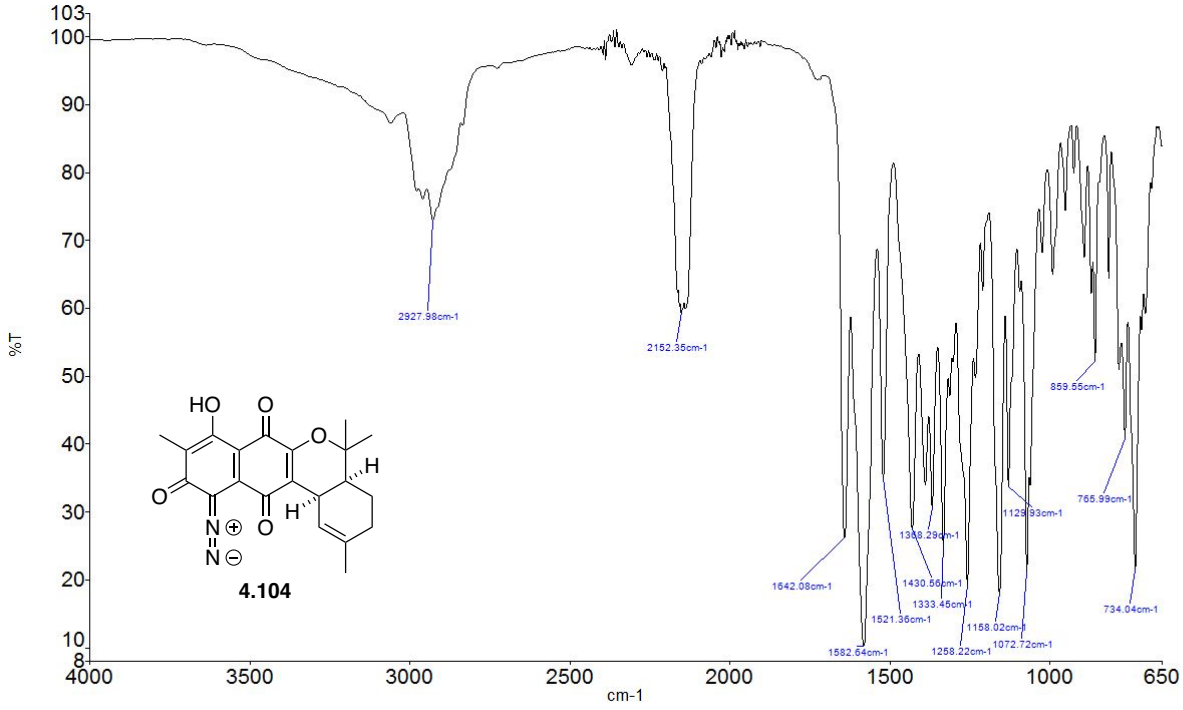

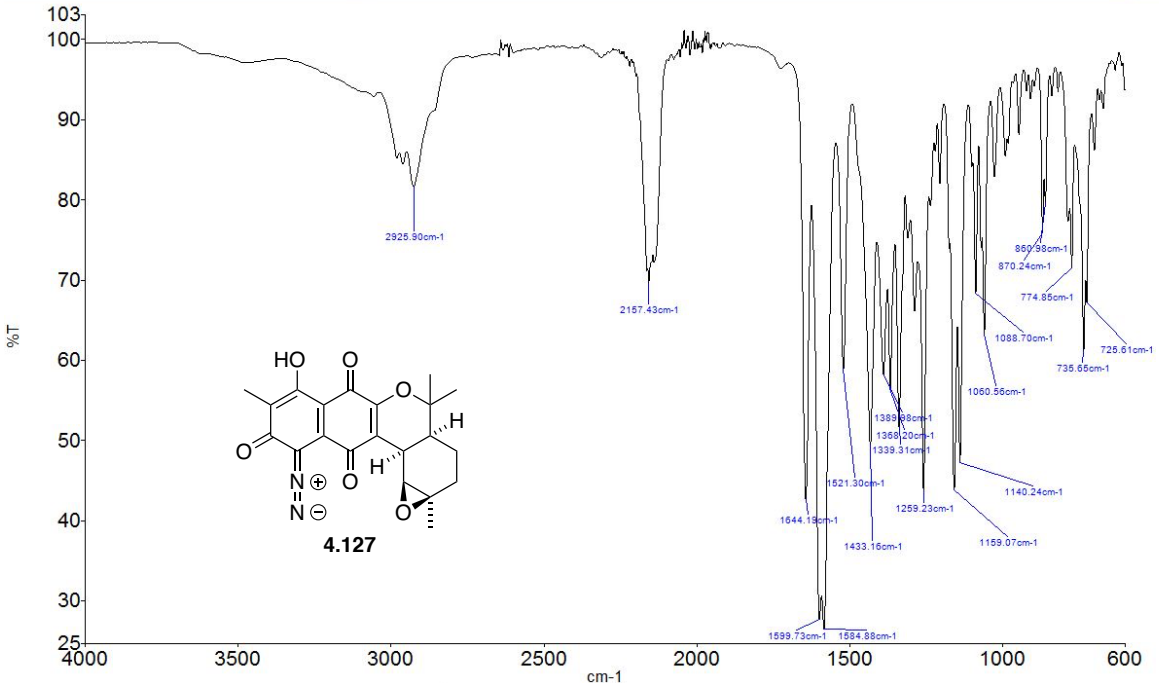
%T
cm-1
2925.90cm-1
2157.43cm-1
1644.19cm-1
1599.73cm-1
1584.88cm-1
1521.30cm-1
1433.16cm-1
1389.98cm-1
1368.20cm-1
1339.31cm-1
1259.23cm-1
1159.07cm-1
1140.24cm-1
1088.70cm-1
1060.56cm-1
870.24cm-1
860.98cm-1
774.85cm-1
735.65cm-1
725.61cm-1
HO
O
O
H
H
N
O
O
4.127

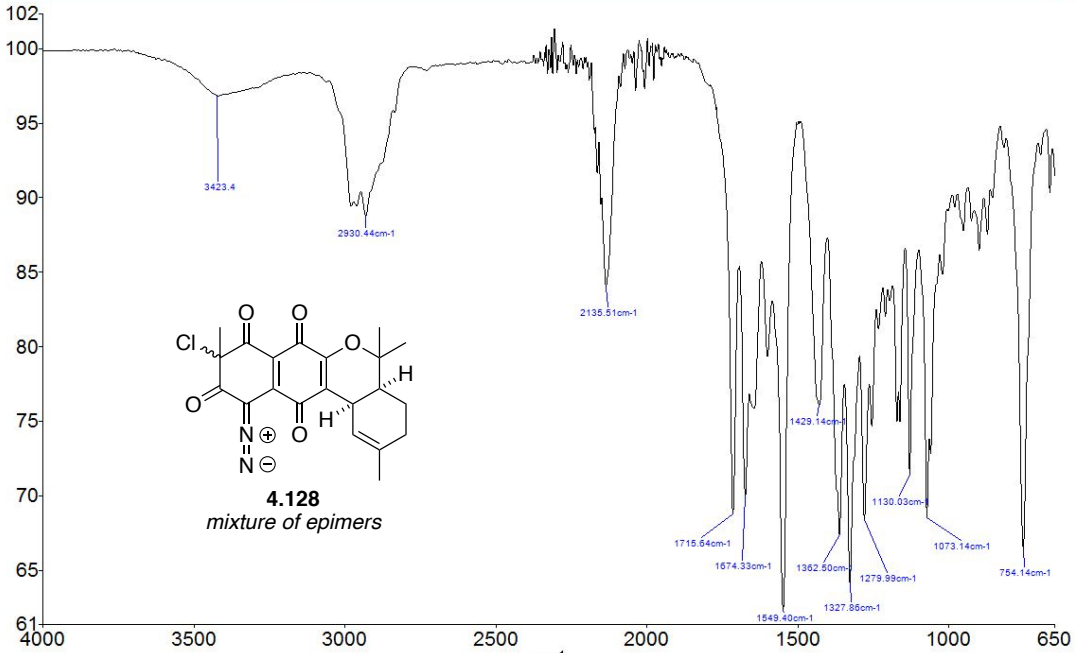
3423.4
2930.44cm-1
2135.51cm-1
1715.64cm-1
1674.33cm-1
1549.40cm-1
1429.14cm-1
1362.50cm-1
1327.86cm-1
1279.99cm-1
1130.03cm-1
1073.14cm-1
754.14cm-1
Cl
O
O
O
O
H
H
N
4.128
mixture of epimers